PROCEEDINGS OF THE

22nd International Symposium on Analytical and Environmental Problems

October 10, 2016

University of Szeged, Department of Inorganic and Analytical Chemistry

Szeged
Hungary

Edited by:
Tünde Alapi
István Ilisz

Publisher:
University of Szeged, Department of Inorganic and Analytical Chemistry, H-6720 Szeged, Dóm tér 7, Hungary

ISBN 978-963-306-507-5

2016.
Szeged, Hungary

The 22nd International Symposium on Analytical and Environmental Problems

Organized by:
SZAB Kémiai Szakbizottság Analitikai és Környezetvédelmi Munkabizottsága

Supporting Organizations
University of Szeged, Department of Inorganic and Analytical Chemistry
Hungarian Academy of Sciences

Symposium Chairman:
István Ilisz, PhD

Honorary Chairman:
Zoltán Galbács, PhD

Organizing Committee:
István Ilisz, PhD
associate professor
University of Szeged Department of Inorganic and Analytical Chemistry
ilisz@chem.u-szeged.hu

Tünde Alapi, PhD
assistant professor
University of Szeged Department of Inorganic and Analytical Chemistry
alapi@chem.u-szeged.hu

Lecture Proceedings

SYNTHESIS AND STRUCTURAL CHARACTERIZATION OF DIMERIC AND POLYMERIC COPPER(II) COMPLEXES WITH SCHIFF BASE AS LIGAND

Ildiko Butà[1*], Diana Aparaschivei[1], Carmen Creţu[1], Liliana Cseh[1], Ramona Tudose[1], Cătălin Maxim[2], Marius Andruh[2], Peter Lönnecke[3], Evamarie Hey-Hawkins[3], Otilia Costişor[1]

[1]*Institute of Chemistry of the Romanian Academy, 24 Mihai Viteazu Bvd.,300223-Timisoara, Romania*
[2]*University of Bucharest, Faculty of Chemistry, Inorganic Chemistry Laboratory, Str. Dumbrava Rosie nr. 23, 020464-Bucharest, Romania*
[3] *Institute of Inorganic Chemistry, Universität Leipzig Johannisallee 29, 04103 Leipzig, Germany*
e-mail: ildiko_buta@acad-icht.tm.edu.ro

Abstract

Polynuclear coordination compounds derived from multidentate Schiff base ligands are a source of new materials with applications in catalysis [1], optoelectronic materials [2], and environmental applications [3]. In extension of our previous studies [4]on polynuclear materials, we report the crystal structures and spectroscopic properties ofdimeric and polymeric copper(II) complexeswith hexadentate Schiff base N,N'-bis[(2-hydroxybenzilideneamino)-propyl]-piperazine (**H_2L**) as ligand. Reaction of $Cu(ClO_4)_2$ hexahydrate with **H_2L** in the presence of triethylamine affords a polymeric structure $[Cu_3\mathbf{L}_2(\mu_3\text{-}ClO_4)_{0.66}](ClO_4)_{1.33}\cdot 1.33CHCl_3$(**1**) in which the perchlorate anion acts as a tridentate ligand in a μ_3-manner binding three $Cu_3\mathbf{L}_2$ units. When NaN_3 was added to the above mentioned reaction mixturea new dimeric assembly$[Cu_6(C_{24}H_{30}N_4O_2)_4(N_3)_2][ClO_4]_2$ (**2**) was obtained in which two azide groups bridge two $Cu_3\mathbf{L}_2$ unitsin an end-to-end fashion. The same dimeric structure was obtained when the polymer **1** was treated with NaN_3.

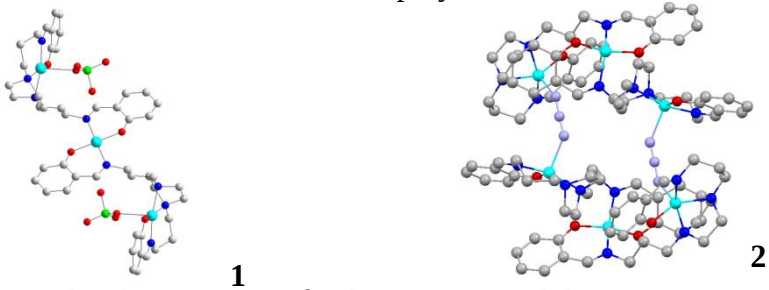

1 **2**

Figure 1. Molecular structure of polymeric (**1**) and dimeric(**2**) copper(II) complexes

Acknowledgements

The authors acknowledge the support of the Romanian Academy, Project 4.1.

References

[1] K.C. Gupta, A. K. Sutar, Coord. Chem. Rev. 252(2008)1420.
[2] C.M. Che, C.C. Kwok, S.W. Lai, A.F. Rausch, W.J. Finkenzeller, N.Y. Zhu, H. Yersin, Chem. Eur. J. 16(2010) 233.
[3] D. Gopi, K. Govindaraju, L. Kavitha, J. Appl. Electrochem. 40(2010) 1349.
[4] C. Cretu, R. Tudose, L. Cseh, W. Linert, E. Halevas, A. Hatzidimitriou, O. Costisor, A. Salifoglou, Polyhedron85(2015) 48.

COMPLEX FORMATION BETWEEN Co-METALLOPORPHYRIN AND SILVER COLLOID IN ACIDIC MEDIA

Anca Lascu[*a], Ionela Creanga[a], Anca Palade[a], Mihaela Birdeanu[b]

[a]*Institute of Chemistry Timisoara of Romanian Academy, 24 M. Viteazul Ave., 300223-Timisoara, Romania,*
[b]*National Institute for Research and Development in Electrochemistry and Condensed Matter, 1 Plautius Andronescu Street, 300224 Timisoara, Romania*
e-mail: ancalascu@yahoo.com

Abstract
Large flower sized nanoparticles of silver were synthesized and hybrid colloids with porphyrins were obtained. Daisy-like round aggregates generated from triangular-shaped silver nanoparticles can be observed, evenly distributed. The complexation of these particles with organic dyes was the main purpose of this work in order to achieve nanomaterials exhibiting wide absorption bands.
The formation of a complex between an acidified Co(II) 5,10,15,20-meso-tetra(3-hydroxyphenyl) porphyrin (**Co-3OHPP**) solution in THF and the silver colloid negatively charged at the surface was proven by analyzing the UV-vis spectra during the experiment.

Introduction
The obtaining ofsilver nanoparticles using non-polluting natural materials is a new trend in science today and thereforevarious natural extracts were used to stabilize the nanosized metal. The reduction with banana peel extract [1] aqueous extract of *Solanum torvum* fruit [2] ora mixture of ascorbic acid and starch were also tested with promising results [3]. In order to prevent the colloids from coagulating, poly(vinyl alcohol), poly(vinylpyrrolidone) or sodium dodecyl sulfate are used to obtain a narrow size distribution of particles [4]. Silver colloids stabilized by cellulose, glass, and quartz supports can be stable for more than 3 weeks [5].
The oxygen-binding behavior of cobalt(II) porphyrin complexes strongly depends on the nature of substituents linked to the porphyrin ring [6].
Our work focuses on obtaining large sized nanoparticles of silver and on forming hybrid materials containing these silver colloids and porphyrins, in order to enhance their optical and biological properties.

Experimental
The method chosen for the obtaining of a sustainable plasmon was adapted from literature [7]. The Co(II) 5,10,15,20-meso-tetra(3-hydroxyphenyl) porphyrin was synthetized as previously mentioned in literature [8].
The silver salt ($AgNO_3$), poly(vinylpirrolidone) (PVP) (Mw=360000), ascorbic acid ($C_6H_8O_6$) and tetrahydrofurane (THF) were purchased from Merck or Sigma-Aldrich and were used without further purification. The water was previously distilled and the ethanol was p.a. grade.
The procedure of obtaining the silver colloid: aqueous solution of $AgNO_3$ (0.6 mL 1M) and poly(vinylpirrolidone) (PVP, Mw=360000, 6 mL, 1% w/w) were added under intense stirring in 30 mL distilled water at room temperature. Ascorbic acid (0.6 mL, 1M) solution was poured at once over the mixture and the stirring was maintained until the solution turned grey. The colloid was investigated by means of UV-vis spectroscopy and AFM measurements.
UV-visible spectra were recorded on a JASCO UV-visible spectrometer, V-650 model (Japan). The surface imaging investigations were done in ambient conditions on a Nanosurf® EasyScan 2 Advanced Research AFM (Switzerland), with samples deposited onto pure silica

plates by slow evaporation of the water. AFM images were obtained in contact mode and are quantitative on all three dimensions.

Results and discussions

The purpose of introducing a large molecular mass polymer into the solution of freshly prepared silver nanoparticles is to prevent them to aggregate and to allow the generation of nanoparticles with various shapes other than spherical, thus enhancing the average surface. Another advantage is that the polymer has no influence upon the light absorption domain and is biocompatible.

As can be observed from the UV-vis spectrum of the colloidal solution of silver nanoparticles (Figure 1), the absorption maximum is located at 424 nm, thus offering information about particle size. It can be estimated that the particles range from 66 to 82 nm[9].

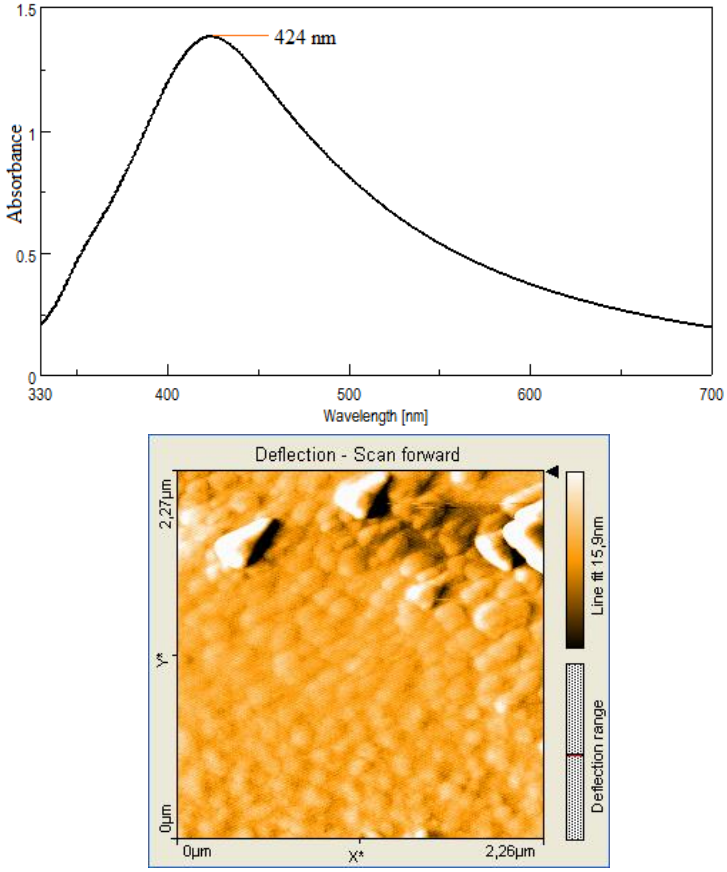

Figure 1. The UV-vis spectrum and 2D AFM imageof water solution of silver nanoparticles

The most conclusive analysis of particle size can be provided by AFM studies. The solution of silver particlesreveals various sizes of nanoparticles, ranging in dimensions from 79 to 290 nm (Figure 1). The formation of larger aggregates by stacking of triangular-shaped particles is also visible (Figure 2).

3D AFM imaging for 2 and 9 µm respectively (Figure 2) reveals the beautiful round flower-like assemblies of silver particles obtained in an environmentally friendly manner.

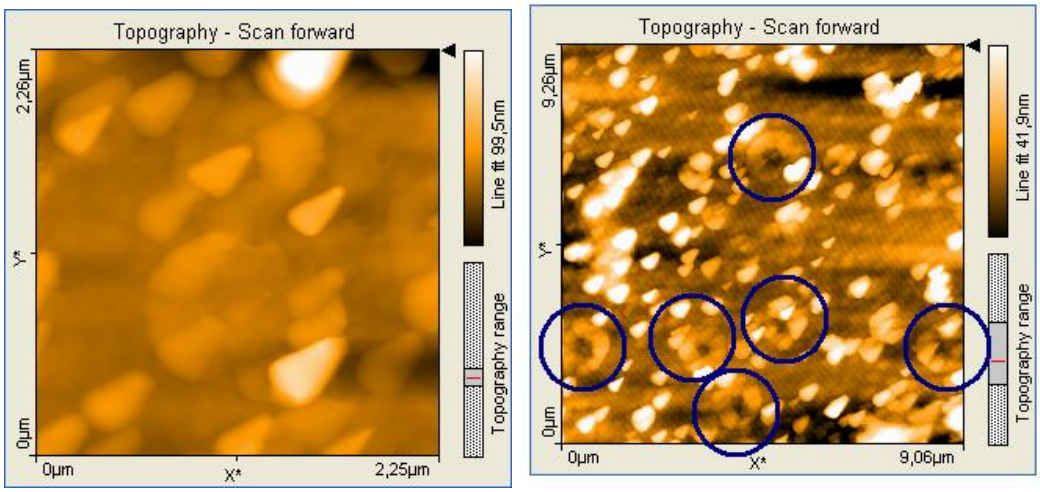

Figure 2. 3D-AFM images of 2 and 9 µm areas of samples measured from water extract of silver colloid

The formation of a complex between these large silver nanoparticles and the Co-porphyrin was attempted as follows: a quantity of 0.18 mg ($2.447x10^{-7}$ mole)Co(II) 5,10,15,20-meso-tetra(3-hydroxyphenyl) porphyrin (**Co-3OHPP**) (M_w=735,65 g/mol)was added to 5 mLTHF and the solution ($c=0.323x10^{-6}$M) was acidified by adding HCl solution (37% wt) until the pH reached 2.This initial solution was added dropwise to 3 mL silver colloid, as follows: 20 µLporphyrin solution in the first ten determinations; then 50 µLporphyrin solution for the next eight determinations. The colloid concentration used in the experiments was $9.375x10^{-5}$M.
After succesive adding of acidified **Co-3OHPP** solution to the silver colloid it can be observed that the intensity of the plasmonic band of the colloid decreases with the increase in porphyrin concentration (Figure 3)as opposed to the case of gold plasmon, where a hyperchromic effect on the Soret band of the **Co-3OHPP-nAu** hybridcan be observed with increasing Co-porphyrin concentration [8].

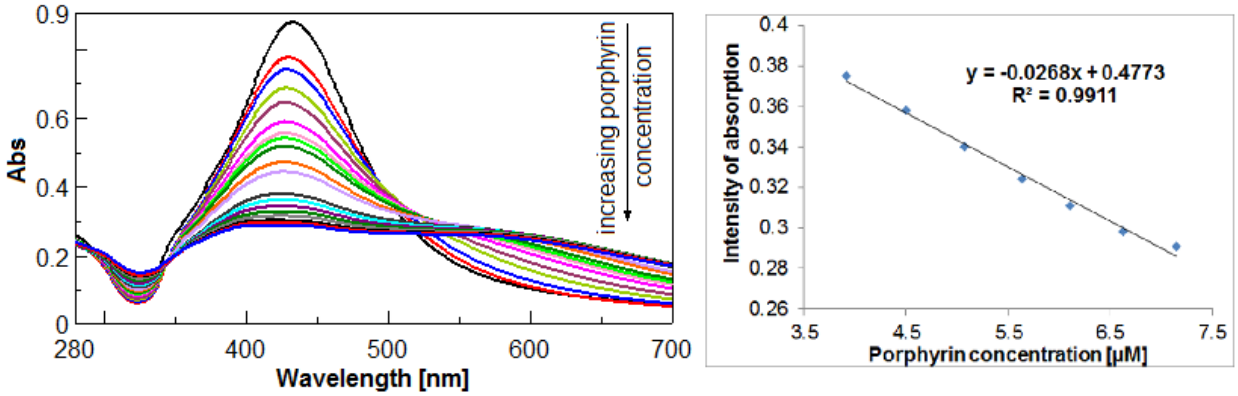

Figure 3. UV-vis spectra of the successive adding of Co-3OHPP to silver colloidand the linear dependence of the intensity of absorption of the nano-silver plasmonic band and the increasing porphyrin concentration

The presence of two isosbestic points, at 350 nm and 570 nm (Figure 3) proves the formation of a complex between the Co-porphyrin and the silver colloidal nanoparticles, indicating at least two equilibrium processes. It can also be observed that the plasmonic band is enlarged having the aspect of a plateau and covers a wide absorption domain with the increase in Co-3OHPP concentration, but the intensity of the absorption is low.

As can be seen in Figure 3, the linear dependence of the intensity of absorption of the nano-silver plasmonic band and the increasing porphyrin concentration can be detected only for a narrow domain of Co-3OHPP concentration, proving that the silver colloid is able to detect with high acuracy only minute quantities of the metalated porphyrin. Co-porphyrins are relevant for human physiology and their trace detection can offer medical information in early diagnosis.

Conclusions

Obtaining large flower sized nanoparticles of silver able to form hybrid colloids with porphyrins was performed. Thus daisy-like round aggregates of triangular-shaped nanoparticles can be observed, evenly distributed in different depths of the colloid. The surface area of these particles is considerable, allowing their use in several technical applications.

The formation of a complex between acidified Co(II) 5,10,15,20-meso-tetra(3-hydroxyphenyl) porphyrin solution in THF and the silver colloid negatively charged at the surface was confirmed by analyzing the UV-vis spectra during the experiment.

References

[1] A. Bankar, B. Joshi, A.R. Kumar, S. Zinjarde, Colloid Surface A: Physicochem. Eng. Aspects 368 (2010)58.
[2] C.H. Ramamurthy, M. Padma, I.D. Samadanam, R. Mareswaran, A. Suyavaran, M.S. Kumar, K. Premkumar, C. Thirunavukkarasu, Colloid Surface B: Biointerfaces 102(2013) 808.
[3] Z. Khan, T. Singh, J.I. Hussain, A.Y. Obaid, S.A. Al-Thabarti, E.H. El-Mossalamy, Colloid Surface B Biointerfaces 102(2013) 578.
[4] G. Carotenuto, G.P. Pepe, L. Nicolais, Eur. Phys. J. B 16(2000) 11.
[5] T. Vo-Dinh, Trends in analytical chemistry 17(1998) 557.
[6] J. Yang, P. Huang, Chem. Mater.12(2000) 2693.
[7] H. Liang, Z. Li, W. Wang, Y. Wu, H. Xu, Adv. Mater. 21 (2009) 1.
[8] E. Fagadar-Cosma, I.Sebarchievici, A.Lascu, I.Creanga, A.Palade, M.Birdeanu, B.Taranu, G.Fagadar-Cosma, J. Alloys Compds, 686 (2016) 896.
[9] A. Slistan-Grijalva, R. Herrera-Urbina, J.F. Rivas-Silva, M. Avalos-Borja, F.F. Castillon-Barraza, A. Posada-Amarillas, Physica E 27(2005) 104.

PHOTODEGRADATION OF DICLOFENAC SODIUM IN AQUEOUS SOLUTION BY ZnO/SnO_2 POWDER MIXTURE CATALYST

Mladenka Novaković[1], Veselin Bežanović[1], Tamara Ivetić[2], Goran Štrbac[2], Ivana Mihajlović[1], Dragana Štrbac[1]

[1]University of Novi Sad, Faculty of Technical Sciences, Department of Environmental Engineering and Occupational Safety and Health, Trg Dositeja Obradovića 6, 21000 Novi Sad, Serbia

[2]University of Novi Sad, Faculty of Science, Department of Physics, Trg Dositeja Obradovića 6, 21000 Novi Sad, Serbia

e-mail: mladenkanovakovic@uns.ac.rs

Abstract

The occurrence of xenobiotics such as drugs, pesticides, personal care products has been widely reported in the last decade. Pharmaceuticals represent emerging micropollutants which are extensively used in medical and veterinary propose. Although pharmaceutical residues are measured in low concentrations, ngL^{-1} in water, they may have negative impacts on ecosystems. The dominant route of pharmaceuticals into environment is by wastewater effluents discharged from treatment plants mainly based on application of biological treatment such as active sludge. The photodegradation of diclofenac sodium under UV irradiation was investigated using ZnO/SnO_2 mixture.After 60 minute of UV exposure, diclofenac was completely degraded.

Introduction

Active pharmaceutical ingredients (APIs) have been defined as important emerging micropollutants, due to its increased use and continuous input into aquatic environment. Pharmaceuticals are biological active substances designed to interact with living organisms. Pharmaceutical residues are transported into water medium by different routes. The wastewater treatment plants (WWTPs) acts as a gateway for human pharmaceuticals to enter water bodies. The existence of pharmaceuticals in surface, ground and drinking water occurs in trace quantities, ppt to ppb (ngL^{-1} - μgL^{-1}). The main therapeutic families detected in water media are: nonsteroidal anti-inflammatory drugs, antibiotics, beta-blockers (β-blockers), antiepileptics, blood lipid lowering agents, antidepressants [1]. Pharmaceuticals in parent or metabolite form are continous infused into water matrices, resulting with pseudo persistence although their half-lives are short.

Present treatment conditions are not effective to handle with this specific class of organic pollutantsdue to variation in their physico-chemical properties. Although pharmaceuticals are ubiquitous in water matrices and have potenial health effects, most of them are not legally regulated. However, three pharmaceuticals: 17b-estradiol, 17a-ethinylestradiol and diclofenac (DCF) are added to the watch list of Directive 2013/39/EU.

Diclofenac (DCF), 2-[2,6-(dichlorophenyl)amino]phenylacetic acid], is non-steroidal anti-inflammatory drug (NSAID) used for inflammation treatment and for pain reduction. Figure 1. shows chemical structure of diclofenac.

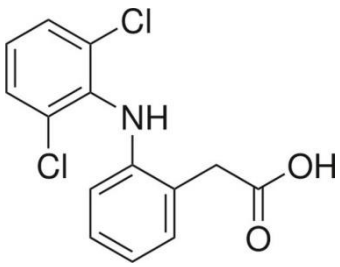

Figure 1. Chemical structure of diclofenac

After consumpiton, diclofenac is eliminated in short period (half life of 2 h). Approximatelly 65% is excetred through urine with six metabolites and 15% remains unchanged after consumption [2]. Diclofenac is used in different forms such eye droping, dermal application and injection. According to investigation, the global consumption was estimated to be 940 tons per year with a daily dose of 100 mg . Diclofenac with log Kow > 3 may be accumulated in tissues of organisms. Diclofenac is detected in effluent water due to its resistence to biodegradation in convetional wastewater plants. Removal efficiency varies from 0-80% because of operating conditions such as sunlight exposure [3]. The presence of –Cl and NH groups in DCF molecule is also a reason of inability of its removal.
Advanced oxidation processes (AOPs) have been proposed as a promising method for removal of recalcitrant pharmaceuticals and other endocrine-disrupting chemicals. The success of advanced oxidation processes depends of persence of oxygen species such as hydroxyl radicals [4]. The main advantage of HO radicals is the non-selective nature and it can contribute to the dectruction of wide range of organic pollutants producing water, carbon dioxide and mineral acids.Among different types AOPs, heterogenous photocatalysis has been mostly studied for photodecomposition of variety pharmaceuticals. The process is based on usage of nanostructured photocatalysis to maximize the absorption of both photons and reactants. One of the most commonly used photocatalysis is titanium oxide (TiO_2) [5-6].
The main propose of this study is to investigate the possibility of photocatalytic application in the presence of ultraviolet irradiation by zinc oxide / tin oxide (ZnO/SnO2) nanoparticles.

Chemicals and reagents
DCF sodium is commercially available and used without further purification. HPLC grade, methanol and acetonitrile were purchased from Sigma Aldrich. Zinc oxide and tin oxide with 99,9% purity and particle size ≤1 μm were also purchased form Sigma Aldrich. The stock solution was prepared by dilution of 25 mg in 25 ml methanol (final concentration of 200 mgL^{-1}). The studied aquaeous solution was distilled water.

Analytical method
The change in DCF concentrations was followed by reverse phase HPLC (Eclipse XDB-C18 (150 x 4.6, particle size 5μm) with diode array detector. The column temperature was adjusted at 25ºC. The mobile phase of the applied isocratic elution consisted of 50% of 0, 1% acetic acid (CH_3COOH) and 50% of acetonitrile (CH_3CN). Flow rate was 0,8 ml min^{-1}. The injection volume of the samples was 10 μL. The maximum wavelength for diclofenac was λ_{max}=276 nm.

Experimental
The initial concentration of analyzed pharmaceutical was 3,4 mgL^{-1}. The ZnO/SnO_2 catalyst load was 40 mg. Experiment was performed in the dark. In order to follow kinetic of photodegradation of diclofenac sodium, different time intervals were applied (in range 5-60 minutes). With a goal to achieve uniform catalyst concentrations in solution, all samples were

stirred at magnetic agitator with 120 rpm speed. The volume of observed samples was 50 ml. Samples were irradiated under UV artificial light. After UV exposure, all samples were filtrated through 0,45 μm Premium Syringe Filter in order to remove nanoparticles from aqueous solution.

Results and discussion

After experiment, results are evaluated with HPLC offline software program. Calibration curve was constructed in range of 1, 5 – 10 mgL^{-1} with high correlation coefficient r^2= 0, 999. Final concentration of analyte was calculated according to peak area. Table 1. shows results obtained from degradation experiment.

Table 1. Results of photodegradation experiment

Time (min)	Area (mAU)	Final concentration (mgL^{-1})
5	42,2	0,99
10	28,9	0,69
20	4,00	0,12
30	1,30	0,05
40	0,72	0,04
50	0,14	0,03
60	0,00	0,00

According to results, concentration of diclofenac decreased with increasing the irradiation time.

In order to investigate possible removal of pharmaceutical, the next equation was used:

$$R(\%) = \frac{c_0 - c_e}{c_0} \text{ x } 100 \qquad (1)$$

Where:

c_0 (mgL^{-1}) is initial concentration of pharmaceutical, and c_e (mgL^{-1}) is the equilibrium concentration of pharmaceutical.

Figure 1. shows percentage of diclofenac removal by time.

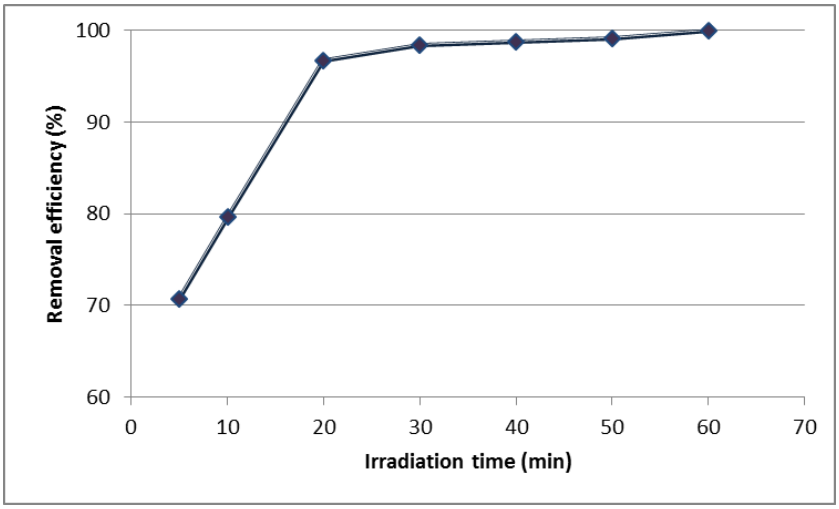

Figure 1. Removal efficiency of diclofenac

Removal efficiency has growing in function of time. After 60 minute of UV exposure, diclofenac was completely degraded.

Conclusion

The possibility of photocatalytic application for diclofenacremoval was investigated. The photodegradation of diclofenac has been studied in aqueous solution (distilled water) using ZnO/SnO_2 nanopowder mixture. Completely removal of DCF was achieved after 60 minutes under UV exposure. According to results, heterogeneous photocatalysis seems to be a satisfied method for removal of diclofenac. In order to optimize photocatalytic process, some of main conditions have to be taken into account such as: concentration of catalyst, time of irradiation, initial concentration of investigated pollutant, effect of pH value, water composition and identification of byproducts. The current practice in wastewater treatment should be improved by integration of advanced technologies in order to achive satisfactory treatment of effluents.

Acknowledgements:

The presented research is partly financed within a project of the Government of Vojvodina "Synthesis and application of new nanostructured materials for the degradation of organic pollutants from municipal landfill leachate in Vojvodina", 114-451-1821/2016-03.

References

[1] M.Papageorgiou, C.Kosma, D.Lambropoulou, Sci.Tot.Environ., 543(2016), pp. 547-569.
[2] Y.Zhang , S.U. Geißen, C. Gal, Chemosphere 73(2008), pp. 1151-1161.
[3] L.Lonappan, S.K. Brar, R.K. Das, M.Verma, R.Y. Surampalli, Environ.Inter. 96(2016), pp. 127-138.
[4]V.C. Sarasidis, K.V. Plakas, S.I. Patsios, A.J. Karabelas, Chem.Engin.J. 239(2014), pp. 299-311.
[5] N.Zhang, G.Liu, H.Liu, Y.Wang, Z.He, G.Wang, J.Hazard.Mater 192(1), 2011, pp 411–418.
[6]C. Martínez, M. Canle L., M.I. Fernández, J.A. Santaballa, J. Faria, J.Applied Catalysis B: Environmental. 107(1-2), 2011, pp 110-118.

MONITORING OF CHLORINE BY NEW METHOD BASED ON FOS IN WATER BODIES

Boris Obrovski[1*], Jovan Bajić[2], Ivana Mihajlović[1], Mirjana Vojinović Miloradov[1], Branislav Batinić[2], Nevena Živančev[1], Miloaš Živanov[2]

[1]University Of Novi Sad, Faculty Of Technical Sciences, Department Of Environmental Engineering, TrgDositejaObradovića6, 21000 Novi Sad, Serbia
[2]University Of Novi Sad, Faculty Of Technical Sciences, Department of Power, Electronic and Telecommunication Engineering, TrgDositejaObradovića 6, 21000 Novi Sad, Serbia
e-mail: borisobrovski@uns.ac.rs

Abstract
Fibre optic sensor (FOS) is used to measure the concentration of total chlorine in samples of surface water, swimming pool water and leachate from MSW landfill. FOS represents new original method which is based on the color of the sample for measurement ofanalyteconcentration. Color sensor converts RGB (Red-Green-Blue) color model to HSV (Hue-Saturation-Value) color model. S and V parameters were used for determination of chlorineconcentrations in selected water bodies. H parameter was used for the calculation of wavelength at which applied sensor measures the concentration of total chlorine. Research was carried out to validate the effectiveness and repeatability of the results obtained with FOS and confirms the capability to use sensor in laboratory controlled conditions. Results obtained with FOS are compared with standard analytical methods (UV-Vis spectrophotometer) to confirm the possibility of using FOS as replacement for standard analytical expensive equipment.

Introduction
Constant contamination of the environment caused by anthropogenic activities requires new improved methods for monitoring of different water bodies. Currently, standard laboratory methods are used for water monitoring, in the absence of better alternatives. They possess certain limiting factors which are related to the use of expensive and specific chemicals, the complexity of the analysis, the loss of the desired analyte in the process of sampling, transportation, extraction and storage. The great disadvantage is impossibility of obtaining *in-situ* and real-time results for the examined water body.
FOS represents inventive equipment for monitoring of aquatic medium. Advantages of FOS compared to the conventional methods are: simple use, low-cost device, small dimensions (which enables measurements where other devices do not have access), resistant to electromagnetic influences and corrosion, enabling measurements in inaccessible and remote areas, possibility to use in high aggressive chemical environments, electric power is not required at sampling points, etc., [1,2,3]. Mentioned advantages allow the use of FOS in the industry, biomedical, civil engineering (construction of dams and buildings), pharmaceutical and many other applications. FOS is used for examination of surface water, groundwater, ocean water, industrial and municipal wastewater, landfill leachate, wastewater from agricultural run-off, acid rain, etc. [4].
In the literature there is a wider range of designed and calibrated FOS that works on different principles. FOS has been developed for measuring of one parameter and as multi-parameter device used for monitoring of the various aqueous solutions. One parameter FOS device were calibrated for measurement of: nitrate [5,6], sodium [7] pH [8], copper [9], potassium [10], BOD (Biological Oxygen Demand) [11]. Multi-parameter sensor devices were designed for measurement of: cyanide, phosphate, sulfate, nitrite, nitrate in aqueous samples [4], metal ions

Co^{2+}, Cu^{2+}, Ni^{2+}, Fe^{3+}, Cd^{2+}, Zn^{2+}, Pb^{2+} and Hg^{2+} in different water bodies [12], measurement of nitrate and ammonium in an aqueous solution [13], prototype field device for measuring organic pollutants in groundwater [14] and orthophosphate, sulfate, nitrite, total chlorine and Cr (VI) in surface water [15].

The aim of this research is to demonstrate the possibility of using laboratory FOS for measurement of chlorine in surface water, swimming pool water and leachate. Chlorine is used for disinfection of drinking water and swimming pool water which are used for recreation and human activities. During disinfection process, toxic and carcinogenic by-products could be generated and could have a negative impact on human health. Contaminated waste water with chlorine compounds could cause pollution of surface and groundwater.

The results obtained by standard analytical methods (UV-Vis spectrophotometer) were compared with the results obtained with the FOS to demonstrate the effectiveness of the sensor and possibility to use for monitoring of various water bodies.

Experimental

Samples of surface water for laboratory analysis were collected from river Danube in the city of Novi Sad, Serbia. Leachate samples were collected from MSW landfill in Zrenjanin, Serbia. Samples of swimming pool water were collected from closed swimming pool in Novi Sad, Serbia. Surface water samples were poured into 1 L plastic bottles, while the samples of leachate and swimming pool water were poured into 1 L glass bottles. All samples were stored in hand refrigerator at 4 ^{0}C, and transported to the laboratory. Analyses were carried out in accredited Laboratory for monitoring of landfills, wastewater and air, Department of Environmental Engineering and Occupational Safety and Health in Novi Sad.

Concentrations of total chlorine in samples were analyzed according to the HACH Method (HACH Method 8167) and measured with UV-VIS spectrophotometer (DR 5000, HACH, Germany).

Operating principle of implemented FOS is the absorption of light. When the light passes through a liquid, certain wavelengths will be transmitted while others are absorbed depending on the color of the tested liquid. Fiber optic sensor detects the color and converts RGB color model in HSV color model. The used sensor determines V and S value and calculates concentration of the parameters of interest, and H value which is used for calculation of wavelength.

The sensor consists of three plastic optical fibres (POFs) that emit red, green and blue components mounted around a central optical fibre collecting light reflected from the mirror. The mirror is located on the underside of the sensor where the optical fiber is compiled. Three light-emitting diodes red, green and blue are set to different frequencies. In this way, detection of the reflected signal is achieved with only one photodetector and three bandpass filters.

Results and discussion

Total chlorine was measured in surface water, closed swimming pool water and leachate by new original FOS method. Results measuredwith FOS were compared with results obtained by standard laboratory methods (UV-Vis spectrophotometer) to demonstrateeffectiveness of applied sensor.

The FOS is calibrated with 4-5 different standard solutions with known concentrations, prepared by diluting standard solution fortotal chlorine. Reference sample with the lowest concentration of residual chlorine have bright pink color and with increasing concentrations of total chlorine, the color of the sample becomes more intense.

FOS converts RGB color model to HSV color model and measure concentration of selected parameter based on color intensity of the sample. Total chlorine concentrations were calculated and determined on the basis of the parameter S, based on calibration curves

obtained with the referent sample. The V value for total chlorine is constant and it is not possible to determine concentrations based on V values with the applied sensor.
Concentrations of total chlorine in Danube river are extremely low and surface water samples were spiked with known concentrations of standard solutions, since the FOS shows some dissipation with lower concentrations. In Table 1are presented the relative differences between total chlorine concentrations measured by UV-Vis spectrophotometer and by FOS in different water bodies.

Table 1. Comparison of total chlorine concentrations obtained by UV-VIS and by FOS forsamples of surface water, swimming pool water and leachate

Samples	UV-Vis [mg/l]	FOS [mg/l]	Relative difference[%]
Surface water	0,165	0,171	3,62
Swimming pool water	0,59	0,562	4,75
Landfill leachate	0.07	1.955	>100%

Based on obtained results, it was determined that FOS can be effectively used to measure the total chlorine concentrations in surface water and swimming pool water. FOS can't be used for determination of total chlorine in leachate from MSW landfill. The influence of matrix, coloration, turbidity, unwanted reactions and high contamination ofleachate samples do not permit use of FOS for this type of water. Removing the color without loss of analyte of interest will allow the use of FOS for wastewater samples.Deviations less than 10% are acceptable and demonstrate the ability to use sensors for monitoringof surface water and swimming pool water.

Conclusion

The further research will be focused on expanding the range of examined parameters. Selection of quality construction components will improve the precision and accuracy of the laboratory device. Increasing the sensitivity of FOS would ensure measurement of low concentrations of selected parameters. FOS is capable to monitor the quality of surface water and especially water from swimming pool.Construction of field device with improved performances will provide higher quality monitoring program and more reliable results which is important in the case of contamination and early responses in order to prevent the contamination of water bodies.

Acknowledgements

The authors acknowledge for the funding provided by the Ministry of Education, Science and Technological Development of Republic of Serbia under project 'Development of methods, sensors and systems for monitoring quality of water, air and soil', number III43008.

References

[1] S. Klainer, R. Thomas, J. Francis, Sensors and Actuators B, 11 (1993) 81-86.
[2] S.S. Ghong, A.R. Abdul Aziz, S.W. Harun, Sensors, 13 (2013) 8640-8668.
[3] A.B.H. Ahmad, Department of Instrumentation and Analytucal Science, UMIST, Manchester, 1994.
[4] S.M. Klainer, J.R. Thomas, J.C. Francis, Sensors and Actuators B, 11 (1993) 81-86.
[5] P.S. Kumar, C.P.G. Vallabhan, V.P.N. Nampoori, V.N.S. Pillai, P. Radhakrishnan, Journal of Optics A: Pure and Applied Optics, 4 (2002) 247-250.

[6] N.A. Aljaber, B.R. Mhdi, S.K. Ahmmad, J.F. Hamode, M.M. Azzawi, A.H. Kalad, S.M. Ali, Journal of Engineering, 04 (2014) 37-43.
[7] F. Buchholz, N. Buschmann, Sensors and Actuators B, 9 (1992) 41-47.
[8] T.H. Nguyen, T. Venugopalan, T. Sun, K.T.V. Grattan, IEEE Sensor Conference, (2009) 89-94.
[9] C.B. Ojeda, F.S. Rojas, Sensors, 6 (2006) 1245-1307.
[10] R. Narayanaswamy, Biosensors and Bioelectronics, 6 (1991) 467-475.
[11] X. Li, F. Ruan, W. Ng, K. Wong, Sensors and Actuators B, 21 (1994) 143-149.
[12] N. Malcik, O. Oktar, M.E. Ozser, P. Caglar, L. Bushby, A. Vaughan, B. Kuswandi, R. Narayanaswamy, Sensors and Actuators B, 53 (1998) 211-221.
[13] P.S. Kumar, PhD Thesis, Cochin University of Science and Technology (2003).
[14] H. Steiner, M. Jakusch, M. Kraft, M. Karlowatz, B. Mizaikoff, T. Baumann, R. Niessner, W. Konz, A. Brandenburg, K. Michel, C. Boussard-Pledel, B. Bureau, J. Lucas, Y. Reichlin, A. Katzir, N. Fleischmann, K. Staubmann, R. Allabashi, J.M. Bayona, Society for Applied Spectroscopy, 57 (2003) 124-130.
[15] B. Obrovski, J. Bajić, I. Mihajlović, M. VojinovićMiloradov, B. Batinić, M. Živanov, Sensors and Actuators B, 228 (2016) 168-173.

NOVEL ASYMMETRIC BENZYLIDENECYCLOHEXANONE PHOTOCHROMIC COMPOUND AS FOOD DYE WITH ANTIOXIDANT PROPERTIES

Iulia Păuşescu[1,2], Ana-Maria Pană[1*], Valentin Badea[2], Cătălin Ianăşi[1], Otilia Costişor[1], Liliana Cseh[1]

[1]*Institute of Chemistry Timisoara of Romanian Academy, 24 M. Viteazul Bvd, 300223, Timisoara, Romania*
[2]*University Politehnica Timisoara, Faculty of Industrial Chemistry and Environmental Engineering, 6 V. Parvan Bvd, 300223, Timisoara, Romania*
ana_maria_pana@ymail.com

Dedicated to the 150th anniversary of the Romanian Academy

Abstract

Nature has always been the provider of compounds with unique properties and amazing application within or outside the living organisms [1]. Color is certainly one of the natural features that have always fascinated researchers from almost all fields of knowledge and compounds with such properties have been isolated from raw materials or have been designed and synthesized based thereon [2]. Flavylium derivatives are natural or synthetic compounds responsible for certain color of fruits and flowers and are able to turn from yellow to red and blue depending on the pH of the media [3]. They are also studied for their photochromic behavior when excited with different wavelengths and their network of chemical transformation has been the subject of many research papers [4,5].

We have focused lately on the synthesis of xanthylium derivatives [6], compounds similar in behavior with flavylium ones with symmetrical and asymmetrical substituents on the aromatic rings. The photochromic behavior of the new asymmetric benzylidene cyclohexanone derivative 4-(p-hydroxybenzylidene)-6-hydroxy-1,2,3,4-tetrahydroxanthylium chloride (HTX)in aqueous solution at different pH values was studied using UV-Vis, NMR and fluorescence spectroscopy. In strong acid environment HTX exhibits purple color and a broad absorption band at about 516 nm, corresponding to the presence of the xanthylium cation, while in basic conditions the solutions are red, with an absorption band at about 596 nm. At pH ranging from 9 to 12 HTX is bluish and suffers spontaneous transformations between species involved in the network of chemical reactions. HTX shows good fluorescence behavior at all pH values. HTX has a good antioxidant character of 55.15% determined by DPPH method. The features described above and its curcumin origin would highly recommend it for application in the field of food colorants.

Acknowledgement: The authors are thankful to the Romanian Academy, Project 4.1.

References

[1] P.Murphy, P. Doherty, The Colors of Nature: An Exploratorium Book, Chronicle Books, 1996.
[2] H. Zollinger, Color Chemistry, Wiley Verlag, Zurich, 2003.
[3] F.Pina, M.J.Melo, C.A.T.Laia, A.J.Parola, J.C.Lima, Chem. Soc. Rev. 41 (2012) 869-908.
[4] F. Pina, J. Agric. Food Chem. 62 (2014) 6885-6897.
[5] V. Petrov, S. Slavcheva, S. Stanimirov, F. Pina, J. Phys. Chem. A 119 (2015) 2908-2918.
[6] A.M. Pană, V. Badea, R. Banică, A. Bora, Z. Dudas, L. Cseh, O. Costişor, J. Photochem. Photobiol. A 283 (2014) 22-28.

MOBILITY OF SELECTED PESTICIDES IN GROUNDWATER

Nevena Živančev[1*], Srđan Kovačević[1], Boris Obrovski[1], Mirjana Vojinović Miloradov[1], Milan Dimkić[1,2]

[1]University of Novi Sad, Faculty of Technical Sciences, Department of Environmental Engineering and Occupational Safety and Health, Trg Dositeja Obradovića 6, Novi Sad, Serbia
[2]Institute for the Development of Water Resources, Jaroslava Černog 80, Pinosava-Belgrade, Serbia
e-mail: nevenazivancev@uns.ac.rs

Abstract
The use of pesticides in plant protection products could result in their occurrence in all environmental mediums. Due to the concern about their environmental impact, the presence of pesticides is monitored in air, soil, water, and also in food and tissues. Jaroslav Černi Institute for the Development of Water Resources has conducted surface and groundwater sampling campaigns, in order to monitor fifteen different pesticides from priority and emerging substances lists. This paper is focused on the results of the groundwater sampling, where the most frequently detected pesticides were herbicide atrazine, fungicide carbendazim and insecticide carbofuran. In this paper, the fact that these pesticides were most frequently detected in groundwater was used for further research of their mobility. The most important process that influences the mobility of pesticides in the environment is the sorption. Therefore, sorption process was observed in the terms of linear sorption coefficient. Multiple linear regressions were used to establish the relationship between the linear sorption coefficient of each pesticide and various soil parameters, that have the highest impact on the sorption process. A thorough understanding of pesticides sorption behavior is crucial for predicting the movement rate of the pesticide in the environment. Information based on these processes will help with predicting the fate of pesticides in the groundwater, but also in the surface waters.

Introduction
Pesticides are substances mostly used in agriculture, to increase the quality and quantity of food. More than 1000 different plant protection products, with over 300 different active ingredients are currently registered for use in Serbia. With increasing the amounts of pesticides being used in the world, the concern about their adverse effects on the environment has also grown. The estimation is that less than 0.1% of the applied pesticide actually reaches the targeted pest, and the rest of the amount enters the environment [1]. The problem with pesticides reaching environmental mediums is also the fact that many of them can persist for long periods of time in an ecosystem.
Information on the quantities of pesticides that reach the environment, and especially the groundwater sources, which are used as sources of drinking water, are extremely important. Therefore, Jaroslav Černi Institute for the Development of Water Resources has monitored the concentrations of fifteen different pesticides in surface and groundwaters of Serbia, from the year 2009 to 2015. In this paper, the results of groundwater sampling campaigns are used. The most frequently detected pesticide in groundwaters in Serbia was herbicide atrazine, with detection in almost 32% of the samples. This herbicide has been banned for use several years ago, but it is still detected in the water samples, due to its persistent nature. It should be highlighted that median concentration of this pesticide in groundwater samples was 3.9 ng L^{-1}, which is a very low concentration. The second most frequently detected pesticide was fungicide carbendazim, which was detected in almost 22% of the samples, and the third most

frequently detected was insecticide carbofuran (in around 6% of the samples). Median concentrations of carbendazim and carbofuran was also very low, 9 and 6 L^{-1}, respectively.
Pesticides may reach the groundwater if they are not effectively retained by the sorption processes in the soil, because these processes are the most influential on the mobility of pesticides. Therefore, the sorption behavior of the three most frequently detected pesticides in groundwaters of Serbia was analyzed in this paper. Sorption process can be represented in the form of sorption coefficient, and in this paper the linear sorption coefficient was chosen for the analysis. The reason for choosing this coefficient is the fact that models predicting pesticides behavior and transport most frequently use this type of coefficient [2]. In this paper, multiple linear regression analysis was conducted, using literature data to set correlation between linear sorption coefficient and soil properties that sorption processes mostly depend on: organic matter content, soil texture and pH of the soil [3-4].

Materials and methods

In this paper, multiple linear regression analysis has been performed for carbendazim, carbofuran and atrazine linear sorption coefficients. This type of analysis is an imporant tool for predicting an uknown value based on the two or more known values.
The multiple linear regression analysis was conducted with a large number of literature data where linear sorption coefficients were gained in the laboratory conditions, and where soil properties values were available, in order to set the correlation between these properties and the sorption coefficient. The database on which this analysis was performed was organized to use only the values where soils had less than 10% of organic matter content, because the main interest of this research are soils in contact with groundwater, where organic content is lower than in the upper layers of soil.
Development of regression equations was performed using Microsoft Excel, with the Solver and Data Analysis Plug-In. The main objective was to develop equations based on the most important soil properties responsible for the sorption behavior of pesticides, that would accurately estimate the linear sorption coefficients for selected pesticides when soil properties are available for a given soil.

Results and discussion

Multiple linear regression analysis for carbendazim showed no significant dependence of linear sorption coefficient on pH, organic matter content or soil texture. It is important to establish which parameters do have an influence on sorption of carbendazim to soil. This should be the subject of further research.
The analysis for carbofuran showed the dependence of linear sorption coefficient (K_d) on pH and organic matter content of the soil, represented as % organic carbon. The following equation (1) is the result of the literature data analysis [5-8], where the coefficient for multiple correlation is 0.66:

$$K_d = -1.80 + 0.33 \cdot (pH) + 0.43 \cdot (\%OC) \pm 0.80 \quad (1)$$

Figure 1. represents the difference between literature data and the values calculated using the previously mentioned equation (1).

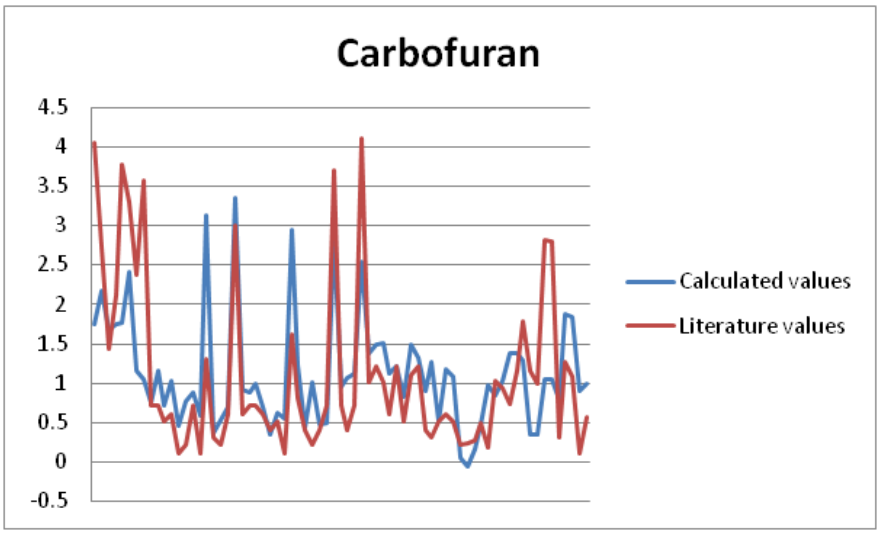

Figure 1. Comparison of calculated and literature data for carbofuran

The multiple linear regression analysis for atrazine showed better results than for carbendazim and carbofuran. The coefficient for multiple correlation was 0.89. The result of the multiple linear regression with literature data [9-11] is the following equation (2):

$$K_d = 1.97 - 0.28 \cdot (pH) + 0.93 \cdot (\%OC) \pm 0.40 \quad (2)$$

Figure 2. represents the difference between literature data and the values gained using the abovementioned equation (2).

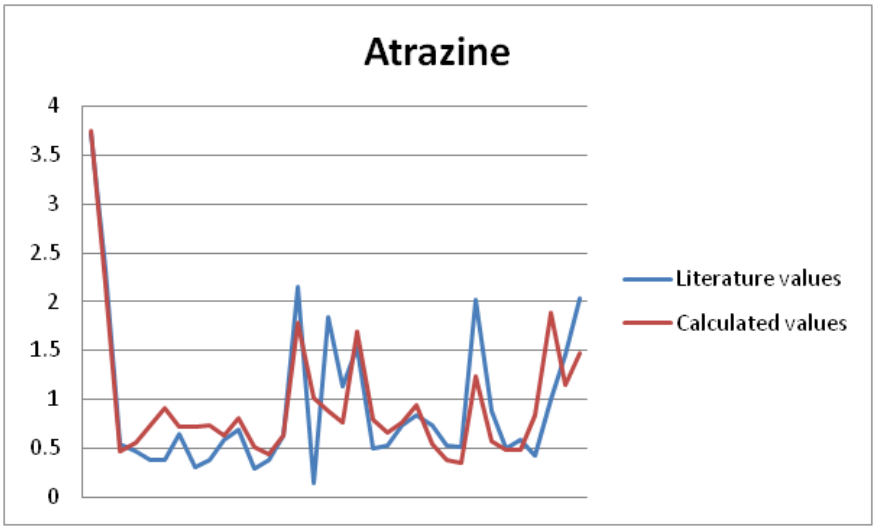

Figure 2. Comparison of calculated and literature data for atrazine

Instead of conclusion

Mobility of pesticides in the groundwater mostly depends on their sorption behavior in the soil. The research of their mobility in the groundwater is highly important in terms of estimating the potential contamination. Due to the fact that movement of pesticides can be slower as the consequence of the sorption processes has resulted in the research of these processes.

In this paper, multiple linear regression was used to correlate the linear sorption coefficient of three selected pesticides to the various soil parameters responsible for sorption. This analysis showed that carbendazim sorption behavior cannot be predicted using a multiple parameter linear equation, because the dependence of the K_d values on soil properties (pH, soil texture

and organic matter content) was insignificant. However, the analyses showed dependence of sorption coefficients on pH and organic matter content (displayed in equations (1) and (2) as % organic carbon) for carbofuran and atrazine. The coefficient for multiple correlation for carbofuran was only 0.66, which is not enough for some serious estimations and predictions. Even more literature data must be examined, but also, some further research should be conducted to establish the connection of sorption coefficent and soil properties.

The best prediction of K_d values through soil properties was for atrazine, where coefficient for multiple correlation was 0.86. However, it is important to continue with the research of atrazine sorption, to better understand the sorption mechanisms and to get even better predictions, which could be used in the assessment of their mobility.

Further research should be focused on establishing the dominant mechanisms for retaining these three pesticides in the soil. This would lead to a better understanding of their mobility in the environment, and more importantly in the groundwater. After gaining a better insight on the sorption of these pesticides, it could be easier to estimate their concentrations in groundwater, and the potential risk for population that gets drinking water from the groundwater sources.

Acknowledgements

This research was supported by the Ministry of Education, Science and Technological Development, Republic of Serbia, under the Project No. TR 37014 and project III 46009.

References

[1] M.Arias-Estévez, E. López-Periago, E. Martínez-Carballo, J. Simal-Gándara, J. C. Mejuto, L. García-Río. *Agr. Ecosyst. Environ.*123(4) (2008) 247-260.
[2] J. M. Köhne, S. Köhne, J. Šimůnek. *J.Contam. Hydrol.* 104(1) (2009) 36-60.
[3] T. Berglöf, T. Van Dung, H. Kylin, I. Nilsson. *Chemosphere* 48(3) (2002) 267-273.
[4] J. P. Gao, J. Maguhn, P. Spitzauer, A. Kettrup. Water. Res. 32(5) (1998) 1662-1672.
[5] M. El M'Rabet, A. Dahchour, M. Massoui, M. Badraoui, M. J. Sanchez-Martin. *Agrochimica* 46 (1-2) (2002) 10-17.
[6] Hsieh, Tsui-Ling, and Ming-Muh Kao J. Hazard. Mater. 58 (1998), no. 1: 275-284.
[7] J. A.Liyanage, R. C.Watawala, A. P. Aravinna, L.Smith, R. S. Kookana, *J. Agr. Food Chem.* 54(5), (2006) 1784-1791.
[8] M. S.Yazgan, R. M. Wilkins, C. Sykas, E. Hoque. *Chemosphere* 60(9) (2005) 1325-1331.
[9] L. J. Krutz, S. A. Senseman, K. J. McInnes, D. A. Zuberer, D. P. Tierney. *J. Agr. Food Chem.* 51(25) (2003) 7379-7384.
[10] Y.Drori, Z.Aizenshtat, B. Chefetz. *Soil Sci. Soc. Am. J.* 69(6) (2005) 1703-1710.
[11] R. M. Johnson, J. Thomas Sims. *Pesticide science* 54(2) (1998) 91-98.

ÚJ Cu-KOMPLEXEK SCHIFF-BÁZISOKKAL, ÉS FIZIKAI-KÉMIAI VIZSGÁLATUK

ifj. Várhelyi Csaba[1], Nagy Renáta-Ildikó[1], Pokol György[2], Korecz László[3], Goga Firuţa[1], Golban Ligia-Mirabela[1], Huszthy Péter[2]

[1] „Babeş-Bolyai" Tudományegyetem, Kémia és Vegyészmérnöki Kar, Kolozsvár
[2] Budapesti Műszaki és Gazdaságtudományi Egyetem, Vegyészmérnöki és Biomérnöki Kar
[3]MTA-Természettudományi Kutatóközpont, Anyag- és Környezetkémiai Intézet, Budapest
e-mail: vcaba@chem.ubbcluj.ro

Abstract
In our research we synthesized novel [Cu(4-benzyl-2-hydroxy-propiophenone)$_2$A], [Cu(ninhydrin)$_2$A] (A = ethylene-diamine, 1,2-, 1,3-propylene-diamine, o-phenylene-diamine) type complexes by reacting copper-acetate with different Schiff-bases in the corresponding solvent. The Schiff-bases were obtained with the condensation of 4-benzyl-2-hydroxy-propiophenone,respectively ninhydrin with diamines. We analyzed their physicochemical properties using mass spectrometry, infrared-, NMR-, UV–VIS-, ESR-spectroscopy, powder-XRD and thermal analysis (TG, DTG and DTA).

The copper(II)-complexes are used as antimicrobial agents. The copper(II)-complexes with aminoacids-, peptides-, chinoxaline-, mono- and bis-semicarbazones ligands are used in cancer therapy. The copper is an essential microelement in the human body. It has a very important role in the convalescence processes.
The objective of the authors is to study the biological activity of the prepared complexes.

Bevezető

A 3 – 6 d átmenetifémek azometin-származékait gyakran párhuzamosan tanulmányozzák ugyanazon ligandummal. A Cu(II)-származékok termikus stabilitása sok esetben kisebb, mint a többi analóg vegyületé, egyes fizikai-kémiai sajátosságaik eltérnek egymástól. Jelentős számú mono- és polinukleáris termék ismeretes 2-, 3- és 4-fogú ligandumokkal. A Cu(II) elektronszerkezete: [Ar]3d^{9}szabad, nem kompenzált „lyukelektronnal" lehetővé teszi a Cu(II)-vegyületek finom szerkezetének tanulmányozását az elektron-spin rezonancia spektrumok segítségével.
A réz-komplexek daganatellenes szerként való felhasználásának egyik nagy előnye, hogy nem annyira mérgezőek az élő szervezetre, mint a tiszta szerves ligandum. Hatásmechanizmusuk azon alapul, hogy katalizálják a szervezetben levő szabad peroxid gyökök felbontását, O_2 molekulává alakítva [1].
N és O atomot tartalmazó Schiff-bázisok általában biológiai aktivitást mutatnak, és nagy az érdeklődés a kutatásukat illetően, a fémionok megkötésének nagyszámú módja miatt. Ismeretes, hogy bizonyos fémek, mint pl. a Cu^{2+} növelik a biológiai aktivitását a biológiailag aktív vegyületeknek, ezért az egyik fő cél a gyógyászatban való alkalmazásuk. Valójában a Schiff-bázisok képesek a fémionok különböző oxidációs állapotait stabilizálni, lehetővé téve ezzel komplexeik széleskörű alkalmazását biológiai, klinikai, analitikai és ipari területeken. Jelentős szerepük van katalizátorként való alkalmazásukban a szerves szintéziseknél [2].
Rengeteg Schiff-bázis állítható elő kondenzációs reakciók útján karbonil-származékokból különféle diaminokkal. A kapott Schiff-bázisok 1:1 arányban reagálnak általában a megfelelő fémionnal, [ML] típusú komplexeket képezve.

Kísérleti rész

Felhasznált anyagok: $CuAc_2$, 4-benzil-2-hidroxi-propiofenon, ninhidrin, etilén-diamin, 1,2-propilén-diamin, 1,3-propilén-diamin,o-fenilén-diamin, Et–OH

Eljárás: először előállítjuk a megfelelő Schiff-bázist 4-benzil-2-hidroxi-propiofenon, ill. ninhidrin etil-alkoholos oldatának és a diamin (en, 1,2-pn, 1,3-pn,o-fen) etil-alkoholos oldatának elegyítésével és keverésével hidegen vagy enyhe melegítéssel (mólarány 2:1). A keletkezett Schiff-bázist leszűrjük, majd etil-alkoholban oldjuk, vagy ha nem válik ki, akkor az oldatot használjuk, és a $CuAc_2$ alkoholos oldatával elegyítjük, majd 1 – 2 órán keresztül forraljuk (mólarány 1:1). A keletkezett terméket lehűtjük, vákuum alatt szűrjük, víz-alkohol (1:1) eleggyel mossuk, és levegőn szárítjuk.

Lejátszódó reakciók [Cu(4-benzil-2-hidroxi-propiofenon)$_2$en], [Cu(ninhidrin)$_2$en]:

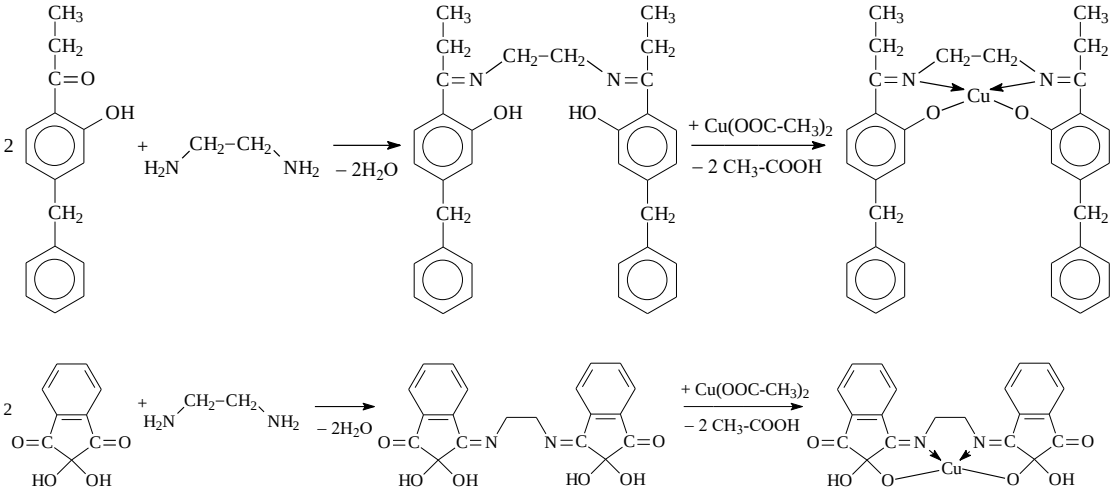

Eredmények és kiértékelés

Az előállított komplexek mikroszkópos jellemzése és előállítási hozama az 1. táblázatban látható.

1. táblázat. Az előállított komplexek mikroszkópos jellemzése, hozama és móltömege.

Sz.	Vegyület	Számít. móltöm.	Hozam (%)	Mikroszkópos jellemzés
1.	[Cu(4-benzil-2-hidroxi-propiofenon)$_2$(en)]	566,20	10,67	Világosabb barna színű, négyzet alapú tűkristályok
2.	[Cu(4-benzil-2-hidroxi-propiofenon)$_2$(1,2-pn)]	580,22	32,75	Sötét barna színű, apró, háromszög alapú hasábok
3.	[Cu(4-benzil-2-hidroxi-propiofenon)$_2$(1,3-pn)]	580,22	31,02	Sötét barna színű, apró, háromszög alapú hasábok
4.	[Cu(4-benzil-2-hidroxi-propiofenon)$_2$(o-fen)]	614,24	34,19	Fekete színű, háromszög alapú hasábok
5.	[Cu(ninhidrin)$_2$en]	441,88	63,63	Sötét barna színű, háromszög alapú hasábok
6.	[Cu(ninhidrin)$_2$(1,2-pn)]	455,91	89,73	Fekete színű, háromszög alapú hasábok
7.	[Cu(ninhidrin)$_2$(1,3-pn)]	455,91	86,78	Fekete színű, háromszög alapú hasábok
8.	[Cu(ninhidrin)$_2$(o-fen)]	489,93	85,93	Barnás-zöld színű, háromszög alapú hasábok

Tömegspektrometria

A tömegspektrumokat Agilent/Technologies 6320 Mass Spectrometer készülékkel rögzítették. A spektrumokban benne van a várt anyagok molekulatömege és bizonyos bomlási fragmenseket is sikerült azonosítani.

Hőbontás (TG, DTG, DTA)

A hőbontást egy 951 TG és 910 DSC kaloriméter (DuPont Instruments) készülékkel végeztük Ar vagy N_2 atmoszférában, 10 K/min fűtési sebességgel (mintatömeg: 4–10 mg).

A nyert adatokból egy általanos bomlási mechanizmust állíthatunk fel:

$[Cu(4\text{-benzil-2-hidroxi-propiofenon})_2A] \rightarrow [Cu(O)_2A] \rightarrow CuO$

$[Cu(ninhidrin)_2A] \rightarrow CuO$

(A = etilén-diamin, 1,2-, 1,3-propilén-diamin,o-fenilén-diamin)

A ninhidrin tartalmú komplexek esetében egyetlen egy meredek lépcső figyelhető meg, a ninhidrinben jelen levő sok oxigén következtében, a bomlás robbanásszerűen megy végbe.

Por-Röntgen diffrakciós mérések

A por-röntgen diffrakciós méréseket egy PANalytical X'pert Pro MPD X-ray diffraktométerrel végeztük. A röntgen diffrakciós mérésekkel a komplexeink kristályosságát vizsgáltuk. Mivel új anyagok, nem tálalhatóak meg a diffraktogramjai a Cambridge-i adatbázisban.

Infravörös spektroszkópiai vizsgálatok

Az infravörös spektrumokat Bruker Alpha FTIR spectrométerrel (Platinum single reflection diamond ATR) vettük fel, szobahőmérsékleten, 4000–400 cm^{-1} hullámszám tartományban. A mintákat szilárd halmazállapotban, elporítva mértük. A főbb IR adatokat a 2. táblázat tartalmazza.

2. táblázat. Az előállított Cu-komplexek IR adatai.

Vegyület / cm^{-1}	ν_{O-H}	ν_{C-H}	$\nu_{C=N}$	ν_{C-Car}	δ_{CH2}	γ_{C-H}	ν_{Cu-N}	ν_{Cu-O}
[Cu(4-benzil-2-hidroxi-propiofenon)$_2$(en)]	-	2978 gy 2938 gy	1609 ie	1574 ie	1498 e 1366 ie	733 ie	489 e	414 k
[Cu(4-benzil-2-hidroxi-propiofenon)$_2$(1,2-pn)]	-	2938 gy 2876 gy	1568 ie	1510 ie	1422 e 1376 ie	741 ie	508 e	469 ie
[Cu(4-benzil-2-hidroxi-propiofenon)$_2$(1,3-pn)]	-	2937 gy 2874 gy	1568 ie	1509 ie	1422 e 1375 ie	741 ie	470 e	427 e
[Cu(4-benzil-2-hidroxi-propiofenon)$_2$(o-fen)]	-	2939 gy 2911 gy	1566 e	1494 ie	1454 e 1361 ie	752 ie	480 k	423 e
[Cu(ninhidrin)$_2$en]	3390 gy	2928 gy 2852 gy	1608 e	1555 ie	1432 ie 1402 ie	753 e	530 e	457 k
[Cu(ninhidrin)$_2$(1,2-pn)]	3194 gy	3077 gy 2930 gy	1669 ie	1585 ie	1405 ie 1340 ie	725 ie	527 e	481 k
[Cu(ninhidrin)$_2$(1,3-pn)]	3214 gy	3076 gy 2973 gy	1670 e	1585 ie	1407 ie 1342 e	724 ie	527 e	482 k
[Cu(ninhidrin)$_2$(o-fen)]	3434 gy	3062 gy 3033 gy	1604 e	1509 e	1463 k 1335 e	774 ie	465 e	428 ie

(ie = igen erős, e = erős, k = közepes, gy = gyenge)

NMR spektroszkópia

A spektrumokat (^1H és ^{13}C NMR) egy Bruker AVANCE spectrométerrel vettük fel 250 MHz (^{13}C: 63 MHz) frekvenciával. Csak a ligandumokra lehet NMR méréseket végezni, mert a réz-komplexek paramágneses tulajdonságúak. A *(4-benzil-2-hidroxi-propiofenon)$_2$A*Schiff-bázisok esetében az aromás gyűrűk protonjainak a jele 6,5 – 7,9 ppm tartományban jelennek meg, az alifás protonok 1 – 4 ppm, ill. a hidroxil-csoport protonjai 12 – 13 ppm között. Az aromás ^{13}C jelek 100 – 165 ppm tartományban, az alifásak pedig 8 – 70 ppm értékeknél. A C=N kettős kötésben levő C-atomok jele 206 ppm érték körül jelenik meg. A *(ninhidrin)$_2$A* esetében az aromás gyűrűk protonjai 7 – 8 ppm tartományban jelennek meg, az alifás protonok 2,5 – 5 ppm, a HO-csoportok protonjai pedig 11 – 12 ppm tartományban. Az aromás ^{13}C jelek 120 – 140 ppm tartományban, a kettős kötésben levő C-atomok jele 207 ppm körüli értéknél található.

Elektronspin-rezonancia (ESR) mérések

Vizsgálatainkat egy Bruker ELEXSYS 500 típusú készülékkel, szobahőmérsékletű és 77 K-re kvencselt („quenchen“: hűtés nagyon alacsony hőmérsékletű folyadékba való mártással) oldatokon végeztük (a mintaszám utáni LN jelzi a 77 K-os mérést). A spektroszkópiai paramétereket szimulációval határoztuk meg (3 táblázat). A szimulációk során figyelembe vettük mindkét réz (^{63}Cu, ^{65}Cu) izotópot (arány: 1:2). Esetenként klaszter képződést is tapasztaltunk. Az **1** (4 N), **3** és a **8**-as minták a spektrumainál a **g** tenzor axiális szimmetriát mutat, a szerkezet négyzetes-planáris. A **7**-es minta szintén négyzetes-planáris de egy enyhe rombos torzulással. A **6**-os számú minta, mind a szobahőmérsékletű, mind a lefagyasztott spektruma szuperpozícióval írható le, azaz két különböző réz-komplex van jelen a rendszerben. Az alacsony hőmérsékletű spektrum azt mutatja, hogy a szimmetria rombos, ami réz-komplexek esetén viszonylag ritka.

3. táblázat. Szimulációval meghatározott ESR spektroszkópiai paraméterek.

Szám	g_x	g_y	g_z	$a_{Cu\,x}$ [G]	$a_{Cu\,y}$ [G]	$a_{Cu\,z}$ [G]	a_{Nx}, a_{Ny} [G]	a_{Nz} [G]
1 LN	2,050436	2,050436	2,192920	22,4401	22,4401	216,6918	13,629	0,002
3 LN	2,048625	2,048625	2,296650	17,8425	17,8425	142,0263	-	-
6	1,952391 2,048546	1,952391 2,048546	1,952391 2,048546	95,0847 99,4422	95,0847 99,4422	95,0847 99,4422	-	-
6 LN	2,018104 2,105629	1,948553 2,075852	1,931618 2,029828	168,9606 44,2337	104,6182 66,2637	94,1495 22,6233	-	-
7 LN	2,070949	2,055280	2,355306	3,9300	21,0940	128,4499	-	-
8 LN	2,051735	2,051735	2,244872	31,5030	31,5030	170,1944	-	-

(a – csatolási állandó)

UV–VIS spektroszkópia

Felvettük komplexeink UV spektrumait 10%-os etil-alkoholos oldatban, valamint pH függvényében, Britton-Robinson puffer-oldatokat használva, és meghatároztuk savassági állandóikat. A tiszt oldatokra kapott hullámhossz értékek: 191, 208 – 229, 275 – 295 nm.

Következtetések

Munkánk során két típusú Schiff-bázissalCu-komplexeket állítottunk elő, melyek várhatóan biológiai szempontból lesznek jelentősek, mint pl. antibakteriális és antitumor hatás.

Köszönetnyilvánítás

A szerzők közül ifj. Várhelyi Csaba köszöni a „Domus Hungarica“ alapítványnak, hogy a számára megítélt évi egy hónapos ösztöndíjakkal lehetővé tette a jelen dolgozat létrejöttét.

Irodalom

[1] M.M. Ibrahim, G.A.M. Mersal, S.A. El-Shazly, A.-M.M. Ramadan, *Int. J. Electrochem. Sci.*,7 (2012)7526

[2] A. Soroceanu, L. Văcăreanu, N. Vornicu, M. Cazacu, V. Rudic, T. Croitori, *Inorganica Chimica Acta*, 442 (2016) 119

PREFERENCES ABOUT CORPORATE SUSTAINABILITY ACTIONS BY BUSINESS ECONOMICS STUDENTS

László Berényi

Institute of Management Science, University of Miskolc, H3515 Miskolc-Egyetemváros, Hungary
email: szvblaci@uni-miskolc.hu

Abstract
The approach and the toolset of corporate social responsibility (CSR) may cover the initiations for achieving a higher level of sustainability. The social and technical context of the topic is complicated thanks to the various interests of the stakeholders. This paper gives additional information by analysing the personal opinions about the necessary corporate focus of CSR activities. The empirical research applies the pairwise comparison method by Guilford for exploring the preference order of business economics students in Miskolc. The results show that the respondents keep the solving of environmental problems by waste reduction and developing greener technologies are priority corporate challenges.

Introduction
Nowadays, the corporate social responsibility (CSR) boosted up the field of sustainable developmentsince it defines the fight against environmental and social problems openly as a business category [1], [2]. Of course the basic question remains whether the efforts lead to true responsibility. Tóth[3] points out that it needs changes and a new approach in business strategy, or it is only a spectacular mask for influencing the consumer behaviour.
Related to green consumer behaviour there are many researches in the fields of sociology and marketing. According to these, the basis of sustainable development is marked as changes in public values, conventions, practices and routines. Pollution can be reduced and prevented, natural resources could be utilised rationally and the acceptance of new technologies can be achieved by changes in consumption and lifestyle behaviour [4], [5].
The importance of a strong engineering approach, including the innovative solutions is not contested [6] but technological efforts are insufficient. In my opinion the achieving a sustainable economy and society strongly requires the consideration of the individual opinions and attitudes next to the common principles and goals. Professional and personal value judgements may differ from each other [7] therefore expectations and models based only on the professional aspect may be misleading. Personal opinions will be reflected in the judgmentin both private and corporate decisions. Moreover, there are distorting factors like group pressure or social expectations that changes the personal values [8]. Researchesin this field– including my results – will help the development of more reliable programmes and actions.

Materials and Methods
Data collection
The data source of the analysis is a survey prepared for higher education students that covers the personal opinions and attitudes about sustainable development and corporate social responsibility (CSR). This paper focuses on one block of the survey that lists 6 issues paired and asks to mark which one should have a higher preference in corporate thinking. The issues are as follows:

- cost reduction
- developing greener technologies

- financial support of environmental protection
- higher income for workers
- supporting schools and kindergartens
- waste reduction.

Method of preference analysis

The survey was prepared for preference analysis by the Guilford-method [9]. This method allows to calculate:

- the personal level of consistency (K) in the order of the factors (0≤K≤1, where 0 is the complete absence of consistency, 1 is the complete consistency, the latter means the responder has a clear list of preferences)
- group-level preference orders on interval-scale (a limitation of the method is that quantified results between groups are not comparable!) between 0 and 100,
- group level consensus by Kendall's coefficient of concordance for pairwise comparison (ν), including the cases K≥0,75.

The maximum level of Kendall's coefficient of concordance is 1, but the minimum is not fixed, it depends on the number of cases (*m*): ν_{even}= -1/(*m*-1) and ν_{odd} = -1/*m*. In order to ensure the comparison, I calculate with a corrected coefficient of consensus as:

$$\nu_{corr.\ i} = 100 * \frac{\nu_i - \nu_{min}}{1 - \nu_{min}} \quad (1)$$

The significance test is as follows (Kindler és Papp 1977:187):

$$u = \sqrt{2\chi^2} - \sqrt{2d_f - 1} \quad (2)$$

where γ shows the sum of values below the main diagonal in the aggregated preference matrix, i.e. the number of non-preferred incidences;*n* is the number of factors and χ^2, d_f:

$$\chi^2 = \frac{4}{m-2}\left\{\sum \gamma^2 - m\sum \gamma + \binom{m}{2}\binom{n}{2} - \frac{1}{2}\binom{n}{2}\binom{m}{2}\frac{m-3}{m-2}\right\} \quad (3)$$

$$d_f = \binom{n}{2}\frac{m(m-1)}{(m-2)^2} \quad (4)$$

Research sample and questions

The analysis is based on the data collection of 2015. The respondents are the business economics students of the University of Miskolc. I applied a random sample with 100 elements from 301 responses.The hypotheses of the analysis:

- the major part of the respondents have an inconsistent preference order,
- environmental issues are more preferred than social ones as corporate challenges,

Results

The results on the personal level of consistency is in Table 1. The hypothesis about inconsistency of preferences are to reject. 46% of the respondents show the maximum value (1,00) and 68% over 0,75. Checking the results by sub-samples the pattern of distribution is similar, there are not groups by gender, age or knowledge level designated where lower values were over-represented.

		Frequency	Percent	Valid Percent	Cumulative Percent
Valid	,00	1	1,0	1,0	1,0
	,125	2	2,0	2,0	3,0
	,25	8	8,0	8,0	11,0
	,375	3	3,0	3,0	14,0
	,50	9	9,0	9,0	23,0
	,625	9	9,0	9,0	32,0
	,75	11	11,0	11,0	43,0
	,875	11	11,0	11,0	54,0
	1,00	46	46,0	46,0	100,0
	Total	100	100,0	100,0	

Table 1. Distribution of consistency level

Figure 1. shows the pairwise results. Environmental issues are regularly preferred. In case of social ones about half and half split can be seen. Cost reduction of corporations is in 'competition' with higher incomes for workers and with supporting the education.

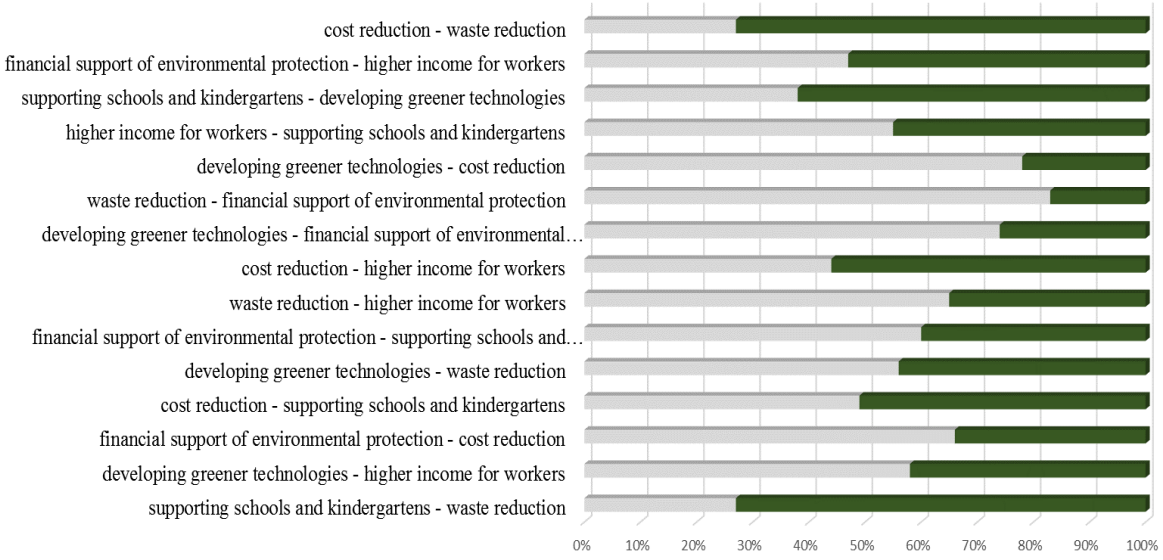

Figure 1. Pairwise comparison of the analysed factors

The results of the analysis by Guilford-method are presented in Figure 2. Importance of waste reduction and developing greener technologies as corporate challenges are prominently above than social issues. Checking the results by sub-samples I could find some differences in weights and order, but the general picture is the same. E.g. women evaluated the greener technologies the highest (100) and waste reduction the second one (90,9). The hypothesis about the higher preferences on environmental issues can be accepted.

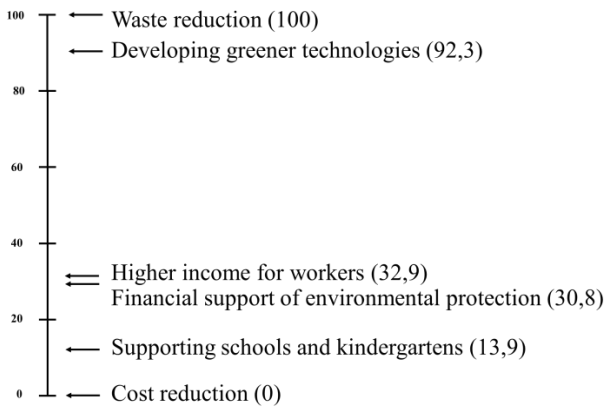

Figure 2. Results of the Guilford analysis

Conclusions

Sustainability is a complex issue: the need for harmony between environmental, social and economic issues is a clear expectation but difficult to achieve. In my research I try to explore the individual and corporate influencing factors of environmentally conscious behaviour. Pairwise comparison applied in this paper allows a nuanced picture than using a Likert-scale based attitude-analysis in exploring the preference orders. Results of the presented analysis point out, that the future management generations (business economics students) have a consistent opinion about the focus points of corporate responsibility. The respondents prefer environmental issues rather than social ones. Analysis of sub-samples by gender, age does not show fundamentally different preferences.

References

[1] M. S. Schwartz, Corporate Social Responsibility: An Ethical Approach, Broadview Press, Buffalo, 2011.
[2] J. Simpson, J. R. Taylor, Corporate Governance Ethics and CSR, Kogan Page Publishers, London, 2013.
[3] G. Tóth,The Truly Responsible Enterprise, KÖVET Association, Budapest, 2007.
[4] Sz. Nagy, I. Piskóti, L. Molnár, A. Marien, The Relationship Between Values and General Environmental Behaviour, Economics And Management 17(1) (2012) pp. 272-278.
[5]K. DudásSchäfferné, A környezettudatosságtöbbszintűértelmezéseés a környezettudatosfogyasztóimagatartásvizsgálata, PhD-értekezés, PTE,Pécs, 2008.
[6] N. Deutsch, Innovations for Sustainability – Challenges and Corporate Actions, In: Proceedings of 10th Annual International Bata Conference for Ph.D. Students and Young Researches, Thomas Bata University, Zlin, 2014, Paper 61.
[7] L. Berényi, Differences of Personal and Professional Opinions – The Example of Environmental Consciousness, In: PiskótiIstván, MolnárLászló (Eds.), Effective innovation and marketing solutions: Theoretical and empirical aspects of innovation marketing, Globe Edit, Saarbrücken, 2016, pp. 143-155.
[8] E. R. Smith, D. M. Mackie, Social Psychology. (3rd ed.), Psychology Press, Hove, 2007.
[9] J. Kindler, O. Papp, Komplexrendszerekvizsgálata: Összemérésimódszerek, MűszakiKönyvkiadó, Budapest, 1977.

APPLICATION RATES OF NEONICOTINOIDS IN SEED COATING AS SOURCES OF ENVIRONMENTAL CONTAMINATION

Mária Mörtl*, Béla Darvas, András Székács

Agro-Environmental Research Institue of National Agricultural Research and Innovation Centre, Herman Ottó u. 15, H-1022 Budapest, Hungary
* e-mail: m.mortl@cfri.hu

Abstract
To assess technical variability in actual dosages, the application rates of neonicotinoid insecticide active ingredients in seed coatings were determined and compared for commercial seeds of different maize varieties. Theeffect oflong storage and coating by unique equipment were assessed. Application rates in different pesticide treatment modes (seed coating, spray or soil granule applications) were also compared. Results indicate that the three technologies utilize similar amounts of the active ingredients per hectare.

Introduction
The use of seed coatings is rapidly increasing throughout the world, as pesticides applied directly to the surface of the seed provide long term protection to crops: the seed coating technology offers an effective method for protecting the seeds during storage or in the soil from pathogens, insects and other pests, and contributes to the uniform stand establishment of a variety of crops produced. Neonicotinoids are nowadays the most widely used insecticides in the world. However, the EU Commission withdrew authorization of three neonicotinoid ingredients (imidacloprid, thiamethoxam and clothianidin) as seed coatings, and restricted their use in 2013 [1]. Based on the environmental risk assessment by the European Food Safety Authority (EFSA) [2], a high risk for bees cannot be excluded unless further restrictions are imposed. According to EU Decision 2015/495 [3] these compounds are now on the watch list and their concentrations in the aquatic environment should be monitored. Reassessment of the above mentioned three neonicotinoids started in 2015 by EFSA with a first publications [4-6], and the risk assessment process is scheduled to be completed by January, 2017. Among neonicotinoids, currently only thiacloprid is authorized in EU for seed coating of maize.

Among the benefits of seed treatment, increased precision and effectiveness are emphasized by placing the crop protection product on the seed to protect it during germination. Estimations claim that the precise application of a crop protection product via seed treatment reduces soil surface exposure by up to 90 percent compared to in-furrow applications and up to 99 percent compared to a surface application [7]. As an environmental impact, lower off-target exposure has been claimed to be expected, yet movement of the neonicotinoid active ingredient in the seed coating in the soil [8], as well as uptake by plants and dispersal in their guttation fluid [9-10] have been evidenced.

Polymers are also applied in seed coatings to bind crop protection products directly to the seed, largely eliminating dust during sowing. It lowers exposure to people who handle and plant the seed, as well as to non-target organisms. Due to its precise application directly to the seed, which is then planted below the soil surface, seed treatment reduces potential off-target exposure to plants and animals. Recommended doses for coating of maize seeds are, however, alarmingly high, 1 mg/seed from thiacloprid (TCL), 1.25 mg/seed clothianidin (CLO) and 0.63 or 1.25 mg/seed from thiamethoxam (TMX). In the current study, to assess true environmental load of neonicotinoids in seed coating, actual levels of neonicotinoid active ingredients TLX, CLO and TMX were determined in coated seeds of various maize varieties.

Experimental

Analyses of samples were carried out on Younglin YL9100 HPLC system equipped with a YL9150 autosampler. A C18 column (150 mm × 4.6 mm i.d., 5µm) was used for the separation at 40ºC. Eluent flow rate was 1.0 ml/min with isocratic elution for 5 minutes (70:30 = A:B eluents, A = 90% water : 10% MeOH, B= MeOH). UV detector signals were recorded at λ=269 nm for CLO and λ=252 nm for TMX. Limits of detections, determined with standard solutions lied at 10 ng/ml for TMX and below 10 ng/ml for CLO.

Samples were obtained from commercially available maize seeds or from those that were coated uniquely on a farm. DECALB 449 (CLO), OCCITAN 380(TMX), and LG 30490 (TCL), were prepared by a relatively new technology, while PR36K67 (CLO) and two MSG seeds were coated earlier. Ingredient contents of coated seeds have been checked by extraction of target compounds from individual seeds with 10 ml of water using ultrasound agitation for 10 minutes, carried out in 10 or 15 replications. Solutions were analyzed after ten-fold or hundred-fold dilution, and filtration through a 0.45 µm hydrophilic polytetrafluoroethylene syringe filter (Labex Ltd, Hungary). Non-coated seeds were used as blank control.

Results and discussion

Results for commercially available new seeds are summarized in Table 1. Analytical determinations indicated that average values are in accordance with current rate of application of CLO or TMX to maize crops (1.25 mg/seed or 0.63 mg/seed), but higher insecticide content was determined for TCL coated seeds, where the recommended dose are 1 mg/seed. High standard deviation (54.3%) observed for Decalb seeds indicates uneven ingredient content. There were more than four-fold difference between lowest and highest value that can also effect the ingredient uptake and individual levels in guttation liquid of maize plants. According to our earlier results average levels in guttation liquid measured in the first period after plantation depend on the amount of ingredient in seed coating material as well. Values determined for plants emerged from commercial seeds (Table 1, line 3) were 50 to 150-fold higher than that of emerged from seeds containing only the 5.4 % of recommended dose (Table 1, line 3)

Table 1. The concentration of three neonicotinoid active ingredients in seed coating on commercial seeds of various maize varieties

Maize variety	Active ingredient	Concentration (mg/seed)	RSD (%)	Number of seeds	Year
DECALB 449	clothianidin	1.217	54.34	15	2013
OCCITAN 380	thiamethoxam	0.605	12.30	10	2013
LG	thiacloprid	1.182	11.15	10	2015

Earlier coated and stored seeds involved in our investigation (see Table 2) contained less insecticides in their coating material compared to the recommended doses. Although deviations were somewhat higher compared to the best values about 10%, they still fall in an acceptable range. There occurred about two-fold differences between the lowest and highest values measured for seeds of maize variety PR36K67 that could have only slight effect to the ingredient uptake and individual levels in the guttation liquid of maize plants.

Uniquely coated maize seeds contained the recommended dose or intentionally less pesticide active ingredient than applied in the usual seed treatment technology. In spite of our expectations, seed coating performed on a farm resulted in similar or somewhat lower values for standard deviations of insecticide content as seeds obtained had previously been in long storage. There occurred less than two-fold difference between the lowest and the highest ingredient content, likely causing no significant differences in levels in maize guttation liquid.

Table 2. The concentration of three neonicotinoid active ingredients in seed coating on commercial seeds after long storage

Maize variety	Active ingredient	Concentration (mg/seed)	RSD (%)	Number of seeds	Year
PR36K67	clothianidin	0.997	24.24	15	2009
MSG-I	thiamethoxam	0.295	18.60	10	2007
MSG-II	thiamethoxam	0.259	15.30	10	2007

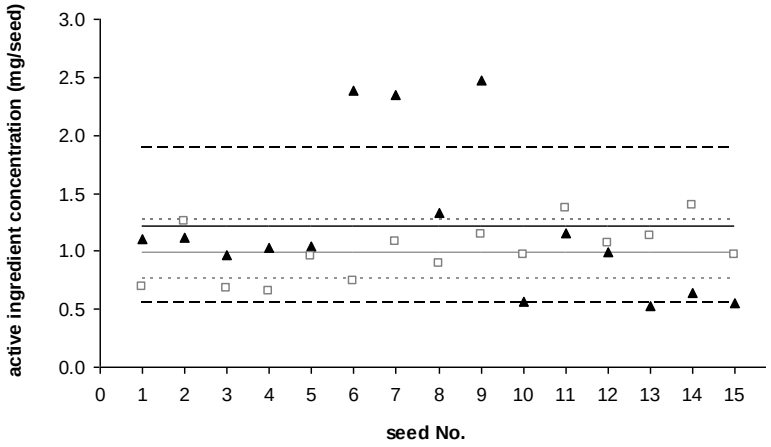

Fig 1. Concentration of active ingredient clothianidin (mg/seed) on individual seeds of maize varieties Decalb 449 (*black triangles*) and PR36K67 (*grey open squares*). Average concentration values (*solid lines*) and standard deviations (*dashed/dotted lines*) determined for 15 seeds are also depicted.

Table 3. The concentration of three neonicotinoid active ingredients in seed coating on uniquely coated maize seeds

Maize variety	Active ingredient	Concentration (mg/seed)	RSD (%)	Number of seeds	Year
1	clothianidin	0.610	16.81	10	2014
2	thiamethoxam	0.145	20.45	10	2014
3	thiacloprid	0.054	9.65	10	2015

Seed coating is considered to be a targeted pesticide delivery method [7] due to being applied directly at the site of the intended protection measure against early insect pests. Application of the active ingredient is secured at the time of sowing, and insecticide efficacy appearing far less dependent on weather conditions than in the case of spay applications. Applied dosages (g of a.i./ha) are also considered to be reduced in seed coating compared to spray or soil granule applications [11], yet this comparison seems to be misleading as it compares different insecticide active ingredients to each other (neonicotinoids in seed coating to carbamate/phenyl-pyrazole compounds (carbofuran, fipronil) in soil disinfectant granules and a chlorinated hydrocarbon (lindane) in spray). Moreover, some of these active ingredients (carbofuran, lindane) are banned in most countries. An approximate comparison of the practically applied dosages of neonicotinoids in seed coating and spray or soil granule formats reveals that seed coating corresponds to 30-85 g active ingredient/ha (0.6-1.22 mg a.i./seed at 50-70 thousand (maize) plants/ha), while typical dosages in spray and in soil granule applications are 20-70 g active ingredient/ha (20-70 mg a.i./l at 1000 l/ha) and 110 g active ingredient/ha (10 g a.i./kg at 11 kg/ha), respectively. This indicates that the three technologies utilize similar amounts of the active ingredients per hectare, and therefore, seed coating is more favorable in terms of pesticide consumption only if spray applications are needed to be used several times during the vegetation period (the number of registered applications is limited in two sprayings per season). Worthy of note that application of seed coating as well

as granules contain insecticide active ingredient in a concentrated form. Thus, their uptake by plants occurs rapidly and high concentrations can be observed in guttation liquid (peak values are often above 100 µg/ml). Due to their good water solubility (e.g. 0.34 g/L and 4.1 g/L for CLO and TMX, respectively), neonicotinoids readily leach into ground and surface water, and consequently are widely detected as pollutants in water resources. Very high contamination rates (up to 100%) were detected in US and Canada in spring. Our environmental monitoring surveys in Hungary showed lower rates: Their occurrence was at 0.017-0.040 ng/ml and 0.040-0.030 ng/ml as diffuse contaminant for CLO and TMX, respectively, and their point source type occurrence at 10-41 ng/ml measured from temporary shallow water bodies [12]. Neonicotinoid uptake processes from different applications and spread of ingredients in the environment are strongly influenced by soil type, and probably soil moisture also affects the transport pattern. According to our previous results of soil column experiments, binding capacity of soils plays an important role in the movement of ingredients [8]. Therefore, contamination of surface waters is more pronounced near to sandy soils, whereas soils of high clay and/or organic matter content retain the components resulting long release of compounds.

Conclusion

Developments in seed coating technology as well as in sowing machines led to decrease of pesticide drift and dust during the sowing of coated seeds. In this way off-target exposure can be eliminated for many species. However, reproducibility of seed coating requires exact technologies and further efforts to ensure controlled doses and environmental effects in the future.

Acknowledgements: This work was supported by OTKA 112978.

References

[1] Commission Implementing Regulation (Eu) No 485/2013
[2] EFSA Journal 2013;11(1):3066-3068.
[3] Commission Implementing Regulation (EU) No 2015/495
[4] EFSA (European Food Safety Authority), 2015. *EFSA Journal***13**(8):4211 (2015), 82 pp.
[5] EFSA (European Food Safety Authority), 2015. *EFSA Journal***13**(8):4210 (2015), 77 pp.
[6] EFSA (European Food Safety Authority), 2015. *EFSA Journal***13**(8):4212 (2015), 70 pp.
[7] The role of seed treatment in modern US crop protection *http://www.cropliffoundation.org*
[8] M.Mörtl, O. Kereki, B. Darvas, et al., *J Chem,***2016** (2016) Article ID 4546584.
[9] V. Girolami, L. Mazzon, A. Squartini, et al., *J Econ Entomol,* **102**(5) (2009) 1808-1815.
[10] M. Mörtl, Á. Vehovszky, J. Győri, et al. *Proc. 21st International Symposium on Analytical and Environmental Problems, Szeged,* Hungary (2015) pp. 52-55.
[11] P. Jeschke, R. Nauen, M. Schindler et al., *J Agric Food Chem***59** (2011) 2897-2908.
[12] A.Székács, M. Mörtl, B. Darvas, *J Chem,* **2015** (2015) Article ID 717948

LIGHT INDUCED SINGLET OXYGEN PRODUCTION AND DETECTION GENERATED BY BACTERIAL REACTION CENTRE-CARBON NANOTUBES COMPOSITES

Anikó Kinka[1], Ateeq Ur Rehman[2], Imre Vass[2], Botond Máthé[1], László Nagy[1], Kata Hajdu[1]

[1]Department of Medical Physics and Informatics, University of Szeged, H-6720 Szeged, RerrichBélatér 1, Hungary
[2]Biological Research Centre of the Hungarian Academy of Sciences, Szeged, H-6726 Szeged, Temesvárikrt. 62, Hungary
e-mail: hajdu.kata@gmail.com

Abstract

Nowadays the photoelectric energy transformation is one of the most promising alternative energy sources. Plants and bacteria have their unique apparatus,the photosynthetic reaction centreprotein (RC)to convert the light into chemical potential. Generation of singlet oxygen accompanying the photochemistry of isolated reaction centre protein of non-sulfur purple bacteria(*Rhodobacter(Rb.) sphaeroides*) have been studied by measuring oxygen uptake by conventional oxygen electrode. In case of oversaturated illuminating conditionsbesides the RC photochemistry the excess energy is captured by triplet states of chlorophyll molecules. The triplet energyisthen dissipated by heat or by sensitizingthe formation of various reactive oxygen species (ROS), especially by singlet oxygen ($^1O_2$). Under these conditions the protein subunits are damaged and the efficiency of photochemistry decreases. The aims of our work are to find conditions in which the concentration of these harmful compounds can be reduced. The possible role of carbon nanotubes (CNT), which are known to quench the singlet oxygen is investigated in the CNT/RC hybrid bio-nanocomposites.

Introduction

During photosynthesis, the light energy is converted into chemical potential in the reaction centre protein (RC) with extremely high efficacy. Under conditions of excess light and/or when the photochemical processes are blocked, reactive oxygen species (ROS, including, e.g., singlet oxygen ($^1O_2$), superoxide anion (O_2^-) and hydroxyl radicals ($OH\cdot$)) are formed inside the complex with large probability.[1,2]ROS components can decrease the efficiency of the photochemical energy conversion, e.g. by reacting with the intracellular components resulting in their degradation (the RC itself as well).

Different mechanisms are developed in nature in order to reduce the ROS concentration, including specific enzyme reactions (e.g. peroxidases, superoxide dismutases) and/or decaying the concentration of long lived excited species (e.g. energy transfer from chlorophyll triplets to carotenoids). Carbon nanotubes (CNT), in artificial systems, are also known to react with singlet oxygen.[3]

Experimental

Carotenoid-less*Rb. sphaeroides* R-26 purple bacterial cells were grown photoheterotrophically. RCs were prepared bydetergent (LDAO:N,Ndimethyldodecylamine-N-oxide, Fluka)solubilization and purified by fractionalized ammonium sulfate precipitation, followed by DEAE Sephacel (Sigma)anion-exchange chromatography.

The photochemical reactions were carried out in a solution that contained 1,3-diphenylisobenzofuran (DPBP), and RC or CNT/RC composite in a 0.5 cm spectroscopic cuvette that was illuminated with 808 nm continuous wave diode laser (DL) light and whole

absorption spectra were measured in every fifteenth seconds by an AVANTES CCD fibre optic spectrophotometer. The reaction mixtures contained DPBF and RC or CNT/RC composite in TRIS buffered (10 mM TRIS, 100 mMNaCl, 0, 03% LDAO, pH:8.0) detergent suspension.

Singlet oxygen concentration was also determined by measuring oxygen uptake with a Clark type electrode (1µM RC; 250 mM histidine; phosphate buffer pH 7; 30 °C; light intensity 500 µE).[4] The effect of carbon nanotubes was detected in blend samples and also after immobilizing the RC on the CNT surface with physical sorption – and chemical binding as well.

Results and discussion

Effect of carbon nanotubes on the equilibrium concentration of $^1O_2$ in RC solutions was determined in two different ways. One method was the use of ROS sensitive DPBF die that has a characteristic spectral change after reacting with singlet oxygen. The other method was the measure of oxygen uptake directly by a Clark type oxygen electrode in the presence of histidine.

Singlet oxygen produced by RC could be detected with the use of DPBF. Figure 1 shows the bleaching of the absorption peak of DPBF at 420 nm in the function of the illumination time. Carotenoid-less R-26 reaction centre wasbound to functionalized and non-functionalized single-walled (SWCNT) and multi-walled (MWCNT) carbon nanotubes with different binding methods indicated on the graph.

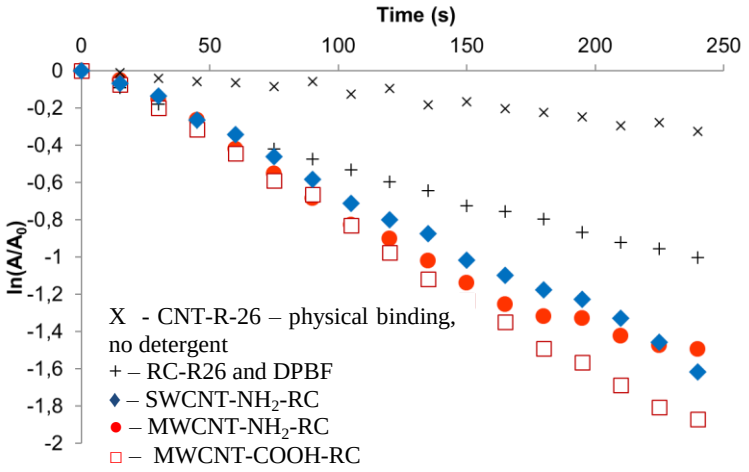

Figure 1. Dose-response curve of absorption change induced by DPBF- $^1O_2$ reaction in carotenoid less (R-26) RCs and CNT/RC suspensionsafter different binding procedure on the surface of amine – and carboxyl functionalized single – and multiwalled carbon nanotubes (SWCNT-NH_2, MWCNT-NH_2, MWCNT-COOH)

On Figure 2 oxygen uptakemeasured with Clark type electrode is shown in the presence of histidine. RCs purified from the carotenoid-less mutant R-26 bacterial strain was used with constant, 1 µM concentration. Carboxyl-functionalised multiwalled carbon nanotubes were applied. Measurements were done using different reaction centre/multi-walled carbon nanotube volume ratios.Three different MWCNT/RC suspensions were prepared.First, RC and MWCNT blend samples, second, RC was bound on the MWCNT with physical sorption and third, RC was bound chemically through the carboxyl-groups of the tubes with the use of crosslinker molecules.Blend samples were measured with four different CNT concentrations and composites were made with two different MWCNT ratios with physical sorption and chemical binding method as well.

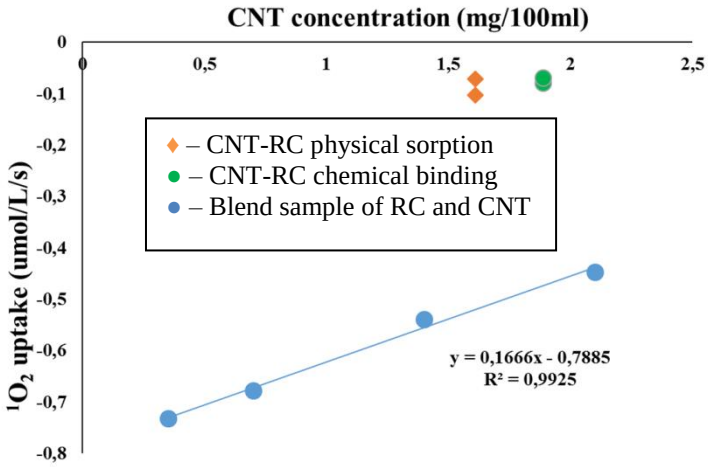

Figure 2. Oxygen uptake in Clark type electrode in the function of MWCNT concentration with three different MWCNT/RC suspensions(Blend samples; MWCNT/RC after physical sorption and MWCNT/RC after chemisorption).[RC]=1 μM.

Conclusion

According to our results with both measuring techniques, MWCNT is able to quench singlet oxygen with bigger efficiency after physical sorption of the RC on the nanotube's surface, than after chemical binding or in the case of the blend samples. This can probably be explained with the smaller diffusion distance between the peptide complexes and the CNTs.
Under our present experimental conditions, we do not see difference in the equilibrium concentration of $^1O_2$ in SWCNT/RC and MWCNT/RC complexes, however, we do see the effect of functionalization. -COOH functionalization shows slightly larger $^1O_2$ production (in line with slightly lower photoactivity of this sample, cf. Fig. 1).

Acknowledgements

This work was supported from OTKA PD116739, from the project Cost Action TD1102 "PHOTOTECH. Photosynthetic proteins for technological applications: biosensors and biochips"and from grant from Switzerland through the SwissContribution (SH/7/2/20). Thanks are due also to the support from "Photosynthesis – Life from Light – Foundation".

References

[1] K.L. J.B. Arellano, Y.A. Yousef, T.B. Melo, S.B.B. Mohamad, R.J.Cogdell, K.R. Naqvi, J. Photochem. Photobiol., 87 (2007) 105-112.
[2] A.F. Uchoa, P.P. Knox, R. Turchielle, N.K. Seifullina, M.S. Baptista, EurBiophys J., 37 (2008) 843–850.
[3] M.A. Hamon, K.L. Stensaas, M.A. Sugar, K.C. Tumminello, A.K. Allred, Chemical Physics Letters, 447 (2007) 1-4.
[4] A.U. Rehman, K. Cser, L. Sass and I. Vass,Bio

LIFE CYCLE ASSESSMENT OF DMSO SOLVENT, COMPARING AN OPEN MANUFACTURING SYSTEM WITH A CLOSED ONE

Anett Zajáros[1*], Klára Szita Tóth[2], Károly Matolcsy[1], Dániel Horváth[3]

[1]ÉMI Non-Profit Llc., H-2000 Szentendre, DózsaGyörgy street 26, Hungary
[2]Institute of World- and Regional Economics, Miskolc University, H-3515 Miskolc-Egyetemváros, Hungary
[3]S-Metalltech 98 Ltd.,H-2000 Szentendre, StégerFerenc alley 20, Hungary
e-mail: azajaros@emi.hu

Abstract
This paper has been elaborated during the project called "DMSO contaminated industrial waste water recycling by distillation" which action connects to the Hungarian water quality improvement program. The dimethyl sulfoxide (DMSO) is frequently used as a solvent for chemical reactions and is also extensively used as an extractant in biochemistry and cell biology. It is known as environmental friendly solvent, and the DMSO can be efficiently recovered from aqueous solutions – even though contaminated with volatile and/or non-volatile impurities – by distillation due to its high boiling point (189 °C). This paper compares two technologies an open and closed system from viewpoint of sustainability, by LCA, in which the DMSO used as solvent, and it was recovered.

Introduction
The factory of the Project Promoter S-Metalltech 98 Ltd. produces arsenic, phosphorus,iodine and fluorine removal adsorber for drinking and technological waters. During the production process 1m^3 high 20 w/w% dimethyl sulfoxide(DMSO) content hazardous waste water is produced daily, which needs to be collected and transferred to the incineration plant to be burned, sothe transferred DMSO need to be replaced with fresh solvent in the production process.This method is really expensive and also has significant negative effect on the environment, due to these reasons the Project Promoter seeks to modernize the production technology regarding both the treatment of the waste water and the solvent replacement (this project is called "DMSO contaminated industrial waste water recycling by distillation").The waste water beside DMSO contains:soluble polymer – ethylene-vinyl alcohol copolymer (EVOH) and minerals such as cerium-hydroxide.

The aims of the project are:

- to reduce the volume of the hazardous waste water,
- to reuse the recovered solvent and water in the production process so to turn the open manufacturing system into a closed one.

The solvent recycling meets with the new initiative of European Environmental Policy as „the Circular Economy" as achieve a new way towards the green and sustainable economy. An EU action plan for „the Circular Economy", the overall objective of resource efficiency can be achieved only through the implementation of circular economy, where the value of products, materials and resources is maintained in the economy for as long as possible, and the generation of waste minimized[5].

Experimental
Dimethyl sulfoxide (DMSO) is a sulfur-containing organic compound; molecule formula: $(CH_3)_2SO$. It exhibits as colorless, odorless, hygroscopic and flammable transparent liquid at

room temperature. It has both high polarity as well as high-boiling point. It also has aprotic and water-miscible characteristics. DMSO is known as environmental friendly solvent that effectively dissolves numerous organic and inorganic chemicals. Its excellent safety characteristics have led to its use for a wide range of purposes, notably as a cleaning agent for electronic components, and as a reaction solvent for pharmaceuticals and agricultural chemicals.Vignes (2000) mentioned as "New" Clean, Unique, Superior Solvent, because it's low toxicity, the outstanding properties of DMSO when compared to competing solvents, and existing and potential applications. It has many benefits comparing with other solvent stated Marti et al. (2013), especially with well chosen recovery process [6]. The solvent recovery in a circular economy results economical benefit [2]and the life cycle assessment of recovery process shows objective result of environmental benefit [3],[1],[4], while the LCSA highlights both of environmental, economic and social effect too [7].

Applied methods during the project:

- qualitative and quantitative analysis of waste water components,
- separate the different types (water, solvent /DMSO/ and other components) with distillation and analyze the efficiency of the separations in laboratory level and also during the manufacturing process,
- prepare sustainability analysis based on technical performance, life-cycle analysis (analyze the environmental, economic and social impacts of these two processes with LCA, LCCA, S-LCA), CAPEX and OPEX in laboratory level and also during the manufacturing process.

This paper focuses to Life Cycle Assessment from aspect of sustainability, where the recovery of DMSO takes 98 % (scenario 1), and where beside this recovery it is used renewable resources too (scenario 2). The functional unit was 1 m^3AsMetadsorber product. The system boundaries were determined from gate to waste treatment. The analysis based on the ISO 14040 standard, ecoinvent database and CML 2001 method.

The flowchartsof two technologies show the differences. The open system results 1 m^3 per day waste water as hazardous waste, what after collection they transport to incineration.

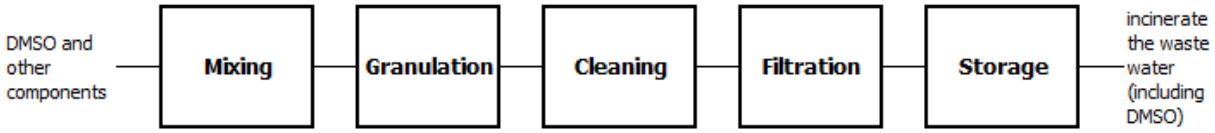

Figure 1. The current manufacturing process (open technology)

The closed technology as a model of circular economy contents a two steps distillation process with 98 % recovered of DMSO and recycled water.

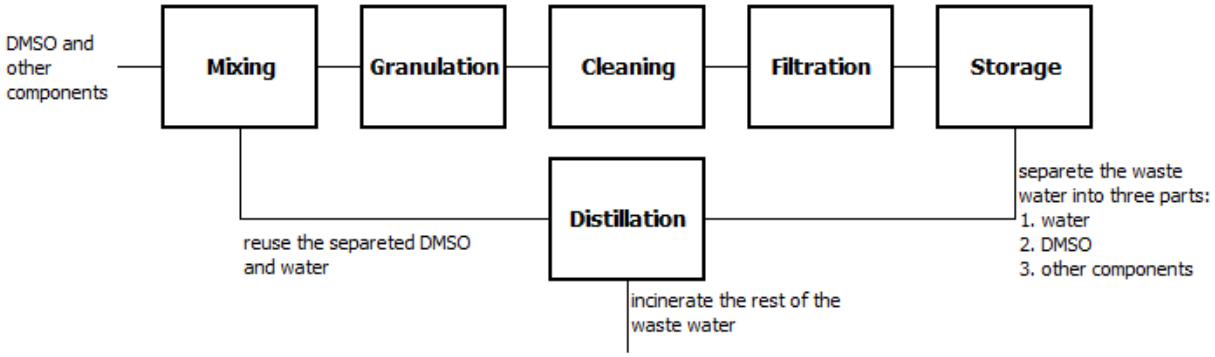

Figure 2. The planned manufacturing process (closed technology)

Results and discussion

The result of analyses shows although the recovery process requires additional electricity and technological equipments, but possible to recover the 98 % of DMSO in quite analytical purity. Comparing the environmental profile of 1 kg DMSO from database and recovery process there are significant differences in every impact category, and it results less environmental impact of closed technology too. There are the greatest differences in the adiabatic potential, global warming potential and ecotoxicity.

Table 1. Comparing Environmental impact of the DMSO(from database) and recovered DMSO, and recovered DMSO with solar PV (RES) (characteristic factors)

	Abiotic Deplation (ADP)	Acidifica-tionPotential (AP)	Eutrophica-tion Potential(EP)	Global WarmingPotential (GWP)	Human Toxicity (HT)	OzonelayerDeplation(ODP)	Photochemi-calOxydation (POP)
	kg Sbeq.	kg SO2 eq.	kg PO4 eq	kg CO2 eq	kg 1,4-DB eq	kg CFC_11 eq.	kg C_2H_4
DMSO	0,021	0,054	0,002	1,272	1,083	1,76E-07	1E-03
DMSO_R'	0,004221	0,002758	0,001693	0,569501	0,345368	3,4806E-08	0,000107
DMSO_R'+SPV	0,002906	0,001834	0,001089	0,395032	0,05917	2,3855E-08	7,18E-05

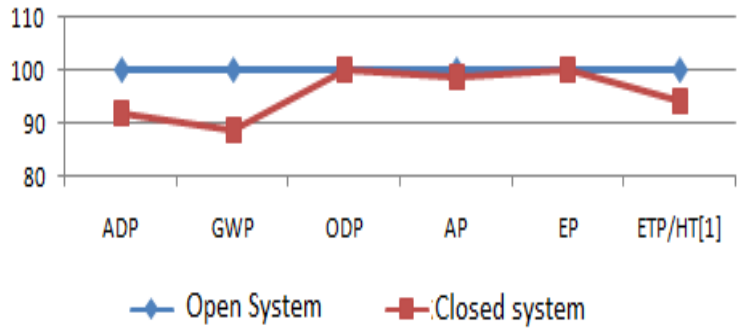

Figure 3. Environmental impact of the two technologies (open technology impact =100 %)

The criteria of sustainability is the following:

LCSA $_{open}$(=LCA+LCC+SLCA) > LCSA $_{closed}$(= LCA + LCC + SLCA),

and each of the three pillars has less impact in the closed system than in the opened one.

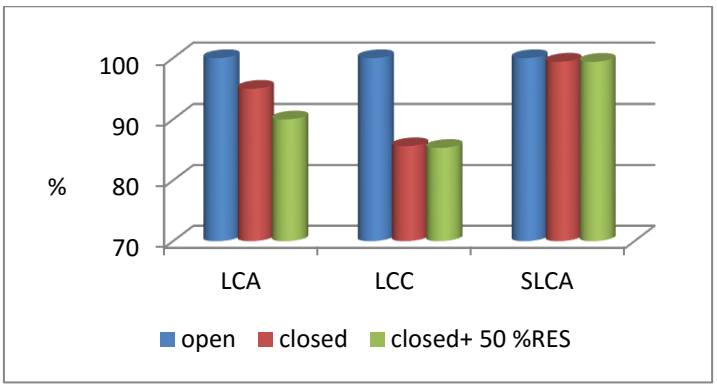

Figure 4. The sustainability assessment of the technologies

Conclusions

In our ongoing project we executed the preliminary measurements and due to these results we found the two-step vacuum distillation as the best solution. Now we are testing the efficiency of the separations in laboratory level and we started the life-cycle analysis and CAPEX, OPEX calculations.

We expected the following results at the end of the project according to preliminary estimates:

- the amount of hazardous waste water could be reduced from 265,2 ton/year to 5,5 ton/year, so with 98%;
- the amount of water used in the manufacturing process could be reduced approximately with 27%.
- the reused amount of the DMSO solvent depends on the efficiency of the distillation process, so its purity.

References

[1]Amelio Antonio, Giuseppe Genduso, Steven Vreysen, Patricia Luis and Bart Van der Bruggen (2014): Guidelines based on life cycle assessment for solvent selection during the process design and evaluation of treatment alternatives† Green Chem., 2014, 16, 3045

[2]Andersen MS (2007): An introductory note on the environmental economics of the circular economy - Sustainability Science,2: 133-140 Springer http://link.springer.com/article/10.1007/s11625-006-0013-6#page-2

[3]Capello Christian, Stefanie Hellweg, Christina Seyler, Konrad Hungerbühler (2005): ecosolvent: A tool for waste-solvent management in chemicalindustry 27th LCA Discussion Forum, 17 November 2005

[4]Gaylord Chemical (2015): Dimethyl sulfoxide recovery: Recovery, System Engineering And Environmental Considerations Gaylord Chemical.org

[5]EEA (2016): Circular economy to have considerable benefits, but challenges remain http://www.eea.europa.eu/highlights/circular-economy-to-have-considerable

[6]Jungho Cho† and Dong Min Kim (2007): Korean J. Chem. Eng., 24(3), 438-444

[7] SzitaTóthné K., J. Roncz (2016): Economic analysis of regional sustainability– Hungary Ch.25. in Fritz Balkau, Stefania Massari, Guido Sonnemann (ed.) 2016: *Life cycle approaches to sustainable regional development*, Taylor & Francis/Routledge in printing

[8] Vignes, Robert (2000):Dimethyl Sulfoxide (Dmso) A "New" Clean, Unique, Superior SolventAmerican chemical society Annual Meeting, August 20-22, Washington

A PRELIMINARY STUDY ON THE POSSIBILITIES TO INDICATE THE EFFECTS OF URBAN STRESS ON MAPLE TREES

Dávid Korányi[1,3], Balázs Palla[1], Éva Stefanovits-Bányai[2], Viktor Markó[1]

[1]Department of Entomology, Szent István University, Faculty of Horticultural Science
[2]Department of Applied Chemistry, Szent István University, Faculty of food Science
[3]Department of Animal Sciences and Animal Husbandry, University of Pannonia, Georgikon Faculty
e-mail: koranyidave@gmail.com

Abstract

Urban trees have an important role to create a more livable environment. These plants are exposed to various types of environmental stresses that might cause decline in their condition and decorative value. The aim of our preliminary study is to study the effects of urban stress factors, mainly the air pollution and pest damage on maple trees. Three maple species were studied: field maple (*Acer campestre*), sycamore maple (*A. pseudoplatanus*) and Norway maple (*A. platanoides*) in four areas in Budapest, Hungary with different traffic density.
The peroxidase (POD) enzyme activity was measured in the leaves by a spectrophotometric method. Phytophagous insects with piercing-sucking mouthparts (Hemiptera) were also collected from the canopy level by beating method.
We found that POD activity was generally the highest in field maples and the lowest in Norway maples with sycamore maples between, but we did not find consistent patterns at each sampling site. The abundance of the collected hemipterans showed similar pattern, but showed no consistent tendency at the various sampling sites and therefore, the abundance of hemipterans did not explain the variation of POD activity. In our study the connection between the POD activity, the air pollution and the abundance of hemipterans remained not fully understood. To clarify this relationship further studies are required.

Bevezetés

A városi környezetbe ültetett fák kiemelt szerepet játszanak egy élhetőbb környezet megteremtésében. A levegő minőségének javítása mellett más ökoszisztéma szolgáltatásban is szerepet játszanak, mint például a zajcsökkentés és a mikroklíma szabályozás [2; 4].
Ezekre a növényekre számos olyan tényező hat, amelyek élettani szempontból káros fiziológiai változásokat idézhetnek elő [16]. Ezen tényezők közé lehet sorolni az utak sózását, a természetes élőhelyekhez viszonyított magasabb hőmérsékletet, a jelentős járműforgalom okozta környezetszennyezést, valamint a rovarok okozta kártételt is [11].
A parkokba díszfaként és a forgalmas utak mentén útsorfaként ültetett fák a környezetüket ért hatásokra érzékenyen reagálnak, így remek bioindikátoroknak mondhatók [12; 14].
Több vizsgálat szerint a különböző stresszenzimek, így a peroxidáz enzim aktivitása remekül reprezentálja a növényeket ért belső változásokat [7; 10; 1]. Ezeknek az enzimeknek számos fontos élettani folyamat szabályozása mellett szerepe van a biotikus és abiotikus stressz tolerancia kialakításában is [9; 5; 6].
A juharfélék (*Aceraceae*) családjába több mint 100 fa- és cserjefaj tartozik [3]. A fajok többsége a klímára kevésbé érzékeny, a szélsőséges talajokat leszámítva a legtöbb helyen fennmarad [13, 8]. Irodalmi adatok alapján a városokba ültetett juharfajok közül a mezei juhar (*Acer campestre*) ellenállóbbnak, míg a korai juhar (*A. platanoides*) és hegyi juhar (*A. pseudoplatanus*) a városi környezettel szemben kevésbé toleránsnak mondható [13,15].
Előzetes vizsgálatunk célja az volt, hogy meghatározzuk három juharfaj városi környezettel szembeni stressztűrő képességét, leveleik peroxidáz enzimativitásának mérésével, illetve a

lombkoronában található szúró-szívó szájszervű rovarok egyedszámának felmérésével.

Anyagok és módszerek

Elővizsgálatunk során három, városi környezetben gyakori juharfaj (mezei, korai és hegyi juhar) stressztűrő képességét vizsgáltuk Budapesten.

Vizsgálatunk a levelek peroxidáz enzimaktivitásának kimutatására irányultak, amellyel a fák stresszeltségére, a városi környezettel (különösen a forgalommal és rovarkártétellel) szembeni toleranciájára kerestük a választ.

A vizsgálathoz négy helyszínen jelöltünk ki fákat: a nagyobb forgalomnak kitett Alkotás utca és a Szent István Egyetem Budai Campusa környékén (Karolina út, Villányi út), valamint a természetesebbnek mondható Budai Arborétumban és a Gellért-hegyen. Minden helyszínen 5-5-5 közel azonos korú mezei, korai és hegyi juharfát jelöltünk ki.

Terepi mintagyűjtés:

A kijelölt fákról laboratóriumi mérés céljára levélmintákat gyűjtöttünk 2016 áprilisában. A begyűjtött leveleket a SZIE Alkalmazott Kémia Tanszékének laboratóriumába való szállítás során hűtőtáskában, illetve a feldolgozásig mélyhűtőben tároltuk.

A vizsgált juharfákon gyakorinak mondható, szúró-szívó szájszervű rovarok (poloskák, levéltetvek, levélbolhák, kabócák és lepkekabócák) rendszeres gyűjtésére is sor került 2015 vegetációs periódusában kopogtatásos módszerrel. A gyűjtött példányokat a SZIE Rovartani Tanszékére szállítottuk, majd meghatároztuk azokat.

A peroxidáz enzim aktivitásának meghatározása:

A gyűjtött leveleket hűtött, 20 mM-os 7,8-as pH-jú Na-acetát puffer (1 % polivinilpirrolidon, 20 % szacharóz, 0,035 % marhaszérum albumin, 10 % Triton X100) és kvarchomok segítségével dörzsmozsárban homogenizáltuk.

A homogenizált mintákat Micro 22R típusú centrifuga segítségével 13000 fordulat/perc fordulatszám mellett, 10 ^{o}C hőmérsékleten, 20 percig centrifugáltuk. Az analízisek a keletkezett felülúszóból történtek.

A mérést Shannon (1966) módszere alapján 0,1 M Na-acetát pufferben (pH=5,0), H_2O_2 szubsztrát és ortidianizidin kromogén reagens (ε=11,3) jelenlétében spektrofotometriásan (λ=460nm) határoztuk meg. Az eredményeket U/ml-ben adtuk meg.

Eredmények és értékelés

A peroxidáz enzimaktivitás méréseinek eredményeit az egyes juharfajokra és helyszínekre vonatkozóan az 1. táblázatban foglaltuk össze.

A három fafaj közül általánosan a mezei juharfák mutatták a legnagyobb ellenállóságot, őket a hegyi és korai juhar követte. Mezei juhar esetében látható, hogy a forgalom által kevésbé terhelt területeken a peroxidáz enzimaktivitás nagyobb, mint a forgalmas utak mentén lévő területeken (Alkotás utca, egyetem környéke). Hegyi juharon fordított mintázatot figyeltünk meg, míg korai juharon a mért értékek nem különböztek jelentősen.

1. táblázat: A peroxidáz enzimaktivitás mérések átlageredményei (egyed/fa ± standard hiba) U/ml-ben

	Mezei juhar	**Hegyi juhar**	**Korai juhar**	**Átlag/helyszín**
Gellért-hegy	9,9 (1,0)	2,1 (0,7)	2,9 (0,9)	5,0
Budai Arborétum	5,4 (2,0)	2,9 (0,8)	3,7 (1,9)	4,0
Alkotás utca	2,0 (1,2)	5,3 (2,3)	2,7 (1,0)	3,3
Egyetem környéke	4,7 (1,7)	6,1 (2,4)	3,0 (1,5)	4,6
Átlag/fafaj	5,5	4,1	3,1	

Összesen 16275 szúró-szívó szájszervű, fitofág rovart gyűjtöttünk, mezei juharon 6880 egyedet, hegyi juharon 5528 egyedet és korai juharon 3867 egyedet. Összességében tehát a legnagyobb peroxidáz aktivitást és rovar egyedszámokat a mezei juharon, a legkisebbet korai juharon figyeltük meg, míg a hegyi juhar köztes értéket vett fel. Az egyes fajok enzimaktivitása és a lombkoronájukban gyűjtött fitofág, szúró-szívó szájszervű rovarok összes egyedszáma viszont nem mutatott hasonlóan egyértelmű összefüggést, ha a négy mintavételi területet külön vizsgáljuk (1. és 2. ábra).

A rovaroknál a kisebb zavarásnak kitett élőhelyek nem különülnek el a nagyobb zavarásnak kitett élőhelyektől (2. ábra). Általános mintázatként mindössze azt állapíthattuk meg, hogy az első három helyszínen mindhárom fafajnál hasonlóan alakult a rovarok egyedszámának mintázata: a legtöbb egyedet a Budai Arborétumban, a legkevesebbet a Gellért-hegyen gyűjtöttük, míg az Alkotás utcában köztes értékeket figyeltünk meg. A negyedik helyszínen viszont kiugróan nagy (mezei juhar) és kifejezetten kis (hegyi juhar) egyedszámokat is mértünk. Összességében a vizsgált élőhelyek forgalmi terhelése, a peroxidáz enzimaktivitás és a rovarkártétel között nem figyeltünk meg egyértelmű összefüggéseket (1. és 2. ábra).

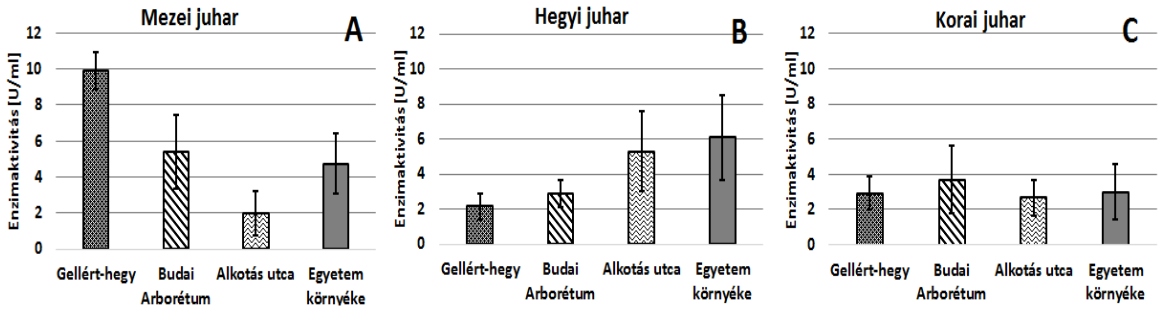

1. ábra: Peroxidáz enzimaktivitás mérések átlagai és szórásai (A) Mezei juhar, (B) hegyi juhar és (C) korai juhar esetében

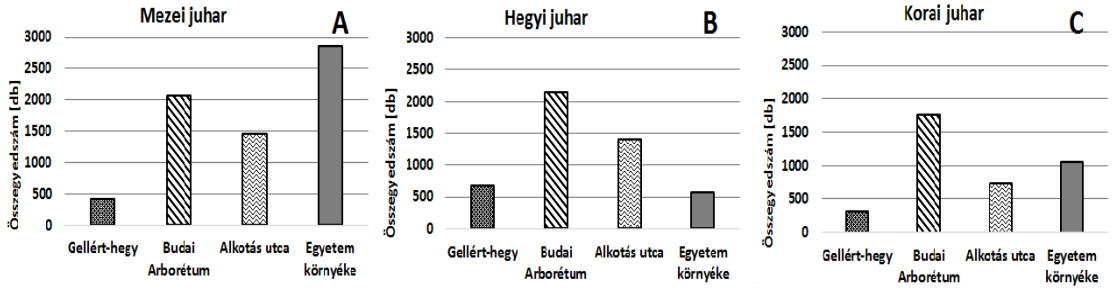

2. ábra: Fitofág szúró-szívó szájszervű rovarok összegyedszámának alakulása (A) mezei juhar, (B) hegyi juhar és (C) korai juharfák lombkoronájában

Következtetés

Vizsgálatunkkal megállapíthatjuk, hogy a mezei juhar ellenállóbbnak bizonyul a városi környezet hatásaival szemben, hiszen már tavasszal egy nagyobb mértékű enzimaktivitással készül fel a stressztényezők hatására keletkező reaktív oxigénformák semlegesítésére. Mindez ugyanakkor egy nagyobb fokú érzékenységet is jelent a másik két juharfajhoz képest.

Hegyi juhar esetében, feltételezzük, hogy a forgalomnak való kitettség jelentősebb hatást gyakorolhat a fák ellenállóságára, mint a növényi nedveket fogyasztó rovarok jelenléte. A fafaj egyedei ugyanis a forgalmas utak közelében mutattak nagyobb enzimaktivitást, annak ellenére, hogy volt olyan forgalmas helyszín, ahol kisebb és kevésbé fogalmas helyszín, ahol nagyobb volt a rovarfertőzöttség.

Elővizsgálatunk alapján a peroxidáz enzimaktivitás a légszennyezés és a rovarkártétel szerint alakuló mintázata nem egyértelmű, sokszor ellentmondásos. Úgy gondoljuk, hogy e két stresszfaktor mellett számos egyéb tényező is szerephez juthat, mint például a mintaterület klimatikus jellemzői, a talaj szennyezettsége, vagy akár a szennyező anyagok összetétele. A fitofág rovarok számának alakulásában továbbá azok természetes ellenségeinek jelenléte, a táj diverzitása és a légszennyezés közvetlen hatásai is meghatározóak lehetnek. Az enzimaktivitás, a rovarok számának alakulása és a légszennyezés közötti egyértelmű kapcsolatok kimutatásához további vizsgálatokra van szükség, amely magába foglalja többek között az újabb, különböző forgalmi terhelésnek kitett helyszínek bevonását, az éven belüli több mérés elvégzését, valamint további stresszmarker fehérjék vizsgálatát.

Köszönetnyilvánítás

Köszönettel tartozunk a SZIE Rovartani Tanszék és Alkalmazott Kémiai Tanszék munkatársainak a minták feldolgozása során nyújtott segítségükért.

Irodalomjegyzék

[1] G. Baycu, D. Tolunay, H. Özden, S. Günebakan, Environmental pollution (2006) 143(3), 545-554.
[2] P. Bolund, S. Hunhammar, Ecological economics (1999),29(2), 293-301.
[3]A. J. Coombes, Trees. Panem-Grafo, Budapest, 1996
[4] F. J. Escobedo, J. E. Wagner, D. J. Nowak, C. L. De la Maza, M. Rodriguez, D. E. Crane, Journal of environmental management (2008) 86(1), 148-157.
[5] SZ. Fekete,Új nemesítésű balkonnövények klímatűrése és peroxidáz aktivitása. Budapesti Corvinus Egyetem, Doktori (Ph.D) értekezés (2008) Budapest
[6] S. S. Gill, N. Tuteja, Plant physiology and biochemistry (2010) 48(12), 909-930.
[7] T. Keller, Forest pathology (1974) 4(1), 11–19.
[8] L. Maráczi L. 2013. Díszfák és díszcserjék védelme. Nyugat-Dunántúli Díszfaiskolások Egyesülete, Szombathely, 2013
[9] D. A. Meloni, M. A. Oliva, C. A. Martinez, J. Cambraia,Environmental and Experimental Botany (2003)49(1), 69-76.
[10] P. Puccinelli, N. Anselmi, M. Bragaloni, Chemosphere (1998) 36(4), 889-894.
[11] G. Ripka, Növényvédelem (2004) 40(7) 385−391.
[12] T. Sawidis, J. Breuste, M. Mitrovic, P. Pavlovic, K. Tsigaridas, Environmental Pollution (2011) 159(12), 3560-3570.
[13] G. Schmidt, I. Tóth, 2006. Kertészeti dendrológia. Mezőgazda Kiadó, Budapest, 2006
[14] S. M. Serbula, T. S. Kalinovic, A. A. Ilic, J. V. Kalinovic, M. M. Steharnik,Aerosol Air Qual. Res. (2013) 13(2), 563-573.
[15] T. Swoczyna, H. M. Kalaji, S. Pietkiewicz, J. Borowski, E. Zaras-Januszkiewicz,Dendrobiology (2010), 63, 65-75.
[16] K. V, Tubby, J. F. Webber.Forestry (2010) 83(4), 451-459.

TiO_2 COATED MEMBRANE SURFACE CHARACTERISATION WITH CONTACT ANGLE MEASUREMENTS

Ildikó Kovács, Szabolcs Kertész, Gábor Veréb, Cecilia Hodúr, Zsuzsanna László*

Department of Process Engineering, Faculty of Engineering, University of Szeged, H-6725 Szeged, Moszkvai krt. 9., Hungary
e-mail: zsizsu@mk.u-szeged.hu

Abstract
In this work a neat polyacrilonitrile ultrafiltration membrane performance was compared to a same but TiO_2 coated membrane during oily water filtration. The fouling mechanisms of the two membranes and the resistances were determined and calculated.It was found that in case of the neat membrane initially intermediate pore blocking occurs that is followed by cake layer formation. The TiO_2 coating proved to be beneficial due to its fouling mitigating effect. With contact angle measurements the membrane wettability changes were monitored,whichoccurred as a result of the TiO_2 coating, oily water filtration and cleaning of the membrane surface by UV irradiation. After 3 hours of UV irradiationthe water flux reached the neat membrane flux, but the residual oil layer on the surface still had a significant effect on the surface wettability.

Introduction
The rapid growth of oil and gas, petrochemical, pharmaceutical, metallurgical and food industries resulted in large oily wastewater production. Physical and chemical wastewater treatment methods are widely investigated, taking into consideration their efficiency, cost, need of additives, equipment and infrastructure, process time, capacity, etc. [4], but most of them are not effective enough to treat stabile oil in water emulsions. Membrane filtration is an efficient process to treat oily wastewaters, without chemical additives and low energy cost compared to traditional separation methods [1, 2, 5]. Ultrafiltration is the most effective treatment, among membrane processes for this purpose [5]. Polymer membranes are the most commonly used type of membranes in water and wastewater treatment. Despite their beneficial qualities, their separation performance, antifouling property and long-time stability need improvement [1-4].
As the membrane fouling is a key problem; in order to minimize it membrane surfaces can be modified with photocatalytic nanoparticles. One way of modifying the membrane is to deposit the particles on the membrane surface [6–8]. TiO_2 is the most commonly used photocatalyst due to its good physical and chemical properties, availability, high photocatalytic activity and desirable hydrophilic properties [6–9]. Increasing the membrane hydrophilicity can increase the membrane fouling resistance [9].Contact angle measurements are commonly used to determine the wettability of a surface. Contact angles also can show an accordance with the surface roughness [10].
The aim of this work was to investigate the effect of TiO_2 coating on a polyacrilonitrile ultrafiltration membrane performance during oily water filtration compared to the neat membrane. Furthermore, to characterize the membrane surface wettability changes by contact angle measurements after TiO_2 coating, oily water filtration, and a cleaning process which consisted of rinsing the membrane surface with water and then irradiating it for 1,2 and 3 hours with UV light.

Experimental

The membrane was a polyacrylonitrile membrane (VSEP, New Logic Research Inc. USA) with 50kDa cut off weight, and membrane surface area 0.00342 m^2. Commercial TiO_2 (AEROXIDE P25, Evonik Industries) was used to coat the membrane surface. The membranes were coated with TiO_2 by filtering through the membrane 25mL, 0.4 g/L catalyst suspension in a dead end cell, at 1 MPa without stirring, that resulted in 0.3mg/cm^2 TiO_2 coating. The filtration was carried out with a Millipore batch filtration unit (XFUF04701, Solvent-resistant Stirred Ultrafiltration Cell, Millipore, USA). For the cleaning cycles with UV irradiation its cap was modified so that the UV light source can be fitted in it. This way a photocatalytic membrane reactor was set up. The UV light source was a low pressure mercury-vapor-lamp (GERMIPAK LightTech, Hungary, 40W, λ=254nm). The filtrations of the model wastewater were carried out at 0.3 MPa transmembrane pressure, without stirring at 20°C.

The model wastewater (oil in water emulsion) was prepared from crude oil (Algyő-area, Hungary) and distilled water. First a 1 wt.% emulsion was prepared by intensive stirring (35000 rpm), then 5 mL of this emulsion was inoculated into 495 mL of distilled water directly below to the transducer of an ultrasonic homogenizer (Hielscher UP200S) resulting the oil in water emulsion (coil=100 ppm). Time of homogenization was 10 minutes, maximal amplitude and cycle was applied while the emulsion was thermostated to 25°C. In case of every filtration 250 mL oily water portion was filtered to volume reduction ratio (VVR) 5. VRR [-], was defined as:

$$VRR = VF / (VF - VP) \quad (1)$$

where VF and VP is the volume of the feed and permeate [m^3] respectively at any time.

Hermia's model was applied to determine the fouling mechanism of each membrane during filtration [11,12]. Resistance-in-series model was applied to analyze resistances that lead to flux decline during the ultrafiltration process[11].

Membrane hydrophobicity was quantified by measuring the contact angle that was formed between the (neat, TiO_2 coated and oily contaminated) membrane surface and distilled water. 10μL water was carefully dropped on the top of the membrane surface. Contact angles were measured using the sessile drop method (Dataphysics Contact Angle System OCA15Pro, Germany). In every case the membrane was sliced up and the entire surface was characterized.

Results and discussion

In the first series of experiments the difference between the fouling propertiesof the neat and TiO_2 coated membranes were investigated. The flux decline in case of the TiO_2 coated membrane was significantly lower compared to the neat membrane(Fig. 1). In the initial stage of the filtration the intermediate pore blocking describes the best the measured data which is followed by the cake layer formation (Fig. 1.a). In case of the TiO_2 coated membrane all blocking models fit the measured data similarly (Fig. 1.b), for that theexplanation lies in the resistances. The calculated resistances give additional information aboutthe mechanism of the fouling. Filtration of oily water through the neat membrane results in a high reversible resistance and irreversible resistance, compared to the TiO_2 coated membrane (Fig. 2), meaning that first complete pore blocking occurs and that is followed by the oil cake layer forms on the membrane surface which can be removed by rinsing the membrane with water. The reversible and irreversible resistances in case of the TiO_2 coated membrane are lower than the membrane resistance, which makes them marginal and explains why the blocking models fit the measured data so closely because none of them occurs to a significant extent (Fig. 1.b and 2).

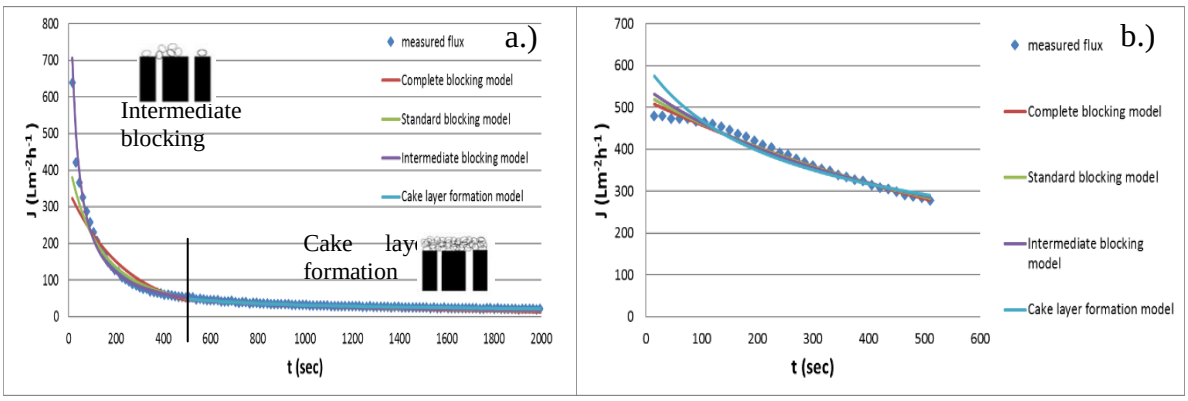

Figure 1. Flux decilne and fitted fouling modells during oily water filtration throught the neat (a) and TiO_2 coated (b) PAN membranes

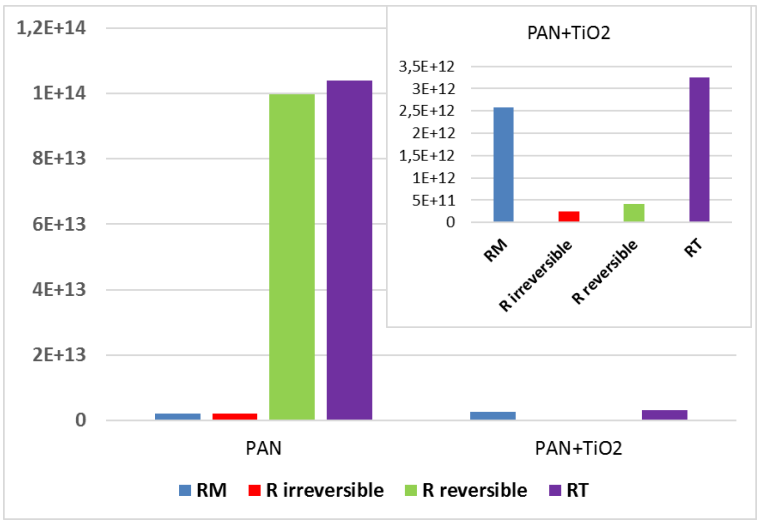

Figure 2. Resistances in case of oily water filtration throught the TiO_2 coated and neat PAN membranes

In the second series of experiments the wettability changes of the membrane during coating, oily water filtration, and UV cleaning were measured to determine if the cleaning process of the surface can be monitored with contact angel measurements. By coating the membrane with TiO_2 the surface wettability increases (Fig. 3), the catalyst forms a hydrophilic layer on the membrane surface.

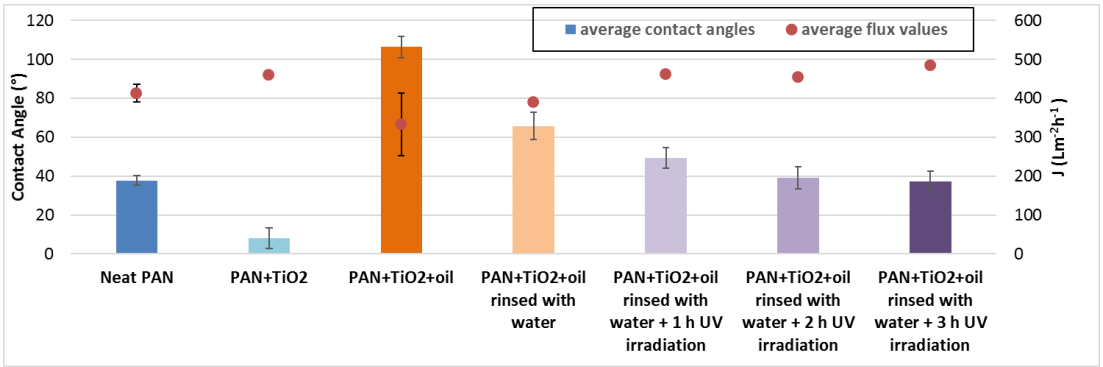

Figure 3. Average contact angles and average flux values of the neat, TiO_2 coated and than fouled and cleaned PAN membranes

The TiO_2 layer does not change the water flux significantly (Fig. 3). During the filtration of

the oily water a hydrophobic oil layer forms on the surface, which results in the decrease of the flux (Fig. 3). By rinsing the membrane surface with water the oil layer can be removed to an extent that results in a flux and hydrophilicity increase (Fig. 3). The wider error bar on the flux of TiO_2 coated membraneduring oily water filtration represents the extent of fouling during filtration.The UV irradiation of the membrane surface with time results in higher flux and hydrophilicity (Fig. 3). After 3 hours the water flux reached the neat membrane flux(Fig. 3). The average hydrofilicity of the membrane after 3 hour is nearly the same as the neat membrane hydrofilicity, but to recover the hydrofilicity of the TiO_2 coated membrane a longer irradiation time is needed. The hydrofilicity increase indicates the degree of the decomposition of the oil layer.

Conclusion

During oily water filtration on the neat polyacrilonitrile membraneinitially intermediate blocking occurs that is followedby cake layer formation, that results in a rapid flux decline. This means that the oil layer acts as an additional filtration layer. By coating the membrane surface with TiO_2, the membrane becomes more resistant to fouling, and does not come to oil cake layer formation. The flux decline during oily water filtration is moderate compared to the neat membrane. The reversible and irreversible resistances are negligible compared to the membrane resistance. The oil that is on the TiO_2 coated membrane surface after filtration significantly increases the membrane surface hydrophobicity that can be reduced by rinsing the membrane surface with water, which results in significant flux recovery. By UV irradiation the surface hydrophilicity can be further increased and total flux recovery can be achieved within 3hours.

Acknowledgements

This project was supported by the János Bolyai Research Scholarship of the Hungarian Academy of Sciences. The authors are also grateful for the financial support provided by the project Hungarian Science and Research Foundation (NKFI contract number K112096).

References

[1] X.S. Yi, S.L. Yu, W.X. Shi, N. Sun, L.M. Jin, S. Wang, B. Zhang, C. Ma, L.P. Sun, Desal., 281 (2011) 179–184.
[2] B. Hu, K. Scott, Chem. Eng. J., 136 (2008) 210-220.
[3] S. Leong, A. Razmjou, K. Wang, K. Hapgood, X. Zhang, H., J. Mem. Sci., 472 (2014)167-184.
[4] M. Padaki, R. S. Murali, M.S. Abdullah, N. Misdan, A. Moslehyani, M.A. Kassim, N. Hilal, A.f. Ismail, Desal., 357 (2015) 197-207.
[5] Y. He, Z. W. Jiang, Filrt. Sep., 45(5) (2008) 14-16.
[6] H. Bai, Z. Liu, D. D. Sun, Chem. Commun. 46 (2010) 6542–6544.
[7] R. Molinari, L. Palmisano, E. Drioli, M. Schiavello, J. Membrane Sci. 206 (2002) 399–415.
[8] E. Bet-moushoul, Y. Mansourpanah, Kh. Farhadi, M. Tabatabaei, Chem. Eng. J. 283 (2016) 29–46.
[9] Y. Mansourpanah, S.S. Madaeni, A. Rahimpour, A. Farhadian, A.H. Taheri, J. Membrane Sci. 330 (1–2) (2009) 297–306.
[10] K.C. Khulbe, C. Feng, T. Matsuura, G.C. Kapantaidakis, M. Wessling, G.H. Koops, J. Membrane Sci.226 (2003) 63–73.
[11]M. C. V. Vela, S. A. Blanco, J. L. García, E. B. Rodríguez, Sep. Purif. Technol. 62 (2008) 489–498.
[12] J. Hermia, Trans. Inst. Chem. Eng. 60 (1982) 183–187.

PHOTOCATALYTIC OZONATION OF MONURON OVER SUSPENDED AND IMMOBILIZED TiO_2

Gergő Simon[a], Tamás Gyulavári[b], Klára Hernadi[b], Zsolt Pap[c,d,e], Gábor Veréb[f], Krisztina Schrantz[a], Tünde Alapi[a]

[a]*Department of Inorganic and Analytical Chemistry, Institute of Chemistry, University of Szeged, Dóm tér 7, H-6720 Szeged, Hungary*
[b]*Department of Applied and Environmental Chemistry, Institute of Chemistry, University of Szeged, Rerrich Béla tér 1, H-6720 Szeged, Hungary*
[c]*Faculty of Physics, Babeş–Bolyai University M. Kogălniceanu 1, RO–400084 Cluj–Napoca, Romania*
[d]*Institute for Interdisciplinary Research on Bio-Nano-Sciences, Treboniu Laurian 42, RO–400271 Cluj-Napoca, Romania*
[e]*Institute of Environmental Science and Technology, Tisza Lajos krt. 103, Szeged HU-6720, Hungary*
[f]*Department of Process Engineering, Faculty of Engineering, University of Szeged Moszkvai krt. 9., H-6725 Szeged, Hungary*
e-mail: gsimon@chem.u-szeged.hu

Abstract

Heterogeneous photocatalysis, using photocatalyst in suspensions and in immobilized form, ozonation, and their combination (photocatalytic ozonation) at various ozone (O_3) concentrations (0–20 mg dm^{-3} O_3 in gas phase) were investigated and compared in the transformation of the herbicide monuron (3-(p-chlorophenyl)-1,1-dimethylurea). Using the photocatalyst (Aeroxide® P25) in immobilized form, the rate of transformation of monuron was considerably lower compared to the case of suspension (1.0 g dm^{-3} TiO_2). O_3 increased the rate of transformation in each case, while the photocatalyst decreased the concentration of dissolved O_3. However, there was no synergistic effect during the combination of heterogeneous photocatalysis and ozonation. The economic feasibility of the treatments was also compared based on the obtained values of Electrical Energy per Order (E_{EO}). The E_{EO} value decreased with the increase of O_3 concentration in each case, and there was no significant difference between the energy requirement of ozonation and its combination with heterogeneous photocatalysis using TiO_2 in suspension at each O_3 concentration.

Introduction

Pesticides are indispensable for agricultural use however, their application can be detrimental due to their usually low biodegradability, resulting in their presence in the soil and waters, including drinking waters. Among them, the group of phenylurea pesticides have received attention due to their biotoxicity [1], while diuron and isoproturon are also listed priority hazardous substances [2]. Their removal from waters is an important task, that often cannot be achieved by regular water treatment methods, and therefore the application of advanced oxidation processes (AOPs), such as ozonation [3,4], or heterogeneous photocatalysis is required [4,5]. It is widely accepted that titanium dioxide (TiO_2) is the most adequate photocatalyst. After purification it is important to get rid of TiO_2 particles, which makes its industrial application a challenge. Therefore numerous attempts have been made to immobilize photocatalysts. While ozonation and heterogeneous photocatalysis are effective processes on their own, their combination – photocatalytic ozonation –under optimum conditions can have a synergistic effect both in oxidation and mineralization efficiency [6,7], and could be more cost effective.

The goal of this study is to investigate the degradation of the phenylurea herbicide monuron by ozonation, heterogeneous photocatalysis– in suspensions and using self-made immobilized catalyst sheets– and their combination(photocatalytic ozonation) at various

O_3concentrations.The economic feasibility of treatments was compared based on the obtained values of Electrical Energy per Order (E_{EO}).

Experimental

Aeroxide P25® (75±5 % anatase and 25±5 % rutile, a^S_{BET}=35–65 m^2 g^{-1}, $d_{anatase}$~25 nm, d_{rutile}~40 nm, Evonik Industries) was used in suspensionor immobilized onto a high-purity alumina ceramic paper (1.6 mm thickness, COTRONICS Co., cat. no.: 300-040-1).Ceramic paper sheets (34.0×14.0 cm, 476.0 cm^2) were immersed in isopropyl alcohol, impregnated with $Ti(OEt)_4$ and then sprayed with ethanol based TiO_2 suspension (c_{P25}=76.9 g dm^{-3}), as described by Veréb, et al. [8].The surface loads of the immobilized TiO_2 correspond to the 1.0 g dm^{-3} suspension concentrations, when TiO_2 was used in aqueous suspension form in photocatalytic measurements.The model contaminant was monuron (> 99%, Sigma-Aldrich), dissolved in ultrapure Milli-Q water. Pure oxygen (99.5%, Messer) was used to saturate the aqueous solutions and to produce O_3.

Scanning Electron Microscopy (SEM) measurements were made using a Hitachi S-4700 Type II FE-SEM instrument.The X-ray diffractograms (XRD) were taken by a RigakuMiniflex II diffractometer using Cu-Kα radiation (λ = 1.5406 Å), equipped with a graphite monochromator. AJASCO-V650 spectrophotometer with an integration sphere (ILV-724) was used for measuring theDiffuse Reflectance Spectroscopy (DRS) spectra of the samples (λ = 300-800 nm).

Agilent 8435 UV-Vis spectrophotometerwas used to measure the concentration of gaseous O_3at 254 nm wavelength ($\varepsilon_{254\ nm}$=2950 mol^{-1} dm^3 cm^{-1}[9]).The concentration of dissolved O_3 was determined spectrophotometrically by the indigo method [10,11]. The concentration of monuron was determined by high performance liquid chromatography (HPLC)equipped with a DAAD detector, using an Agilent 1100 modular HPLC system with a LiChroCART® C-18 column (250 mm×4 mm, 5 µm particle size) andmethanol/water (60:40 V/V %) mixture (1.0 cm^3 min^{-1} flow rate) as eluent. The quantification wavelength was 244 nm.

The experiments were carried out in a recirculation reactor system described by Kovács, et al. [4]. The light source was a fluorescent UV lamp (λ_{max}=365 nm, 15 W, GCL303T5/365 nm, LightTech) with a photon flux of 1.20(±0.06)×$10^{-5}$$mol_{photon}$ s^{-1} [4]. Ozoniser (Ozomatic Modular 4HC, max. 95 W) was used to produce 5, 10, 15, 20 mg dm^{-3}gaseous O_3.

The effectiveness of treatments were evaluated based on the E_{EO}values reflecting the electric energy in kilowatt hours [kWh] required todegrade the volume [e.g.: 1 m^3]of contaminated water[12].E_{EO} values [$kWhm^{-3}order^{-1}$] is calculated using the following formula in a batch system:

$$E_{EO} = \frac{P \times t \times 1000}{V \times \lg(c_i/c_f)} \quad (1)$$

where P is the rated power [kW] of the AOT the system, V is the volume [dm^3] of water treated in the time$t$ [h], c_i, $c_f$arethe initial and final concentrations [mol dm^{-3}],and lg is the symbol for the decadic logarithm.

Results and discussion

SEM micrographs provide, that increasing the amount of the immobilized photocatalyst, larger aggregates of nanoparticles formed. XRD measurements were performed in order to determine the exact P25 loading of the ceramic sheet. The real loading and equivalent suspension concentrations of the samples are listed in Table 1.To verify the optical properties of the ceramic papers, DRS spectra were recorded. In case of the $Ti(OEt)_4$ impregnated sheet the band-gap value calculatedwas 3.9 eV (320 nm), which is close to the value registered for amorphous titanium oxide hydroxide. After the addition of P25, the registered dR/dλ curves and the evaluated band-gap values corresponded to P25.

Table 1 Nominal and measured loads and equivalent suspension concentrations for the prepared ceramic sheets with immobilized photocatalyst

Sample name	Nominal loading ($\times10^{-3}$ mg cm^{-2})	Nominal eq. susp. c. (g dm^{-3})	Measured loading ($\times10^{-3}$ mg cm^{-2})	Measured eq. susp. c. (g dm^{-3})
P25-1	1.55	1.0	1.51	0.97

Table 2 The initial transformation rates of monuron and the corresponding dissolved O_3 concentrations (determined in Milli-Q water without monuron)

		Initial rates of transformation (r_0($\times10^{-8}$moldm^{-3} s^{-1})) and dissolved O_3 concentration (c_{O_3}(mg dm^{-3}))				
c_{O_3} in gas phase (mg dm^{-3})		0	5	10	15	20
O_3	r_0	–	6.9±0.4	14.8±0.5	24.4±1.6	41.7±4.5
	c_{O_3}	–	*2.0±0.1*	*3.8±0.1*	*5.1±0.1*	*10.3±0.0*
susp. TiO_2/O_3	r_0	24.4±2.2	31.7±2.6	42.5±4.2	49.6±4.7	68.1±6.8
	c_{O_3}	–	*1.3±0.0*	*2.0±0.1*	*4.1±0.1*	*7.8±0.3*
im. TiO_2/O_3	r_0	8.1±1.0	16.1±1.5	24.8 ± 4.1	34.6±1.5	49.8±4.1
	c_{O_3}	–	*1.2±0.0*	*2.21±0.1*	*4.1±0.3*	*8.9±0.2*

O_3: ozonation; ***susp. TiO_2/O_3*:** combination of ozonation and heterogeneous photocatalysis when P25 was applied in suspension; ***im. TiO_2/O_3***: combination of ozonation and heterogeneous photocatalysis when P25 was immobilized on ceramic paper

The increasing amount of O_3 enhanced the degradation rate of monuron(c_0=5.0×10^{-4}moldm^{-3}). The suspended catalysts proved to be more effective compared to the immobilized form in all processes. Addition of 20 mg dm^{-3}O_3 increased the rate of transformation by up to ~6 times compared to photocatalysis using immobilized P25 without O_3 addition, whereas in the case of suspended P25 the increase is only ~3 times. Comparing the data determined at 20 mg dm^{-3}O_3 concentrations, the effect of the photocatalyst on the monuron transformation rate and on dissolved O_3 concentration is found to be more significant in suspension than in immobilized form. TiO_2decreased the concentration of dissolved O_3 in both cases, indicating that the improved reaction rates are probably due to the reactive radicals produced by the photocatalytic degradation of O_3. Moreover the O_3 can also enhance the efficiency of heterogeneous photocatalysis as a very effective electron scavenger inhibiting efficiently the recombination of pohotogenerated charges. However, there was no significant synergism in the case of photocatalytic ozonation under the experimental conditions applied in this work.

To compare the economic efficiency of the applied AOPs the values of E_{EO} were calculated. The total E_{EO} values decreased with the increase of O_3 concentration in each case. At lower O_3 concentrations (0, 5, 10 mg dm^{-3}), the application of immobilized TiO_2results in significantly higher values than ozonation or its combination with heterogeneous photocatalysis using TiO_2 suspensions (Fig. 4c). It has to be noted however,that the energy requirement of filtration was not taken into account, which would make the use of immobilized catalysts more preferable. At higher O_3 concentrations (15 and 20 mg dm^{-3}), there was no significant difference between the energy requirements. There is no significant difference between the energy requirement of ozonation and its combination with heterogeneous photocatalysis using TiO_2 in suspensions at each O_3 concentration, however the rate of transformation of monuron is enhanced in the case of the combined method.

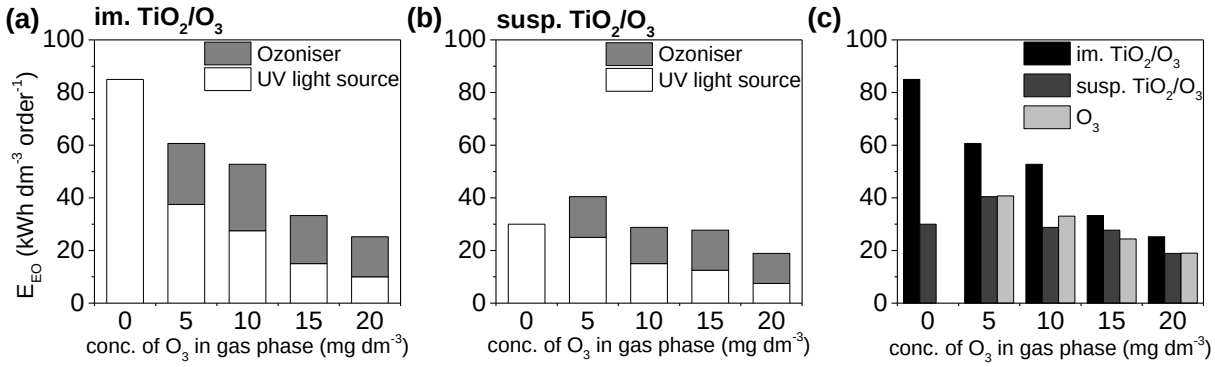

Figure 4 The E_{EO} values determined in the case of using immobilized TiO_2 (a), suspended TiO_2 (b) (white: the part of E_{EO} required by the UV light source; grey: the part of E_{EO} required by the ozoniser) and the total E_{EO} values determined in the case of investigated processes (c)

Conclusion

In this study photocatalytic ozonation of monuron over suspended and immobilizedTiO2was investigated. O_3 increased the rate of transformation in each cases, however there was noynergistic effect during the combination of heterogeneous photocatalysis and ozonation. The photocatalyst decreased the concentration of dissolved O_3. TheE_{EO}value decreased with the increase of O_3 concentration in each case. At higher O_3 concentrations (15 and 20 mg dm^{-3}) there was no significant difference observed between E_{EO} values of the methods.

Acknowledgements

G. Veréb acknowledges the support of the JánosBolyai Research Scholarship of the Hungarian Academy of Sciences.K. Schrantz acknowledges the supportof the European Union and the State of Hungary, co-financed by the European Social Fund in the framework of TÁMOP 4.2.4. A/1-11-1-2012-0001 'National Excellence Program'.T. Alapi acknowledges the support of the European Union and the State of Hungary, co-financed by the European Social Fund in the framework of TÁMOP-4.2.4.A/2-11/1-2012-0001 'National Excellence Program'.The financial support of the Swiss Contribution (SH7/2/20) is acknowledged and greatly appreciated.

References

[1] H. Mestankova, B. Escher, K. Schirmer, U. von Gunten, S. Canonica, Aquat. Toxicol., 101 (2011) 466-473.
[2] F.J. Benitez, C. Garcia, J.L. Acero, F.J. Real, World Acad. Sci. Eng. Technol., 3 (2009) 648-656.
[3] A.L. Tahmasseb, S. Nélieu, L. Kerhoas, J. Einhorn, Sci. Total Environ., 291 (2002) 33-44.
[4] K. Kovács, J. Farkas, G. Veréb, E. Arany, G. Simon, K. Schrantz, A. Dombi, K. Hernádi, T. Alapi, J. Environ. Sci. Health, B., (2016) 1-10.
[5] R.R. Solís, F.J. Rivas, A. Martínez-Piernas, A. Agüera, Chem. Eng. J., 292 (2016) 72-81.
[6] M.J. Farré, M.I. Franch, S. Malato, J.A. Ayllon, J. Peral, X. Domenech, Chemosphere, 58 (2005) 1127-1133.
[7] F.J. Beltrán, F.J. Rivas, O. Gimeno, J. Chem. Technol. Biotechnol., 80 (2005) 973-984.
[8] G. Veréb, Z. Ambrus, Z. Pap, K. Mogyorósi, A. Dombi, K. Hernádi, React. Kinet., Mech. Catal., 113 (2014) 293-303.
[9] E.J. Hart, K. Sehested, J. Holoman, Anal. Chem., 55 (1983) 46-49.
[10] H. Bader, J. Hoigné, Water Res., 15 (1981) 449-456.
[11] C.F. Chiou, B.J. Mariñas, J.Q. Adams, Ozone Sci. Eng., 17 (1995) 329-344.
[12] J.R. Bolton, K.G. Bircher, W. Tumas, C.A. Tolman, Pure Appl. Chem., 73 (2001).

PURIFICATION OF INDUSTRIAL WASTEWATER WITH THE COMBINATION OF OZONATION AND MEMBRANE SEPARATION

Zakar Mihály[1], Veréb Gábor[1], Hodúr Cecília[1], Keszthelyi-Szabó Gábor[1], Lakatos Erika[2], László Zsuzsanna [1]

[1] *Department of Process Engineering, Faculty of Engineering, University of Szeged, H-6724 Szeged, Moszkvai krt. 9.*

[2] *Institute of Food Sciences, Széchenyi István University, H-9200 Mosonmagyaróvár, Lucsony Srt. 15-17.*

e-mail:zsizsu@mk.u-szeged.hu

Abstract

The development of effective and economic purification methods for the treatment of hydrocarbons contaminated waters is an intensively investigated research area. Especially complicated the purification of stable oil in water emulsions ($d_{oil\ droplets}$<2 μm). Advanced oxidation processes, membrane separation and their combination are also promising methods. In the present study pre-ozonation combined with membrane microfiltration(PES, d_{pore}=0,2 μm) was applied for the purification of stable oil in water emulsions (c_{oil}=100 ppm; $d_{oildroplets}$<2 μm). The effects of applied pressure, stirring speed, time of ozonation and water matrix were also investigated. Fluxes were measured during the experiments, the removal efficiency was determined turbidity and TOC measurements.

Keywords: *oil contaminated water, ozonation, membrane separation*

Összefoglalás

Napjaink egyik igen fontos kutatási területe a szénhidrogénekkel szennyezett vizek hatékony és gazdaságos kezelésére alkalmas víztisztító módszerek fejlesztése. Különösen nehézkes a kis cseppméretű, stabil olaj/víz emulziók kezelése. Ígéretes módszerek többek között a nagyhatékonyságú oxidációs eljárások, a membrán szeparáció és ezen módszerek kombinációi is. Jelen tanulmányban ózonos előkezelést követő mikroszűrést (PES, d=0,2μmalkalmaztunk stabilolaj/vízemulzió(c_{olaj}=100 ppm; d<2μm) tisztítására. Vizsgáltuk a szűréssoránalkalmazottnyomáséskevertetésisebesség, az ózonos előkezelési idő valamint a vízmátrix hatását. Mértük azelérhetőfluxusokat valamint jellemeztük azeltávolításihatékonyságokatzavarosság és TOC mérésekkel.

Kulcsszavak: *olajszennyezettvizek, ózonkezelés, membránszűrés*

Bevezetés

Napjainkbansajnos még mindig igen komoly kihívását jelentenek az olajszármazékokat tartalmazó ipari szennyvizek hatékony és gazdaságos kezelése [1]. Különösen nagy kihívást jelentenek a vízzel stabil emulziót képző olajszennyezések eltávolítása [2]. A szerves vízszennyezők eltávolítására számos területen folynak kutatások, ezek egyik ígéretes területe a membránszűrés alkalmazása [3]. A membrán eltömődése (amely jelentősen megnöveli a szűrés energiaigényét, költségeit, illetve csökkenti a membrán élettartamát) azonban jelentős limitáló tényező, így a kutatások napjainkban főként a membráneltömődés mértékének csökkentésére fókuszálnak. A membránszeparáció és a nagyhatékonyságú oxidációs eljárások kombinálása új lehetőségeket nyit meg, mivel a szennyező anyagok részleges oxidációja révén egyes esetekben kedvezően befolyásolható a szennyező anyagok felületi töltése, hidrofil/hidrofób jellege illetve a membrán felületén kialakuló koncentráció-polarizációs határréteg vastagsága és/vagy szerkezeti kompaktsága [4-6]. Jelen munkában ózonos előkezelést alkalmaztam olaj/víz emulziók mikroszűrése során.

Alkalmazott anyagok és módszerek

A kezelendő modellszennyvíz 100 ppm olajtartalommal (ásványi kőolaj, Algyő) rendelkező olaj/víz emulzió ($d_{olajcsepp} < 2\mu m$) volt, melynek előállításához desztillált vizet, illetve egyes esetekben modell termálvizet használtunk. A modell termálvíz előállításához $NaHCO_3$-ot(2,259 g/L), NH_4Cl-ot (53,449 mg/L), $CaCl_2$-ot(19,11 mg/L), KCl-ot (20,88 mg/L), NaCl-ot (93,5 mg/L), $FeCl_3$-ot (4,49 mg/L) valamint $MgSO_4$ -ot (35,31 mg/L) használtunk fel.

Az ózon előállítását egy *BMT 802X* típusú német gyártmányú ózongenerátorral végeztük tiszta oxigénből (*Messer*; 3.5 tisztaság).A szűréshez 7,6 cm átmérőjű membránnal szerelhető szakaszos szűrést biztosító kevertetett cellás *Millipore* membránszűrőt használtunk, melybe 0,2 µm pórusátmérőjű *VSEP* gyártmányú poliéterszulfon (PES) anyagú membránt helyeztünk.

A permeátumok teljes szerves széntartalmát (TOC) egy *Analytik Jena N/C 3100* típusú készülékkel határoztuk meg, míg a minták zavarosságát egy *Hach 2100N*típusú zavarosságmérővel mértük.

Eredmények és értékelésük

Jelen munka első lépéseként különböző nyomásértékek (1, 2, 3 bar) és kevertetési sebességek (50, 200, 350 rpm) alkalmazása mellett szűrtük az emulziót és megállapítottuk, hogy 1 bar transzmembrán nyomás és 350 rpm kevertetési sebesség alkalmazásakor kaptuk a legnagyobb relatív fluxusértékeket. Megállapítható, hogy olajemulziók PES membránnal történő mikroszűrése során kiemelt fontossága van az intenzív kevertetésnek (az olajcseppek megtapadásának megakadályozása érdekében), és nem célszerű a nagy nyomás alkalmazása, mivel a nyomás emelésével nem csak az ellenállás mértéke nőtt meg, de a fluxusok abszolút értéke is csökkent.

Az ózonos előkezelés idejének a relatív fluxusokra gyakorolt hatását vizsgálva megállapítható, hogy mind desztillált vízben, mind modelltermálvízben előállított olajemulziók esetén egy rövid idejű (5 perces) ózonkezelés (35±5 mg/L elnyelt ózon) megnöveli a szűrés során mérhető fluxust ugyanakkor az előkezelés idejének növelésével nem érhető el további kedvező hatás a fluxusértékek vonatkozásában (**1. ábra**).

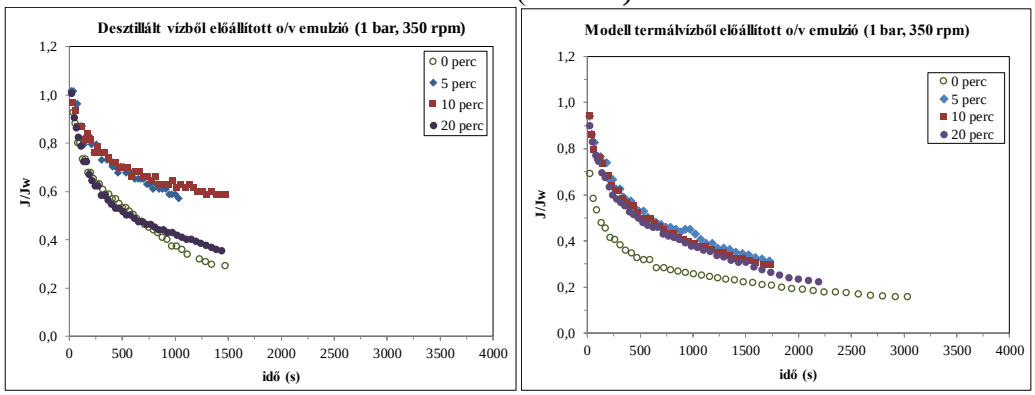

1. ábra Az ózonos előkezelés hatása a relatív fluxusra az emulziók mikroszűrése során

A desztillált víz felhasználásával előállított stabil olajemulzió szűrése során mért igen csekély irreverzibilis ellenállás tovább csökkent az 5 perces ózonos előkezelés hatására, de még jelentősebb volt a reverzibilis ellenállás csökkenése (**2. ábra**). Modelltermálvíz esetén az ózonnal nem előkezelt emulzió szűrése során (szemben a desztillált víz felhasználásával készített olajemulzióval) igen jelentős irreverzibilis ellenállást mértünk mely nagymértékben csökkenthető volt a rövid idejű ózonos előkezeléssel a membránfelületre erősen feltapadó olajréteg csökkentése által (**2. ábra**). Ugyanakkor az ellenállás értékek alapján megállapítható az is, hogy az ózonos előkezelés idejének növelése már növeli a teljes ellenállás mértékét (**2. ábra**).

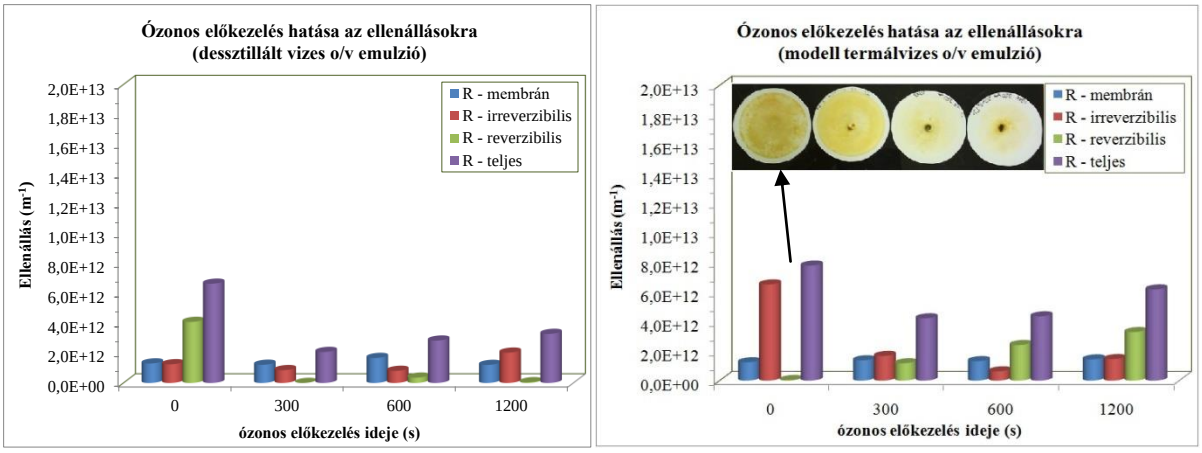

2. ábra Az ózonos előkezelés hatása az ellenállásokra

Megállapítható, hogy az ózonos előkezelés a zavarosságértékek vonatkozásábannem befolyásolja számottevően a mikroszűréssel kivitelezhető kiváló tisztítási hatékonyságot (>98%) az olajcseppekvisszatartásának köszönhetően, ugyanakkor a TOC értékek vonatkozásában az ózonos előkezelés idejének növelésével számottevően csökken a tisztítási hatékonyság, ami az oxidáció hatására képződő vízoldható komponenseknek tulajdonítható, melyek átjuthatnak a mikroszűrő membránon (**3. ábra**). Megjegyzendő azonban, hogy a relatív fluxusértékek illetve az ellenállások vonatkozásában egyaránt kedvező, rövid idejű (5 perces) előkezelés esetén a tisztítási hatékonyságban bekövetkezett csökkenés még igen csekély mértékű.

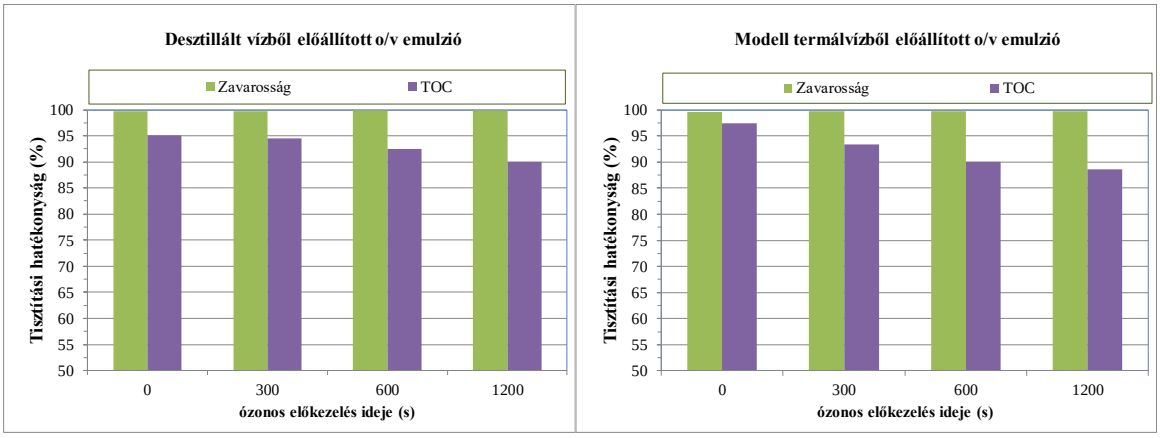

3. ábra Az ózonos előkezelés hatása a tisztítási hatékonyságra

Konklúziók

Összességében megállapítható hogy megfelelő nyomásviszonyok és megfelelő intenzitású kevertetés esetén rövid idejű ózonos előkezeléssel elérhető a membránok eltömődésének csökkentése úgy, hogy az előkezelés okozta tisztítási hatékonyságban bekövetkezett csökkenés ne legyen számottevő. Fontos továbbá, hogy a víz iontartalmának jelentős megnövelésével megnő az emulzió okozta irreverzibilis ellenállás, ami azonban szintén jelentősen lecsökkenthető egy rövid ózonos előkezeléssel (35±5 mg/L elnyelt ózon).

Köszönetnyilvánítás
A munka a Bolyai János Kutatási Ösztöndíj és a Nemzeti Kutatási, Fejlesztési és Innovációs Hivatal (NKFI témaszám: K112096)támogatásával készült is.

Referencia

[1] Freeman, H.M. Industrial Pollution Prevention Handbook, McGraw-HillInc.: USA(1995)
[2] Chakrabarty B., Ghoshal A.K., Purkait M.K.Ultrafiltration of stable oil-in-water emulsion by polysulfone membrane, Journal of Membrane Science (325)(2008) 427-437.
[3] Chang I.-S., Chung C.-M., Han S.-H. Treatment of oily wastewater by ultrafiltration and ozone, Desalination (133)(2001) 225-232.
[4] Kiss Zs.L., Kocsis L., Keszthelyi-Szabó G., Hodúr C., László Zs. Treatment of oily wastewater by combining ozonation and microfiltration, Desalination and Water Treatment (55/13)(2014) 3662-3669.
[5] Nguyen S.T., Roddick F.A. Pre-treatments for removing colour from secondary effluent: Effectiveness and influence on membrane fouling in subsequent microfiltration, Separation and PurificationTechnology (103)(2013) 313–320.
[6] Van Geluwe, S., Braeken, L., Van der Bruggen, B. Ozone Oxidation for the alleviation of membrane fouling by natural organic matter: a review, Water Research (45)(2011) 3551-3570.

TREATMENT OF OIL CONTAMINATED WATERS BY (PHOTO-)FENTON REACTION AND THEIR EFFECTS ON MEMBRANE FILTRATION

Veréb Gábor, Bozóki Renáta, Kovács Ildikó, Kertész Szabolcs, Hodúr Cecília, László Zsuzsanna

Department of Process Engineering, Faculty of Engineering, University of Szeged, H-6724 Szeged, Moszkvaikrt. 9.
*e-mail:*verebg@*mk.u-szeged.hu*

Abstract
In the present study crude oil contaminated (100 ppm oil content; $d_{oil\ drops}$< 1.5μm) water was purified by Fenton reaction, UV/H_2O_2 combined treatment and by photo-Fenton reaction. Among the investigated advanced oxidation processes, photo-Fenton treatment showed emergent purification efficiency, which resulted 53% decline of chemical oxygen demand after 120 min of treatment. It can also be concluded that after the treatment with photo-Fenton reaction, adjusting the pH to 7, iron-hydroxide was precipitated, which adhered the residual oily contaminants, which increased the flux during the microfiltration of the pre-treated water.

Keywords: *oil contaminated water, Fenton, photo-Fenton, UV/H_2O_2, membrane filtration*

Összefoglalás
Jelen munkában kőolajjal szennyezett vizet (100 ppm olajtartalom;$d_{olajcsepp}$<1,5 μm) tisztítottunk Fenton reakcióval, UV/H_2O_2 kombinált kezeléssel és foto-Fenton reakcióval.A vizsgált nagyhatékonyságú oxidációs eljárások közül kiemelkedő hatékonyságú volt a foto-Fenton kezelés, mellyel 120 perc kezelési idő alatt 53%-kal sikerült csökkenteni a víz kémiai oxigénigényét. Megállapítható továbbá, hogy a foto-Fenton kezelés után a pH megemelésével (pH~7) kicsapódó vas-hidroxid megkötötte a maradék olajszennyezést, és ezáltal jelentősen megnőttaz előkezelt víz mikroszűrése során elérhető fluxus.

Kulcsszavak: *olajszennyezettvizek, Fenton, foto-Fenton, UV/H_2O_2, membránszűrés*

Bevezetés
Az ipari szennyvíztisztításon belül kiemelt fontosságú a(megfelelő tisztítás nélkül komoly környezeti károkat okozó) olajjal szennyezett vizek tisztítása. A legnagyobb kihívást a nanométeres tartományba eső olajcseppek eltávolítása jelenti.
Lehetséges kezelési módszerek a nagyhatékonyságú oxidációs eljárások. Alver és munkatársainak [1] 2015-ös publikációja alapján (melyben olíva olaj előállítása során keletkező szennyvizet tisztítottak) az olajszennyezett vizek kezelésére alkalmas lehet az egyszerűen kivitelezhető Fenton-reakció. Tony és munkatársai olajfinomítóból származó szennyvizet 75% fölötti tisztítási hatékonysággalkezeltek foto-Fenton eljárással [2].Egy másik tanulmányban foto-Fenton eljárás és flotáció kombinálásával 99%-os tisztítási hatékonyságot értek el [3].
A membránszeparáció szintén hatékony módszere az olajjal szennyezett vizek tisztításának [4], azonban a szűrés során az olajcseppek okozta membráneltömődés és az ebből adódó fluxuscsökkenés jelentős limitáló tényező. A nagyhatékonyságú oxidációs eljárások és a membránszeparáció kombinálásával további előnyök is elérhetőek lehetnek, mint például a fluxuscsökkenés mértékének visszaszorítása, a membrán amortizációjának lassítása és/vagy hatékonyabb tisztítás [5]. Jelen tanulmányban Fenton, UV/H_2O_2 és foto-Fenton kezeléseket alkalmaztunk kis cseppméretű ($d_{olajcsepp}$<1,5 μm) olaj/víz emulziók tisztítására és vizsgáltuk a kezelések mikroszűrésre gyakorolt hatását is.

Alkalmazott anyagok és módszerek

Kísérleteinkhez 100 ppm olajtartalommal (ásványi kőolaj, Algyő) rendelkező olaj/víz emulziót ($d_{olajcsepp}$< 1,5 µm)használtunk, melynek pH értékét (H_2SO_4 oldattal) 4-re állítottuk, majd 98 ppm$Fe(SO_4)$•$7H_2O$-ot (*Spectrum 3D*; c=0,353 M Fe^{2+}) és 300 ppm H_2O_2-ot (*Sigma-Aldrich)*adtunkhozzá (nFe^{2+}: nH_2O_2= 1:25). Az emulzióból megfelelő időközönként vett minták pH értékét(1 m/m%-os NaOH oldattal) 7-re állítottuk és a maradék hidrogén-peroxidotkataláz enzim(*Sigma-Aldrich*) hozzáadásávalbontottuk el. A foto-Fenton eljárás során254 nm-en sugárzó UV fénycsővel (*Lighttech*; 10W) világítottuk meg az emulziót.

A szűréshez 7,6 cm átmérőjű membránnal szerelhető szakaszos szűrést biztosító kevertetett cellás *Millipore* membránszűrőt használtunk, melybe0,2 µm pórusátmérőjű *VSEP* gyártmányú poliéterszulfon (PES) anyagú membránt helyeztünk és a szűrések során ötszörös sűrítési arányt (VRR=5) alkalmaztunk.

A permeátumok kémiai oxigénigényének jellemzéséhez kálium-dikromáttal történő oxidáción alapuló tesztcsöveket (Hanna Instruments), egy *Lovibond ET 108* roncsoló egységet (2 óra roncsolás 150°C-on), valamint egy *Lovibond COD Vario*spektrofotométert használtunk.

Eredmények és értékelésük

A 100 ppm-es olaj emulziót Fenton reakcióval kezelve a kezdeti 255 mg/L-es kémiai oxigénigény, 6 óra kezelési idő után222 mg/L értékre csökkent, ami mindösszesen 13%-os tisztítási hatékonyságot jelent (**1/a ábra**). A még H_2O_2-ot is tartalmazó és a kataláz enzimmel kezelt (H_2O_2-ot már nem tartalmazó) minták KOI értékeinek különbsége alapján egyértelmű az is, hogy a hidrogén-peroxidnak is csak csekély része bomlott el(**1/a ábra**).

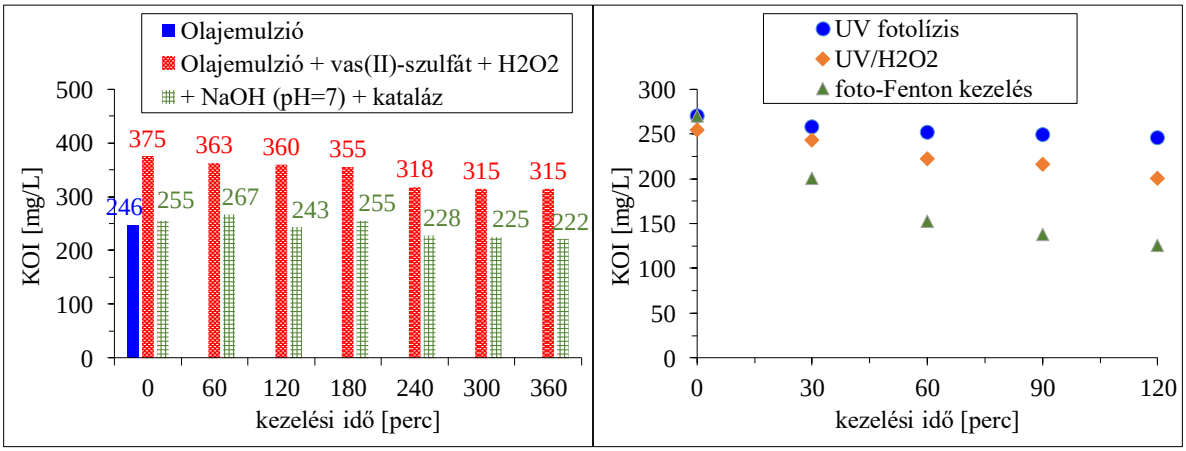

1/a ábra: Kezelés Fenton-reakcióval; **1/b ábra:** Kezelés UV fotolízissel, UV/H_2O_2 kezeléssel és foto-Fenton reakcióval

A tisztítás intenzifikálására UV/H_2O_2 illetve foto-Fenton eljárás alkalmazásával folytattuk kísérleteinket (**2/b ábra**).A 120 perces kísérletek során az alkalmazott 254 nm-en sugárzó UV fényforrás önmagában (fotolízis) is eredményezett egy csekély mértékű (9%-os) kémiai oxigénigény csökkenést. Ugyanakkor a 300 ppm hidrogén-peroxidot is tartalmazó emulzió UV besugárzásával végzett kísérlet (UV/H_2O_2) során a 120 perces kezelés hatékonysága 21%-ra emelkedett,míg a vas(II)-szulfátot is tartalmazó emulzió ugyancsak 120 perces foto-Fenton kezelése soránmár 53%-os tisztítási hatékonyságot mértünk.Megjegyzendő továbbá, hogy a kísérletek elvégzése során a minták pH=7-re történő állításakor apró vöröses-barna színű csapadék (vas-hidroxid) képződött, amihez az olajcseppek is hozzákötődtek.

Vizsgáltuk a 100 ppm kőolajat tartalmazó modell szennyvízmikroszűréssel kivitelezett tisztíthatóságát is előkezeletlen és 120 percig foto-Fentonreakcióval előkezelt emulziók esetén

egyaránt. A kísérletek során mért fluxusgörbéket ábrázoltuk a **2/a ábrán**. A foto-Fenton reakcióval előkezelt olaj emulzió esetén jelentősen nagyobb a szűrés során mérhető fluxus. A szűréséhez szükséges idő az előkezelés hatására 58 percről 15 percre csökkent a VRR=5 sűrítési arány eléréséig.

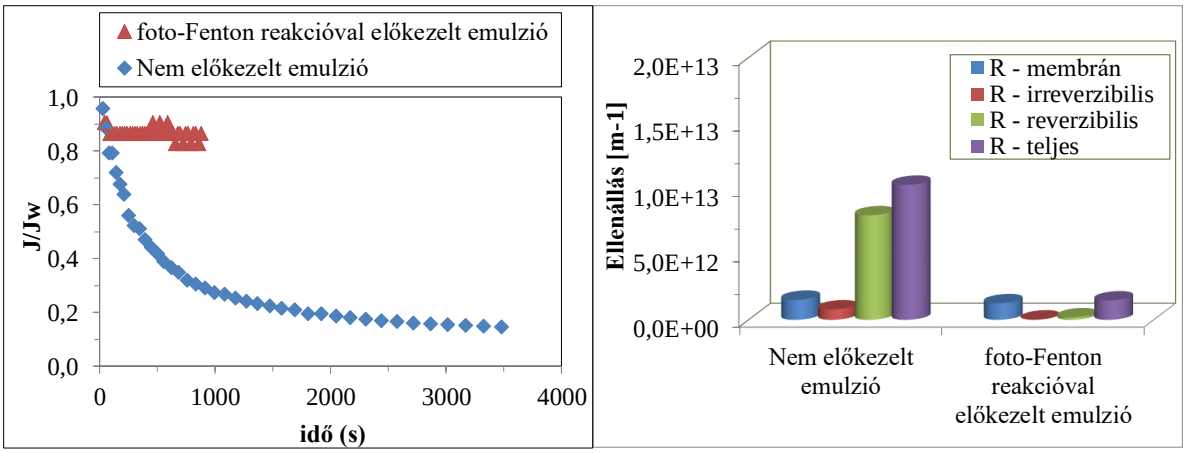

2/a ábra: Előkezeletlen és foto-Fenton reakcióval előkezelt modell szennyvíz szűrése során mérhető relatív fluxusok; **2/b ábra:** A mikroszűrés során mért ellenállások

A membránszűrések során mérhető teljes ellenállás három fő részre osztható:a membrán saját ellenállására, egy (a lemosható olajrétegből illetve a koncentráció-polarizációs rétegből adódó) reverzibilis- és egy (a membrán felületére tartósan feltapadó-, illetve a pórusokat eltömítő olajból adódó) irreverzibilis ellenállásra. Az irreverzibilis ellenállás mindkét esetben kisebb volt a membrán saját ellenállásánál, illetvea foto-Fenton reakcióval előkezelt olaj emulzió esetén még kisebb volt, mint az előkezeletlen emulzió esetén. A reverzibilis ellenállás azonban a nem előkezelt emulzió esetén a teljes ellenállás jelentős része (77,4%-a), míg az előkezelt emulzió esetén ez az ellenállástípus is elhanyagolhatóan csekély mértékű. A teljes ellenállás mértéke 86%-al volt csökkenthető az előkezelés hatására az előoxidált és koagulált olajcseppeknek köszönhetően.
A mikroszűréssel elérhető tisztítási hatékonyság97 ill. 98 % voltaz általunk alkalmazott 0,2 µm pórusátmérőjű PES hidrofil membránnal az előkezeletlen és a foto-Fenton reakcióval előkezelt olajszennyezett vizek esetén.

Következtetések

A kőolajjal szennyezett víz (c_{olaj}=100 ppm) Fenton-reakcióval történő tisztítása (19,7 ppm Fe^{2+} és 300 ppm H_2O_2;nFe^{2+}: nH_2O_2 = 1:25) a 6 órás kezelési idő alattmindösszesen 13%-os tisztítási hatékonyságot eredményezett. Ultraibolya fotolízissel (254 nm-es UV fényforrás alkalmazásával) már 120 perc alatt 9%-ot csökkent az emulzió kémiai oxigénigénye, míg UV/H_2O_2 kombinált módszer alkalmazásával (300 ppm H_2O_2) 120 perc után21%-os tisztítási hatékonyságot mértünk. A 19,7 ppm Fe^{2+} hozzáadásával kivitelezettfoto-Fenton reakció alkalmazásakor ugyanennyi idő alattmár 53%-kal sikerült csökkenteni a modell szennyvíz kémiai oxigénigényét.
Mikroszűréssel (0,2 µm pórusátmérőjű PES membrán alkalmazásával) a vizsgált modell szennyvíz kémiai oxigénigénye 97%-kal csökkenthető, de a szűrés során a fluxus számottevően lecsökken. Ugyanakkor a foto-Fenton reakciókkal előkezelt emulzió esetén a pH érték 7-re történő állításakor képződő vas-hidroxid csapadékon az olajcseppek megkötődnek, ami jelentős mértékben megnöveli a szennyvíz mikroszűrése során elérhető fluxust, illetve számottevően csökkenti a membrán eltömődését, megnövelve annak élettartamát, miközben a tisztítási hatékonyság (98%)nem csökken.

Köszönetnyilvánítás
A munka a Bolyai János Kutatási Ösztöndíj, illetve a Nemzeti Kutatási, Fejlesztési és Innovációs Hivatal (NKFI témaszám: K112096) támogatásával készült.

Referencia
[1] A.Alver, E.Bas, A. Kilic, M.Karatas, ProcessSafety and EnvironmentalProtection98 (2015) 319–324.
[2]M. A. Tony, P. J. Purcell, Y. Q. Zhao, A. M. Tayeb& M. F. El-Sherbiny, Journal of Environmental Science and Health Part A 44(2009) 179–187.
[3] S. S. Silva, O. Chiavone-Filho, E. L. B.Neto, Journal ofEnvironmental Management147 (2014) 257-263.
[4]H. Shokrkar, A. Salahi, N. Kasiri, T. Mohammadi, Chem. Eng. Res. Des., 90 (2012) 846-853.
[5] Z. L. Kiss, L. Kocsis, G. Keszthelyi-Szabó, C. Hodúr, Z. László, Desal. Wat. Treat., 55 (2014) 3662-3669.

Poster Proceedings

CANCER RISK ASSESSMENT OF ANATOMY LABORATORY WORKERS

Dragan Adamovic[1*], Mirjana Vojinovic- Miloradov[1], Savka Adamovic[2], Jelena Radonic[1], Maja Turk- Sekulic[1], Sabolc Pap[1], Boris Obrovski[1]

[1]University of Novi Sad, Faculty of Technical Sciences, Department of Environmental Engineering and Occupational Safety and Health, Trg Dositeja Obradovića 6, 21000, Novi Sad, Serbia
[2]University of Novi Sad, Faculty of Technical Sciences, Department of Graphic Engineering and Design, Trg Dositeja Obradovića 6, 21000, Novi Sad, Serbia
e-mail: draganadamovic@uns.ac.rs

Abstract
Formaldehyde (FA) is a chemical traditionally used in pathology and anatomy laboratories as a tissue preservative. Several epidemiological studies of occupational exposure to FA have indicated an increased risk of various types of cancer in industrial workers, embalmers and pathology anatomists. Based on the available data IARC, the International Agency for Research on Cancer, has recently classified FA as a human carcinogen. This paper presents the results of the quarterly monitoring of concentration levels of formaldehyde in the working premises of the Department of Anatomy at the Medical Faculty. Air monitoring was performed in order to evaluate occupational exposure to FA. The measurements of concentration levels of formaldehyde were conducted at five locations inside the Department in order to assess the exposure level and cancer risk of students and employees of the institution. The level of exposure to FA was evaluated near the breathing zone of workers. The calculations indicate an extremely high level of cancer risk of the employees. The values obtained in all measuring places are significantly higher than those recommended by international expert organizations. When it comes to students, risk levels are in range with those recommended by international organizations.

Introduction
At room temperature, formaldehyde (FA) is a flammable and colorless gas with a strong pungent odor. It is also a naturally occurring biological compound present in all cells, tissues and body fluids. The highest level of human exposure to this aldehyde occurs in occupational settings. Because of its widespread use a relatively large number of workers are exposed to FA. Based on available data the International Agency for Research on Cancer (IARC) classified FA as carcinogenic to humans (group 1) [1]. Epidemiological studies of industrial workers, embalmers and pathology anatomists have associated FA exposure with elevated risks for cancers at various sites, including nasal cavities, lung, brain, pancreas and lymphohematopoietic system [2-4]. Occupational exposure to FA occurs mainly in anatomy laboratories where it is used for the preservation of tissues and specimens. During operations with anatomical specimens, absorption of FA occurs mainly through inhalation. Inhaled FA primarily affects the upper airways; the severity and extent of physiological response depends on its concentration in the air [5].
FA is most commonly available commercially as a 30–50% (by weight) aqueous solution, commonly referred to as ‘formalin’. In dilute aqueous solution, the predominant form of FA is its monomeric hydrate, methylene glycol. In more concentrated aqueous solutions, oligomers and polymers that are mainly polyoxymethylene glycols are formed and may predominate. Methanol and other substances (e.g. various amine derivatives) are usually added to the solutions as stabilizers, in order to reduce intrinsic polymerization. The concentration of methanol can be as high as 15%, while that of other stabilizers is of the order of several

hundred milligrams per litre. Concentrated liquid FA–water systems that contain up to 95% FA are also available, but the temperature necessary to maintain the solution and prevent separation of the polymer increases from room temperature to 120°C as the concentration in solution increases [6].

Experimental

This paper presents the results of the quarterly monitoring of concentration levels of formaldehyde in the working premises of the Department of Anatomy at the Medical Faculty. The measurements of concentration levels of formaldehyde were conducted at five locations inside the Department in order to assess the exposure level and cancer risk of students and employees of the institution.

FA has been continuously sampled during 8 hours by using the air sampler PRO EKOS 401-x. The device was mounted at a height equivalent to the breathing zone, approximately 1.50 m above the floor. The air was infiltrated through the Drechsel bottles with diffuser frit containing absorption solution for FA (95 cm^3 concentrated sulfuric acid and 0.5 cm^3 1% hromotropic acid). The air flow was set on 0.5 $dm^3 \cdot min^{-1}$.

In the presence of concentrated sulfuric acid, chromotropic acid (1,8 dihydroxynaphthalene-3,6-disulfonic acid) reacts with FA to give a red-violet hydroxydiphenylmethane derivative. The resulting chromophore can be analyzed by UV/VIS spectroscopy. Upon the sampling completion it was necessary immediately to determine the FA concentration, as the intensity of purple color of the absorption solution remains stable only for a few hours. The samples have been analyzed in an accredited laboratory of the Department of Environmental Engineering and Occupational Safety and Health, Faculty of Technical Sciences in Novi Sad by using the UV/VIS spectrophotometer DR 5000 HACH LANGE. The absorption intensity was determined by UV/VIS spectrometry at 580 nm. Based on the determined concentrations of FA and the amount of air transmitted through the absorbing solution, the FA concentrations in air at 5 different sampling locations were calculated.

Cancer risk assessment

Cancer risk is predicted as an increase of the possibility of cancer development during one's life span as a result of exposure to a carcinogen substance. As part of the health risk assessment, as a consequence of exposure to FA, an evaluation of cancer risk has been conducted on the employees of the Department, as well as the students who attend Anatomy classes as an obligatory course at the first year of the Faculty of Medicine.

Cancer risk (CR) was estimated by chronic daily intake (CDI) multiplied by the Slope Factor (SF) according to the Integrated Risk Information System (IRIS) [7,8]. The slope factor is an estimate of probability of an individual developing cancer as a result of lifelong exposure to a particular level of a potential carcinogen [9].

Slope factor (SF) turns the expected value of a daily intake of a substance throughout one's lifetime directly into risk of developing cancer. If we assume that the slope factor is constant (especially in low doses), the risk is directly related to the intake.

$$CR = CDI \times SF$$

According to the IRIS system, the slope factor in this study of formaldehyde is 0.0455 $mg \cdot kg^{-1} \cdot day\text{-}1$ (USEPA) [7].

For the calculation of the CDI, certain values have been assumed according to USEPA [10].

$$CDI = \frac{(CA \times IR \times ED \times EF \times L)}{(BW \times ATL \times NY)}$$

The values used for the calculation of CDI of employees and students are shown in the Table 1. IR of 1.02 $m^3 \cdot h^{-1}$ (average inhalation) was used, in accordance with the Exposure handbook factors [10].

Table 1. The data necessary for the calculation of cancer risk of employees and students

Parameter	Description	Value (employees)	Value (students)	Unit
CA	Contaminant concentration			$mg \cdot m^{-3}$
IR	Inhalation rate, adult	1.02	1.02	$m^3 \cdot h^{-1}$
ED	Exposure duration	40	4	$h \cdot week^{-1}$
EF	Exposure frequency	36	30	$week \cdot year^{-1}$
L	Length of exposure	40	1	years
BW	Body weight, man/woman	70/60	70/60	kg
ATL	Average time of life, man/woman	69/72	69/72	years
NY	Number of days per year	365	365	$days \cdot year^{-1}$

Results and discussion

Based on the data of FA concentration levels, cancer risk of the employees of the Department, as well as the students who attend classes at the Department, has been calculated. The student exposure is significantly lower than that of the employees, considering the significantly shorter time period of their exposure to FA. The results of the calculations of cancer risk of employees and students are shown in Table 2 and Table 3, respectively. During the calculations of cancer risk, the fact that the first year students are exposed to formaldehyde 4 hours a week over 30 teaching weeks and the fact that the student attendance at the premises of the Department is limited to classrooms 1 and 2 have been taken into consideration.

Table 2. Exposure to formaldehyde (CDI) and cancer risk (CR) of employees at the examine locations.

Sampling site	Classroom 1	Classroom 2	Prepare room	Storage room	Break room
C (ppm)	1.20	0.86	1.90	5.73	0.67
CA ($mg \cdot m^{-3}$)	1.47	1.06	2.34	7.05	0.82
CDI ($mg \cdot kg^{-1} \cdot day^{-1}$) men	0.049	0.035	0.078	0.235	0.027
CDI ($mg \cdot kg^{-1} \cdot day^{-1}$) women	0.051	0.037	0.081	0.242	0.028
CR men (40 years of exposure)	2.24E-03	1.61E-03	3.55E-03	10.69E-03	1.25E-03
CR women (40 years of exposure)	2.31E-03	1.66E-03	3.66 E-03	11.03E-03	1.29E-03

The calculations indicate an extremely high level of cancer risk of the employees at the Department of Anatomy. The values obtained in all measuring places are significantly higher than those recommended by international expert organizations. The US Environmental Protection Agency (US EPA) proscribes an acceptable risk level value of the order 10^{-6} (1 in 1,000,000), while NIOSH proscribes a significantly higher level of the order 10^{-3} (1 in 1,000). Generally, US EPA uses the 1 in 10, 000 to 1 in 1,000,000 risk range as a target range within which the agency strives to manage risk. The EPA uses the 1 in 10,000 risk level as an appropriate cut-off level for decisions on whether risk management action is required at a site [11].When it comes to students, risk levels are in range with those recommended by international organizations.

Table 3: Exposure to formaldehyde (CDI) and cancer risk (CR) of students at the examined locations

Sampling site	Classroom 1	Classroom 2
C (ppm)	1.20	0.86
CA ($mg \cdot m^{-3}$)	1.47	1.06
CDI students men ($mg \cdot kg^{-1} \cdot day^{-1}$)	10.23E-05	7.37E-05
CDI students women ($mg \cdot kg^{-1} \cdot day^{-1}$)	11.44E-05	8.24E-05
CR students men	4.66E-06	3.36E-06
CR students women	5.21E-06	3.75E-06

Conclusion

This paper points to the presence of formaldehyde with concentration levels significantly higher than those prescribed and recommended by international expert organizations. What stands as a direct consequence to exposure to formaldehyde is an extremely high risk of cancer development, primarily with tenured employees of the Department who spend a lot of time in rooms contaminated by high formaldehyde concentration levels. In order to ensure optimal working conditions and to reduce employees' risk of exposure to formaldehyde it is strongly recommended to Department to install effective ventilation system in working premises or to use the less toxic chemical cocktails in the processes of embalming and preserving of anatomical specimens.

Acknowledgements

This research was supported by the Ministry of Education, Science and Technological Development, Republic of Serbia (III46009).

References

[1] IARC, 2006. IARC Monographs on the Evaluation of Carcinogenic Risks to Human, 88: World Health Organization, Lyon
[2] Coggon, D., Harris, E.C., Poole, J., Palmer, K.T., 2003. J. Natl. Cancer Inst. 95, 1608–1615
[3] Stone, R.A., Youk, A.O., Marsh, G.M., Buchanich, J.M., McHenry, M.B., Smith, T.J., 2001. J. Occup. Environ. Med. 43, 779–792
[4] Pinkerton, L.E., Hein, M.J., Stayner, L.T., 2004. Occup. Environ. Med. 61, 193– 200
[5] Keil, C.B., Akbar-Khanzadeh, F., Konecny, K.A., 2001. Appl. Occup. Environ. Hyg. 16, 967–972
[6] Swami, P.C., R. Raval, M. Kaur, J.Kaur, British J. of Oral and Maxillofacial Surg. 54: 351–352 (2016).
[7] U. S Env. Prot. Agency (USEPA). EPA/540/189/002. Washington, DC: EPA Press; 1989.
[8] U. S Env. Prot. Agency (USEPA). Integrated risk information system, Available at http://www.epa.gov/iris (accessed April 19, 2016).
[9] U. S. Env. Prot. Agency (USEPA) Risk assessment guidance for superfund (RAGS) Part A: Chapter 7 (toxicity assessment) and 8 (risk characterization)(1996)
[10] U. S. Env. Prot. Agency (USEPA). Exposure factors handbook. Washington, DC: US Government Printing Office; 1997. EPA/600/8-89/43.
[11] Kootenay Boundary Comm. Health Serv. Soc. Acceptable level of humana health risks resulting from smelter conataminants in the trail areaKootenay Boundary Health Nelson, BC (2001).

EVALUATION OF COPPER CONTENT IN SOIL AND ZEA MAYS L. GRAINS, IN A ROMANIAN POLLUTED AREA

Simion Alda[1], Liana Maria Alda[1]*, Teodor Cristea[1], Diana Moigradean[1], Maria Rada[2], Claudia Sirbulescu[1], George Andrei Draghici[3], Luminita Pirvulescu[1]

[1]Banat University of Agricultural Sciences and Veterinary Medicine "King Mihai I of Romania" 300645 Timisoara 119, Calea Aradului, Romania;
[2]"Victor Babes" University of Medicine and Pharmacy Timisoara, Piata Eftimie Murgu, 300041 Timisoara, Romania;
[3]"Vasile Goldis" Western University of Arad, Str. Liviu Rebreanu, nr. 86, Campusul Universitar "Vasile Goldis" Arad, Romania;
e-mail: lianaalda@yahoo.com

Abstract

The heavy metal contamination of soil is one of the most pressing concerns in the debate about food security and food safety in Europe. Maize, also known as corn, constitute a staple food in many regions of the world. The aim of this paper was to determine the capacity of maize (*Zea mays* L.*)* grainstoaccumulate Cu, in order to evaluate the potential risk for human consume and to obtained informations regarding the soil pollution in this area. The studied area was Tarnaveni (Mures County, Romania). In soil, the copper content, calculated on the dry basis, ranged from 13.17 ppm to 52.96 ppm for 0-20 cm depth and from 14.01 to 44.82 ppm for 20-40 cm depth. The soil copper contents are exceeding the value of 20 ppm (the normal contents in soil, for Romania) but do not exceed the value of 100 ppm (the Alert threshold values for Romania). Regarding the copper content ($mgKg^{-1}$ dry weight) in corn, the values are between 4.87 to 25.40 ppm, and five from seven samples exceed the permissible limit of copper for plants (10 mg/kg recommended by WHO). This study allows to obtain informations regarding the copper pollution level in this area.

Introduction

The heavy metal contamination of soil is one of the most pressing concerns in the debate about food security and food safety in Europe [9].

Maize, also known ascorn, constitute a staple foodin many regions of the world. Maize crop presents a high yield potential. Maize meal is also used as a replacement for wheat flour, to makeother baked products.

Literature contains numerous data on the distribution of copper in soil and plants cultivated in different geographical areas [1,2,3,4,5]. The crop of *Zea mays* L. is heavy-metal tolerant, has high metal accumulating ability in the foliar parts with moderate bioaccumulation factor. So, maize is capable of continuous phytoextraction of metals from contaminated soils by translocating them from roots to shoots [11].

The main man-made releases of copper are from coal-fired power stations, metal production, waste incinerators, sewage treatment processes and from the application of agricultural chemicals.

Excess copper in soils is toxic to some micro-organisms, disrupting nutrient-cycling and inhibiting the mineralisation of essential nutrients such as nitrogen and phosphorus[12].

The permissible limit of copper for plants is 10mg/kg recommended by WHO [10].

The aim of this paper was to determine the capacity of maize (*Zea mays* L.) grainstoaccumulate Cu, in order to evaluate the potential risk for human consume and to obtained informations regarding the soil pollution in this area.

Experimental

The prelevations points are located in Tarnaveni area (Mures County, Romania).Soil and maize samples were collected from seven familiarly farms located in the studied area. From each prelevation points (PP) were collected soil (0-20 cm and 0-40 cm depth) and maize samples.

The minerals determination was made by FAAS. After calcination we made the solubilisation of the inorganic matter in nitric acid 0.5 N up to 50 ml. The solutions obtained were used for FAAS determinations [7]. Determination of pH has been accomplished in watery suspension in report with the soil: water of 1:2.5.

Results and discussion

The pH of soil in prelevations points soil varies between 6.56 to 8.73.

The results regarding copper content in soil and maize, were expressed in ppm ($mgKg^{-1}$dry weight).

In Table 1 are presented, for copper, the Normal contents in soil, the Alert threshold values for Romania and the Intervention threshold values for Romania (Order 756/1977) [8].

Table 1. Heavy metals total contents in soil (mg/kg DW)

Heavy metals total contents in soil (mg/kg DW)		
NC*	ATV**	ITV***
20	100	200

* Normal contents in soil, for Romania(Order 756/1977) ;
**Alert threshold values for Romania(Order 756/1977) ;
***Intervention threshold values for Romania (Order 756/1977)

The Cu contents ($mgKg^{-1}$ dry matter) in maize (*Zea mays* L.)grains and corresponding soils are presented in Table 2. Each value in the tabel is an average of 3 replicates.

In soil, Cu ranged from 13.17 ppm to 52.96 ppm for 0-20 cm depth and from 14.01 to 44.82 ppm for 20-40 cm depth.

According to Table 1 and Table 2, the copper soil contents are exceeding 20 ppm (the normal contents in soil, for Romania) but do not exceed 100 ppm (the Alert threshold values for Romania).

Regarding the copper content ($mgKg^{-1}$ dry weight) in corn, the values are between 4.87 to 25.40 ppm, and five from seven samples exceed the permissible limit of copper for plants (10 mg/kg recommended by WHO).

Table 2. Average values mg/kg dry weight (ppm) of total copper contents in maize grains and corresponding soils

Prelevation Point	**Soil pH**		**Cu(ppm) in soil**		**Maize grains**
	0-20 cm	20-40 cm	0-20 cm	20-40 cm	Cu(ppm)
PP1	8.68	8.73	13.17	14.01	19.83
PP2	8.23	8.15	47.29	43.75	22.74
PP3	7.87	7.98	52.96	44.82	20.01
PP4	7.97	7.74	27.56	29.14	4.87
PP5	7.67	7.74	23.14	21.61	5.64
PP6	7.95	8.13	27.06	29.95	25.40
PP7	6.56	6.58	29.64	29.77	13.57

Analysing the Figure 1, we can conclude that the Cu contents in the soil influences the evolution of the copper maize contents for all seven locations.

Our research is in accord with other studies [5, 6,11].

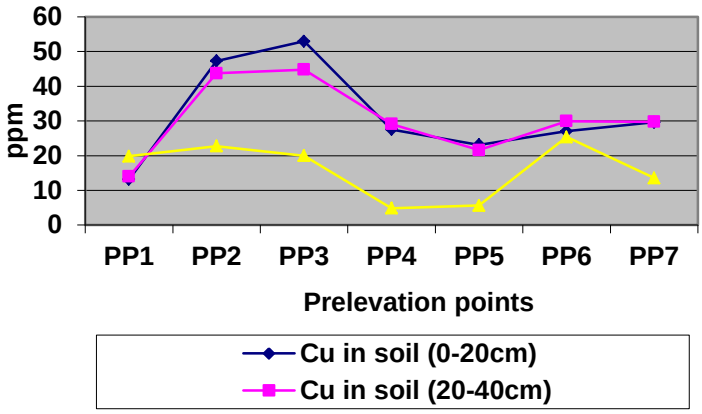

Figure 1. Graphical representation of Cu contents in maize and corresponding soil
Legend: PP =Prelevation Point

Conclusion

In soil, copper ranged from 13.17 ppm to 52.96 ppm for 0-20 cm depth and from 14.01 to 44.82 ppm for 20-40 cm depth.
The copper soil contents are exceeding the value of 20 ppm (the normal contents in soil, for Romania) but do not exceed 100 ppm (the Alert threshold values for Romania).
Regarding the Cu contents ($mgKg^{-1}$ dry weight) in corn, the values are between 4.87 to 25.40 ppm, and five from seven samples exceed the permissible limit of copper for plants (10 mg/kg recommended by WHO).
This study allows to obtain informations regarding the copper pollution level in this area.

References

[1] S.Alda, Agrotehnica si herbologie, Editura Eurobit, (2004).
[2] S.Alda, Herbologie speciala, Editura Eurobit, (2007).
[3] D. M. Bordean, Journal of Horticulture, Forestry and Biotechnology, 16(2), (2012),106-111.
[4] D. M. Bordean, I. Gergen, M. Harmanescu, L Pirvulescu, M. Butur, C. I. Rujescu, J. Food Agric & Environ, 8(2), (2010), 1054-1057.
[5] I.Gogoasa, G. Oprea, I. Gergen, E. Alexa, A. Cozma, D.M. Bordean, D. Moigrădean, L.M. Alda, Journal of Agroalimentary Processes and Technologies, Vol. 15, No 1, (2009), 172-176.
[6] I.Gogoasa, A. Mircescu, G. Oprea, D.M. Bordean, L.M. Alda, M. Rada, S.Alda, I. Gergen, lda, Journal of Horticulture, Forestry and Biotechnology, Vol. 15, No 4, (2011), 13-16.
[7] R. Lacatusu, A.R Lacatusu, Carpth. J. of Earth and Environmental Science, 3, (2008),115–129.
[8] Monitorul Oficial al Romaniei, No. 303 bis/ 6 XII 1997/ OM 756/1997, (1997).
[9] G.Tóth, T. Hermann, M. R. Da Silva, L. Montanarella, Environment international, 88,(2016), 299-309.
[10] H. Zaigham, A.Zubair, U.K.Khalid, I.Mazhar, U.K.Rizwann, Z.Jabar et al. Research Journal of Environmental and Earth Sciences, vol 4, (2012),5.
[11] R. A. Wuana, F. E. Okieimen, African Journal of General Agriculture, 6(4), (2010), 275-287.
[12] http://apps.sepa.org.uk/spripa/Pages/SubstanceInformation.aspx?pid=104.

THEORETICAL CONSIDERATION REGARDING THE CONTAMINATED SOIL

Mihaiela Andoni[1]*, Georgeta-Maria Simu[1], Germaine Savoiu-Balint[1], Anca Dragomirescu[1], Oana Raluca Pop[1]

[1]Faculty of Pharmacy, University of Medicine and Pharmacy "Victor Babeş" Timişoara, 3000040 Timişoara. P-ţa Eftimie Murgu nr.2, România
e-mail: andoni.mihaiela@umft.ro

Abstract
This artice represent a small review of the main methods for decontamination of soil infected with toxic chemicals. Are presented several methods such as: isolation of contaminated area, separation methods, electrochemical methods, phytoremediation and photocatalytic remediation of soil contaminated with toxic chemicals.

Introduction
It is known that many inorganic chemicals and organic especially are very toxic to the environment and human body[1]. Inorganic combinations are eliminated from the body, but some affect internal organs such as the liver and kidneys, but the organic compounds mostly cannot be removed[2]. They accumulate in the body and their cumulative effect becomes obvious after a few years. Therefore, there are studies on the mechanisms of action of toxic compounds. It is important to establish environmental remediation processes because they found a growing accumulation of toxic compounds, which represent a real risk factor[3]

Experimental
There are several general methods of environmental remediation that we review:
a. *Isolation of contaminated area*
Isolation can be done using barriers of steel, cement, bentonite and plastered walls that can be placed both horizontally and vertically. This insulation of contaminated areas is done to reduce infiltration of contaminated water in areas where perhaps it cannot yet penetrate. Contaminated soil solidification technologies are pretty much used. Solidification is the physical encapsulation of toxic compounds into a solid matrix, solidification being preceded by chemical reactions that reduce mobility of contaminants[4].
b. Method of separation
Mechanical separation is necessary for the classification of soil particles based on their size. To achieve such separations are used: cyclones which separates particles larger than 10-20 μm by centrifugal force from the particles smaller, separation through a fluidized bed in which the particles smaller than 50 μm are found at the top of the fluidized bed and are extracted in countercurrent in a column upright, gravity *separation* by *flotation* process which is based on separating under the action of terrestrial gravitational field, of the particles with average density lower than water, *magnetseparation* is based on the magnetic properties of metals and can be used for the separation of ferrous materials.
Pyrometallurgical separation using high temperature furnaces where toxic compounds are volatilized from contaminated soil. This process is applicable to soil with high concentrations of toxic compounds. These compounds are then recovered.
Chemical separation is applied either for detoxification or to reduce ion mobility. The method is usually used for wastewater. Ions are subject to reduction processes.
Separation using additives is a method used for the separation of toxic compounds. You can use natural zeolites that form an important class of natural aluminosilicate. They have great ability to remove highly toxic compounds.

c. Electrochemical separation

Electrochemical process involves passing a current of low intensity between an anode and a cathode implanted in contaminated soil. Ions and small particles loaded together with ground water are transported between the electrodes. An applied potential difference between the electrodes initiates the process. When current passes directly through the ground, ions migrate towards the electrodes, cations to cathode and anions to anode. This effect is used in electrochemical remediation If using an ion exchange membrane the process is called electrodialysis[5]. The principle of the method is shown in Figure 1

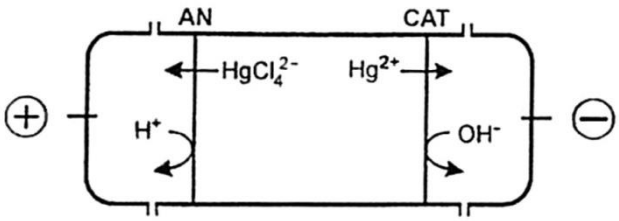

Figure 1. The principle of mercury contaminated soil remediation by electrodialysis
AN = anion exchange membrane; CAT = cation exchange membrane

d. Photocatalytic remediation

It was taken as example to remedy such wastewater with a high content of mercury. Heterogeneous photocatalysis is a promising method for remediation of wastewater with a high content of mercur.TiO_2 is known as a photocatalyst by means of which mercury is removed from aqueous solutions. All remediation processes in the presence of TiO_2 are carried out in the absence of oxygen[6]. The reaction mechanism is as follows:

$$TiO_2 + h\nu \rightarrow 2e^- + 2h^+$$

$$Hg^{2+}(aq) \leftrightarrow Hg^{2+}(ads)$$

$$Hg^{2+}(ads) + 2e^- \rightarrow Hg^0(ads)$$

$$2H_2O \leftrightarrow 2H^+ + 2OH^-$$

$$2OH^- + 2h^+ \rightarrow H_2O + \tfrac{1}{2} O_2$$

Total reaction: $Hg^{2+}(aq) + H_2O \xrightarrow[TiO_2]{h\nu} Hg^0(ads) + 2H^+ + \tfrac{1}{2} O_2$

e. Remediation by biochemical processes

Metals extraction techniques include microorganisms' bioextraction, biosorbtion and processes of oxidation / reduction. *Bioextraction* is via microorganisms such as *Aspergillus niger* fungus that can produce citric acid and gluconic acid. They can function both as acids and adjusts the pH as well as complexing agents for mercury. *Biosorbtion* represents a biological treatment in which the adsorption of mercury in biomass represented by algae and bacterial cells that can be dead or alive *The processes of oxidation/reduction* .are also made by microorganisms. For the mercury exist sulfate-reducing bacteria (SRB) forming insoluble mercuric sulfide, according to the reactions:

$$CH_3COOH + SO_4^{2-} \rightarrow 2HCO_3 + HS^- + H^+$$

$$H_2S + Hg^{2+} \rightarrow HgS + 2H^+$$

f.Phytoremediation

Plants like *Thlaspi, Urtica, Chenopodium* are able to accumulate toxic compounds and may be considered as a method of treating contaminated soil. The method is suitable for soils that do not contain high concentrations of toxic substances. Schematic process (Figure 2):

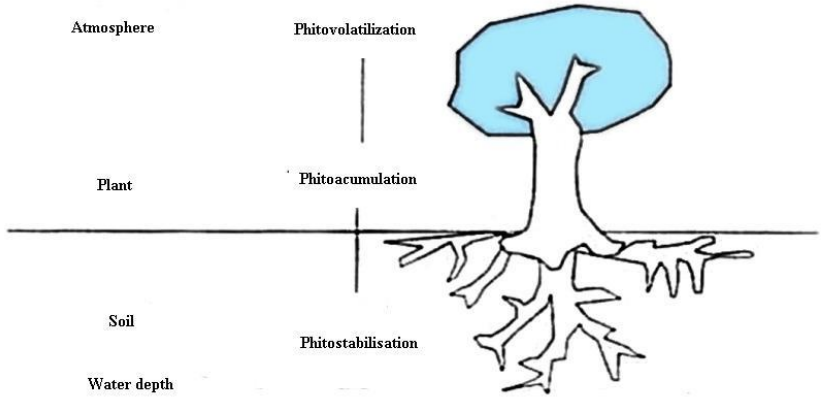

Figure 2. Schematic diagram of the process of phytoremediation of soils contaminated with mercury

g. Remediation of soil by washing with various agents

The solutions used for extraction is infiltrated into the ground using flooding from surface, sprinkler irrigation, pool infiltration etc. Use water with various additives. Process diagram is shown in Figure 3:

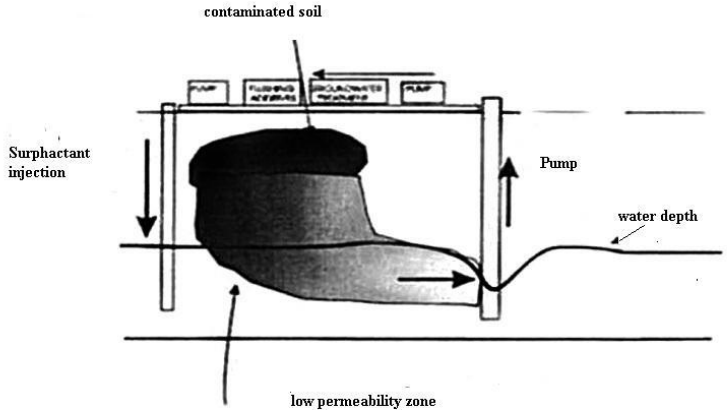

Figure 3. Remediation of soil by washing with various agents diagram

Results and discussion

For the isolation of contaminated area the vertical barrier reduce movement of deep waters contaminated with toxic substances or prevents deep penetration of contaminated water in contaminated areas. To prevent the transport of toxic compounds through this barrier it must be covered with a glue or a low permeability layer. If this barrier cannot be placed is required an extraction system of deep water to avoid toxic compounds passing through the barrier. Use mud walls, geomembranes and walls with multiple layers. Most used are mud walls because they are the most readily available and the cheapest. A horizontal barrier are not yet widely used and has not yet been demonstrated efficiency. In any case these barriers can be used as a horizontal dividing line for contaminated area so you do not need excavation Vitrification is a process of solidifying soil requiring thermal energy. Involves inserting electrodes into the ground. Through these electrodes must be able to pass electricity, and solidification occurs through cooling.

Mechanical separation methods are increasingly being used, especially as methods of

decontamination of soil run-up. They prepare the soil particles, it groups them classified so that it can be applied specific decontamination processes. Following the separation pyrometallurgically it forms a slag that contains heavy metals that can be recovered in this way. Sometimes it is necessary as a pretreatment to reduce the volume of soil to be subjected to pyrometallurgical separation.bChemical treatments can be made in situ by injecting reactants in deep waters, but there is a risk of introducing other contaminants.Experiments were performed on soils contaminated with mercury, and then treated with the zeolite. As a result of experiments and found that the treatment of the soil with zeolites reduces the amount of toxic compounds by up to 80%. Reducing the concentration of mercury is attributed zeolites ability to immobilize mercury ions acting as natural ion exchangersIf electrochemical remediation is an example in which the cations are H^+ and Hg^{2+} and OH^- anions are represented and $HgCl^{4-.}$ The contaminated soil is placed between anion exchange membrane and cation exchange membrane. Efficiency remedy depends on the current density electrodyalitic During the mercury ions move from one side of the contaminated soil to another forming an ion front. This procedure is applied mainly in sandy soilsIf photocatalytic remedy when presented for extracting mercury complexing agents may be employed for mercury, allowing its extraction and if present oxygen in solution. The reaction may occur even under sunlight.

Conclusion

We wanted to make a review of the main methods for decontamination of soil infected with toxic chemicals. Some methods have been applied to contaminated soils in different geographic areas with relatively successful results Attempts to develop new effective methods for decontaminating soil infected with toxic chemicals are done.

References

[1]. M. Andoni, A.. Dragomirescu, A.Iovi, I. Ursoiu, A. Negrea, L.Lupa, P.Negrea, M. Ciopec, Revista de chimie 60 (2009) 424

[2] M. Andoni, A.Iovi, P. Negrea, L.Lupa, A.Negrea, M. Ciopec, Revista de chimie 59 (2008)779

[3] M.Andoni, A.Iovi, P.Negrea, A.Negrea, L..Lupa, M. Ciopec, Revista de chimie 59 (2008) 653

[4] C. Borza, C.Oancea, R. Mateescu, G. Balint-Săvoiu, C. Cristescu, M.Andoni, G.M. Simu, M. Butur, C. Dehelean, E.A. Pauncu, Journal of Foof Agriculture&Environment 9 (2011) 175

[5] M. Andoni, J.M. Pătrașcu, C.A. Dehelean, G.M. Simu, C.Soica, D. Antal, R. Pop, Croatica Chemica Acta 88 (2015), 241

[6] M. Andoni, M. Medeleanu, M. Stefanut, A. Cata, I. Ienascu, C. Tanasie, R.Pop, Journal of Chemical Srbian Society 81 (2016) 177

NEW CARBOXYSALICYLALDEHYDE SCHIFF BASE LIGAND AND ITS COPPER(II) COMPLEXES

Diana Aparaschivei[1,*], Ildiko Buta[1], Ana-Maria Pană[1], Iulia Păuşescu[2], Valentin Badea[2], Liliana Cseh[1], Otilia Costişor[1]

[1]Institute of Chemistry Timisoara of Romanian Academy, 24 M. Viteazul Bvd, 300223, Timisoara, Romania;
[2]University Politehnica Timisoara, Faculty of Industrial Chemistry and Environmental Engineering, 6 V. Parvan Bvd, 300223, Timisoara, Romania
e-mail: diana.aparaschivei@gmail.com

Dedicated to the 150th anniversary of the Romanian Academy

Abstract

Metal-organic frameworks have become a subject of great interest lately because of their interesting features and applications in the field of catalysis, magnetism and biological studies [1]. Coordination polymers are most commonly the creators of such frameworks, and researchers have devoted great effort to the design of metal-generated networks with tailored properties [2,3].

Our group has recently been involved in the development of by-design structures based on 3d metal coordination complexes derived from Schiff based ligands [4]. Salen-based complexes of 3d metals, in which the Schiff base presents the carboxy substituent on the aromatic moiety, generate infinite coordination polymers in the presence of alkaline bases [5]. In this respect, we have obtained new carboxysalicylaldehyde Schiff base ligand, namely N,N'-bis(5-carboxy-salicylidene-aminopropyl)piperazine (CBPP), characterized by NMR and FTIR spectroscopy and TG analysis. Copper(II) complexes of CBPP were synthesized by direct or template synthesis, isolated and characterized by FTIR; preliminary results suggest the formation of polymeric structures.

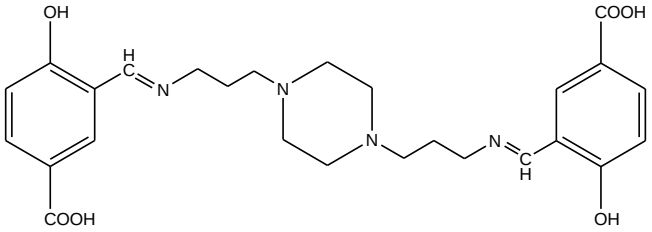

Fig. 1. CBPP structure

Acknowledgement

The authors acknowledge the support of the Romanian Academy, Project 4.1.

References

[1] L.L. Liu, C.X. Yu, W. Zhou, Q.G. Zhang, S.M. Liu, Y. F Shi, Polymers 8(1) (2016) 3.
[2] A. Bilici, I. Kaya, F. Doğan, J. Polym. Sci. A, 47(2009) 2977.
[3] S.V. Kolotilov,O. Cador, F. Pointillart, S. Golhen, Y. Le Gal,K.S. Gavrilenko, L. Ouahab, J. Mater. Chem. 20 (2010) 9505.
[4] C. Cretu, R. Tudose, L. Cseh, W. Linert, E. Halevas, A. Hatzidimitriou, O. Costisor, A. Salifoglou, Polyhedron 85 (2015) 48.
[5] A. Bhunia, P.R. Roesky, Y. Lan, G.E. Kostakis, A.K. Powell, Inorg. Chem. 48 (2009) 10483.

PHYTOCHEMICAL CHARACTERISTICS AND ANTIOXIDANT CAPACITY OF FRUIT EXTRACTS OF DIFFERENT *PRUNUS* SPECIES

Boris Popović[1], Ana Teresa Serra[2], Bojana Blagojević[1*], Ružica Ždero Pavlović[1], Dubravka Štajner[1], Catarina M.M. Duarte[2]

[1]*Faculty of Agriculture, University of Novi Sad, Trg Dositeja Obradovića 8, 21000 Novi Sad, Serbia*
[2]*Instituto de Tecnologia Quimica e Biologica, Universidade Nova de Lisboa, Av. da Republica, EAN, 2780-157 Oeiras, Portugal*
e-mail: bojana.blagojevic@polj.uns.ac.rs

Abstract

Fruits are one of the major sources of polyphenol compounds in human diet. These compounds are known to have many health-promoting activities, especially anticancer, antiradical and antioxidant effects. In this work, seven different *Prunus* species traditionally grown in south Bačka region of Vojvodina were investigated: blackthorn (*P. spinosa*), plum (*P. domestica*), apricot (*P. armeniaca*), cherry plum (*P. cerasifera*), sweet cherry (*P. avium*), sour cherry (*P. cerasus*) and mahaleb cherry (*P. mahaleb*). Freeze-dried fruits were evaluated in terms of their phytochemical characteristics and bioactivity, determining total content of phenolics, flavonoids and anthocyanins, total antioxidant capacity and antiproliferative effect on human colon cancer cells (HT29). Blackthorn fruits are the richest in phenolic and flavonoid contents, while mahaleb cherry and sweet cherry had much higher content of total anthocyanins than other examined species. Apricot and cherry plum fruits had the lowest levels of polyphenol compounds, but very high antiproliferative effect, almost the same as blackthorn. This indicates that not only polyphenol compounds contribute to antiproliferative effects. Concerning total antioxidant activity, blackthorn, sweet cherry, sour cherry and mahaleb cherry showed the highest capacity of scavenging DPPH radical and ferric reducing activity power.

Introduction

Regular consumption of fruits has been associated with reduced risk of developing cancer, neurodegenerative diseases, cardiovascular diseases, diabetes and other chronic diseases. These benefits are often attributed to their various phytochemical content and strong antioxidant activity. Fruits are abundant in phenolic compounds, plant secondary metabolites, which greatly contribute to their health promoting effects.[1,2]Health effects of polyphenols are often attributed to their antioxidant activity which is mediated by a variety of mechanisms, including reduction or scavenging of ROS, chelation of transition metal ions and inhibition of enzymes involved in oxidative stress.[3]

Prunus L. genus belongs to Amygdaloideae (or Prunoideae) subfamily of Rosaceae family. The subfamily Amygdaloideae differs from other rosaceous subfamilies by having a drupe, a fleshy fruit with a stony endocarp or stone. This genus includes the plums, cherries, peaches, apricots and many other stone fruits which are widely consumed and present good sources of phytochemicals in human diet.[4]

There are earlier reported many bioactivities and phytochemicals of *Prunus* species.[5-8] Within this context, the aim of this work was to evaluate and compare the antioxidant and antiproliferative effects of seven *Prunus* species traditionally grown in Serbia,in south Bačka region of Vojvodina, in an effort to distinguish promising functional fruits.

Experimental

It were assessed freeze-dried fruit extracts of seven different *Prunus* species: blackthorn (*P. spinosa*, genotype B1), plum (*P. domestica*, cultivar Čačanska rodna), apricot (*P. armeniaca*, cultivar DM), cherry plum (*P. cerasifera*, wild type), sweet cherry (*P. avium*, wild type), sour cherry (*P. cerasus*, cultivar Oblačinska) and mahaleb cherry (*P. mahaleb*, wild type). For spectrophotometric assays 50% acidic methanol (1% HCOOH) fruit extracts were prepared and water extracts were used for determination of antiproliferative activity.

Total phenolic content (TPC) in fruit extracts was determined spectrophotometrically according to the Folin–Ciocalteu method.[9] The results were expressed as milligram of gallic acid equivalents per gram of dry weight (mg GAE/g DW).

Total favonoid content (TFC) was measured using aluminium chloride assay and results were expressed as milligram of quercetin equivalents per gram of dry weight (mg QE/g DW).[10]

Total anthocyanin content (TAC) was determined by pH differential method and expressed as cyaniding-3-glucoside equivalents per gram of dry weight (mg CGE/g DW).[11]

Total antioxidant activity was determined using scavenging effect on 2,2-diphenyl-1-picrilhydrazyl (DPPH) radical[12] and measuring the ferric reducing activity power (FRAP).[13] Results of DPPH assay were given as reciprocal value of IC_{50} (the concentration of extract required to scavenge 50% of radical) and for FRAP test in milligram of ascorbic acid equivalents per gram of dry weight (mg AAE/g DW).

Antiproliferative activity (APA) assay was performed using human colon cancer cells HT29.[14] Cell proliferation was determined using the colorimetric MTT assay. Results were expressed as reciprocal value of ED_{50} (effective dose), the amount of sample necessary to decrease 50% of the cellular viability.

Results and discussion

In this present work, fruits of seven *Prunus* species, were compared by the content of phenolic compounds and antioxidant activities, as well as antiproliferative potential against human cancer cells from colon (HT29).

The content of total phenolic, flavonoid and anthocyanin compounds are presented in Table 1. Blackthorn fruits were the richest in phenolic and flavonoid contents (30.32 mg GAE/g DW and 3.24 mg QE/g DW), while mahaleb cherry and sweet cherry had much higher content of total anthocyanins (11.11 and 9.76 mg CGE/g DW) than other examined species.

Table 1. Total phenolic, flavonoid nad anthocyanin contents of fruit extracts*

Common name	Latin name	TPC (mg GAE/g DW)	TFC (mg QE/g DW)	TAC (mg CGE/g DW)
blackthorn	*P. spinosa*	30.32 ± 3.70	3.24 ± 0.09	4.65 ± 0.08
plum	*P. domestica*	8.79 ± 0.70	0.59 ± 0.01	0.25 ± 0.02
apricot	*P. armeniaca*	3.60 ± 0.06	0.22 ± 0.01	0.01 ± 0.00
cherry plum	*P. cerasifera*	2.92 ± 0.09	0.20 ± 0.01	0.18 ± 0.01
sweet cherry	*P. avium*	20.04 ± 0.34	2.68 ± 0.02	9.76 ± 0.00
sour cherry	*P. cerasus*	17.76 ± 0.03	0.95 ± 0.01	3.94 ± 0.08
mahaleb cherry	*P. mahaleb*	18.82 ± 0.12	3.64 ± 0.14	11.11 ± 0.28

*Values are expressed as means of three replications ± standard deviation.
Abbreviations: TPC-Total phenolic content; TFC-Total flavonoid content; TPC-Total anthocyanin content; GA-Gallic acid, Q-Quercetin; CG-Cyanidin-3-glucoside; E-equivalents.

Extracts of all fruits showed good antioxidant and antiproliferative activities, but blackthorn was distinguished as much better than the others, especially in scavinging DPPH radical and

ferric reducing antioxidant power as shown in Figure 1. Very high antioxidant activity was also noticed for sweet cherry, sour cherry and mahaleb cherry fruit extracts.

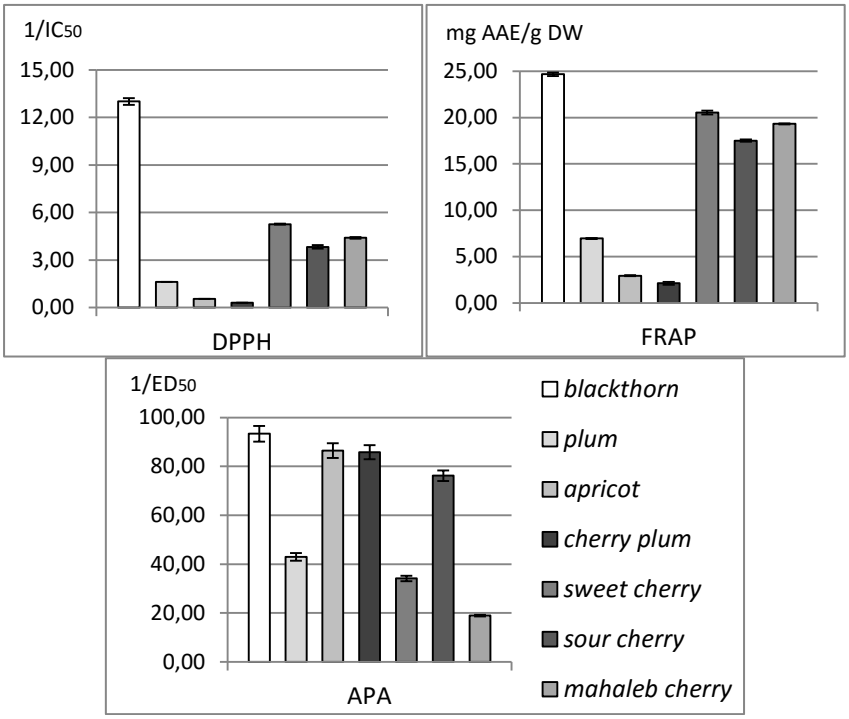

Figure 1. Scavenging activity on DPPH radical, ferric reducing antioxidant power (FRAP), and antiproliferative activitiy (APA) on human colon cancer cells HT29 of different *Prunus* species.

The lowest values of total phenolics, flavonoids and anthocyanins were assessed in apricot and cherry plum fruit extracts and these two fruit extracts showed much lower antioxidant capacity comparing to other species. On the other hand, apricot and cherry plum fruit extracts very strongly inhibited proliferation of HT29 cells, almost as strong as blackthorn, which was the most effective species (Figure 1).This suggests that not only polyphenol compounds contribute to antiproliferative effect, but some other phytochemicals, as well.

Conclusion

The present investigation was carried out to compare phytochemical characteristics and antioxidant and antiproliferative activities of seven*Prunus* species commonly used in human diet.According to obtained data, all examined *Prunus* species showed remarkable antioxidant and antiproliferative effects.Results obtained for apricot and cherry plum fruits, indicates that not only polyphenol compounds contribute to antiproliferative effect, because these two fruit extracts greatly inhibited proliferation of HT29 human colon cancer cells, but were not so abundant with total phenolic compounds and did not show so high antioxidant capacity as the other ones. Among all species, blackthorn was distinguished by the best potential to be used as a source of functional ingredients, but the potential of other species, should not be neglected, also.

Acknowledgements

This research is a part of IPA Planttrain project (HUSBR/1203/221/173) and the Project No III 43002 which is financially supported by the Ministry of Education, Science and Technological Development, Republic of Serbia.

References

[1] N. Balasundram, K. Sundram, S. Sammam, Food Chem. 99 (2006) 191.
[2] K.B. Pandey, S.I. Rizvi, Oxid. Med. Cell. Longev. 2 (2009) 270.
[3] P. Sharma, A.B. Jha, R.S. Dubey, M. Pessarakli, J. Bot. 2012 (2012) Article ID 217037.
[4] S. Lee, J. Wen, J. Am. Bot. 88 (2001) 150.
[5]A.T. Serra, A.A. Matias, A.P.C. Almeida, M.R. Bronze, P.M. Alves, H.C de Sousa, C.M.M. Duarte, J. Supercrit. Fluids. 55 (2011) 1007.
[6] M.A. Schmitz-Eiberger, M.M. Blanke, LWT 46 (2012) 388.
[7] O.E. Campbell, O.I. Padilla-Zakour, Food Res. Int. 54 (2013) 448.
[8] B.M. Ruiz-Rodríguez, B. de Ancos, C. Sánchez-Moreno, V. Fernández-Ruiz, M. de Cortes Sánchez-Mata, M. Cámara, J. Tardío, Fruits 69 (2014) 61.
[9] E.A. Ainsworth, K.M. Gillespie, Nat. Protoc. 2 (2007) 875.
[10] C. Chang, M. Yang, H. Wen, J. Food Drug Anal. 10 (2002) 178.
[11] J. Lako, V.C. Trenerry, M. Wahlqvist, N. Wattanapenpaiboon, S. Sotheeswaran, R. Premier, Food Chem. 101 (2007) 1727.
[12] C. Sánchez-Moreno, J.A. Larrauri, F. Saura-Calixto, J. Sci. Food Agr. 76 (1998) 270.
[13]I.F.F. Benzie, J.J. Strain, Methods Enzym. 299 (1999) 15.
[14] A.T. Serra, R.P. Feliciano, M.R. Bronze, C.M.M. Duarte, J. Funct. Foods. 2 (2010) 46.

ACCUMULATION OF HEAVY METALS IN *VICIA FABA* BEANS

Despina – Maria Bordean, Diana Raba*, Sofia Pintilie, Dan Raican, Andrei Catargiu, Aurica Breica Borozan, Luminita Pirvulescu, Luminita Cojocariu

Banat University of Agricultural Sciences and Veterinary Medicine "King Mihai I of Romania" 300645 Timisoara 119, Calea Aradului, Romania;
*e-mail: dianaraba@yahoo.com

Abstract
The levels of heavy metals like lead, cadmium, zinc, chromium, iron, nickel etc., were examined in *Vicia faba*beans(broad beans) sold in supermarkets from Timisoara, Romania.
The beans have been analyzed for fife heavy metals (Pb, Cd, Cu, Ni and Zn) using AAS. Research findings show that some of the samples present contamination with lead, cadmium and a very high content of nickel. Statistical analysis reveals the tendency of broad beans to be a good bio accumulator of nickel.

Introduction
Vicia faba L is one of the oldest crops grown by man, used as a source of protein in human diet, as fodder [1] and forage crop for animals, and for available nitrogen in the biosphere [12]. Faba beans are the best source of vegetable protein legumes [10]. It is well known that replacing meat with legumes decreases saturated fat in the diet and reduce cardiovascular risk [12].
Lead (Pb), Cadmium (Cd), Copper (Cu), Nickel (Ni) and zinc (Zn) are heavy metals which are affecting the plants differently, being essential elements for cellular metabolism (Cu, Zn, Ni) and also considered as non-essential (Cd, Pb).

Experimental
Samples collection and preparation
Vicia faba beans samples were collected from four local supermarkets.
The collected *Vicia faba* beans were washed with distilled water to remove dust particles and were oven dried at 105°C to constant weight and prepared for analysis as described by Bordean D.M.et al, 2012 [2]. All glass wares and containers required for experimentations were first washed with distilled water followed by soaking in 10% nitric acid for few hours.
Heavy metal analysis
The heavy metals content in *Vicia faba beans* was carried out in HNO_3 solution resulted by ash digestion [2, 9]. The dry ash process was carried out in a muffle furnace by increasing the temperature stepwise of up to 550°C and then keeping at this temperature for 4.30 hours. The metal content in the in the obtained solutions were determined by flame atomic absorption spectrophotometry and were expressed as $mgkg^{-1}$ d.w. (dry weight).
Statistical analyses were performed by using MVSP software package.

Results and discussion
The results of the heavy metals performed analysis are presented in figure 1.
According to the data, the studied heavy metals concentrations seem to be similar to the values present in analyzed *Vicia faba* beans originated from other countries and are under the recommended maximal limit (*table 1*), for copper and zinc content. Two of the analyzed samples present high content of lead (A: 0.27 [$mgkg^{-1}$ d.w] respectively C: 0.58 [$mgkg^{-1}$ d.w]) and one sample presents contamination with cadmium (B: 0.22 [$mgkg^{-1}$ d.w]). Interesting is the high content of nickel in three of the samples (A, B and C).

According to Ghosh et al, 2013 [8], the presence of Nickel ranges from 0.200 to 5.833 ppm in various vegetables, while Cempel M and Nikel G, 2006 consider that "Nickel levels in foodstuffs generally range from less than 0.1 mg/kg to 0.5 mg/kg" [3].
The high content of Ni in beans is confirmed by Sharma AD., 2013 which affirms that legumes like beans, peas, lentils, peanut, soya beans and chickpeas are "foods with high nickel content irrespective of the soil content" [11].

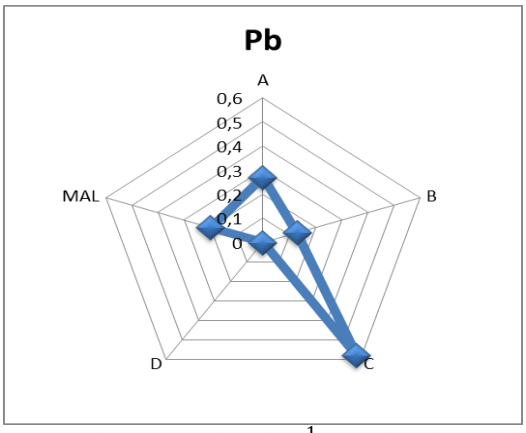

Lead content [mgkg^{-1} d.w.] in broad beans

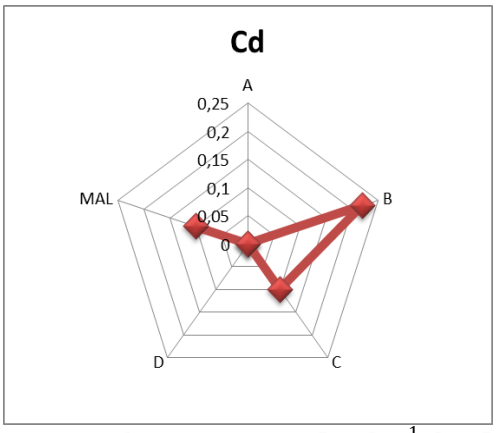

Cadmium content [mgkg^{-1} d.w.] in broad beans

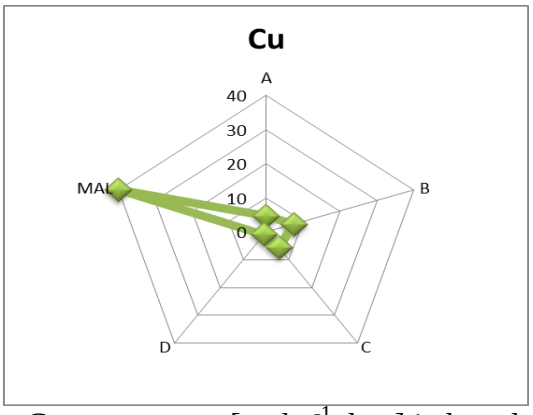

Copper content [mgkg^{-1} d.w.] in broad beans

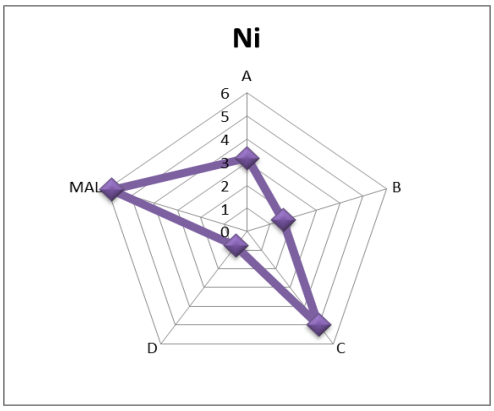

Nickel content [mgkg-1 d.w.] in broad beans

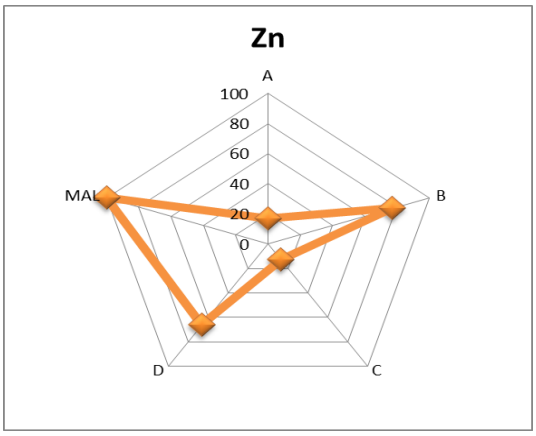

Zinc content [mgkg-1 d.w.] in broad beans

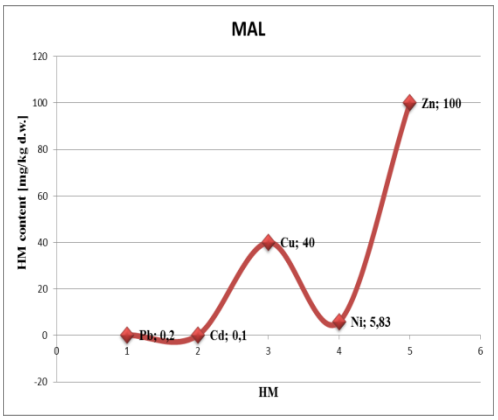

Maximum allowable limits (MAL) in vegetables

Figure 1. Graphical representation of heavy metal content in *Vicia faba* beans

Legend: A, B, C, D = the supermarkets from where the *Vicia faba* beans were collected

Table 1: Standard conditions for Atomic Absorption Spectrophotometer and safe limits of heavy metals in *Vicia faba* beans

Element	Standard conditions for AAS, λ [nm]	Safe limits [mgkg^{-1} d.w.]	References
Pb	217.0	0.2	[5]
Cd	248.3	0.05 0.1	[14] [4]
Cu	324.8	10 40	[4] [7]
Ni	232.0	-	-
Zn	228.8	100	[13]

The graphical representation of Principal components analysis (PCA) using transposed standardized data is presented in figure 2 and it is suggesting that the heavy metals: lead and nickel present high contamination potential for the *Vicia faba* beanssamples species available on the Romanian market (*figure 2*).

PCA as a statistical technique was chosen to find the characteristic patterns of heavy metals data in the analyzed samples.

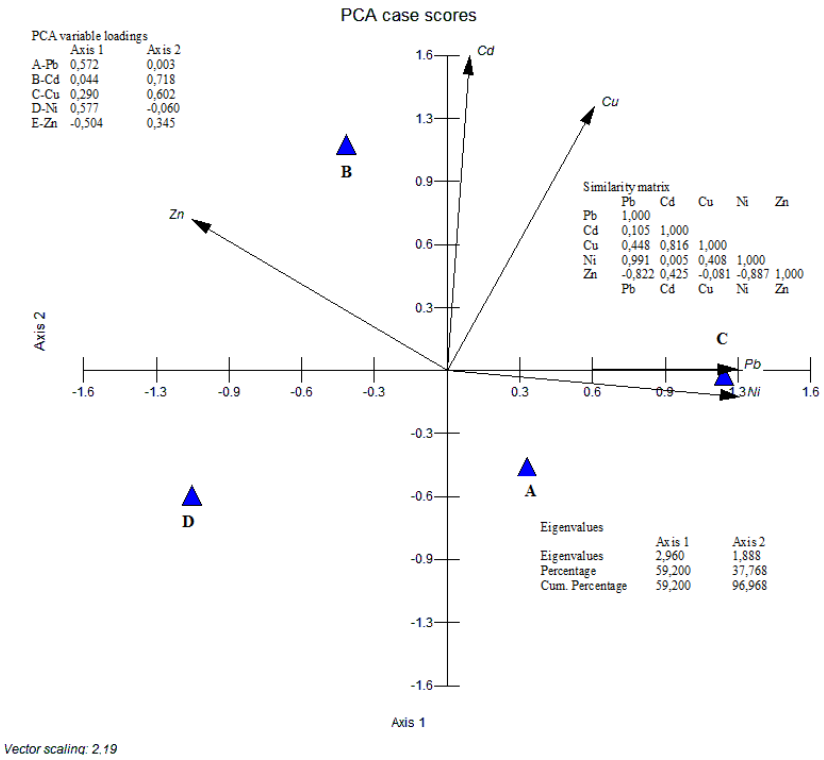

Figure 2. Biplot of the principal component analysis of heavy metals content data

Conclusions

Heavy metals analysis is of big importance in vegetables and fruits, but in special in plants with high accumulation potential like beans, peas, root vegetables, cabbage, tomatoes and nuts. Statistical analysis reveals the tendency of broad beans to be a good bio accumulator of nickel.

Acknowledgements
All authors are principal authors, have equal rights and have contributed evenly to this paper. The present work was funded by the project "*Study of synergic bioactivity of some antioxidant mixes fortifications with the role to fortify patients with Parkinson's disease*", No 47/12.11.2015, financed by Antiparkinson Association from Romania.

References

[1]Alda S., Agricultural techniques and herbology (in rom.lang.), (2004), Edit. Eurobit Timişoara
[2]D.M.Bordean, F.N.Ciobanu, D. Nica, I. Gergen, A.B. Borozan, L. Pirvulescu, S. Alda, N.Filimon – *Statistical evaluation of heavy metal content in some capsicum varieties available on the Romanian market* (2012), available online at: http://leto.mgk.u-szeged.hu/RARD/2012-1/34-17.pdf.
[3]M. Cempel, G.Nikel, Polish J. of Environ. Stud. Vol. 15, No. 3 (2006), pp.375-382, http://www.pjoes.com/pdf/15.3/375-382.pdf
[4]Codex Alimentarius Commission (CAC). 1993. Joint FAO/WHO Food Standards Program, (1995), p. 391
[5]Codex Alimentarius Commission (CAC). Evaluation of certain food additives and contaminants. FAO/WHO, Codex stan. 230-2001, Rev, 1-2003, (2003),Rome.
[6]Codex general standard for contaminants and toxins in food and feed (CODEX STAN 193-1995), (1995), available online at http://www.fao.org/fileadmin/user_upload/livestockgov/documents/1_CXS_193e.pdf
[7]FAO/WHO, Codex Alimentarious Commission. Doc No. Cx/FAC 96/17 Joint FAO/WHO foodstandards programme. Codex general standard for contaminants and toxins in foods (1996)
[8]R. Ghosh, R. Xalxo, M. Ghosh,. Curr. World Environ (2013); 8(3). doi :http://dx.doi.org/10.12944/CWE.8.3.13
[9]Lacatusu, R, Lacatusu, AR., Carpth. J. of Earth and Environmental Science, (2008), 3, pp.:115–129.
[10]E.Molina, A.B.Defaye, D.A.Ledward, in Food Hydrocolloids 16, (2002), pp. 625-632.
[11]AD. Sharma, Indian Journal of Dermatology. 2013;58(3):240. doi:10.4103/0019-5154.110846.
[12]AK Singh and BP Bhatt, *Hort Flora Research Spectrum* 1-3, (2012), pp.267-269;
[13]USDA 2003, Zinc in foods-draft for comments. Foreign Agricultural Service (GAIN Report) # CH3043, China, Peoples Republic of FAIRS, products specific MRL., p1 and 2
[14]J. M. Walker, Regulation by other countries in foods and the human environment, Proceeding, No.2 "Cadmium Accumulation in Australian Agriculture". National Symposium, Canberra, 1-2 March 1988, Australian Government Publishing Service, Canberra, (1988), pp.176- 85.

HYDROTHERMAL CRYSTALLIZATION OF MICROMETRIC HYDROXYAPATITE FOR BIOMEDICAL APPLICATIONS

Alexandra Ioana Bucur*, Raul Alin Bucur, Corina Orha, Paula Svera

National Institute for Research and Development in Electrochemistry and Condensed Matter, no 144 A. Paunescu Podeanu Street, Timisoara 300569
e-mail: corr_bucur@yahoo.com

Abstract
The paper presents the synthesis of hydroxyapatite by chemical reaction of calcium nitrate tetrahydrate and diammonium hydrogen phosphate, followed by hydrothermal crystallization at 200-230°C and 24/72 hours. The obtained white powders were characterized by X-Ray Diffraction, Scanning Electron Microscopy and Atomic Force Microscopy, revealing the formation of crystalline hydroxyapatite with microsized lamella shaped crystals, when the crystallization took place in acidic environment.

Introduction
Synthetic calcium phosphates are widely used biocompatible materials due to their similarity with the natural hydroxyapatite (HA, $Ca_{10}(PO_{4)6}(OH)_2$), present in the hard tissues of the human body. Among the calcium phosphate compounds, HA presents excellent properties as a bioactive material for human implants [1]. HA has been synthesized by a variety of methods like precipitation, hydrolysis, sol-gel, solid state reactions, etc [2-4]; among these methods, in recent years, the hydrothermal method [5, 6] has gained an increasingly important role due to a series of advantages, like: a) relatively low processing temperatures (typically below 350°C), comparing to calcination where high temperatures are required; b) short time, comparing to the sol-gel method; c) the autoclave is a closed system, so outside influences, like airborne impurities, are eliminated; d) there is no need for organic additives (which might alter the biocompatibility properties). Hydrothermal method seems to offer a better control over particles size, chemical composition and morphology, and thus its use has continuously extended over the last decades [7]. Most of the studies of HA synthesis aim at fabricating nanoparticles; the aim of the present study was to achieve microparticles of HA, to be used for future construction of biocomposites.

Experimental
The synthesis was performed usinganalytical grade reagents, namely calcium nitrate tetrahydrate $Ca(NO_3)_2.4H_2O$ (Sigma Aldrich) and diammonium phosphate $(NH_4)_2HPO_4$ (Reactivul Bucuresti) as Ca and P ions precursors, dissolved in distilled water so as to yield 0.05 M solutions. The Ca/P molar ratio of 10/6 was achieved by mixing the appropriate amounts of precursor solutions. The P precursor was added dropwise onto the Ca precursor, under magnetic stirring, followed by 30 minutes stirring. Then the reaction mixture was poured into a teflon liner, which was introduced into a steel autoclave and placed in the oven at temperatures ranging between 200 and 230°C and times of 24 and 72 hours, in order to follow the influence of time and temperature on the crystallization product. Since the pH of the reaction media is acidic, in the range 5-6 (measured with a pH-meter), in order to observe the difference introduced by a pH change, one synthesis was performed with pH adjustment, using ammonia (the pH value was brought to 8).
After the time spent in the oven, the reaction product was cooled to room temperature naturally, extracted and washed with distilled water for 5-6 times, until pH has returned to neutral, and dried at 60°C for 4 hours.

The resultant white powder was subjected to physico-chemical characterization by means of x-ray diffraction technique, using a PANalytical X'Pert Pro MPD Diffractometer with Cu anode, working parameters 45 kV and 30 mA. Images of the samples were obtained using a PANalyticalInspect S scanning electron microscope coupled with an energy dispersive X-Ray analysis detector (EDX) at 3000x magnification (powder samples were supported on glass holders and coated with Ag). Atomic force microscopy was performed on a MultiView 1000 scanner from Nanonics Imaging Ltd., in intermittent mode, using 20 nm radius tip doped with chromium, for the HA1 sample, scanned on a 10x10 μm scale. The analyzed sample was diluted in ethanol and dropwise added to the glass substrate

Results and discussion

The xrd results are presented in Figure 1, where the names of the samples are correlated with experimental parameters as follows:

Name	Synthesis (pH, temperature (°C), time(h))
HA1	5.35; 200; 72
HA2	5.83; 230; 24
HA3	8; 220; 24

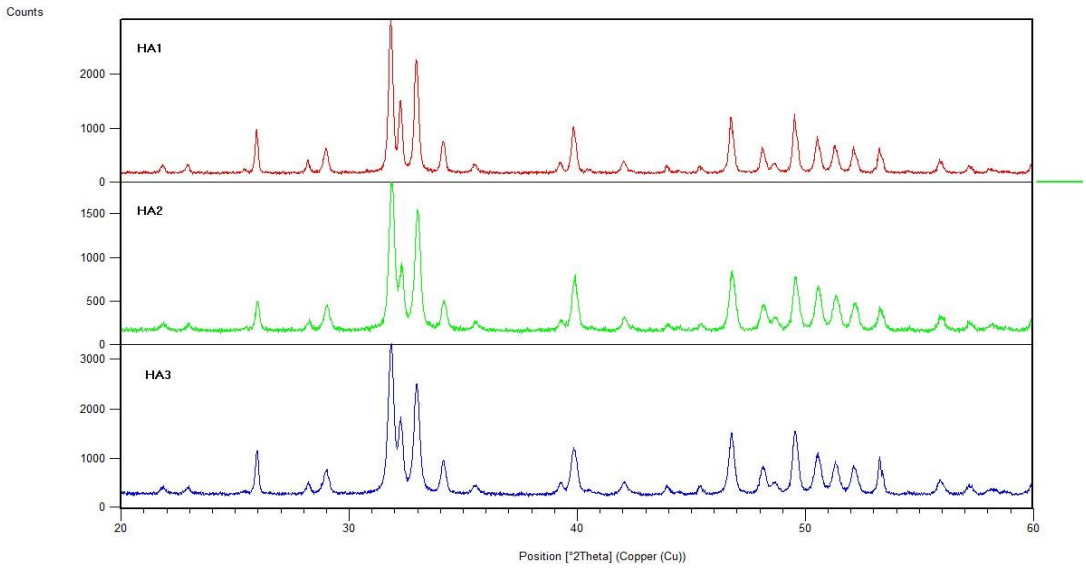

Figure 1. X-ray diffractograms of HA samples

As can be seen in the diffractograms, the samples are crystalline and have been identified as hydroxyapatite; no other crystalline phase is present in any of them. Comparing the peaks intensities, one can conclude that increased time of hydrothermal crystallization (72h, compared to 24h) implies a better crystallization of the samples, and the pH increase also leads to an increase in the crystallinity degree.

The SEM images of the crystalline HA samples are presented in Figure 2. Synthesized in acidic condition,HA1 and HA2 samples present an elongated morphology, plate-like (lamellas). The crystals in the HA1 sample are micrometric-sized (10-20 μm) with uniform distribution of dimensions (most of the crystals appear to be broken, probably during the washing and drying procedures). The 30 degrees difference in the processing temperature between samples HA1 and HA2 seems not to matter; instead, the time difference of 48 hours seems of great importance, since the distribution of the crystals in the HA2 sample belongs to a smaller range; just a small number of them appear in the range of tens of microns. Most of

the crystals appear as wires with lengths of a few microns (≤5μm); some of the crystals appear as agglomerations. The pH difference is too small to count for such a big difference in the sample morphologies. This statement seems to be in agreement with the XRD results, where HA2 sample is a little less crystalline than HA1 sample, which means it needs a longer time to complete the crystallization process.

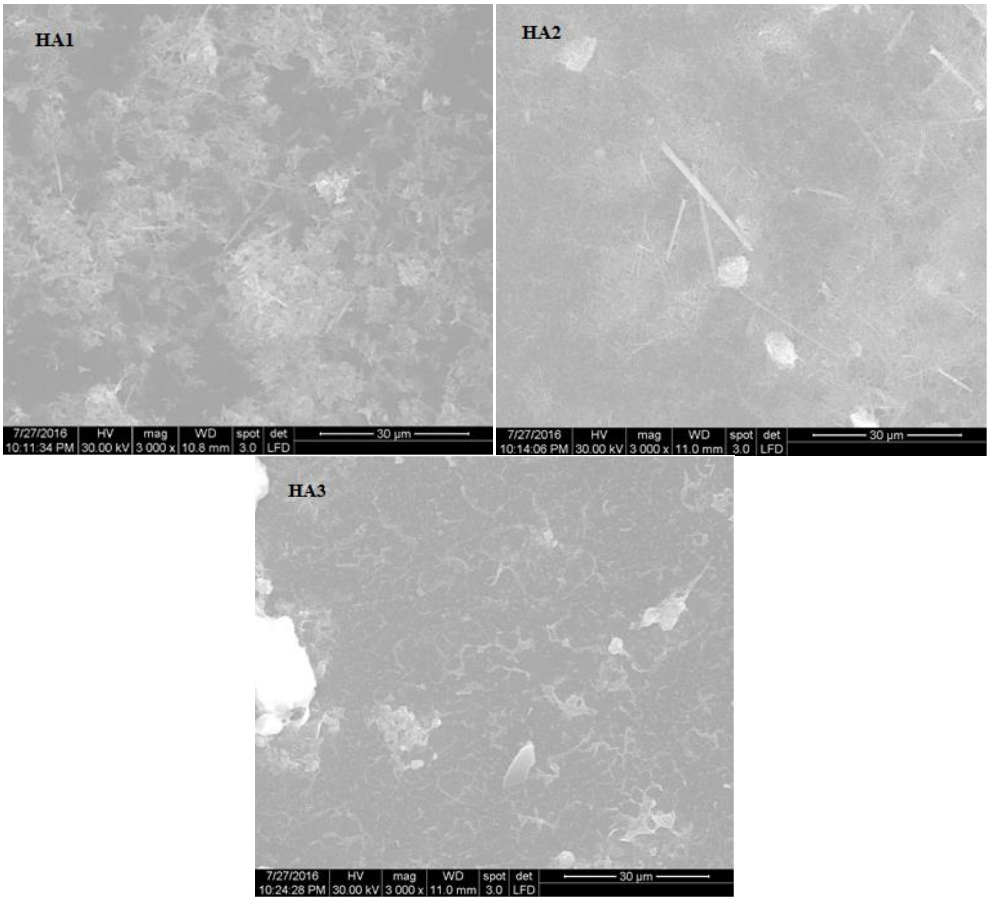

Figure 2. SEM images of HA1, HA2 and HA3 samples

Regarding the sample HA3, the SEM image presents agglomerations of very small crystallites. Correlating this image with the XRD result, one can conclude that sample HA3 contains agglomerated nano-crystallites which, even if very well crystallized, are highly compacted (literature mentions this problem in fabricating nano-HA). The "slice" that appears on the image of the HA3 sample comes from an impurity, because it is an isolated appearance. Some results of the morphologic analysis by AFM of the HA1 sample are presented in Figure 3: image(left), measured profile (center) and 3D image (right). The AFM results confirmed the presumption of micrometric lamellas formation; the left image shows broken lamellas, which is in agreement with the SEM image for the HA1 sample, and could also be observed in the AFM 3D image (right). The profile (center image) from the selected area was recorded along the green line in the left image. The measured base-width of the crystal was around 700 nm and the maximum height of the measured lamella was around 25 nm. The measured profile is actually a reprezentation of the lamella half-cross-section, with relatively sharp lateral facets and waved top. Even if the top surface appears as smooth on the SEM images, the AFM shows that the actual surface is rather rough, which is a quality required for a bioceramic to be used in medical implants. The AFM confirms the formation of a crystalline material, with crystalls in the micrometer-domain.

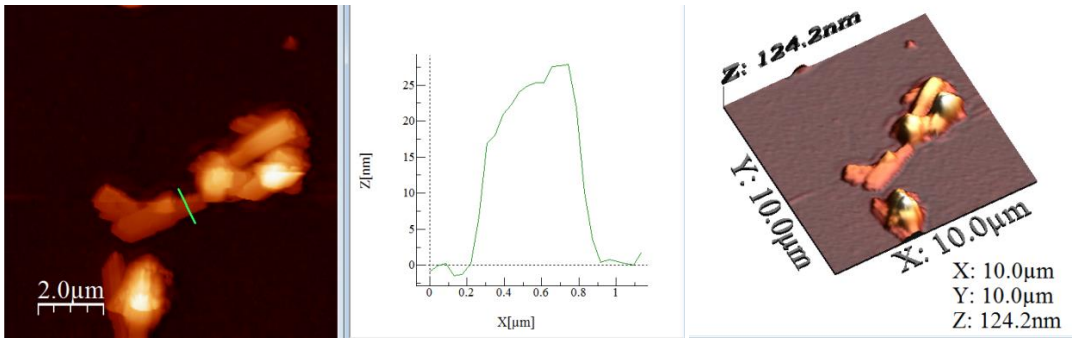

Figure 3. AFM results of the HA1 sample: image(left), profile (center) and 3D image (right)

From this study of HA synthesis and crystallization, we can conclude that variations of temperature in the range 200-230 do not introduce much difference in the results. Instead, the change of pH from 5-6 to 8 will introduce a big difference, and so is the variation in the crystallization time, from 24 to 72 hours.

Conclusions

The conclusions of this study are:

1. Crystalline rough hydroxyapatite can easily be fabricated by a facile one-step hydrothermal route
2. Temperatures in the range 200-230°C are to be used
3. pH in the range 5-6 is to be used, if micrometric crystals are desired
4. longer crystallization times lead to longer crystals (72h results are promising)
5. potential future investigation directions may regard lower temperatures crystallization (100-200°C) and/or longer time (>72h) studies

References

[1] M. Sadat-Shojai, M.-T. Khorasani, E. Dinpanah-Khoshdargi, A. Jamshidi, Acta Biomater 9(8) (2013) 7591-7621

[2] K. Agrawal, G. Singh, D. Puri, S. Prakash, J. Miner. Mater.Charact.Eng. 10(8)(2011)727-734

[3] Koutsopoulos, S, J. Biomed. Mater. Res. 62(4) (2002) 600-612

[4] V. Sinitsyna, A. G. Veresov, E. S. Kovaleva, Yu. V. Kolen'ko, V. I. Putlyaev, Yu. D. Tret yakov, Russ. Chem. Bull. International Edition 54(1) (2005) 79-86

[5] Y. Yang, Q. Wu, M. Wang, J. Long, Z. Mao, X. Chen, Cryst. Growth Des 14 (2014) 4864−4871

[6] M. Kamitakahara, T. Nagamori, T. Yokoi, K. Ioku, J Asian Ceram Societies 3(3) (2015) 287-291

[7]R. E. Riman, W. L. Suchanek, K. Byrappa, C.-W. Chen,P. Shuk, C. S. Oakes, Solid State Ionics 151 (2002), 393– 402

ENERGY HARVESTING FROM BICYCLE VIBRATIONS USING FLEXIBLE LEAD-FREE PIEZOELECTRIC MATERIALS

Bucur Raul Alin*, Farkas Iuliana, Bucur Alexandra Ioana

National Institute for Research and Development in Electrochemistry and Condensed Matter, Condensed Matter Department, No. 1 Plautius Andronescu, 300224 Timisoara, Romania.
**e-mail: raul_alin_bucur@yahoo.com*

Abstract
A piezoelectric flexible patch, based on $(K_{0.5}Na_{0.5})(Nb_{0.85}Sb_{0.05}Ta_{0.1})O_3$ doped with 0.5 mol% $GdMnO_3$ piezoelectric ceramic was studied. The ferroelectric and piezoelectric measurements performed shows good material properties of the studied compound. The application considered is an electric energy harvester from the rotation of a bicycle wheel. A maximum output power of 4.522 mW was obtained, sufficient to light a LED or charge a rechargeable battery.

Introduction
Perovskite ferroelectric materials are considered nowadays very interesting, due to their extraordinary piezoelectric proprieties, with application in the field of sensors, actuators and transducers. $(K,Na)NbO_3$ perovskite ferroelectric materials are considered promising materials as alternative environmental friendly piezoelectrics [1, 2, 3], envisioned to replace current lead based materials based on $Pb(Zr,Ti)O_3$. The latest finding shows that $(K,Na)NbO_3$ piezoceramics can reach a value for the charge coefficient of d_{33} = 490 pC/N [4], superior to some lead based compositions.
Current renewable energy technologies are based on wind power or solar energy. A new field that recently emerged is based on recovering energy from different sorts of vibration. The conversion of mechanical energy into electrical energy can be done by electromagnetic induction, electrostatic induction or by direct piezoelectric effect, using piezoelectric materials [5]. The piezoelectric materials used for electric energy harvesting can be ceramics, polymeric or composite. Functionally, there are two types of piezoelectric materials: monolithic, with one active part and bimorph, with two active components (the piezoelectric material and a metal or plastic substrate). Structurally, a bimorph can be fabricated using a polymeric material (such as PVDF [6]), a ceramic material or a mixture of piezoelectric ceramics (particles or fibers) and polymers, known as composite materials [7].
The purpose of this work is to fabricate and characterize a flexible piezoelectric materials based on $(K_{0.5}Na_{0.5})(Nb_{0.85}Sb_{0.05}Ta_{0.1})O_3$ doped with 0.5 mol% $GdMnO_3$ ceramics. The energy harvesting application proposed consists of a bicycle, where a flexible piezoelectric patch was mounted on the wheel. The AC voltage obtained was converted into DC using an electronic converter, and then the electric energy is stored in a rechargeable battery.

Experimental
A flexible piezoelectric electric energy harvester was obtained based on $(K_{0.5}Na_{0.5})(Nb_{0.85}Sb_{0.05}Ta_{0.1})O_3$ doped with 0.5 mol% $GdMnO_3$ (noted KNNST-0.5GM) piezoelectric ceramics. A solid state reaction was used to obtain the intended compound, starting from K_2CO_3 (99%; Scharlau), Na_2CO_3 (99%; Scharlau,), Nb_2O_5 (99%; Merck), Gd_2O_3 (99%; Fluka), Mn_2O_3 (99%; Sigma-Aldrich), Sb_2O_5 (99%; Merck) and Ta_2O_5 (99%; Merck). The samples were first calcined at 880º C for five hours, then mixed with a 5 mass% PVA binder, cold pressed at 200 MPa into disk samples of 10 mm in diameter and 0.5 mm thickness, and sintered at 1090°C for 3 hours. Flexible piezoelectric patches were obtained by

metal soldering a rectangular shaped piezoelectric ceramic to a thin metal plate, and then glue bonded to a large flexible fiber glass substrate. X-ray diffraction was obtained using a PanAnalytical X'Pert Pro MPD diffractometer (Netherlands). The temperature dependence of the dielectric constant and dielectric loss was obtained 1 kHz, using an Impedance/LRC meter TEGAM model 3550 (Geneva, OH, USA). The hysteresis loop was obtained at 100 Hz, using a Sawyer-Thomson capacitive voltage divider, coupled with an Atten ADS 1152CML digital storage oscilloscope (Helmond, Netherlands). The piezoelectric properties were measured using the resonance method with an impedance analyzer Agilent E5100A (Amstelveen, Netherlands).

Results and discussion

Figure 1 shows the X-ray diffraction pattern of $(K_{0.5}Na_{0.5})(Nb_{0.85}Sb_{0.05}Ta_{0.1})O_3$ – 0.5 mol% $GdMnO_3$ sintered ceramics. The pattern obtained was indexed as pure perovskite using the JCPDS-ICDD file number 01-071-2171, with a mixture of orthorhombic and tetragonal crystalline structure at room temperature, identified from the splitting of [200] and [020].

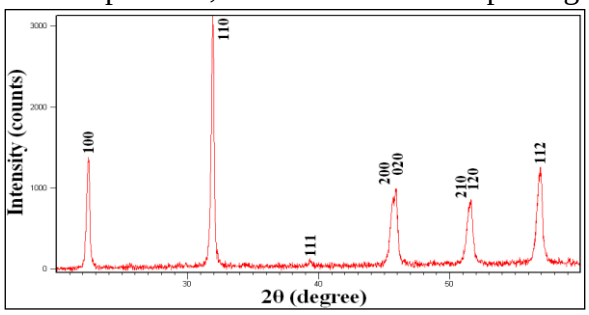

Figure 1. X ray diffractions of KNNST-0.5GM

The variation of dielectric constant and dielectric loss for KNNST-0.5GM ceramics, in terms of temperature, is presented in figure 2. The dielectric spectroscopy measurements were performed from room temperature up to 430º C, at 1 kHz. From X-ray diffraction we have concluded that the system crystallize in a mixture of orthorhombic and tetragonal phases at room temperature. At 60º C, the system re-crystallizes in tetragonal symmetry, than at 260º C, the Curie temperature of the composition, the system distorts to cubic symmetry. All phase transitions are marked by inflexions points in figure 2. Similar behavior was observed for the dielectric loss variations. At room temperature a small dielectric dissipation factor was measured, of 0.09, where at high temperature, the factor increases exponentially up to 0.22.

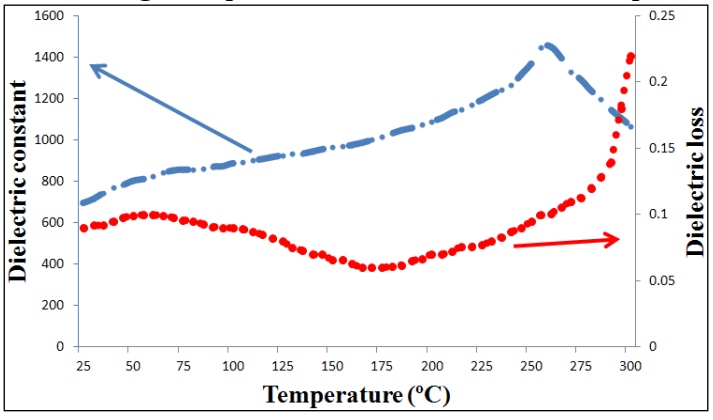

Figure 2. Temperature dependence of the dielectric constant and dielectric loss

KNNST doped with 0.5 mol% $GdMnO_3$ shows good ferroelectric properties, as proved in figure 3. The remnant polarization measured was 14.5 $\mu C/cm^2$, with a polarization saturation value of 28 $\mu C/cm^2$. Also, for a maximum electric field applied of 50 kV/mm, the coercive field measured was 14 kV/cm

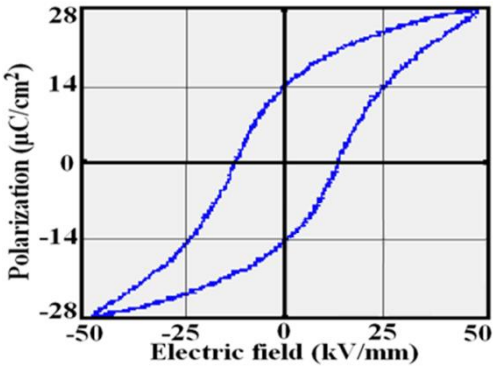

Figure 3. Room temperature hysteresis loop of KNNST-0.5GM ceramics.

After poling in silicon oil at room temperature, for 30 minutes at 4 kV/mm, the samples were aged for 1 day.For a complete determination of piezoelectric coefficients from resonance and anti-resonance curves, both radial mode and length mode oscillations were used. The piezoelectric properties are presented in table 1.

Table 1. Piezoelectric properties of KNNST-0.5GM.

Q	k_{31}	k_p	S^E_{11} [10^{-12} m^2/N]	S^E_{12} [10^{-12} m^2/N]	S^D_{11} [10^{-12} m^2/N]	d_{31} [10^{-12} C/N]	g_{31} [10^{-3} Vm/N]	k_{33}	d_{33} [10^{-12}C/N]	g_{33} [10^{-3} Vm/N]	S^D_{33} [10^{-12} m^2/N]	S^E_{33} [10^{-12} m^2/N]
102	0.18	0.41	10.5	4.6	9.98	52.3	7.3	0.43	147	10.8	11.9	13.6

In order to obtain a flexible piezoelectric patch a thin disk of 0.5 mm thick was obtained. Than it was cut into a rectangular shape and silver bonded to a thin metal sheet, serving as reinforcement for the ceramic. This subassembly was finally glue bonded to a flexible carbon fiber substrate. The length of the substrate was chosen in such a way that the transversal oscillation applied to the piezoelectric material do not produce cracks (figure 4).

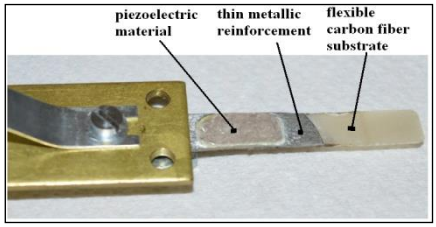

Figure 4. Flexible piezoelectric patch.

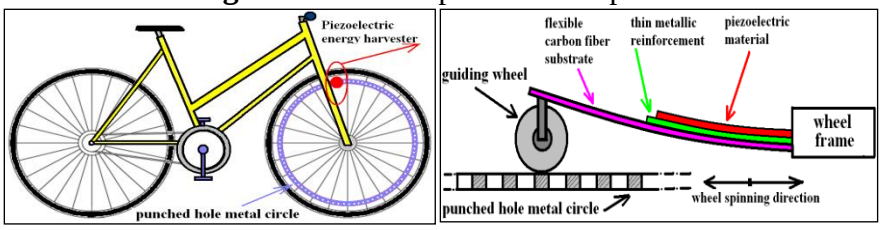

Figure 5. Design of a bicycle piezoelectric harvester

In order to obtain the vibrations needed for the patch to generate electric energy, a system based on a force cantilever was proposed, as seen in figure 5. The patch is initially compressed; the guiding wheel attached to one end of the piezoelectric patch has the possibility to roll across a fixed punched whole metal circle clamped to the wheel on the bicycle. While passing through a whole, the patch will be decompressed and the resulting internal deformation of the piezoelectric material will produce an alternative current voltage signal. The electric current obtained can be directly used to light a LED, or guided through a diode bridge to recharge a direct current battery.

The output voltage generated by the piezoelectric harvester, measured with an digital

oscilloscope is presented in figure 6. Three wheel rotational speeds were considered, for which the output power was calculated in table 2. The maximum output power obtained was 4.522 mW for the highest rotational speed. As a LED requires at optimum operation conditions around 25 mW, the output power obtain by the proposed flexible piezoelectric harvester show that lead free materials based on KNN can be successfully considered for energy harvesting, along with solar power and wind power.

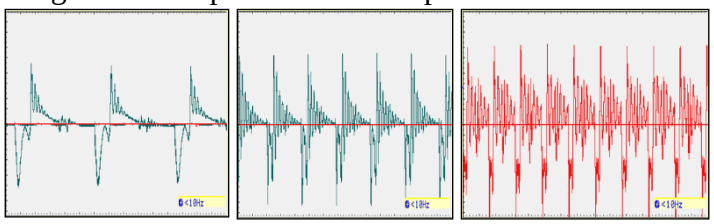

Figure 6. Mesured output voltage of the piezoelectric patch, at three wheel rotational speeds.

Table 2. Power output measured for three wheel rotational speeds.

Speed	Voltage (V)	Current (mA)	Power output (mW)
I	5.8	0.042	0.2436
II	7.4	0.180	1.332
III	10.3	0.439	4.522

Conclusion

A flexible piezoelectric patch was obtained based on $(K_{0.5}Na_{0.5})(Nb_{0.85}Sb_{0.05}Ta_{0.1})O_3$ doped with 0.5 mol% $GdMnO_3$ piezoelectric ceramics. The pattern obtained from X-ray diffraction shows a mixture of orthorhombic and tetragonal phases at room temperature, results confirmed by dielectric spectroscopy. A good ferroelectric behavior was observed, along with good piezoelectric properties. The piezoelectric harvester was mounted onto to a bicycle wheel and was able to produce a maximum power output of 4.522 mW.

References

[1] Y. Hou, M. Zhu, F. Gao, H. Wang, H. Yan, J. Am. Ceram. Soc. 87 (2004) 847–850.
[2] R.A. Bucur, A.I. Bucur, Proceedings of the 21st International Symposium on Analytical and Environmental Problems, 2015, Szeged, 147-150.
[3] R.A. Bucur, I. Badea A.I. Bucur, D. Novaconi, Proceedings of the 20th International Symposium on Analytical and Environmental Problems, 2015, Szeged, 113-117.
[4] X. Wang, J. Wu, D. Xiao, X. Cheng, T. Zheng, B. Zhang, X. Lou, J. Zhu, J. Mater. Chem. A 2 (2014) 4122–4126.
[5] S. Roundy and P. K. Wright, Smart Mater. Struct. 13(5), 1131–1142 (2004).
[6] Tim R. Dargaville, Mathias C. Celina, Julie M. Elliott, Pavel M. Chaplya, Gary D. Jones, Daniel M. Mowery, Roger A. Assink, Roger L. Clough, Jeffrey W. Martin, Sandia report, SAND2005-6846 Unlimited Release, November 2005.
[7] A. Gupta, I. Rathod, A. Sharma, International Journal in Management and Social Science Vol.03 Issue-02, February, 2015.

MAIN PHYSICAL-CHEMICAL CHARACTERISTICS OF PRESSED HAM COMMERCIALIZED IN TIMIS COUNTY

Gabriel Bujancă, Teodor Ioan Trașcă, Adrian Riviș, Alexandru Rinovetz, Corina Miscă, Corina Costescu, Călin Jianu, Ioan David, Ariana Velciov

[1]*Banat's University of Agricultural Sciences and Veterinary Medicine ofTimisoara, Faculty of Food Processing Technology, 300645-Timisoara,Calea Aradului 119, Romania, Phone: +40-256-277327; Fax: +40-256-277261,*
e-mail: gabrielbujanca@yahoo.com

Abstract
The paper proposes the study of some quality characteristics of pressed ham by standard methods of package, a widely spread product int the Western area of Romania (Timis county) as well. The samples were evaluated in terms of admissibility of sensory, physical, chemical and microbiological indicators, known by the consumer through various information methods. There have been identified and quantified, the following characteristics: water content, NaCl, NO2, fat and protein percentage, and among those with potential pathogenic microorganism interest: Coliforms, Escherichia coli, Salmonella, Staphylococcus coagulase-positive. The maximum limits for admissibility were recorded in water (75.5 to 78.4% (up to 80% max.)), NaCl (3.0-3.3% (3.5% max.)), a moderate protein (16 6% (up to 13% max.)), and modest limits lipids (3.6 to 4.0% (up to 16% max.)) and for NO2 the values are below the admissibility limit. As for microbiological analyzes, the obtained values, they prove the product as being fit for consumption.

Keywords: pressed ham, physical-chemical characteristics, quality of pressed ham, microbiological contamination of pressed ham.

Introduction
The preserving of pork leg as ***ham*** has a long history, with*Cato the Elder*writing about the "*salting of hams*" in his *De Agri Cultura* tome around 160 BC [1].
Cooked (pasteurized) and pressed ham falls into the specialties category, characterized by an exclusive presence of pork meat (pork leg). By the specific manufacturing technology, the end product, takes the form and shape of the pasteurization vessel. [2]. There is a very complex relationship between the constituents of meat products, such as moisture, protein, and fat, which provide the desired sensory attributes, especially in terms of texture (tenderness, cohesiveness, chewiness) and color [3,4]. The study characterizing the quality hams, applying a multi-disciplinary approach. Ham sensory profile depending as physico-chemical, aromatic, morphological and textural characteristics [5]. Among porcine meat products, cooked ham has the highest level of consumption in several European countries, making it an economically important product. Besides the current technological guidelines adopted in the different countries for the production of cooked ham, genetic aspects together with breeding conditions of pigs play a crucial role on the quality of finished product [6,7]. The evaluation of physicochemical detectable parameters of ham represents an important tool to define and characterize this product. For example, the moisture level measured in cured-cooked ham might represent a performing and informative parameter used to classify the product [8,9]. The final quality of the product results from a combination of different properties that involve raw and processed meat [10,11]. This research was carried out to define the quality parameters of pressed hams from pig,of different origin, and processed under commercial guidelines. Our

aim was to highlight the organoleptic, physico-chemical and microbiological characteristics of the different kinds of cooked ham and show the differences useful for characterizing the product.

Materials and methods

Materials: Six samples of pressed ham were analyzed from different producers of Timiș county. Samples were collected according to law, in the period June-July 2015.

Methods: For quality assessment of the pressed ham obtained from pork leg were checkedpackaging and labeling, organoleptic characteristics, physico-chemical and microbiological quality of six assortment of finished product. Samples were subjected to sensory (appearance, color, consistency, taste and smell), physical-chemical (water, salt, protein, fat and NO_2content) and microbiological examination (coliforms, *Escherichia coli*, *Salmonella*, Staphylococcus coagulase-positive).

Measurements were carried out according to the following standards:

- Water content: SR ISO 1442:2010;
- Sodium chloride content: SR ISO 1841-2: 2000;
- NO_2 content: SR EN 12014-3: 2005;
- Fat content: SR ISO 1443:2008;
- Coliforms: SR ISO 4831/92 and 4832/92;
- *Escherichia coli*: SR ISO 7251/96;
- *Salmonella*: SR EN 12824/2001;
- Staphylococcus coagulase-positive: SR ISO 6888/92.

Results and discussions

External examination revealed that all samples were submitted data necessary to identify the product, they were not cracked, shell was smooth and clean.The products had a round section.

The contents were examined from a sensory, physical-chemical and microbiological point of view.

Direct microscopic examination of smears made from the contents of each sample did not reveal the presence of a number of microscopic germs in the field, over the allowed limit.

Sensory characters corresponded to STAS: *appearance*: the contents of containers filled entirely, showed no air pockets, form in the section was cylindrical; *color*: light pink, specify to boiled meat; *consistency*: normal, specify to boiled meat, good behavior at slicing; *taste* and *smell*: pleasant, specifically the cooked meat and spices, without foreign taste and smell.

In the physical-chemical analysis of the samples were considered the following conditions of admissibility: Water – maximum 80%; NaCl – maximum 3.5%; Protein– minimum 13%; NO_2 – maximum 7 mg/ 100 g product; Fat – maximum 16%.

The physical-chemical and microbiological characteristics of the analyzed samples are shown in the following tables and charts:

Table1. Main physico-chemical characteristics of examined pressed ham samples

Sample / Characteristics	1	2	3	4	5	6
Water	78.4	75.6	76.0	76.6	77.2	75.5
NaCl	3.3	3.0	3.2	3.2	3.1	3.0
Proteins	13.9	16.1	16.2	15.7	15.3	16.6
NO_2	5.5	5.3	4.9	6.0	5.8	6.1
Fat	3.7	3.8	3.7	3.9	3.6	4.0

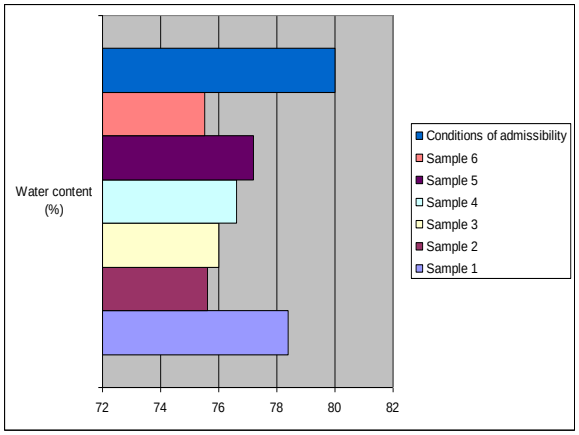

Figure 1. Water content of analyzed pressed ham samples

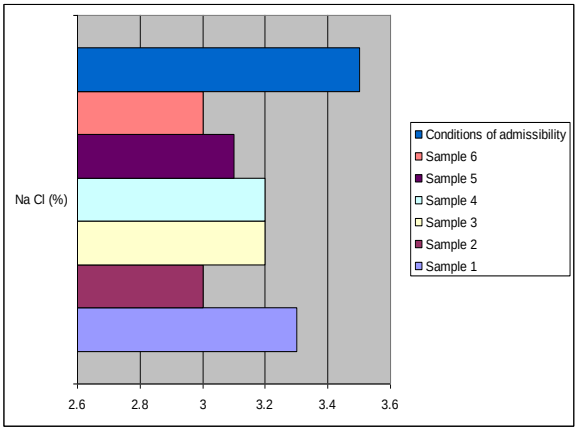

Figure 2. NaCl content of analyzed pressed ham samples

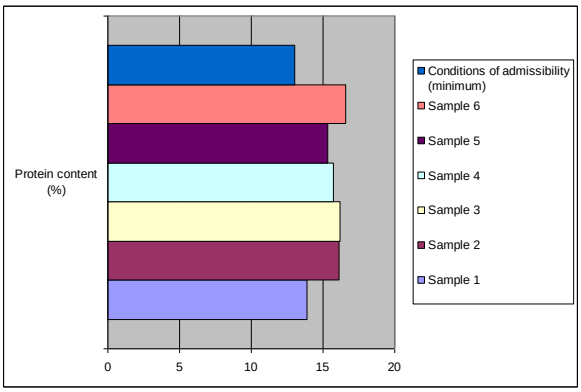

Figure 3. Protein content of analyzed pressed ham samples

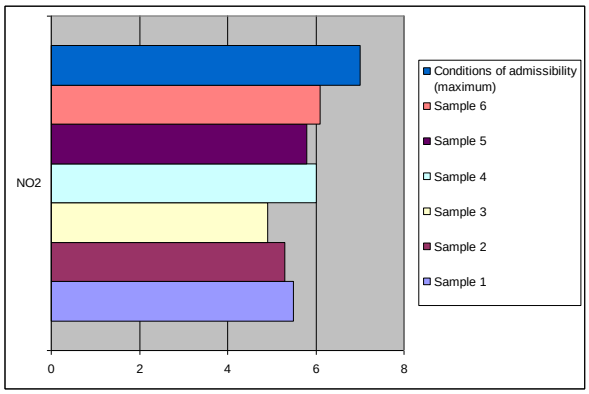

Figure 4. NO_2 content of analyzed pressed ham samples

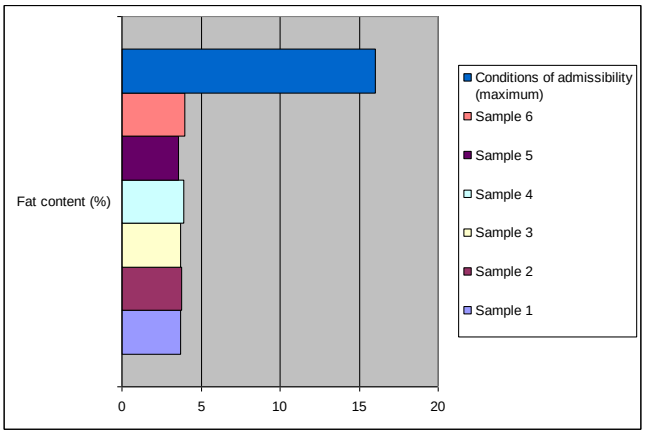

Figure 5. Fat content of analyzed pressed ham samples

Table 2. Microbiological composition of examined pressed ham samples

Sample / **Microorganisms**	**1**	**2**	**3**	**4**	**5**	**6**
Coliforms/g	53	0	31	14	67	22
***Escherichia coli*/g**	2	0	0	0	5	0
***Salmonella*/25 g**	Absent	Absent	Absent	Absent	Absent	Absent
Staphylococcus coagulase-positive	2	0	3	0	6	0

Water contained in the analyzed products did not exceed the maximum allowablelimit, values hovering between 75.5% and 78.4%.
The percentage of protein exceeded the allowable minimum limit of 13% in all cases. This demonstrates the high quality of these products.
The fat content was not exceeded in any case and so the legislation is respected.
The percentage of sodium chloride has been hovering around 3.1%, a value that is within the maximum limit of 3.5% stipulated by STAS.
Medium nitrites content was 5.6 ppm, under the 7 ppm imposed limit.
Determined microorganisms were present in very small quantities, fits within the legal limits.

Conclusions

The experimental results lead to the following conclusions:

- all analyzed pressed ham samples had labels under current law;
- packaging did not show any defect;
- the microbiological examination did not reveal the presence of any class of pathogens beyond the limits imposed by the law;
- physical-chemical parameters were within the specific limits of the product;
- analyzed products are optimal for consumption, not putting consumers' health at risk.

References

[1] Callow, E. H., 1947, British Journal of Nutrition,1(2-3), p. 269-274.
[2] Mircea, C., Tehnologia preparatelor din carne, Editura Universitatii Lucian Blaga, 2000.
[3] Francine Gomes Basso Los**,** Daniel Granato**,** Rosa Cristina Prestes**,** Ivo Mottin Demiate, 2014, Food Sci. Technol (Campinas) 34(3), 577-584.
[4] Cheng et al., 2005. Journal of Food Engineering, 67(4), 427-433.
[5] Monica Laureati et al., 2014.Meat Science, 96(1), 288–294.
[6] Lindahl, G.,Henckel, P.,Karlsson, A.H.and Andersen, H.J.,2006. Meat Sci.72, 613–623.
[7] Moretti, V. M., Bellagamba, F., Paleari, M. A., Beretta, G., Busetto, M. L., & Caprino, F. 2009.Journal of Food Quality,32(1), 125-140.
[8] Pedrelli, R.,Barbieri, G.,Franceschini, M.andPizza, A.,2005.Ind. Conserv. 80, p. 159–171.
[9] Casiraghi, E.,Alamprese, C.andPompei, C.,2006. Food Sci. Technol.40,164–169.
[10] Mcdonald, K.,Sun, D.andKenny, T.,2001.J. Food Eng.47,139–147.
[11] Santos, C.et al.,2004.Food Chem. 88, p. 123–128.

DEVELOPMENT AND VALIDATION OF NEW MULTIRESIDUE METHOD FOR THE DETERMINATION OF MULTICLASS PESTICIDE RESIDUE USING LC-MS/MS IN ONIONS

Bursić Vojislava[1], Vuković Gorica[2], Ilin Žarko[1], Jelena Perenčević[3], Adamović Boris[1], Zeremski Tijana[4], Tanasković Snežana[5]

[1]University of Novi Sad,Faculty of Agriculture, Trg Dositeja Obradovića 8, 21000 Novi Sad, Serbia
[2] Institute of Public Health, Bul. despota Stefana 54a, 11000 Belgrade, Serbia,
[3] Agricultural Professional Service Sombor, Staparski put 35, 25000 Sombor
[4] Institute of Field and Vegetable Crops, Maksima Gorkog 30, 21000 Novi Sad, Serbia
[5]Faculty of Agronomy, University of Kragujevac, Cara Dušana 34, 32000 Čačak, Serbia
e-mail: bursicv@polj.uns.ac.rs

Abstract

The LC-MS/MS was used in the ESI+ mode. The method was set for the detection of six multiclass pesticides in a single injection. The validation procedure for the method was in accordance with SANTE /11945/2015and it was carried out using blank onion samples spiked with a pesticide mix solution at four levels: 0.01, 0.02, 0.1 and 0.2 μg/mL, with carbofuran–D3 as the internal standard. The linearity of the method was investigated in the range from 0.01 to 0.20 mg/kg. The obtained R^2values for all investigated pesticides (formetanate hydrochloride, spirotetramat, spinosad, dimethomorph, metalaxyl-Mand mandipropamid)were higher than 0.99.The recoveries ranged from96.2 to 101.45 with the precision lower than 8.00%. The LODs were calculated using the Agilent MassHunter B.04.00 software, and the LOQs were experimentally set at 0.01 mg/kg.

Introduction

Onion (*Allium cepa*L.) is one of the most significant vegetables and belongs to the family *Alliaceae*[1]. Onion has weak competitive strength towards weeds which, in return, can lower the yield and the quality of the onion and in the extreme cases totally annihilate the crop. On the other hand, the onion has to be treated, against pathogens such as *Sclerotiumcepivorum, Botrytis allii*, *Botrytis cinerea*, *Botrytis squamosa*, *Peronospora destructor*, *Alternariaporri* and including viruses and bacteria. It also has to be protected against numerous pests such as species belonging to families *Scarabaeidae*, *Elateridae*, *Noctuideae*, *Triozabrassicae* and*Hylemia antique*, *Ceuthorrynchussaturalis*, *Frankliniellaoccidentalis* and *Thripstabaci*. Onion bulbs are quite often treated during the storage with the preparations containing maleic hydrazide which prevents germination[2].

Obtaining high and quality yields of agricultural plants is the ultimate goal of modern agricultural production. To achieve these results the use of pesticides is indispensable[3].In Serbia the formulations of four insecticides, 21 fungicides, 20 herbicides and two growth regulators were registered for use in onions[4].

The growing concern for human health related to pesticide residues in food, greatly changed the strategy of crop protection with a special emphesis on the quality and safety of food [5]. That is why the paper will deal with the validation of the multi-residue method for the determination of formetanate-hidrohlorid, spirotetramat, spinosad, dimethomorf, metalaxil-M and mandipropamidresidues in onions by liquid chromatography tandem mass spectrometry (LC-MS/MS) according to SANTE/11945/2015.

Materials and methods

Chemicals and apparatus. All reagents used were of analytical grade, >95% purity. Acetonitrile was purchased from Fisher Chemical (Leics, UK) and methanol (Ultra Gradient HPLC Grade) was purchased from J.T. Baker (Deventer, the Netherlands). Water was deionized (>18 M/cm) by the Elga Maxima system. QuEChERS Extraction Packets, EN Method (BondElute, P/N 5982-7550, Agilent Technologies) was used for extraction and Dispersive SPE, Fruits and Vegetables packets (BondElute, P/N 5982-5056, Agilent Technologies) for cleanup samples.The certified pesticide analytical standards of formetanate-hidrohlorid, spirotetramat, spinosad, dimethomorf, metalaxil-M and mandipropamid were purchased from Dr. Ehrenstorfer. Standard stock solutions were prepared in acetonitrile (1.0 mg/mL), while the working standard was in concentration of 10 µg/mL. This solution was used as spiking solution and also to prepare the standard solutions to obtain the calibration curves, by dilution with mixture of methanol and water (50/50,V/V; with 0.1% formic acid).

The LC-MS/MS analysis was performed on the Agilent 1200 HPLC system (Agilent Technologies, Waldronn, Germany) with an automatic degasser, a binary pump and an auto sampler connected to the Agilent 6410B Triple-Quad LC/MS system. The chromatographic separation was performed on the Zorbax XDB C18 analytical column of 50×4.6mm and 1.8 µm particle size (Agilent Technologies, the USA), which was maintained at 30 °C. The LC flow was maintained at 0.4 mL/min, the injection volume was 5 µL. The mobile phase gradient program started at 90% of B (water with 0.1% formic acid) held for 2 min, then decreases to 10% at 15 and 5% at 17 min, held for 3 min. The mobile returned to the initial composition at 5.0 min and equilibrated for another 5 min before the next injection. Electrospray ionisation was performed in the positive mode with the following parameters: resolution Q1 and Q3-wide (0.3 units) spray voltage-2000 V, gas temperature-325 °C, vaporizer-220 °C, gas flow (N_2)-5 L/min; nebuliser gas (N_2)-40 psi; the MassHunter software (version B.04. QQQ Agilent Technologies) controlled the LC-MS/MS system and processed the data. The data acquisition was in multiple reactions monitoring (MRM) mode. The ion transitions and mass parameters monitored for each analyte are listed in Table 1.

Validation

Linearity study, LOD and LOQ determinations: The evaluation of the analytical curves' linearity was done based on injections of the standard solutions prepared in organic solvent (mixture methanol and water) and also in blank union extract, atthe concentrations 10, 25, 50, 100 and 200 ng/mL, where this sequence was injected three times (n = 3). The corresponding range of pesticide concentrations in union extract were from 0.01 to 0.20 mg/kg. The limit of detection (LOD) was determined as the lowest concentration giving a response of three times the average baseline. The ratio signal/noise in the obtained chromatograms for the LOD was calculated by MassHunter Qualitative Software. The real LOQ was based on the accuracy and precision data, obtained via the recovery determinations and was defined as the lowest validated spike level meeting the requirements of a recovery within the range 70–120% and RSD≤20%.

Accuracy and precision (recovery experiments): The main goal of the recovery experiments is to determine the method accuracy, via comparison of the real concentration of each pesticide measured by performing the complete procedure with the known pesticide concentration initially added to the matrix. The method precision is expressed as the repeatability (RSD%) of the recovery determinations at the four differentspiking levels (10, 50, 100 and 200 mg/kg).The spiking procedure with 6 pesticides, added to blended and homogenized union, was done three times (n=3) at each spike level and also the blank union matrix analysis was performed two times. This blank extract was also used for preparationof standard solutions in matrix.

Extraction procedure

10g sample + 10mLMeCN + 100µL ISTD (10 µg/mL Carbofuran-D3)

↓ Shake vigorously for 1 min

Add 4g $MgSO_4$,1g NaCl, 1g Na_3Citrate dihydrate, 0.5g Na_2HCitrat sesquihydrate
Shake tube immediately for 1 min

↓ Centrifuge for 5 min at 3000 g

Transfer 5 ml of the extract into a PP tube contained $MgSO_4$,PSA
Shake for 30s

↓ Centrifuge for 5 min at 3000 g

Transfer 200µL into a vial, evaporate to dryness
Reconstitute in 200µL of mobile phaseLC-MS/MS →

Results

The validated method which uses the LC-MS/MS provides appropriate linearity, a very high sensitivity, good repeatability and can be applied with the high reliability to the analysis of pesticide residues in trace levels [7].Before the calibration andquantification of pesticides it was necessary to set an acquisition method. The determination of the acquisition method comprises: setting chromatographic conditions, determining the precursor and product ion so called monitoring mode of ion transfer (MRM or SRM), determining the fragmentation energy (Frag.) and the energy of collision cell (CE). For setting the MRM MassHunter Optimizer Softvere Version B03.01 (Agilent Technologies 2010) and Agilent G1733AA MassHunter Pesticide Dynamic MRM Database were used.

Table 1. Retention times, MRM and CE, Frag, R^2 and average recoveries of studied pesticides

Pesticide	**MRM (m/z)**	**Product ion (m/z)**	**Frag. (V)**	**CE (V)**	**Rt (min)**	**R^2**	**Avr. recovery ±RSD (%)**
formetanate	222.1	165.1 (93.1)	120	15 (36)	11.597	0.9997	98.5±4.25
metalaxil-M	280.2	220.1(192.1)	90	9 (13)	15.760	0.9978	96.2±7.19
dimethomorf	388.1	301.1(165.0)	120	30 (20)	17.024	0.9992	97.6±6.47
spirotetramat	374.0	302.0(330.0)	100	20 (20)	17.497	0.9999	99.8±5.36
mandipropamid	412.1	328.0(356.0)	100	5 (11)	18.677	1.0000	100.0±3.88
spinosad	732.5	142.0(98.0)	140	35 (55)	23.673	0.9999	101.4±2.32

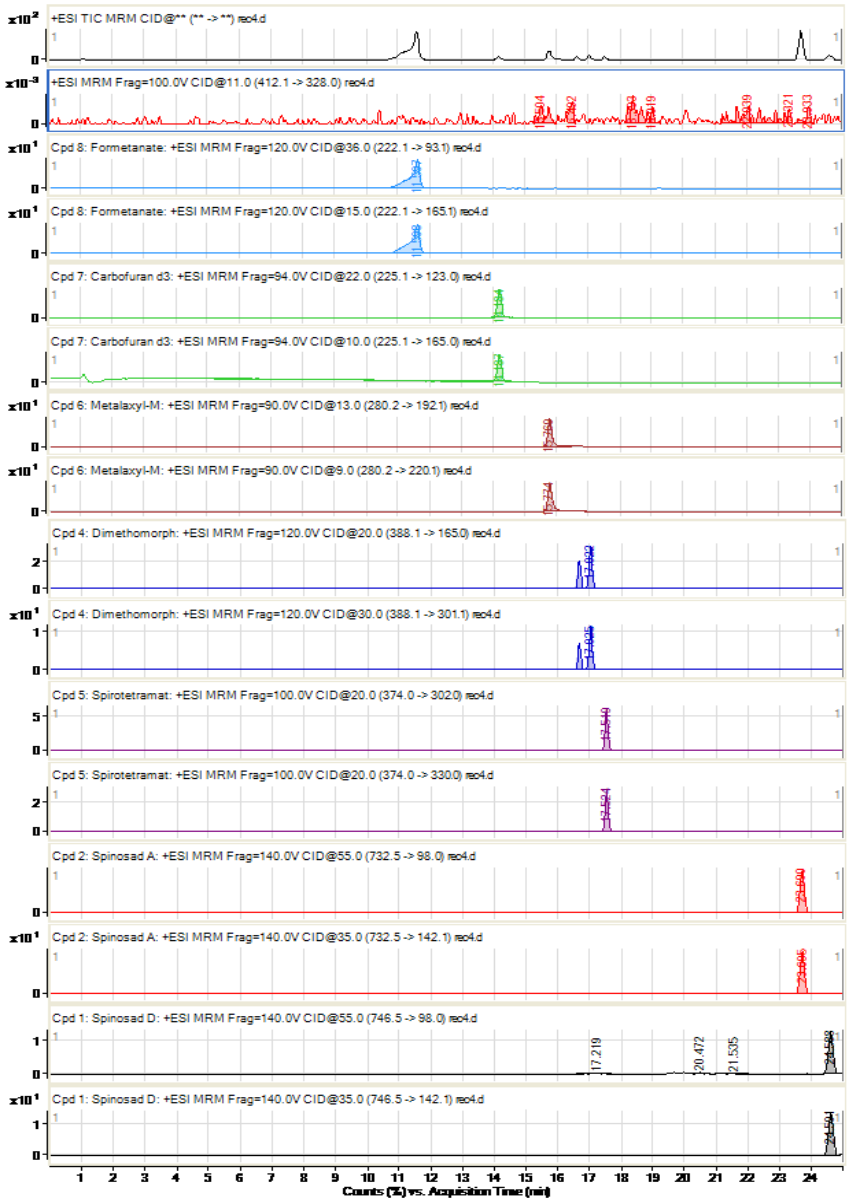

Figure 1. TIC chromatogram and MRM chromatograms of analysed pesticides

The methodlinearity was investigated in the range from 0.01 to 0.2 mg/kg. The obtained correlation coefficients (R^2) were higher than 0.99 for all investigated pesticides.The recoveries were in the 96.2-101.4% range and were characterized by precision lower than 8%.The LOQs of 0.01 mg/kg confirm that the method is appropriate for the determination of pesticide residuesaccording to the regulations of the Serbian and EU MRLs(Maximum Residue Levels).

Conclusions

A very fast, easy, cheap, robust and efficient multiresidue method, based on QuEChERS procedures and LC–MS/MS analysis, has been developed and validated for onion samples. The performance characteristics for the majority of the six studied pesticides were acceptable, according to the most recent EU guidelines for method validation. Good linearity of the calibration curves was obtained the range from 10 to 200 ng/mL, with $R^2 \geq 0.99$. Recoveries were in the range 96.2–101.4%, with RSD≤7.19%. The method has been proved to be successful as a real quantitative, multiresidue method for pesticide residues analysis in onion,

which is known to be a difficult matrix. It can be recommended for routine application in monitoring studies or surveys.

Acknowledgments
The authors acknowledge the financial support of the Ministry of Education and Science, Republic of Serbia, Project Ref. TR31036.

References
[1] Bursić V., Lazić S., Šunjka D., Ilić Z., Vuković S. (2010), Determination of maleic hydrazide residues in onion, Field and Vegetable Crops Research, 47 (1), 267-272.
[2] Ilić Z., Filipović-Trajković R., Lazić S., Bursić V., Šunjka D. (2011). Maleic hydrazide residues in the onion bulbs induce dormancy and hamper sprouting for long periods, Journal of Food, Agriculture and Environment, vol. 9 (1): 113-118.
[3]Baličević R., Rozman V., Raspudić E., Brmež M., Lončarić Z., Bursić V., Ravlić M., Sarajlić A., Lucić P. (2015): Upotreba sredstava za zaštitu bilja na obiteljskim poljoprivrednim gospodarstvima na području istočne Hrvatske. 50th Croatian and 10th International Symposium on Agriculture, Opatija, Croatia, Proceedings, 49-53.
[4] Savčić-Petrić S. (2015). Plant protection products on the Serbian market (2015), Plant Doctor.
[5] Bursić V., Vuković G., Čabilovski R., Meseldžija M., Popović A., Baličević R., Budić N. (2015). Determination of pesticide residues in *Cucurbitaceae* falily, Plant doctor, 43, 3, 272-280.
[6] SANTE/11945/2015, Guidance document on analytical quality control and method validation procedures for pesticides residues analysis in food and feed.
[7]Vuković G., Stereva D., Bursić V., Mladenova R., Lazić S. (2012). Application of GC-MSD and LC-MS/MS for the determination of priority pesticides in baby foods in Serbian market, LWT – Food Science and Technology, 49, 312-319.

EQUILIBRIUM OF PHENOL AND CHROMATE ADSORPTION ON IONIC LIQUID FUNCTIONALIZED Zn-Al LAYERED DOUBLE HYDROXIDE

Laura Cocheci, Lavinia Lupa, Alin Golban, Rodica Pode

Faculty of Industrial Chemistry and Environmental Engineering, Politehnica University of Timisoara, 300223 Timisoara, 6 Parvan Blv., Romania
e-mail: laura.cocheci@upt.ro

Abstract
A Zn_3Al-type layered double hydroxide (LDH) was impregnated with methyltri-n-butylammonium chloride (IL) in order to obtain a functionalized material (IL-LDH). Both materials were utilized as adsorbents for phenol and chromate from water. The results show that the functionalized material has better adsorption capacities than the starting material. Four equations (Langmuir, Freundlich, Langmuir-Freundlich and Redlich-Peterson) were taken into consideration in order to describe the adsorption equilibrium.

Introduction
Ionic liquids (IL) are a group of new organic salts that exist as liquids at a low temperature (<100°C). An important feature of ILs is their immeasurably low vapor pressure. For this reasons, they are called "green" solvents, in contrast to traditional volatile organic compounds. ILs have many attractive properties, such as chemical and thermal stability, nonflammability, high ionic conductivity, and a wide electrochemical potential window. Therefore, they have been extensively investigated as solvents or co-catalysts in organic and anorganic synthesis and extractants for metals and organic compounds [1-3]. The main disadvantage of ILs is the possibility of their decomposition in water with release of extractants, therefore the immobilization of the extractants in suitable supports is a solution to prevent these drawbacks [4].
Layered double hydroxides (LDH), also called hydrotalcite-like materials or anionic clays, have layered structure and tunable properties. The general formula of layered double hydroxides is:
$[M^{II}_{1-x} M^{III}_{x} (OH)_2]^{x+} [A^{n-}_{x/n} \cdot mH_2O]^{x-}$
where: M^{II} is a divalent cation (Mg^{2+}, Mn^{2+}, Zn^{2+}, Ni^{2+}, Fe^{2+}, Co^{2+}, Cd^{2+}, Cu^{2+} etc.), M^{III} a trivalent cation (Al^{3+}, Fe^{3+}, Ga^{3+}, In^{3+}, Cr^{3+} etc.) and A^{n-} charge compensating anions (NO_3^-, Cl^-, SO_4^{2-}, ClO_4^- etc.). Due to the positive charged brucite-like layer and the exchangeable anions and water in the interlayer space, these materials have attracted much attention because of their properties as catalysts, catalyst precursors, adsorbents, flame retardants and matrices for biosensors [5-9].
This paper focuses on the study of equilibrium adsorption of phenol and chromate from water. As adsorbents were utilized two materials: Zn_3-Al – layered double hydroxide and ionic liquid functionalized Zn_3-Al - layered double hydroxide.

Experimental
LDH was prepared from analytical grade reagents by co-precipitation under oversaturation method, described by Cavani et al. [10]. The molar ratio Zn^{2+} : Al^{3+} in the starting solution was 3 : 1. A part of the solid material obtained after synthesis was impregnated with methyltri-n-butylammonium chloride (IL). The impregnation method implies 10 minutes of ultrasonication using a IL : LDH ratio of 1 : 10 (w/w). The phase composition of the samples was established by X-ray diffraction using a Rigaku Ultima IV diffractometer (40 kV, 40 mA) using Cu Kα radiation. Fourier transform infrared (FT-IR) spectra were performed over a

range of wavenumber from 4000 to 400 cm^{-1} on a Shimadzu IRPrestige-21 FT-IR spectrophotometer.

All adsorption experiments were performed by contacting 50 mL of solutions containing phenol from 5 to 200 mg/L or Cr(VI) from 5 to 100 mg/L with the adsorbents samples corresponding to a solid : liquid ratio of 1g/L. The phenol and chromium removal were conducted in an batch shaker model Julabo, at 25±2 °C, in order to reach the adsorption equilibrium for 6 hours. At equilibrium, the solid was separated by filtration. Phenol and chromate concentrations in aqueous solution were spectrophotometrically determined at 510 nm and 540 nm, respectively, by means of colorimetric methods [11]. Phenol or chromium uptake by the sorbent was calculated by using the following equation:

$$q_e = (C_0 - C_e)\, V/m$$

where q_e is the adsorption loading of sorbent material at equilibrium (mg/g), V the volume of solution (L), C_0 (mg/L) and C_e (mg/L) the initial and equilibrium concentrations of phenol or Cr(VI), respectively, and m is the mass of adsorbent (g).

Results and discussion

The diffractogram of IL-LDHis presented in Figure 1.The basal peaks corresponding to (003), (006) planes, which are typical of the layered double hydroxides, were present at low 2θangle values. At 2θ angles ranging from 60 to 65° were present the peaks corresponding to (110) and (113) planes, also characteristic of the layered double hydroxides. The presence of ionic liquid at the LDH surface is envisaged by the FT-IR spectra of the materials, presented in Figure 2. The typical absorption bands for layered double hydroxides were present for both LDH and IL-LDH materials. In addition, the presence of two absorption bands of IL molecule, typical of C-H stretching modes, at 2968 and 2869 cm^{-1}, in the IL-LDH spectra confirm that the IL impregnation of LDH was successful.

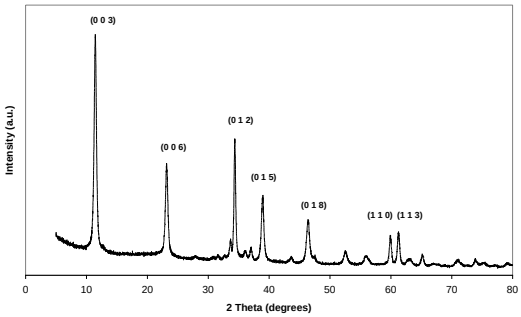

Figure 1. The XRD pattern of IL-LDH

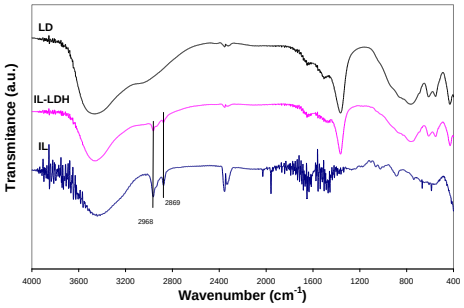

Figure 2. The FT-IR spectra of LDH, IL-LDH and IL

The results of adsorption equilibrium of phenol and chromate onto LDH and IL-LDH are presented in Figure 3 and Figure 4, respective.

The four mathematical models used to describe the adsorption behavior are presented in Table 1. The values of the equilibrium isotherm parameters and correlation coefficients obtained after non-linear regression fitting are listed in Table 2 and Table 3. The correlation coefficients are a measure of the goodness-of-fit and confirm the representation of the experimental data by the Langmuir–Freundlich model.

The maximum adsorption capacities of IL-LDH are higher that of LDH. The isotherm of phenol adsorption on LDH presented a “S” shape, that suggested a low affinity of phenol for this material, while the isotherm of phenol adsorption on IL-LDH are far from the equilibrium plateau at up 200 mg/L, the maximum concentration employed (Figure 3).

The isotherm of chromate adsorption on LDH presented a typical Langmuir plateau, while the adsorption on IL-LDH have not reach the equilibrium at up 100 mg Cr(VI)/L (Figure 4).

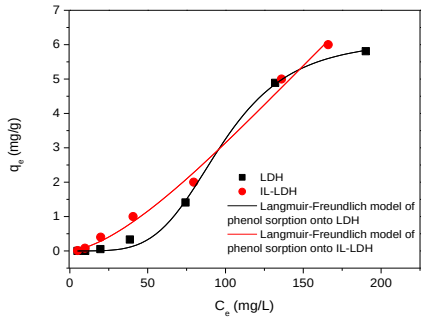

Figure 2. Adsorption equilibrium of phenol

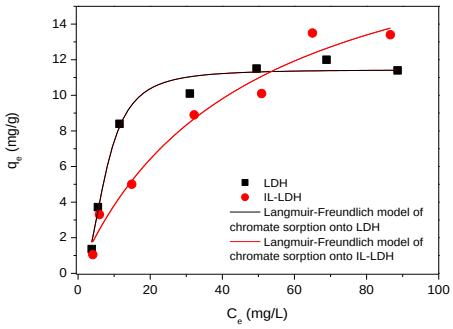

Figure 3. Adsorption equilibrium of chromate

Table 1. The mathematical expressions of the isotherms used for the modelling of the adsorption experiments

Model	Equation
Langmuir (L)	$q_e = q_{\max} \frac{K_L \cdot C_e}{1 + K_L \cdot C_e}$
Freundlich (F)	$q_e = K_F \cdot C_e^{1/n}$
Langmuir-Freundlich (L-F)	$q_e = q_{\max} \frac{(K_{LF} \cdot C_e)^n}{1 + (K_{LF} \cdot C_e)^n}$
Redlich-Peterson (R-P)	$q_e = q_{\max} \frac{K_{RP} \cdot C_e}{1 + (K_{RP} \cdot C_e)^n}$

where q_e is the sorption loading of sorbent material at equilibrium (mg/g); C_e the equilibrium concentration of Cr(VI) (mg/L); q_{max} maximum sorbed quantity (mg/g); n is the non-homogeneity factor; K – constant).

Table 2. Equilibrium isotherm parameters for phenol adsorption

Model	**q_{max}**	**K**	**n**	**R^2**
LDH				
Langmuir	16.9	$2.32 \cdot 10^{-3}$	-	0.8888
Freundlich	-	$6.16 \cdot 10^{-3}$	0.758	0.9549
Langmuir-Freundlich	6.16	32.3	2.32	0.9985
Redlich-Peterson	2.40	$1.36 \cdot 10^{-2}$	3.29	0.9837
IL-LDH				
Langmuir	119	$3.00 \cdot 10^{-3}$	-	0.9664
Freundlich	-	447	0.0926	0.9437
Langmuir-Freundlich	29.7	$5.40 \cdot 10^{-3}$	1.55	0.9947
Redlich-Peterson	24.0	$3.60 \cdot 10^{-3}$	0.56	0.9742

Table 3. Equilibrium isotherm parameters for chromate adsorption

Model	q_{max}	K	n	R^2
LDH				
Langmuir	14.0	$7.93 \cdot 10^{-2}$	-	0.9278
Freundlich	-	2.47	2.69	0.8243
Langmuir-Freundlich	11.4	$12.9 \cdot 10^{-2}$	2.39	0.9856
Redlich-Peterson	20.2	$4.06 \cdot 10^{-2}$	1.31	0.9508
IL-LDH				
Langmuir	20.9	$2.22 \cdot 10^{-2}$	-	0.9640
Freundlich	-	1.05	1.70	0.9610
Langmuir-Freundlich	21.5	$2.09 \cdot 10^{-2}$	0.98	0.9741
Redlich-Peterson	20.4	$2.32 \cdot 10^{-2}$	0.97	0.9647

Conclusion

A layered double hydroxide Zn_3Al-type was synthesized and functionalized by impregnation with ionic liquid. The two obtained materials were characterized in order to prove the layered structure and the presence of the organic compound (ionic liquid). The structural characterization confirm that the IL impregnation of LDH was successful.

The adsorption experiments of phenol and chromate on the two materials were conducted batchwise. Four equilibrium models were used to describe the adsorption behavior. The non-linear fitting of the experimental data reveals that the Langmuir-Freundlich model approximated the experimental data in all the cases.

The ionic liquid functionalized layer double hydroxide presents higher adsorption capacities that layer double hydroxide alone.

Acknowledgements

This work was supported by a grant of the Romanian National Authority for Scientific Research and Innovation, CNCS - UEFISCDI, project number PN-II-RU-TE-2014-4-0771.

References

[1] H. Zhao, S. Xia, P. Ma, J. Chem. Technol. Biotechnol., 80 (2005) 1089
[2] S. Pandey, Anal. Chim. Acta, 556 (2006) 38
[3] N. Ding, M. Li, L. Zhao, C. Lu, S.L. de Rooy, I.M. Warner, J. Hazard. Mater, 192 (2011) 1350
[4] X. Sun, Y. Ji, J. Chen, J. Ma, J. Rare. Earth., 27 (2009) 932
[5] Z. Chang, N. Zhao, J. Liu, F. Li, D.G. Evans, X. Duan, C. Forano, M. de Roy, J. Solid State Chem., 184 (2011) 3232
[6] P. Kustrowski, D. Sulkowska, L. Chmielarz, P. Olszewski, A. Rafalska-Lasocha, R. Dziembaj, React. Kinet. Catal. Lett., 85 (2005) 383
[7] F.A. He, L.M. Zhang, Compos. Sci. Technol., 67 (2007) 3226
[8] M.C. Costache, M.J. Heidecker, E. Manias, G. Camino, A. Frache, G. Beyer, R.K. Gupta, C.A. Wilkie, Polymer, 48 (2007) 6532
[9] T. Zhan, Y. Song, X. Li, W. Hou, Materials Science and Engineering C, 64 (2016) 354
[10] F. Cavani, F. Trifiro, A. Vaccari, Catal. Today, 11 (1991) 173
[11] Eaton A.D., Clesceri L.S., Rice E.W., Greenberg A.E. (Eds.), Standard Methods for the Examination of Water and Wastewater, 21th Edition, American Public Health Association, Washington, DC, 2005

EVALUATION OF PHYSICO-CHEMICAL CHARACTERISTICS FOR SOME PINEAPPLE AND MANGO FRUITE COMPOTE

Cozma Antoanela[1], Velciov Ariana[1], Petcu Mihaela[1], Cretescu Iuliana[2], Vlad D. Mircov[1], Micula Lia[1], Popescu Sofia[1*]

[1]Banat's University of Agricultural Science and Veterinary Medicine Timişoara, "King Michael I of Romania" Timisoara 119 Calea Aradului, 300 645, Timisoara,Romania
[2]Victor Babes University of Medicine and Pharmacy from Timisoara, Romania
e-mail: antoanelacozma@yahoo.com, sofiapopescu@yahoo.com

Abstract
Fruits are vegetable foods that can be consumed both fresh or processed into juices, syrups, jams, fruit compotes, etc.A popular form often used for preserving fruit in cold periods, are fruit compotes. Pineapples and mango fruit are consumed fresh, cooked, juiced and also can be preserved. The aimof the study was to evaluate physicochemical characteristics (pH, total soluble solids (TSS), conductivity and viscosity) in case of some exotic fruit compotes. In the experimental part were analyzed different samples of pineapple and mango fruit compote prepared by us, simply just from fruit, with sweetener and with the addition of brown sugar. The pH was measured using a pH meter mark OP-211/2 connected with combined electrode OP-0808P according to the AOAC methods, the total soluble solids using a refractometer Abbe. Electrical conductance was determined by conductometer OK 112 and viscosity using Ubbelohde-type viscometer.

Introduction
Increasing tendency for fruits consumption worldwide and also inour country showsthe weight thatthey haveheldor holdthem inour diet. In case of fruits, not onlygood looks, nicecolorortasteand aromasareconsidered to be important, but especiallytheir nutritional value,richin sugars,vitaminsand mineralsneededin the diet ofthe human body.The fruit represents the group of foods with vegetable origin, very precious from nutritional point of view, rich in carbohydrates, cellulose, minerals and organic acids, needed daily for the human body. Being sources of vitamins: A, B1, B5, C, enzymes and fiber, they should not be missing from a rational nutrition. [6].Fresh fruit represents the products of great importance in the rational diet, and for the fact that in certain periods are missing, they should be consuming preserved in various forms.The fruits are foods that can be consumed both fresh or processed (preserved) into different types of sorts like juices, syrups, jams, fruit compotes, etc. [3].A popular form often used for preserving fruit are fruit compotes. Fruit compotes are canned food prepared from whole fruit divided into a sugar syrup through thermal treatment packed and hermetically closed. Have been developed methods that do not reduce the qualities and value of fruit and the addition of sugar, pectin, or some food acids, improves taste and increases their energy value. [5].
Also the addition of sugar syrup determines a significantly improved alkalinity of the product and also allows the consumption of the product. The fruit compote is considered one of the most healthiest, very popular food in autumn and winter being found in the cuisine of many nations. Pineapple [*Ananas comosus* (L.) Merr. Family:Bromeliaceae] and Mango [*Mangifera indica*(L.) Merr. Family:Anacardiaceae] are the third most important tropical fruit in the world after Banana and Citrus. They have exceptional juiciness, vibrant tropical flavor and immense health benefits. Pineapple and mango fruit is a rich source of natural antioxidant, vitamins and minerals having good nutraceutical and medicinal value**.** [4]. Mature fruit contains 14% of sugar, a digesting protein enzyme, bromelain, and also citric and malic acid, vitamin A and B,

copper, manganese and dietary fibre. Fresh pineapple contains minerals as Calcium, Chlorine, Potassium, Phosphorus and Sodium [6].Pineapple contains considerable amount of calcium, potassium, vitamin C, carbohydrates, crude fibre, water and different minerals that is good for the digestive system and helps in maintaining ideal weight and balanced nutrition.The fruit compote is not only tasty but also very healthy because can add missing vitamins diet during the cold season and may well have other curative properties.

Experimental

The aimof the study was to assess the physicochemical characteristics pH, total soluble solids content (TSS), electrical conductivity (G) and viscosity (η) in case of some exoticpineapple and mango fruit compotes.

In the experimental part were analyzed different samples of pineapple and mango fruit compote prepared by us, simply just from fruit, with sweetener and with the addition of brown sugar. Pinneaple and mango fruit were purchased from a hypermarket in March 2016 in the city of Timisoara (Romania). pH represents a measure of the acidity or basicity of a solution. It was defined as the cologarithm of the activity of dissolved hydrogen ions (H+).The pH of the juices was measured using a pH meter mark OP-211/2 connected with combined electrode OP-0808P according to the AOAC methods.The total soluble solids (TSS)and the refractive index were obtained using the refractometry method with the Abbe refractometer corrected to the equivalent reading at 20°C (AOAC, 1995).Electrical conductance (G) was determined by conductometer OK 112 and viscosity using the Ubbelohde-type viscometer.

Results and discussion

Figures1 to 4 show the effect of the different type of fruit compote on theanalyzedphysicochemical characteristics. The fruite compote was prepared in March.

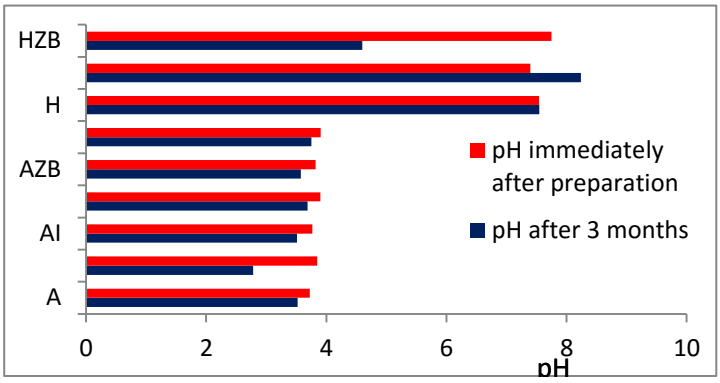

Figure 1. Determination of pH in case of different type of compote samples

From figure 1 we can see thatthevalue of pH decreases from March to June. In March the obtained data provide similar pH values,the lowest pH value was obtained forpineapple fruit compote with sweetener (3.77) and the highest value formango with brown sugar (3.91).

The lowest values of ph were obtained for the mango compote in June(2,783)and the highest value of pH is on mango with brown sugar (3,75). The pHvalue decrease from March to June and the explanation is due to the fermentationprocess. The addition of other compounds (sweetener or brown sugar) in the fruit processing help to conserve the compote caracteristics (pH) for a longer time.

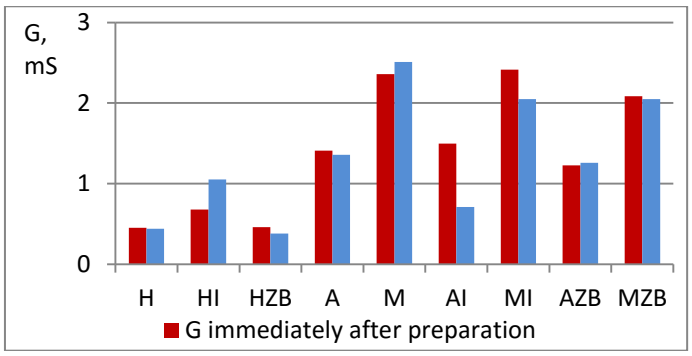

Figure 2. Determination of conductivity for different type of compote samples

In March the lowest value of the conductivity was obtained for the pinneaple fruit compote (1,41mS) and the highest value for mango with sweetener (2,41mS) while in June the lowest value was determined for the pinneaple fruit with sweetener (0,71mS) and the highest electric conductivity was obtained for mango with sweetener (2,05 mS). After 3 month the values shows that the conductivity decrease for the sweetener and brown sugar fruit compotes.

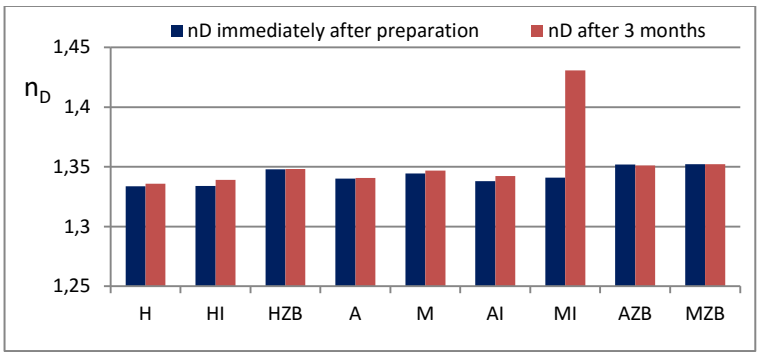

Figure 3. Determination of the refractive index for the different type of compote samples

Pineapple contains 81.2 to 86.2% moisture, and 13-19% total solids, of which sucrose, glucose and fructose are the main components [4]. Sugar (sucrose) is a carbohydrate which naturally occurs in fruits and vegetables.[2].Carbohydrates represent up to 85% of total solids where as fibre makes up for 2-3%. The refractive index of a carbohydrate solution increases with the concentration increasing. High concentration of sugar in fruit samples gives high value of refractive index and brix. TSS varies from 10% to 14% brix depending upon the stage of maturity and season [1]

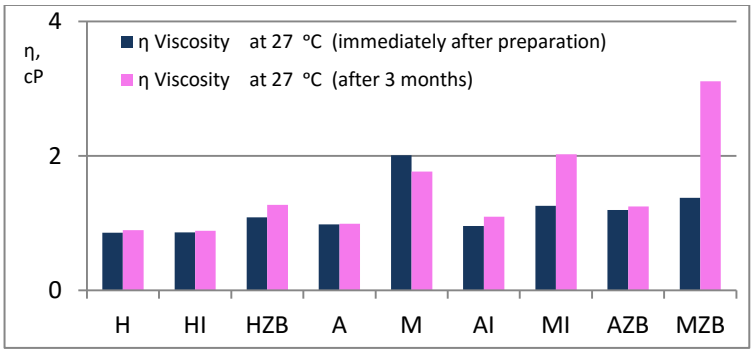

Figure 4. Determination of viscosity for different type of compote samples

The results obtained in March and June shows that the viscosity of the compote in case of sweetener and brown sugar adittion increase in this period (3 month) because of a higher level of glucides.The increasing is more visible for the mango fruit compote.

Conclusion

The addition of sweetener and brown sugar in fruit samples preserved better the fruite compote, **pH** is more stabile while electric conductivity **(G)** and refractive index **(n)**values presents small differences between samples.The viscosity increase in the samples with the sweetener and brown sugar addition, after 3 month. The effect on the viscosity is more visible on the mango compote with brown sugar followed by sweetener.

The effect of different type of fruit compote on theanalyzedphysicochemical characteristics is more significant for the pH and viscosity values.

References

[1] Cretescu Iuliana, Caprita Rodica, Munteanu Oana, Velicevici Giancarla, Duma-Copcea Anisoara, Cozma Antoanela, 2014,Determination of total soluble solid (TSS) in concentrated and diluted fruit juices by refractometric method, PROCEEDINGS of the international conference — „Horticulture in quality and culture of life „

[2] Cozma Antoanela,Petcu Mihaela, Velicevici Giancarla, Cretescu Iuliana, Evaluation of physicochemical characteristics on commercially available carrot juice and carrot juice mixed with other fruit, Journal of Horticulture, Forestry and Biotechnology, Volume 19(1), pag.158-161, 2015.

[3] Cretescu Iuliana, Petcu Mihaela, Cozma Antoanela, Velicevici Giancarla - Evaluation of physicochemical characteristics of some commercially available fruit compote, Research peopleand actual tasks on multidisciplinary sciences 24-28 June 2015, Lozenec, Bulgaria

[4]Md. Farid Hossain, Shaheen Akhtar, Mustafa Anwar - Nutritional Value and Medicinal benefits of Pineapple, International Journal of Nutrition and Food Sciences, 2015; 4(1): 84-88, Science Publishing Group

[5]Joy, P.P. 2010. Benefits and uses of pineapple. Pineapple Research Station, Kerala Agricultural University, Kerala, India[http://www.kau.edu/prsvkm/Html/BenefitsofPA.htm]

[6]Dull, G. G. 1971.The pineapple: general. In: A. C. Hulme (Ed.). The biochemistry of fruits and their products, Academic Press, New York. vol. 2: p. 303-324.

$Y_{0.5}Ca_{0.5}BaCo_4O_7$ PEROVSKITE ELECTRODES WITH CATALYTIC EFFECT FOR METHANOL AND ETHANOL ELECTROOXIDATION IN ALKALINE MEDIA

Victor Daniel Craia-Joldes, Mircea Laurenţiu Dan, Delia Andrada Duca, Nicolae Vaszilcsin

University Politehnica Timişoara, Faculty of Industrial Chemistry and Environmental Engineering, 300223, Parvan 6, Timisoara, Romania
e-mail: daniel.craia@fitt.ro

Abstract
In this paper, preliminary data of methanol and ethanol anodic oxidation on $Y_{0.5}Ca_{0.5}BaCo_4O_7$ perovskite electrode in aqueous alkaline solution (1 M KOH) are presented. Electrocatalytic activity of methanol and ethanol anodic oxidation becomes a serious issue, especially due to the utilization of 114 layered cobalt perovskite electrodes in fuel cells. In order to elucidate the mechanism of methanol (MOR) and ethanol oxidation reactions (EOR) which occur at this perovskite electrodes interface, advanced studies are required. Electrochemical behavior has been studied by cyclic voltammetry, chronoamperometry and chronopotentiometry. Obtained results have shown that $Y_{0.5}Ca_{0.5}BaCo_4O_7$ perovskite electrodes are suitable as anodes in fuel cells.

Introduction
Direct alcohol fuel cells (DAFCs) are electrochemical devices that convert the chemical energy of methanol and ethanol electrooxidation in electrical one [1]. DAFCs are promising auxiliary power sources in transportation, portable electronics, and other modern applications [2,3]. They belong to alkaline fuel cells (AFCs) family [4]. Methanol and ethanol electrooxidation efficiency is a continuous challenge from research point of view. Platinum is known for its highest catalytic activity of MOR and EOR compared to other pure metals in alkaline media. An advantage of alkaline fuel cells is the potential use of non-Pt catalysts as electrodes [5]. Noble metal (Au) and non-noble metals (Cd, Pb, Bi, Ti) were investigated as anode for alcohol oxidation in alkaline media [4]. Latterly, electronically conducting mixed oxides were tested as anode materials; oxides of V, Fe, Ni, In, Sn, La and Pb were used [6]. In recent years, studies on various transition metal mixed oxides have shown that perovskite oxides can be used as fuel cell electrodes [6].
In this paper, new aspects of MOR and EOR on $Y_{0.5}Ca_{0.5}BaCo_4O_7$ electrode have been studied using cyclic voltammetry. Also, a mechanism was proposed for both electrochemical oxidation reactions. The results are expected to provide basic information in order to understand the mechanism of MOR and EOR on cobalt layered perovskites type 114 electrodes.

Experimental
$Y_{0.5}Ca_{0.5}BaCo_4O_7$ perovskite was obtained using solid state reaction, mixing Y_2O_3, $CaCO_3$, $BaCO_3$ and $CoO_{1.38}$ precursors (all reagents were Aldrich p.a. min 99,99%) according to the stoichiometric cations ratio. Perovskite powder was prepared in two steps: decarbonation at 600°C, fired in air for 48 h at 1100°C and then quickly removing from furnace and set room temperature. After reground, the mixture was pressed into discs (1 cm^2) and sintered at 1100°C for 24 h in air.
Electrochemical tests were performed at room temperature using a SP-150 potentiostat/galvanostat (Bio-Logic, SAS, France). A 100 mL typical glass cell was equipped with three electrodes: working electrodes consisting of $Y_{0.5}Ca_{0.5}BaCo_4O_7$ perovkites samples,

Ag/AgCl reference electrode (E_{ref} = 0.197 V vs NHE) and two graphite rods counter electrodes. In electrochemical experiments, the exposed surface of working electrode was 0.2 cm^2. All potentials are given versus the reference electrode.
Cyclic voltammograms (CVs) were recorded at different scan rate, between 5 and 500 mV s^{-1}. 1 M KOH solution (prepared using Merck KOH, p.a.) ensured the alkaline media used in all experimental studies, in which 0.06 M methanol and ethanol concentration was added, prepared from Sigma-Aldrich reagent p.a. min 99.8%.

Results and discussion
Figures 1 and 2 presents CVs recorded at different scan rates, between 500 and 5 mV s^{-1}, in alkaline solutions, in a wide range of the potential (+1.75 and -1.75 V), in the presence of methanol (Figure 1) and ethanol (Figure 2). It can be observed a significant anodic peak between -0.50 and +0.25 V and a cathodic current plateau in -1.25 – -1.70 V potential range. These are associated to formadehyde/formate redox couple in alkaline medium for methanol solution, acetaldehyde/acetate redox couple for ethanol solution and Co(II) to Co reduction/oxidation for KOH solution. MOR and EOR characteristic peaks are distinguished only if scan rare is less than 10 mV s^{-1}.

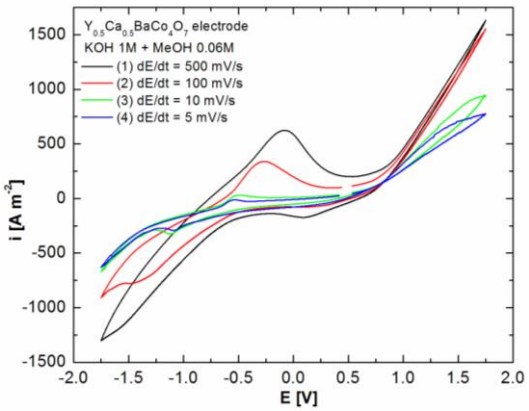

Figure 1. CVs recorded on $Y_{0.5}Ca_{0.5}BaCo_4O_7$ electrode in 1 M KOH with 0.06 M methanol at different scan rates.

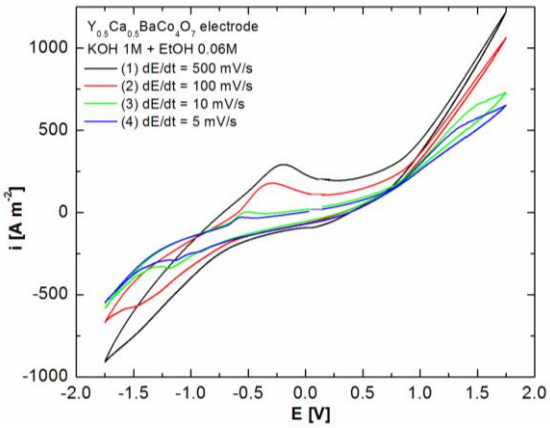

Figure 2. CVs recorded on $Y_{0.5}Ca_{0.5}BaCo_4O_7$ electrode in 1 M KOH with 0.06 M ethanol at different scan rate.

Cyclic voltammetric studies have shown that it is possible to separate the peaks associated with the all electrochemical processes occurring at the interface perovskite electrode-alkaline electrolyte only if the potential scan rate is around 5 mV s^{-1}, as shown in Figure 3.

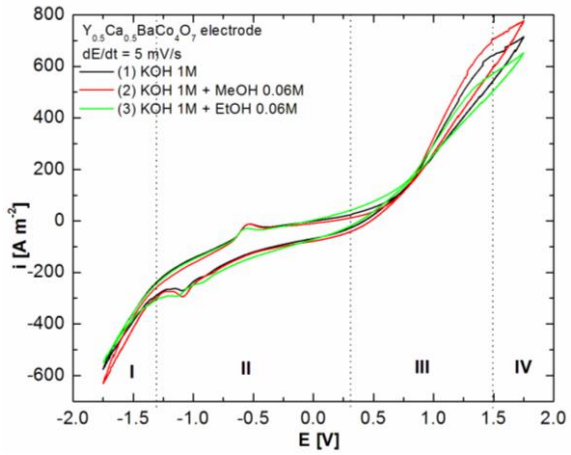

Figure 3. CVs recorded on $Y_{0.5}Ca_{0.5}BaCo_4O_7$ electrode in 1 M KOH in the absence (1) and in the presence of 0.06 M methanol (2) and ethanol (3), at 5 mVs^{-1} scan rate.

Analysing CVs depicted in Figure 3, there is possible to partition the voltammograms in four potential domains:

I - HER domain;

II - Co^{2+}/Co redox couple domain in alkaline solution from inside of perovskite (1), formaldehyde/formate (2) and acetaldehyde/acetate (3) ions redox couple domain;

III – Co^{2+} oxidation to Co^{3+} in $Y_{0.5}Ca_{0.5}BaCo_4O_7$ electrode (1), MOR (2) and EOR (3) on 114 layered cobalt perovskite surface domain;

IV - OER domain.

Variation of open circuit potential (OCP) after cyclic voltametric experiments for $Y_{0.5}Ca_{0.5}BaCo_4O_7$ electrode in alkaline solution without and with methanol and ethanol are presented in Figure 4. Chronopotentiometric measurements were performed for 60 minutes.

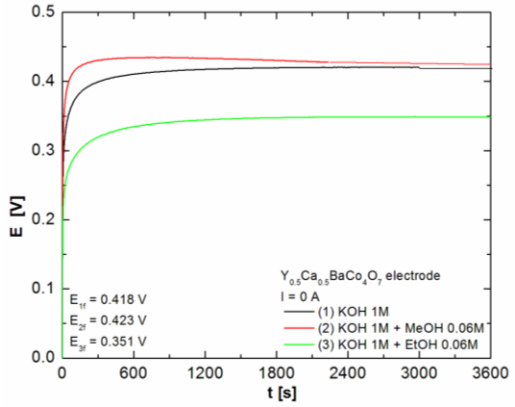

Figure 4. OCP for $Y_{0.5}Ca_{0.5}BaCo_4O_7$ electrode in 1 M KOH (1) without and with 0.06 M methanol (2) and ethanol (3).

Chronoamperometric studies had as starting point the CVs shown in Figure 3. Analysing these curves, +0.75 V potential value, corresponding to the MOR, OER and perovskite oxidation in alkaline solution (domain III from Figure 3) was chosen to carry out the chronoamperometric measurements. The results are presented in Figure 5 for 60 minutes oxidation time.

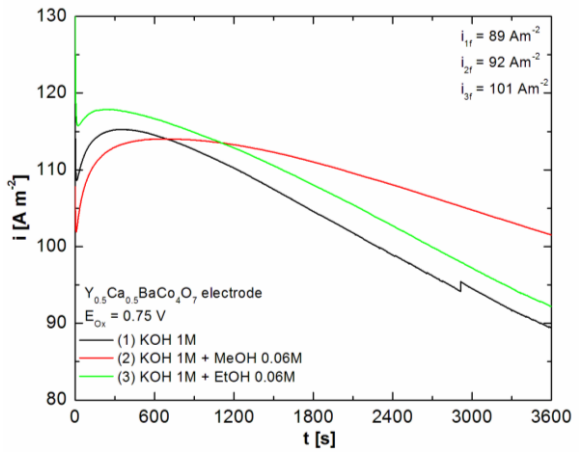

Figure 5. Chronoamperometric measurement at E = + 0.75 V for $Y_{0.5}Ca_{0.5}BaCo_4O_7$ oxidation (1), MOR (2) and EOR (3).

Conclusion

Preliminary data presented in this paper confirmed the possibility to oxidize methanol and ethanol in alkaline media on an $Y_{0.5}Ca_{0.5}BaCo_4O_7$electrode. The potential domain for MOR, EOR and $Y_{0.5}Ca_{0.5}BaCo_4O_7$perovskite oxidation in alkaline electrolyte is the same.

From the perspective of using this electrode type as anode material in alkaline direct alcohol fuel cells with methanol or ethanol electrolyte, the possibility to oxidize alcohols directly on their surface offer a good reason to continue experimental studies in this domain.

Acknowledgements

This work was partially supported by University Politehnica Timisoara in the frame of PhD studies.

References

[1] E. Antolini, J. Power Sources 170 (2007) 1.
[2] C. Lamy, A. Lima, V. LeRhun, F. Delime, C. Coutanceau, J.M. Leger, J Power Sources 105 (2002) 28.
[3] C. Bianchini, P.K. Shen, Chem. Rev. 109 (2009) 4183.
[4] A. M. Sheikh, K. Ebn-Alwaled Abd-Alftah, C. F. Malfatti, JMEST, 1(3) (2014) 1.
[5] E. Antolinia, E.R. Gonzalez, J Power Sources 195 (2010) 3431.
[6] M.S. Ekrami-Kakhki, Z. Yavari, J. Saffari, S. Ali Ekrami-Kakhki, JEE 4 (2016) 88

BEHAVIOR OF BIPYRIDINE DERIVATIVE Cu(I) COMPLEXES IN DONOR SOLVENTS

Carmen Cretu[1*], Diana Aparaschivei[1], Valentin Badea[2], Elisabeta I. Szerb[1], Otilia Costisor[1]

[1]*Institute of Chemistry of the Romanian Academy, 24 Mihai Viteazu Bvd., 300223-Timisoara, Romania,*
[2]*Faculty of Industrial Chemistry and Environmental Engineering, University Politehnica Timisoara, 2 Vasile Pârvan Bvd., 300223-Timisoara, Romania*
e-mail: cretucami@yahoo.com

Dedicated to the 150th anniversary of the Romanian Academy

Abstract
Cu(I) complexes are known as highly emissive compounds having interesting fluorescence applications[1].Theluminescence is generated by more intense metal to ligand charge transfer (MLCT) electronic transitions for Cu(I), affording longer excited-statelifetimes compared to transient d-d excited state of Cu(II)[2].Herein we report the behavior of two bipyridine derivative Cu(I) complexes containing phenanthroline and biquinoline ligands, respectively, in donor solvents as dimethylsulfoxide and acetonitrile.The Cu(I) phenanthroline complex (**1**) is unstable in solution,due to oxidation of Cu(I) to Cu(II) in time, accompanied by change in coordination geometry from tetrahedral to trigonal bipyramidal. The Cu(I) biquinoline complex (**2**) is more stable in donor solvents,the stability increasing at low temperatures with the stabilization of tetragonal geometry of Cu(I).In case of biquinoline ligand, this kind of geometry is stabilized by the bulky aryl substituentsatαposition with respect to the pyridine nitrogen.

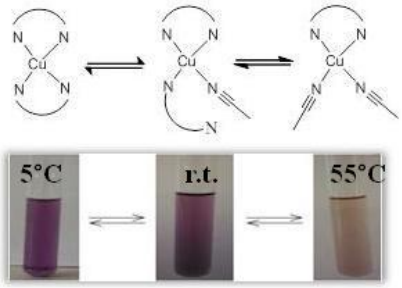

The proposed mechanism of dissociation of **2** in AcCN with increasingtemperature

Acknowledgment
We are thankful to the Romanian Academy (Project 4.1.) for the financial support.

References:

[1] J. Nitsch, C. Kleeberg, R. Fröhlich, A. Steffen, *Dalton Trans.* 44(15) (2015) 6944.
[2] N. Armaroli, G. Accorsi, F. Cardinali and A. Listorti, in Photochemistry and Photophysics of Coordination Compounds I, ed. V. Balzani and S. Campagna, 280 (2007) 69.

A LOW COST LINEAR PARABOLIC CONCENTRATOR SYSTEM– PHOTOREACTOR FOR PHOTOCATALYTIC PROCESSES THAT USES NATURAL SOLAR LIGHT

Daniel Ursu[1], Cristina Mosoarca[1*], Radu Banica[1]

[1]*National Institute for Research and Development in Electrochemistry and Condensed Matter, no 144 A. PaunescuPodeanu Street, Timisoara 300569*
e-mail: mosoarca.c@gmail.com

Abstract
PdS/CdS based photocatalysts exhibit high efficiency in water splitting reaction. Due to the fact that the band gap value of CdS is 2.4 eV, the photocatalytic process may be performed using visible light at temperatures between 20 and 80°C. From our previous work we noticed that the yield of water splitting process, using this type of photocatalysts increases with the increase of temperature from 20 to 60°C. To increase the temperature of the photocatalystsuspension at higher values than the environment temperature, an irradiance greater than 1000 W/m^{2}is needed. In this paper we present the design and construction of an inexpensive solar collector –photoreactorassembly, by which the optimal temperature of photocatalystsuspension can be maintained,even in low solar irradiance conditions.

Introduction
Photocatalysisthat uses solar energy is utilized the most often todegrade the wastewater organic content into carbon dioxide and water and in the water splitting reaction [1]. For these processes the following types of photoreactors[2] are used: Inclined Plane Photoreactor, Double Skin Sheet Photoreactor and Parabolic trough Photoreactor. The first two types of photoreactors do not need the solar tracking devices. The Parabolic trough Photoreactor needs, at least one axis tracking system. The Inclined Plane Photoreactor and the Double Skin Sheet Photoreactor can utilize the direct and diffuse radiation. Due to the fact that they do not use concentrated solar light, these photoreactors cannot function at temperatures much higher than that of the environment. Also the functioning of these photoreactors during the winter is problematic. The Parabolic trough Photoreactor functions in concentrated light making the high temperature photocatalysis possible, also a fraction of the solar energy may be saved as heat [3]. In this study a low cost tubular photoreactor – linear parabolic concentrator assembly is presented. This system is utilized for the water splitting reaction with simultaneous heat recovery.

Experimental
In this paper we are presenting the design and construction of an inexpensive linear parabolic concentrator – photoreactor system, which can be utilized for photocatalytic processes that need natural solar light. The total price of the concentrator – photoreactorsystem is lower than 200 Euros.Due to the fact that the photocatalytic process is a discontinuous one(determined by the necessity of the photocatalyst periodic replacement) the photoreactor design has to fulfill at least some criteria, like: the photocatalytic process must take place in a visible range transparent flask apart from the photocatalystfueling tank, the separation and storage of the produced hydrogen and the simple and efficient delivery.In order to satisfy these necessities, the constructive solution of a tubular, glass photoreactor, equipped with a cooling mantle, positioned in the focus of a cylindrical parabolic concentrator, was chosen. This set-up is placed on a dual axis solar tracker device. The system has two recirculating fluid pumps, one dedicated to the photocatalyst suspension and the other to the cooling fluid.

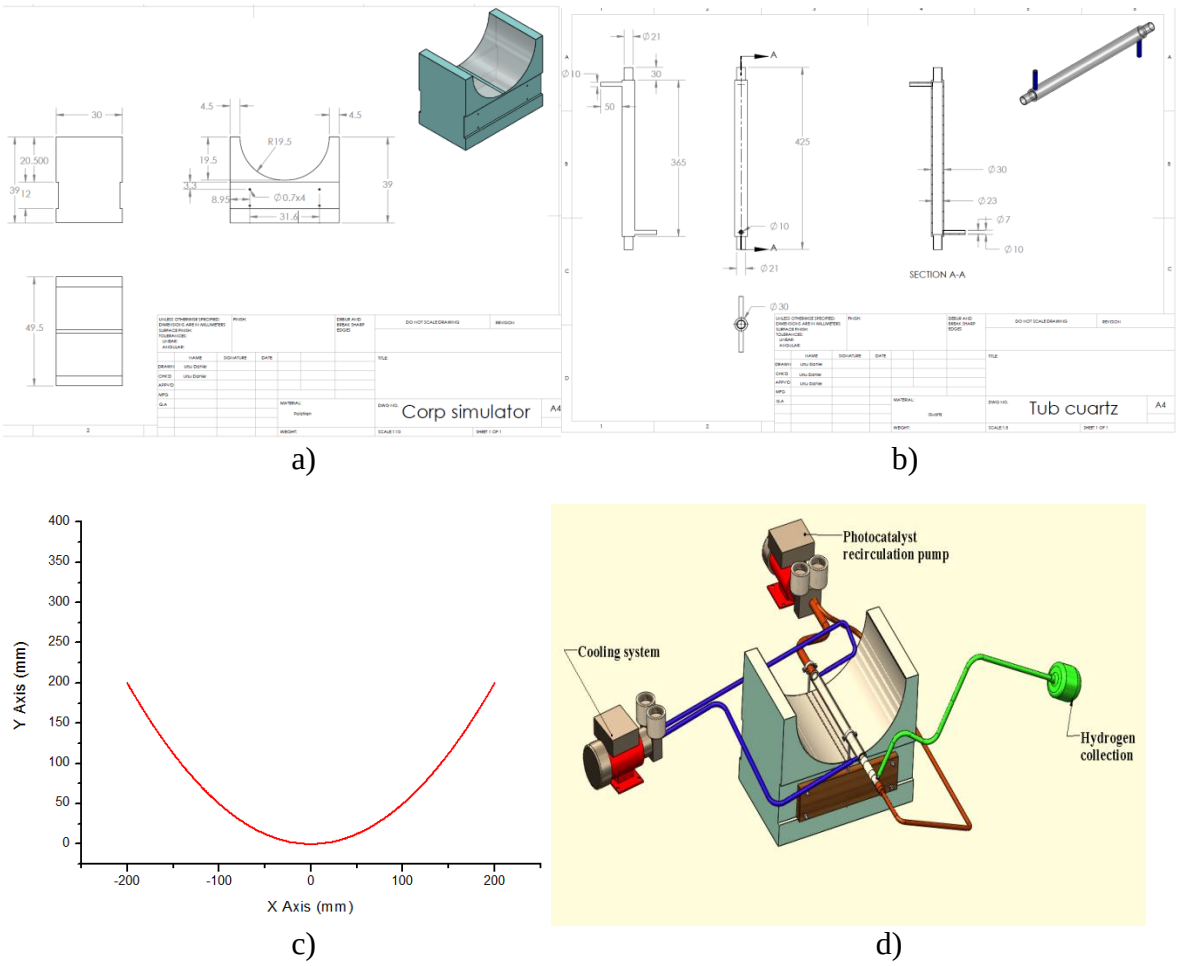

Fig. 1. Constructive sketches of the radiation caption body (a), the light collection tube (b), the details by which the parabolic body was cut (c) and of the 3D assembly (d)

The radiation collector tube (figure 1b) is made from borosilicate glass and has two entries and two exits for two recycling pumps mounting, one for the photocatalyst suspension and the second for the cooling water recycling. On the branch of cooling water recycling, the mounting of an air-water heat exchanger is necessary. A tank,having thermal buffer role,may be integrated in the system for avoiding the high temperature variations during its adjustment with the help of a PID controller.The linear parabolic body was cut in expanded polystyrene and covered with aluminum foil having 94% reflectance at a 500 nm wavelength. The parabolic concentrator has a 400 mm diameter and a depth of 200 mm. The focal axis is placed at a 50 mm distance from the bottom. The length of the linear parabolic body is 300 mm.

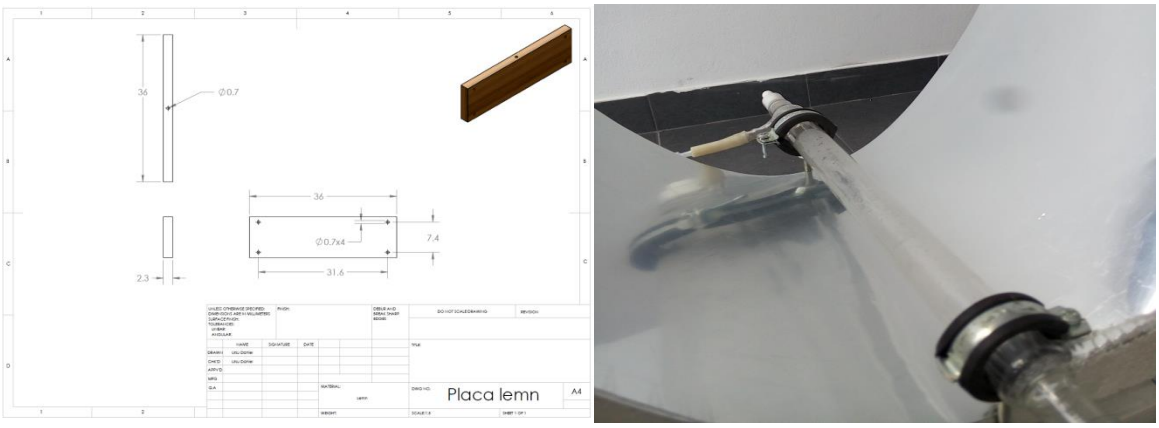

a) b)

Fig. 2. The construction sketch for the wooden boards (a) and parabolic concentrator – photoreactor overview

The glass photoreactor with cooling mantle is mounted with the help of two metallic rings through the medium of two threaded bars fixed in two wooden boards (figure 1d and 2a). These are attached on the sides of the polystyrene body, so as to the glass photoreactor can be lowered towards the bottom of the concentrator, into the focus.

Conclusions

In this paper, theconstruction sketches, for a linear parabolic concentrator system – photoreactor assembly, with a cost lower than 200 Euros, where presented. It can be employed in photocatalytic reactions that utilize the natural solar light. The body of the linear parabolic concentrator is manufactured out of expanded polystyrene, covered with a reflective aluminized mirror. The tubular photoreactor, made from glass is equipped with a cooling mantle and fixed through two threaded bars, as so being mobile in the plane which encompasses the bottom and the focal axis of the parabolic concentrator.

Acknowledgements

This work was carried out through the Partnerships in priority areas - PN II program, developed with the support of MEN - UEFISCDI, project no. PN II PT PCCA-2013-4-1708.

References

[1] L. Bora, V. Mittal, S. Dasgupta, R. Vadgama, J. of Basic and App. Eng. Res. 2, (2015) 1242

[2] L. Bora, P. Padmanabhan, A. Kumar, R. VadgamaJ. of Basic and App. Eng. Res. 2, (2015) 1246

[3] C. Navntoft, J. of Solar Energy Eng.129, (2007.) 127

PHOTOCATALYTIC EFFICIENCY OF $LiInO_2$ IN DEGRADATION OF ALPRAZOLAM FROM WASTEWATERS

Ljubica Đačanin Far*[,1], Tamara Ivetić[1], Svetlana Lukić-Petrović[1], Dragana Štrbac[2], Nina Finčur[3], Biljana Abramović[3]

[1]University of Novi Sad, Faculty of Sciences, Department of Physics, Trg Dositeja Obradovica 4, 21000 Novi Sad, Serbia
[2]University of Novi Sad, Faculty of Technical Sciences, Department of Environmental Engineering and Occupational Safety and Health,Trg Dositeja Obradovica 6, 21000 Novi Sad, Serbia
[3]University of Novi Sad,Faculty of Sciences, Department of Chemistry, Biochemistry and Environmental Protection, Trg Dositeja Obradovica 3, 21000 Novi Sad, Serbia
e-mail: ljubica@df.uns.ac.rs

Abstract

Alprazolam is a widely consumed psychiatric pharmaceutical from the benzodiazepinesgroup, thathas been continuously introduced into the environment throughwastewaters, being a potential risk to living organisms. Furthermore, alprazolam is highly resistant to photodegradation, with degradation half-time of 228 sunny days [1].

Lithium-indium oxide is a high density (5.9 g/cm^3), wide band-gap semiconductor with promising applications for scintillating detection of solar neutrinos as well as for efficient phosphorescence when doped with different rare earth ions. Here we report for the first time the photocatalytic efficiency of $LiInO_2$ powder, synthesized using a simple solid-state chemistry procedure at relatively low temperature of 700°C. Materials structure was examined by X-ray diffraction,that confirmed materials tetragonal structural form (space group: $I4_1/amd$) with no impurity phases. Optical band-gap of 3.99 eV was estimated from the diffuse-reflectance spectrum. Photocatalytic efficiencywas examined under both simulated solar and UV radiation. Photodegradation kineticsshowed $LiInO_2$ powderhas a good potentialfor UV-activated degradation of alprazolam.

References

[1] V. Calisto, M.R.M. Domingues, V.I. Esteves, Photodegradation of psychiatric pharmaceuticals in aquatic environments - kinetics and photo-degradation products, Water Res. 45 (2011) 6097–6106

ELECTROCHEMICAL OXYGEN INTAKE/RELEASE PROCESS OVER $YBaCo_2Fe_2O_{7.5}$ ELECTRODES IN AQUEOUS SOLUTIONS

Mircea Laurenţiu Dan, Andrea Kellenberger, Nicolae Vaszilcsin

University Politehnica Timişoara, Faculty of Industrial Chemistry and Environmental Engineering, 300223, Parvan 6, Timisoara, Romania
e-mail: mircea.dan@upt.ro

Abstract
The present study proves that $YBaCo_2Fe_2O_{7.5}$ perovskite has high performance for oxygen storage capacity in aqueous solutions by electrochemical oxidation. This perovskite is a promising candidate for applications requiring efficient oxide ion conductivity or large oxygen storage capacity is. The oxygen intake/release propriety of $YBaCo_4O_7$ has been studied by cyclic voltammetry and chronoamperometry in alkaline and neutral aqueous electrolytes.

Introduction
$YBaCo_4O_7$ cobalt perovskite, originally discovered by Valldor and Andersson, shows remarkable ability for intake/release oxygen [1-4]. In order to increase $YBaCo_4O_7$ stability, the control of chemical composition is one of the most promising methods. Perovskite $YBaCo_4O_7$ supports different types of cation substitutions, of which the most important are: Ca and smaller atoms such as rare earth elements (Dy, Ho, Er, Tm, Yb and Lu), able to substitute Y and Fe, Zn, Al and Ga with Co [5]. The substitution of half number of cobalt ions with iron ions was proposed, forming the new compound $YBaCo_2Fe_2O_{7+\delta}$, where δ=0.5.
Oxygen nonstoichiometry in $YBaCo_2Fe_2O_{7.5}$ perovskite structure is influenced by the oxygen content variations depending of cobalt or iron ions average number of oxidation which affects the oxygen permeability and diffusion [6]. From electrochemical point of view, $YBaCo_4Fe_2O_{7.5}$ oxidation/reduction studies in aqueous solutions can be attractive due to his oxygen insertion/release capacity.
In the present work, the oxygen intake/release capacity of $YBaCo_2Fe_2O_{7.5}$ perovskite in alkaline and neutral solutions using electrochemical methods was studied.

Experimental
$YBaCo_2Fe_2O_{7.5}$ layered perovskite was obtained using solid state reaction, mixing the precursors Y_2O_3, $BaCO_3$, $Fe_3O_4$and $CoO_{4/3}$ (all, Normapur 99,9%) according to the stoichiometric cations ratio. After decarbonation at 1000°C the powder was reground and fired in air at 1200°C. The obtained mixture was pressed into discs (1 cm^2) and sintered at 1100°C in air. The structure of obtained perovskite was checked by X-Ray powder diffraction (Philips X-pert Pro). Using this preparation method in air all iron ions from the perovskite structure are found at maximum oxidation number +3.
The electrochemical studies were carried out using BioLogic SP150 potentiostat/galvanostat. The electrochemical cell was equipped with two graphite counter electrodes, working electrode ($YBaCo_2Fe_2O_{7.5}$ disc with 1 cm^2 exposed area) and a saturated Ag/AgCl electrode as reference.

Results and discussion
In order to show the peaks associated with the electrochemical processes occurring at $YBaCo_2Fe_2O_{7.5}$ - aqueous solution interface, cyclic voltammetry was used.
Cyclic voltammograms recorded in 1 mol L^{-1} KOH, between -2.0 and +1.5 V/Ag/AgCl with 500 mV s^{-1} scan rate, are depicted in Figure 1, starting from OCP. Peak (1) can be associated

with Co^{2+} ions oxidation reaction inside of perovskite structures. When the potential becomes more positive, a plateau (2) characteristic for oxygen evolution reaction can be observed. The others peaks correspond to adsorbed oxygen reduction or Co^{3+} reduction (3), Fe^{3+} or Co^{2+} ions reduction (4), hydrogen evolution reaction (5) and Fe^{2+} or Co metallic oxidation (6).

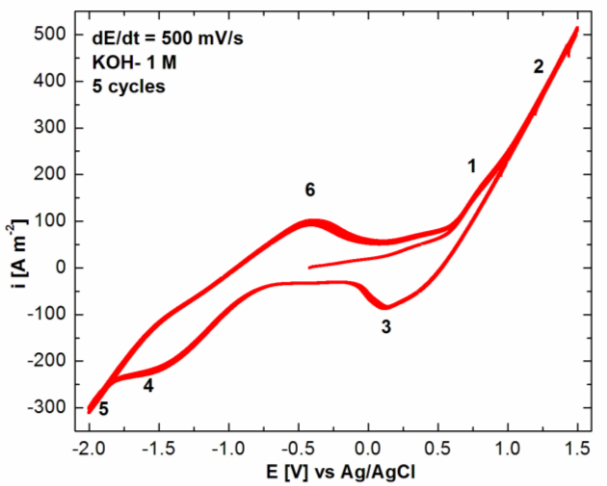

Figure 1. Cyclic voltammograms plotted on $YBaCo_2Fe_2O_{7.5}$ in alkaline aqueous solutions.

Similarly, in figure 2 are presented cyclic curves plotted in 0.5 mol L^{-1} Na_2SO_4 at 500 mV s^{-1} scan rate. Peaks are (1) and (2) are associated with Co^{2+} oxidation.

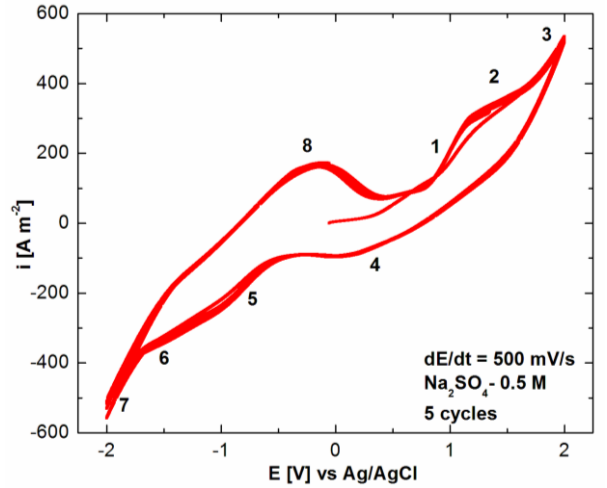

Figure 2. Cyclic voltammograms plotted on $YBaCo_2Fe_2O_{7.5}$ in neutral aqueous solutions.

Global reactions at the electrode/electrolyte interface at anodic polarization can be describes by equation (1) in alkaline solution and equation (2) in neutral one:

$$YBaCo_2Fe_2O_{7.5} + 2\delta HO^- \rightarrow YBaCo_2Fe_2O_{7.5+\delta} + \delta H_2O + 2\delta e^- \quad (1)$$

$$YBaCo_2Fe_2O_{7.5} + \delta H_2O \rightarrow YBaCo_2Fe_2O_{7.5+\delta} + 2\delta H^+ + 2\delta e^- \quad (2)$$

In both electrolytes, anodic oxidation process of $YBaCo_2Fe_2O_{7.5}$perovskite consists in oxygen insertion in oxide structure, assigned to Co^{2+} oxidation (3) [3,4]:

$$Co^{2+} \rightarrow Co^{3+} + e^- \quad (3)$$

In preliminary studies, chronoamperometric measurements had as a starting point the cyclic voltamograms shown in Figure 1 and 2. Analyzing these curves, three potential values were chosen for the chronoamperometric measurements in alkaline solution: two values correspond with the compound oxidation plateau: (1) E = + 0.25 V and (2) E = + 0.50 V and (3) E = +1.00 V, corresponding to the oxygen release process on electrode surface. For neutral electrolyte were chosen only two potential values (1) E = +1 V and (2) E = + 1.50 V, both corresponding to perovskite oxidation. All potentials values are given versus the reference electrode (E_{ref} = 0.197 V vs NHE). Chronoamperometric studies were performed for 15 minutes. Graphical results are presented in figure 3 for alkaline solutions and 4 for neutral media.

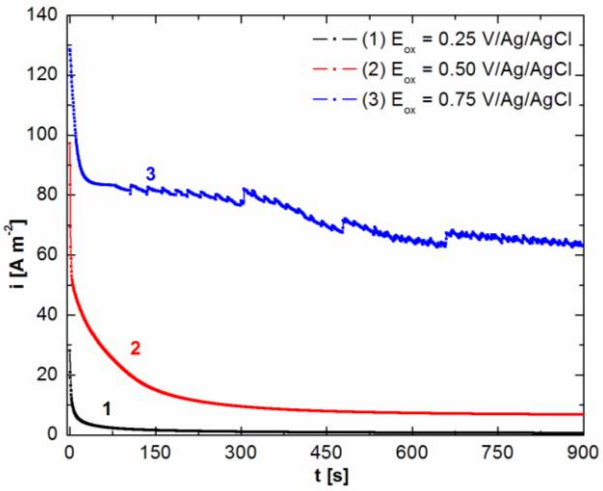

Figure 3. Chronoamperometric studies on $YBaCo_2Fe_2O_{7.5}$ electrode, in alkaline solutions.

Analyzing graphical data can conclude the following aspects: at +0.25 and +0.50 V potential values, the only process occurring at perovskite interface is oxidation. If chronoamperometric measurements are carried out at +0.75 V, value characteristic for oxygen evolution reaction on perovskite electrode surface, the curve shape (3) indicates that oxygen evolution reaction occurs simultaneously with $YBaCo_2Fe_2O_{7.5}$ oxidation.

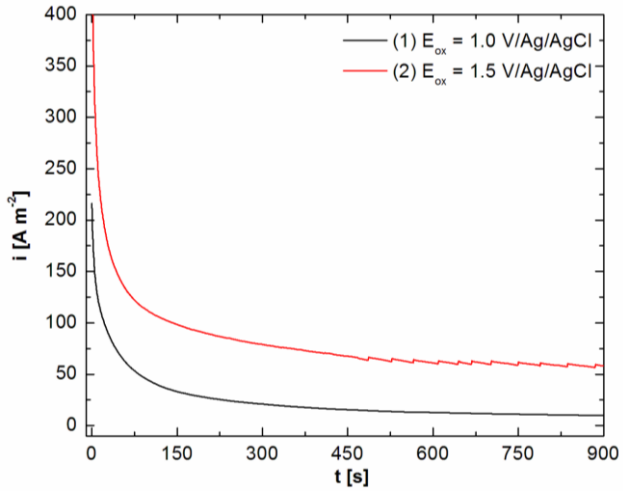

Figure 4. Chronoamperometric studies on $YBaCo_2Fe_2O_{7.5}$ electrode, in alkaline solutions.

Conclusion

Experimental data have proven the oxygen uptake/release capability of $YBaCo_2Fe_2O_{7.5}$ at lower temperature range using cyclic voltammetry. The results showed the possibility to increase the oxygen content in $YBaCo_2Fe_2O_{7.5}$ using chronoamperometry.

Acknowledgements

This work was partially supported by University Politehnica Timisoara.

References

[1] M. Valldor, M. Andersson, Solid State Sci. 4 (2002) 923-931.
[2] O. Chmaissem, H. Zheng, et al., J. Solid State Chem., 181 (2008) 664.
[3] M. Dan, N.Vaszilcsin, A. Kellenberger, N. Duteanu, Studia Univ. Babes-Bolyai, Chemia, 56(1) (2011) 119.
[4] M. Dan, N.Vaszilcsin, A. Kellenberger, N. Duteanu , J. Solid State Electrochem., 15(6) (2011) 1227.
[5] O. Parkkima, H. Yamauchi, M. Karppinen, Chem. Mater., 25(4) (2013) 599.
[6] M. Dan, N.Vaszilcsin, N. Duteanu, Studia Univ. Babes-Bolyai, Chemia, LX (4) (2015) 165.

SKELETAL NICKEL BASED 6 LAYERS PLATINUM NANOPARTICLES ELECTRODE WITH CATALYTIC EFFECT FOR ETHANOL ELECTROOXIDATION IN ALKALINE MEDIA

Mircea Laurentiu Dan, Delia Andrada Duca, Nicolae Vaszilcsin

University Politehnica Timişoara, Faculty of Industrial Chemistry and Environmental Engineering, 300223, Parvan 6, Timisoara, Romania
e-mail: mircea.dan@upt.ro

Abstract

In this paper, preliminary aspects of ethanol electrocatalytic oxidation on skeletal nickel based 6 layers platinum nanoparticles electrode in aqueous alkaline solution have been investigated using voltammetric studies. Ethanol oxidation reaction (EOR) was studied by cyclic and linear voltammetry.

Introduction

Recently, from the alkaline fuel cells (AFCs) existing types, direct ethanol fuel cells (DEFCs) had part of huge development and many resources were invested for this purpose, because ethanol is less toxic compared to methanol and can be easily produced in large quantity [1]. The electrode material effect on the electrocatalytic activity of ethanol oxidation is of continuing interest.

Platinum is known to be the optimum electrocatalyst for ethanol oxidation in different fuel cells, because it is chemically stable in both acid and alkaline electrolytes [1,2]. For oxidation of various organic compounds, especially for saturated alcohols, nickel has been reported as an efficient anode material [1]. It was demonstrated that platinum and nickel alloys materials exhibit superior characteristics as against of single metal materials in the catalysis of organic compounds oxidation [1]. Skeletal nickel electrode, due to its morphology and considerable porosity, was considered suitable as anode in fuel cells as catalyst for different anodic reactions [3,4].

Besides pure platinum, nickel and skeletal nickel electrodes, as well as other nickel-based electrodes, like skeletal nickel based 6 layers platinum nanoparticles, have been tested for many reactions of applied interest, such as hydrogen evolution reaction, or methanol and sulphite anodic oxidation. All processes were studied in alkaline media [5].

In this paper, a skeletal nickel based 6 layers platinum nanoparticles electrode as electrocatalyst for ethanol oxidation in an alkaline solution has been used.

Experimental

Electrochemical tests were performed at room temperature using a SP-150 potentiostat/galvanostat (Bio-Logic, SAS, France). A 100 mL typical glass cell was equipped with three electrodes: skeletal nickel based 6 layers platinum nanoparticles working electrodes, Ag/AgCl reference electrode and two graphite rods counter electrodes. For performed experiments, working electrode exposed surface was 0.5 cm^2.

Skeletal nickel electrode was prepared using thermal arc spraying technique. Skeletal nickel-platinum based electrodes have been prepared by spray pyrolysis technique.

Different concentrations of ethanol were added: 0.125, 0.25, 0.5, 1 and 2 mol L^{-1} in the alkaline media (1 mol L^{-1} KOH). All reagents were prepared from Sigma-Aldrich p.a. min 99.8%

Results and discussion

Cyclic voltammograms plotted at 500 mV s^{-1} scan rate, in +0.70 ÷ -1.20 V potential range, on skeletal nickel based 6 layers platinum nanoparticles electrode in 1 mol L^{-1} KOH solution with different ethanol concentrations, between 0.125 and 1 mol L^{-1}, are shown in figure 1. Starting from open circuit potential (OCP) the characteristics processes for metallic electrode/ethanol added in alkaline solution, depicted in CVs are: ethanol oxidation reaction and oxygen evolution reaction on anodic branch, adsorbed oxygen reduction and reduction of ethanol oxidation products (acetate, acetaldehyde, etc.) on the backward scan. Specific anodic and cathodic peaks corresponding to acetaldehyde/acetate redox couple are observed between -0.50 and 0.00 V potential values. When the potential values are more negative than -1.00 V, hydrogen evolution reaction occurs on the surface of the working electrode. Anodic characteristic peak for oxidation of acetaldehyde to acetate are also inserted in the figure.

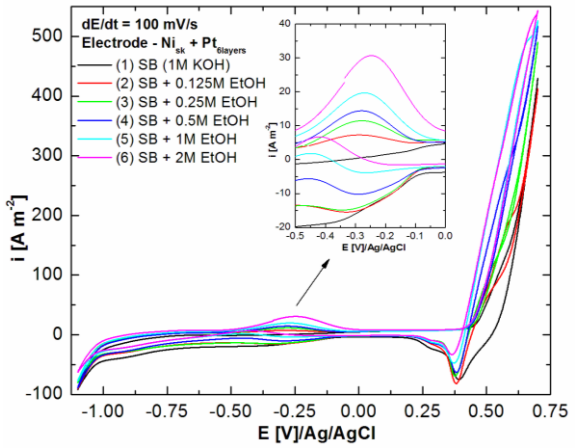

Figure 1. CVs recorded on Ni_{sk} + $Pt_{6layers}$ electrode in 1 mol L^{-1} KOH without and with different concentration of ethanol, scan rate: 100 mV s^{-1}.

In figure 2, cyclic voltammograms recorded on skeletal nickel based 6 layers platinum electrode in 1 mol L^{-1} KOH + 0.25 mol L^{-1} ethanol solution, with 10 mV s^{-1} polarization speed are presented, starting from OCP, in different potential range, from +0.70 to -1.20 V value. Anodic plateau for ethanol oxidation are also inserted.

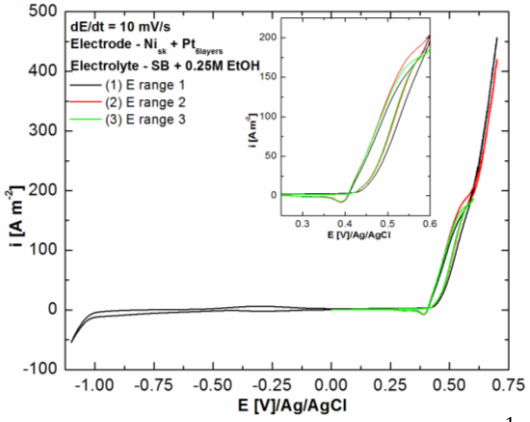

Figure 2. CVs recorded on Ni_{sk} + $Pt_{6layers}$ electrode in 1 mol L^{-1} KOH with 0.25 mol L^{-1} ethanol, in different potential ranges, scan rate: 10 mV s^{-1}.

To study acetaldehyde/acetate redox process, cyclic voltammograms (10 cycles) were recorded in -0.50 ÷ 0.00 V potential range, on skeletal nickel based 6 layers platinum electrode, in 1mol L^{-1} KOH + 0.125mol L^{-1} ethanol solution, with 100 mV s^{-1} scan rate.

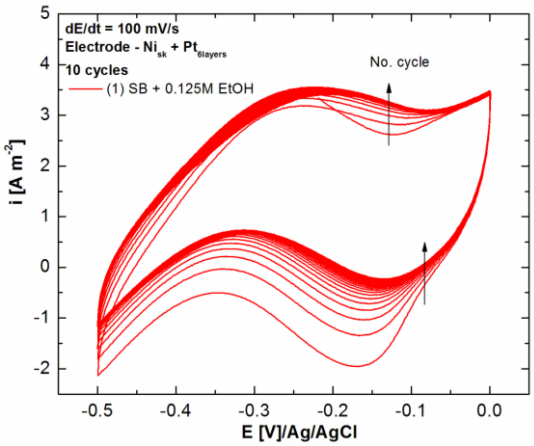

Figure 3. CVs (10 cycles) for acetaldehyde/acetate redox couple, on Ni_{sk} + $Pt_{6layers}$ electrode, in 1 mol L^{-1} KOH with 0.125 mol L^{-1} ethanol, scan rate: 100 mV s^{-1}.

The experimental technique which confirmed the advantages of skeletal nickel based 6 layers platinum electrode compared to platinum or skeletal nickel electrodes is linear voltammetry recorded at very low scan rate (1 mV s^{-1}). Obtained curves plotted on platinum and skeletal nickel based 6 layers platinum electrodes are shown in figure 4.

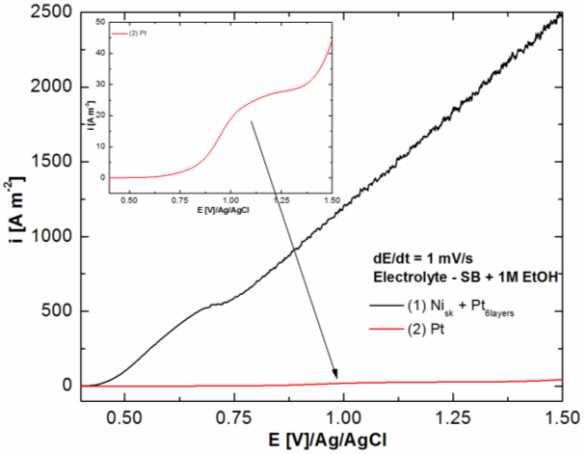

Figure 4. LVs (anodic domain) on Ni_{sk} + $Pt_{6layers}$ and Pt electrodes in 1 mol L^{-1} KOH with 1 mol L^{-1} ethanol, scan rate: 1 mV s^{-1}.

Figure 5 presents curves recorded on skeletal nickel and skeletal nickel based 6 layers platinum electrodes in same conditions.

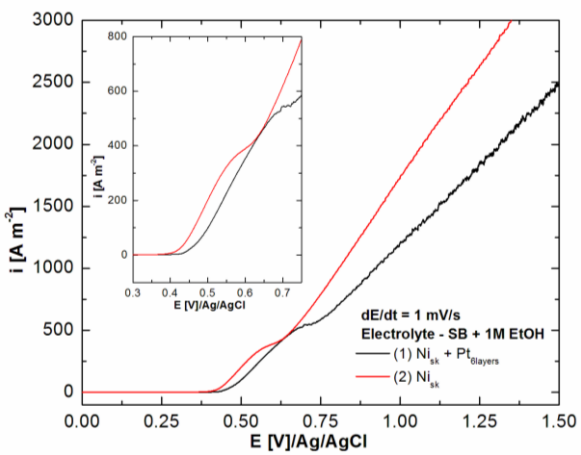

Figure 5. LVs (anodic domain) on Ni_{sk} + $Pt_{6layers}$ and Ni_{sk} electrodes in 1 mol L^{-1} KOH with 1 mol L^{-1} ethanol, scan rate: 1 mV s^{-1}.

Conclusion

In this study, skeletal nickel based 6 layers Pt nanoparticles prepared using spray pyrolysis has been tested for ethanol oxidation reaction. Cyclic and linear voltammetry used as electrochemical analysis techniques confirm an increased activity for studied process in alkaline media. Preliminary results demonstrate this type of electrodes can be a promising anode for DEFC.

Acknowledgements

This work was partially supported by University Politehnica Timisoara in the frame of PhD studies.

References

[1] C. Xu, L. Cheng, P. Shen, Y. Liu, Electrochem. Commun. 9 (2007) 997.
[2] J.J. Huang, W. S. Hwang, Y. C. Weng, T. C. Chou, Mater. Trans., JIM 50 (5) (2009) 1139.
[3] A.F. Enache, N. Vaszilcsin, M.L. Dan, Chem. Bull. "POLITEHNICA" Univ. (Timisoara) 61(75) 1 (2016) 7.
[4] M.L. Dan, N. Vaszilcsin, A.F. Enache, Chem. Bull. "POLITEHNICA" Univ. (Timisoara) 61(75) 1 (2016) 18.
[5] A. Iacob, M. Dan, A. Kellenberger, N. Vaszilcsin, Chem. Bull. "POLITEHNICA" Univ. (Timisoara) Volume 59(73) 2 (2014) 42.

CHEMISTRY AND PHOTOCHEMISTRY OF NOVEL AROMATIC SPIROKETALS DERIVED FROM 2,6-BIS(5-BROMO-2-HYDROXYBENZYLIDENE)CYCLOHEXANONE

Livia Deveseleanu-Corîci[1], Sergiu Şova[2], Valentin Badea[3], Otilia Costişor[1], Liliana Cseh[1*]

[1]Institute of Chemistry Timisoara of Romanian Academy, 24 Mihai Viteazul Bvd, 300223 Timisoara, Romania
[2]Inorganic Polymers Group, Petru Poni Institute of Macromolecular Chemistry, Iasi, Romania
[3]Politehnica University of Timisoara, Faculty of Industrial Chemistry and Environment Engineering, 6 Vasile Pârvan Bvd, 300223 Timisoara, Romania
e-mail:lili_cseh@yahoo.com

Abstract

Natural colorants such as flavylium and xanthylium derivatives have attracted considerable interest in the last decades due to their potential health effects and replacement of synthetic pigments. In addition, these type of compounds exhibit versatile photochromic properties by switching from a variety of colourswhen submitted to different external stimuli[1-3].

The aim of the present work was to design novel photochromic systems based on xanthylium derivatives. Therefore, we have synthesized and characterized 2,6-bis(5-bromo-2-hydroxybenzylidene)cyclohexanone. The network of chemical reactions when submitted to light and different pH values has been investigated. A new colorless compound 3,11-dibromo-7,8-dihydro-6H-chromeno[3,2-d]xanthenes(Scheme 1) isolated from the equilibrated solution of *trans*-chalcone specie in methanolhave been isolated and fully characterized by NMR and X-ray diffraction. The rate of the reaction increased when the solution of *trans*-chalcone was exposed to sunlight. The spiroketal form was stable at in neutral and basic conditions, while at low pH values it converts into xantylium cationic form.

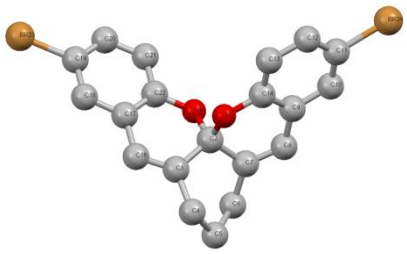

Scheme 1. Crystal structure of 3,11-dibromo-7,8-dihydro-6H-chromeno[3,2-d]xanthenes

Acknowledgements

The authors acknowledge the support of the Romanian Academy, Project 4.1. t

References

[1]. X. Guo, J. Zhou, M. A. Siegler, A. E. Bragg and H. E. Katz, Angew. Chem., 54 (2015) 1.
[2]. F. Pina, M. J. Melo, C. A. T. Laia, A. J. Parola, J. C. Lima, Chem. Soc. Rev., 41(2012) 869.
[3]. A. M. Diniz, C. Pinheiro, V. Petrov, A. J. Parola, F. Pina, Chem. Eur. J., 17 (2011) 6359.

COMPARATIVE STUDIES FOR 2-PROPANOL ELECTROOXIDATION ON PLATINUM AND NICKEL ELECTRODES IN ALKALINE MEDIA

Mircea Laurentiu Dan, Delia Andrada Duca, Nicolae Vaszilcsin, Nicoleta Maria Dragomir

University Politehnica Timişoara, Faculty of Industrial Chemistry and Environmental Engineering, 300223, Parvan 6, Timisoara, Romania
e-mail: d_nicoleta16@yahoo.com

Abstract
In this paper, new aspects of 2-propanol oxidation electrocatalytic effect on platinum and nickel electrodes, in aqueous alkaline solution was investigated using voltammetric studies. 2-propanol oxidation reaction has been studied by cyclic and linear voltammetry.

Introduction
Small alcohols electrooxidation from C1 - C3 group has been intensely studied, mainly because of their possible use in fuel cells [1]. Methanol, although extensively used, is toxic inflammable with low boiling point and is not a primary fuel. Ethanol isn't toxic and can easily be obtained from sugar and biomass [1,2]. The use of alcohols with longer chains for applications in fuel cells can also be attractive considering the high energy content emitted in fuel [3]. 2-propanol is the smallest secondary alcohol and far less toxic than methanol. Its electrochemical oxidation has aroused great interest due to its particular molecular structure [4,5]. Alcohols with more than two carbon atoms in their structure have several isomers and special features of non-CO adsorption [6]. When the onset potentials for oxidation of different alcohols were compared, the performance of 2-propanol was superior as against of methanol and ethanol [7]. The possibility to use 2-propanol as electrolyte in direct alcohols fuel cells (DAFCs) has been reported since 1995 [8].
Platinum has been extensively investigated as electrocatalyst for 2-propanol electrooxidation in both acid and alkaline electrolytes. Pt is easily poisoned by the reaction intermediates [9]. Also, platinum high price and limited supply constitute a major barrier for DAFCs development, other materials with similar catalytic properties being necessary [4,10]. Nickel is a good electrocatalyst for methanol and ethanol oxidation in alkaline electrolyte. However, there is little information on the electrocatalytic properties of 2-propanol oxidation on nickel in alkaline medium.
In this paper, comparative studies for 2-propanol electrooxidation on platinum and nickel electrodes in alkaline media are presented using different electrochemical methods, such as: cyclic voltammetry, linear polarization and chronoamperometry.

Experimental
Electrochemical tests were performed at room temperature using a SP-150 potentiostat/galvanostat (Bio-Logic, SAS, France). A 100 mL typical glass cell was equipped with three electrodes: Pt/Ni working electrodes, Ag/AgCl reference electrode and two graphite rods used counter electrodes. For performed experiments, the exposed surface of working electrode was 0.5 cm^2. Different concentrations of 2-propanol were added: 0.125, 0.25, 0.5, 0.75 and 1 mol L^{-1} in 1 mol L^{-1} KOH, all prepared from Sigma-Aldrich reagent p.a. min 99.8%.

Results and discussion

Cyclic voltammograms recorded on platinum electrode, between -1.5 and +2.0 V/Ag/AgCl, at 50 mV s^{-1} scan rate, in 1 mol L^{-1} KOH with different 2-propanol concentration, are depicted in Figure 1, starting from open circuit potential (OCP). Potential domain associated with 2-propanol oxidation on platinum electrode is between +0.7 and +1.8 V.

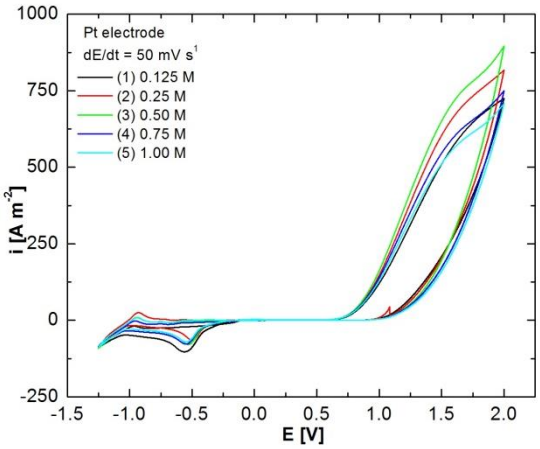

Figure 1. Cyclic voltammograms plotted on platinum electrode in 1 mol L^{-1} KOHwith different concentration of 2-propanol, scan rate: 50 mVs^{-1}.

In order to study the electrochemical processes occurring at platinum electrode surface in 1 mol L^{-1}KOH with 0.75 mol L^{-1} 2-propanol, cyclic voltammograms (3 cycles)were recorded, starting from OCP, in the potential range between -1.00 and +0.60V, at 50 mVs^{-1} scan rate, when current density is small, few A m^{-2}. Platinum oxides formation/dissolution on electrode surface and oxidation/reduction of different intermediate products formed in 2-propanol electrooxidation were followed.

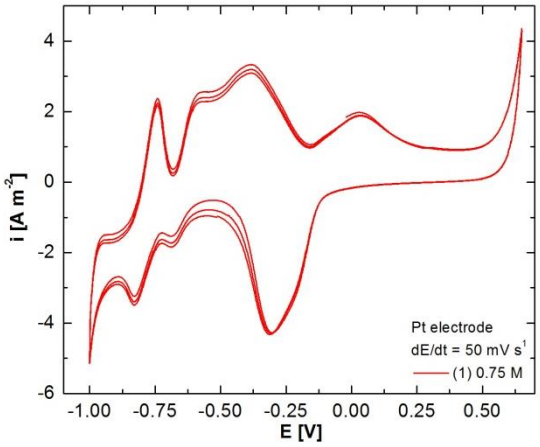

Figure 2. Cyclic voltammograms plotted on platinum electrode in 1 mol L^{-1} KOH with 0.75 mol L^{-1}2-propanol, scan rate: 50 mVs^{-1}.

Similarly, in figure 2 are presented cyclic curves plotted in 1 mol L^{-1}KOH with different concentrationof 2-propanol, on nickel electrode, between -1.4 and +0.6 V/Ag/AgCl potential range,at 50 mV s^{-1} scan rate. Potential domain characteristic for 2-propanol electrooxidationis between +0.4 and +0.6 V, depending on the alcohol concentration added in electrolyte solution.

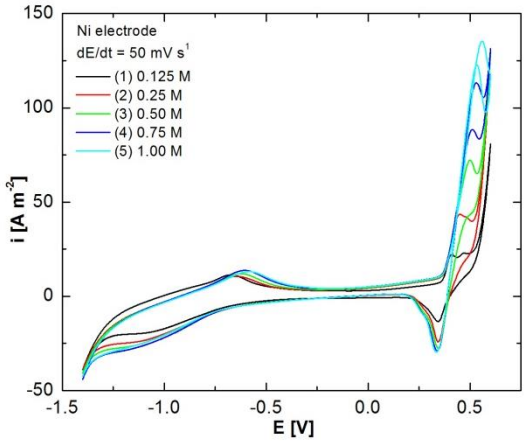

Figure 3. Cyclic voltammograms plotted on nickel electrode in 1 mol L^{-1} KOH solutions with different concentration of 2-propanol, scan rate: 50 mVs^{-1}.

Linear voltammograms plotted at low scan rate (1 mV s^{-1}) in 1 mol L^{-1} KOH + 0.75 mol L^{-1} 2-propanol, on both platinum and nickelelectrodes are shown in figure 4 a and b. The curves shape indicates only one oxidation process on electrode surface.

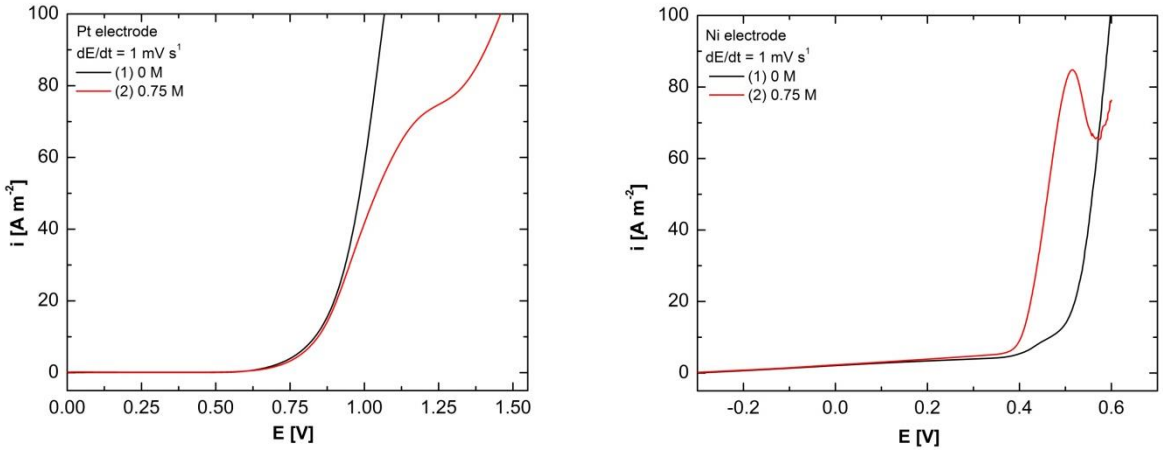

a) b)

Figure 4. Linear voltammograms plotted on platinum (a) and nickel (b) electrode in 1 mol L^{-1} KOH + 0.75 mol L^{-1} 2-propanol, scan rate: 1 mV s^{-1}.

On metallic electrode, especially platinum, 2-propanol electrooxidation in alkaline medium can be described by following reactions [4]:

$$CH_3CHOHCH_3 + 2HO^- \rightarrow CH_3COCH_3 + 2H_2O + 2e^- \quad (1)$$

$$CH_3COCH_3 + 16HO^- \rightarrow 3CO_2 + 11H_2O + 16e^- \quad (2)$$

The overall reaction is:

$$CH_3CHOHCH_3 + 18HO^- \rightarrow 3CO_2 + 13H_2O + 18e^- \quad (3)$$

S.G. Sun and Y. Lin demonstrated that equation (1) is a fast reaction, and acetone oxidized into CO_2 is a relatively slow reaction [12].

Chronoamperometric measurements had as starting point the linear voltamograms shown in figure 4 a and b. Analyzing these curves, three potential values were chosen for the 2-propanol electrooxidation in alkaline solution on each electrode:

(1) E = + 1.00 V, (2) E = + 1.25 V and (3) E = +1.50 V for platinum electrode;

(1) E = + 0.40 V, (2) E = + 0.45 V and (3) E = +0.50 V for nickel electrode.

All potentials values are given versus the reference electrode (E_{ref} = 0.197 V vs NHE). Chronoamperometric studies were performed for 60 minutes. Graphical results are presented in figure 5 a and b. Also, chronoamperometric comparative data recorded on both platinum and nickel electrodes, in alkaline electrolyte without and with 0.75 mol L^{-1} 2-propanol are presented. Anodic oxidation of 2-propanol at different potential values are inserted in figures.

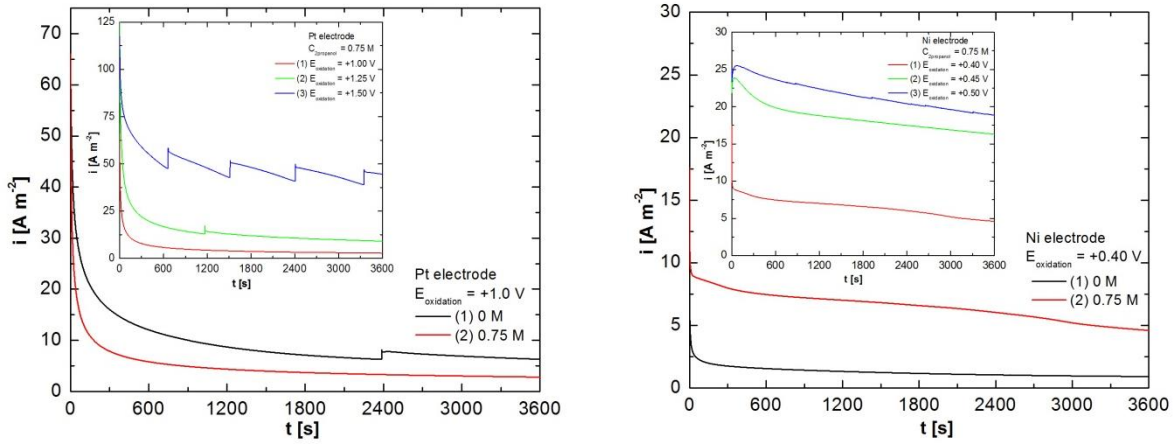

a) b)

Figure 5. Chronoamperometric studies on platinum (a) and nickel (b) electrode 1 mol L^{-1} KOH in the absence and presence of 0.75 mol L^{-1} 2-propanol.

Analyzing graphical data recorded on platinum electrode can conclude that at +1.00 and +1.25 V potential values, the only process occurring at the interface is 2-propanol oxidation. If chronoamperometric measurements are carried out at +1.50 V, the curve shape indicates oxygen evolution reaction on electrode surface.

Conclusion

In this study, platinum and nickel electrodes have been tested for 2-propanol electrooxidation reaction. Cyclic voltammetry, linear polarization and chronoamperometry used as electrochemical analysis techniques confirm an increased activity for studied process in alkaline solution.

Acknowledgements

This work was partially supported by University Politehnica Timisoara in the frame of PhD studies.

References

[1] M. S. Ureta-Zanartu, C. Berríos, T. Gonzalez, F. Fernandez, D. Baez, R. Salazar, C. Gutierrez, Int. J. Electrochem. Sci., 7 (2012) 8905.
[2] F. Maillard, F. Gloaguen, F. Hahn, J. M. Leger, Fuel Cells, 2 (2002) 143.
[3] S. S. Gupta, J. Datta, J. Chem. Sci. 117(4) (2005) 337.
[4] J. Ye, J. Liu, C. Xu, S. P. Jiang, Y. Tong, Electrochem. Commun. 9 (2007) 2760.
[5] P.T.A. Sumodjo, E.J. Silva, T. Rabochai, J. Electroanal. Chem. 271 (1989) 305.
[6] H. B. Hassan, TOELECJ 1 (2009) 19.
[7] S.LJ. Gojkovic, A.V. Tripkovic, R.M. Stevanovic, J. Serb. Chem. Soc. 72(12) (2007) 1419.
[8] J.T. Wang, S. Wasmus, R.F. Savinell, J. Electrochem. Soc. 142 (1995) 4218.
[9] C.G. Lee, M. Umeda, I. Uchida, J. Power Sources 160 (2006) 78.
[10] M.E.P. Markiewicz, D.M. Hebert, S.H. Bergens, J. Power Sources 161 (2006) 761.
[11] S.G. Sun, Y. Lin, J. Electroanal. Chem. 375 (1994) 401.

STUDIES ON THE POSSIBILITY OF USING EXPIRED CEFTRIAXONE DRUG AS ADDITIVE IN ACID ELECTROPLATING BATHS

Delia-Andrada Duca, Nicolae Vaszilcsin, Mircea Laurenţiu Dan

University Politehnica Timişoara, Faculty of Industrial Chemistry and Environmental Engineering,300223, Pârvan 6, Timişoara, România
e-mail: duca.delia@gmail.com

Abstract
In this paper, preliminary data obtained using ceftriaxone (CEFTR) as additive in copper and nickel electrodeposition from acid baths are presented. Electrochemical behaviour of ceftriaxone and introductory information about the way its presence in the metalselectrodeposition bath influences the electrode processes have been obtained by cyclic voltammetry on platinum electrode. Inhibitory effect of ceftriaxone in the electrolyte solutions used in copper and nickel deposition processes was studied by linear voltammetry.

Introduction
Considering the appreciable amount of unused and expired medical products available worldwide and the non-environmental friendly storage and neutralization techniques currently practiced, researchers seek for new ways of using non-compliant drugs [1-3].
Currently, the active substances from drugs are successfully used as corrosion inhibitors [4].They act similar to the levelling agents added in the galvanic baths. Due to increasing coverage with organic substance because of adsorption onto metal surface, additives increase the metal deposition overpotential. Regarding the morphology of cathodic deposits, blocking active sites on the surface during electrodeposition results in nucleation rate enhancement.As it is known,this leads to more smooth cathodic deposits [5].
Research purpose is to harness CEFTR, the active substance from expired cefort, as additive in copper and nickel deposition from acid baths. Copper coatings are used for galvanotechnics purposes in manufacturing printed circuit boards, pattern and photogravures and very often as interlayer for nickel deposition [6]. Watts type bath is the most commonly used for nickel deposition. Nickel coatings are often used in decorative purposes and for their anticorrosive properties [7-9].
Coating properties are improved by additives. These are in general organic molecules which influence the physical and mechanical properties of cathodic deposits [10,11]. Similar compounds are found in active substances from drugs.
According to its structure, ceftriaxone sodium,a cephalosporin antibiotic, is a promising additive. It is the active substance found in cefort. Its systematic (IUPAC) name is:(Z)-7-[2-(2-aminothiazol-4-yl)-2-methoxyimi-noacetamido]-3-[(2,5-dihydro-6-hydroxy-2-methyl-5-oxo-1,2,4-triazin-3-yl)thiomethyl]-3-cephem-4-carboxylic acid, disodium salt, sesquaterhydrate [12].

Experimental
To characterize ceftriaxone voltametric behaviour in acid media (0.5 mol L^{-1} H_2SO_4 and 30 g L^{-1} H_3BO_3 + 0.5 mol L^{-1} Na_2SO_4 solutions), cyclic voltammetry (CV) on platinum electrode was performed. CVs were recorded at 50 mV s^{-1}.
In order to determine ceftriaxone influence on copper and nickel deposition processes, linear voltammograms (LVs) were drawn on copper and nickel electrodes in electrolyte solutions containing 5 g $L^{-1}M^{2+}$ ions, in 25 – 65^{o}C temperature range.
In experimentalstudies, ceftriaxone sodium (Figure 1), the active substance from commercial

drugcefort was used.

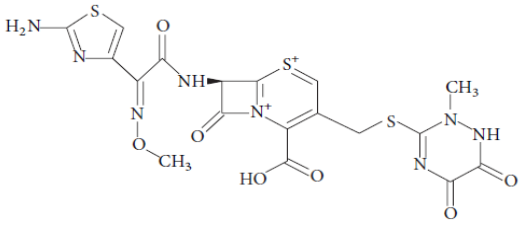

Figure 1. Ceftriaxone sodium chemical structure [13].

All reagents used in experimental studies were of analytical grade. Copper and nickel working electrodes werepolished with different grit emery papers, ultrasonic cleaned, washed with distilled water and dried.

Electrochemical measurements were performed using a PARSTAT 2273 potentiostat/galvanostat in a thermostatic three-electrode glass cell equipped with: Pt/Cu/Ni working electrodes with 1 cm^2 exposed area, Ag/AgCl reference electrode and two graphite counter electrodes. All further potential values given in this paper are versus the reference electrode ($E_{Ag/AgCl}$ = 0.197 V).

Results and discussion

In order to determine CEFTR electrochemical behavior, CVs were recorded with different scan rates, on platinum electrode, in blank solution and solutions with different concentrations of CEFTR, between 10^{-6} – 10^{-3} mol L^{-1}.

To simulate the pH values fromindustrial deposition baths, as blank solutions, 0.5 mol L^{-1} H_2SO_4 have been used for copper deposition, and 30 g L^{-1} H_3BO_3 + 0.5 mol L^{-1} Na_2SO_4 solution (BS) for nickel deposition.

In figure 2, CVs recorded at 50 mV s^{-1} scan rate on Pt electrode, in 0.5 mol L^{-1} H_2SO_4 in the absence and presence of 10^{-3} mol L^{-1} CEFTR are presented.

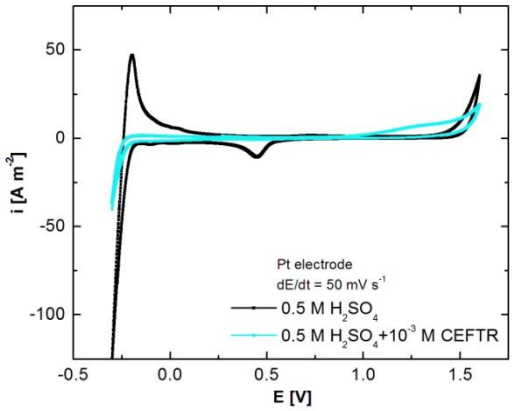

Figure 2. CVs on Pt electrode, in 0.5 mol L^{-1} H_2SO_4 without/with 10^{-3} mol L^{-1} CEFTR, 50 mV s^{-1} scan rate.

Figure 3 presents CVs recorded at scan rate of 50 mV s^{-1} on Pt electrode, in BS in absence and presence of 10^{-3} mol L^{-1} CEFTR.

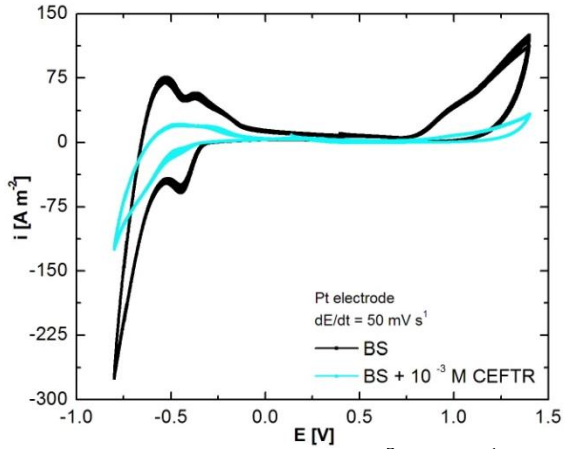

Figure 3. CVs on Pt electrode, in BS without/with 10^{-3} mol L^{-1} CEFTR, 50 mV s^{-1} scan rate.

Comparing voltammograms drawn in the samepotentialrange, from both figures 2 and 3 it can be observed a decrease of current density associated to characteristic processes when using CEFTR as against blank solution. Also, ashift of cathodic peaks to more negative potentials and of anodic peaks to more positive potentials can be seen.

CEFTR effect on copper and nickel deposition processes was studied at temperatures between 25 and 65°C by linear voltammetry. LVs were drawn at 5mV s^{-1} scan rateon Cu (Figure 4) and Ni electrode(Figure 5) in 5 g L^{-1} Cu^{2+} (from H_2SO_4 + $CuSO_4$), respectively Ni^{2+} ions (from H_3BO_3 + $NiSO_4$ + $NiCl_2$)electrolyte solutions.

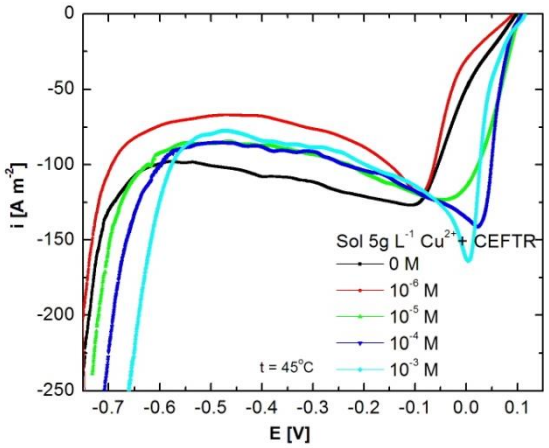

Figure 4. LVs in 5 g L^{-1} Cu^{2+} inthe absence and presence of different CEFTR concentrations,5 mV s^{-1} scan rate.

Analysing above LVs,ceftriaxone addition in the electrolyte solution leads to a shift of copper and nickel deposition potential values because ofthe organic molecule absorptiononto the metal surface.

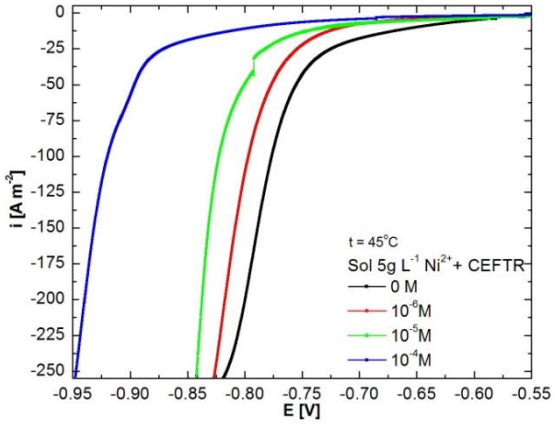

Figure 5. LVs in 5 g $L^{-1}Ni^{2+}$ inthe absence and presence of different CEFTR concentrations,5 mV s^{-1} scan rate.

Conclusion

Preliminary studies shows that ceftriaxone from expired cefort can be recycled as additive in copper and nickel electrodeposition from acid baths.

Ceftriaxone addition in the electrolyte solution inhibits both anodic and cathodic studied processes.

Acknowledgements

This work was partially supported by University Politehnica Timisoara in the frame of PhD studies.

References

[1] M.A. Kozak, J.R. Melton, S.A. Gernant, M.E. Snyder, Res. Social Adm. Pharm. 12 (2) (2015) 336.
[2] A.Y.C.Tong, B.M. Peake,R. Braund, Environ. Int. 37 (2011) 292.
[3] Ruhoy I.S., Daughton C.G., Environ. Int. 34 (2008) 1157.
[4] G. Gece, Corros. Sci. 53 (2011) 3873.
[5] G.A. di Bari, in: M. Schlesinger, M. Paunovic (Eds), Electrodeposition of Nickel,Modern Electroplating, Fifth Edition, Wiley, Hoboken, New Jersey, 2010, pp. 79-114.
[6] T. Chang, Y. Jin, L. Wen, C. Zhang, C. Leygraf, I. O. Wallinderb, J, Zhangc,Electrochim. Acta, 211 (2016) 245.
[7] B. Szczygiel, M. Kolodziej, Electrochim. Acta, 50 (2005) 4188.
[8] T. Sakamoto, K. Azumia, H. Tachikawaa, K. Iokibea, M. Seoa, N. Uchidac, Y. Kagayac, Electrochim. Acta, 55 (2010) 8570.
[9] E. Rudnik, M. Wojnicki, G. Wloch, Surf. Coat. Technol., 207 (2012) 375.
[10] E. M. Oliveira, G. A. Finazzi, I. A. Carlos, Surf.Coat. Techn.200 (2006) 5978.
[11] S. L. Wang, L. L. Hong, W. W. Yu, Acta Metall. Sin. 21 (2008) 269.
[12] K. Parfitt, The complete drug reference, Thirty-second edition, Pharmaceutical Press USA, 1999, pp. 175.
[13] R. Ethiraj, E. Thiruvengadam, V. S. Sampath, A. Vahid, J. Raj, Int. Sch. Res. Notices 2014 (2014) 1.

SKELETAL NICKEL ELECTRODE WITH CATALYTIC EFFECT FOR ETHANOL ELECTROOXIDATION IN ALKALINE MEDIA

Delia Andrada Duca, Mircea Laurentiu Dan, Nicolae Vaszilcsin

University Politehnica Timişoara, Faculty of Industrial Chemistry and Environmental Engineering, 300223, Parvan 6, Timisoara, Romania
e-mail: duca.delia@gmail.com

Abstract
The aim of this investigation is to examine ethanol anodic oxidation on a skeletal nickel electrode in aqueous alkaline solution (1 mol L^{-1} NaOH). Electrocatalytic activity for ethanol anodic oxidation becomes a serious issue, especially due to the utilization of skeletal nickel electrodes in fuel cells. In order to understand the oxidation mechanism on the surface of these types of electrodes, comprehensive researches were necessary. Electrochemical behavior has been studied by cyclic and linear voltammetry.

Introduction
Alkaline fuel cells (AFCs) commonly use a potassium hydroxide aqueous solution as electrolyte [1]. Also, sodium hydroxide can be used but has a disadvantage because of sodium carbonate lower solubility, obtained as secondary product, compared to potassium carbonate [1]. Compared to AFCs which use H_2/O_2, direct alcohol fuel cells (DAFCs) are more compact without the heavy and bulky external fuel reformer and can be used to power electric vehicles [2]. Liquid fuels, such as small alcohols from C1 - C3group, featuring higher volumetric and gravimetric energy densities and better energy efficiency, are easily handled, stored and transported in comparison with gaseous fuels [2].
Ethanol can be produced on a massive scale from biomass feed stocks originating from agriculture (first-generation bioethanol), forestry and urban residues (second-generation bioethanol) [3,4]. The advantage of using ethanol as fuel consists in a large volume energy capacity of 6.3 kWh/L, which is higher than of hydrogen (2.6 kWh/L) or methanol (4.8 kWh/L) [5].
A significant challenge in the development of direct ethanol fuel cells (DEFCs) technologies is the manufacture of highly active catalysts for ethanol oxidation reaction (EOR). Platinum is the most commonly used catalytic metal in DEFCs because has excellent properties in ethanol adsorption and dissociation [3]. However, the cost of platinum is a major impediment in DEFCs commercialization [3]. Pd has similar catalytic properties with Pt, making it very attractive for long-term industrial applications. In this series, other tested catalysts were Pt-M and Pd-M binary or ternary alloys obtained by adding metallic elements such as: Ru, Sn, Ir, Bi, Rh, Mo, Fe, Co, Cu, Ni, Au, Ag, etc [3]. Since 1970, nickel and nickel-based electrodes have been used in fundamental and practical studies for the small alcohols oxidation in alkaline media [6]. Nickel based electrocatalysts are considered low-cost materials and making the DEFC a potentially low cost technology compared to fuel cells with platinum or platinum based catalysts [7].
In this paper, a skeletal nickel electrode was used as electrocatalyst for ethanol oxidation in alkaline media.

Experimental
Electrochemical tests were performed at room temperature using a SP-150 potentiostat/galvanostat (Bio-Logic, SAS, France). A 100 mL typical glass cell was equipped with three electrodes: samples of skeletal nickel as working electrodes, Ag/AgCl reference

electrode and two graphite rods as counter electrodes. For performed experiments, the exposed surface of working electrode was 0.2 cm^2. All potentials are given versus the reference electrode (E_{ref} = 0.197 V vs SHE).Different concentrations of ethanol (0.125, 0.25, 0.5, 1 and 2 mol L^{-1}) were added in 1 mol L^{-1} NaOH electrolyte solution.

Results and discussion

Cyclic voltamograms recorded in alkaline solutions, in the absence and presence of ethanol, in a wide range of potential (from -1.20 to +0.75 V), at 500 mV s^{-1} are presented in figure 1. Starting from open circuit potential (OCP) towards anodic polarisation it is observed an anodic plateau associated with EOR. When the electrode potential is over +0.60 V, oxygen evolution reaction (OER) on skeletal nickel surface can be observed. On the backward scan, a pronounced cathodic peak associated with adsorbed oxygen reduction or reduction of ethanol oxidation products, was recorded. At more negative than -1.10 V electrode potential values, hydrogen evolution reaction (HER) occurs.

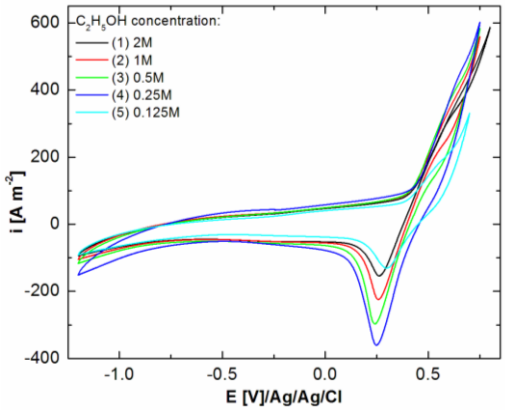

Figure 1. CVs recorded on Ni_{sk} electrode in 1mol L^{-1}NaOH without and with different concentration of ethanol, scan rate:500 mV s^{-1}.

For better identification of EOR characteristic potential domain, figure 2 presents the anodic plateau of cyclic voltammograms recorded on skeletal nickel electrode in 1 mol L^{-1} NaOH with different concentrations of ethanol, at 500 mV s^{-1} scan rate.

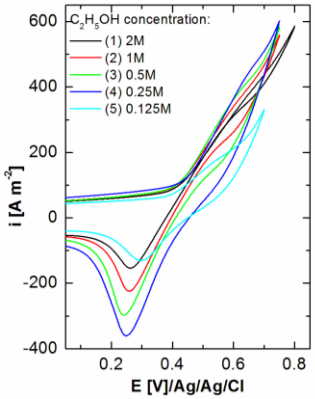

Figure 2. CVs (anodic domain) recorded on Ni_{sk} electrode in 1mol L^{-1}NaOH without and with different concentrations of ethanol, scan rate:500 mV s^{-1}.

Scan rate influence on cyclic curves shape plotted on skeletal nickel electrode in 1mol L^{-1}NaOH solution with 1 mol L^{-1}ethanol are depicted in figure 3.

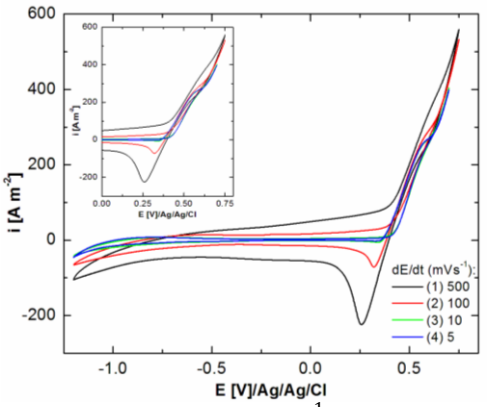

Figure 3. CVs recorded on Ni_{sk} electrode in 1mol L^{-1}NaOH with 1 mol L^{-1}ethanol at different scan rates.

Cyclic voltammograms recorded at 100 mV s^{-1} scan rate on skeletal and smooth nickel electrodes in 1 mol L^{-1} NaOH with 0.25 mol L^{-1} ethanol solution are presented comparatively in figure 4.

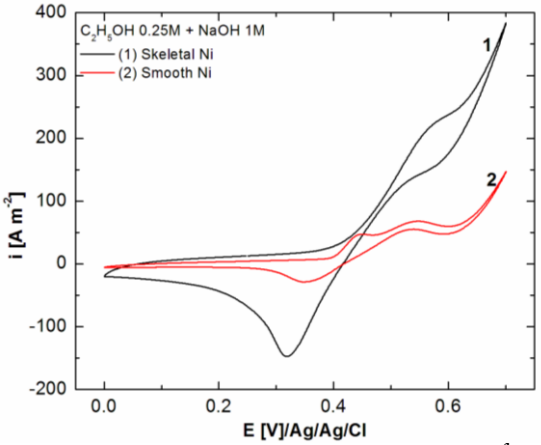

Figure 4. CVs recorded on Ni_{sk} and Ni electrodes in 1 mol L^{-1} NaOH with 0.25 mol L^{-1} ethanol, scan rate: 100 mV s^{-1}.

Other electrochemical experimental technique which confirmed the advantage of skeletal nickel electrode compared to smooth nickel electrode as catalyst for EOR is linear voltammetry recorded at very low scan rate (1 mV s^{-1}). Obtained curves are shown in figure 5. The curves shape indicates only one oxidation process on both electrodes surface. Specific parameters (oxidation range potential and limiting current density) for are presented in table1.

Table 1. Electrochemical parameters from EOR:

Electrode	**E_{ox} range [V]**	**$i_{lim.ox}$ [A m^{-2}]**
Skeletal nickel	0.42 ÷ 0.57	135
Smooth nickel	0.44 ÷ 0.60	23

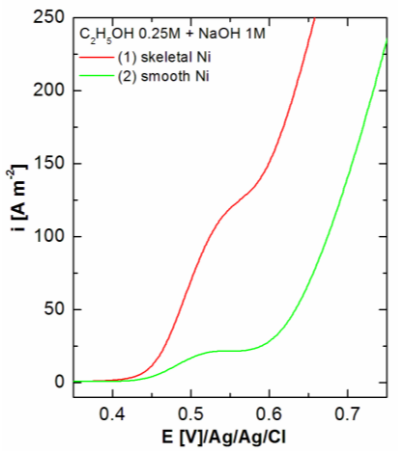

Figure 5. LVs (anodic domain) recorded on Ni_{sk} and Ni electrodes in 1 mol L^{-1} NaOH with 0.25 mol L^{-1} ethanol, scan rate: 1 mV s^{-1}.

Conclusion

In this paper, new aspects of ethanol oxidation reaction on skeletal nickel electrode are presented. The used electrode has a high surface area and increased catalytic activity for EOR in alkaline media. Also, comparative cyclic and linear voltammetric studies on skeletal and smooth nickel electrodes are shown.

A thoroughgoing study is necessary for EOR complete characterization by chronoamperometric method and electrochemical impedance spectroscopy. Furthermore, EOR optimum characteristic parameters will be accessible.

Acknowledgements

This work was partially supported by University Politehnica Timisoara in the frame of PhD studies.

References

[1] M. Cifrain, K. Kordesch, in: W. Vielstich, H. A. Gasteiger, A. Lamm (Eds), Handbook of Fuel Cells – Fundamentals, Technology and Applications, Volume 1: Fundamentals and Survey of System, John Wiley & Sons, Ltd. ISBN: 0-471-49926-9, 2003, pp.268

[2] W. Zhou, Z. Zhou, S. Song, W. Li, G. Sun, P. Tsiakaras, Q. Xin, Appl. Catal., B. 46 (2003) 273.

[3] Y. Wang, S. Zou, W.B. Cai, Catalysts 5 (2015) 1507.

[4] E. Antolini, J. Power Sources 170 (2007) 1.

[5] Z. Zhang, L. Xin, K. Sun, W. Li, Int. J. Hydrogen Energy 36 (2011) 12686.

[6] A.F.B. Barbosa, V.L. Oliveira, J. van Drunen, G. Tremiliosi-Filho, J. Electroanal. Chem. 746 (1) (2015) 31.

[7] E. Antolini, E.R. Gonzalez, J. Power Sources 195 (2010) 3431

COMPARATIVE ANALYSIS OF CHLOROPHYLL AND CAROTENOID PIGMENTS CONTENT OF ARUGULA (*ERUCA SATIVA*) AND LETTUCE (*LACTUCA SATIVA*) LEAVES

Delia-Gabriela Dumbravă[1*], Camelia Moldovan[1], Diana-Nicoleta Raba[1], Viorica-Mirela Popa[1], Despina-Maria Bordean[1]

[1]Faculty of Agrofood Products Technology, Banaţs University of Agricultural Science and Veterinary Medicine "King Michael I of Romania" fromTimisoara, Romania
e-mail: delia_dumbrava@yahoo.com

Abstract
The aim of this study was to analyze the chlorophyll and carotenoids content of fresh arugula (*Eruca sativa*, Ruca variety) and lettuce (*Lactuca sativa*, Marilena variety) leaves from the Romanian market. The pigments concentration in the analyzed samples was determined by a spectrophotometric method. In both analyzed samples, chlorophyll "a" predominates to chlorophyll "b". The highest content of chlorophyll pigments was found in leaves of arugula: 31.47 mg/g, while in the lettuce leaves was found a concentration of 27.14.Arugulaleavesare alsothe richestincarotenoids (245.50 μg/g).

Introduction

In recent years, increasing awareness concerning the promotion and protection of health exerted by the bioactive compounds from plant products, has resulted in increased attention to green leafy vegetables as vital components of the daily diet [1].
Green leafy vegetables are an excellent source of fiber, folate, carotenoids and chlorophylls. This plants has also a high content of vitamins C and K and minerals, are rich in antioxidants and removes free radicals from the body, before becoming dangerous [1,2].
Chlorophyll is a specific pigment for green vegetables, which plays a critical role in photosynthesis. It is a fused polycyclic aromatic hydrocarbon; has a structure similar to heme, but contains magnesium instead of iron. There are several different forms of chlorophyll which are in different proportions depending on plant [3]. Until the present we known 12 chlorophylls types, of which the most well researched are chlorophylls a and b [4]. Chlorophyll a is greenish –yellow in solution and chlorophyll b is blue- green [3]. In the green normal leaves, there is a greater amount of chlorophyll a than b, the report of which is 2: 0.7 [4]. All forms of chlorophyll are oil-soluble. Among the therapeutic effects of chlorophyll can include: stimulating the immune system, help prevent cancer, help combat anemia, purifying the blood and the organism, help to rejuvenate and energize the body, normalize blood pressure, combating bad odors, bad breath as well as body odor [3].
Carotenoids are pigments without nitrogen with a polyisoprene structure, universal spread both in the plant and animals tissues. There are two major types of carotenoids: hydrocarbon class and oxygenated class or xanthophylls. These compounds cause a yellow, orange or red color in the tissues where they are, due to the large number of conjugated double bonds which they contain [5]. Carotenoid pigments are synthesized only by plants. Until the present have been identified over 700 carotenoid compounds. Is known the essential role of carotenoids for plants: in the process of photosynthesis, in breathing, in fertilization, in transferring of absorbed energy from chlorophyll, in protection against destructive photooxidation. Also carotenoid compounds involved in the smooth running of important biochemical processes in animals and human life: in the vision (provitamins A), growing and breeding; more recently have been recognized protective effects of carotenoids against serious disturbances such as:

cancer, heart disease, and were stimulated intensive research on the role of carotenoids as antioxidants and as regulators of the immune response system [6].
Arugula (*Eruca sativa*) is an edible plant of the family *Brassicaceae* (cabbage family). From arugula are consumed: the leaves (rich in chlorophyll, vitamin C, glucosides and potassium), flowers and seeds (for flavored mustards) [7,8]. Arugula possess anti-secretory, cyto-protective, aphrodisiac and anti-ulcer properties [9].
Lettuce (*Lactuca sativa*) is worldwide cultivated, being one of the most consumed green leafy vegetable in the raw form, for its pleasant taste and high nutritional value. It is a rich source of important bioactive compounds such as carotenoids, chlorophylls, vitamins, polyphenols, minerals [10].
In this work we aimed to analyze the content of chlorophyll a, chlorophyll b and total carotenoids in leaves of arugula and lettuce from the Romanian market.

Experimental

For this study were purchased from the Romanian market following materials: leaves of arugula (*Eruca sativa*)- Ruca variety and lettuce (*Lactuca sativa*)- Marilena variety.

Chlorophyll pigments analysis

Determination of chlorophyll pigments in the studied plants was done by a spectrophotometric method [11].
The vegetal samples were weighed on analytical balance and then were subjected to trituration with quartz sand in the presence of acetone 80% (v/v). The obtained homogenate was then centrifuged at 3500 rpm, for 5 minutes, and the supernatant was collected in amber glass containers. The precipitate was taken up with solvent until the extract is no longer present any coloration. The combined supernatants were analyzed at 646 nm and 663 nm in a UV-VIS Spectrophotometer Perkin Elmer Lambda 25.
According to the relationship of Lichtenthaler and Wellburn [12], chlorophyll content was quantified as follows:

$$Chl\ a = 12.21 \cdot (A_{663}) - 2.81 \cdot (A_{646}),$$

$$Chl\ b = 20.13 \cdot (A_{646}) - 5.03 \cdot (A_{663}),$$

$$Chl_{total} = 17.32 \cdot (A_{646}) + 7.18 \cdot (A_{663}),$$

where: Chl a - chlorophyll in mg/l,
Chl b - b chlorophyll in mg/l,
Chl_{total} - total chlorophyll content in mg/l,
A663 - absorbance of the sample at 663 nm,
A646 - absorbance of the sample at 646 nm.

Carotenoid pigments analysis

Determination of the carotenoid pigments was carried out spectrophotometrically, using the same acetone extracts as for chlorophylls analysis.
Calculation of the carotenoid content in the studied raw materials was based on the relationship[]:

$$Carotenoids = [(1000 \cdot A_{470}) - (3{,}27 \cdot Chl\ a) - (1{,}04 \cdot Chl\ b)] / 229$$

where: Chl a - chlorophyll in mg/l,
Chl b - b chlorophyll in mg/l,
A_{470} – absorbance of the sample at 470 nm.

Results and discussion

Results on chlorophyll content in the analyzed samples are shown in Figure 1.

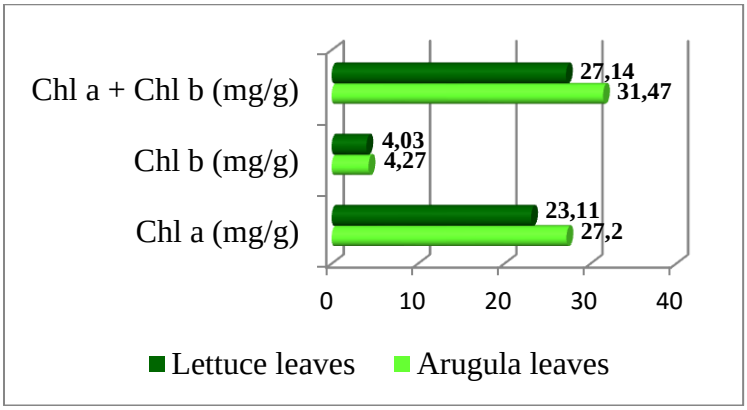

Figure 1. Content of chlorophyll pigments in the analyzed samples

From the experimental results is seen that, for both analysed plants, chlorophyll apredominates to chlorophyll b. Arugula leaves are the richest in chlorophyll pigments (chlorophyll a: 27.20 mg/g; chlorophyll b: 4.27 mg/g), but in the case of lettuce values are only slightly smaller (chlorophyll a: 23.11 mg/g; chlorophyll b: 4.27 mg/g).
The results concerning the carotenoid pigments content in the arugula and lettuce leaves are showed in figure 2.

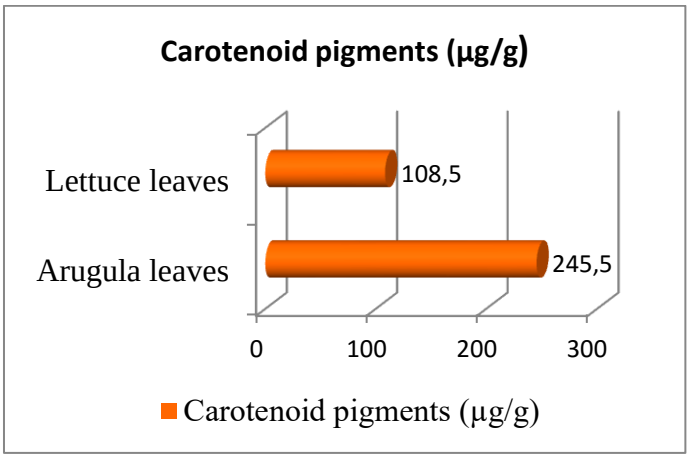

Figure 2.- Carotenoid pigments content in the analysed samples

From the above values is observed that the leaves of arugula (245.5 µg carotenoids/g) are of 2.26 times more rich in carotenoids than lettuce leaves (108.5 µg/g).

Conclusion

1. Spectrophotometric analysis of chlorophyll pigments revealed that both in arugula leaves and in the lettuce leaves, chlorophyll a predominates versus chlorophyll b.
2. The concentrations of chlorophyll pigments in the leaves of arugula and lettuce are close in value, arugula having slightly higher amounts than lettuce.
3. Carotenoids are found in amounts of over than two times higher in the arugula leaves than in lettuce leaves.

References

[1] F.I., Smith,P., Eyzaguirre, African Journal of Food, Agriculture, Nutrition and Development, 7(3), (2007) pp. 1-8.
[2] K.A. Steinmetz, J.D. Potter, Epidemiology. Cancer Causes Control, 1991, 2, pp. 324-57.

[3] A.L. İnanç, Chlorophyll: Structural properties, health benefits and its occurrence in virgin olive oils, Akademik Gıda, 9(2), (2011) pp. 26-32.
[4] N. Sălăgeanu, Fotosinteza, Ed. Academiei Române, Bucureşti, 1972.
[5] V. Tămaş, G. Neamţu, Pigmenţi carotenoidici şi metaboliţi, vol. 1, Ed. Ceres, Bucureşti, 1986.
[6] D.G. Dumbravă, Contribuții la studiul, izolarea și purificarea pigmenților caotenoidici din material vegetale, Ed. Politehnica, Timișoara, 2008, pp.8-9.
[7] F. Nuez, J.E.Hernández Bermejo. Neglected horticultural crops, 1994, pp. 303-332. In: Hernándo Bermejo JE, León J (Eds.). Neglected Crops: 1492 from a different perspective. Plant Production and Protection Series 26. FAO, Rome, Italy.
[8] D. Pignone, C. Gómez-Campo. Eruca, 2011 pp. 149-160. In: Kole C (Ed). Wild crop relatives: genomic and breeding resources, oilseeds. Springer-Verlag, Berlin, Heidelberg, Germany.
[9] S. Alqasoumi, T. Al Howiriny, M. Al Yahya, R. Syed. Rocket "*Eruca sativa*": A salad herb with potential gastric anti ulcer activity. World J Gastroentero, 15, (2009) pp.1958-1965.
[10] R. Cruz, P. Baptista, S. Cunha, J.A. Pereira, S. Casal, Carotenoids of Lettuce (*Lactuca sativa* L.) Grown on Soil Enriched with Spent Coffee Grounds,Molecules,17, (2012) pp. 1535-1547.
[11] I. Ianculov, R. Palicica, M. Butnariu, D. Dumbravă, I. Gergen, Obţinerea în stare cristalină a clorofilei din cetină de brad (*Abies alba*) şi de pin (*Pinus sylvestris*), Revista de Chimie,56(4), (2005) pp 441-443.
[12] H.K. Lichtenthaler, A.R. Wellburn, Determinations of total carotenoids and chlorophylls a and b of leaf extracts in different solvents. Biochemical Society Transactions, 11, (1983) pp 591 – 592.

ANODIC OXIDATION OF SULPHITE IONS ON SMOOTH NICKEL BASED 1 LAYER PLATINUM NANOPARTICLES IN ALKALINE SOLUTION

Andreea Enache, Mircea Laurentiu Dan, Nicolae Vaszilcsin

University Politehnica Timişoara, Faculty of Industrial Chemistry and Environmental Engineering, 300223, Parvan 6, Timisoara, Romania
e-mail: enacheandreeafloriana@gmail.com

Abstract
In this paper, nickel based 1 layer platinum nanoparticles electrode (Ni-Pt_{1layer}), prepared by spray-pyrolysis technique, it has been tested in order to obtain a complete characterization for the process of anodic oxidation of sulphite to sulphate in alkaline media. This process was investigated by cyclic voltammetry technique and linear polarization. The present study concerns the preliminary evaluation of electrocatalytic properties for this type of electrode toward the electrochemical oxidation of sulphite.

Introduction
In a world with limited resources, the dominant model for economic growth based on rising resource consumption and pollutants emission, no longer tenable [1]. In this context, the concept of "green economy" has offered the opportunity to change the way society handles the interaction between environmental and economic areas. To enable the society to build and sustain a green economy concept associate " green nanotechnology " aims to exploit innovations in materials science and engineering to develop products and processes that are energy efficient as well as economically and environmentally sustainable [1].
Nanotechnology has a significant impact in fuel cells domain, which are devices able to convert chemical energy into electrical one [2]. Nanomaterials can be very efficient electro-catalysts for oxidation / reduction reactions in fuel cells because of high active surface area [3, 4]. Platinum nanoparticles have been considered as the best catalyst for application in fuel cells [5]. Nanomaterials conteining platinum alloys have been the subject of research because of high electrocatalytic activity and chemical resistance [6]. Platinum is one of the rarest and most expensive metals. It has high corrosion resistance and numerous catalytic applications including automotive catalytic converters and petrochemical cracking catalysts. Platinum nanoparticles are used to reduce the amount of metal needed for various applications.
Electrochemical oxidation of sulphite in aqueous solution is an important issue for the industrial sector. The mechanism for this reaction has been extensively studied for application to the hybrid sulfur cycle (Hys), also known as Westinghouse cycle, for hydrogen production [7, 8], this process being also applied to remove the sulphite from exhaust gases (flue gas desulfurization) [9, 10], electrogenerative oxidation [11] and the analytical determination of sulfur compounds concentrations [12]. Many aspects of this reaction have also interest in fundamental electrocatalysis [13].
Sulphur dioxide - oxygen fuel cells present an important role due to the possibility to produce both electric energy and sulphuric acid.
In this paper, cyclic voltammetry and linear polarization techniques were used in order to characterize the sulphite anodic oxidation in alkaline solutions on skeletal nickel based platinum nanoparticles electrode.

Experimental

Electrode preparation

Platinum salt precursor solution used for platinum nanoparticles deposition has been prepared with chloroplatinic acid hexahydrate ($H_2PtCl_6 \cdot 6H_2O$) and isopropanol (Sigma-Aldrich, 99.7%).

Platinum nanoparticles were deposited on smooth nickel substrate by spray-pyrolysis technique using an ultrasonic nebulizer SONO-TEK Corporation Exacta Coat. After deposition, the electrodes were heated at 350°C during 30 minutes to obtain the platinum nanoparticles [14].

Electrochemical measurements

Electrochemical measurements were performed with a SP 150 Bio-Logic potentiostat/galvanostat in a three-electrode electrochemical cell consisting of Ni-Pt_{1layer} as working electrode with surface area of 0.5 cm^2. Two graphite roads were used as counter electrodes placed symmetrically to the working electrode and Ag/AgCl as reference electrode.

Electrochemical experiments were carried out in 1 mol L^{-1} NaOH solution (prepared with Merck NaOH, p.a.) with and without Na_2SO_3 (Merk, p.a. 98%). Electrolyte solutions with different concentrations of Na_2SO_3 were prepared, as follow: 10^{-3}, 10^{-2} and 10^{-1} mol L^{-1}.

Cyclic voltammograms have been registered with 5 - 500 mV s^{-1} scan rate. Linear polarization curves have been recorded with 1 mV s^{-1} scan rate.

Results and discussion

Cyclic voltammetry studies

A typical cyclic voltammograms recorded on Ni-Pt_{1layer}electrode in alkaline solution with different concentration of Na_2SO_3 are presented in Figure 1.

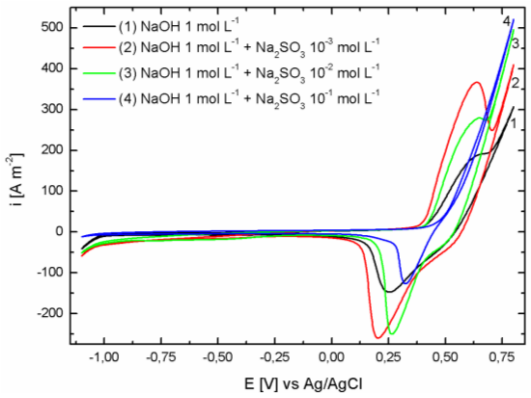

Figure 1. Cyclic voltamograms recorded on Ni-Pt_{1layer} electrode in 1 mol L^{-1} NaOH without/with different concentration of Na_2SO_3 at 500 mV s^{-1}.

On the catodic plateau the only process visible is the hydrogen evolution reaction (HER) according to the equation (1):

$$2H^+ + 2e^- \rightleftarrows H_2 \qquad (1)$$

Sweeping the potential in the anodic region, at potential range between 0.35 - 0.70 V vs. Ag / AgCl it was observed a pick that can be associated with the formation of an oxide on the electrode surface followed by oxidation of sulphite and oxygen evolution reaction.

The most generally accepted mechanisms for oxygen evolution reaction (OER) on various electrodes, including nickel based platinum nanoparticles, involve reactions with one of the electron charge transfer steps rate-determining [15]:

$$OH^- \rightleftarrows OH_{ads} + e^- \qquad (2)$$

$$OH_{ads} + OH^- \rightleftarrows O_{ads}^- + H_2O \quad (3)$$

$$O_{ads}^- \rightleftarrows Oads + e^- \quad (4)$$

$$O_{ads} + O_{ads} \rightleftarrows O_2 \quad (5)$$

Cyclic voltammograms plotted with high scan rate (50 mV s^{-1}) on Ni-Pt_{1layer}electrode in alkaline electrolyte with different amounts of Na_2SO_3 are shown in Figure 2.

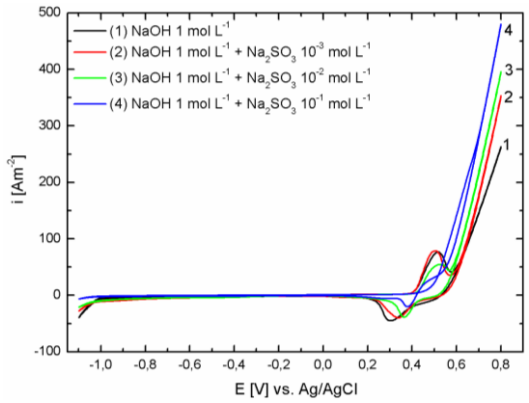

Figure 2. Cyclic voltamograms recorded on Ni-Pt_{1layer} electrode in 1 mol L^{-1} NaOH without/with different concentration of Na_2SO_3 at 50 mV s^{-1}.

On cyclic curves plotted at 50 mV s^{-1}shown in Figure 2 for 1 mol L^{-1} NaOH solutions in the absence and presence of different concentrations of Na_2SO_3 it can be observed the OER potential value is shifted to more negative potentials in the presence of SO_3^{2-} ions.
The decrease of scan rate from 500 mV s^{-1} at 50 mV s^{-1} provides the opportunity to point out the identification of the SO_3^{2-} ions oxidation processes occurring at the interface working electrode/electrolyte solution in the potential range between +0.5 and +0.7 V vs. Ag/AgCl.
Linear voltammetry studies

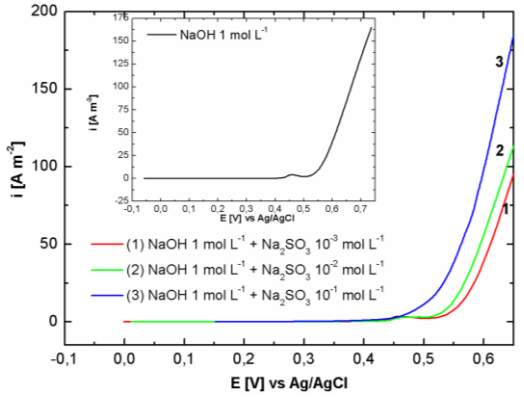

Figure 3. Linear voltammograms recorded on Ni-Pt_{1layer} electrode in 1 mol L^{-1} NaOH with different concentration of Na_2SO_3 at 1 mV s^{-1}; linear voltamograms in 1 mol L^{-1} NaOH inserted.

Linear voltammetry technique was applied to validate the results presented above. Curves registered at low scan rate (1 mV s^{-1}) in alkaline media with different concentrations of SO_3^{2-} ions are shown in Figure 3.From the analysis of linear voltammograms, specific potential ranges of oxidation processes that occur at the interface electrode/electrolyte solution (SO_3^{2-} ions oxidation and OER) have been emphasized. The electrochemical oxidation of sulphite to sulphate ions in alkaline media can occur following two possible mechanisms, presented by

Skavas [16] where sulphite anion is oxidized to sulphate in two successive steps, each implying one electron transfer or sulphite anion is oxidized to sulphite radical wich can interact and form dithionate ions $S_2O_6^{2-}$. Finally, these ions disproportionates in SO_4^{2-} and SO_3^{2-}.
The OER mechanism on Ni-Pt_{1layer}electrode takes place following reactions (2) – (5) and SO_3^{2-} ions oxidation is conducted directly in alkaline electrolyte by a chemical irreversible process when the molecular oxygen was produced on electrod surface.

Conclusion

Ni-Pt_{1layer} electrodeprepared by spray-pyrolysis technique has been characterized by different techniques in order to its applicability as an electrocatalytic material in fuel cells for the oxidation of sulphite ions in alkaline solution. The insertion of platinum nanoparticles has a significant effect on the activity of the studied reaction and the experiments presented have confirmed the possibility to oxidize electrochemicaly SO_3^{2-} to SO_4^{2-} on smooth nickel based platinum nanoparticles electrode.

Acknowledgements

This work was partially supported by Politehnica University Timisoara in the frame of PhD studies.

References

[1] I. Iavicoli, V. Leso, W. Ricciardi, Environ. Health, 13 (2014) 78.
[2] X. Chen, C. Li, M. Grätzel, R. Kostecki, S.S. Mao., Chem. Soc. Rev. 41 (2012) 7909-7937.
[3] J. Zhang, C.M. Li, Chem. Soc. Rev. 41 (2012) 7016-7031.
[4] Y. Qiao, C.M. Li, J. Mater. Chem. 21 (2011) 4027-4036.
[5]C.J. Zhong, J. Luo, B. Fang, B.N. Wanjala, P.N. Njoki, R. Loukrakpam, J. Yin, Nanotechnology, 21 (2010) 062001-10.
[6] V. Mazumder, M. Chi, K.L. More, S. Sun, J. Am. Chem. Soc. 132 (2010) 7848-7849.
[7] H. Kohler, D.L. Piron, G. Belanger, J. Electrochem. Soc. 134 (1987) 120.
[8] D.L. Piron, H. Kohler, N. Masse, J. Electrochem. Soc. 132 (1991) 445.
[9] I.R.Moraes, M. Weber, F.C. Nart, Electrochim. Acta. 42 (1997) 617.
[10] C. Quijada, J.L.Vazquez, Recent Res. Dev. Electrochem. 3 (2000) 137.
[11] S.E. Lyke, S.H. Langer, J. Electrochem. Soc. 138 (1991) 1682.
[12] E.T. Seo, D.T. Sawyer, Electrochim. Acta. 10 (1965) 239.
[13] J.A. Allen, G. Rowe, J.T. Hinkley, S.W. Donne, Int. J. Hydrogen Energy 39 (2014) 11376 – 11389.
[14]Iacob A., Dan M., Kellenberger A., Vaszilcsin N., Chem. Bull. "Politehnica" Univ. Timisoara, Romania, 59 (73), (2014) 42-45.
[15] U.G. Akano, Oxygen Evolution Reactions on Nickel, Nickel Oxide Electrodes Using Galvanostatic Methods, Doctoral Thesis, 1980, McMaster University, Department of Engineering Physics, Hamilton, Ontario.
[16] E. Skavas, T. Hemmingsen, Electrochim. Acta. 52 (2007) 3510-3517.

SKELETAL NICKEL BASED 6 LAYERS PLATINUM NANOPARTICLES ELECTRODE WITH CATALYTIC EFFECT FOR ANODIC OXIDATION OF SULPHITE IN ALKALINE SOLUTION

Andreea Enache, Mircea Laurentiu Dan, Nicolae Vaszilcsin

University Politehnica Timişoara, Faculty of Industrial Chemistry and Environmental Engineering, 300223, Parvan 6, Timisoara, Romania
e-mail: enacheandreeafloriana@gmail.com

Abstract
In this paper, anodic oxidation of sulphite ions on skeletal nickel based 6 layers platinum nanoparticles electrode ($Ni_{sk} – Pt_{6layers}$) in aqueous alkaline solution was investigated by cyclic voltammetry and linear polarization. The present research is essential to understand the mechanism of reaction on this electrode.
The preliminary results presented in experimental part confirm the high catalytic activity of $Ni_{sk} – Pt_{6layers}$ for sulphite electrooxidation process and offer the possibility to use this type of electrodes in alkaline fuel cells.

Introduction
Since the 1990s, nanocatalisys emerged as one area at the interface between homogeneous and heterogeneous catalysis, which provide unique solutions to fulfill the conditions required for process improvement [1, 2].
Lately, the attention of researchers was directed towards the nanostructured materials for innovative applications in energetic industry. These materials possess promising properties for energy harvesting, conversion and storage [3].
Currently, nanoparticles represent key components in the development of energy technologies, which play an important role in replacing fossil fuels by renewable energy resources. It is therefore necessary to grow techniques for preparing larger volume of nanoparticles, that would be advantageous in terms of costs and considering that performance and commercialization of fuel cells depends on electrode material properties [4].
Nanoparticles are used as electrocatalysts in fuel cells and other electrochemical converters. The desire is to increase activity per unit area and to reduce the required amount of catalyst material whose cost is high. Performance and commercialization of fuel cell depend on electrode materials [4].
Electrochemical oxidation of sulphite in aqueous solution became an important subject for industry and environment. This process has been investigated throughout time and it has gained further interest recently due to the participation of this reaction in the Hybrid Sulfur (HyS) cycle for hydrogen production [5–9].
In this paper, cyclic voltammetry and linear polarization techniques have been used in order to describe the sulphite anodic oxidation mechanism in alkaline solutions on skeletal nickel based 6 layers platinum nanoparticles electrode.

Experimental
Electrode preparation
Chloroplatinic acid hexahydrate ($H_2PtCl_6 \cdot 6H_2O$) and isopropanol (Sigma-Aldrich, 99.7%) were used for preparation of platinum salt precursor solution.
Platinum nanoparticles were deposited on skeletal nickel substrate by spray-pyrolysis technique using an ultrasonic nebulizer SONO-TEK Corporation Exacta Coat. After

deposition, the samples were heated at 350°C for 30 minutes to obtain the platinum nanoparticles [10].

Electrochemical measurements

SP 150 Bio-Logic potentiostat/galvanostat in a three-electrode electrochemical were used for electrochemical measurements. The cell consists of Ni_{sk} – $Pt_{6layers}$ as working electrode with 0.5 cm^2active surface area, two graphite roads as counter electrodes placed symmetrically to the working electrode and Ag/AgCl as reference electrode.

Electrochemical experiments were performed in 1 mol L^{-1} NaOH solution (prepared using Merck NaOH, p.a. min. 99.8%) in the absence and presence of Na_2SO_3 (Merk, p.a. min. 98%).Na_2SO_3 concentrations added were: 10^{-3}, 10^{-2} and 10^{-1} mol L^{-1}.

Cyclic voltammograms were plotted at different scan rate between 5 and 500 mV s^{-1}. Linear polarization curves were registered at 1 mV s^{-1} scan rate.

Results and discussion

Cyclic voltammetry studies

Cyclic voltammograms plotted with high scan rate (500 mV s^{-1}) on Ni_{sk} – $Pt_{6layers}$ electrode in alkaline electrolyte with different amounts of sodium sulphite are shown in Figure 1.

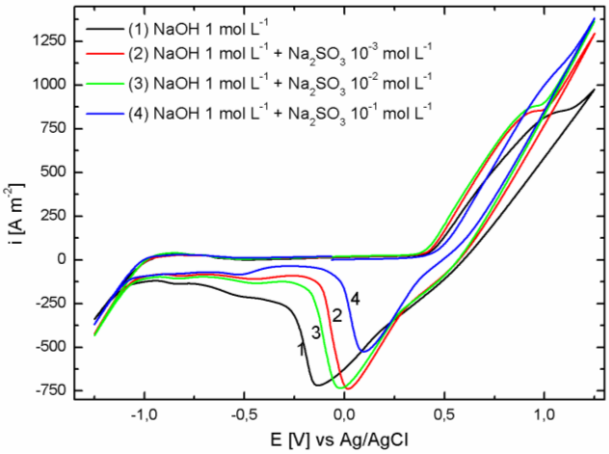

Figure 1. Cyclic voltamograms recorded on Ni_{sk} – $Pt_{6layers}$ electrode in 1 mol L^{-1} NaOH without/with different concentration of Na_2SO_3 at 500 mV s^{-1}.

Applying electrical current through electrode/electrolyte solution system, hydrogen evolution reaction (HER) is the only process visible on the cathode plateau. Sweeping potential to more positive values, within a range between +0.45 ÷ +1.15 V vs. Ag / AgCl can be seen a pick that may be associated with the formation of an oxid layer on the electrode surface followed by sulphite oxidation and oxygen evolution reaction (OER).

First identification of SO_3^{2-} ions oxidation process occurring at the interface working electrode/electrolyte was possible when the scan rate was decreased at 50 mV s^{-1} (Figure 2).

On cyclic curves registered at 50 mV s^{-1}in 1 mol L^{-1} NaOH solutions without and with Na_2SO_3 it can be observed in characteristic potential range for anodic oxidation of sulphite ions between +0.45 and +0.75 V vs. Ag/AgCl. It can be also noted that OER potential value is shifted to more negative values in solutions with SO_3^{2-}ions.

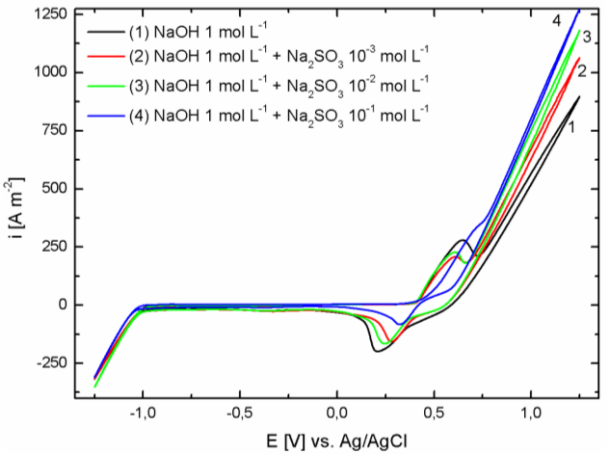

Figure 2. Cyclic voltamograms recorded on $Ni_{sk} - Pt_{6layers}$ electrode in 1 mol L^{-1} NaOH without/with different concentration of Na_2SO_3 at 50 mV s^{-1}.

Linear voltammetry studies

Linear voltammetry technique was applied to obtaine the dependence of current density versus electrode potential for anodic plateau at low scan rate (1 mV s^{-1}) in alkaline solutions with and without SO_3^{2-} (Figure 3).

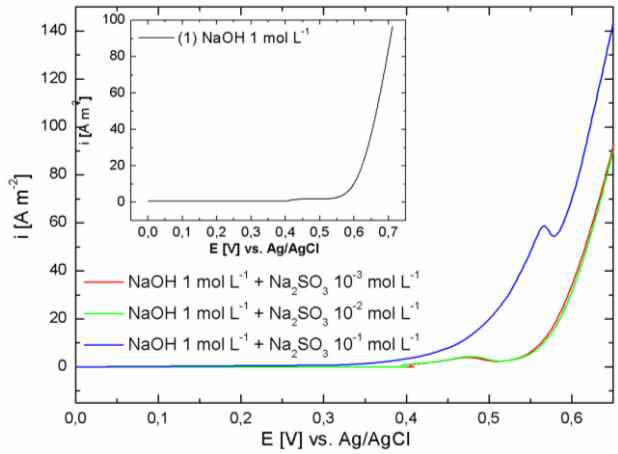

Figure 3. Linear voltammograms recorded on $Ni_{sk} - Pt_{6layers}$ electrode in 1 mol L^{-1} NaOH without/with different concentration of Na_2SO_3 at 1 mV s^{-1}; linear voltamograms in 1 mol L^{-1} NaOH inserted.

From linear voltammograms analysis, potential ranges of both oxidation processes that occur on anodic plateau (SO_3^{2-} ions oxidation and OER) have been highlighted. The curves shape indicates only one oxidation process on electrode surface.

Skavas [11] descriebed two possible mechanisms for electrochemical oxidation of sulphite to sulphate ions in alkaline media. According to this mechanism, sulphite anion is oxidized to sulphate in two successive steps, each implying one electron transfer.

On the other hand, sulphite anion is oxidized to sulphite radical which can interact forming dithionate ions $S_2O_6^{2-}$. Consecutively these ions disproportionates in sulphate and sulphite ions.

Conclusion

Ni_{sk} – $Pt_{6layers}$electrodeprepared by spray-pyrolysis technique has proved to be a promising catalyst for sulphite anodic oxidation. The platinum nanoparticles insertion has a significant effect on the studied process. The experiments presented have confirmed the possibility to oxidize electrochemicaly SO_3^{2-} to SO_4^{2-} on this type of electrode.

The possibility to oxidize sulphite ions provides a very good reason to continue studies regarding the use of Ni_{sk} – $Pt_{6layers}$as catalyst in alkaline fuel cells.

Acknowledgements

This work was partially supported by Politehnica University Timisoara in the frame of PhD studies.

References

[1] J.M. Thomas, Chem. Cat. Chem. 2 (2010) 127–132.
[2] D. Astruc, Nanoparticles and Catalysis, Wiley-VCH Verlag GmbH, Weinheim, Germany, 2008 pp. 1.
[3] J. Liu, G. Cao, Z. Yang, D. Wang, D. Dubois, X. Zhou, G.L. Graff, L.R. Pederson, J.G. Zhang, Chem. Sus. Chem. 1 (2008) 676–697.
[4] A. Islam, A.K. Bhuiya, Asia Pac. J. of Energy and Environ. 1 (2), (2014) 107.
[5] J.A. Staser, J.W. Weidner, J. Electrochem. Soc. 156 (1), **(**2009)B16–21.
[6] J.A. Staser, J.W. Weidner, J. Electrochem. Soc. 156 (7), (2009) B836–841.
[7] F. Jomard, J.P. Feraud, J.P. Caire, Int. J. Hydrogen Energy, 33 (4), (2008)1142–1152.
[8] J.A.Staser, R.P. Ramasamy, P. Sivasubramanian, J.W. Weidner, Electrochem. Solid-State Lett. 10 (11), **(**2007) E17–19.
[9] J.A. O'Brien, J.T. Hinkley, S. Donne, Electrochem. Soc., 215th ECS Meeting (2009) Abstract 403.
[10]A. Iacob, M. Dan, A. Kellenberger, N. Vaszilcsin, Chem. Bull. "Politehnica" Univ. Timisoara, Romania,59 (73), (2014) 42-45.
[11] Skavas E., Hemmingsen T., Electrochim. Acta, 52 (2007) 3510-3517.

IMPROVED QUALITY FACTOR IN (K,Na)NbO_3 BASED UNVIRONMENT FRIENDLY PIEZOCERAMICS

Iuliana Farkas*, Alexandra Ioana Bucur, Raul Alin Bucur

National Institute for Research and Development in Electrochemistry and Condensed Matter, Condensed Matter Department, No.1 Plautius Andronescu, 300224 Timisoara Romania.
e-mail: iulia_b24@yahoo.com

Abstract
Perovskite crystalline structures of (1-x)($K_{0,5}Na_{0,5}$)NbO_3 – x$GdMnO_3$ (KNN – xGM) were obtained by solid state reaction. The phase purity was confirmed by X-ray diffraction. The homogeneity of the samples was studied by S.E.M investigations. From hysteresis loops we can observe that the ferroelectric quality depends on the concentration of the dopants. Good piezoelectric properties, along with an excellent quality factor were observed for the doped samples.

Introduction
Ferroelectric ceramics are known for their widespread applications like capacitors, piezoelectric actuators, sensors and transducers etc [1, 2, 3]. The development of lead-free piezoelectric ceramics as substitutes for Pb(Zr, Ti)O_3 is recent [4], due to the high toxicity of lead based materials. Ferroelectric materials such KNN (($K_{0,5}Na_{0,5}$)NbO_3) are investigated for their excellent electric properties and also for their non-toxic behavior.
Current studies on KNN materials are focusing on the improvement of material proprieties. Material improvement can be accomplished by chemical substitution [5], alteration of phase transitions [6] or structural material alterations [7]. In this paper we are considering the use of $GdMnO_3$ doping, on improving ferroelectric and piezoelectric proprieties of KNN.

Experimental
($K_{0,5}Na_{0,5}$)NbO_3 – x$GdMnO_3$, where x= 0 mol%, 0,25mol%, 0,75mol%, 1 mol%, 1,5 mol% and 2,5 mol% were obtained by solid state method in air, starting from K_2CO_3 (99%; Scharlau, Sentmenat, Spain), Na_2CO_3 (99%; Scharlau), Nb_2O_5 (99%, Merck, Darmstadt, Spain), Gd_2O_3 (99%; Fluka, Buchs, Switzerland) and Mn_2O_3 (99%, Sigma-Aldrich, St. Louis, USA). The powders were calcined at 880ºC for 5h. After mixing with 5 mass% polyvinyl alcohol binder solution, samples with different geometries (accordingly to the dimensional requirement of each measurement) were cold-pressed at 200Mpa. The sintering was performed at 1090ºC for 3h. The crystalline structure of the sintered samples was examined by long time x-ray diffraction using a PanAnalytical X'Pert Pro MPD difractometer. The bulk density was measured using the Archimedes method. The microstructure of the sintered samples was investigated using scanning electron microscope model Inspector S Phillips (FEI, Netherlands). Silver electrodes were deposited onto the samples using Emitech K975X thermal evaporator (Ashford, UK). The hysteresis loop of each composition was obtained at 100Hz using a Sawyer-Thomson capacitive voltage divider, coupled with an Atten ADS 1152CML digital storage oscilloscope (Helmond, Netherlands). For the piezoelectric measurements, the samples were polled at 120 - 190ºC in a silicon oil bath, under a direct current electric field of 4 kV/mm, for 10 min.

Results and discussion
The X-ray diffraction patterns presented in figure 1 confirmed that all obtained samples of KNN ceramics are indexed as perovskite with an orthorhombic crystalline structure. We

observe from the x-ray diffraction that the presences of the signals from some secondary phases are getting more visible as the doping percent increases.

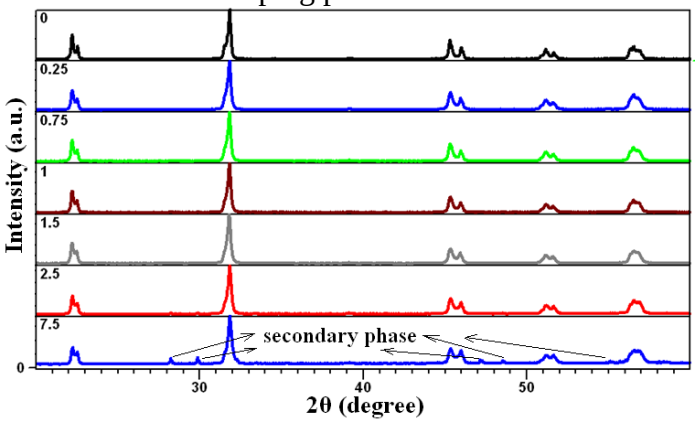

Figure 1. X-ray diffraction patterns of KNN material obtained

Figure 2 presents the variation of bulk density for the sintered samples. Compared to the reference sample KNN with a relative density of of 4.21 g/cm^3, as the doping percent increases, the density also increases almost linearly. Starting from a value of 4.28 g/cm^3 for KNN-0,25GM, the bulk density increases up to 4.4 g/cm^3 for KNN-2.5GM.

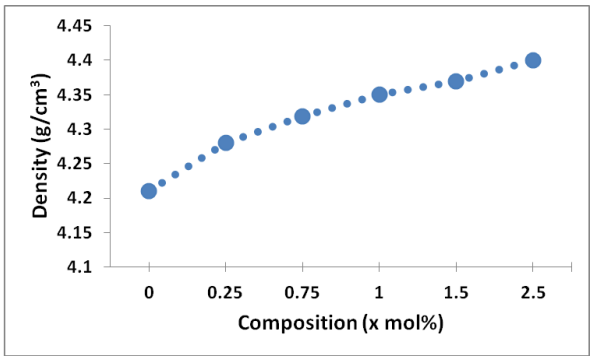

Figure 2. Variation of bulk density

The microstructure of KNN–xGM ceramics sintered at 1090ºC is shown in figure 2. As we can observe, $GdMnO_3$ inhibit the grain growth. From around 3 μm for KNN, the crystallite size decreases to around 1 μm for KNN-2.5GM. The grain morphology changed from smooth cubical grains for KNN-0GM, to round cornered grains for KNN-2,5GM.

The dielectric properties of KNN-xGM relative to the temperature, are presented in figure 4. Two distinctive inflexions can be noticed in the figure, associated with two phase transition temperatures. At around 200ºC a ferroelectric orthorombic to tetragonal phase transition is present, and also at around 400ºC a paraelectric tetragonal to cubic phase transition exists. The variation of the real part of the dielectric constant confirm that at room temperature the ceramic crystalise in orthorombic symetry. The addition of $GdMnO_3$ do not produce any significant alteration of the transition temperatures and assures a good dielectric loss, with a value below 0,5 at room temperature.

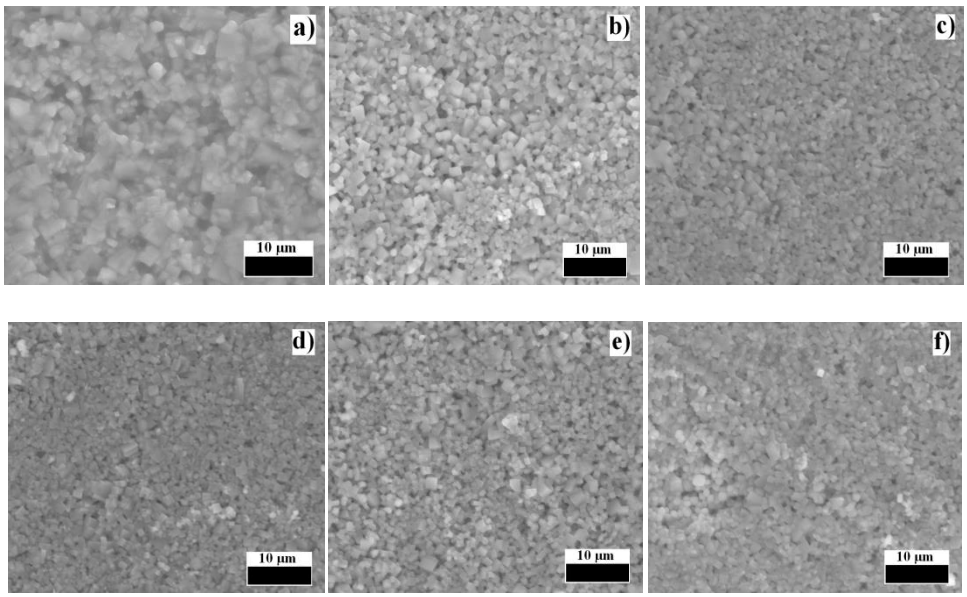

Figure 3. Surface morphology of (a) KNN – 0GM. (b) KNN – 0,25GM , (c) KNN-0,75GM, (d) KNN- 1GM, (e) KNN- 1,5 GM, (f) KNN – 2,5 GM sintered ceramics.

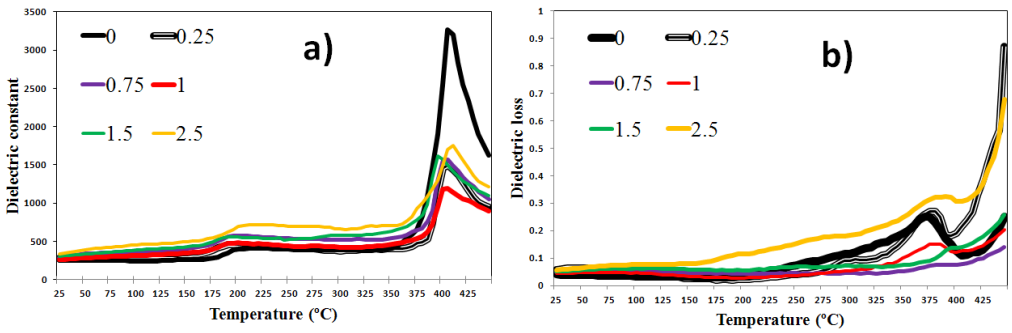

Figure 4. Temperature dependence of the dielectric constant (a) and dielectric loss (b) for thin disks of doped KNN ceramics.

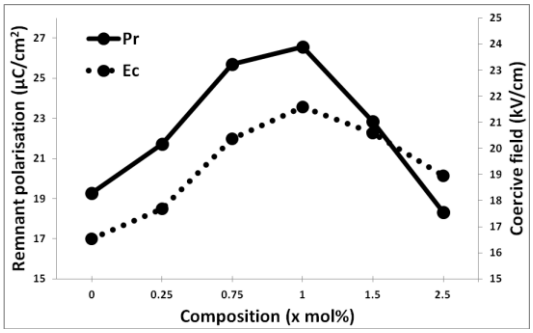

Figure 5. Remnant polarization and coercive field of KNN-xGM ceramics.

The ferroelectric properties were evaluated in terms of remnant polarization and coercive field variations presented in figure 5. All values were derived from hysteresis loops obtained with a Sawyer-Thomson capacitive voltage divider. At room temperature, for the reference sample values of 19.28µC/cm^2 and 16,53 kV/cm were measured for remnant polarization, respectively coercive field. As GM percent increases, both values increases up to 26,56µC/cm^2, respectively 21,58 kV/cm for KNN-1GM. Beyond this composition, the ferroelectric properties degrade, with a drop in both values down to 18.31µC/cm^2, respectively 18,95 kV/cm.

In figure 6, the variations of the main piezoelectric properties are presented across the compositions studied. All values presents similar trends to the variation of remnant polarization and coercive field, hence we can conclude there is a optimum composition of KNN-xGM, where all ferroelectric and piezoelectric properties are maximum: KNN-1GM. Starting with values of d_{33}= 89,2 pC/N, k_{33}= 0,475, Q_m= 407.07 and k_p= 0,347 for the reference sample KNN, the values increases to d_{33}= 97,1 pC/N, k_{33}= 0,482, Q_m= 1180 and k_p= 0,426. Beyond this composition, all value degrade significantly down to d_{33}= 83 pC/N, k_{33}= 0,433, Q_m= 592.07 and k_p= 0,37. The results show that $GdMnO_3$ addition contribute in a small extent to the charge constant and coupling factor growth, but to a large extent to the increase of the mechanical quality factor Q_m.

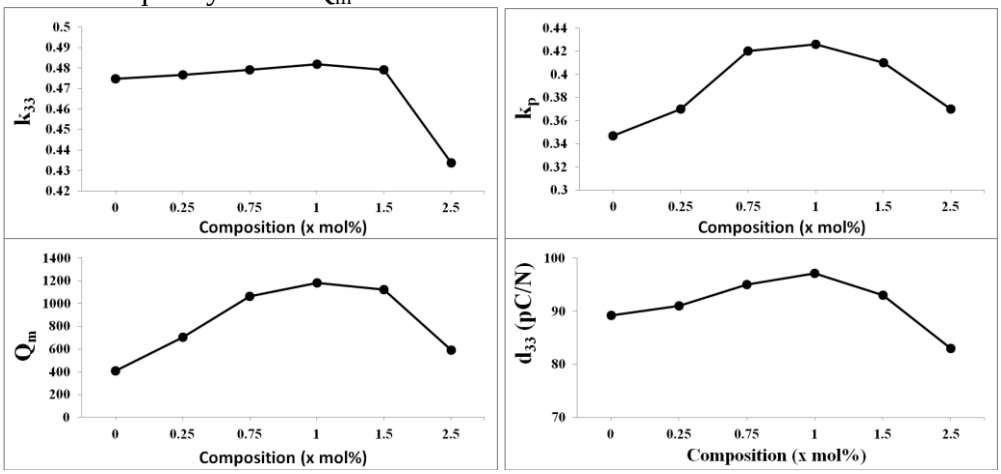

Figure 6. Piezoelectric properties of KNN-xGM ceramics.

Conclusion

$(1-x)(K_{0,5}Na_{0,5})NbO_3$ – $xGdMnO_3$ceramics were obtained by solid state reaction with orthorhombic perovskite crystalline structure at room temperature. The addition of $GdMnO_3$ decreases the grain size and increases the bulk density. While maintaining good dielectric loss values, the addition of $GdMnO_3$ do not produce any significant shift in the transition temperature. Also, $GdMnO_3$ addition improves in small measure the values of k_{33}, k_p, respectively d_{33}, and significantly increases the mechanical quality factor.

References

[1] Hong, J.; Yoo, J.; Lee, K.; Lee, S.; Song, H., Jpn. J. Appl. Phys. 2008, 47, 2192–2194.
[2] Lee, T.; Kwok, K.W.; Li, H.L.; Chan, H.L.W, Sens. Actuators A Phys. 2009, 150, 267–271.
[3] Shen, Z.Y.; Li, J.F.; Chen, R.M.; Zhou, Q.F.; Shung, K.K. J. Am. Ceram. Soc. 2011, 94, 1346–1349.
[4] Li, J.F.; Wang, K.; Zhu, F.Y.; Cheng, L.Q.; Yao, F.Z., J. Am. Ceram. Soc. 2013, 96, 3677–3696.
[5] Lu, L.; Gong, Y.Q.; Gong, L.J.; Dong, H.D.; Dong, H.; Yi, X.F.; Zheng, X.J., Mater. Des. 2012, 33, 362–366.
[6] Toshio, K.; Yuan, Y.; Fumito, Materials 2010, 3, 4965–4978.
[7] Fu, J.; Zuo, R.Z.; Wang, X.H.; Li, L.T., J. Alloys Compd. 2009, 486, 790–794.

INFLUENCE OF STRUCTURAL AND TOPOGICAL CONNECTIVITY INDICES ON DIELECTRIC PROPERTIES OF BLENDS BASED ON QUATERNIZED POLYSULFONES: THEORETICAL APPROACH

Anca Filimon[1*], Adriana Popa[2]

[1]*Department of Physical Chemistry of Polymers,"Petru Poni" Institute of Macromolecular Chemistry, Aleea Grigore Ghica Voda 41 A, 700487 Iasi, Romania*
[2]*Institute of Chemistry Timisoara of Romanian Academy, Mihai Viteazul Blv. 300223 Timisoara, Romania*
e-mail: capataanca@yahoo.com

Abstract

Cationic polysulfones containing quaternary ammonium side groups (PSFQ), synthesized by reaction of the chloromethylated polysulfone (CMPSF) with a tertiary amine, N,N-dimethylbutylamine (DMBA), are considered to be suitable for a wide range of applications from the electronic field. Additionally, quaternized polysulfone-based composites with optical and electrical properties represent a challenge for researchers. Therefore, it is of interest to find out whether PSFQ can be designed for specific applications in blends with polyvinyl alcohol (PVA) and to establish their impact on the different properties. Thus, in the present study the cationic polysulfone PSFQ was analyzed in combination with PVA, which is supposed to improve among the other properties, such as hydrophylicity, flexibility, and the optical ones [1].In this context, the thermoplastic characteristics (*e.g.*,the refractive index and dielectric constant)were evaluated using the structural and topological techniques of spatial arrangement of the constituent atoms from analyzed polymer [2], by means the zero-order connectivity indices and first-order connectivity indices (Table 1).

Table 1. Zero-order connectivity indices, ${}^0\chi$,and ${}^0\chi^v$, and first-orderconnectivity indices, ${}^1\chi$and ${}^1\chi^v$, as well as the theoretical values of the refractive index, n_{th}, and dielectric constant, ε_{th}, for different mixing ratio of PSFQ/PVA blend

Sample	Parameters					
	${}^0\chi$	${}^0\chi^v$	${}^1\chi$	${}^1\chi^v$	n_{th}	ε_{th}
PSFQ	52.054	43.439	34.680	24.785	1.580	2.496
PVA	2.284	1.732	0.986	0.666	1.500	2.250
PSFQ/PVA						
75/25	39.612	33.012	26.256	18.755	1.5600	2.434
50/50	27.169	22.585	17.833	12.725	1.5400	2.372
25/75	14.726	12.158	9.409	6.695	1.5200	2.310

Data obtained emphasize the effects generated by the molecular structure, electrostatic repulsions between charge groups, and/or intermolecular interactions; a slightly decrease of n and ε with increasing of the PVA content was observed, this being useful for certain applications that involves a lower polarizability for the final products. Consequently, results will be useful in predicting of the special properties of these polymers in order to obtain high performance materials with applications both in electronic and optical field.

References

[1] Roddecha, Z. Dong, Y. Wu, M. Anthamatten, J. Membr. Sci. 389, (2012) 478.
[2] J. Bicerano, Prediction of Polymer Properties, Marcel Dekker, New York, 1993.

SYNERGISTIC EFFECTS OF STRUCTURAL CHARACTERISTICS OF QUATERNIZED POLYSULFONE/CELLULOSE ACETATE PHTHALATE BLENDS ON SURFACE PROPERTIES

Mihaela Dorina Onofrei[1], Adriana Popa[2], Anca Filimon[1]
[1] *"Petru Poni" Institute of Macromolecular Chemistry, Aleea Grigore Ghica Voda 41 A, 700487 Iasi, Romania Romania*
[2] *Institute of Chemistry Timisoara of Romanian Academy, Mihai Viteazul Blv.,300223 Timisoara, Romania*
e-mail: capataanca@yahoo.com

Abstract

An alternative in order to obtain of new complex polymeric materials is represented by the blending polymers, thus creating a balance between the properties of individual components. New quaternized polysulfones (PSFQ)/cellulose acetate phthalate (CAP) blends were investigated for establishing the structural and compositional characteristics with impact on the surface properties. In this context, the synergistic effects generated by the charged groups from the alkyl radical of the quaternized polysulfones, flexible and hydrophilic nature of CAP in casting solution of polysulfone significantly influenced the surface tension parameters, surface free energy, and topographic reorganization. Moreover, the CAP composition, as well as the history of the formed films provide the controlling surface properties and are responsible for performance properties of the final membranes.

In order to understand the correlation between the structural particularities and the resulting properties a deep analysis of the morphology must be performed (Figure 1).

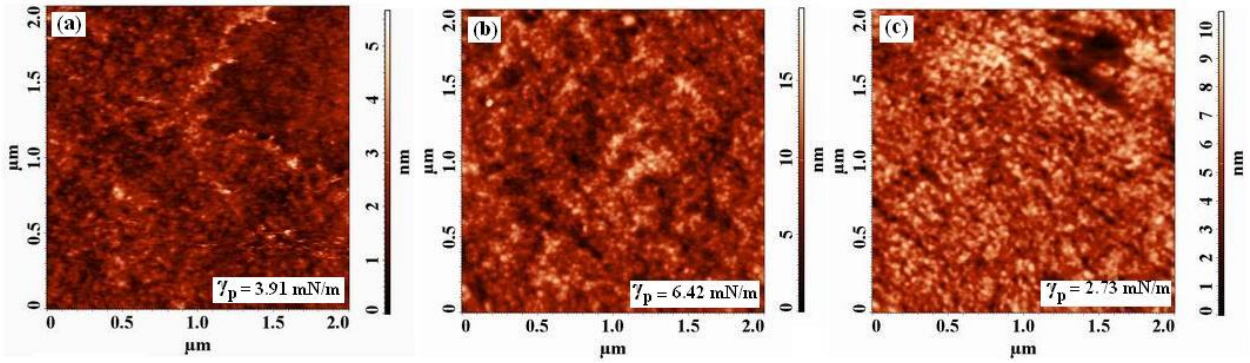

Figure 1. 2D images of topography performed by atomic force microscopy for samples: (a) PSFQ, (b) CAP, and PSFQ/CAP blend at 50/50 w/w composition. Variation of polar components of total surface tension, γ_p

Varying the polymer blend composition in the casting solutions were modified the morphological characteristics and pore numbers, as well as surface energy characteristics. These results indicate that apart from the history of the films formed from solutions in NMP, the nature of the functional groups spread all along the chain and charge density of the PSFQ, affects these parameters.

It can be concluded that, the resulted data are important in designing of PSFQ/CAP blends, with controllable porosity and hydrophilicity, as potential performance materials used in biomedical fields.

PARTIAL LEAST SQUARES MODEL OF MOULTING ACCELERATING COMPOUNDS WITH INSECTICIDE ACTIVITY AGAINST LEPIDOPTERAN SPECIES[†]

Simona Funar-Timofei[1*], Alina Bora[1], Ana Borota[1], Daniela Ionescu[2],Luminita Crisan[1]

[1]*Institute of Chemistry Timisoara of the Romanian Academy, Bul. Mihai Viteazu 24, 300223 Timisoara, Romania*
[2]*University of Medicine and Pharmacy, Faculty of Pharmacy, P-ta Eftimie Murgu 2-4, 300034 Timisoara, Romania*
e-mail: timofei@acad-icht.tm.edu.ro

Abstract

In this study the insecticidal activity of a series of 33 dibenzoylhydrazinederivatives, expressed as the pEC_{50}activity measured *in vitro*, based on an ecdysone-dependent reporter assay using cell lines derived from one lepidopteran species (the cotton leafworm *Spodoptera littoralis*), was correlated with structural descriptors using the partial least squares (PLS) approach. The data set was energy pre-optimized by molecular mechanics calculations using the MMFF94s force field. Several 0D, 1D, 2D and 3D descriptors were calculated for the minimum energy conformers. A two-components PLS model was obtained with acceptable statistical quality ($R^2X(Cum) = 0.705$, $R^2Y(cum) = 0.821$ and $Q^2(Cum) = 0.793$) for modeling the insecticidal activity. The model goodness of fit tested with the Y-randomization test indicated a stable model. Specific dibenzoylhydrazine structural features supplying information about topological distances and descriptors sensitive to any conformational change influence the insecticidal activity.

Introduction

Dibenzoylhydrazine compounds are insect growth regulators that act through the induction of an early and lethal larval molting process in vulnerable insects that belong to the species of Lepidoptera and Coleoptera [1]. These compounds are effective in the pest control because they activate the steroid receptor complex of ecdysone type at lower concentrations than the natural hormone, and because the insect cannot remove them efficiently from its body. As consequence, a constant state of ecdysteroid signaling is displayed in the insect, which avoids it to complete the molting process and for which a decrease in ecdysteroid signaling is required. Because the insect stays permanently trapped in the molting process and is unable to feed, it dies in the period of a few days from desiccation and starvation.

The importance of the unusual high affinity for the ecdysone receptor of lepidopteran insects of dibenzoylhydrazine non-steroidal ecdysone agonists has been recognized [2]. The molecular mechanism of action of ecdysteroids, was not explained until now because one of the three interaction sites of the hormone-receptor model is not present in some active compounds [3].

The objective of this paper is to determine the structural features of a series of 33 dibenzoylhydrazine ecdysone agonists [4] (Table 1), which influence the lethal larval molting process in susceptible insects that belong to the orders of one lepidopteran species, namely the cotton leafworm *Spodoptera littoralis*. The quantitative relationship between chemical features and the ecdysone agonistic activitywas determinedby means of the partial least squares (PLS) approach.

[†] Dedicated to the 150th anniversary of the Romanian Academy

Table 1. The smiles notation of dibenzoylhydrazine analogue structure and their experimentalinsecticidal (pEC_{50}) and predicted activity values (pEC_{50pred}) obtained using the PLS method

No	Smiles	pEC_{50}	pEC_{50pred}
1	CC(C)(C)N(NC(=O)C1=CC=CC=C1)C(=O)C1=CC=CC=C1	5.89	6.14
2	CCC1=CC=C(C=C1)C(=O)NN(C(=O)C1=CC(C)=CC(C)=C1)C(C)(C)C	8.66	7.53
3	COC1=CC=CC(C(=O)NN(C(=O)C2=CC(C)=CC(C)=C2)C(C)(C)C)=C1C	8.22	8.23
4	CC(C)(C)N(NC(=O)C1=CC=C(Cl)C=C1)C(=O)C1=CC=CC=C1	6.34	6.65
5	CC1=CC(=CC(C)=C1)C(=O)N(NC(=O)C1=C(C)C2=C(OCCC2)C=C1)C(C)(C)C	8.58	8.41
6	CC(C)(C)N(NC(=O)C1=CC=CC=C1)C(=O)C1=C(C=CC=C1)C(F)(F)F	6.1	5.99
7	CC(C)(C)N(NC(=O)C1=CC=CC=C1)C(=O)C1=C(Cl)C(Cl)=C(Cl)C=C1	5.28	5.34
8	CC(C)(C)N(NC(=O)C1=CC=CC=C1)C(=O)C1=C(Cl)C(Cl)=C(Cl)C=C1	6.3	6.99
9	CC(C)(C)N(NC(=O)C1=C(F)C=CC=C1)C(=O)C1=C(Cl)C=CC=C1	6.54	6.08
10	CC1=C(C=CC=C1)C(=O)NN(C(=O)C1=C(Cl)C=CC=C1)C(C)(C)C	6.36	6.98
11	CC(C)(C)N(NC(=O)C1=CC(F)=CC=C1)C(=O)C1=C(Cl)C=CC=C1	6.34	5.54
12	CC(C)(C)N(NC(=O)C1=CC(Cl)=CC=C1)C(=O)C1=C(Cl)C=CC=C1	5.77	5.82
13	CC(C)(C)N(NC(=O)C1=CC=C(Br)C=C1)C(=O)C1=C(Cl)C=CC=C1	6.36	6.32
14	CCCC1=CC=C(C=C1)C(=O)NN(C(=O)C1=C(Cl)C=CC=C1)C(C)(C)C	7.13	6.45
15	CC(C)C1=CC=C(C(NN(C(C)(C)C)C)C(C2=C(Cl)C=CC=C2)=O)=O)C=C1	7.76	6.81
16	COC1=CC=C(C=C1)C(=O)NN(C(=O)C1=C(Cl)C=CC=C1)C(C)(C)C	6.47	6.06
17	CC(C)(C)N(NC(=O)C1=CC=CC=C1)C(=O)C1=CC=CC=C1	8.15	7.78
18	CC1=CC(=CC(C)=C1)C(=O)N(NC(=O)C1=CC=C(C=C1)C(C)(C)C)C(C)(C)C	7.79	8.20
19	CC1=CC(=CC(C)=C1)C(=O)N(NC(=O)C1=C(C)C(C)=CC=C1)C(C)(C)C	6.96	7.24
20	CCC1=CC=C(C=C1)C(=O)NN(C(=O)C1=CC=CC=C1)C(C)(C)C	4.66	5.14
21	CCOC1=C(C=CC=C1)C(=O)N(NC(=O)C1=CC=C(OC)C=C1)C(C)(C)C	5.02	5.00
22	CCOC1=C(C=CC=C1)C(=O)N(NC(=O)C1=CC=C(Cl)C=C1)C(C)(C)C	5.16	5.27
23	CCOC1=C(C=CC=C1)C(=O)N(NC(=O)C1=CC=C(CC)C=C1)C(C)(C)C	5.76	6.02
24	CC1=CC(C(=O)N(NC(=O)C2=CC=CC=C2)C(C)(C)C)=C(Cl)C(C)=C1	6.47	6.60
25	CCC1=CC=C(C=C1)C(=O)NN(C(=O)C1=C(Cl)C(C)=CC(C)=C1)C(C)(C)C	5.95	6.13
26	CCCCC1=CC=C(C=C1)C(=O)NN(C(=O)C1=C(Cl)C(C)=CC(C)=C1)C(C)(C)C	5.69	6.36
27	COC1=CC=C(C=C1)C(=O)NN(C(=O)C1=C(Cl)C(C)=CC(C)=C1)C(C)(C)C	5.87	6.04
28	CC1=CC=C(C=C1)C(=O)NN(C(=O)C1=C(Cl)C(C)=CC(C)=C1)C(C)(C)C	5.45	6.02
29	CCCCCC1=CC=C(C=C1)C(=O)NN(C(=O)C1=C(Cl)C(C)=CC(C)=C1)C(C)(C)C	5.97	6.10
30	CC1=CC(C(=O)N(NC(=O)C2=CC=C(Cl)C=C2)C(C)(C)C)=C(Cl)C(C)=C1	7.17	7.52
31	CC1=CC(C(=O)N(NC(=O)C2=CC=C3OCCCC3=C2C)C(C)(C)C)=C(Cl)C(C)=C1	8.27	8.35
32	CC1=C2CCCOC2=CC=C1C(=O)NN(C(=O)C1=C(Cl)C=CC=C1)C(C)(C)C	6.49	6.00
33	CCCCCC1=CC=C(C=C1)C(=O)NN(C(=O)C1=C(Cl)C=CC=C1)C(C)(C)C	5.11	4.92

Material and methods

Definition of target property and molecular structures

A series of 33 dibenzoylhydrazine analogues (Table 1) was used, having the insecticidal activity pEC_{50} measured *in vitro*, based on an ecdysone-dependent reporter assay using cell lines derived from the lepidopteran speciesthe cotton leafworm *Spodoptera littoralis*,as dependent variable.

These insecticides were energy pre-optimized by molecular mechanics calculations using the MMFF94s force field included in the OMEGA (version 2.5.1.4, OpenEye Scientific Software, Santa Fe, NM. http://www.eyesopen.com) software [5, 6]. Structural 0D, 1D, 2D and 3D descriptors were calculated for the minimum energy structures using the DRAGON (Dragon Professional 5.5 (2007), Talete S.R.L., Milano, Italy) and InstantJchem (which was used for structure database management, search and prediction) (InstantJchem 6.0.0, 2013, ChemAxon (http://www.chemaxon.com) software

The Partial Least Squares (PLS) method

Projections to latent structures (PLS) represent a regression technique for modeling the relationship between projections of dependent factors and independent responses. In this approach data analysis features link a block (or a column) of response variables to a block of explanatory variables [7]. The relationship between the dependent and independent variables is described as a latent variable approach [8]. The PLS approach leads to stable, correct and highly predictive models even for correlated descriptors [9].PLS calculations were performed by the SIMCA package (SIMCA P+ 12.0.0.0, May 20 2008, Umetrics, Sweeden, http://www.umetrics.com/). The QSAR matrix (including the dependent and independent matrices) was analyzed in a first step by the principal component analysis (PCA) [10],and subsequently by the partial least squares(PLS)approaches. The squared correlation regression coefficient R^2, and the squared cross-validated correlation coefficient, Q^2, are the most important statistical parameters that provide a measure of the quality and validity for the final PLS model, while the Variables Importance in the Projection (VIP) values and the sign of the variables' coefficients are more relevant in explaining the activity mechanism. The significant principal components were selected by 7 cross-validation groups.

The Y-randomization test is a widely used technique that displays the robustness of a QSAR model, being a measure of model overfit. The dependent variable (biological activity) is randomly shuffled and a QSAR model is built using the same descriptor matrix. The obtained PLS models (after 999 randomizations) must have the minimal R^2 and Q^2 values[11].

Results and discussion

A statistical analysis of the dibenzoylhydrazine analogues was performed using the calculated variables.A PCA model was built for the whole X matrix (including N=33 compounds and X = 1462 descriptors). From the total of 7 significant principal components resulted from this analysis, the first three components already explained 61.7% of the information content of the descriptor matrix. PLS calculations were, also, performed using the same program forthe same dataset.

Table 2. The coefficients in descending order of VIP values for the two principal components of model M2.

No	Variable ID*	CoefCS[2]	VIP[2]	No	Variable ID*	CoefCS[2]	VIP[2]
1	BEHe2	0.07	0.98	8	Mor32p	0.20	1.22
2	BELm1	0.10	1.01	9	Mor32v	0.19	1.21
3	F09[C-C]	0.05	0.94	10	R4u	0.14	1.07
4	G3m	0.17	0.88	11	R5u	0.12	0.95
5	Infective-80	0.16	0.94	12	RDF085v	0.08	0.84
6	Mor02m	0.11	0.80	13	VEA1	0.11	0.97
7	Mor29e	0.17	1.01	14	VEA2	0.20	1.08

*BEHe2-highest eigenvalue n. 2 of Burden matrix / weighted by atomic Sanderson electronegativities, BELm1-lowest eigenvalue n. 1 of Burden matrix / weighted by atomic masses, F09[C-C]-frequency of C-C at topological distance 9, G3m-3st component symmetry directional WHIM index / weighted by atomic masses, Infective-80 - Ghose-Viswanadhan-Wendoloski antiinfective-like index at 80%, Mor02m-3D-MoRSE - signal 02 / weighted by atomic masses, Mor29e-3D-MoRSE - signal 29 / weighted by atomic Sanderson electronegativities, Mor32p-3D-MoRSE - signal 32 / weighted by atomic polarizabilities, Mor32v-3D-MoRSE - signal 32 / weighted by atomic van der Waals volumes, R4u-R autocorrelation of lag 4 / unweighted,R autocorrelation of lag 5 / unweighted, R5u-Radial Distribution Function - 8.5 / weighted by atomic van der Waals volumes, VEA1-eigenvector coefficient sum from adjacency matrix, VEA2-average eigenvector coefficient sum from adjacency matrix

The statistical results of the PLS model: $R^2_Y(CUM) = 0.837$ and $Q^2(CUM) = 0.613$ obtained for three principal components demonstrated the model overfit ($R^2_{X(CUM)}$ and $R^2_{Y(CUM)}$ are the cumulative sum of squares of all the X and Y values). This inconvenience was overstepped by excluding the noise variables from this model (e.g. coefficient values insignificantly different from 0). Thus, a robust model, M2 (N= 33 and X= 14) with two latent variables, which explaines70.5% of the information content of the descriptor matrix, $R^2_Y(CUM) = 0.821$ and $Q^2(CUM) = 0.793$ was obtained.
All selected variables in M2(Table 2) had VIP values greater than 1 and were considered to be the most relevant for the model.For the test set the Y-randomization procedure was applied using the SIMCA-P+ 12.0 software (for the final PLS model). It gave the following intercept (PLS) values of the regression lines obtained by the correlation between the calculated R^2, respectively Q^2 values of the original Y-variable and the shuffled Y-variable, respectively: 0.134 for the R^2_Y line and -0.249 for the Q^2_Y line. The slope values close to zero indicate stable models.

Conclusion

The final modelof dibenzoylhydrazine non-steroidal ecdysone agonists obtained using the PLS method have good statistical parameters.The most important molecular descriptors for the insecticidal activity are related to the geometric representation of molecules, providing information on interatomic and topological distances, structural fragments, descriptors sensitive to any conformational change, antiinfective drug-like index having a qualifying range that covers approximately 80% of the drugs studied.

Acknowledgements

This project was financially supported by Project 1.1 of the Institute of Chemistry of the Romanian Academy. Access to the Chemaxon Ltd. and OpenEye Ltd. software are greatly acknowledged by the authors.

References

[1] L. Swevers, T. Soin, H. Mosallanejad, K. Iatrou, G. Smagghe, Insect Biochem. 38 (2008) 825.
[2] T. Soin, M. Iga, L. Swevers, P. Rougé, C.R. Janssen, G. Smagghe, Insect Biochem. 39 (2009) 523.
[3] N. Ferro, J.E. Tacoronte, T. Reinard, P. Bultinck, L.A. Montero, J. Mol. Struct.-THEOCHEM 758 (2006) 263.
[4] T. Soin, E. De Geyter, H. Mosallanejad, M. Iga, D. Martín, S. Ozaki, S. Kitsuda, T. Harada, H. Miyagawa, D. Stefanou, G. Kotzia, R. Efrose, V. Labropoulou, D. Geelen, K. Iatrou, Y. Nakagawa, C.R. Janssen, G. Smagghe, L. Swevers, Pest. Manag. Sci.66 (2010) 526.
[5]. P.C.D. Hawkins, G.A. Skillman, G.L. Warren, B.A. Ellingson, M.T. Stahl, J. Chem. Inf. Model. 50(2010) 572.
[6]. P.C.D. Hawkins, A. Nicholls, J. Chem. Inf. Model. 52 (2012) 2919.
[7] H. Wold, in: S. Kotz and N.L. Johnson (Eds.), Encyclopedia of Statistical Sciences, (Vol. 6), Wiley, New York, 1985, pp. 581.
[8] L. Eriksson, J. Gottfries, E. Johansson, S. Wold, Chemom. Intel. Lab. Syst.73 (2004) 73.
[9] A. Höskuldsson, J. Chemometrics 2(3) (1998) 211.
[10] M. Daszykowski, K. Kaczmarek, V. Heyden, B. Walczak, Chemom. Intell .Lab. Syst. 85 (2007) 203.
[11] P.P. Roy, S. Paul, I. Mitra, K. Roy, Molecules 14(2009) 1660.

ASPECTS OF THE HOMEOSTASIS CHANGES INDUCED BY THE GALLIUM COMPLEX C(24) IN EXPERIMENTS ON RATS

Zeno Gârban[1,2], Ioniţă Hortensia[3], Gârban Gabriela[2,4], Muselin F.[2,5], Baltă Cornel[6], Simiz Eliza[7], Ujhelyi Robert[2,8]

[1]Department of Biochemistry and Molecular Biology (former), Faculty of Food Products Technology, University of Agricultural Sciences and Veterinary Medicine of Banat "King Michael I of Romania" Timişoara, Calea Aradului No. 119, RO-300 645 Timişoara, Romania
[2]Working Group for Xenobiochemistry, Romanian Academy-Branch Timişoara, Bd. M.Viteazu Nr.24, RO-300 223 Timişoara, Romania
[3]Clinic of Hematology-Oncology, Faculty of Medicine, „Dr. Victor Babeş" University of Medicine and Pharmacy, Timişoara, Romania
[4]Laboratory of Environment and Nutrition, National Institute of Public Health - Branch Timişoara, Romania
[5]Faculty of Animal Sciences and Biotechnology, University of Agricultural Sciences and Veterinary Medicine of Banat "King Michael I of Romania" Timişoara, Romania
[6]Faculty of Medicine, West University „Vasile Goldiş" Arad, Romania
[7]Faculty of Veterinary Medicine, University of Agricultural Sciences and Veterinary Medicine of Banat "King Michael I of Romania" Timişoara, Romania
[8]Medical Department, S.C. CaliVita International, Timişoara, Romania
e-mail.: zeno.garban@yahoo.com

Abstract
The action of the Ga complex C(24) on some serum biochemical parameters in rats was studied in two different day times, i.e. morning and evening. There were analyzed : total serum proteins (PRO); serum albumin (ALB); serum non-protein nitrogenous compounds, i.e. uric acid (UA), creatinine (CRE), blood ureea nitrogen (BUN); calcemia and magnesiemia. The obtained values and calculation of differences made possible to evidence homeostasis changes occurring in two direction: conditioned by time (choronobiochemistry) and conditioned by the administered xenobiotic (i.e. the studied Ga complex).

Keywords:homeostasis, serum biochemical parameters, gallium complex C(24)

Introduction
Investigations regarding blood biochemical parameters are of special interest to metabolomics and metallomics because blood is the main tissue that transports the metabolites and xenobiotics (including the pharmaceutical ones, too) in the organism.
Such studies can allow to evidence and monitor homeostasis changes caused by various chemical xenobiotics of nutritional (e.g. food contaminants) and pharmaceutical interest (chemotherapeutics) and can offer useful information in elucidating their structures, properties, mechanism of actionat molecular and tissue level (Gielen and Tienkink, 2005).
All the above mentioned investigations are of importance in nutrition, toxicology, pharmacology and, evidently in biochemistry and xenobiochemistry (Testa, 1995). In the last two decades there were performed numerous investigations on Ga compounds in order to use them in therapy, implicitly in certain form of cancer (Haiduc and Silvestru, 1989; Collery et al., 2002).
Certain studies had in view distinctly the following inorganic compounds: gallium nitrate, chloride and sulfate (Bernstein, 1998; Chitambar, 2012). Also, there were investigated the effects induced by some organometallic compounds as: gallium maltolate,gallium 8-quinolinolate (Collery et al., 2002), gallium protoporphirin IX (Arivett et al., 2015).

The aim of this study was to evidence the effects induced in rats by the new gallium complex C(24) considered as a xenobiotic.

Experimental

Chemicals.

Experiments were performed on the actions of the organometallic gallium complex with the formula: [NEt3H][Ga{PPh(2-SC6H4)2-k3S,S',P}-{PPh(2-SC6H4)2-k2S,S'}]

This complex is noted usually C(24) and has a molecular weight of 820.71 Da - details see Vălean et al., 2009. The gallium complex C(24) was solved in a mixture of co-solvents consisting of: water-ethanol-polyethylen glycol (PEG) 400. In biomedical experiments and in some pharmaceuticals the usage of PEG is a regular practice (Milton, 1992; Gârban et al., 2013 a). In this study there were used ethanol-C_2H_5-OH with the molecular weight46.07producedbyS.C."P.A.M. Corporation" S.R.L., Romaniaandpolyethyleneglycol HO $(C_2H_4)_nH$ with the molecular weight380-420and density of1.13g/cm^3, produced bySCharlabSL., Pol. Ind. Mas d`enCisa, Sentmenat, Barcelona, Spain.

Experimental design.

In this study Wistar strain albino rats weighing 100-120 g were used. They were fed with commercial dry pellets manufactured by S.C. Freman Oradea and received tap water *ad libitum*. Two series of animals were composed: a morning (m) one - administration of substance at 7 a.m. and an evening (e) one - administration of substance at 7 p.m. Each series consisted of two groups (each with 6 animals): control (C) and experimental (E) . Animals of morning control group C_m and evening control group C_e were injected intraperitoneally (i.p.) with physiological saline 1 mL / 100 g b.w. Animals of morning experimental group E_m and evening experimental group E_e were injected i.p. with a solution containing the Ga complex C(24) dissolved in the core-solution a „co-solvent" containing Et-OH 40% : PEG 400 at the ratio 1: 1.5 (practically the solvent for the Ga complex, i.e. its carrier).The concentration of the administered gallium complex C(24) in solution was 0.25 mg/mL, each animal receiving 1 mL / 100 g b.w. (i.e. 2.5 mg/kg b.w.). During the injection of the substances the animals were anesthetized by inhalatory administration of Anesteran (Rompharm Co. Bucharest). At the end of the experiment, i.e. at 48 hrs the animals were anesthetized again and blood samples were collected for biochemical and hematological analysis. Determinations were carried out in identical conditions in the morning / evening. The investigations were in accordance with the ethical standards laid down in the Council Directive 86/609/EECregarding the protection of animals used for experimental and other scientific purposes.

Investigation of the biochemical parameters.

The biochemical parameters were determined by spectrophotometric methods used in clinical chemistry. For this purpose the biochemical "Spotchem" Analyzer was used with specific reagent strips manufactured by „Arkray Factory Inc." (Koji-Japan). Thus, the followings were considered: total serum proteins (PRO); albumin (ALB); non-protein nitrogen compounds, i.e. uric acid (UA), creatinine (CRT), blood urea nitrogen (BUN); calcemia and magnesiemia. Details on the analytical methods were presented in a previous paper (Gârban et al., 2013 b).

Statistical evaluation.

Analytical data were processed by determining the mean values (X) and standard deviations (SD). To analyse the differences between group means the analysis of variance (ANOVA) test was applied by using a SSPS IBM Statistic 19.0 software package.

Results and discussions

The experiments presented in this paper pursued to highlight possible disturbances in the homeostasis of the mentioned serum biochemical parameters induced by the new gallium complex C(24).

It is known that certain gallium compounds are used not only in the treatment of tumors but also in some infective diseases (Antunes et al., 2012). Usage of Ga(III) as compound with anti-infective action is considered as a "Trojan Horse" strategy in the interactions occurring in the living tissue (Arivett et al., 2015) .

One of issues was to assess the "effects conditioned by time"- with importance in chronobiochemistry- both in case of control groups C_m and C_e and of experimental groups E_m and E_eThese effects were denotedas (ΔX_1) and represent the differences between the means of the morning and evening parameters. A second issue was the evaluation of the "effects conditioned by the substance" (the xenobiotic with gallium) and denoted as (ΔX_2) being the differences between the means of control groups and experimental groups.

Results of investigations concerning serum proteins and albumin in rats injected with the gallium complex C(24) are given in Table 1.

Normal values of proteinemia and albuminemia in rats, according to Car et al. (2006) are 5.5-6.6 g/dL respectively 4.0-4.8 g/dL. Other literature data give different values, e.g. 5.6-7.6 g/dL for total serum proteins and 3.8-4.8 g/dL for serum albumin (http://www.ratfanclub.org./values.html).

Our data for PRO and ALB showed a mild evening increase in case of control groups and an evening decrease in the experimental groups (ΔX_1). The obtained values were statistically non-significant. These findings could be attributed to the chronobiological specificity of protein synthesis in animals (Gârban, 2015). Such data were mentioned in humans, too (Haus et al. 1993).

Table 1 Homeostasis changes in serum protein and albumin

Serum parameters	UM	Groups (n=6)	X ± SD	Groups (n=6)	X ± SD	ΔX_1
PRO	g/dL	C_m	5.72 ± 0.30	C_e	5.90 ± 0.34	+ 0.18
		E_m	5.67 ± 0.24	E_e	5.65 ± 0.33	- 0.02
		ΔX_2	- 0.05	–	- 0.25	–
ALB	g/dL	C_m	3.18 ± 0.32	C_e	3.26 ± 0.08	+ 0.08
		E_m	3.08 ± 0.13	E_e	2.88 ± 0.27	- 0.20
		ΔX_2	- 0.10	–	- 0.38	–

Analyzing the obtained data of PRO and ALB in the experimental groups versus to those of control groups one can observe that the gallium complex C(24) induceda light decrease (see ΔX_2) both in the morning and evening series.

Concerning the results of serum non-protein nitrogen metabolites, i.e. uric acid (UA), creatinine (CRE) and blood urea nitrogen (BUN) as well as those of calcium and magnesium are presented in Table 2.

Table 2 Homeostasis changes in the serum non-protein nitrogen metabolites, calcium and magnesium

Serum parameters	UM	Groups (n=6)	X ± SD	Groups (n=6)	X ± SD	ΔX_1
UA	mg/dL	C_m	0.64 ± 0.09	C_e	0.62 ± 0.08	- 0.02
		E_m	0.70 ± 0.12	E_e	0.64 ± 0.09	- 0.06
		ΔX_2	+ 0.06	–	+ 0.02	–
CRE	mg/dL	C_m	0.58 ± 0.08	C_e	0.60 ± 0.15	+ 0.02
		E_m	0.62 ± 0.10	E_e	0.63 ± 0.15	+ 0.01
		ΔX_2	+ 0.04	–	+ 0.03	–
BUN	mg/dL	C_m	15.66 ± 3.26	C_e	16.83 ± 3.43	+ 1.17
		E_m	19.83 ± 4.16	E_e	17.66 ± 3.72	- 2.17
		ΔX_2	+ 4.17	–	+ 0.83	–
Calcium	mg/dL	C_m	11.48 ± 0.31	C_e	11.23 ± 0.19	- 0.25
		E_m	11.46 ± 0.38	E_e	11.68 ± 0.42	+ 0.22
		ΔX_2	- 0.02	–	+ 0.45	–
Magnesium	mg/dL	C_m	1.96 ± 0.22	C_e	1.95 ± 0.12	- 0.01
		E_m	1.82 ± 1.54	E_e	1.96 ± 0.05	+ 0.14
		ΔX_2	- 0.14	–	+ 0.01	–

The results of the experiment showed chronobiochemical changes in the control groups by the increase of the evening values of CRE and BUN as well as the decrease of UA. In case of experimental groups UA and BUN decreased while CRE increased in the evening series. As to the values of Ca and Mg an evening decrease in the control groups and increase in the experimental groups were found (see ΔX_1). Chronobiological changes by Ga involvement in substitution of Fe, Ca, Mg, etc. were reported by Bernstein (1998).

When evaluating the effects induced by the gallium complex C(24) - evidenced by the differences ΔX_2 - one can remark increases of UA, CRE, BUN in all experimental groups. Values of serum Ca and Mg showed a decrease in the morning and increase in the evening. Experiments on rats by i.p. injection of Ga salts (nitrate) made by Chitambar (2012), showed a decrease in serum Ca and inhibition of bone resorbtion.

This evaluation of homeostasis changes explains, per se, the interest toward the effects conditioned by time and induced by various chemical compounds (xenobiotics) in the animal organism which can be extrapolated to humans, too.

Conclusions

1. Data conditioned by time (chronobiochemical) highlighted in control groups C_m and C_e a mild increase of PRO, ALB, CRE and BUN while in case of experimental groups E_m and E_e only CRE, Ca and Mg increased. These data have predictive character for the study of the chronopharmacological applications.
2. The results conditioned by the xenobiotic (i.e. the gallium complex) showed decrease of PRO and ALB while UA, CRE and BUN increased. These data point out the action of Ga C(24) on the renal function. In case of Ca and Mg a morning decrease and evening increase were found.

Acknowledgements

These investigations were performed with apparatus obtained by the financial support of the Romanian Ministry for Education, Research, Youth and Sports – National Authority for

Scientific Research, PN–II-ID–PCCE–2008–1 (Project Nr.2 / 2010, code CNCSIS ID–PCCE 140). The authors express thanks to Dr.Pascu Corina, Dr.Ghibu George-Daniel, Dr.Avacovici Adina-Elena for their technical assistance.

References

[1] Antunes C.S. Luisa, Imperi F., Minandri Fabrizia, Visca P. -Antimicrob Agent Chemother, 2012, 56(11), 5961-5970.
[2] Aoki Y., Lipsky M.M., Fowler B.A. Toxicol. Appl. Pharmacol.,1990, 106(3), 462-468.
[3] Arivett B.A., Fiester S.E., Ohneck Emily J., Penwell W.F., Kaufman Cynthia M., Relich R.F., Actis L.A. - Antimicrob Agents Chemother, 2015, 59, 7657-7665
[4] Arumugam G., Shanthi P., Sachdanandam P. - Exp. Oncol., 2006, 28(2), 141-145.
[5] Bernstein L. - Pharmacological Reviews, 1998, 50(4), 665-682.
[6] Car B.D., Eng V.M., Everds E. Nancy, Bounous I. Denise - in „The laboratory rat" (Suckow M.A., Weisbroth S.H., Franklin C.L. (Eds.), Elsevier Academic Press, Burlington, 2006, pp. 127-146.
[7] Chitambar C.R.- Future Med. Chem., 2012, 4(10), 1257-1272
[8] Collery P., Keppler B., Madoulet C., Desoize B. - Critical Reviews in Oncology/Hematology, 2002, 42, 283-296.
[9] Gârban Gabriela, Silaghi-Dumitrescu R., Ioniţă Hortensia, Gârban Z., Hădărugă Nicoleta-Gabriela, Ghibu G.-D., Baltă C., Simiz F.-D., Mitar Carmen - Biol.Trace Elem.Res., 2013 a, 155, 3, 387-395
[10] Gârban Z., Silaghi-Dumitrescu R., Ghibu G.-D., Baltă C., Ioniţă Hortensia, Avacovici Adina, Gârban Gabriela, Hădărugă Nicoleta, Simiz Eliza, Muselin F., Brudiu Ileana - in Proceedings of the 19th International Symposium on Analytical and Environmental Problems, (Galbacs Z. Ed.), SZAB, Szeged, 2013 b
[11] Gârban Z. - *Biochemistry: Comprehensive treatise*. *Vol. I. Basics of biochemistry* (in romanian), 5th edition, Editura Academiei Române, Bucureşti, 2015.
[12] Gielen M., Tiekink E.R.T. (Eds.) – Metallotherapeutic drugs and metal-based diagnostic agents : The use of metals in medicine, J. Wiley and Sons Ltd., Chichester, 2005.
[13] Haiduc I., Silvestru C. - Organometallics in Cancer Chemotherapy, Vol. I, Main Group Metal Compounds, CRC Press Inc., Boca Raton, FL, 1989.
[14] Halberg F. - Am. J. Anat., 1983, 168(4), 543-594
[15] Milton J.H. - Poly(Ethylene Glycol) Chemistry : Biotechnical and Biomedical Applications, Plenum Press, New York, 1992.
[16] Testa B.-Metabolism of Drugs and Other Xenobiotics, Academic Press, New York, 1995.
[17] Vălean Ana-Maria, Gómez-Ruiz S., Lönnecke P., Silaghi-Dumitrescu I., Silaghi-Dumitrescu Luminiţa, Hey-Hawkins Evamarie - New J. Chem., 2009, 33, 1771-1779.
[18] *** - Council Directive 86/609/EEC of 24 November 1986 on the approximation of laws, regulations and administrative provisions of the Member States regarding the protection of animals used for experimental and other scientific purposes, Official Journal of the European Union, L 358 , 18/12/1986.
[19] *** http://www.ratfanclub.org./values.html. Accessed September 20, 2015

STUDY REGARDING COFFEE BREW METAL CONTENT

Ioan Gogoaşă[1], Levente Sipos[1], Adina Negrea[2], Liana Maria Alda[1], Corina Costescu[1], Maria Rada[3], Dana Velimirovici[3], George Andrei Draghici[3], Mihaela Ostan[1], Despina-Maria Bordean[1*]

[1]Banat's University of Agricultural Science and Veterinary Medicine "King Mihai I of Romania", Romania
[2]PolitehnicaUniversity - Timisoara, Romania
[3]Victor BabesUniversity of Medicine and Pharmacy, Timisoara, Romania
e-mail: despina.bordean@gmail.com

Abstract
This paper contains data regarding the concentration of some essential mineral elements in certain coffee brews and their mineral supply in the daily-recommended diet. We determined, through flame atomic absorption spectrometry, the concentration of Na, K, Ca, Mg, Fe, Mn, Zn and Cu in brews made with five assortments of coffee. The mean values of the concentrations determined experimentally – 34.90 mg/L (Ca), 21.49 mg/L (Mg), 1.180 mg/L (Na), 522 mg/L (K), 0.158 mg/L (Fe), 0.206 mg/L (Mn), 0.146 mg/L (Zn), 0.027 mg/L (Cu) – allowed the calculus of their mineral supply. Data show that an intake of 300 mL coffee brew covers in a small measure the daily recommended intake of essential elements; therefore, coffee brews cannot be taken into account as far as their mineral supply is concerned.

Introduction
Coffee, an energising drink with pleasant flavour and taste, is one of the most appreciated drinks in the world: about 40% of the world's population drink coffee [6, 10]. Its popularity is increasing due to its numerous beneficial effects on the human body. Recent research show that moderate consumption of coffee is beneficial to human health since it decreases the risk of mortality, prevents the development of colon-rectal cancer, liver lesions and degenerative cirrhosis, and progressive and chronic diseases such as Alzheimer's and Parkinson's disease, type 2 diabetes and coronary heart diseases [3, 8]. Its nutrition and therapy properties are due to the main biological active compounds – carbohydrates, lipids, nitrogenous compounds, vitamins, alkaloids, phenolic compounds and minerals [8].
Roast coffee contains appreciable amounts of minerals – 3.5-4.5% in Arabica and 4.6-5.0 in Robusta [7]. Literature contains numerous data regarding the mineral concentration of different assortments of coffee used to prepare the drink [1, 2, 5, 6, 9], as well as information regarding the analysis techniques and methods used to determine the concentrations of mineral elements in green coffee, roasted and ground coffee, instant coffee and coffee brews [10]. In a study by R. Ashu and B. S. Chandravanshi [1], it is shown that coffee beans (roasted and ground) used to prepare the drink contain important amounts of essential minerals; their distribution is very uneven and it depends on the coffee assortment, country of origin, roasting method, etc. Analysing the distribution of some mineral elements in different brands of coffee powder used to prepare drinking coffee, I. Gogoaşă et al. [5] obtained results comparable to those of Ramato Ashu and Bhagwan Singh Chandravanshi. The concentrations of the analysed elements showed the following values: Ca (1270-1650), Mg (1050-1270), Na (37.31-103.6), K (13800-17500), Fe (24.0-49.0), Mn (13.85-17.50), Zn (5.60-6.70) and Cu (8.20-9.90) and very small amounts (insignificant) of Pb and Cd.
The important concentrations of essential elements determined in different types of coffee used to prepare drinking coffee prompted the investigation of such contents in coffee drinks and the assessment of the mineral supply of such drinks.

The goal of this experiment was to determine the concentration in Ca, Mg**,** Na, K, Fe, Mn, Zn and Cu in brews with five types of ground coffee to assess their mineral supply in the daily-recommended diet and the possibility of using them as supplementary (alternative) sources of essential element.

Experimental

To carry out the experiment, we used brews of five types of powder coffee – Jacobs-Aroma, Jacobs-Krönung, Doncafé-Elita, Fort-Strong Coffee and Nova Brasilia – purchased from local supermarkets from Timisoara, Romania. To prepare the brew, we used 6 g of ground coffee on which we poured 150 mL boiling distilled water [14] that we let to settle for 10 minutes. After removing the coffee grounds with filter paper, the coffee brew was evaporated until almost dry, after which it was added 25 mL solution of HNO_3 0.5 N and evaporated until almost dry. The last operation was repeated, and then the samples were added distilled water and used to determine the concentrations in essential elements. The concentrations of Na, K, Ca, Mg, Fe, Mn, Zn and Cu were determined using flame atomic absorption spectrometry with a Varian AA 240 FS flam atomic absorption Spectrometer. Working parameters such as wavelength, air-acetylene flow, number of readings/determination, volume of un-nebulised sample are recommended by the manufacturer.

Results and Discussion

Results (mean concentrations of samples analyzed in triplicate) of the analysis of essential mineral elements depending on coffee brew are shown in Table 1.

Table 1. Concentration of Na, K, Ca, Mg, Fe, Mn, Zn and Cu in coffee brews (mean values)

Description	Essential elements, mg/L							
	Ca	**Mg**	**Na**	**K**	**Fe**	**Mn**	**Zn**	**Cu**
Jacobs - Aroma	32.87	19.45	1.296	478	0.184	0.229	0.160	0.026
Jacobs-Krönung	39.62	23.75	1.591	543	0.182	0.257	0.163	0.032
Doncafé-Elita	30.46	19.67	0.554	459	0.159	0.178	0.136	0.025
Fort-Strong Coffee	35.51	23.06	1.288	582	0.174	0.175	0.149	0.029
Nova Brasilia	36.04	21.50	1.173	546	0.091	0.189	0.124	0.023
Mean value	***34.90***	***21.49***	***1.180***	***522***	***0.158***	***0.206***	***0.146***	***0.027***

As shown in Table 1 above, the levels of concentration of the analysed bio elements are neatly inferior to the concentrations of the same elements in ground coffee [5]. This is fully justified because the quantum of mineral elements extracted in aqueous brews depends not only on their concentration in the coffee used to prepare the brew, but also on the coffee matrix, on the physical and chemical features of each bio element and, last but not least, on the conditions of preparing coffee brews [1, 13, 14].The distribution of elements in aqueous coffee brews is very uneven: the mean values of their concentrations range within 1.189 mg/L (Na) and 522 mg/L (K) in macroelements, i.e. 0.027 mg/L (Cu) and 0.206 mg/L in microelements. Among macroelements, K is the best represented (522 mg/L), followed by Ca, Mg and Na that have lower values: 34.90, 21.49, and 1.180 mg/L, respectively.

Microelements were determined in much lower concentrations than macroelements: the best represented was Mn (0.206 mg/L), followed by Fe and Zn (in concentrations close to 0.158, i.e. 0.146 mg/), and Cu (0.027 mg/L), respectively.

These experimental values are supported by other researchers in the field [1, 2, 3, 13, 14].

Mean concentrations of mineral elements in the analysed coffee brews (Table 1) and recommendations regarding the necessary mineral elements in humans' daily diet (Table 2) allowed the calculus of the mineral supply of coffee brews per 300 mL of coffee.

Table 2. Reference values regarding the necessary mineral elements in the recommended daily diet [16]

Specification	Mineral supply (%)							
	Na	K	Ca	Mg	Fe	Mn	Zn	Cu
Males aged 19-50	0.02	3.33	1.05	1.53	0.59	2.68	0.40	0.91
Females aged 19-50	0.02	3.33	1.05	2.01	0.26	3.43	0.55	0.91

In our experiment, a daily intake of 300 mL coffee brew (two medium-size coffee cups) supplies minerals in the daily recommended diet for males and females aged 19-50 as shown in Table 3 below.

Table 3. Mineral supply (mean values) corresponding to a daily intake of 300 ml (two cups) of coffee brew

Specification	Mineral element (mg/day)							
	Na	K	Ca	Mg	Fe	Mn	Zn	Cu
Males aged 19-50	0.02	3.33	1.05	1.53	0.59	2.68	0.40	0.91
Females aged 19-50	0.02	3.33	1.05	2.01	0.26	3.43	0.55	0.91

Data shown in Table 3 above show that mineral supply and the degree of coverage of the recommended daily intake of Na, K, Ca, Mg, Fe, Mn, Zn and Cu, corresponding to an intake of 300 mL coffee brew (prepared as shown above), has low and very low values ranging between 0.02% Na and 3.43% Mn. However, we should mention the supplies of potassium (3.33%), manganese (2.68% in males and 3.43% in females) and magnesium (1.53% in males and 2.01% in females); the supplies of natrium, zinc, iron, copper and calcium are insignificant.

We can, therefore, say that mineral supply of the analysed coffee brews has low and very low values and do not contribute appreciably to the necessary mineral supply in the daily diet. This is confirmed by literature [2, 3, 6, and 12].

The supply of minerals can increase slightly with the increase of the amount of coffee used to prepare coffee brew, but this is not always recommended.

Conclusion

Mean concentration of the bio elements in the analysed coffee brews have lower values than the coffee used to prepare the drinks; it varies within broad limits ranging between 1.189 mg/L (Na) – 522 mg/L (K) in macroelements and 0.027 mg/L (Cu) – 0.206 mg/L (Mn) in microelements.

The distribution of essential elements in coffee brews is uneven and it has much lower values than the matter used to prepare them. In general, the distribution of the essential elements follows a descending trend: K>> Ca> Mg> Na, and Mn> Fe≅ Zn>> Cu, respectively.

In our experiment, the mineral supply in the daily-recommended diet of experimental coffee brews had very low values ranging between 0.02% in sodium, 3.33% in potassium and 3.43% in manganese.

Finally, we can say that the analysed coffee infusions are of no importance from the point of view of their mineral supply and cannot be considered appreciable sources of bio elements.

Acknowledgements

We thank Prof.Dr.Eng. Petru Negrea for ICP-MS spectrometry, Politehnica University - Research Institute for Renewable Energy (ICER) – Timisoara.

References

[1]. R. Ashu and B. S. Chandravanshi, Concentration levels of metals in commercially available Ethiopian roasted coffee powders and their infusions, Bull. Chem. Soc. Ethiop., 25(1), pp. 11-24 (2011)

[2]. F. Demir, N. Selvi, A.S. Kıpçak, Ö. D. Özdemir, M. B. Pişkin, E. M. Derun, The Investigation of the Element Contents in the Turkish Coffees, CBU J. of Sci., Volume 11, Issue 3, pp. 423-428

[3]. M. M. Fercan, A.S. Kipcak, O.D. Ozdemir, M.B. Piskin, E. Moroydor Derun, Determination of the Element Contents in Turkish Coffee and Effect of Sugar Addition, International Journal of Chemical, Molecular, Nuclear, Materials and Metallurgical Engineering, Vo:10, No:1, pp. 112-115, (2016).

[4]. M. E. Gillies, J. A. Birkbeck, Tea and coffee as sources of some minerals in the New Zealand diet, Am J Clin Nutr., 8(6), pp. 936-942, (1983)

[5]. I. Gogoasa., A. Pirvu, L. M. Alda, A. Velciov, M. Rada, D. M. Bordean, D. Moigradean, S. Alda and I. Gergen, The Mineral Content of Different Coffee Brands, JOURNAL of Horticulture, Forestry and Biotechnology, Volume 17(4), pp. 68– 71, (2013).

[6]. M. Grembecka, E. Malinowska, P. Szefer., Differentiation ofmarket coffee and its infusions in view of their mineral compositionSci. Total Environ., 383, pp. 59-69, (2007)

[7]. A. Gure, Investigation of Metals in Raw and RoastedIndigenous Coffee Varieties in Ethiopia, ADDIS ABABA UNVERSITY, OFFICE OF REASERCH ANDGRADUATE PROGRAM, JULY,pp. 1-65, (2006)

[8]. J. V. Higdon. and F. Balz, Coffee and Health: A Review of Recent Human Research, Critical Reviews in Food Science and Nutrition, 46, pp. 101–123, (2006)

[9]. M. J. Martin, F., A.G. Gonzalez, Characterization of Arabica and Robusta RoastedCoffee Varieties and Mixture Resolution According to Their Metal Content, Food Chem.,66, pp. 365-370, (1999)

[10]. P. Pohl, E., M., Welna, A. Szymczycha-Madeja, Determination of Elementar composition of coffeeusing instrumenta metods, Food Annal. Methods, 6, pp. 598-613, (2013)

[11]. W. M. N. Ratnayake, R. Hollywood, E. O'Grady, B. Starvic, Lipid Content andComposition of Coffee Brews Prepared by Different Methods, Food Chem. Toxicol.,31, pp. 263-269, (1993).

[12]. B. Suseela, S. Bhalke, A.V. Kumar, R.M. Tripathi, V.N. Sastry, Daily intake of trace metals through coffeeconsumption in India, Food Addit Contam., 18(2), pp. 115-20, (2001).

[13]. E. Stelmach, P. Pohl, A. Szymczycha-Madeja, The suitability of the simplified method of the analysis of coffeeinfusions on the content of Ca, Cu, Fe, Mg, Mn and Zn and the study of theeffect of preparation conditions on the leachability of elements into thecoffee brew, Food Chemistry, 141, pp. 1956–1961, (2013).

[14].A. Szymczycha-Madeja,M. Welna and P. Pohl, Solubility and Bioaccessibility of Ba, Ca, Cr, Cu, Fe, Mg, Mn, P, Sr and Zn in Slim Coffee Infusions by in vitro Gastrointestinal Digestion, J. Braz. Chem. Soc.,Vol. 26, No. 9, pp. 1781-1789, (2015).

[16].*ttps://fnic.nal.usda.gov/sites/fnic.nal.usda.gov/files/uploads/recommended_intakes_individuals.pdf*

GERMINATION ENERGY AND SEED GERMINATION - VALID PARAMETERS OF HEAVY METAL PRESENCE IN WATER

Sonja Gvozdenac[1]*, Vojislava Bursić[1], Jelena Tričković[2], Dušica Jovičić[3], Aleksandra Petrović[1], Dejan Prvulović[1], Dušan Marinković[1]

[1]University of Novi Sad, Faculty of Agriculture, Trg Dositeja Obradovića 8, Novi Sad, Serbia
[2]University of Novi Sad, Faculty of Science, Trg Dositeja Obradovića 3, Novi Sad, Serbia
[3]Institute for field and vegetable crops, Maksima Gorkog 30, Novi Sad, Serbia
email: sonjag@polj.uns.ac.rs

Abstract
The use of water polluted with heavy metals for irrigation can cause phytotoxic effects and affect crop production. An important step in mitigating possible negative effects is certainly a continuous monitoring of water quality, assessment of risk for crops by biotests, right choice of test plant and selection of parameters that reliably indicate the changes in the environment. The aim of this study was to assess indicators potential of germination energy (GE) and seed germination (G) of five cultivated plants (sorghum, cabbage, sunflower, beans and buckwheat) in detection of metal (Cr, Pb and Cd) presence in water. A filter paper method according to ISTA was used. Metals were applied in series of concentrations including maxmium allowable concentrations (MAC's). Chromium significantly inhibited G and GE of sunflower seeds in treatments with 2000 µg/l, while lead caused such effects of GE and G of sorghum and sunflower in amounts exceeding 50 µg/l (two times less than MAC), and of cabbage and buckwheat at 200µg/l. Cadmium significantly inhibited GE and G of beans at 0.1 µg/l (100 fold less than MAC).The overall results suggest that GE and G can be considered as valid parameters for the detection of certain metal presence in water, in amounts exceeding MAC such as Pb (sorghum and sunflower seeds) and Cd (beans seeds).
Key words: germination energy, germination, seeds, metals, crops, phytoindicators

Introduction

Contamination of irrigation water is a pronounced problem in agricultural and industrial regions. Generally the use of such water can cause phytotoxic effects and affect crop production, due to high levels of pollutants, especially metals. To mitigate negative consequences it is necessary to carry out continuous monitoring of water quality and assess the risk to crops. An important step is certainly a right choice of test organism and selection of parameters that reliably indicate changes in water. It is familiar that some plants are very sensitive to high content of pesticides, heavy metals and organic substances in soil and water. They react with different morphological and physiological changes and are successfully used as bioindicators of water contamination, as test plants in bioassays for contamination detection and in assessment of ecotoxicological risks [1; 2; 3]. Most of the standardized phyto-toxicity tests and a number of authors point out germination as a valid parameter which indicates changes in water quality [4; 5; 6]. It has advantages such as ease of implementation and assessment, low cost and a convenience for wide range of substances and large number of samples. The aim of this study was to assess indicators potential of germination energy and seed germination of five cultivated plant species (sorghum, cabbage, sunflower, beans and buckwheat) in detection of metal (Cr, Pb and Cd) presence in water.

Materials and methods

In bioassay, the folowing test species were chosen: sorghum (*Sorghum bicolor* L.), cabbage (*Brassica oleracea* var.capitata), sunflower (*Heliantus anuus* L.), beans (*Phasolus vulgaris* L.)

and buckwheat (*Fagopyrum esculentum* Moench). The effect of water quality was evaluated according to changes in germination energy –GE and seed germination – G (%) of tested species, in bioassay which was carried out according to a standard filter paper method described by ISTA (2011), with slight modifications. Heavy metals were applied at following rates, including the MAC in [7], [8] and [9]Cr (100-4000 µg/l); Pb (1-200 µg/l) and Cd (0.01-200 µg/l).Data were analyzed using Duncan's multiple range test, for 95% confidence interval, in software SPSS version 17.0.

Results and discussions

In bioassay, seeds of test plants responded in inhibition or stimulation of GE and G, depending of the metal and applied rate. This is in accordance with [10], indicating that the sensitivity of plants to certain contaminants (e.g. heavy metals) in water depends on the concentration and the type of pollutants, but also on the development stage (germination, emergence, vegetative growth). Significant inhibition of sunflower seeds G was recorded in treatments with 2000 µg/l of chromium. However, this metal stimulated GE and G of beans seeds at rates 200-2000 µg/l (Tab. 1). Given indicates that GE and G of tested species are not valid indicators of Cr water contamination. In literature, the presented results differ. [11] showed that germination of maize and rice was inhibited with the distillery effluent containing high amounts of heavy metals (Cd, Cr, Ni and Zn). [12] reported that Cr in amount 50-250 g/l did not affect germination of sunflower seeds, but it delayed the time of germination. According to [13] Cr stimulated germination of buckwheat seeds at 40-160 ppm.

Tab. 1 Germination energy and germination of test plants depending on the applied rate of Cr

Parametar	Rate (µg/l)	Sorghum	Cabbage	Beans	Sunflower	Buckwheat
Germination energy (%)	4000	98.50 ±0.50 a	97.25 ±0.25 a	96.00 ±1.00 b	95.50 ±0.50 b	98.00 ±0.00 a
	2000	99.00 ±1.00 a	98.00 ±1.00 a	97.75 ±0.75 a	95.50 ±1.50 b	98.00 ±1.00 a
	1000	99.00 ±1.00 a	99.25 ±0.25 a	98.50 ±0.50 a	97.50 ±0.50 ab	98.00 ±1.00 a
	500*	99.50 ±0.50 a	99.00 ±0.00 a	98.75 ±0.75 a	97.50 ±0.50 ab	98.50 ±0.50 a
	200	99.50 ±0.50 a	99.75 ±0.75 a	95.75 ±0.75 a	97.25 ±0.75 ab	98.50 ±0.50 a
	100	99.75 ±0.75 a	99.50 ±0.50 a	96.50 ±0.50 ab	97.75 ±1.75 ab	98.50 ±0.50 a
	control	99.00 ±1.00 a	99.75 ±0.75 a	96.00 ±1.00 b	99.75 ±0.75 a	99.00 ±1.00 a
	F value	**0.95ns**	**5.17ns**	**6.69***	**10.61****	**0.74ns**
Germination (%)	4000	98.50 ±0.50 a	97.25 ±0.25 a	96.00 ±0.00 a	95.50 ±0.50 b	98.00 ±1.00 a
	2000	99.00 ±0.00 a	99.00 ±1.00 a	97.75 ±0.75 a	95.50 ±1.50 b	98.50 ±0.50 a
	1000	99.00 ±0.00 a	98.00 ±0.00 a	98.50 ±0.50 a	97.50 ±0.50 ab	98.50 ±0.50 a
	500*	99.50 ±0.50 a	99.25 ±0.25 a	98.75 ±0.50 a	98.00 ±0.00 a	98.50 ±0.50 a
	200	99.50 ±0.50 a	100.00 ±0.00 a	98.75 ±0.75 a	97.50 ±0.50 ab	98.50 ±1.50 a
	100	99.75 ±0.75 a	99.75 ±0.75 a	97.75 ±0.75 a	98.00 ±1.00 a	98.75 ±0.75 a
	control	99.50 ±0.50 a	100.00 ±0.00 a	97.25 ±0.25 a	99.75 ±0.75 a	99.50 ±0.50 a
	F value	**0.95ns**	**8.08ns**	**3.47ns**	**14.36****	**1.14ns**

Mean values ±SD; Values with the same letter in the column are on the same level of significance; **p<0.01;* p<0.05; ns p>0.05; Bold values in Rate column are MAC values according to the [9]*

Lead significantly inhibited GE and G of sorghum and sunflower seeds at rates exceeding 50 µg/l (2 fold less than MAC) and of cabbage at 200 µg/l. Given that MAC according to [8] is 10 µg/l and [9] is 100 µg/l, GE and G of sorghum and sunflower seeds can be considered valid parameters in Pb contamination detection (Tab. 2). [14] reported significant inhibition of sunflower seeds germination by Pb at 40 and 50 ppm in water i.e. 50 and 60 ppm in soils. [15] also point out that Pb negatively affects seeds germination.

Tab. 2 Germination energy and germination of test plants depending on the applied rate of Pb

Parametar	Rate (µg/l)	Sorghum	Cabbage	Beans	Sunflower	Buckwheat
Germination energy (%)	200	94.50 ±0.50 b	83.50 ±0.50 b	96.50 ±2.50 a	78.25 ±0.25 b	96.00 ±1.00 a
	100**	95.00 ±2.00 b	88.50 ±0.50 a	97.50 ±1.50 a	79.00 ±1.00 b	97.00 ±0.50 a
	50	95.00 ±0.00 b	91.75 ±0.75 a	97.75 ±0.75 a	78.25 ±0.25 b	97.00 ±1.00 a
	10*	96.00 ±1.00 ab	92.25 ±0.25 a	98.00 ±1.00 a	84.50 ±0.50 ab	98.50 ±0.50 a
	5	97.25 ±0.25 a	92.00 ±0.00 a	97.75 ±1.75 a	89.50 ±0.50 a	99.00 ±2.00 a
	1	98.00 ±1.00 a	92.00 ±1.00 a	98.00 ±0.00 a	88.25 ±0.25 a	98.75 ±1.75 a
	control	98.75 ±0.75 a	93.75 ±0.75 a	98.25 ±1.25 a	90.25 ±0.25 a	98.75 ±0.75 a
	F value	**4.49****	**7.06****	**0.37ns**	**9.97****	**3.13ns**
Germination (%)	200	94.50 ±0.50 b	83.50 ±0.50 b	96.50 ±2.50 a	78.25 ±0.25 b	96.00 ±1.00 a
	100**	95.00 ±0.00 ab	88.50 ±0.50 ab	97.50 ±1.50 a	79.00 ±1.00 b	97.00 ±0.50 a
	50	95.00 ±1.00 ab	92.00 ±0.00 a	97.75 ±0.75 a	78.25 ±0.25 b	97.00 ±1.00 a
	10*	96.00 ±0.00 ab	92.25 ±0.25 a	98.00 ±1.00 a	84.50 ±0.50 ab	98.50 ±0.50 a
	5	98.00 ±1.00 a	93.00 ±0.00 a	97.75 ±1.75 a	89.50 ±0.50 a	99.00 ±2.00 a
	1	98.75 ±0.75 a	93.50 ±0.50 a	98.00 ±0.00 a	88.25 ±0.25 a	98.75 ±1.75 a
	control	98.75 ±1.75 a	95.00 ±0.00 a	98.25 ±1.25 a	90.25 ±0.25 a	98.75 ±0.75 a
	F value	**6.68****	**8.64****	**0.37ns**	**9.97****	**3.13ns**

Mean values ±SD; Values with the same letter in the column are on the same level of significance; **p<0.01;* p<0.05; ns p>0.05; Bold values in Rate column are MAC values according to [8]* or [9]**.

Cadmium significantly inhibited GE and G of bean seeds at 0.1 µg/l (less than MAC), of sunflower at 100-200 µg/l and of buckwheat seeds at 200 µg/l. According to these results only GE and G of bean seeds are valid parameters in detection of Cd presence in water in amounts exceeding MAC (Tab. 3). Several authors indicate that Cd inhibits seeds germination of a number of plant species [16, 17]. [18] reported that germination of sorghum seeds is not sensitive parameter for Cd toxicity, while [19] point out germination as the most suitable for Cd toxicity detection.

Tab 3. Germination energy and germination of test plants depending on the applied rate of Cd

Parametar	Rate (µg/l)	Sorghum	Cabbage	Beans	Sunflower	Buckwheat
Germination energy (%)	200	93.00 ±2.00 a	95.00 ±2.00 a	50.00 ±1.00 d	80.00 ±1.00 c	92.00 ±2.00 b
	100	93.00 ±1.00 a	96.00 ±1.00 a	91.00 ±0.50 c	92.00 ±2.00 b	96.00 ±1.00 a
	10**	94.00 ±1.00 a	96.00 ±1.00 a	92.00 ±0.00 bc	95.00 ±1.00 ab	96.00 ±1.00 a
	1	94.00 ±0.00 a	96.00 ±1.00 a	92.00 ±2.00 bc	96.00 ±0.00 ab	97.00 ±0.50 a
	0.1	95.00 ±0.00 a	96.50 ±0.50 a	92.00 ±2.00 bc	97.00 ±1.00 ab	98.50 ±0.50 a
	0.01	95.00 ±1.00 a	96.00 ±0.00 a	97.00 ±1.00 a	99.00 ±1.00 a	99.50 ±0.50 a
	control	95.00 ±2.00 a	96.50 ±0.50 a	98.00 ±1.00 a	99.00 ±1.00 a	99.00 ±1.00 a
	F value	**1.20ns**	**0.97ns**	**146.04****	**32.71****	**14.43****
Germination (%)	200	93.00 ±2.00 a	95.00 ±1.00 a	78.00 ±0.00 c	82.00 ±0.00 d	95.00 ±2.00 b
	100	93.00 ±1.00 a	96.00 ±0.00 a	91.00 ±2.00 b	92.00 ±2.00 c	96.00 ±1.00 ab
	10**	94.00 ±1.00 a	96.00 ±1.00 a	92.00 ±2.00 b	95.00 ±1.00 b	96.00 ±1.00 ab
	1	94.00 ±0.00 a	97.00 ±1.00 a	92.00 ±2.00 b	96.00 ±0.00 ab	97.00 ±0.00 a
	0.1	95.00 ±0.00 a	97.00 ±1.00 a	92.00 ±2.00 b	97.00 ±1.00 ab	99.00 ±0.00 a
	0.01	95.00 ±1.00 a	97.00 ±2.00 a	97.50 ±1.50 a	99.00 ±1.00 a	99.00 ±1.00 a
	control	95.00 ±2.00 a	97.00 ±0.00 a	98.00 ±1.00 a	99.00 ±1.00 a	99.00 ±0.00 a
	F value	**1.20ns**	**3.25ns**	**26.85****	**27.13****	**8.68****

Mean values ±SD; Values with the same letter in column are on the same level of significance; **p<0.01;* p<0.05; ns p>0.05; Bold values in Rate column are MAC values according to [9]**

Conclusions

Based on the obtained results, Cr significantly inhibited G of sunflower seeds in treatments with 2000 µg/L but stimulated GE and G of beans at 200-2000 µg/l; Pb significantly inhibited GE and G of sorghum and sunflower at 50 µg/l (2 fold less than MAC) and higher rates, of cabbage and buckwheat at 200 µg/l; Cd significantly inhibited GE and G of beans at 0.1 µg/l

(less than MAC), of sunflower at rates 100-200 µg/l and of buckwheat seeds at 200 µg/l. The overall results suggest that GE and G can be considered as valid parameters for the detection of certain metal presence in water, in amounts exceeding MAC: sorghum and sunflower seeds for Pb and beans seeds for Cd.

Acknowledgements
This research work was carried out with the support of the Ministry of Education, Science and Technological Development of the Republic of Serbia and financed from a Project III 43005.

References
[1] Angelopoulos K., Paraskeva C.A., Emmanouil C., 2009. Phytotoxicity of olive mill wastewater fractions and their potential use as a selective herbicide, paper work.
[2] Kungolos A., Emmanouil C., Bakopoulou A., Petala M., 2011. Environ Sci Pollut Res., 74:188-194.
[3] Gvozdenac S., Inđić D., Vuković S., Bursić V., Tričković J., 2014. J.Anim. Plant Sci. 24(2): 614-619.
[4] OECD Guideline for Testing of Chemicals 208. 1984. Terrestrial Plants, Growth Test.
[5] AFNOR X31-203/ISO 11269-1. (1993) Determination des effets des pollutants sur la flore du sol: Méthode de mesurage de l'inhibition de la croissance des racines.
[6] Mahmood S., Hussain A., Saeed Z., Athar M., (2005). Int. J. Environ. Sci. Tech., 2(3):269-274.
[7] Directive 2008/105 EC of the European Parliament and of the Council (OJ L 348, 84-97).
[8] ICPDR – The Danube Basin district IC/084
[9] Regulation on allowable amounts on hazardous and harmfull substances in soil and water for irrigation and methods for theis analysis ispitivanja (Official gazette RS 23/94).
[10] Liu T.F., Wang T., Sun C., Wang Y.M., 2009. J. of Hazardous Materials, 163:344-348.
[11] Pandey N., Sharma C.P., 2002. Plant Sci., 163:753-758.
[12] Atta M.I., Gulshan A.B., Ahmad N., Saeed S., 2014. Journal of Agricultural and Biological Science, 9(2):46-50.
[13] Jamal S. N., Iqbal M. Z. and Athar M., 2006. Int. J. Environ. Sci. Technol., 3:53-58.
[14] Chhotu D., Madhusudan J., Fulekar H., 2008. Environmental Engineering and Management Journal, 7(5):547-558.
[15] Zhang R., Wang Kai-Xuan, 2011. Journal of Shanxi Datong University (Natural Science Edition), 2011-01
[16] Raziuddin F., Akmal M., Shah S. S., Mohammad F. and Zhou W., 2011. Pak. J. Bot., 43(1):333-340.
[17] Aydinalp C., Marinova S., 2009. Bulgarian Journal of Agricultural Science, 15(4):347-350.
[18] An Y., 2004. Soil ecotoxicity assessment using cadmium sensitive plants, Environmental pollution, 127: 21-26.
[19] Correa A.X.R., Rorig L.R., Verdinelli M.A., Cotelle S., Ferard J.F., Radetski C.M., 2006. Sci. Total Environ., 357:120-127.

PHOSPHORUS IN A HILL PERMANENT GRASSLAND ECOSYSTEM IN SPRING BY PRINCIPAL COMPONENTS & CLASSIFICATION ANALYSIS

Monica Harmanescu

Faculty of Agriculture, Banat's University of Agricultural Sciences and Veterinary Medicine "Regele Mihai I al Romaniei" from Timisoara, Calea Aradului 119, PC 300645, Romania
e-mail: monica.harmanescu@yahoo.com

Abstract
The aim of the present study was to extract information regarding the phosphorus content in a permanent grassland ecosystem, influenced anthropic by two different agricultural systems: exclusive mineral fertilisation and sheep manure farming management. The research was made in spring, in a hill region of Romanian Banat. Principal Components & Classification Analysis (PC&CA) was performed for statistical interpretation of data. The first two principal components described around 90% of the total variance. Forages total phosphorus content was positive correlated to the sheep manure farming system (0.84), and to the grassland soil phosphorus, total content (0.88) and mobile form (0.65).

Introduction
The phosphorus in vegetal cell is required for the proteic metabolism, in the glucides transfer to the root [1], in biological oxidation and photosynthesis processes [2], in the transmission of hereditary characters [3], ensuring the formation of buffer systems, etc. [4]. An optimum phosphorus content in plants stimulates their regeneration after forage harvesting [1].So, it is justified the necessity to monitorthe phosphorus content in grassland ecosystem and supplementing it in case of necessity [5, 7]. For the environment health it is recommended to verify the existing phosphorus in grassland soil, to assure the phosphorus balance: inputs versus outputs [12]. The application of mineral and/or organic fertilizers influences positively the grassland forage production [11], being preferable to use organic fertilisers, for replace or reduce to the minimum the mineral fertilisers application [3]. The aim of this issue was to quantify in spring the quantity of phosphorus content in a Banat hill permanent grassland ecosystem, after sheep manure or mineral fertilizers application since 2003.

Experimental
A grazed and mowed hill permanent grassland, situated in Romanian Banat County (45°12'N; 21°60'E) on a Calcic Luvisol, was organisedas experimental field in 2003. A complete randomised block design with 5 replications was used; 25 m^2/trial. The fermented sheep manure was applied at two years in three different trials: 20 t/ha, 40 t/ha and 60 t/ha (P2, P3, and P4). Total phosphorus content of sheep manure was 5156 ppm (at U=61%). Mineral fertilisers were applied yearly: NPK complex, ammonium nitrate, superphosphate, and potassium salt. Doses of 100 kg/ha N + 50 kg/ha P_2O_5 + 50 kg/haK_2O were applied in P5; 150 kg/ha N + 50 kg/ha P_2O_5 + 50 kg/ha K_2O in P6 trial; (100+100) kg/haN +50 kg/ha P_2O_5 + 50 kg/ha K_2O in P7. P1 trial was not fertilised. In the studied region the clime is temperate continental with Mediterranean influences [9]. In 2008 theannual average temperature was around 12°C and annual average rainfall around 802 mm [14].
The floristic composition of the permanent grassland covering in May 2008 was determined using gravimetric method. The plants samples were harvested from 1 m^2 for each grassland trial, at 3 cm above soil. For the multivariate matrix computational process was used the following floristic code: 0 for 0%; 1 for 0.1-10%; 2 for 11-20%; 3 for 21-30%; 4 for 31-40%; 5 for 41-50%; 6 for 51-60% species participation.

Humus content was determined by Walklay – Black – Gogoasa method; and available phosphorus (mobile form) of soil was quantified using Egner-Riehm-Domingo method [13]. Total calcium content was determined by atomic absorption spectrometry [6] and total phosphorus content at 450 nm [10]. PC&CA was performed for multidimensional data analysis by StatSoft - STATISTICA VERSION 10.

Results and discussion

The *Festuca rupicola* grass participation in permanent grassland covering, after floristic code application, were 4, 2, 1, 1, 6, 2, 1 for P1, P2, P3, P4, P5, P6, respectively P7. In *Lathyrus pratensis*leguminous case the values were 1, 0, 0, 1, 0, 0, 1, while for *Trifolium repens* were 1, 4, 5, 5, 0, 0, 1 in P1, P2, P3, P4, P5, P6, respectively P7 trials.

The total calcium content of grassland forages varied between 6579 ppm (P6) to 25535 ppm (P2). In forages cut from organic P3 and P4 trials, the total calcium content was 21237ppm, respectively 18521 ppm, and for the mineral fertilised trials P5 and P7 were 7566 ppm and 6799 ppm. In forages harvested from unfertilised conditions the total calcium content was 14911 ppm, smaller than sheep manure management, and higher than mineral fertilized trials.

Total phosphorus content of grassland forages from P1 to P7 trials was556 ppm, 890 ppm, 1237 ppm, 1289ppm, 875 ppm, 821 ppm, respectively 967 ppm. In grassland soil, the total phosphorus content in P1 – P7 ecological conditions were: 65 ppm, 113 ppm, 133 ppm, 166ppm, 122 ppm, 130 ppm, and 133 ppm, while mobile form of phosphorus quantified 58.3ppm, 53.6 ppm, 61.6 ppm, 87.6 ppm, 61.7 ppm, 49.2 ppm and 70.7 ppm.

Soil grassland pH in spring of 2008 varied in range 6.1 – 6.3 in organic farming system (P2 – P4), and 5.7 – 5.9 in exclusive mineral fertilised trials (P5 – P7), reported to the conditions of unfertilised case (P1) with 6.1. Considering this information, it is obviously that mineral fertilizers application acidified the grassland soil in raining and temperature natural conditions of Romanian Banat.

The grassland soil humus contentsin P1 – P7 trials, differentiate reported to the anthropic influence of fertilizers application, were: 5.8 %, 5.6 %, 6.1 %, 7.2 %, 6.5 %, 6.2 % and 6.2 %.

All these experimental data were used to perform the matrix, following the procedures of multidimensional PC&CA. The active variables were: forages total calcium content (ppm); forages total phosphorus content (ppm); soil total phosphorus content (ppm) and soil phosphorus mobile form (ppm);soil pH; soil humus (%); and the fertilisation data. The supplementary variables were considered the participation in grassland covering of *Festuca rupicola*, *Lathyrus pratensis* and *Trifolium repens*. The matrix cases were considered all the seven trials. The matrix data were interpreted via the correlation matrix.

The eigenvalues of the PC1 and PC2 were 5.62 and 3.36. In accordance with the data, the first two principal components described around 90% of the total variance. High positive influence in PC1 had forages total calcium content (0.86), forages total phosphorus content (0.61), soil pH (0.97), *Trifolium repens* participation in spontaneous covering (0.94), and sheep manure fertilisation (0.92). The mineral fertilisation data had high negative influence in PC1, varying from -0.86 to -0.90. Soil phosphorus mobile form had a positive contribution in PC1 (0.51). The highest negative influence in PC2 had: soil total phosphorus content (-0.89); soil humus (-0.87); forages total phosphorus content (-0,69) and soil phosphorus mobile form (-0.69). The cases and variables distribution on PC1 x PC2 plane are shown in Figure 1 and Figure 2.

Using the PC&CA facilities, it is obviously that all the three cases of the ecological conditions of grassland ecosystem, modified anthropic by exclusive mineral fertilisation (P5, P6 and P7), present similitudes and were classified in a distinct group reported to the organic farming system (P2, P3 and P4) and unfertilised trial (P1). In the soil and clime conditions of Banat spring, the sheep manure fertilisation system play a key role to the total phosphorus content of forages, heaving a significant statistic correlation (0.84). Organic farming system influences

positively also the soil pH (0.82) and the forages total calcium content (0.66).

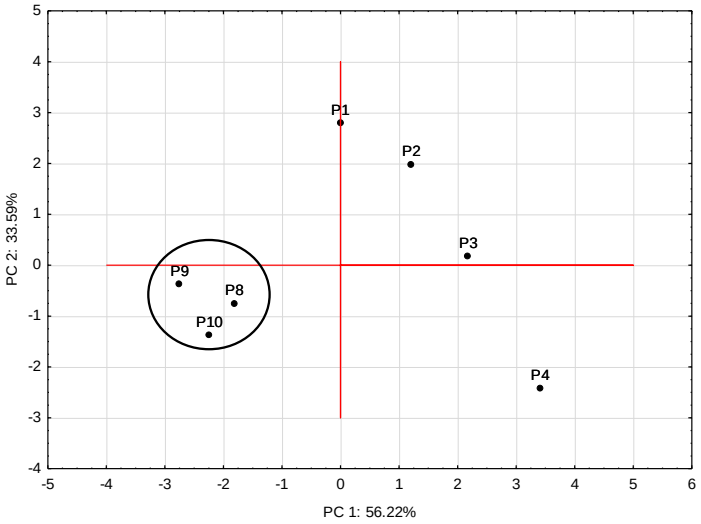

Figure 1.PC&CA cases distribution on PC1 x PC2 plane

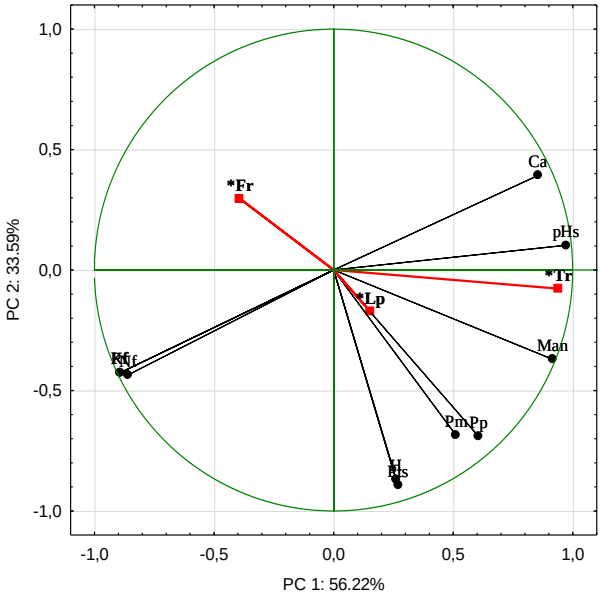

Figure 2. PC&CA variables distribution on PC1 x PC2 plane

The variables correlations reflected o positive coefficient between total phosphorus content of forages and soil total phosphorus content and soil mobile formof phosphorus (0.88, respectively 0.65). A positive correlation coefficient was find also between total content and mobile form of soil phosphorus (0.60). The soil mobile form of phosphorus was positive influenced by the organic fertilizer application (0.65) and soil humus content (0.81). Analogously, the soil total phosphorus contentwas positive correlated to the soil humus (0.75). With regard to the selected plants participation in the permanent grassland covering, it can say that *Trifolium repens*had the highestpositive correlation to the sheep manure application in organic farming system (0.92). *Lathyrus pratensis* participation to the grassland floristic composition was positively correlated to the mobile form of soil phosphorus(0.66).

Conclusion

In Banat environmental conditions of 2008 spring the organic farming system with fermented sheep manure had a positive influence on the forages total phosphorus content (0.84). Positive

correlation coefficients were found between forages total phosphorus content and soil total phosphorus content (0.88) and soil mobile form of phosphorus (0.65).
In studied hill permanent grassland, the soil total phosphorus content and soil mobile form of phosphorus had a positive correlation (0.60). The soil humus influenced also positively the soil mobile form phosphorus (0.81) and the soil total phosphorus content (0.75) in the hill Romanian Banat grassland ecosystem.

Acknowledgements
All the results used for multidimensional statistical interpretation of this issue were obtained for PhD thesis in Agronomy realised byHarmanescu Monica (*On the influence of substances flows on the quality of forage from grassland*, 2006-2009), *Banat's University of Agricultural Sciences and Veterinary Medicine from Timisoara*, coordinator Prof.PhD.Eng. Alexandru Moisuc, with the financial support of a Grant BD/CNCSIS Romania (www.cncsis.ro), 2007–2009.

References
[1] C. Barbulescu, Producerea si pastrarea furajelor, Editura Didactica si Pedagogica, Bucuresti, 1971.
[2] C. Barbulescu, Gh. Motca, Pajistile de deal din Romania, Editura Ceres, Bucuresti, 1987.
[3] B.S. Coulter, S. Lalor edit., Major and micro nutrient advice for productive agricultural crops, 3rd Edition, Teagasc, Oak Park, Co Carlow, 2008.
[4] A.R. Dîrlea, Citologie si biologie celulara, Editura Solness, 2000.
[5] S. Fortune, J.S. Robinson, C.A. Watson, L. Philipps, J.S. Conway, E.A. Stockdale, Response of organically managed grassland to available phosphorus and potassium in the soil and supplementary fertilization: field trials using grass– clover leys cut for silage, Soil Use and Management 21 (2005) 370–376.
[6] M. Harmanescu, L.M. Alda, D.M. Bordean, I. Gogoasa, I. Gergen, Heavy metals health risk assessment for population via consumption of vegetables grown in old mining area; a case study: Banat County, Romania, Chemistry Central Journal 5 (2011) 64.
[7] P. Haygarth, B.L. Turner, A. Fraser, S. Jarvis, T. Harrod, D. Nash, D. Halliwell, T. Page, K. Beven, Temporal variability in phosphorus transfers: classifying concentration-discharge event dynamics, Hydrology and Earth System Sciences 8(1) (2004) 88-97.
[8] A.L. Heathwaite, P. Griffiths, P.M. Haygarth, S.C. Jarvis, R.J. Parkinson, Phosphorus loss from grassland soils: implications of land management for the quality of receiving waters, Freshwater Contamination (Proceedings of Rabat Symposium S4, April-May 1997), IAHS Publ. no. 243 (1997) 177-186.
[9] Gh. Ianos, Geografia solurilor cu noţiuni generale de pedologie,Edited by Universitatea de Vest, Timisoara, 2005.
[10] P.G. Jeffery, *Metode chimice de analiză a rocilor*, Editura tehnică, Bucureşti, 1983.
[11] I. Rotar, M. Cirebea, F. Pacurar, R. Vidican, A. Malinas, O. Ranta, Mineral and organic fertilisation influence on Festuca rubra – Agrostis capillaris natural meadow, Romanian Journal of Grassland and Forage Crops, No.13 (2016) 39-46.
[12] C. Rumpel, A. Crème, P.T. Ngo, G. Velásquez, M.L. Mora, A. Chabbi, The impact of grassland management on biogeochemical cycles involving carbon, nitrogen and phosphorus, Review, Journal of Soil Science and Plant Nutrition 15 (2) (2015) 353-371.
[13] E. Stoica coord., C. Rauta, N. Florea, Metode de analiza chimica a solului, Bucuresti, 1986.
[14] Meteorological Station Archive, Oravita (Caras-Severin), for the climatic data.

SIMULTANEOUS FLUORIDE AND ARSENIC REMOVAL FROM GROUNDWATER BY USING ALUMINUM SACRIFICIAL ANODE

Monica Ihos[1*], Florica Manea[2], Rodica Pode[2]

[1]National R&D Institute for Industrial Ecology - ECOIND - Timisoara Branch, P-ta Regina Maria Nr.1, Et.2, 300004Timisoara, Romania,
[2]"Politehnica" University of Timisoara, Faculty of Industrial Chemistry and Environmental Engineering, Bv. Vasile Pârvan Nr.6, 300223 Timisoara, Romania
e-mail: monica_ihos@yahoo.com

Abstract
The simultaneous removal of fluoride and arsenic in groundwater collected from three deep wells situated in Western part of Romania was carried out by electrocoagulation (EC) with aluminium sacrificial anode. The current density was of 156, 480 and 780 A/m^2, respectively and the electrolysis time 60 min. The removal efficiency of fluoride and arsenic was determined based on their residual concentration. Also, the specific energy consumption was calculated and it was in the range of 0.14 - 1.40 kWh/m^3.

Introduction
Groundwater is one of the most important sources of drinking water in the world. The most significant inorganic pollutants in the groundwater that have harmful effects on human health are fluoride and arsenic. However it should be noted that fluoride has beneficial effects on human health in the range of 0.5 - 1 mg/l in drinking water, and above 1.5 mg/l represents a risk of dental fluorosis and progressively higher concentrations lead to increasing risks of skeletal fluorosis. Also, the guideline value for arsenic is 10 μg/L [1].
Many people in the world are subjected to drinking water that contains concomitant fluoride and arsenic. The effects following the concomitant exposure to fluoride and arsenic need comprehensive studies because in the human body these pollutants may function independently or can act as synergistic or antagonistic to one another [2]. Salgado-Bustamante et al. have studied the effect of exposure to fluoride and arsenic on the pattern of expression of apoptosis and inflammatory genes by immune cell. The results show that the combined exposure to arsenic and fluoride has a different effect on gene expression than the exposure to arsenic or fluoride alone [3].
Research was carried out in order to develop technologies that are able to remove simultaneously fluoride and arsenic: adsorption [4-9] and electrochemical methods [10, 11].
In the last years electrocoagulation (EC) has been considered as water treatment for drinking purposes because of electrochemical methods advantages such as versatility, energy efficiency, easy operation, automation and environmental compatibility.
The purpose of this paper was to remove simultaneously the fluoride and arsenic in groundwater from the West of Romania by EC with aluminium as sacrificial anode.

Experimental
The groundwater was collected from three deep wells situated in Western part of Romania. The characteristics of groundwater are presented in Table 1.
The working solutions were prepared from the groundwater by adjusting the pH to 7 with NaOH p.a., adding NaCl p.a.so that its concentration was 0.01 M. Also, NaF p.a. was added so that the concentration of fluoride was 5.08 and 10 mg/L, respectively.
The EC experiments were carried out in a plexiglass cell with horizontal electrodes. The sacrificial anode was made of aluminium with an active surface area of 78.4 cm^2. The cathode

was a wire mesh grid made up of 3 mm diameter stainless steel wires. The distance between the electrodes was 5 mm.

Volumes of 500 ml working solutions were introduced in the cell, and the current density was of 156, 480 and 780 A/m^3, respectively. Electrolysis duration was 60 minutes and samples were taken at every 10 minutes.

The fluoride concentration was determined by using a Thermo Scientific Orion fluoride ion selective electrode. TISAB II solution was used as a buffer to maintain the pH and background ion concentrations. The detection limit for fluoride is 0.02 mg/L. Arsenic concentration was measured on a Varian SpectrAA atomic absorption spectrophotometer equipped with hydride system. Argon carried AsH_3 to a 900 ˚C quartz cell where arsenic was quantified at 197.2 nm. The detection limit for arsenic is 0.1 μg/L.

Table 1. Characteristics of groundwater

Parameter	Unit of measurement	Groundwater		
		1	2	3
Depth	m	110	250	300
Turbidity	NTU	2.47	0.01	0.02
Conductivity	μS/cm	780	750	540
pH	pH units	7.6	7.9	7.9
Ammonia	mg/L	0.291	0.519	2.31
Nitrate	mg/L	< 0.074	< 0.074	< 0.074
Nitrite	mg/L	< 0.026	< 0.026	< 0.026
Chemical oxygen demand (COD-Mn)	mgO_2/L	< 1.6	< 1.6	< 1.6
Hardness	German degree	9.1	2.9	6.4
Chloride	mg/L	58.1	41.1	20.6
Sulphate	mg/L	5.40	4.58	4.39
Iron	mg/L	0.880	0.210	0.208
Manganese	mg/L	0.355	0.089	0.118
Arsenic	μg/L	71.6	98.4	99.5
Fluoride	mg/L	0.093	0.539	0.017

Results and discussion

Figures 1-3 show the fluoride removal efficiency versus electrolysis time at 156, 480 and 780 A/m^2, respectively. Regardless of fluoride concentration in the groundwater, as the electrolysis time and the current density increased, the fluoride removal efficiency increased. This finding is in accordance with the fact that in EC (sacrificial anode aluminium) the removal of the pollutants is managed by aluminium hydroxide yielding in solution. According to Faraday's Law, the amount of aluminium hydroxide is directly proportional to the charge passed into solution. The pollutants removal occurs by formation of pollutant-aluminium hydroxo-complexes. As the amount of aluminium hydroxide is larger the adsorbed pollutant amount will be larger.

The results listed in Table 2 show that simultaneously with fluoride removal, the arsenic was efficiently removed too. The arsenic residual concentration in the groundwater collected from the three deep wells after 60 min of electrolysis and 780 A/m^2, regardless of fluoride/arsenic mass ratio in the untreated groundwater is under 10 μg/L.

In Table 3 specific energy consumption for 60 min of electrolysis and the applied current density in the EC are presented. The values are in accordance with those reported in the literature [10].

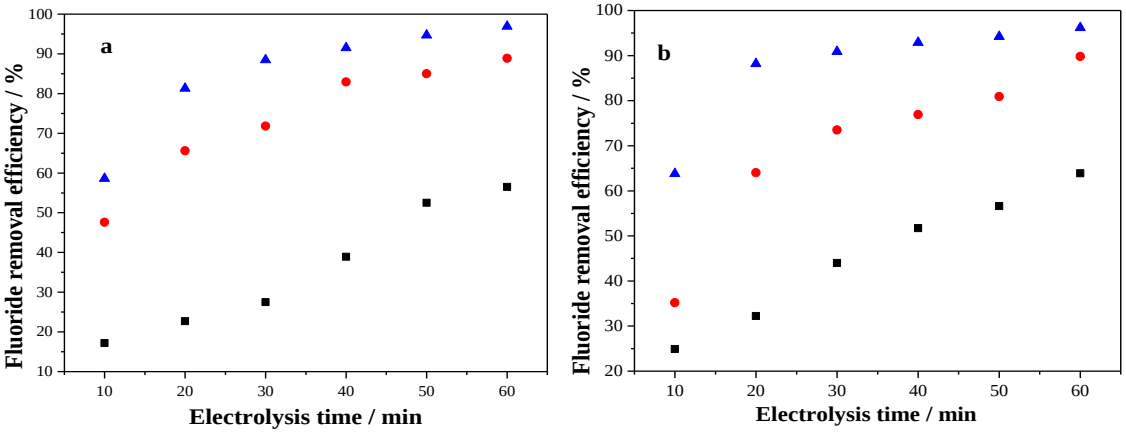

Figure 1. Fluoride removal efficiency versus electrolysis time for groundwater 1 current density: (■) - 156 A/m^3; (●) – 480 A/m^3; (▲) – 780 A/m^3; pH_{ini}=7; $conc_{ini}$: **a.** 10 mg/L F^-; **b.** 5.08 mg/L F^-

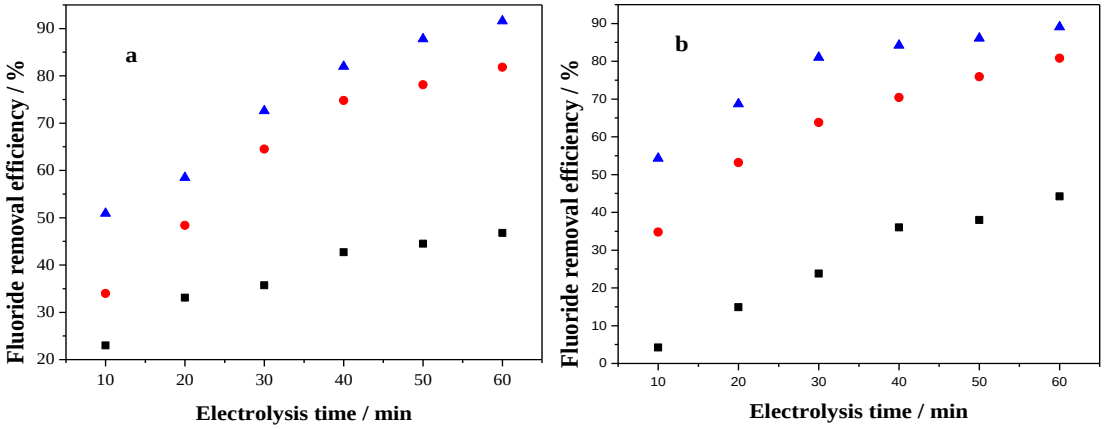

Figure 2. Fluoride removal efficiency versus electrolysis time for groundwater 2 current density: (■) - 156 A/m^3; (●) – 480 A/m^3; (▲) – 780 A/m^3; pH_{ini}=7; $conc_{ini}$: **a.** 10 mg/L F^-; **b.** 5.08 mg/L F^-

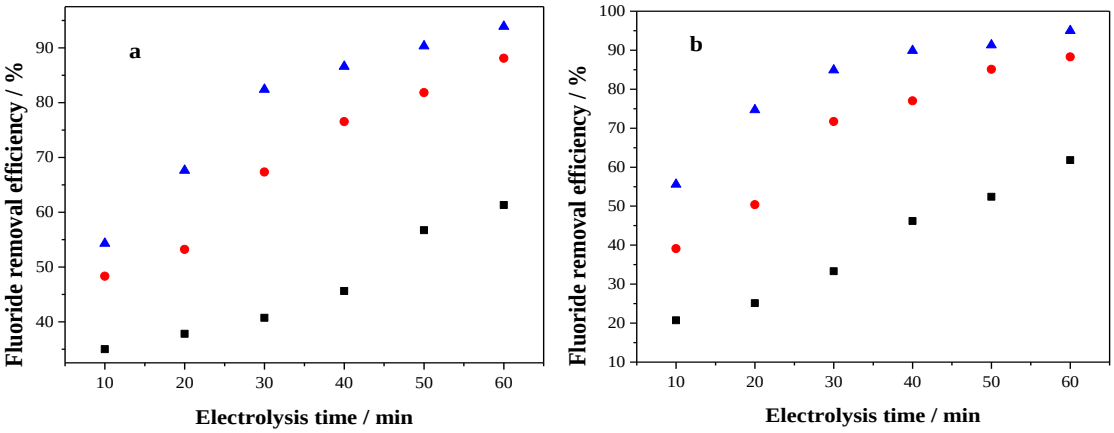

Figure 3. Fluoride removal efficiency versus electrolysis time for groundwater 3 current density: (■) - 156 A/m^3; (●) – 480 A/m^3; (▲) – 780 A/m^3; pH_{ini}=7; $conc_{ini}$: **a.** 10 mg/L F^-; **b.** 5.08 mg/L F^-

Table 2. Arsenic concentration in treated groundwater for 60 min of electrolysis and current density of 780 A/m^3

Groundwater	Fluoride/arsenic mass ratio in untreated groundwater	Arsenic concentration in untreated groundwater/ µg/L	Arsenic concentration in treated groundwater/ µg/L	Arsenic removal efficiency / %
1	140	71.56	< 0.1	> 99.9
2	102	98.36	7.39	92.5
3	101	99.47	2.07	97.9
1	71	71.56	2.75	96.2
2	52	98.36	1.10	98.9
3	51	99.47	1.69	98.3

Table 3. Specific energy consumption for 60 min of electrolysis

Current density / A/m^3	Cell voltage / V	Current intensity / A	Treated groundwater / L	Specific energy consumption / kWh/m^3
156	0.9	0.08	0.5	0.14
480	1.4	0.24		0.67
780	1.8	0.39		1.40

Conclusion

EC proved to be effective in simultaneous removal of fluoride and arsenic from the groundwater collected from three deep wells situated in Western part of Romania regardless of the fluoride/arsenic mass ratio. The residual concentration of fluoride and arsenic in treated groundwater were under the threshold limits stipulated in Law 458/2002 concerning the drinking water quality: 1.2 mg/L and10 µg/L, respectively. The removal efficiency of fluoride was in the range of 90-97% and of arsenic 93-99.9% for 60 min of electrolysis and current density of 780 A/m^3 regardless of where the groundwater was collected from.

Acknowledgements

This work was financed by Programme Nucleu through the project PN 16 25 03 07.

References

[1] W.H.O., Guidelines for Drinking Water Quality, fourth edition, 2011.
[2] S.Chouhan, S.J.S. Flora, Indian J. Exp. Biol. 48(7) (2010) 666.
[3] M. Salgado-Bustamante, M.D. Ortiz-Perez, E. Calderon-Aranda, L. Estrada-Capetillo, P. Nino-Moreno, R. Gonzalez-Amaro, D. Portales-Perez, Sci. Total Environ. 408 (2010) 760.
[4] R. Liu, W. Gong, H. Lan, T. Yang, H. Liu, J. Qu, Sep. Purif. Technol. 92 (2012) 100.
[5] Y. Tang, J. Wang, N. Gao, J. Environ. Sci. 22(11) (2010) 1689.
[6] V. Kumar Rathore, D. Kumar Dohare, P. Mondal, JECE. 4 (2016) 2417.
[7] R. Liu, L. Zhu, Z. He, H. Lan, H. Liu, J. Qu, Colloids Surf., A. 466 (2015) 147.
[8] V. Kumar, N. Talreja, D. Deva, N. Sankararamakrishnan, A. Sharma, N. Verma, Desalination 282 (2011) 27
[9] R. Devi, E. Alemayehu, V. Singh, A. Kumar, E. Mengistie, Bioresource Technol. 99 (2008) 2269.
[10] A. Guzman, J. L.Nava, O. Coreno, I. Rodriguez, S. Gutierreza, Chemosphere 144 (2016) 2113.
[11] X. Zhao, B. Zhang, H. Liu, J. Qu, Chemosphere 83 (2011) 726.

TOXIN PRODUCTION BY *PSEUDOMONAS SYRINGAE* PATHOVARS ORIGINATING FROM SWEET CHERRY

Iličić Renata[1], Balaž Jelica[1], Vlajić Slobodan[1], Jošić Dragana[2], Ognjanov Vladislav[1]
[1]*University of Novi Sad, Faculty of Agriculture, Trg Dositeja Obradovića 8, 21000 Novi Sad, Serbia.*
[2]*Institute of Soil Science, Teodora Drajzera 7, 11000 Belgrade, Serbia.*
e- mail:renatailicic@gmail.com

Abstract
Pseudomonas syringae pathovars *syringae* and *morsprunorum* race 1, causal agents of sweet cherry die back were investigated for their toxin production. Total of 155 strains isolated from diseases sweet cherries from several location in Vojvodina Province, Serbia were used. In previous study the strains were identified as a pv. *syringae*(79 strains, based on presence/absence of *syrB* and *syrD* genes) and as a pv. *morsprunorum* race 1 (76, presence *cfl*gene)based on molecular identification.In this study, bioassay for syringomycin production showed that 64 strainsamong pv. *syringae*produced toxin, and 15 have not in the presence of syringomycin sensitive organisms*G. candidum*,*S. cerevisiae*and *R. pilimanae.* However, using bioassay for coronatine production on the potato slices only few strains out of 76 pv. *morsprunorum* race 1 strains produced coronatine.

Introduction
Bacterial canker caused by *P. syringae* is one of the most serious diseases of stone fruit trees. Diseases of fruits trees caused by pathovars *syringae* and *morsprunorum* result in significant economical losses especially in the past few years in the growing of sweet cherry. The disease usuallymanifestsin the form ofdrying buds, shootsand branches, followed by the cancers formation. Barkon infected treesandbrancheshas darklyreddish color, sags and crack. Cankers and necrosis can be associated with orange-brown gummosis[4]. Identification of *P. syringae* pathovars is based on classical bacteriological test LOPAT[11], GATTatests[10], pathogenicity tests, additional biochemical tests and various molecular techniques of PCR [2; 15; 3; 14; 8;6; 7]. *Pseudomonas syringae* pathovars produces several well-characterized phytotoxic compounds. According to literature *P. s.* pv. *syringae* produces a toxin of the lipodepsipeptide group syringomycin and pv. *morsprunorum* race 1 toxin coronatine [13; 3; 9].Both toxins have been implicated as virulence factors in the diseases induced by these bacteria. The ability to produce syringomycin examines in the use of indicator fungi *Geotrichum candidum*[10]. Also can be applied and *Rhodotorula pilimanae* and *Saccharomyces cerevisiae.*Völksch et al. (1989) reported another bioassay on the potato slices for the detection of the presence of toxins (coronatine) specific for *P. s.* pv. *morsprunorum* (race 1). Genes responsible for syringomycin synthesis (*syrB*) and syringomycin secretion (*syrD*) are specific to the pv. *syringae*, whereas coronatine production gene (*cfl*) is specific to the *P. s.* pv. *morsprunorum* race 1 [2; 15; 3; 7]. The aim of this study was to identify*P. syringae* pvs. strains originating from sweet cherry by testing their toxin production using bioassays.

Experimental
Strains of pv. *syringae*(79 strains) and pv. *morsprunorum* race 1 (76 strains) were grownon NSA (Nutrient-Sucrose-Agar) for 2 days at 26°C. In previous study the strains were identified as a pv. *syringae*(79 strains) and as a pv. *morsprunorum* race 1 (76)[5]based on molecular identification. **Syringomycinproduction.** Strains were streaked on Potato Dextrose Agar medium (PDA)in the form of the circle and grown for 24 hours at 26°C. Cultures of

syringomycin sensitive organisms *Geotrichum candidum*,*Saccharomyces cerevisiae*and *Rhodotorula pilimanae* were cultivated also for 2 days at 25°C. The surface of the medium was sprayed with a suspension of the indicator organism spores prepared in sterile distilled water (SDW). After incubation (2 days), clear zones of fungi growth inhibition were observed around bacterial colonies as an indication of syringomycin production. **Coronatine production.** For the coronatine production bioassay on the potato slices were performed. Bacterial suspension were prepared in SDW and applied onpotato slices. Visualization of *coronatine production*was confirmed by hypertrophy of the tissue slices caused by bacteria.

Results and discussion

Phytotoxins of *P. syringae* pvs. coronatine, syringomycin, syringopeptin are the most studied, and each contributes significantly to bacterial virulence in plants. Some of them appear as a consequenceof particular toxin production, such as chlorosis (coronatine, phaseolotoxin, and tabtoxin) or necrosis (syringomycin and syringopeptin) [1]. Coronatine induces stunting and hypertrophy of plant tissue and is important for virulence of the pathovars that produce it [2]. Bioassay for syringomycin production showed that,in the presence of allsyringomycin sensitive organisms,64 strain of pv. *syringae*produced toxin, and 15 (T23, T24, T25, T26, T27, T28, T29, KBNS85, KBNS86, KBNS88, KBNS89, KBNS90, KBNS91, KBNS92, KBNS94) have not (Figure 1). Strains of pv. *morsprunorum* race 1 in the same test were negative. According to our previous study using multiplex-PCR method by implementation of both genes *syrB*and*syrD,* genes were not detected (strains T20, T1, T23, T24, T25, T26, T27, T28, T29). In bioassay strains T23, T24, T25, T26, T27, T28, T29 also were negative, these can be interpreted by the absence or suppression of genes for syringomycin secretion. In strains T20 and T1 presence of syringomycin was detected in the case of all indicators, although genes were not amplified. However, eight strains (KBNS85, KBNS86, KBNS88, KBNS89, KBNS90, KBNS91, KBNS92, KBNS94) in bioassay were also negative, but both genes (*syrB*and*syrD*) were successfully detected using m-PCR [5]. This indicated a higher sensitivity of PCR method in comparison with bioassay test. Variability among isolates originating from the stone fruit species according to bioassay test were reported by other authors [12; 3; 9]. Roos and Hattingh (1983) suggest that the syringomycin production is specific for pv. *syringae*, but the 30.2% of tested isolates (intermediate forms) also were positive for syringomycin production. Kaluzna (2011) points out that isolates pv. *morsprunorum* (races 1 and 2) reacting negatively, and that most isolates pv. *syringae* produces syringomycin, however for individual isolates pv. *syringae* reaction is negative, as confirmed by our results. Bioassay on the potato slices for the detection of toxins (coronatine) specific for *P. s.* pv. *morsprunorum* (race 1) performed in all tested strains (76) were positive for only few strains, which was comfirmed by hypertrophy of the tissue slices caused by bacteria. Völksch et al. (1989) noted variability in this test, which can occur depending on the potato cultivar and the age of tuber tissue. According to obtained results this test is not completely reliable and adequately, because *cfl*- coronatine production gene was successfully detected in the case of all pv. *morsprunorum* race 1strain (76).

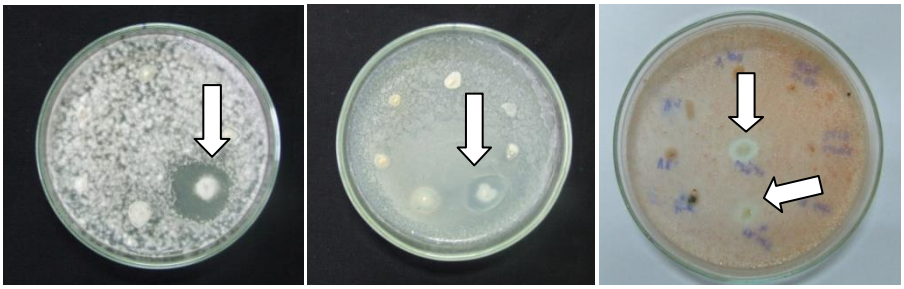

Figure 1. Syringomycin production. Zones of fungi growth inhibition (*G.candidum*; *S.cerevisiae*and *R. pilimanae*)

Conclusion

In bioassay for syringomycin production 64 stains among pv. *syringae*produced toxin, and 15 have not.On the potato slicesonly few strains of pv. *morsprunorum* (race 1) produced toxin coronatine. Bioassays for toxin production can be useful for *P. syringae*pathovars differentiation, but only with implementation of some PCR methods. Obtained results indicated a higher sensitivity of PCR method used in previous study in comparison with bioassay test.

Acknowledgements

This work was supported by Serbian Ministry of Education, Science and Technological Development, Project No. III46007 and TR31038.

References

[1] C.L. Bender, F. Alarcón-Chaidez, D.C. Gross, Microbiol. Mol. Biol. Rev. 63 (1999) 266–292.
[2] S. Bereswill,P. Bugert, B. Volksch, M. Ullrich, C. Bender, K. Geider, Appl. Environ. Microbiol. 8 (1994) 2924-2930.
[3] A. Bultreys, I. Gheysen, Appl. Environ. Microbiol. 65 (1999) 1904-1909.
[4] A. Bultreys, M. Kaluzna**, J. Plant Pathol.** 92 (1, Supplement), (2010) S1.21-S.1.33.
[5] R. Iličić, PhD thesis, Faculty of Agriculture Novi Sad, Serbia (2016).
[6]R. Iličić, J. Balaž, D. Jošić, V Congress of the genetic society. Kladovo, Serbia, Proceedings, (2014) 218.
[7] R. Iličić, J. Balaž, V. Stojšin, D. Jošić, Genetika 48 (2016) 1 285-295.
[8] Ž. Ivanović, S. Stanković, S. Živković, V. Gavrilović, M. Kojić, Đ. Fira, Eur. J. Plant Pathol.134 (2012) 191-203.
[9] M. Kaluzna, Research Institute of Horticulture, Pomology Division Pomologiczna 96-100 (2011) Skierniewice. pp. 18.
[10] B.A. Latorre, A.L. Jones, Phytopathology 69(1979) 335-339.
[11] R.A. Lelliott, E. Billing, A.C. Hayward, J. Appl. *Bacterial.* 29(3) (1966) 470-489.
[12] I.M.M. Roos, M.J. Hattingh, Plant. Dis. 67 (1983) 1267-1269.
[13] I.M.M. **Roos, M.J.** Hattingh, Phytopathology 77 (1987) 1253-1257.
[14] M. Scortichini, U. Marchesi, M.T. Dettori, M.P. Rossi, Plant Pathol. 52 (2003) 277-286.
[15] K.N. Soresten, K.H. Kim, J.Y. Takemoto, Appl. Environ. Microbiol.64 (1998) 226-320.
[16] B. Völksch, F. Bublitz, W. Frieche, J. Basic Microbiol. 29 (1989) 463-468.

ENHANCED ADSORPTION OF METHYL ORANGE FROM AQUEOUS SOLUTIONS USING A FUNCTIONALIZED STYRENE-DIVINYLBENZENE COPOLYMER

Roxana Istratie[1], Roxana Băbuţă[1], Adriana Popa[2], Cornelia Păcurariu[1], Marcela Stoia[1]

[1] *Politehnica University Timişoara, Faculty of Industrial Chemistry and Environmental Engineering, 6 Pîrvan Blv., RO-300223, Timişoara, România*
[2]*Institute of Chemistry Timişoara of Romanian Academy, Romanian Academy, 24 MihaiViteazul Blv., RO-300223, Timişoara, România*
e-mail: roxi_istratie@yahoo.com

Abstract
The adsorption efficiency of the styrene-divinylbenzene copolymer functionalized with carboxylic acid groups (SDVBF) was investigated for methyl orange (MO) removal from aqueous solutions. The effects of contact time and of the initial concentration on the amount of MO adsorbed were studied. The kinetics of MO adsorption onto SDVBF copolymer was described by the pseudo-second order model. It was demonstrated that Redlich-Peterson model is the most suitable to describe the adsorption of MO onto SDVBF copolymer. The maximum adsorption capacity of the SDVBF adsorbent, resulted from the Langmuir isotherm was 53.12 mg g^{-1}.

Introduction
The widespread use of dyes generates large amounts of waste water, producing toxicological problems related to environmental protection [1]. Their presence, even in small quantities, causes changes in terms of waters color, besides the cumulative effect, reducing the amount of light that reaches the aquatic environment thus complicating the process of photosynthesis [2,3]. Most dyes are used in industries such as textiles, paper, plastics, cosmetics, paints, leather, food and pharmaceutical industries [2,3].
Over time there were developed many techniques for the removal of dyes from wastewater such as: flocculation [4], precipitation [5], coagulation [6], separation membranes [7] electrolysis [8], photolysis [9] and adsorption [10]. Among these methods, adsorption is considered by many authors as a superior technique because of high efficacy, low implementation cost, wide availability and simplicity in terms of design [11].
In this study we investigate the adsorption efficiency of the styrene-6.7%divinylbenzene copolymer functionalized with carboxylic acid groups (SDVB-F) for the removal of methyl orange (MO) from aqueous solutions.

Experimental
The preparation and characterization of the functionalized copolymer was presented in our previous work [12]. The adsorption experiments were performed at 25°C, in a thermostated shaker with an operating speed of 200 rpm and at the natural pH of the solution.
The MO concentration was monitored using a UV–Vis SHIMADZU spectrophotometer. The absorbance values were measured at the wavelength of maximum absorbance of 464 nm.

Results and discussion

The effect of different initial concentrations, ranging from 100 to 600 mg L^{-1}, on the adsorption of MO onto SDVBF copolymer is shown in Fig. 1.

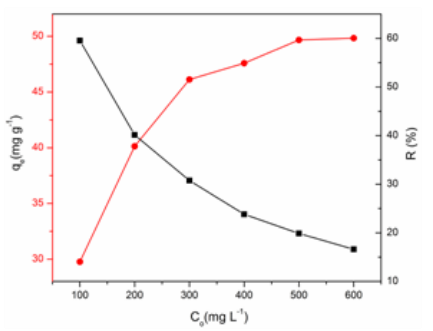

Figure 1. Effect of initial concentration on MO adsorption ontoSDVBF: m= 2 g L^{-1}.

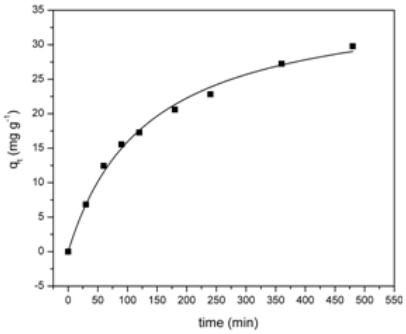

Figure 2. Effect of contact time on MO adsorption onto SDVBF: C_0= 100 mg L^{-1},m=2 g L^{-1}.

The results are in accordance with the literature data, showing the increase of the amount of MO adsorbed at equilibrium and the decrease of the percentage of the pollutant removal with increasing the initial concentration which indicates that the MO removal is concentration dependent.

The amount of MO adsorbed onto SDVBF as a function of contact time is presented in Fig. 2.It can be observed the fast increase of the adsorbed amount of MO in the first 200 min of the process. This behavior can be explained by the large number of initially available vacant sites on the SDVBF surface, sites which are gradually occupied in time as a result of sorption process. It can be seen that equilibrium was reached in about 6 h.

The adsorption kinetics experiments were conducted at 25 °C, 100 mg L^{-1} initial concentration of MO and 2 g L^{-1} adsorbent dose.

The experimental data were fitted with four kinetic models namely Lagergren pseudo-first order, Ho and McKay pseudo-second-order, Elovich and intraparticle diffusion model proposed by Weber and Morris. The fitting plots of the MO adsorption data to the four kinetic models are shown in Fig.3. and the kinetic parameters are listed in Table 1.

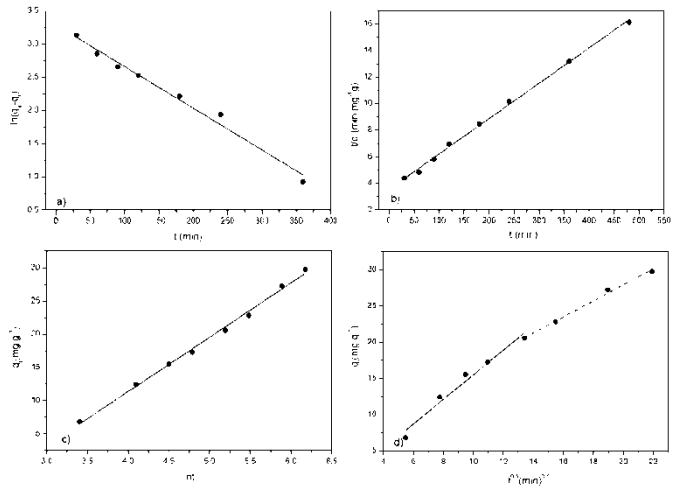

Figure 3. Adsorption kinetics of MO onto SDVBF: a) pseudo-first-order; b) pseudo-second-order; c) Elovich equation; d) intraparticle diffusion model.

Table 1. Kinetic parameters for the adsorption of MO onto SDVB-F.

Kinetic model	Kinetic parameters	
Pseudo-first-order model	$q_{e,calc.}$ (mg g^{-1})	26.84
	$q_{e,exp.}$ (mg g^{-1})	29.77
	$k_1 \cdot 10^3$ (min^{-1})	6.28
	R^2	0.98205
Pseudo-second-order model	$q_{e,calc.}$ (mg g^{-1})	37.56
	$q_{e,exp.}$ (mg g^{-1})	29.77
	$k_2 \cdot 10^4$ (g mg^{-1} min^{-1})	2.00
	R^2	**0.99733**
Elovich model	α (mg g^{-1} min^{-1})	0.60
	β (g mg^{-1})	0.12
	R^2	0.99484
Intraparticle diffusion model (second linear portion)	k_i (mg g^{-1} $min^{-0.5}$)	1.10
	c (mg g^{-1})	5.83
	R^2	0.99147

The linear plots of t/q versus t, and the values of the determination coefficients (R^2) close to unity (Table 1) indicate that the adsorption kinetics of MO is properly described by the pseudo-second-order model. The plot of q_t versus $t^{0.5}$ is not linear over the entire time range, which means that the adsorption mechanism of MO onto SDVBF is not controlled only by the intraparticle diffusion.

The experimental equilibrium data were fitted by the most used isotherm models namely: Langmuir, Freundlich and Redlich-Peterson. The fitting of the equilibrium experimental data of MO with the three isotherm models are shown in Fig.4, and the theoretical parameters of isotherms along with the corresponding determination coefficients (R^2) and Chi-square values (χ^2)are listed in Table 2.

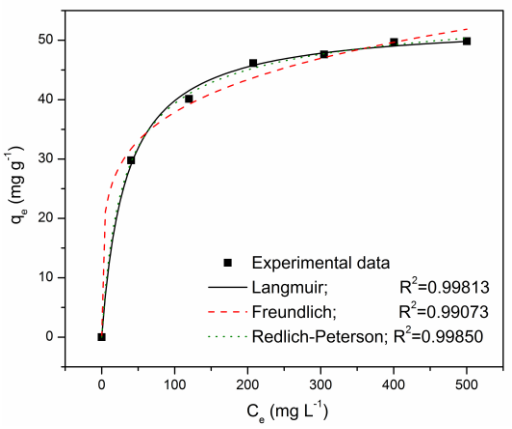

Figure 4. Isotherm plots for the adsorption of MO onto SDVBF.

Comparing the R^2 and χ^2 values of the analyzed isotherms (Table 2), it follows that the Redlich-Peterson model is the most suitable to describe the adsorption of MO onto SDVBF.

It can be noticed the maximum adsorption capacity of the SDVBF resulted from the Langmuir isotherm of 53.12 mg g^{-1}, which is higher as compared with other results reported in the literature regarding the adsorption of MO onto different adsorbents [13].

Table 2. Isotherm parameters values for the adsorption of MO onto SDVBF.

Isotherm model	Parameter	Pollutant
		MO
Langmuir	q_m (mg g^{-1})	53.12
	K_L (L mg^{-1})	0.030
	R^2	0.99813
	χ^2	0.60769
Freundlich	K_F (((mg$^{1-(1/n)}$L$^{1/n}$)g^{-1}))	15.41
	n	5.120
	R^2	0.99073
	χ^2	3.01319
Redlich-Peterson	K_{RP} (L mg^{-1})	1.947
	α_R((L mg^{-1})$^{\beta}$)	0.049
	β	0.954
	R^2	0.9985
	χ^2	0.48748

Conclusion

The styrene-divinylbenzene copolymer functionalized with carboxylic acid groups has shown good adsorption capacity for removal MO from aqueous solutions. The kinetic studies indicated that the adsorption of MO onto SDVBF followed the pseudo-second-order model and the equilibrium adsorption data were best fit by the Redlich-Peterson isotherm.

Acknowledgements

This work was supported by a grant of the Romanian National Authority for Scientific Research and Innovation, CNCS – UEFISCDI, project number PN-II-RU-TE-2014-4-0514.

References

[1] I. M. S. Pillaia, S. K. Guptaa, M. K. Tiwari, J. Environ. Sci. Heal. A. 50 (3) (2015) 301.
[2] G. Z. Kyzas, N. K. Lazaridis, M. Kostoglou, Chem. Eng. J. 248 (2014) 327.
[3] L. Fan, C. Luo, X. Li, F. Lu, H. Qiu, M. Sun, J. Hazard. Mater. 215-216 (2012) 272.
[4] A. Szygułaa, E. Guibalb, M.A. Palacína, M. Ruiza, A. M. Sastrec, J. Environ Manage. 90(10) (2009) 2979.
[5] M.X. Zhu, L. Lee, H. H. Wang, Z. Wang, J. Hazard Mater. 149(3) (2007) 735.
[6] M. Khayet, A. Zahrim, N. Hilal, Chem. Eng. J. 167 (2011) 77.
[7] E. Alventosa-deLara, S. Barredo-Damas, M. Alcaina-Miranda, M. Ibbora-Clar, J. Hazard. Mater. 209-210 (2012) 492.
[8] L. Wang, J. Hazard. Mater. 171 (2009) 577.
[9] O. Ruzimuradov, K. Sharipova, A. Yarbekova, K. Saidova, M. Hojamberdievb, R.M. Prasadc, G. Cherkashininc, R. Riedelc, J. Eur. Ceram. Soc. 35(6) (2015) 1815.
[10] J. Tian, P. Tian,G. Ning, H. Pang, Q. Song, H. Chenga, H. Fanga, RSC Advences 7 (2015) 5123.
[11] B. Tanhaei, A. Ayatia, M. Lahtinenb, M. Sillanpää, Chem. Eng. J. 259 (2015) 1.
[12] C. Păcurariu, G. Mihoc, A. Popa, S. G. Muntean, R. Ianoş, Chem. Eng. J., 222 (2014) 218.
[13] X. Luo, L. Zhang, J. Hazard Mater.171(2009)340.

THE EFFECT *ORIGANUM VULGARE* L. ESSENTIAL OILS ON WEED SEED GERMINATION

Bojan Konstantinović, Nataša Samardžić, Milena Popov, Milan Blagojević

University of Novi Sad, Faculty of Agriculture,Department for Environmental and Plant Protection, Trg Dositeja Obradovića 8, 21000 Novi Sad, Serbia
e-mail: bojank@polj.uns.ac.rs

Abstract

Oregano is a common name for products derived from more than 60 plant species which mostly belong to the families Lamiaceae and Verbenaceae. Within the genus Origanum, forty-two species and forty-nine taxa (species, subspecies and varieties) divided into 10 groups were classified. The largest number comes from the Mediterranean and it is of local character. [4].
In recent years, interest for use of natural compounds in control of weed species keeps growing. Natural compounds with allelopathic effect generally represent the products of secondary metabolism and are known as allelochemicals. Allelochemicals are safer than synthetic herbicides primarily because they are biodegradable and have a minimal detrimental impact on the environment [7].
During 2016, the allelopathic effect of oregano essential oil was studied on germination of some plant species such as: rucola (*Eruca sativa* Mill.), onion (*Alium cepa* L.), kohlrabi (*Brassica oleracea*var.*gongylodes* L.) and kale (*Brassica oleracea* var. *sabauda*, L.). Seeds of the mentioned weed species were treated with different concentrations of oregano essential oil in the amount of 200 µl/ml, 400 µl/ml, 600 µl/ml and 800 µl/ml. Distilled water was used as a control. The obtained results indicate that the increase in concentrations of the essential oil results with the reduction in germination of onion and kohlrabi plant seeds, and also with the increase in its inhibitory effects. For kale and rucola seeds a deviation in correlative inhibition of germination at a concentration of 600 µ/ml was established, while the average seed germination was higher than at a lower concentration of 400 µ/ml.

Introduction

Essential oils have a significant role in the reduction of herbivores and parasites, so that in addition to the pharmaceutical, food and cosmetic industries, they have found the application also in the protection of ecosystems, humans, animals and foods [8]. Essential oils are complex, unstable natural compounds with a strong odour and represent secondary metabolites of aromatic plants. They are the most frequently separated by steam or hydrodistillation. In nature, they protect plants from bacteria, viruses, fungi, insects and herbivores. Essential oils have a role in attracting of certain insects to for the purpose of dispersion of pollen and seed, but for some other insects they can be repellents. They can be synthesized in all plant organs, and are kept in secretory cells, channels, cavities, epidermal cells or glandular trichomes [1][6]. In warm climate, the content of essential oil is higher. Therefore it is often said that essential oils are products of Helios synthesis. From the other hand, there really exist ‘’chemical races’’ in many of aromatic plants [3].
Oregano (*Origanum vulgare* L.) is perennial, herbaceous plant of aromatic smell and taste. Numerous studies have confirmed antibacterial, fungicidal, antiviral and antioxidative properties of oregano. It is strongly antiseptic, and its essential oil (5%) the tincture with rosemary is used for outside rubbing in treatments of rheumatism and diseased joints [2].
There are two basic oregano species that grow in the region of Serbia. The first one is *Origanum vulgare* subsp. *vulgare* L., oregano or wild marjoram (wild marjoram – or "blue" oregano - for blue flowers). It is used for the production of oils for cosmetic purposes, and the

most frequently as an adjunct to massage oils. It is extraordinary antiseptic. It is used in the form of teas - as a medicinal herb. It is not used as a spice, except in special cases, as a surrogate to real oregano. It is added to alcoholic drinks that obtain specific taste and antiseptic property of this plant. The fabric industry uses it also for getting products of special lilac colour. In Serbia this plant is wild, but it is also cultivated. Mountain areas are the most suitable for its growth, although it can also be found on terrains of lower altitude. It is widely distributed, and the studies have shown that oregano of the highest quality grows in the region of Zlatibor.

Beside allelopathic effect to weed species, essential oils of aromatic plants can have a negative impact on cultivated plants. Due to their negative influence, studies on the impact of essential oils are desirable in order to get to know possibilities and restrictions of their use in agricultural production in advance. The phytotoxic potential of essential oils ant their pure components have been studied earlier, and in many previous studies, it has been documented that essential oils and their compounds delay germination and inhibit the growth of weed seedlings and also seedlings of cultivated plants. These studies have to be taken into account when considering the application of essential oils in the system of food production, as well as ways of its use in order to achieve a minimum adverse effect on cultivated plants or way of use by which such negative effect would be avoided.

Experimental

In the trial the essential oil of oregano was used (*Origanum vulgare* L.) which are the most common components were carvacrol with 85% and thymol with 5%, while all other components were represented with less than 1%.

Plant species whose seeds were used for the studies on influence of oregano (*O. vulgare* L.) essential oil to germination and growth of seedlings were the following: rucola (*Eruca sativa* Mill.), onion (*Alium cepa* L.), kohlrabi (*Brassica oleracea*var.*gongylodes* L.) and kale (*Brassica oleracea* var. *sabauda* L.).

Petri dishes were filled with fifteen seeds per dish; seeds were placed on two layers of filter paper and covered with the third one. Seeds were treated by 200 µl/ml, 400 µl/ml, 600 µl/ml and 800 µl/ml of essential oil concentrations. The laboratory test was accomplished in four replications.

After placing of seeds into Petri dishes and impregnation with distilled water and different concentrations of oregano essential oils, Petri dishes were relocated into a climatic chamber. The test was monitored on daily basis, and after four days, germinated seeds of chosen plants were numbered, and length of seedlings was measured in millimetres.

Results and discussion

Seed germination can be defined as the emergence and development of seminal embryos of the most important structures that are, depending on plant species that are under convenient conditions for growth and development, capable of producing a normal plant. Many biotic and abiotic factors influence on seed germination, as well as on the main component of seed quality – germination [5].

In Table 1 are presented average values of rucola (*E. sativa* Mill.) seed shootings achieved by treatment with different concentrations of oregano essential oils. Given data present lack of germinated seeds after treatment with the highest oregano essential oil concentration of 800 µl/ml, and also there is a deviation in gradual successive reduction in germination with increasing concentrations, meaning that the applied concentration of 600 µl/ml resulted with higher germination than after use of the essential oil concentration of 400 µl/ml.

Table 1 Influence of different concentrations of oregano essential oil on germination of rucola (*E. sativa* Mill.) seed.

	Control	200 µl/ml	400 µl/ml	600 µl/ml	800 µl/ml
Rucola	6.73	1.53	0.23	0.48	0

The same inhibitory effect of the essential oil in concentrations of 200 µl/ml and 400 µl/ml was established after treatment of onion (*A.cepa* L.) seed, with the average values of shootings of 0.11 mm, as well as the inhibitory effect after seed treatment with different concentrations of 600 µl/ml and 800 µl/ml, for which the identical average values of shootings length of 0.26 mm were recorded.

Table 2 Influence of different concentrations of oregano essential oil on germination of onion (*A. cepa* Mill.) seed.

	Control	200 µ/ml	400 µ/ml	600 µ/ml	800 µ/ml
Onion	2.3	0.11	0.11	0.26	0.26

In Table 3 are presented average values of shooting length of kohlrabi (*B. oleracea*var.*gongylodes* L.) seeds, obtained by their treatment with different concentrations of oregano essential oil in control with distilled water. It was found that the average length of shooting reduced with the increase of oregano essential oil concentration, i.e. shootings were the longest when sprayed by the concentration of 200 µl/ml, and the shortest after application of the highest concentration of the essential oil of 800 µl/ml.

Table 3 Influence of different concentrations of oregano essential oil on germination of kohlrabi (*B. oleracea*var.*gongylodes* L.) seeds.

	Control	200 µl/ml	400 µl/ml	600 µl/ml	800 µl/ml
Kohlrabi	12.4	1.45	1.01	0.78	0.13

In Table 4 is presented the influence of different concentrations of oregano essential oils on kale (*B. oleracea* var. *sabauda* L.) seeds. Given data show that the highest average length of seedlings was achieved after spraying with the lowest concentration of 200 µl/ml, and the lowest shootings length was obtained after use of the highest concentration of the essential oil of 800 µl/ml; and also there is a deviation in gradual successive reduction in germination with increasing concentrations, meaning that the applied concentration of 600 µl/ml resulted with higher germination than after application of the essential oil concentration of 400 µl/ml.

Table 4 Influence of different concentrations of oregano essential oil on germination of kale (*B. oleracea* var. *sabauda* L.) seeds.

	Control	200 µ/ml	400 µ/ml	600 µ/ml	800 µ/ml
Kale	18.2	1.23	0.30	0.36	0.11

Conclusion

Oregano is an aromatic, medicinal and spice plant. With the increase in studies of its properties, new knowledge on its usefulness arises. Because of this, it is increasingly demanded by domestic and foreign markets. Numerous studies have confirmed antibacterial, fungicidal, antiviral and antioxidative properties of oregano due to which it is widely used in traditional medicine.

The processing of the obtained results showed that oregano essential oil had a significant influence on germination of rucola, onion kohlrabi and kale seeds. All four studied plant

species did not show tolerance to treatment with the essential oil. The obtained results clearly revealed that with the increase of the essential oil concentration its inhibitory action also increased to germination of seeds of tested plants, excepting rucola and kale seeds for which there is a deviation in the gradual successive reduction in germination with increasing concentrations. For this seed, the deviation in correlative inhibition of shooting after spraying with the concentration of 600 μ/ml is obvious, while the average germination of seeds was higher than after use of lower concentration of 400 μ/ml.

Results of this study showed that in decision making on the use of oregano essential oil in the production of the studied plant species, the attention must be paid in regard to the inhibitory effect of the essential oil to germination of seeds and length of seedlings. Also, further analysis and studies should be encouraged and supported, not only on oregano essential oil, but on all essential oils on different plant species in order to find new, harmless, and sustainable strategies in plant protection as an alternative to synthetic chemical compounds, thus preventing the occurrence of environmental pollution as well as many other adverse effects of chemical plant protection.

References

[1] A.Angioni, A.Barra, V. Coroneo, S.Dessi, P.Cabras, Journal of Agricultural and Food Chemistry 54 (2006) 4364-4370.

[2] H.Baydar, O.Sagdic, G.Ozkan, T. Karadogan, Food Control, 15 (2004) 169-172.

[3] SM.Gorunović, BP.Lukić, Farmakognozija. Farmaceutski fakultet, Univerzitet u Beogradu, Beograd (2001).

[4] J.H. Ietswaart, A taxonomic revision of the genus Origanum (Labiatae). PhD thesis. Leiden University Press, The Hague (1980).

[5] D.Jovičić, Z.Nikolić, D.Petrović, M.Ignjatov, K.Taški-Ajduković, M.Tatić, Institut za ratarstvo i povrtarstvo. 48 (1) (2011) 163-170.

[6] V.Masotti, F.Juteau, J.Bessiere, J.Viano, Journal of Agricultural and Food Chemistry 51 (2003) 7115-7121.

[7] S.Topal, I.Kocaçalşkan, Allelopathic effects of dopa against four weed species. DPU Fen Institute of science, 11 (2006) 27-32

[8] M.Vučinić, J.Nedeljković-Trailović, S.Trailović, S.Ivanović, M.Milovanović, D.Krnjaić, Veterinarski glasnik, 65 (2011) 433–441.

SORPTION-DESORPTION BEHAVIOUR OF HYDROPHOBIC ORGANIC COMPOUNDS ON DANUBE SEDIMENT

Marijana Kragulj Isakovski[1], Jelena Tričković[1], Jasmina Agbaba[1], Srđan Rončević[1], Aleksandra Tubić[1], Miljana Prica[2], Božo Dalmacija[1]

[1]University of Novi Sad, Faculty of Sciences, Trg Dositeja Obradovića 3, 21000 Novi Sad, Serbia
[2]University of Novi Sad, Faculty of Technical Sciences, Trg Dositeja Obradovica 6, 21000 Novi Sad, Serbia
e-mail: marijana.kragulj@dh.uns.ac.rs

Abstract
The sorption-desorption hysteresis of naphthalene and phenanthrene onto Danube sediment was investigated. Hysteresis indices (*HI*) are calculated for three equilibrium concentration (C_e=1%, 5% i 50% of the solubility in water). The results of sorption-desorption hysteresis indicated that it exists for both investigated sorbates on the Danube sediment. For more hydrophobic compound, phenanthrene ($\log K_{OW}$< 4.55) hysteresis is less pronounced in comparison with naphthalene ($\log K_{OW}$< 3.36). In the case of naphthalene, the existence of hysteresis may be due to irreversible pore deformation of the sorbent which causes the formation of meta-stable states in the sorbate mesopores.

Introduction
Sorption is one of the major processes influencing the fate of hydrophobic organic compounds (HOCs) in soils and sediments. It has been shown that sorption of HOCs is directly related to soil/sediment organic matter (SOM), and SOM comprises of two important heterogeneous sorption domains: a “rubbery”, soft, or amorphous and a “glass”, hard, or condensed domain [1]. In addition, investigating sorption reversibility can provide additional information on sorption and desorption mechanisms. Understanding the mechanism of desorption is an essential step towards assess the risk of releasing of pollutants from sediment which is important in assessing the risk of the release of pollutants into the aquatic environment [2].
The aim of this study was to determine sorption-desorption characteristics of the Danube for two selected polycyclic aromatic hydrocarbons (PAHs). Adsorption-desorption hysteresis, the mismatch between the sorption and desorption isotherms, was investigated for naphthalene and phenanthrene on the Danube sediment.

Experimental
Characterization of sediment
The organic carbon (OC) content was determined by TOC analyzer (LiquiTOCII, Elementar, Germany) after acid pre-treatment of the sediment to remove inorganic carbon. The multi-point BET (Brunauer–Emmett–Teller) specific surface area (SSA) of Danube sediment was determined by nitrogen adsorption at 77 K by Autosorb iQ Surface Area Analyzer (Quantachrome Instruments, USA). Samples were outgassed at 200 ºC for 2 h before running the isotherms. Mesopore volumes (V_{mes}) were derived from desorption isotherms using the BJH (Barrett–Joyner–Halenda) model. Micropore volumes of both sorbents were calculated by t-test method.
Physicochemical properties of PAHs
Two PAHs (naphthalene and phenanthrene) were used as sorbates. Both PAHs(purity > 99%) were purchased from Sigma-Aldrich Chemical Company. The physicochemical properties of the chosen PAHs are summarized in Table 1.

Table 1.*Physicochemical properties of selected PAHs*[3]

Compounds	*MW (g/mol)*	*logK_{ow}*	*S_w (mg/l)*	*V_i*
Naphthalene	128.17	3.36	30	1.09
Phenanthrene	178.23	4.55	1.6	1.45

MW, molecular weight (g/mol); K_{OW}, octanol-water partition coefficient; S_W, water solubility (mg/l); V_i, McGowan volume in units of (cm^3/mol)/100.

Sorption-desorption isotherms

All sorption-desorption isotherms were run in duplicate at room temperature (20 ± 2ºC). The sorption isotherms were performed in conventional batch sorption experiments in 40 ml vials with Teflon lined septa. The background solution was 0.01 M $CaCl_2$ in deionized water with 100 mg/l NaN_3 as biocide. Initial concentrations of PAHs ranged from 0.005 to 1.0 mg/l. The solid/solution ratio was adjusted to result in 20-80% uptake of given organic compound. Head space in the vials was kept at a minimum in order to minimize the loss of compounds during the experiment due to evaporation. The procedure was as follows: in vials which contained premeasured sorbent and background solution, a certain volume of methanol stock solution of PAHs was spiked and equilibrated at room temperature by continuous shaking for 7 days. After the completion of sorption, vials were centrifuged at 3000 rpm for 15 minutes, and the aliquots of the clear supernatant were taken for PAHs analysis. Control vials, prepared similarly but with no sorbent, were run simultaneously for assessing the loss of sorbate due to processes other than sorption (evaporation, adsorption on the walls of the vials, degradation). The results showed that the total uncertainty was less than 5% of the initial concentrations. Desorption was conducted by sequential decant-refill steps, after the completion of the sorption experiments, which involves replacement of an aqueous solution that is in equilibrium with fresh background solution, which does not contain sorbate, after which the vials reach new equilibrium. Dilution factors were determined by measuring the mass of the vials before and after the addition of fresh portions of background solution. By calculating the mass balance based on the equilibrium sorbate concentrations, the masses removed of the supernatant solution and the portions added background solution, provided data on the amount of sorbate desorbed in the desorption, and data were collected to fit desorption isotherms.

PAHs in the supernatants were analyzed after liquid-liquid extraction with hexane (J.T.Baker, for organic residue analysis). PAHs were analyzed by gas chromatography with mass spectrometric detection (GC/MS, Agilent 7890A/5975C) on a HP-5MS column (J&W Scientific) with phenathrene-d10 as internal standard.

Data analysis

The sorption data were fitted with the Freundlich isotherm:

$$q_e = K_F \cdot C_e^n \quad (1)$$

where q_e and C_e are the solid phase and aqueous phase equilibrium concentrations (in mg/kg and mg/l, respectively); K_F and the exponent n are the Freundlich sorption coefficient [expressed as (mg/kg)/(mg/l)^n].

Sorption-desorption hysteresis was explored using Hysteresis Index (*HI*) as proposed by Huang et al. [4]:

$$HI = \frac{q_e^{\,d} - q_e^{\,s}}{q_{es}} /_{T,C_e} \quad (2)$$

where q_{es} and q_{ed} are solid-phase solute concentrations for the single cycle sorption and desorption experiments, respectively, and the subscripts T and C_e specify constant temperature and residual aqueous phase concentration, respectively.

Results and discussion

Characterization of Danube sediment

Danube sediment has average mesopore radius about 11.4 nm, while the results of t-test methods clearly show that sediment does not contain micropores. Additionally, the SSA and pore volume (PV) were 3.19 m^2/g and 0.018 cm^3/g, respectively. OC content of Danube sediment is 1.21%. Based on these results it can be concluded that the Danube sediment represents a typical sandy aquifer material with low OC content.

Sorption-desorption hysteresis

Sorption reversibility provides an additional insight into the sorption mechanisms, as well as structural properties of the sorbent governing the specific sorptive behaviour of the sorbate. The sorption-desorption hysteresis was quantified for each sorption and desorption isotherms using the hysteresis index (*HI*) (eq. 2). Hysteresis indices were calculated using Freundlich's parameters obtained from the sorption and desorption of the three sorbate equilibrium concentrations (C_e=1%, 5% i 50% of the solubility in water). The calculated *HI* values are represented in Table 2.

Table 2.*Sorption-desorption hysteresis for investigated PAHs on the Danube sediment*

Compounds	*HI*		
	C_e*(mg/l)* S_W		
	0.01 S_W	*0.05* S_W	*0.5* S_W
Napthalene	0.65	1.02	1.70
Phenanthrene	0.45	0.31	0.11

The more pronounced sorption-desorption hysteresis was observed for naphthalene. Interestingly, Danube sediment showed a more pronounced hysteresis for naphthalene (*HI* = 1.70 to 0.65) than phenanthrene (*HI* = 0.45 to 0.11), which may indicate that the smaller naphthalene remains trapped after penetrating into the pores of the sorbent. In this case, hysteresis can be explained as follows: in low concentrations, sorption may be the result of surface interactions. Surface-bound molecules are probably desorbed much faster. However, as the concentration of sorbate increases, the increased concentration gradient causes molecules that penetrate deeper into the pores of sorbent and organic matter causing the creation of pores in which they are trapped, resulted in the pronounced hysteresis. Since the sediment has mesopores with average radius of about 114 Å, the pore volumes can be calculated and is equal to 6.20 10^6 A^3. Volume of one molecule of naphthalene is about 187 $Å^3$ which means that "irreversible entrapment" can be the cause of the observed sorption-desorption hysteresis.

For phenanthrene, desorption increased with increasing concentration. Hysteresis can be explained as follows: at lower concentration of phenanthrene sorption is results interaction between molecules of phenanthrene with condensed domain of SOM, while at higher concentrations molecules of phenanthrene can interact with soft domain of SOM.

Additionally, Sander et al. [5] point out that desorption hysteresis was widely reported for organic contaminants from soils/sediments, and was attributed to irreversible pore deformation of the sorbent by the sorbate and the formation of meta-stable states of sorbate in fixed mesopores.

Conclusion

In this study, the sorption-desorption behaviour of two compounds from the group of the PAHs on Danube sediment was investigated. Sorption-desorption hysteresis exists for both PAHs. The more pronounced sorption-desorption hysteresis was observed for naphthalene on the Danube sediment which may be due to irreversible pore deformation of the sediment which causes the formation of meta-stable states in the sorbate mesopores. Further research should be focused on a more detailed characterization of the organic matter in the sediment to better define the sorption behaviour. Understanding these results will be useful for exposure and risk assessment of investigated PAHs in aquifer materials and groundwater.

Acknowledgements

The authors gratefully acknowledge the support of the Provincial Secretariat for Higher Education and Scientific Research, Republic of Serbia, Autonomous Province of Vojvodina (Project No. 114-451-2263/2016).

References

[1] K. Sun, B. Gao, Z. Zhang, G. Zhang, Y. Zhao, B. Xing, Environ. Pollut. 158, (2010) 3520.
[2]B. Pan, D.H. Lin, H., Mashayekhi, B. Xing, Environ. Sci. Technol. 42, (2008) 5480.
[3] C. Niederer, R.P. Schwarzenbach, K.U. Goss, Environ. Sci. Technol. 41, (2007) 6711.
[4] W. Huang, H. Yu, W.J. Weber Jr, Con. Hyd.31, (1998) 129.
[5] M. Sander, Y. F. Lu, J. J. Pignatello, J. Environ. Qual. 34, (2005) 1063.

CORROSION INHIBITION PROCESS OF CARBON STEEL IN HYDROCHLORIC ACID BY CRONOX

Mihaela Alexandra Labosel, Andra Tamas, Mircea Laurentiu Dan

University Politehnica Timişoara, Faculty of Industrial Chemistry and Environmental Engineering, 300223, Parvan 6, Timisoara, Romania
e-mail: mihaela.labosel@gmail.com

Abstract
The aim of this investigation is to examine the inhibitory effect of CRONOX toward the corrosion of carbon steel corrosion in 1M hydrochloric acid solution. Weight loss and potentiodynamic polarization techniques were used in this work to evaluate the inhibition efficiency of the tested inhibitor. Also, Tafel method for determining of the kinetic parameters, scanning electron microscopy, all of them providing complete information about the mode of action of the inhibitors; simultaneously, has been studied, the CRONOX inhibiting efficiency with increasing temperature.

Introduction
Carbon steel corrosion process in hydrochloric acid solution is extensively studied because the industrial applications of acid solutions especially in pickling rescaling and cleaning process of steel surface [1,2]. Inhibitors are generally used to reduce the corrosive attack on metallic materials acting on metal dissolution [3]. They are single or mixtures organic compounds, which have nitrogen, oxygen and sulfur atoms in their molecular structure [4]. Inhibitory effect consist in formation of a physical and/or chemical adsorption film barrier on the metal surface [1,5].
CRONOX is a commercial corrosion inhibitor which has composition presented in Table 1. CRONOX corrosion inhibitor supplied are used in the subsea oil and gas industry. CRONOX is a water soluble, oil insoluble corrosion inhibitor concentrate designed for application in water based drilling mud systems and as a packer fluid inhibitor [6,7].

Table 1. Inhibitor composition [6,7]:

Ingredients	**Wt%**
Methanol	30 - 60
Fatty acids	10 - 30
Polyoxyalkylenes	10 - 30
Modified thiourea polymer	10 - 30
Propargyl alcohol	5 - 10
Olefin	1 - 5

Experimental
The working electrode was a cylindrical disc cut from a carbon steel sample. HCl reagent was used for the preparation of aggressive solutions. To determine the inhibitor effect of CRONOX on the corrosion rate of carbon steel in 1M HCl solution, in preliminary studies presented in this paper, 0.1% inhibitor was used.
The cyclic voltammetry, linear polarization (Tafel polarization method) and weight loss methods were used in order to notice the inhibitive properties of CRONOX on the carbon steel corrosion process. The electrochemical studies were recorded using a SP150 BioLogic potentiostat/galvanostat.

Results and discussion

The electrochemical behavior of CRONOX in 1 M HCl electrolyte was studied by cyclic voltammetry on platinum electrode. In figures 1 and 2 are presented CVs recorded in test solution without and with 0.1% inhibitor at different scan rate.

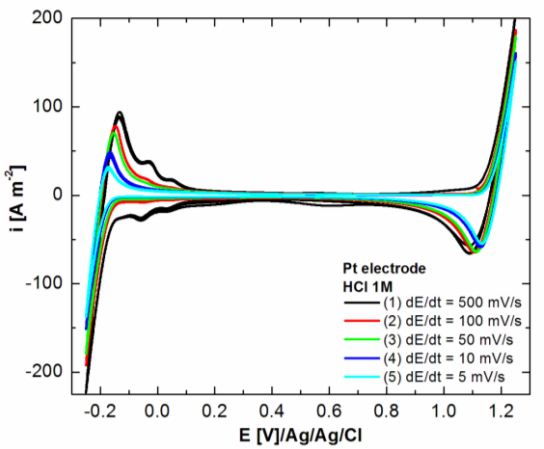

Figure 1. CVsrecorded on Pt electrode in 1 M HCl solution, at different scan rate.

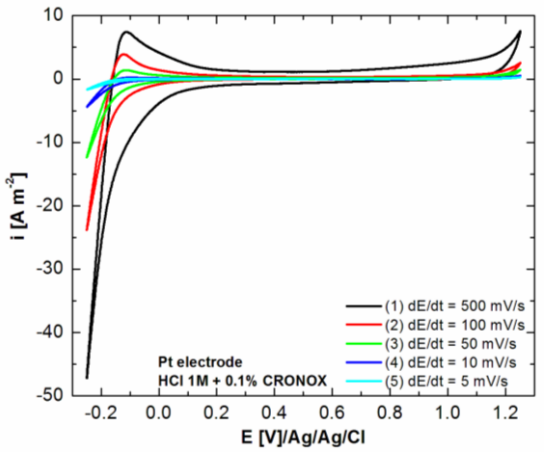

Figure 2. CVsrecorded on Pt electrode in 1 M HCl + 0.1% CRONOX solution, at different scan rate.

The manner in which CRONOX can be a corrosion inhibitor for carbon steel in 1 M HCl solution and its effect on corrosion rate can be estimated by Tafel method from linear polarization curves recorded without and with 0.1% inhibitor at temperatures range between 298 and 338 K, as shown in figures 3 and 4.

Numerical values of the corrosion current density (i_{corr}) variation, corrosion potential (E_{corr}), anodic Tafel slope (b_a), cathodic Tafel slope (b_c) and polarization resistance (R_p) were obtained from polarization profiles by extrapolating potentiodynamic curves from figures 3 and 4 using BioLogics software.The inhibition efficiency (*IE*) has been calculated using equation (1). All obtained values are presented in Table 2.

$$IE(\%) = \left(\frac{i^{o}_{corr} - i^{inh}_{corr}}{i^{o}_{corr}}\right) \times 100 \qquad (1)$$

where $i^{0}_{corr}$and i^{inh}_{corr} are the uninhibited and inhibited corrosion current densities, respectively.

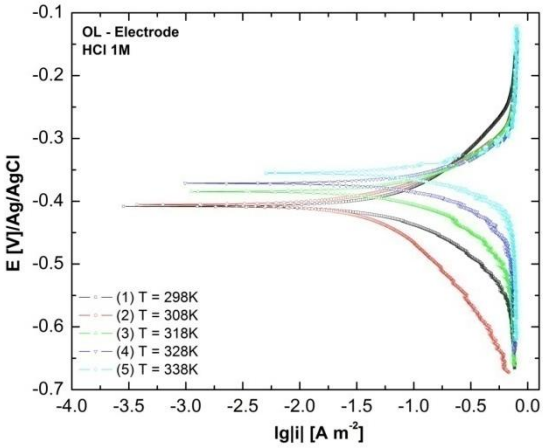

Figure 3. LVs recorded on carbon steel electrodes in 1 M HCl solution, scan rate: 1 mV s^{-1}.

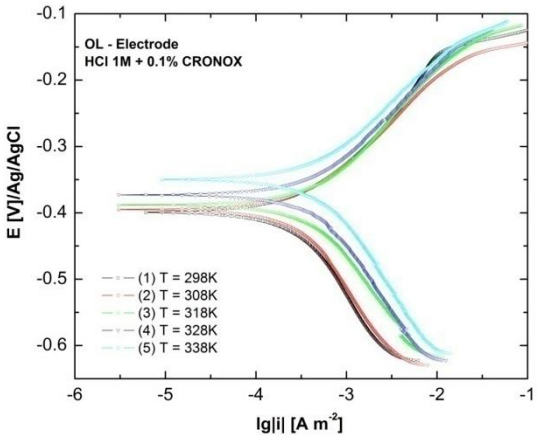

Figure 4. LVs recorded on carbon steel electrodes in 1 M HCl + 0.1% CRONOX solution, scan rate: 1 mV s^{-1}.

Table 2. Polarization parameters for test electrodes corrosion process in 1 M HCl solution in the absence/presence of CRONOX at different temperatures:

Electrolyte	**T [K]**	**i_{corr}, [μA cm^{-2}]**	**E_{corr}, [mV]**	**$-b_c$, [mV dec^{-1}]**	**b_a, [mV dec^{-1}]**	**R_p, [Ω]**	**v_{corr}, [mm an^{-1}]**	***IE*, %**
SB (HCl 1M)	298	**5.314**	-406	175	165	1.338	**109**	-
	308	**9.861**	-394	162	158	1.708	**569**	-
	318	**13.51**	-385	154	149	0.846	**158**	-
	328	**22.13**	-372	141	137	0.733	**259**	-
	338	**23.4**	-366	134	124	0.398	**273**	-
SB + 0.1% Cronox	298	**0.044**	-421	163	156	214	**0.452**	**99.17**
	308	**0.067**	-415	156	154	194	**0.647**	**99.32**
	318	**0.079**	-411	148	153	179	**0.834**	**99.42**
	328	**0.088**	-401	142	148	164	**0.933**	**99.60**
	338	**0.102**	-391	140	145	147	**1.026**	**99.56**

The gravimetric measurements of carbon steel discs samples immersed in 1 M HCl, in the absence and presence of 0.1% CRONOX inhibitor, were investigated and determined after

240 hours of immersion, at 298 K. The corrosion rate of carbon steel (W_L) and the inhibition efficiency (*IE*) obtained are shown in Table 3.

Table 3. The inhibition efficiency obtained by weight loss method:

CRONOX conc. [%]	**W_{corr} [mg cm^{-2} h^{-1}]**	***IE* [%]**
0	1.192	-
0.1	0.035	**98.28**

Conclusion

CRONOX inhibition efficiency has been studied by two different methods: weight loss and linear polarization, both giving comparable values. This compound exhibited excellent inhibition performance as carbon steel inhibitor in 1 M HCl.

Acknowledgements

This work was partially supported by University Politehnica Timisoara.

References

[1] M. Abdallah, B.A.AL Jahdaly, O.A. Al-Malyo, Int. J. Electrochem Sci., 10 (2015) 2740.
[2] M. Lagrene, B. Mernari, M. Traisnel, F. Bentiss, Corros.Sci., 44(2002) 573.
[3] M. Abdallah, B.H. Asghar, I. Zaafarany, A.S. Fouda, Int. J. Electrochem. Sci., 7 (2012) 282.
[4] N. Labjar, S. El Hajjaji, M. Lebrini, M. S. Idrissi, C. Jama, F. Bentiss, J. Mater. Environ. Sci. 2 (4) (2011) 309.
[5] F. Bentiss, M. Lagrrene, M. Traisnel, Corrosion, 56(2000) 733.
[6] http://www.subsea.org/products/specification.asp?prod=1306.
[7] http://doc.ccc-group.com/msds/english/241046.pdf.

SELF-MEDICATION IN STUDENTS
EGYETEMI HALLGATÓK ÖNGYÓGYSZEREZÉSI SZOKÁSAI

Lehel Máthé[1], Péter Szabó[2], János Máthé[3*]

[1]Department of Pharmacology and Clinical Pharmacy ,[3]Department of Biochimistry University of Medicine and Pharmacy, Tirgu-Mures, Romania, str Marinescu nr 38,[2]student e-mail: lehelmathe@gmail.com

Abstract
Self-medication empowers patients to treat or prevent short term or chronic illnesses which they consider not requiring the consultation of a physician or may be treated by the people after an initial medical diagnosis.[1]The prevalence rates are high all over the world; up to 68% in European countries.[2]Various previous studies have shown that self medication practices are more common in women, who live alone, have a lower socioeconomic status, have more chronic diseases, have psychiatric conditions or are of younger ages.[3]The youth is especially exposed to the media and the increased digital advertising world of pharmaceuticals.Our objective was to determine the prevalence, attitude and knowledge of self-medication amongst medicine and pharmacy university students in Tirgu-Mures, Romania.

Bevezető
Szakmai körökben öngyógyításnak vagy öngyógyszerezésnek nevezzük, amikor az emberek saját maguk döntenek arról, hogy hogyan és milyen módszerekkel gyógyítják az önmaguk által felismert panaszokat. Az öngyógyítás egyik eszköze a nem receptköteles gyógyszerek vásárlása és szedése, ami számos előnnyel jár.[4] Az emberek ezáltal temérdek időt takaríthatnak meg.
A lakosság egyre jelentősebb része első- és gyakran egyetlen állomásként a gyógyszertárat keresi fel, ha gyógyszerre vagy tanácsra van szüksége. Egyre többen az orvos megkerülésével, gyakran a reklámok hatására kezdenek öngyógyításba. Ekkor a gyógyszerész figyelme, szakértelme rendkívül fontossá válik, hiszen ő az egyetlen személy, aki még hozzáértően beavatkozhat. A gyógyszerész-beteg beszélgetések 31%-ban észlelhető a gyógyszerreklámok hatása.[5]
A betegségek 95%-át először vény nélküli gyógyszerekkel kezelik.[6]
Célul tűztük ki, hogy felmérjük a marosvásárhelyi Orvosi- és Gyógyszerészeti Egyetem diákjainak vény nélküli gyógyszerek szedésére vonatkozó szokásait, és a reklámok befolyásoló hatását.

Anyag és módszer
Az adatok gyűjtésénél egy általunk szerkesztett kérdőívet használtunk “Az egyetemisták öngyógyszererézi szokásai” címmel 2015 április-május hónapokban. A kérdések első fele zárt kérdéssor: nem, életkor, hallgatói státus, származási hely, krónikus betegségek-, illetve ezek kezelése. Az utána következő kérdések az utolsó évben fellépő akut betegségekre, orvosi ügyeletre- vagy családi/szakorvosi rendelő felkeresése, valamint orvos által felírt vények kiváltására vonatkoztak. A következő kérdések a hallgató otthoni „gyógyszerdoboz”-ának tartalmára, az OTC gyógyszerek ismeretére és vény nélküli kiváltásuknak gyakoriságára, valamint azok lehetséges mellékhatásaikról és interakcióikról kutakodtak. A kérdéscsomag utolsó felében az egyetemisták tünettani ismeretére voltunk kíváncsiak, vagyis hogyan következtetnek különböző panaszokból, hogyan állítanak fel hirtelen egy munkadiagnózist, függetlenül attól hogy az az általános műveltségükből vagy tanult ismeretekből származnak.
Összesen 647 kérdőívet sikerült összesíteni, amiből 254 általános orvosis diák, 161 fogorvosis

és 202 gyógyszerész hallgató volt. Az adatokat Microsoft Excel táblázatba csoportosítottuk és különböző statisztikai számításokat végeztünk.

Eredmények

Az egyetemi hallgatók átlagéletkora 22,3 év volt. A 647 diák nagyrésze lány (75,58%) volt. A legtöbben az orvosi karról képviseltették magukat (39,26%). Összeségében elmondható, az egyetemi hallgatók ritkán keresik fel családorvosukat, átlagban évente egyszer, de azt is a kötelező rutin-ellenőrzés miatt. De otthoni gyógyszerdobozzal majdnem mindenki rendelkezik, és ezáltal nagyszámban öngyógszerezést is folytatnak. (51,13%). Otthoni gyógyszertartalékaik átlagban 4-5-féle készítményt tartalmaznak.(1. ábra) Magasabb százalékban a lányok és az orvosi kar diákjai rendelkeznek gyógyszerekkel. Jó jelnek számít, hogy nagyon magas (90%) az aránya azoknak, akik elolvassák bevétel előtt a használati utasításokat.

A megkérdezett diákok 300 különféle OTC és vényköteles gyógyszerrel rendelkeztek kereskedelmi nevüket illetően. Gyógyszercsoportra szűkítve ez max 12-féle hatóanyag-csoportot jelent. Leggyakrabban gyulladáscsökkentőket, lázcsillapítókat, fájdalomcsillapítókat, görcsoldókat, vitaminokat, prokinetikumokat, vizeletferttőtlenítő szereket és figyelem-antibiotikumokat használtak öngyógyítás céljából.

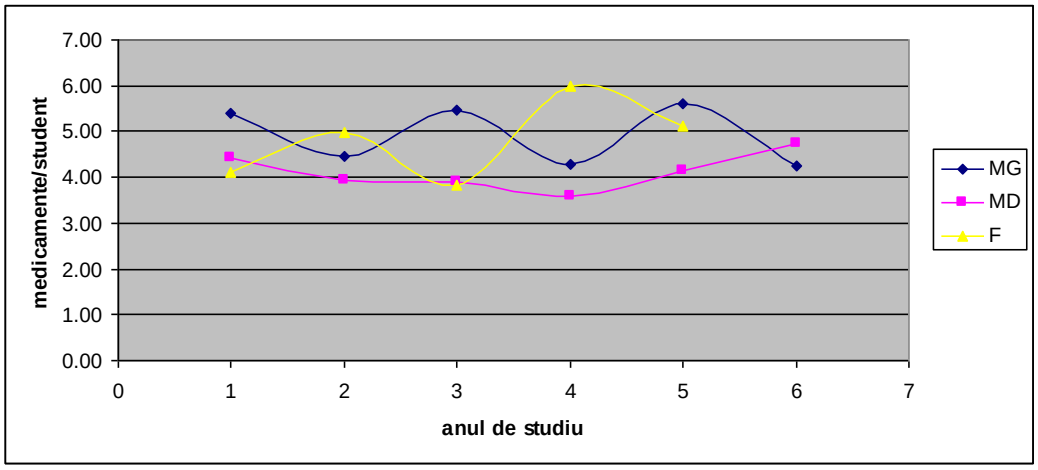

1.ábra Hányféle gyógyszerrel rendelkeznek a tanúlmányi év és szak függvényében (MG-ÁOK,MD-FOK, F-Gy)

A vényköteles antibiotikumokat 22,47%-ban öngyógyító célból használták a hallgatók. Nagyobbrészt a férfiak (27,22%) használtak orvosi előírás nélkül antibiotikumokat és ezek közül is a leggyakrabban penicillinszármazékokat. (2. ábra) A végzős diákok nyúltak öngyógyító antibiotikumokhoz gyakrabban, érdekes módon ez a legmagasabb a fogorvosi kar végzős hallgatói esetében volt. (3.ábra)

Érdekes módon az egyetemi hallgatók gyógyszerszedése a vizsgaidőszakban megsokszorozódott, ez főleg vitaminok és táplálékkiegészítők formájában manifesztálódott. (4.ábra)

A 489 hölgy közül 11,24% szedett fogamzásgátlót 85,45%-ban orvosi konzultáció után.

A tünetek csoportjába tartózó kérdések közül kiemelendő a meghűléses panaszokra közel a hallgatók 10%-a rögtön antibiotikummal indítana, s mindezt öngyóhyító céllal. Ha láz is társul a tünetekhez akkor már majdnem 40%-a gondolja úgy a hallgatóknak hogy a saját gyógyszerdobozából antibiotikumot kell szednie. Ugyancsak nagyon gyakori a kombinált készítmények használata szaktanács és recept nélkül.(50% feletti a használat megfázásos panaszokra).

Említésre méltó a Romániában vényköteles metamizol végzős gyógyszerészhallgatók körében a vény nélküli magas százalékú (60%) használat.
Vizeletfertőzés esetén a hölgy-hallgatók 80%-a semmilyen szakembertől nem kér tanácsot és saját felelősségére antibiotikummal, mégpedig valamilyen floxacin-származékkal kezdi el a kezelést.

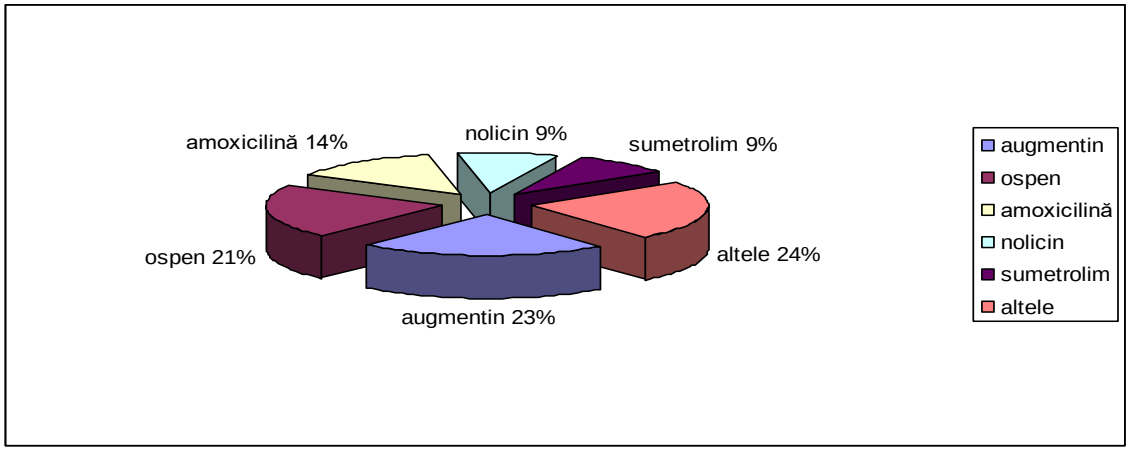

2.ábra A leggyakrabban használt antibiotikumok százalékos megoszlása

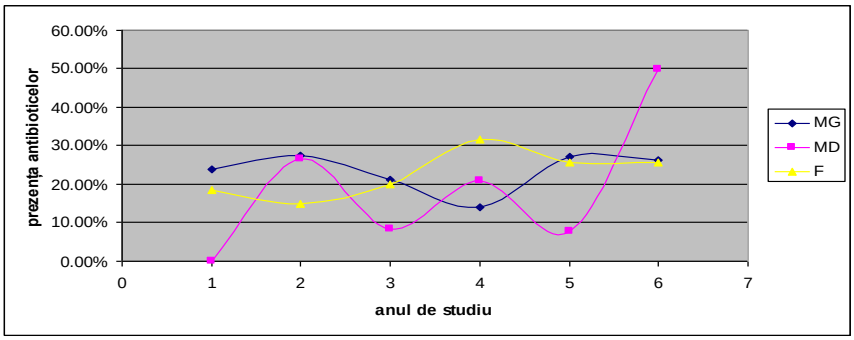

3.ábra A különböző karok antibiotikum használata

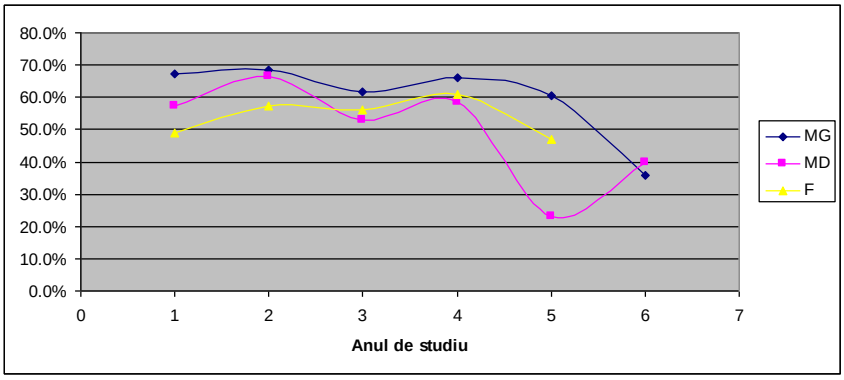

4.ábra Vitaminok és táplálákkiegészítők fogyasztása vizsgaidőszakban

A leggyakrabban a vizsgaidőszakban fellépő gyomorfájásos panaszokra a már vény nélkül is kapható proton-pumpa bénítókat használják mindhárom kar diákjai. A hasmenést és a hányingert is 80% felett saját maguk kezelik.
Megint csak gondolkodásra késztető a stressz, szorongás, illetve nyugtalanság magas százalékú öngyógyító kezelése (70% feletti) 29%/-ban vényköteles szerekkel.(5.ábra)

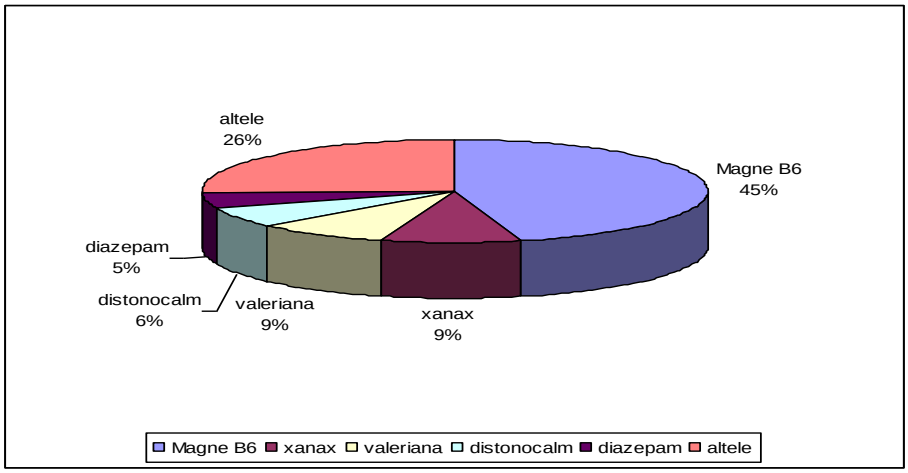

5.ábra Az egyetemi hallgatók stresszoldásra használt gyógyszerei

Konklúziók

Az öngyógyítás egy rég használatos módszer, egy vény nélkül kapható gyógyszeres terápia, melynek azonban korlátai vannak és ennek így is kell lenni.

Egy speciális fiatalokból álló csoportot néztünk, akik a témának tudói lesznek, de most tanulmányaik különböző fokán állnak.

A diákok öngyógyszerezési szokásai nem különböznek nagyban az átlagpopuláció bibliografikus adataitól és nagyon jól korrelál az elmondott panaszokkal.[7] Mégis külön kiemelendő az antibiotikumok és más vényköteles gyógyszerek könnyed használata. Egyrészt a saját gyógyszerdobozukhoz való nyulás következtében, másrészt patikákból való vénynélküli megszerzés révén.

Bibliográfia

[1]EU, Commission Communication 'Safe, innovative and accessible medicines: A Renewed Vision for the Pharmaceutical Sector', http://eur-lex.europa.eu/LexUriServ/LexUriServ.do?uri=COM:2008:0666:FIN:en:PDF. 2008. 5

[2]JF Bretagne, MB Richard, C Honnorat, A Caekaert, P Barthelemy. French national survey of 8000 adults. Presse Med 2006; 35:23-31

[3]A Figueiras, F Caamano, JJ Gestal-Otero. Sociodemografic factors related to self-medication in spain. Eur J Epidemiol 2000;16:19-26

[4]Gy Borjádi, P Juhász: Marketingpirula recept nélkül, Galenus Kiadó, Budapest, 2003. 13-14

[5]E Németh, A Horváth, Cs Major: New challenge in the communication of healing: The increasing effects of advertisments. Psychology & Health 2006, 21:110

[6]PA Emelia, L Richardson-Campbell, L Kennedy-Malone: Self-medication with over-the-counter drugs among elderly adults. Journal of Gerontological Nursing. 2003, 29:8-10

[7]M Wazaify:Societal perspectives on over-the-counter medicines,Fam Practice 2005;22:175

THE DOMINANT WEEDS IN INTENSIVE ORCHARDS

Branka Ljevnaić-Mašić, Slavko Gudurić, Ljiljana Nikolić, Dejana Džigurski, Aleksandra Petrović

Faculty of Agriculture, University of Novi Sad, Trg D. Obradovića 8, 21000 Novi Sad, Serbia
e-mail: brana@polj.uns.ac.rs

Abstract
The main prerequisite for the proper and timely implementation of measures of weed control and their suppression is the knowledge of their basic biological characteristics. Therefore, the aim of this study was floristic and taxonomic analysis, and also analysis of the biological characteristics of the dominant weeds in intensive orchards, which are cultivated according to the principles of conventional agricultural production, around the Irig village (Vojvodina Province, Serbia). It was identified a total of 18 weed species. Classes Magnoliopsida and Liliopsida are preset with 83.33% and 16.67% species, respectively. In the analyzed weed flora were recorded the presence of 16 invasive species for Europe and 4 invasive species for the Vojvodina Province. The largest number of species are weed-ruderal plants (50.00%), followed by ruderal weeds (22.22%).Majority of the analyzed weed species bloomed from June to September. The biological spectrum of the flora indicates the dominance of theropytes (T - 61.10%).

Introduction
Natural conditions in Serbia are extremely favorable for growing fruit [1].Serbia is one of the few countries, that at a relatively small area, has favorable environmental conditions for the cultivation of all continental species of fruit trees [1, 2].Fruits are a food of high nutritional value and significant raw material for different products. Fruit growing also allows a rational use of agricultural land. A larger area under the fruit trees positively influences to the microclimate of the place and prevents soil erosion on slopes.
However, one of the biggest problems in agricultural production is a control of weeds. The weeds in orchards inflict great damage during production. Their presence significantly reduces the yield and impairs the quality of the fruit. In intensive production, the aim is to destroy weeds or at least brought them into the balance with the crop [3].The composition of weeds in orchards is varied making it difficult to correct choice of herbicides for their control.Great influence on the efficiency of most herbicides have climatic factors.Better results are obtained under conditions of higher soil moisture and pre-treated soil [4].The basic prerequisite for the choice of appropriate measures of weed control is the knowledge of the biological and ecological characteristics of weeds [5, 6, 7, 8, 9].Therefore, the aim of this study was floristic and taxonomic analysis, and also analysis of basic biological characteristics of the dominant weed species in the orchards around the Irig village (Vojvodina Province, Serbia), cultivated according to the principles of conventional agriculture.

Experimental
Investigation of weed flora in intensive orchards of plums, peaches and apricots, were carried out during the vegetation period 2013-2014, around the Irig village ((Vojvodina Province, Serbia). Weed species were determined according to standard identification keys[10, 11, 12, 13]. The taxonomic affiliation of species is according to [14]. Characterization of invasive species for Europe and for Vojvodina Province are according to [15]and [16]. The categorization of weeds by habitat type is according to [17], and for a species *Consolida*

regalis Gray according to [18]. Time of flowering is according to [17], and for a species *Consolida regalis* Gray according to [19]. Life forms are according to [20].

Investigation area

Irig village (45°10' 19°86') is located in the north of the Republic of Serbia, in terms of moderate continental climate. Summers are very hot, with a lack of moisture, and winters are long and harsh. Autumn and spring are moderately warm and short [21]. The average air temperature is 10.9 °C.

Results and discussion

In the weed flora of intensive orchards was identified a total of 18 species.All weeds are included into the phylum Magnoliophyta (11 families, 10 orders, 8 superorders, 7 subclasses and 2 classes),Tab. 1. The greatest number of weeds belongs to the class Magnoliopsida (83.33%). The most common are the representatives of the family Asteraceae (27.78%) and Poaceae (16.67%). In the analyzed weed flora were recorded the presence of 16 invasive species for the Europe (88.88%) according to [15]. Four species (22.22%) are invasive for the Vojvodina Province [16]: *Amaranthus retroflexus* L., *Consolida regalis* Gray, *Panicum crus-galli* L. and *Stenactis annua* L. (Tab. 1). Considering on the huge problems that invasive weed species do to grown plants, it is necessary constantly monitoring of their numbers which is very important in order to prevent their uncontrolled proliferation. Special attention must be paid to adventitious and cosmopolitan weeds because their intensive spread makes a big problems on grown plants and native species in general [22].The largest number of weed species belongs to weed-ruderal plants (50.00%), followed by ruderal (22.22%) and segetal weed species (16.67%).The least number of species belong to meadow weeds (11.11%),Tab. 1.Majority of the analyzed weed species bloomed from June (VI) to September (IX), Tab. 1.The longest flowering period has *Capsella bursa-pastoris* (L.) Medik. (IV-XI). The shortest flowering period have *Rubus caesius* L., *Panicum crus-galli* L. and *Calamagrostis epigeios* (L.) Roth.The biological spectrum indicates on the therophytic character of the weed flora (therophytes - 61.10%),Tab. 1.The most abundant are therophytes T_4, i.e. annuals plants which germinate in the Spring, with the maturing at the end of Summer (33.33%). Geophytes (22.22%) and hemicryptophytes (16.67%) are also recorded. Similar results were obtained by [3].The domination of therophytes indicates on instability of weed community due to the intensive agro-technical measures in the investigated agroecosystem[23, 5].

Conclusion

Investigetion of weed flora in intensive orchards around Irig village, cultivated according to the principles of conventional agriculture, it was found a total of 18 weed species. Sixteen species are invasive for Europe and four for Vojvodin Province. All species are included into phylum Magnoliophyta (class Magnoliopsida - 83.33% and class Liliopsida - 16.67%). The most common are the representatives of the family Asteraceae (27.78%).Majority of the analyzed weed species belongs to weed-ruderal plants (50.00%). The greatest number of recorded weed species bloomed from June to September. The study weed flora shows the therophytic character (T - 61.10%) with prevalence of annual plants that germinate in the Spring, with the maturing at the end of Summer (T_4 - 33.33%).

Acknowledgements

This study is part of the project TR31027 titled »Organic agriculture: Improvement of production by use of fertilizers, biopreparates and biological measures" subsidized by the Ministry for Education and Science of the Republic of Serbia.

Table 1. The dominant weed species in intensive orchards with categorization according to the habitat, time of flowering and life forms (Irig village, Serbia)

Phylum	Class	Subclass	Superorder	Order	Familia	Plant species	Categorization according to the habitat	Time of flowering	Life form
Magnoliophyta	**Magnoliopsida**	Ranunculidae	Ranunculanae	Ranunculales	Ranunculaceae	***Consolida regalis* Gray ***	S	V-IX	T_2
				Papaverales	Papaveraceae	*Papaver rhoeas* L. *	S	V-VI	T_2
		Caryophyllidae	Caryophyllanae	Caryophyllales	Amaranthaceae	***Amaranthus retroflexus* L. ***	KR	VI-IX	T_4
					Chenopodiaceae	*Chenopodium album* L. *	KR	VI-XI	T_4
			Polygonanae	Polygonales	Polygonaceae	*Polygonum aviculare* L. *	R, KR	V-X	T_4
		Rosidae	Rosanae	Rosales	Rosaceae	*Rubus caesius* L.	KR	V	H_3
		Asteridae	Asteranae	Asterales	Asteraceae	*Artemisia vulgaris* L. *	R, LK, ŠK	VII-IX	H_5
						Erigeron canadensis L. *	R	VI-X	T_4
						Cirsium arvense (L.) Scop. *	KR	VI-VII	G_3
						***Stenactis annua* L. ***	R	VI-X	T_4
						Taraxacum officinale L. *	KR, LK	IV-IX	H_3
		Dilleniidae	Capparanae	Capparales	Brassicaceae	*Capsella bursa-pastoris* (L.) Medik. *	KR	IV-XI	T_1
						Sinapis arvensis L. *	KR	V-IX	T_3
		Lamiidae	Lamianae	Solanales	Convolvulaceae	*Convolvulus arvensis* L. *	KR	VI-IX	G_3
				Lamiales	Lamiaceae	*Mentha arvensis* L. *	LK, ŠK	VI-IX	G_2
	Liliopsida	Commelinidae	Poanae	Poales	Poaceae	*Bromus commutatus* Schrad. *	KR	V-VI	T_2
						Calamagrostis epigeios (L.) Roth.	LK, ŠK	VII	G_1
						***Panicum crus-galli* L. ***	S	VI	T_4
Σ	**2**	**7**	**8**	**10**	**11**	**18**			

Legend: *- invasive species for the Europe; bold - invasive species for the Vojvodina Province; Legend: KR - weed-ruderal plant; R – ruderal weed; LK – meadow weed; ŠK – forest weed; S – segetal weed; I-XII – month; T – therophyte; G – geophyte; H - hemicryptophyte

References

[1] D. Nikolić, Z. Keserović, N. Magazin, S. Paunović, R. Miletić, M. Nikolić, J. Milivojević. Stanje i perspektive razvoja voćarstva u Srbiji. Zbornik radova i apstrakata XIV Kongresa voćara i vinogradara Srbije sa međunarodnim učešćem. Vrnjačka Banja, Srbija. (2012), 3-22.

[2] Statistički godišnjak Republike Srbije. (2015)(available at: http://webrzs.stat.gov.rs/WebSite/userFiles/file/Aktuelnosti/StatGod2015.pdf)

[3] D. Džigurski, B. Ljevnaić-Mašić, Lj. Nikolić. Dominantni korovi pri organskoj proizvodnji breskve - *Prunus persica* Batsch. (Rosaceae A. L. De Jussieu 1789, Rosales). Zbornik izvoda XXVI Nacionalne konferencije Procesna tehnika i energetika u poljoprivredi - PTEP 2014, 6-11. april 2014, Kladovo, Srbija. (2014), 39-40.

[4] J. Jocković J. Suzbijanje korova u voćnjacima. Bilten Poljoprivredne stručne službe, Šabac. (2010), 1-5.

[5] D. Kovačević. Njivski korovi-biologija i suzbijanje. Poljoprivredni fakultet, Univerzitet u Beogradu. (2008), 1-506.

[6] Lj. Nikolić, D. Džigurski, B. Ljevnaić-Mašić, R. Čabilovski, M. Manojlović. Bulgarian Journal of Agricultural Science. (2011), 17(6), 736-743.

[7] B. Ljevnaić-Mašić, Lj. Nikolić, D. Džigurski. Acta Biologica Jugoslavica, serija G: Acta herbologica. (2012), 21(1), 41-50.

[8] D. Džigurski D., Lj. Nikolić, B. Ljevnaić-Mašić. Journal on Processing and Energy in Agriculture. (2013), 17(3), 130-133.

[9] B. Ljevnaić-Mašić, D. Džigurski, Lj. Nikolić. Journal on Processing and Energy in Agriculture. (2013), 17(1), 33-38.

[10] M. Josifović (ed.). Flora SR Srbije. I-IX, SANU, Beograd. (1970-1977)

[11] M. Sarić (ed.). Flora Srbije. X, SANU, Beograd. (1986)

[12] M. Sarić (ed.). Flora Srbije I. SANU, Beograd. (1992)

[13] S. Jávorka and V. Csapody Icanographie der Flora des Südostlichen Mitteleuropa. Akademiai Kiado, Budapest. (1975)

[14] A. Takhtajan. Flowering Plants. Second Edition. Springer. (2009), 1-906.

[15] DAISIE. Delivering Alien Invasive Species Inventories for Europe.(2016) (available at: http://www.europe-aliens.org/speciesSearch.do)

[16] IASV.Lista invazivnih vrsta na području AP Vojvodine = List of invasive species in AP Vojvodina [Internet]. Version 0.1 beta. Anačkov G, Bjelić-Čabrilo O, Karaman I, Karaman M, Radenković S, Radulović S, Vukov D & Boža P, editors. Department of Biology and Ecology. Novi Sad, Serbia. (2011) (available at: http://iasv.dbe.pmf.uns.ac.rs)

[17] M. Čanak, S. Parabućski, M. Kojić. Ilustrovana korovska flora Jugoslavije. Matica srpska, Novi Sad, Srbija. (1978)

[18] M. Kojić, A. Stanković, M. Čanak. Korovi - biologija i suzbijanje, Institut za zaštitu bilja, Poljoprivredni fakultet, Novi Sad, Srbija. (1972)

[19] J. Kovačević. Korovi u poljoprivredi - Herbicidi. Nakladni zavod Znanje. Zagreb. (1976), 1-750.

[20] M. Ujvárosi. Gymnövények. Mezőgazdasági Kiado, Budapest, Hungary. (1973)

[21] P. Katić, D. Đukanović, P. Đaković. Klima SAP Vojvodine. Poljoprivredni fakultet, Novi Sad, OOUR Institut za ratarstvo i povrtarstvo, Novi Sad. (1979), 1-237.

[22] S. Vrbničanin, B. Karadžić, Z. Dajić-Stevanović. Adventivne i invazivne korovske vrste na području Srbije. Acta Herbologica. (2004), 13(1), 1-12.

[23] M. Kojić, B. Šinžar, R. Stepić. Korovska vegetacija severozapadne Srbije. Zbornik radova Poljoprivrednog fakulteta. (1988), 32-33(589), 83-107.

COMPARATIVE STUDY OF SOME HONEY TYPES COLLECTED FROM UNPOLLUTED AREAS OF TIMIS COUNTY

Velciov Ariana – Bianca, Popescu Georgeta – Sofia, Cozma Antoanela, Riviș Adrian, Bujancă Gabriel

University of Agricultural Sciences and Veterinary Medicine of Banat "King Mihai I of Romania" Timisoara
Faculty of Food Processing Technology Food Science Department 300645, Timisoara, Calea Aradului, nr. 119, Roumania
e-mail:ariana.velciov@yahoo.com

Abstract

This research followed to achieve some physico-chemical properties for natural food based on honey and dried fruits. The honey samples were represented by three 3 different types of bee honey: multiforal and unifloral species - Acacia flower (lat. Robinia pseudoacacia), and Linden flower (lat. Tilia cordata) – bought directly from the producers originally from unpolluted areas in Timis County. In honey samples we added dried fruits: apricots (lat. Prunus armeniaca) and figs (lat. Ficus carica). For these samples, refractive index, water content - based on nD values, total solid content, and acidity were determined.

Based on nd values between 1.4811 – 1.49, the water content shows values from 18.61% and 22.54%, respectively from 81.39%, until 77.46% in case of total solid content, and acidity had values between 2.1 and 3.53 acidity degrees.

The principal purpose of this study was to bring more data to the knowledge of some types of honey originating from unpolluted area of Timis county in terms of physical properties, and also how different additions can contribute to increasing the nutritional value of these products.

Introduction

Honey is a sweet natural food product, obtained by honey bees from sugary solution of nectar flowers[1, 2]. Due to its unique nutritional and medicinal qualities, honey is one of the most widely sought products. These attributes are due to the influence of a large number of substances (about 200) - mainly sugars (glucose and fructose and other types), proteins, minerals, phytochemicals (organic acids, vitamins, enzymes), that provide beneficial properties. Honey composition, aroma, color and flavour depends in a large measure on the climatic conditions but also on the types of flowers [4].

Some unpolluted area from Timis County are well-known as melliferous variety sources, this is why our samples were harvested in those areas.

Recent studies are revealed a growing interest for new food products with an increased nutritional values, so since honey has been used from the ancient times not only as a sweet food product but also as therapeutic agent, because of multiples functional actions, we try to obtain some information in these area.

Nowadays, honey with different addition is considered as a food supplement with bioactive and innovative characteristics. From these foundations, we can consider that honey enriched with small amounts of dried fruits could be taking into consideration as functional food [5].

Experimental

Honey samples

In this study, we used 3different types of unifloral and multifloral honey samples collected from beekeepers from different parts of Timis County.Samplesobtained werestored for 30 days at 22–25°Croom temperatures.

The honey samples with addition of dried fruits were obtained by mixing the three types of honey (Acacia, Linden and multifloral) with dried figs and dried apricots in ratio 1/10 (dried fruits/honey - w/w).

Analytical procedures

Refractive index (nD) values were determined by an Abbe – type refractometer that was first calibrated with doubled distilled water. Measurements were made after the honey was reaching a constant temperature in the refractometer, in triplicate and the average value was taking into consideration for experimental part,

Water content (moisture) of the honey samples were calculated from index values by using the expression developed by Abu-Jdayil et al., [6, 7].

$$\%Water = 608.277 - 395.743 \cdot nD$$

Total solid content (TSC) can be determined from moisture content as below:

$$\text{Total solids / Dry matter} = 100 - \%\ \text{Moisture}$$

The method for determination of acidity was by titration with NaOH 0,1 N in the presence of phenolphtalein [8]. The results were expressed in acidity degrees.

All determinations were performed in triplicate, calculating their arithmetic mean of three separate determinations. The data were statistically analyzed using the program Microsoft Excel.

Results and discussion

The obtained data regarding water content in honey samples with addition of dried apricots and figs according to refractive index (nD) are represented in fig. 1.

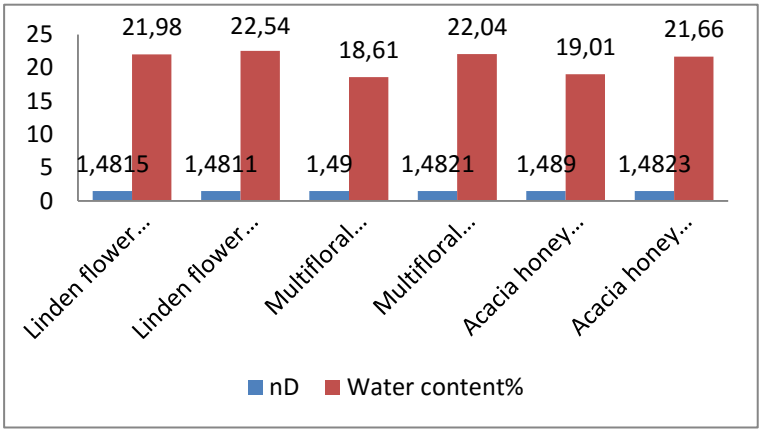

Fig. 1 Refractive index (nD) and water content (%), in honey samples with addition of dried fruits

Refractive indexes of honey samples were between 1.4811 (Linden flower honey with dried apricots) and 1.49 (Multifloral honey with dried figs).
Water content is a parameter related to the maturity of honey and temperature. In the present study water content values are between 18.61% and 22.54%. Except for two samples – multifloral honey with dried figs and acacia honey with dried figs, all the other four samples were having water content values higher than values allowed by European Community regulations [9].
Water content is a quality parameter, important for honey shelf life. The different values in water content are depending on the season in regions with high relative humidity, physical properties of honey, but also could be modified during honey processing [10].
In fig. 2 we are presenting total solid content (TSC) values.

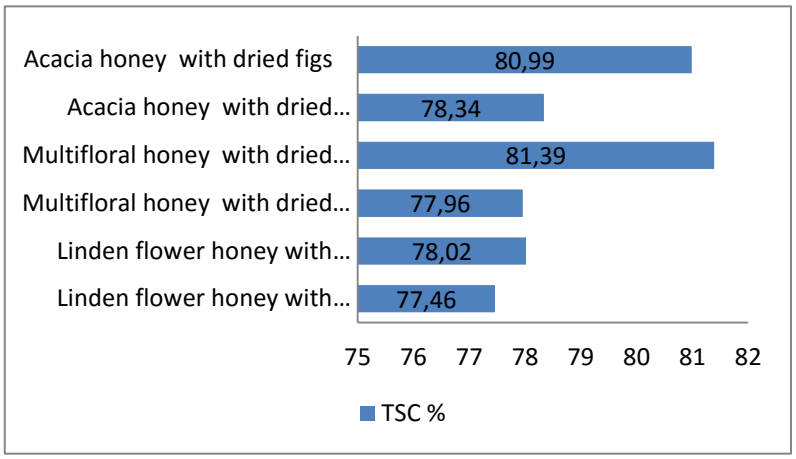

Fig. 2 Total solid content (TSC) % in honey samples with dried fruits

From the analysed data presented above, we can observe that the highest value of the total solid content was found in multifloral honey with dried figs, – 81.39%, and the lowest value were found in linden flower honey with dried apricots – 77.46%.
Determination of acidity (°),in honey samples with addition of dried fruits are presented in Fig. 3.

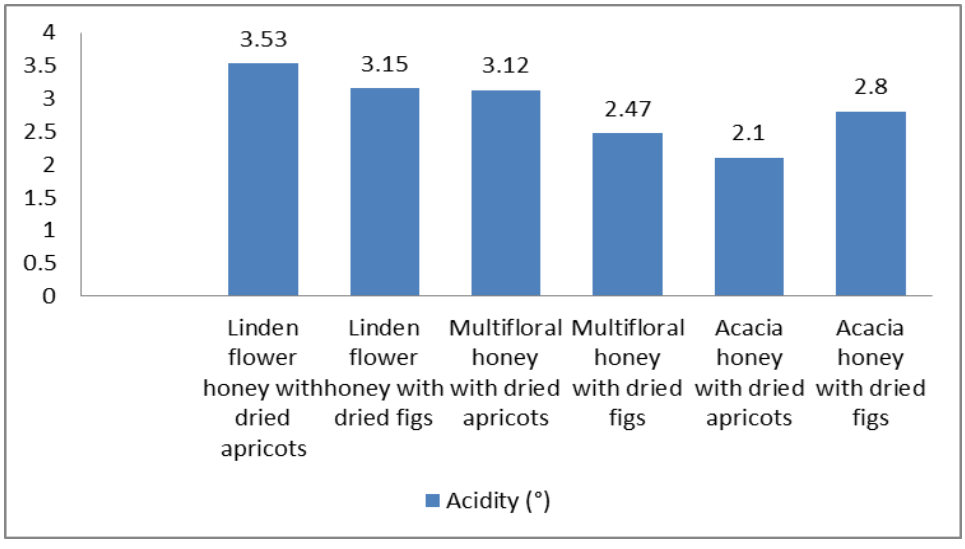

Fig. 3 Acidity degreesin honey samples with dried fruits

The acidity (low pH) contributes to antimicrobial activity of honey [11]. The values of acidity were between 2.1 – 3.53 acidity degrees (in acacia honey with dried apricots respectively in linden flower honey with dried apricots).

Conclusions

Recently, much interest in the health benefits of dried fruits used as admixtures to different types of honey has been revealed. The physical properties of three types of honey samples originating from Banat County, in which we added dried figs and apricotswere determined and used to evaluate their behavior.

The antimicrobial properties of honey may be attributed to the low acidity values, and the percentage water content can be an important parameter used to access quality of honey samples.

The obtained data could be used for future research because of results that are suggesting that honeys enriched with small amounts of dried fruits could be potential functional foods.

References

[1] Missio da Silva P., Gauche C., Gonzaga L.V., Costa A.C.O. – Honey, Chemical composition, stability and authenticity, Food Chemistry, 196, (2016), 309-323;

[2] White J. W. – Composition of honey in E. Crane (Ed.), Honey, a comprehensive survey (Vol. 5, pp. 157-206), London, UK, Heinemann.

[3] Chakir A., Abderrahmane R., Marcazzan G.L., Ferazzi P. – Physicochemical properties of some honeys produced from different plants in Morocco, *Arabian Journal of Chemistry*, 2011, doi: 10.1016/j.rabic.2011.10.013;

[4] Escuredo O., Miguez M., Fernández – González M., Seijo M.C. – Nutricional value and antioxidant activity oh honeys produced in a European Atlantic area, Food Chemistry, 138, (2013), 851-856;

[5] Osés S.M., Pascual – Maté A., Fernández – Muiño M.A., López – Díaz T.M., Sancho M.T. – Bioactive properties of honey with propolis, Food Chemistry 196, (2016), 1215-1223;

[6] Abu – Jdayil B., Abd Al – Majeed G., Al – Malah K.I., Dhahera Z. – Heat effect on rheology of Light – and dark – colored honey, J. Food Engr., 51 (1), (2002), 33-38;

[7]James O.O., Mesubi M.A., Usman L.A., Yeye S.O., Ajanaku K.O., Ogunniran K.O., Ajani O.O., Siyanbola T.O. – Physical characterization of some honey samples from North-Central Nigeria, *International Journal of Physical Sciences*, 2009, 4(9), 464-470;

[8]Bogdanov S. – Harmonized methods of the European Honey Commission, International Honey Commission, 2002;

[9]*** The Council of the European Union, 2002 – Council Directive 2001/110/EC of 20 December 2001 relating to honey. Official Journal of the European Communities 72, 37-47;

[10] Bogdanov S., Ruoff K., Persano Oddo L. – Physico – chemical methods for the characterization of unifloral honeys: a review, Apidologie, 35 (2004), S4-S17;

[11] Moldovan C., Raba D., Dumbravă D.,Popa M., Drugă M.- Sensorial and physicochemical properties of some honey with various natural admixtures, pp. 545 -552 *in Nano, Bio and Green-Technologies for a Sustainable Future*, Conference Proceedings, 15th International Multidisciplinary Scientific Geoconf SGEM 2015, Albena 2015, Bulgaria;

[12] Velciov A.B., Riviş A., Costescu C.I., Pintilie G.S., Jidic A.M. - Physico-chemical evaluation of honey fortified with oleaginous seeds, *Bulletin UASVM Food Science and Technology*, 2014, 71(2), 213-214, ISSN-L 2344-2344.

PRELIMINARY *IN SILICO* INVESTIGATION OF COX 2 SELECTIVE INHIBITORS[1]

Luminita Crisan, Liliana Pacureanu

Department of Computational Chemistry, Institute of Chemistry of Romanian Academy, Timişoara, Mihai Viteazul Avenue, 24, 300223 Timişoara, Romania
pacureanu@acad-icht.tm.edu.ro

Abstract
We report herein an attempt to generate QSAR models for a large number of structurally diverse compounds (1078 compounds) whose affinities for cyclooxygenase-1 (COX-1) and cyclooxygenase-2 (COX-2) were experimentally determined. Initially, individual QSAR models for COX-1 (M1) and COX-2 (M2) for biological activity were developed. A selectivity QSAR model, M3 was then developed using as dependent variable Y the differences in pIC50 values between COX-1 and COX-2. The statistical results for all three models showed a satisfactory to good statistical parameters where the values for squared correlation coefficient (coefficient of determination) for the training set are: M1: 0.872, M2: 0.797 respectively M3: 0.739. The predicted values of affinity in the case of all three models selected M1, M2 and respectively M3, are very good 84.88%, 91.12%, 79.59% which lead to very small diffrences between observed and predicted biological activity/selectivity (less than 0.5 logarithimic units).

Keywords: COX-1, COX-2, QSAR

Introduction
Prostaglandin synthesis is promoted by the cyclooxygenase (COX), which during the '90 it was discovered that this enzyme exist in two isoforms: COX-1 which is responsible for protection of kidney and maintenance of gastric mucosal integrity function whereas COX-2 is implicated in the pathophysiological reactions including inflammation and pain[1]. Nonsteroidal anti-inflammatory drugs (NSAIDs) are the most frequently used drugs to treat pain, inflammation and cancers [2]. Cyclooxygenase inhibitors have been divided over time in (1) nonselective inhibitors, which shows a similar affinity for both COX-1 and COX-2, i.e. aspirin which block irreversibly the enzyme by acetylation of Ser530, (2) nonselective acting as competitive with arachidonic acid, i.e. diclofenac, indomethacin, ketoprofen, naproxen, ibuprofen, phenylbutazone, and meclofenamate [3], (3) nonselective, which inhibit preferentially COX-2, i.e. etodolac, meloxicam, nabumetone and nimesulide. Side effects resulting from the use of these inhibitors in the treatment of various diseases can lead to severe complications and increased costs of their relief [3]. In last years, it was demonstrated that COX-1 isoform, but not COX-2, is over-expressed in diverse human pathologies (ovarian, skin and colon cancer as well as in other cancer types) [4]. Thus, finding new drugs that are selective COX-2 and not inhibit COX-1 is a widely investigated topic which attracts a great interest nowadays. The present work reports the attempt to address the phenomenon of selectivity of COX-2 inhibitors by generating robust and predictive QSAR models for a large set of compounds in order to reliably predict novel selective COX-2 inhibitors.

[1] Dedicated to the 150th anniversary of the Romanian Academy

Material and Methods

Dataset selection and preparation

A number of 5900 inhibitors of cyclooxygenase-2 (COX-2; Assay ID: CHEMBL230) and 3763 inhibitors of cyclooxygenase-1 (COX-1; Assay ID: CHEMBL221) were downloaded from ChEMBL database [5]. 1145 Compounds were selected which have experimental activities for both enzymes COX-1 and COX-2. All these molecules were filtered using *BlockBuster software* available in FILTER module [6-13] from OpenEye package. Totally, 1078 compounds passed the filter criteria (HBA=0÷13, HBD=0÷9, MW=130÷781, RBN=0÷16, XLogP=-3.0÷6.85, 2dPSA=0÷205) and were used further in the QSAR analysis. The experimental activity for both protein is expressed in IC50 (nM) and for QSAR modeling it was transformed into negative logarithm of inhibitory concentrations, pIC50, and used later as a dependent variable. In order to obtain a selectivity QSAR model the Y values were obtained by taking the differences between pIC50 measured against COX-2 and COX-1. The LigPrep module [14] and ConfGen [15] from Schrödinger package [16] were used to generate the tautomers and ionization states in the pH range of 7.2±0.2, and conformational sampling.

QSAR models generation

QSAR modeling was performed with AutoQSAR module from Schrödinger package [15]. The QSAR models are constructed using different machine learning algorithms and multiple automatically generated random training and test sets. As function of the quality of QSAR models on the training and test sets, a score rank have been implemented. The predicitivity performance of AutoQSAR generated models is close or better than previously published results but show the advantage of reduced time, costs and expertise.

For each individual QSAR model generated (M1 for COX1, M2 for COX2, and M3 for selectivity, modeling the difference between pIC_{50}COX-2– pIC_{50}COX-1, as dependent variable) multiple QSAR models were generated using different methods. These models are ranked based on high values of the statistics parameters fortraining and test set and the best ten models are listed.

Results and discussion

Linear regression models were built using 809 (75%) compounds in training set and 269 compounds in test set (25%). The independent variable matrix X contain binary fingerprints descriptors (radial, linear, dendritic, molprint2D) and canvasMolDescriptors, whereas the Y matrix contained experimental values for COX-2 affinity for the model M1, experimental affinities for COX-1 in the case of model M2 and the selectivity values for COX2 for M3 model. For each case ten models were generate and the best one was selected (see Table1 and Figures1, 2, 3).

Table1. Statistical results for the best linear QSAR models

	M1	M2	M3
# *	5	5	5
R^2	0.872	0.797	0.739
SD	0.461	0.464	0.689
Q^2	0.675	0.738	0.729
RMSE	0.705	0.685	0.841

* # = The number of PLS factors used in the partial least squares regression model; R^2 = R-squared value for the coefficient of determination for the training set; SD = Standard deviation of the model; Q^2 = the squared value of the regression coefficient for the test set;RMSE = Root-mean-square error for the test set predictions.

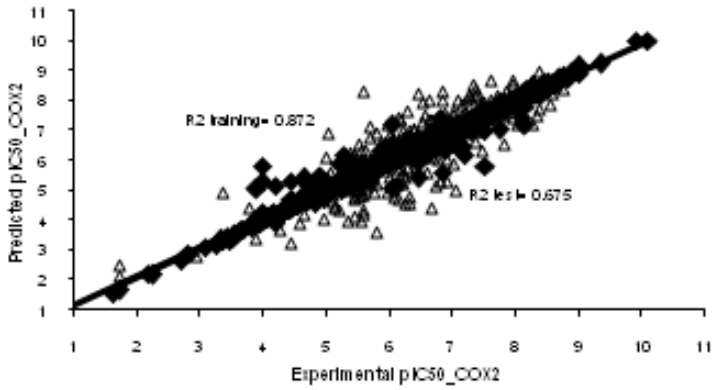

Figure 1. Plot of experimental versus predicted pIC_{50} values for model M1 (black squares – training setcompounds, white triangles – test compounds)

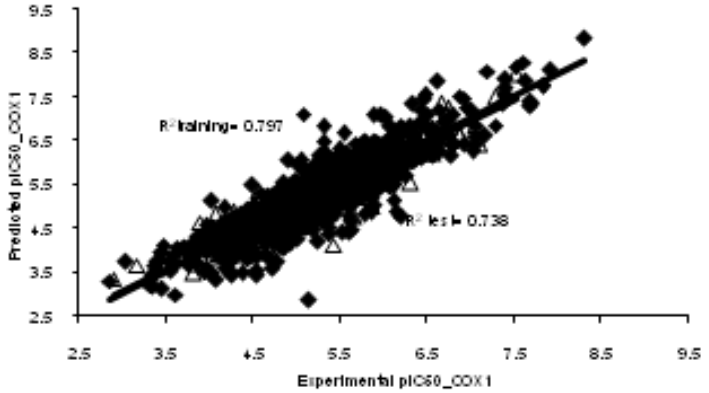

Figure 2. Plot of experimental versus predicted pIC_{50} values for model M2 (black squares – training compounds, white triangles – test compounds)

.

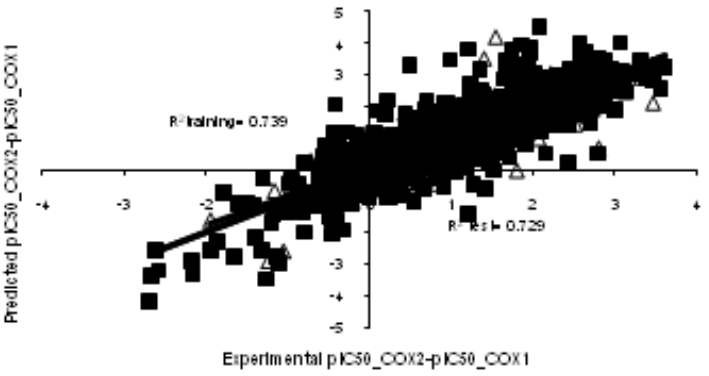

Figure 3. Plot of experimental versus predicted pIC_{50} values for model M3 (black squares – training compounds, white triangles – test compounds)

The best statistical results were obtained for the PLS model M1 while the best predictive power we observed in the case of the PLS models M2 and M3 models. The predicted values of affinity/selectivity of all QSAR models are very good: 84.88%, 91.12%, and 79.59% of inhibitors of the M1, M2 and respectively M3 models are predicted very well with a diffrence smaller than 0.5 logarithimic units between observed and predicted biologiocal activity/selectivity.

Conclusions

A set of structurally diverse 1078 compounds downloaded from ChEMBL have been engaged to develop quantitative structure - activity, respectively selectivity QSAR models to correlate the structural features with the affinity/selectivity against COX-2 enzyme. The statistical performances of the QSAR models are reasonably satisfactory. The correlation coefficient (R^2) is higher than 0.800 for model M1 and higher than 0.700 for models M2 and M3.

Acknowledgements

This project was financially supported by Project 1.2 of the Institute of Chemistry of the Romanian Academy. Access to the OpenEye Ltd. software are greatly acknowledged by the authors.

References

[1] W.L. Smith, D.L. Dewitt, Adv. Immunol. 62 (1996) 167.
[2] A.R. Chopade, F.J. Sayyad, N.S. Naikwade, 1st ed. LAP Lambert Academic Publishing; 2011.
[3] D. L. Simmons, R. M. Botting, T. Hla, Pharmacol. Rev. 56 (2004) 387.
[4] M.G. Perrone, P. Malerba, J. Uddin, P. Vitale, A. Panella, B.C. Crews, C.K. Daniel, K. Ghebreselasie, M. Nickels, M.N. Tantawy, H.C. Manning, L.J. Marnett, A. Scilimati, Eur. J. Med. Chem. 80 (2014) 562.
[5] A.P. Bento, A. Gaulton, A. Hersey, L.J. Bellis, J. Chambers, M. Davies, F. Krüger, Y. Light, L. Mak, S. McGlinchey, M. Nowotka, G. Papadatos, R. Santos, J. P. Overington, Nucleic Acids Res.42 (2014) D1083.
[6] R. Wang, F. Ying, L. Lai, J. Chem. Inf. Comput. Sci. 37 (1997) 615.
[7] P. Ertl, B. Rohde, P. Selzer, J. Med. Chem.43 (2000) 3714.
[8] C. A. Lipinski, F. Lombardo, B. W. Dominy, P. J. Feeney, Adv Drug Deliv Rev23 (1997) 3.
[9] W. J. Egan, K. M. Merz, J. J. Baldwin, J. Med. Chem.43(2000) 3867.
[10] D. F. Veber, S. R. Johnson, H. Y. Cheng, B. R. Smith, K. W. Ward, K. D. Kipple,J. Med. Chem.45 (2002) 2615.
[11] Y. C. Martin, J. Med. Chem.48 (2005) 3164.
[12] T. Fawcett, Pattern Recognit. Lett. 27 (2006) 861.
[13] FILTER version 2.0.2: OpenEye Scientific Software, Santa Fe, NM. www.eyesopen.com.
[14] LigPrep, version 3.9, Schrödinger, LLC, New York, NY, 2016.
[15]ConfGen, version 3.7, Schrödinger, LLC, New York, NY, 2016.
[16] Schrödinger, LLC, New York, NY, 2016-3.

ACCUMULATION OF CADMIUM IN THE GRAIN OF DIFFERENT CULTIVARS OF WHEAT

Ivana Maksimović[1], Marina Putnik-Delić[1], Vojislava Momčilović[2], Srbislav Denčić[2], Imre Kádár[3], Rudolf Kastori[1]

[1]University of Novi Sad, Faculty of Agriculture, Trg Dositeja Obradovića 8, Novi Sad, Serbia
[2]Institute of Field and Vegetable Crops, Maksima Gorkog, 30, Novi Sad, Serbia
[3]Research Institute for Soil Science and Agricultural Chemistry of the Hungarian Academy of Sciences, Herman Ottó ú. 15. Budapest, Hungary
e-mail: ivanam@polj.uns.ac.rs

Abstract
Cadmium (Cd) is in higher concentrations toxic for all living organisms. Therefore, the knowledge on the accumulation of Cd in edible parts of plants is important for health. Genotypes of different crops may differ significantly with respect to accumulation of Cd. Hence, the aim of this research was to assess its accumulation in the grains of genetically diverse wheat genotypes, originating from different parts of the world. In two years, average concentration of Cd ranged from 0.0270 to 0.0403 mg/kg DM and it was significantly below the toxic level. The highest concentration of Cd was recorded in cultivar Bezostaja 1, while the other genotypes differed only slightly in accumulation of Cd in the grain.

Introduction
Many organic and inorganic substances contribute to environmental pollution. Amongst them, heavy metals play important role. The most abundant antropogenic sources of soil pollution by Cd are transport vehicles, mines, ore smelters, metal industry, municipal solid and liquid wastes and others. Significant pollutants of arable land may also be phosphoric fertilizers, application of Cd-laden sludge, and to a lesser extent, manure, compost and atmospheric precipitates.
Cadmium, similarly to the other heavy metals, is in higher concentrations toxic to all living organisms, including plants (Kastori et al., 1997), soil microorganisms, humans and animals (Vapa and Vapa, 1997). Therefore, prevention of pollution by Cd and prevention of its entry into the food chain has a remarkable significance for the environment and health.
The accumulation of mineral substances in plants and their organs depends on genetic background, environmental conditions and the interaction of genotype and environment. Plant species differ in their abilities to uptake, accumulate and transport various mineral elements to different organs, as well as by their sensitivity to deficiency or excess of mineral substances. Differences exist also between genotypes and lines (Clark, 1983). Considering the large global importance of wheat production in the diet of the human population and partly of domesticated animals, as well as the toxicity of Cd, we felt justified to examine the variability of Cd accumulation in the grain of different genotypes of wheat grown in the same environmental conditions.

Material and methods
Eight genotypes of wheat, originating from different parts of the world, were used in the experiment, which was conducted at the experiment field of the Institute of Field and Vegetable Crops in Novi Sad, in 2011 and 2013.

The soil at the experimental field was classified as a calcic, gleyic chernozem (Loamic, Pachic – CH-cc.gl-Ip.ph (IUSS Working Group WRB, 2015)). Concentration of Cd in the soil was significantly lower than the maximally allowed (2 mg/kg) and even lower from the usual concentration of Cd (0.2 to 1 mg/kg) (Tab. 1). Monthly mean air temperature during vegetation in 2010/11 was 8.5 °C, and in 2012/13 it was 9.9 °C. Sum of average day temperatures was slightly higher in 2012/13. Higher amount of precipitation during 2012/2013 than 2010/2011 (591 and 388 mm, respectively), significantly affected average wheat yield at the experimental field and in the entire region of Vojvodina. In 2011 average wheat yield was 4.88 whereas in 2013 it was 5.91 t/ha.

Table 1. Cadmium concentration in different horizons of the soil profile at the experimental site(mg/kg)

		Ekstraction agent	
Horizon	Depth (cm)	[1]EDTA	[2]HNO_3
Ap	0-20	0.206	0.703
A	20-35	0.208	0.753
AC	35-117	0.088	0.773
CG	117-195	0.084	0.777

Form: [1] - soluble; [2] - total

The genotypes were harvested at crop maturity. After digestion of grain wholemeal in a mixture of 10 ml HNO_3 (65%) and 2 ml of H_2O_2 (30%) using the microwave technique, the concentrations of total Cd were determined by inductive coupled plasma emission spectrometer, in Research Institute for Soil Science and Agricultural Chemistry of the Hungarian Academy of Sciences, Budapest. Statistical analyses were done with program XLSTAT- Pro (demo version, Version 03.02.2009).

Results and discussion

Concentration of Cd in examined wheat genotypes in two experimental years ranged from 0.0270 to 0.0403 mg/kg DM (Tab. 2).

Table2. Cadmium concentration in grains of eight wheat cultivars(mg/kgDM)

Wheat cultivars	**Origin**	**Years**		**Average**
		2011	**2013**	
Panonnia	SRB	0.0375^{cd}	0.0201^{e}	0.0288^{b}
Bankut 1205	HUN	0.0420^{bcd}	0.0202^{e}	0.0311^{b}
Bezostoja 1	RUS	0.0605^{a}	0.0201^{e}	0.0403^{a}
Siete Cerros	MEX	0.0440^{bc}	0.0180^{e}	0.0310^{b}
Florida	USA	0.0340^{d}	0.0200^{e}	0.0270^{b}
Renan	FRA	0.0332^{d}	0.0225^{e}	0.0278^{b}
Condor	AUT	0.0475^{b}	0.0195^{e}	0.0335^{b}
Bolal	TUR	0.0395^{bcd}	0.0200^{e}	0.0298^{b}
Mean		0.0423^{a}	0.0201^{b}	0.0312
Min		0.0332	0.0180	0.0270
Max		0.0605	0.0225	0.0403
Standard deviation		0.0082	0.0011	0.0039
Variation coefficient (%)		19.51	5.73	12.67
Standard error		0.0031	0.0004	0.0015

Means with a common letter are not significantly different ($p > 0.05$)

In Bezostaja 1 concentration of Cd was significantly the highest, whereas the other genotypes differed insignificantly with respect to Cd (Tab 2, Fig 1). The difference in concentration of Cd in wheat grains was not higher than about 1.5 times within each year. At least in part, this may be explained by the fact that vegetative plant parts of a species (and genotype) in general differ in their chemical composition to a greater extent than generative parts. Measured concentrations of Cd are in line with concentrations of Cd found in wheat grown in different parts of the world (Kabta-Pendias and Pendias, 2000). The difference in Cd concentration in grains between two experimental years was statistically significant. In average, in dry 2011 concentration of Cd was much higher than in humid 2013 (0.0423 and 0.0201 mg/kg DM, respectively). Minimum and maximum concentrations in 2011 were also much higher than in 2013 (Tab. 2).
According to the literature, wheat grain formed in humid years contains less nutritive and other elements than in dry years. Moreover, soil humidity affects differently concentration of nutrients in particular plant parts (Kastori, 1981), which may be the consequence of higher yield and therefore so-called biological "dilution" effect. Indeed, Bogdevitch and Mikulich (2008) explain by dilution effect lower concentration of radionucleides found in wheat grain of high yield.

Table 3. Analysis of variance of Cd concentration in wheat grains

Source	df	SS	MS	F-count	F-table		P-value
					0.05	0.01	
Rep*Y	4	0.050	0.012	0.39^{ns}	2.71	4.07	0.8112
Year (Y)	1	0.006	0.006	476.34^{**}	4.20	7.64	0.0000
Cultivar (C)	7	0.748	0.107	0.82^{**}	2.36	3.36	0.0096
C*Y	7	0.917	0.131	4.15^{**}	2.36	3.36	0.0030
Error	28	0.884	0.032				

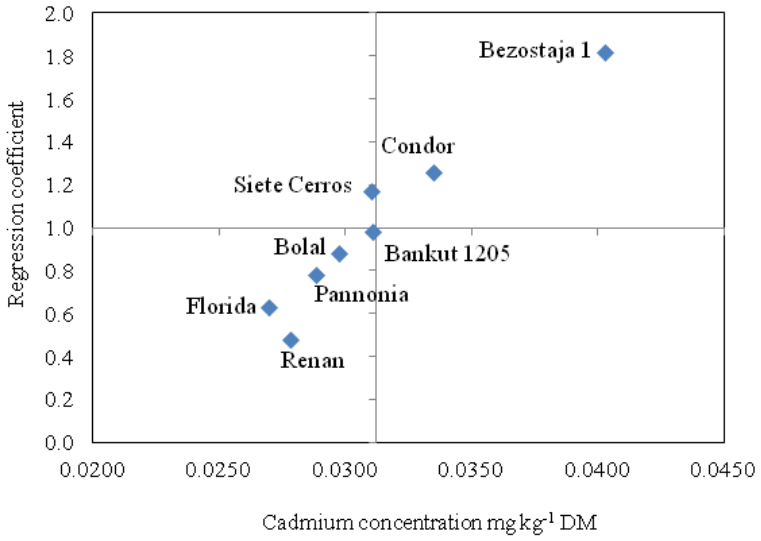

Figure 1. Relation between Cd concentrations in grains of wheat cultivars and the Finlay and Wilkinson's b regression coefficient

There is a close correlation between Cd concentration in the soil and in the grain of wheat (Hornburg and Brümmer, 1986), indicating its good upward mobility in plants (Verkleij and Schat, 1990). The concentrations of Cd in the grain of tested wheat genotypes were significantly

below the allowed maximum concentration (0.5 mg/kg DM). This can be explained by a low concentration of soluble Cd with respect to total Cd in the soil (Tab. 1) and low transport rate of Cd from vegetative to generative organs in plants, which was recorded even on soils heavily contaminated with Cd (Leita et al., 1996).

Conclusion

Concentration of Cd in the grain of wheat genotypes of various origin, in temperate continental climate conditions, on calcic, gleyic chernozem soil, that contained low concentration of Cd, in two years, ranged in average from 0.0270 to 0.0403 mg/kg DM. Significantly the highest concentration of Cd was found in the grain of Bezostaja 1. Among the other seven genotypes concentration of Cd in the grain was not statistically different. It can be concluded that genotypes originating from different parts of the world differed only slightly in the accumulation of Cd in the grain and that concentrations of Cd in the grain in all tested genotypes were significantly below toxic levels.

References

[1] I. Bogdevitch, V. Mikulich, Yield and quality of spring wheat grain related to P status of luvisol loamy sand soil and fertilization. Zemes Ukio Mokslai. 15 (2008) 47-54.
[2] R. B. Clark, Plant genotype differences in uptake, translocation, accumulation and use of mineral elements required for plant growth. Plant Soil 72 (1983) 175-196.
[3] V. Hornburg, G. W. Brümmer, Cadmium availability in soil and content of wheat grain. In: Anke, M. et al. (eds.) 5thSpurenelement Symposium on Iodine and other Trace Elements. F. Schiller University, Jena, (1986) 916-921.
[4] IUSS Working Group WRB (2015): World Reference Base for Soil Resources 2014, update 2015, International soil classification system for naming soils and creating legends for soil maps. World Soil Resources Reports No. 106: FAO, Rome.
[5] A. Kabata-Pendias, H. Kabata, Trace Elements in Soils and Plants. CRC Press, Boca Raton, Florida, (2000).
[6] R. Kastori, N. Petrović, I. Arsenijević-Maksimović, Heavy metals and plants. In: Kastori, R. (ed.) Heavy Metals in the Environment. Naučni institut za ratarstvo i povrtarstvo, Novi Sad, (1997) 197-257. (in Serbian).
[7] R. Kastori, Content and distribution of biogenic elements in wheat. In. Belić, J. (ed.) Physiology of Wheat. Serbian Academy of Sciences and Arts, Vol. DXXXVI (1981) 80-101. (in Serbian)
[8] L. Leita, M. de Nobili, S. Cesco, Analysis of intercellular cadmium forms in roots and leaves of bush bean. J. Plant Nutr. 19 (1996) 527-533.
[9] M. Vapa, Lj. Vapa, Heavy metals and animals. In: Kastori, R. (ed.) Heavy Metals in the Environment. Naučni institut za ratsrtvo i povrtarstvo, Novi Sad, (1997) 261- 301. (in Serbian).
[10] J. A. C. Verkleij, H. Schat, Mechanisms of metal tolerance in higher plants. In: Shaw, A. J. (ed.) Heavy matal tolerance in plants – Evolutionary aspects. CRC Press Inc. Boca Raton, Florida, (1990) 179-193.

Cd ACCUMULATION IN *PARMELIA SPP.* SPECIES

Masu Smaranda[1], Amalia Raluca Dumbrava[2]

[1]National R & D Institute for Industrial Ecology, ECOIND,
Branch of Timisoara, 300004, 1 Regina Maria Square, Timisoara, Romania
[2]Administration of Natural Park Portile de Fier, 90 Banat street, Orsova, Romania
e-mail: andamasu@yahoo.com

Abstract
Lichens are a group of organisms with a large geographical spread. They live permanently with their surrounding environment. They show a great sensitivity to the composition and concentrations of the substances found in the environment.The concentration of metals in the environment can dramatically affect the lichens' health. The aim of this study was to determine the degree of bioaccumulation of Cd in the tissue of the *Parmelia spp.* species of lichens from synthetic aqueous environments with different concentrations of Cd between 20-50 $mg \cdot L^{-1}$.The study was conducted in the laboratory on samples of lichen the acacia support. The lichens originatefrom a Natural Reservation in the South-West of Romania. The bio-accumulation of Cd was tracked over a period of 16 weeks of exposing the lichens to pollution with synthetic solutionsat pH =3.5, simulating acid rain. The lichens have bio-accumulated amounts of Cd between 4,0-4.9$mg \cdot kg^{-1}$D.M. The studies on the lichens metal bioavailability could further enhance their utility as environmental bio-prospections and for air quality biomonitoring tools.

Introduction
In 1867 Schwendener announced to the scientific world his hypothesis that lichen was formed by two separate organisms, a fungus and an algae. It was later reported that lichens are symbiotic association between the algae *Cianobacteriae* or *Chlorophyceae* and *Ascomiycetes* fungus, or in rare occasions with *Basidiomycetes or Pycomycetes* fungus.Algae provides nutrients and the fungus provide water and minerals. Lichens are spread out all over the globe: trees, bushes, rocks, walls, rots, etc. Lichens were designated as species with high potential for environmental monitoring characteristics modifications 1-4]. The basis of this consideration are the following aspects: long life, slow growth and ability to accumulate certain pollutants in ambient air, in wet and dry deposition [5]. Lichens differ in their sensitivity to various substances in the environment. Was noted that lichens are relatively resistant to metal pollution [6].Lichens in areas with low rainfall, which obtain most of their water from fog and dew, are particularly vulnerable to air quality and weather pattern changes[7].Fog, which often increases with increasing elevation, contains higher levels of dissolved ions, including H^+, than precipitation rain or snow. Although the effects of occult deposition from fog on lichen communities have not yet been critically examined, acid fog has been implicated in changes to cryptogamic plants [8].According to recent studies, lichens are the best indicators for low and moderate bioaccumulation of metals in industrial and urban areas. Metal content in lichens were correlated with the level of annual air pollution.Considering the previous reports in the literature [1, 6-7], the current study evaluates the bioaccumulation of cadmiumin a artificial polluted environment.Cd is a component of fly-ash and presumably travels long distances in the atmosphere; its presence can be correlated with power plants, industrial centers, etc. [7].Higher metal concentrations were recorded in the higher rainfall autumn season compared with spring for most metals. An inter-species comparison of several hundred measurements confirmed the

higher affinity of *Parmelia spp*. for Cd.In order to improve data quality inbio-prospectionsandbiomonitoring environmental, it is suggested to analyses lichens tissue and the introduction species like *Parmelia spp.* in monitoring the presence or absence of Cd in air [9-10].

Experimental

Experimental study aim to evaluate the ability of lichens to incorporate metals in case of exposure to acidic synthetic solutions. The studied lichens were *Parmelia spp.*Lichens have been taken with acacia wood support from a Natural Reservation in the South-West of Romania. Lichens were placed in three beakers and have been sprayed periodically with nutrient solutions and polluting synthetic solutions. Nutritional solutions contain sodium acetate, urea and dipotassium hydrogen phosphate. Polluting synthetic solutions having pH=3.5 contain cadmium in concentrations of 2.0-5.0mg $\cdot L^{-1}$. The experiment lasted 16 weeks. The structure of the experiment is shown in Table 1.

Table 1 Polluting solution characteristics and the experiment structure

Polluting synthetic solution characteristics	Experiment's variants		
	P 1	P 2	P 3
Type	s 1	s 2	s 3
pH simulating acid rain	3.5	3.5	3.5
Cd content [mg·L^{-1}]	2.0	4.0	5.0

The metal content of lichens samples was analyzed before and after experiment. Lichens were separated by wooden cuticle and were washed twice with double distilled water. Then, the lichens were dried for 3 days at room temperature. It was weighed an amount of 1.2 g lichens and was kept at a constant temperature (60°C) to constant weight (3-4 hours).Then the tissue was hand-milled to homogenize. It was weighed amount 0.25-0.50g of powder, then acclaimed at 550°C for 90 min. The resulting ash was dissolved on the sand bath using a mixture of 5:1 hydrochloric acid (37% Merck, Germany) and HNO_3 (69% Merck Germany) The solid residue was taken up in 3ml HCl 1: 1 and filtered through Sartorius filter papers 2-206 FT.The crucible was washed 3 times with 3 ml of HCl 1:1. The washing solutions were filtered. All the resulting solutions were transferred into flasks of 25 ml and bring to volume with HCl 1: 1. Metals analyses were performed with an AAS spectrometer type Avanta.The certified reference material BCR 482 lichen (IRMM) Geel Belgium was used to validate the analytical determinations.Determination of metals in wood support of lichens was similarly analyzed.

Results and discussion

Table 2 presents the initially amount of metals in the studied lichens.Initially lichens showed no detectable Cd and Cr in tissues. Nickel may occur in some tissue samples, such as in sample P 1. Initially Fe content in lichen samples was included in the range 1925.4-3845.0mg·kg^{-1} D.M. The amount of Pb was in the range 30.6-45.2 mg·kg^{-1} D.M.The amount of Zn was 7.5-31.1 mg·kg^{-1} D.M., of the copper and of 7.6-12.7 mg·kg^{-1} D.M.It is observed from the Table 2 that the quantities of metals in analyzed lichens, determined before starting the experiment, are correlated with the values reported by The certified reference material BCR 482 lichen[11].

Table 2 The initially amount of metals in the lichens, *Parmelia spp.* [mg·kg^{-1} D.M.]

No	Experiment's variants	**Metals [mg·kg^{-1} D.M.]						
		Cd	Cr	Cu	Fe	Ni	Pb	Zn
1	P 1	*	*	117 ±2.0	3845.0 ±43.5	7,8 ±2.3	30,6 ±3.1	16,7 ±2.7
2	P 2	*	*	7,6 ±1.7	1925,4 ±33.8	*	37,7 ±4.6	22,7 ±3.7
3	P 3	*	*	12,7 ±1.9	2864,0 ±42.8	*	45,2 ±4.6	31,1 ±3.2
4	The certified reference material BCR 482 lichen [11]	0.56	4.12	7.03	-	2.47	40.9	100.6

*Below detection limit ,** 3 replicates for each metal anal;yzed

In Table 3 is indicates the concentrations of metals initially determined on woody acacia support for *Parmelia spp.* The acacia support does not contain Cd and Ni ions, but contain Cr which was not adsorbed into the studied lichens. In the case of other metals, respectively Cu, Fe, Pb and Zn, the found amounts on acacia support are correlated with initial quantities of these metals in the tissue of lichens.

Table 3 Initially range of metals ccontent on woody acacia support for *Parmelia spp.*

No.	Experiment's variants	Metals content min.-max. [mg·kg^{-1} D.M.]							
		Cd	Cr	Cu	Fe	Mn	Ni	Pb	Zn
1	acacia wood support	*	5.9-9.5	5.1-9.3	863.5-1775	22.3-29.0	*	22.9-55.7	9.8-18,6

*Below detection limit

In Table 4 are presented the metal concentrations determined in the tissue *of lichens Parmelia spp*. after 16 weeks exposure in the laboratory to artificial pollution with a single pollutant - cadmium.Initially lichen samples do not contain Cd. This metal was bio-accumulated in time the tissue of lichens.

Table 4 *Parmelia spp.*metal content after 16 weeks exposure in the laboratory to artificial pollution with a single pollutant - cadmium

No.	Experiment's variants	**Metals content [mg·kg^{-1} D.M.]					
		Cd	Cr	Cu	Fe	Pb	Zn
1	P 1	4.37 ±0.3	*	12.67 ±2.4	2698 ±46.4	30.6 ±6.2	22.1 ±4.3
2	P 2	4.90 ±0.4	*	9.74 ±1.9	2750 ±34.7	37.7 ±28	20.3 ±5.1
3	P 3	4.0 ±0.2	*	14.5 ±4.1	3021 ±52.6	45.2 ±5.7	37.3 ±3.9

*Below detection limit, **3 replicates for each metal analyzed.

Several hundred measurements confirmed the affinity of *Parmelia spp.* for higher Cd content [9-10]. The amount of Cd bio-accumulate in the tissue of lichens was between 4.0-4.9mg·kg^{-1} D.M.In 16 weeks of exposure to laboratory environmental pollution using aqueous solutions with different concentrations of Cdand pH=3.5 simulating acid rain, bioaccumulation of Cd levels reached a plateau at 4.45 ± 0,45mg·kg^{-1} D.M. The cadmiumbioaccumulation in lichen tissues pollution exposed has reached a limit value, relatively constant. In Table 5 it is shown

comparatively the appearance of lichens *Parmelia spp*. after 16 weeks of exposure to laboratory pollution with synthetic solutions having a single pollutant - Cd.It can be observed that after 16 weeks exposure to pollution with synthetic solution of Cd at concentrations of 2-4$mg \cdot L^{-1}$ the color of lichens was changed from greenish-gray, to greenish with brown spots (see table 5 samples P1 and P2). Exposure to environments more polluted with cadmium produced dramatic alteration of lichens with their surface restriction and from greenish-gray at brown color modification (see table 5 sample P 3).

Table 5 Lichens *Parmelia spp.* appearance of the experimental variant after 16 weeks

Experiment's variants	The appearance of the lichens (*Parmelia spp.*)	
	Initial	After 16 weeks.
P1	Greenish-gray	Greenish with brown spots
P 2	Greenish-gray	Greenish with brown spots
P 3	Greenish-gray	Brown and surface restriction

Conclusions

Lichens of the *Parmelia spp.* species exposed 16 weeks to artificial polluting environments with Cd acid aqueous solutions at pH= 3.5, have confirmed the high affinity for Cd. Levels of cadmium bioaccumulation after 16 weeks of exposure, in laboratory experiment, to polluted environments with aqueous solutions with different concentrations of Cd, reached a plateau at 4.45 ± 0.45$mg \cdot kg^{-1}$ D.M.The cadmiumbioaccumulation in lichen tissues pollution exposed has reached a limit value, relatively constant.After 16 weeks of exposure to pollution with synthetic cadmium solution at concentrations of 2-4$mg \cdot L^{-1}$ and pH=3.5 simulating acid rain, the color of lichens was changed from greenish-gray to greenish with brown spots. Exposure to more polluted environments as 5$mgCd \cdot L^{-1}$ had dramatic effects on lichenswith their surface restriction and color modification.The lichens studies of metal bioavailability could further enhance utility as environmental bio-prospections and air quality bio-monitoring tool.

References

[1] M.E.Conti, G.Cecchetti, Environ. Pollut. 14(2001) 471.
[2] H.A. Carreras, E.D.Wannaz, C.A. Perez, M.I. Pigmata, Environ, Res. 97 (2005) 50.
[3] A.M.Rusu, G.C.Jones., P.D.J. Chimodes, O.W. Purvis,Environ. Pollut. 143 (2008) 81.
[4] M.O. Obiakor, C.D. Ezeonyejiaku,Am. J. Life. Sci. Res. 1(2013) 59.
[5] T.H. Nash,Lichen Biology Cambridge University Press, Cambridge UK (1996).
[6] J. Garty, Crit. Rev. Plant Sci.20 (2001) 309.
[7] M.E. Hale, Lichens as bioindicators and Monitors of Air Pollution in the Flat Tops Wilderness Area. Colorado. Final Report USFS Contract No. ON RFP R2-81-SP35 (1981).
[8] P.A.Wolseley, P.W. James, Acidification and the Lobarion: a case for biological monitoring. *In*: P. A. Wolselely, and P.W. James. (eds.). The Effects of Acidification on Lichens 1986-1990. CSD Report 1247. The Nature Conservancy Council, Peterborough, UK.(1992).
[9] R. Bargagli, F.Monaci, F Borghini, F. Bravi,C. Agnorelli, Environ Pollut. 116 (2002) 279.
[10] P.L. Nimis, S. Andreussi,E.Pittao, Sci. Tot. Environ. 275(2001) 43.
[11] EC-IRMM, (Revised: 2007), The certified reference material BCR 482 lichen, European Comission- Joint Research Centre,Institute for Reference Materials and Measurements,Brussels, Belgium (1995).

THE USE FLY ASH IN-SITU PHYTOREMEDIATION OF CRUDE OIL POLLUTED SOILS

Masu Smaranda[1*], Dragomir Nicolai[2]

[1]National R & D Institute for Industrial Ecology ECOIND. Branch of Timisoara. 300004. 1 Regina Maria Square. Timisoara. Romania
[2]Banat´s University of Agricultural Sciences and Veterinary Medicine "King Michael I of Romania" from Timisoara,, 300645, Timisoara, Calea Aradului 119, Romania
e-mail: andamasu@yahoo.com

Abstract

The phytoremediation of lands polluted with oil products are generally applied in situ as a non-destructive technique. The process of phytoremediation participates in improving the agronomic characteristics of degraded soils. The content of petroleum products in the studied soils ranged between 70.45-120.32g·kg^{-1} D.M. The experimental study block consisted of in- situ variants located on land polluted by crude oil. The experimental variants were: variants of polluted soil unfertilized / fertilized with 50 t ·ha^{-1} sewage sludge. In addition, for the variants fertilized with sewage sludge an extra 50 t·ha^{-1} fly ash originating from power plants was used. From the mixture of meadow plants used for the phytoremediation, the species *Lolium spp.* and *Medicago spp.* formed a coating plant layer on the variant fertilized with a mix of sewage sludge with fly ash, which covered up to 90% of the sown area. Effectiveness of the reduction of petroleum products in the soil was over 48% in three months time. The phytoremediation can be promoted with good results for the recovery of oil polluted soils with the use of treatments with sewage sludge and fly ash.

Introduction

The premises of the application of the method to restore damaged soils using crops, namely phytoremediation, are simple. However, as for the application any other methods, further research is needed. In this case, research is needed on the plant species in order to choose the most effective one. Additionally, the features of the polluted space, of the probable risks, of the applicationcosts, partial and final results etc. must be defined[1-5].Adding fertilizer to soils polluted with petroleum products is a variant of the phytoremediation technique, which is applied to increase the efficiency of biodegradation achieved by plants. The soil polluted with oil products, has an excess of carbon compounds. Nitrogen and phosphorus are often limiting factors in the process of biodegradation of hydrocarbons in polluted soils. Therefore, a balance of nutrients can reduce competition for nutrients between plants and microorganisms. Consequently, in soils polluted and fertilized, the efficiency of biodegradation of petroleum products will increase [5-6]. Flyash from fossil coal combustion in power plants are now byproducts, known mostly as waste. Fly ash have been recognized as a potential improver of the destroyed soil in that it presents minerals that contribute to plant growth. Mineral substances essential for plant growth are almost all in ionic form and have a positive impact on the physicochemical properties of damaged soil [7]. From this point of view, fly ash is considered a useful adjuvant for increasing crop production, especially in the case of the phytoremediation of damaged soils and waste dumps [8]. Discoloration of the wastewater with power plant fly ash was reported by a large number of researchers. Based on this information,the area available for the absorption of some pollutant components from the soil was studied. The studies were then extended to the

adsorption of the pollutants from the soil and reduction of their stress to the plants [9]. Finally, it should be noted that, although the technique of phytoremediation can be a cost-effective option, it requires a longer time than other alternative technologies to achieve clean soil characteristics and stability of cultures [10].The aim of this study is to optimize the process of phytoremediation of soils polluted with petroleum products using sewage sludge as fertilizer and fly ash resulting from the burning of fossil coal in power plants.

Experimental

The experimental study was done on soils contaminated with petroleum products (Total Petroleum Hydrocarbon-TPH) with concentration in the range of 70.45 – 120.32 $g \cdot kg^{-1}$D.M.. The experimental block is located within the following coordinates: 46°16' 96.66" N, 21° 43' 46.1" E and 150melevation. The experimental block includes the variants: 1). Polluted soil with petroleum products, fertilized with sewage sludge in the amount of 50$t \cdot ha^{-1}$**- PN**; 2). Polluted soil with petroleum products fertilized with sewage sludge in the amount of 50$t \cdot ha^{-1}$, and fly ash in the amount of 50t $\cdot ha^{-1}$**- PNC**; Soil polluted with petroleum products **-P.** Sewage sludge come from the Municipal Water Treatment Station. Fly ash come from burning fossil coal in the power plant. The surface of an experimental allotment was 20m^2. The experimental variants are separated from each other by spaces of 1 m. For the experimental studies are selected meadow plant species on experimental variants of the polluted lands: *Loliumperenne* and *Medicago sativa*. The quantity of seeds used for sowing is of 18-20$kg \cdot ha^{-1}$. Coverage of the cultivated area with different meadow plant species was established using the Braun-Blanquet abundance-dominance scale [11]. In table 1 are presented sewage sludge and fly ash characteristics.

Table 1 Sewage sludge and fly ash characteristics determined according to the methods of the national standards (3 replicates for each parameters)
* coal, non bioavailable

Organic matter[%]	Nutrients		Metals content [$mg \cdot kg^{-1}$D.M.]						
	N[%]	P[%]	Cr	Cu	Fe	Mn	Ni	Pb	Zn
Sewage sludge									
32.4 ±4.1	1.015 ±0.3	1.437 ±0.3	34.5 ±3.0	82.7 ±9.4	898.8± 34.5	200.1 ±14.3	77.1± 5.9	13.2 ±2.6	65.5± 6.3
Fly ash									
0.2-2.0*	< 0.05	< 0.02	69.1 ±4.1	119.4 ±11.0	2450.1 ±134.5	173.6 ±22.3	90.3± 15.7	28.8 ±5.5	80.9± 6.1

Results and discussion

The emergence stage The first plants sprung from a mixture of seeds sown were from *Lolium perenne* species. The plants sprouted on the variant fertilized in the absence/presence of fly ash, two weeks after seeding. After the emergence, the surface covered with plants of variant PNC (fertilized with sewage sludge mixed with fly ash) was two times larger than the area of the variant fertilized in the absence of fly ash. To note that the variant of soil polluted and untreated, plants emerge 30-45 days later than those emerging on fertilized variants. Plants of the leguminous species *Medicago sativa* sprouted after two months from seeding, on the variants fertilized in the absence / presence of fly ash.

Development stage for harvest 1. Plants of *Lolium spp*. grow exclusively in the first two months of vegetation on the experimental variants studied. *Lolium spp.* reaches 90% in the experimental variant fertilized with fly ash at the end of the 2nd month. On the variant fertilized in the absence of fly ash, the presence of *Lolium spp.* was 20% lower than when using the addition of fly ash. The culture established on the experimental variant fertilized with sewage sludge in the presence of fly ash had healthy looking plants that were heavily twinned. The culture established on the experimental variant fertilized in the absence of fly ash has had some ailing plants with yellow,necrotic leaves.On the non-fertilized variant meadow plants grow in rare clumps.

Maturity stage - harvest 1. Mowing took place two months from the emergence of plants when they reached maturity. Harvest was formed from *Lolium perenne* plants. Figure1 shows the quantity of *Lolium spp.* harvested on the experimental variants

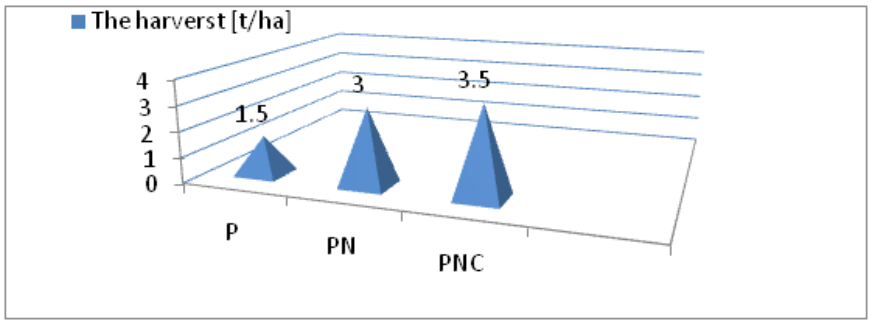

Figure 1. The quantity of *Lolium spp.* harvested on the experimental variants. **Harvest 1**

Development stage for harvest 2. After mowing, the presence of the leguminous species will gradually increase in the meadow plant culture used for phytoremediation. On the third month of vegetation, on experimental variant fertilized with sewage sludge in the presence of fly ash, the surface covered by *Medicago sativa* reached 30% of the total area covered with meadow plants. The presence of *Lolium spp.* plants will be reduced to 50% compared to the previous month. The meadow culture established on 80% of the variant experiomental surface is resistant to the torrid heat and drought conditions. On the experimental variant fertilized with sewage sludge but not treated with fly ash, the surface covered with leguminous plants will reach 20% of the total cultivated area. In this case too, the leguminous species presence of the total covered area will be achieved by reducing the presence of grass plant *Lolium spp.* Figure 2 shows the vegetal layer formed on the experimental variant fertilized in the presence / absence of fly ash after mowing.It is seen from Figure 2 the healthy aspect of the culture established on the fertilized experimental variant in the presence of fly ash *vs.* the aspect of culture established on the experimental variant fertilized without the addition of fly ash.The meadow culture established on the experimental variant fertilized with sewage sludge in the absence of fly ash has had some ailing plants with yellow leaves In addition emerged in the meadow culture clamps of plants that have dried after harvesting.


a)

b)

Figure 2 The aspect of the culture established on a) the fertilized experimental variant in the presence of fly ash, b) the experimental variant fertilized without the addition of fly ash.

Conclusions

The advantages of using as amendment fly ash from thermal power plants in the process of phytoremediation with meadow grass plants are that they resulted in: 1. Emergence of plants 30-45 days earlier than the fertilized experimental variant not treated with fly ash; 2. The forming of a rich vegetal layer with healthy plants even from the first stages of development; 3.*Lolium spp.*culturepresence was 20% higher than culture in the absence of the addition of fly ash;4. Increase the yields by 14.2%; 5.Presence of leguminous plants with 10-15% more *vs*. presence of leguminous the experimental variant not treated with fly ash; 6. Maintaining of the vegetation under conditions of a summer characterized by low rainfall and very high long time heat.

References

[1] A. van Epps, (2006). Phytoremediation of petroleum hydrocarbons,EPA, USA
[2] K. E. Gerhardt, X. D. Huang, B. R. Glick, B. M. Greenberg, Plant Sci. 176(2009) 20.
[3] R.S. A. Kitamura, L. T. Maranho, Revista Latino-americana de Ciotehnologia Ambiental y Algal 7 (2016) 1.
[4] H.Ikeura, S. Ozawa, M. Tamak, Journal of International Scientific Publications 10 (2016) 265.
[5] B.Basumatary, S. Bordoloi, H.P. Sarma, Water, Air, Soil Poll. 223(2012) 3373.
[6] S. Masu, N. Dragomir, M. Popa, J. Environ.Prot. Ecol. 14**(2013)** 901.
[7] P.Kishor, A.K. Ghosh, D. Kumar, Asian Journal of Agricultural Research 4 (2010) 1.
[8] N.Merkl, R. Schultze-Kraft, M. Arias, Int. J. Phytoremediat. 7(2005) 217.
[9] G.S. Gupta, G. Prasad, V.H. Singh, Water Res. 24(1990) 45.
[10] R.K.Kamath, J.A. Rentz, J.L. Schnoor, P.J.J. Alvarez, Chapter 16,Phyremediation of hydrocarbon-contaminated soils: principles and applications, Stud. Surf. Sci. Catal. 151(2004) 447.
[11] D.A.Wikum, G.F.Shanholtzer, Environ. Manage. 2(1974) 323.

DRINKING WATER QUALITY IN CITY OF BANJA LUKA, BOSNIA AND HERZEGOVINA – CASE STUDY

Ljiljana Stojanović Bjelić[1 *], Jelena Slijepčević Babić[1], Dragana Nešković Markić[2], Maja Sremački[3], Jovana Bondžić[4] and Mirjana Vojinović Miloradov[3]

[1]Pan-European University for Multidiscipline and Virtuel Studies, Pere Krece 13, Banja Luka, Republika Srpska, BiH
[2]Faculty of Ecology, Independent University, 78101 Banja Luka, Republika Srpska, BiH
[3]University of Novi Sad, Department of Environmental Engineering and Occupational Safety, Faculty of technical sciences, Trg Dositeja Obradovića 6, Novi Sad, Serbia
[4]University of Novi Sad, Disastre Risk Reduction Research Center, Department of Civil Engineering, Faculty of technical sciences, Trg Dositeja Obradovića 6, Novi Sad, Serbia
e-mail: ljilja_stojanovic@blic.net

Abstract
The paper presents the situation of system for public drinking water facilities "Waterworks" of Banja Luka city, including the current situation and new projects and facilities. The goal of the case study is to analyse and evaluate the results of basic physicochemical parameters of drinking water produced during the period of two years – 2013 and 2014. The data includes the seasonal sampling champagnes of two years, during the months January, April, Jul and October. It is important to have continual and controlled monitoring and evaluation of the wells, raw water wells and drinking water quality therefore it can be affected under negative impact of the dynamic natural change and anthropogenic activities. According to basic physicochemical parameters the population of Banja Luka is drinking water of good quality. During the research correlation and covariance of basic physicochemical parameters was evaluated.

Introduction
Water is an elementary component of every living being, strategic and economic resource of the area development. Supplying the population with sufficient amounts of high quality and hygienically safe drinking water is one of the basic prerequisites of good health. In addition, to well-known physiological significance for life, water plays a major role in human pathology because through it can transmit many infectious diseases that are manifested as a waterborne disease. Drinking water of low quality can have hazardous and illicit health effect.Valorisation of the quality of drinking water is done by controlled recommended values acorrding to national law and bylaws. The most important global act which refers to drinking water quality guidelines is the act of World Health Organization *Strategy on water quality and health [1]*.Banja Luka is the largest city in Republika Srpska entity, and second largest in Bosnia and Herzegovina. It is located in the north western part of the country. The city lies on the River Vrbas and it is the source of raw water for drinking water production [2]. According to the 2013 census the Settlement of Banja Luka has 150,997 inhabitants [3] while the City of Banja Luka, which represents Banja Luka's wider area (municipality), has 199,191 inhabitants [4].Banja Luka covers some 96.2 km^2 of land on the banks of Vrbas River. The city is located at 44.78°N 17.19°E. Banja Luka is at 163 m above sea level, surrounded by hills. The source of the Vrbas River is about 90 km to the south. The tributary rivers Suturlija, Crkvena, and Vrbanja flow into the Vrbas at Banja Luka. Adopted technology at the new facility "Novoselija 2" of Water Supply in Banja Luka, is derived based on the results of the pilot plant, and based on the research of water

quality of the river Vrbas and analysis of the existing plant.Raw water of Vrbas River is the primary source for production of drinking water for Banja Luka city area.The system of wells accounts for 35 l/s and from facility "Novoselija 1" 700 1/s.For more complex procedures that are required in the organization of water supply of larger towns and cities hydrological research requires a careful examination of hydrological and hydraulic characteristics of underground aquifers with wells, as well as knowledge of the physicochemical and microbiological characteristics of water.

Figure 1: Waterworks Banja Luka - Novoselija 2

Before the construction of all equipment and supporting facilities for water supply are carefully examined for the risk factors, because the properties of the water must be met strict national and international criteria for drinking water quality. In the first phase of field investigation examined the conditions in which the water is located, reveals the possible existence of direct and indirect pollutants that can distress the quality of water.

Experimental

Field tests include studies of physicochemical properties of water and controlling of water samples according to national and international standard methods and prepared for further laboratory analysis [5]. Table 1 show the limit values for basic physicochemical parameters which refer to drinking water quality [6].

Table 1. Limit values for basic physicochemical parameters [6]

Physicochemical parameters	Treated water	Raw water
Temperature [°C]	8-12	
Odour [-]	no	
Taste[-]	no	
Silicate turbidity [mg]; Turbidity [NTU]	< 5 ; < 1,2	< 10 ; < 2,4
Colour [Pt-Co°]; Water containing humic matter	10 ; (-)	20° ; < 40 °
pH [-]	6,8-8,5	6,8-8,5
TSS [mg/l]	< 800	< 1000
$KMnO_4$, [mg/l]; Water containing humic matter	< 8 ; (-)	< 12 ; < 20
Chemical oxidation demand [O_2/l]	< 2	< 3
Electroconductivity [μScm^{-1}]	< 500	< 600
Dissolved oxygen [%]	85	85

When constructed water supply systems by-law provides guidelines for analyses of wells, raw water quality and, after compulsory disinfection procedure, drinking water.

Examination and control of the physicochemical and microbiological properties should be performed according to strict rules and national recommendations. Permanent and continual quality monitoring provides insight into the changes in quality of water.

In BiH, the quality of drinking water is defined by the guidelines of the by-law on the sanitary quality of drinking water with maximum levels of physicochemical and microbiological components of drinking water [6].The characteristic flow on the gaging station can range from 1218 to 13 m^3/s. The catchment area is characterized by significant rainfall caused large

fluctuations in water level. The flow can be high in the spring and in the autumn, a "small" in the summer and winter period. The main capacity of the source (about 1000 l/s drinking water) is in Novoselije, located about 6 km upstream from the city centre, on the right bank of the river Vrbas.At the source "Novoselija 'drinking water is produced in two ways:
"New Plant" - the abstraction of water through open catchment situated on the river Vrbas and then the treatment of raw water by a conventional method, with capacity of 600 l/s (Phase I facilities). A technological process consists of coagulation with aluminium sulphate, filtration at a rapid sand filters, clean and disinfection with chlorine in the final stage and dispatched to a consumer via Ø 1000 mm pipeline [7]. Sludge removal is performed automatically, and clarification phase is carried out the method of coagulation. To reduce the natural turbidity aluminium sulphate is diminutively used ($Al_2(SO_4)_3x18H_2O$).Filtration takes place in the filter station containing quick-sand filters gravity. Due to the constant requests for connection to the water supply of new consumers and to meet the needs of a sufficient quantity of hygienic drinking water in the period up to 2020, access to the expansion of production capacity by construction of the second phase of the "Novoselija 2", additional 800 l/s [6].

Results and discussion

Based on the results of the comparative analysis of the drinking water quality from the "Waterworks" Banja Luka for the period 2013/2014, it can be concluded that the parameters are within the reference range according to the *Bylaw on the sanitary quality of drinking water* (Of. Gazette of R.S. no. 75/15). In 2013/2014 624 water samples were collected for analyses, 312 samples per year. All analytical analyses of samples were carried out in the Laboratory "Waterworks" Banja Luka. All the results are shown in the Figure 2.

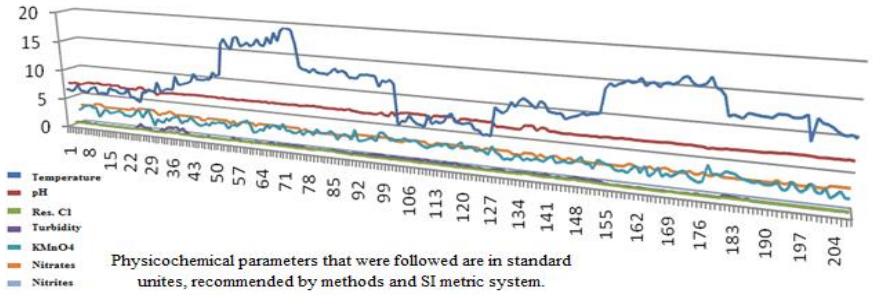

Figure 2. Results of physicochemical parameter analyses

Physicochemical parameters that were followed are in standard unites, recommended by methods and SI metric system.The statistical data for the basic physicochemical parameters in the form of correlation and covariance parameters are shown in the tables 2 and 3.The water temperature in the in 2013 ranged from 5.1 to 20.9 C, and during 2014 from 17.4 to 6.1ºC. The pH value ranged from 7.39 to 8.24. The water is free from ammonia and manganese. In the sample from January 2013 $Fe^{3+}_{(aq)}$ appears in the amount of 0.03 mg/l, while in 2014 iron is found repeatedly in the values of 0.01- 0.02 mg/l, which is within the limits prescribed by the Regulations. The value of nitrate in this period was stable and ranged from 2.7 mg/l NO_3 to 3.5 mg/l. Water is a tasteless and odourless. According to results the concentration of chlorine is in the range of 0.5 to 0.7, while the concentration of residual chlorine in the supply pipeline ϕ 1000 the range from 0.30 to 0.60 mg /l.It should be noted that in January and April 2013 turbidity increase was recorded. Turbidity in 2013 ranged from 0.10 to 1.37 NTU, while the values for 2014 ranged from 0.08-1.08 NTU.

Table 2. Calculation of correlation of basic physicochemical parameters

	T	pH	Res. Cl	Turbidity	$KMnO_4$	Nitrates	Nitrites	EC 20ºC
T	1							
pH	-0.4266626	1						
Res. Cl	-0.166355	0.0458896	1					
Turbidity	-0.2046064	0.0012955	0.2277727	1				
$KMnO_4$	0.0254763	0.0776327	-0.0762613	0.1730386	1			
Nitrates	-0.3829857	0.1980637	0.0879477	0.2385592	-0.0222994	1		
Nitrites	-0.2668514	-0.2178082	0.1743107	0.1433833	-0.1383575	0.154945	1	
EC 20ºC	0.0795733	0.2379349	0.0257393	-0.1350725	0.2002378	-0.1857596	-0.2114198	1

Table 3. Calculation of covariance of basic physicochemical parameters

	T	pH	Res. Cl	Turbidity	$KMnO_4$	Nitrates	Nitrites	EC 20ºC
T	13.65678							
pH	-0.346817	0.048382						
Res. Cl	-0.036039	0.000592	0.003437					
Turbidity	-0.169294	6.38E-05	0.00299	0.05013				
$KMnO_4$	0.051398	0.009322	-0.00244	0.021151	0.298034			
Nitrates	-0.330734	0.01018	0.001205	0.012482	-0.002845	0.054607		
Nitrites	-0.001357	-6.59E-05	1.41E-05	4.42E-05	-0.000104	4.98E-05	1.89E-06	
EC 20ºC	5.375841	0.956763	0.027585	-0.552866	1.998406	-0.793559	-0.005317	334.203

Conclusion

During the researched period the basic physicochemical parameters of the quality of the final product were within the national standards. According to the efficient system of raw water conditioning and continuous monitoring of the system, the drinking water in Banja Luka that is distributed to the population is of hygienic and adequate healthy quality level. The system for conditioning water in the "Water Supply" Banja Luka managed on the optimal way, the increase of turbidity was minimised and disinfection have been successfully optimised, and therefore the population of Banja Luka have access to satisfactory quality of drinking water. Even in the "emergency" situations when extreme care and good organization is require, the facility "Novoselija" is successful managed.

References

[1] Strategy on water quality and health, World Health Organization, 2010
[2] General information about Banja Luka, http://www.banjaluka.rs.ba/
[3] Census of population, households and dwellings in BH 2013, on the territory of Republika Srpska - Preliminary results, www.rzs.rs.ba
[4] Preliminary Results of the 2013 Census of Population, Households and Dwellings in BiH.
[5] Đukić Z. i Zmijanjac M. „Water quality of Banja Luka water supply system with aspects chemical control", Conference "Water quality management, water losses and rational consumption of water in the water supply system to another technology and measuring devices", Pale, Jahorina (2003)
[6] Official Gazette RS, br.75/15, "Bylaw on sanitary safety of drinking water"
[7] Bjelić Stojanović Lj, PhD thesis "Model prekograničnog uticaja sliva rijeke Vrbas na rijeku Savu" 2014, Faculty of technical sciences, Univeristy of Novi Sad

METEOROLOGICAL AND SYNOPTIC INTERPRETATION AT THE REPRESENTATIVE STATIONS FROM WESTERN ROMANIA DURING THE SUMMER OF 2014

[1]Vlad Dragoslav Mircov, [2]Nichita Iuliana Anca, [2]Irina Moisescu Constantin Alexandru, [1]Antoanela Cosma, [1]Anisoara Barbalan, [1]Adela Grozavescu

1 Faculty of Agriculture, USAMVB "Regele Mihai I al Romaniei" din Timisoara, 119, Calea Aradului, 300310, Timisoara, Romania
2 CMR Banat Crisana, 15, Gheorghe Adam, 300310, Timisoara, Romania
e-mail:vlad.mircov@yahoo.com

Abstract
In Romania, droughts occur on the background of specific synoptic configurations. It is, mainly, about the persistence of an anti-cyclone field due to the coverage of our country by some backward cyclones (of the east-European Anti-cyclone, the Azores Anti-cyclone, the Scandinavian Anti-cyclone, or the North-African Anti-cyclone), i.e. on the existence of a high pressure field because of an anti-cyclone belt made by the union of the Azores Anti-cyclone with the East-European Anti-cyclone.

Introduction
In Romania, more exactly in Western Romania, the summer of 2014 was rich in extreme meteorological phenomena, particularly periods associated rather to high atmospheric instability that marked all three summer months than to hot periods (they occurred only twice in the Banat-Crişana region). As a result, we can say that the summer of 2014 was rainy. To support this allegation, we present, in this study, an analysis of each summer month: pressure level at soil surface, geo-potential height at 500 level hPa, standard deviations of mean air temperature and of precipitations compared to the normal multi-annual values (reference interval: 1961-2013).

Materials and methods
We used data supplied by four representative meteorological stations in the Banat-Crişana Region – Oradea, Arad, Timişoara and Reşiţa – and we pointed out the deviations in relation to normal multi-annual values. Synoptic characterisation was done with maps of soil level pressure that show the distribution of cyclones and anti-cyclones and maps of altitudes with geo-potential at 500 hPa, i.e. at about 5,500 m.

Results and discussion
The summer 2014 was a cold one at the beginning, with minimum temperatures in plateaus of 5°C. In June, there was a single short hot interval (6-11 June), when maximum temperature was in Oradea (35.8ºC in Oradea). June is well known for being unstable, with quick shifts from nice, hot weather to unstable, cooler periods. The largest monthly amount of precipitations is supposed to fall in June(figure 1). June 2014 partially fit this pattern. The amounts of precipitations were slightly below multi-annual values in the Western Plain and Northern Crişana, while those in Southern Banat were in excess(6).

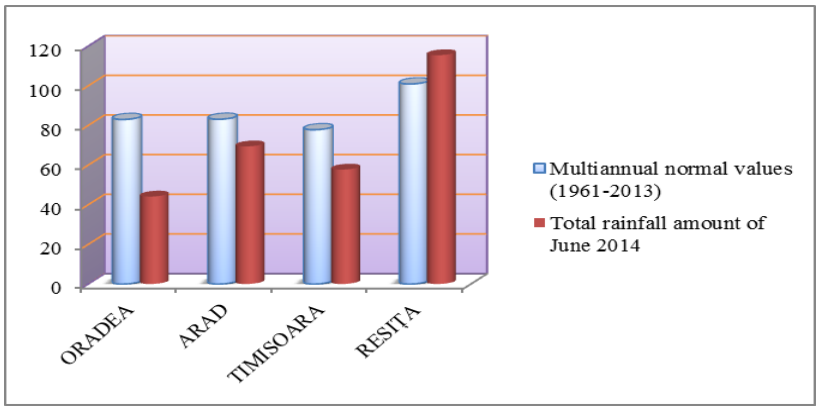

Figure 1. Precipitations in June 2014 compared to normal multi-annual values

As for the synoptic context, at the level of 500 hPa, on June 25, 12:00 GMT, it was on the ascending slope of the geo-potential thalweg (figure 2). At soil level, there was an area of low pressure extended from the central basin of the Mediterranean Sea (4) with several nuclei, whose cloud systems affected Western Romania.

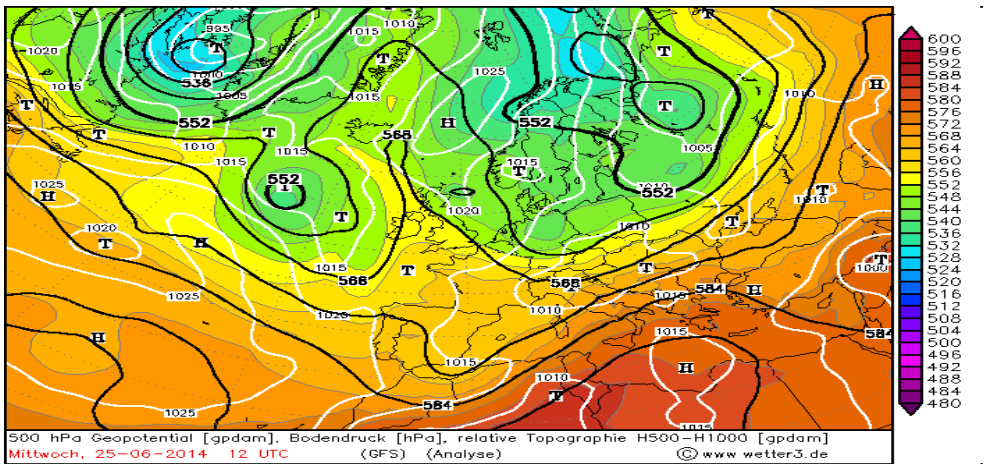

Figure 2. Geo-potential at 500 hPa and pressure at soil level on June 25, 2014, 12:00 GMT

Mean air temperature in July 2014 was close to the normal value of this month, but without intense, prolonged heat waves as in previous years. Temperatures were rather modest, partly because of heavy nebulosity (figure3). Though there were many hot days, the thermal threshold of heat was reached only once (35.1ºC on July 20, in Chișineu-Criș).

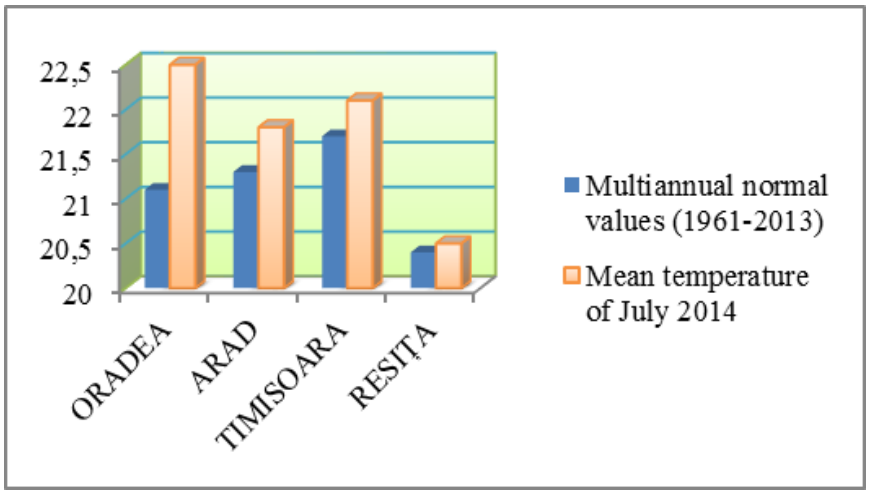

Figure 3. Mean air temperatures in July 2014 compared to normal multi-annual values

July 2014 was special from the perspective of precipitations. The amounts of precipitations were twice or even thrice larger than normal multi-annual values, so that we can speak of records.July 2014 was also the month with the most serious floods in Banat in the last years(6). The precipitations in excess on July 30 and 31 (for instance, in the Timiş County, 141.2 l/m^2 in Moravița and 127.8 l/m^2 in Gătaia) had devastating effects. Emergency Situations Inspectorates supplied the following data:

- Timiş County: 465 displaced people, 150 flooded households, 1 fallen house, County Road 588 linking Denta and Gătaia – closed;
- Caraş-Severin County: 4 dead people, 11 flooded houses, 96 flooded courtyards and gardens.

In August, the weather was influenced by an intense activity of the Iceland Depression. Its frontal systems reached our country and caused larger amounts of precipitations in the Crișana Region (114.0 l/m^2 in Ștei, 165.4 l/m^2 in Șiria-Cetate, 210 l/m^2 in Stâna de Vale), amounts recorded mainly in hill and mountain areas.

Comparing the mean air temperatures with the normal multi-annual values, we can see that mean deviations of air temperature ranged within normal limits, little above mean values in Crişana and with slightly negative deviations in Banat (up to 0.3°C), but not significant. As for the precipitations (figure 4), the amounts of water were above multi-annual values.

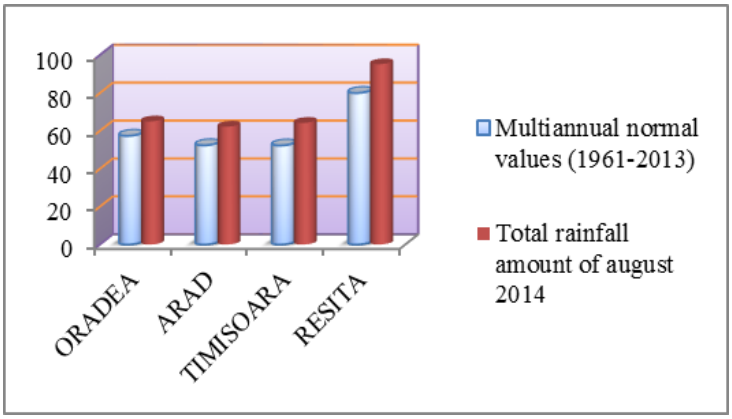

Figure 4. Precipitations in August 2014 compared to normal multi-annual values

Conclusion

Thermal deviations in the summer of 2014 had exceptional features. There was a quick dynamics of meteorological conditions that generated higher temperatures for a short period (2-3 days), followed by lower temperatures (during intense cyclone activity in the area) and by higher temperatures repeatedly. On the other hand, the distribution of precipitations and amounts of precipitations recorded (with exceptional values in July) stirred the interest of specialists. The amounts of precipitations in June and July, though not equally large, were also above multi-annual values. In June, there was a single short hot interval (6-11 June), when maximum temperature was in Oradea. July 2014 was special from the perspective of precipitations.

Comparing the mean air temperatures with the normal multi-annual values, we can see that mean deviations of air temperature ranged within normal limits, little above mean values in Crişana and with slightly negative deviations in Banat (up to 0.3°C), but not significant. As for the precipitations, the amounts of water were above multi-annual values.

References

[1] Bogdan Octavia, (2005), Caracteristici ale riscurilor climatice de pe teritoriul României, Mediul Ambiant Nr 5 (23).

[2] Croitoru, Adina-Eliza, Toma, Florentina-Mariana (2010), Trends in precipitation and snow cover in central part of Romanian Plain, in Geographia Technica, 1.

[3] Mircov D. Vlad, 2006, Climate features in 2005,Lucrări ştiinţifice Agricultură vol XXXVII,Timişoara

[4] Mircov D. Vlad, Nichita Cristian, 2015 – Curs de Meteorologie si Climatologie, Edit. Eurobit, Timisoara.

[5] ***, (2008), Clima României, Administraţia Naţională de Meteorologie, Bucureşti.

[6] ***, Arhiva Centrului Meteorologic Regional Banat-Crișana din Timișoara.

OVERVIEW OF WASTE GLASS CONTAINER MANAGEMENT IN SERBIA ACCORDING TO THE DECREE ON ESTABLISHMENT OF CONTAINER WASTE REDUCTION PLAN

Zorica Mirosavljević[1*], Dragana Štrbac[1,2]

[1]University of Novi Sad, Faculty of Technical Sciences, Department of Environmental Engineering, 21000Novi Sad, Trg Dositeja Obradovića 3, Serbia
[2]University of Novi Sad, Faculty of Sciences,Department of Physics, 21000Novi Sad, Trg Dositeja Obradovića 3, Serbia
e-mail: zoricavojnovic@uns.ac.rs

Abstract
The aim of this paper is to assess the current state of waste glass container management (WGCM) in Serbia, as developing country, by analyzing a legal framework: National Waste Management Strategy and Law on Packaging and Packaging Waste Management. The analysis is mostly based on the available data from Serbian Environmental Protection Agency (SEPA). According to the Specific National targets of packaging and packaging waste, for 2016, minimum percentage for the glass containers recycling is 25%, indicating that the current situation of WGCM is not satisfactory, because only 16% from produced glass containers are recycled, not for making the new bottles, but only for making glass cullet for some other purpose.

Introduction
In view of the deteriorating ecological situation in Serbia and abroad, the problem of utilization of solid household waste, which keeps occupying large areas, is very urgent. The interest in glass waste, whose share in solid household waste reaches 5 – 6%, has grown lately in Serbia. Glass waste remains resistant to atmospheric precipitation for many years, therefore, its storage on urban dumping areas is economically ineffective. Glass is used for many purposes, but in the waste system glass is predominantly found as a beverage and food containers with a relatively short lifetime before ending up in the waste [1]. An efficient glass collection and recycling scheme is an important driver to move towards a circular economy where waste is not dumped but become the essential raw materials used to manufacture new products, same or some other new products. The management of packaging and packaging waste is regulated by the Law on Packaging and Packaging Waste [2].
Evaluating how to avoid or dispose of waste in more environmentally respectful ways has become critical to waste management. Landfill space is becoming increasingly scarce and the assimilative capacity of Earth is reaching its limits, but landfilling is still the most common method of managing waste [3, 4]. The objective of a landfill is to safely dispose of solid waste for a long timeframe as it is actually a long-term storage of inert waste and a place of decomposition for biodegradable waste. This decomposition means emissions are inevitable and controlling these is an important aspect of the landfilling process [5]. Container glass, also called packaging glass, is the product used for packaging primarily food products. Glass is distinctive in its claim to be 100% recyclable [6, 7]. Container glass waste can be used instead of raw material as input for the manufacture of new glass. It can be mixed with raw materials or theoretically used as the only input for new glass manufacture, although in practicality only about 80% of new container glass input can be cullet, which is crushed glass used as an ingredient in glass manufacture [8].

The legislation of waste management contains various requirements to recycling of waste and sets political targets for recycling in order to minimize the environmental damage caused by waste management. Long-term strategy of Republic of Serbia in the area of environment protection shall mean the improvement of population's living quality by providing desirable conditions of environment and conservation of nature based on sustainable environment management. Key steps shall include strengthening of the existing and development of new measures for establishment of integrated waste management system, further integration of environmental policy into other sector policies, acceptance of extended individual responsibility for environment and more active participation of public in decision making processes. The National Waste Management Strategy shall be a fundamental document providing requisites for rational and sustainable waste management at the Republic of Serbia level. The Strategy has to be supported by large number of implementation plans for management of specific waste streams (biodegradable, packaging and other). Establishment of economic instruments and financial mechanisms shall be necessary in order to provide for the system for national and international investments into long-term sustainable activities. Also, the Strategy shall consider needs for institutional strengthening, legislation development, regulations implementation at all levels, education and development of public awareness. The objective of this paper was to compare and analyze the current percent of glass container recycling according to the legal framework, such as decree on establishment of waste reduction plan.

Experimental

All flows and processes associated with glass containers consumed and discarded in Serbia in 2014 are within the system boundary in this paper. The year 2014 was chosen because the data from this year were the most recent available data. The official data were used from Serbian Environmental Protection Agency (SEPA) [9], from the Report on the management of containers and containers waste in the Republic of Serbia (Table 1.).

Table 1. Official data about waste glass container amount from Serbian Environmental Protection Agency in 2014 [9]

	Operator 1 (t)	Operator 2 (t)	Operator 3 (t)	Operator 4 (t)	Operator 5 (t)	Operator 6 (t)	Total (t)
The amount of glass containers released on the market	28,013.9	21,603.4	769.6	1,408.1	1,748.0	1,693.7	55,236.8
The amount of glass containers taken by operators	4,589.0	3,296.4	129.1	284.9	384.2	263.7	8,947.2
The amount of recycled waste glass container	4,589.0	3,296.4	129.1	284.9	384.2	263.7	8,947.2

The license for container waste management has 6 operators in Serbia. The operator is obliged, on behalf of its members, to provide that: the local utility company regularly takes municipal container waste, to regularly receive and collect container waste that is not municipal waste from

end users, to ensure reuse, recycling or disposal in accordance with the Law.

Law on Packaging and Packaging Waste Management (Official Gazette of RS, no. 36/09) sets forth environmental requirements which packaging must meet in order to be marketed; packaging and packaging waste management, reporting on packaging and packaging waste, economic instruments, as well as other relevant issues with regard to packaging and packaging waste management. The Law also regulates imported packaging, produced, i.e. marketed packaging, as well as packaging waste generated in the course of business activities on the territory of the Republic of Serbia, regardless of its origin or purpose, and used packaging material.

The Decree on establishing a plan to reduce container waste for the period 2015 – 2019 defines the targets for recovery and recycling.

Tabela 2. Recycling and recovery targets under Serbian legislation for the period 2015. – 2019.

		Specific recycling targets				
		2015	**2016**	**2017**	**2018**	**2019**
Paper/cardboard	%	35,0	40,0	45,0	50,0	60,0
Plastic	%	13,0	17,0	19,0	21,0	22,5
Glass	%	19,0	25,0	31,0	37,0	43,0
Metal	%	23,0	29,0	34,0	39,0	44,0
Wood	%	10,0	12,0	13,0	14,0	15,0

Results and discussion

Quantities of recovered container waste again by operators, waste types and manner of treatment, are shown in Table 1, and then these data are used to obtain a realistic picture of the WGCM in Serbia, which is shown in Figure 1.

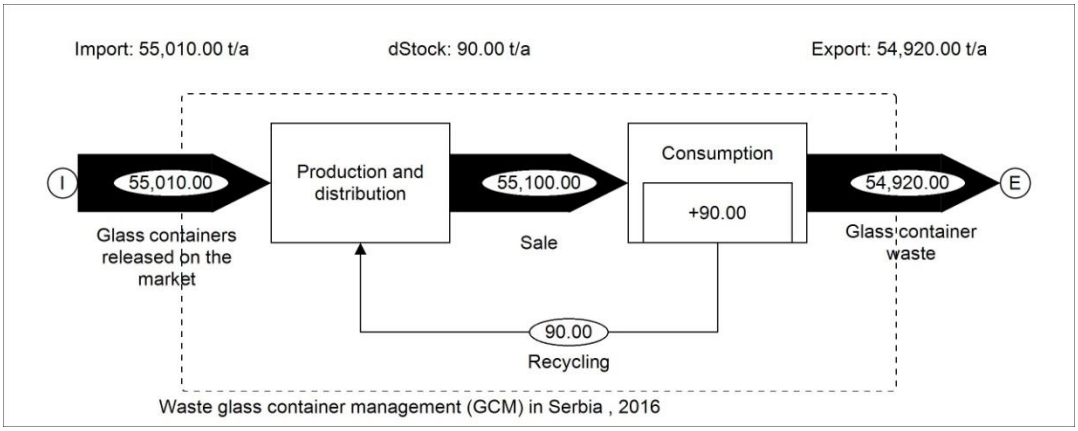

Figure 1. Waste glass container management (WGCM) in Serbia

The amount of glass containers released on the market is approximately 55,237 tons per year, of which 46,290 tons ends up in landfill, and only less than 9,000 tons of waste glass goes to recycling process. It means that only 16% from produced glass containers are recycled, not for making the new bottles, but only for making glass cullet for some other purpose.

According to the Specific National targets of packaging and packaging waste for 2016 [10],

minimum percentage for the glass containers recycling is 25%, indicating that the current situation of WGCM in Serbia, with reached only 16% of glass recycling, is not satisfactory.

Conclusion

Well planned waste management systems, may reduce imports of glass containers and increase the economy of the country. Based on EUROSTAT's statistical data, the glass container waste generation per inhabitant has steadily increased since 1998 and the price of glass cullet has increased over the years as the amount put on the market has also increased, which can contribute to economic development in Serbia in the field of WGCM.

From the aforementioned reasons, it is necessary to Serbia continue work on activities aimed at raising awareness and capacity of legal persons, to closer involvement of the public utility companies in local governments in the implementation of the system of packaging and packaging waste and aimed to more intensive inspection over the implementation of the Law on packaging and packaging waste. In the future, the results of these examples could be useful for the implementation of changes in the WGCM system in Serbia.

References

[1] H.Christensen Thomas: Solid Waste Technology & Management Volume 1. In: WILEY, A John Wiley and Sons, Ltd., Publication, Department of Evironmental Engineering. Technical University of Denmark, Lyngby, Denmark (2011)
[2] Official Gazette RS, no. 36/09
[3] United Nations. UN Statistics.
http://unstats.un.org/unsd/environment/wastetreatment.htm (2011). Accessed 25 December 2015
[4] P. T. Williams: Waste Treatment and Disposal, Second Edition. John Wiley & Sons Ltd, West Sussex, England (2005)
[5] P. White, M. Franke, P. Hindle: Integrated Solid Waste Management: A lifecycle inventory. Chapman & Hall London, U.K. (1995)
[6] The Glass Recycling Company. The Glass Recycling Company.
http://www.gpi.org/recycling/glass-recycling-facts (2015). Accessed 20 September 2015
[7] R.G.C. Beerkens, H.A.C. van Limpt, G.Jacobs,: Energy efficiency benchmarking of glass furnaces. Glass Science and Technology. (44) (2004)47-57
[8] U.S. EPA, U. S. E. P. A. Solid Waste Management: A Local Challenge with Global Impacts https://www3.epa.gov/climatechange/(2002). Accessed 20 December 2012.
[9] Serbian Environmental Protection Agency, Report on the management of containers and containers waste in the Republic of Serbia in 2014.
[10] Waste Management Strategy for the period 2010.-2019., Government of Republic of Serbia, Ministry of Energy, Development and Environmental Protection of Republic of Serbia.

CHANGES IN THE QUALITY IN TOMATO FRUIT DUE TO HOME-SCALE FREEZING

Diana Moigradean*, Mariana-Atena Poiana, Liana-Maria Alda, Ioan Gogoasa, George-Andrei Draghici

Faculty of Food Processing Technology, Banat's University of Agricultural Sciences and Veterinary Medicine „King Michael I of Romania" from Timisoara, Calea Aradului 119, Timisoara, RO 300645, Romania
e-mail: dimodean@yahoo.com

Abstract
The aim of the study was to evaluate the effect of home-scale freezing in the quality of tomato fruit cultivated in field conditions, in Romanian west area.Freezing is one of the oldest and most widely used methods of vegetables preservation.Tomatoes were analyzed fresh and stored frozen in domestic freezer at -18^{0}C for 2-6 months until analysis. Tomatoes were analyzed regarding moisture, sugar, lycopene content,ascorbic acid, phenolic compounds and total antioxidant capacity. Most important losses due to 6 months home-scale freezing were recorded for lycopene content (47%) followed by vitamin C content (20%), total antioxidant capacity (16%) and phenolic compounds content (13%). The freezing process has no to much effect on the nutritional compounds but for the best quality, use the tomato fruit within short time.

Introduction
Tomato (*Lycopersicum esculentum*) is the most popular and widely cultivated seasonal fruit vegetable crop; it is grown in the backyard of most people's home [12].
Tomatoes produced in climatic conditions of Romanian country is highlighted by high sugar content, acidity, ascorbic acid and carotenoids, especially the tomatoes produced in the field the months from July to September, due to high temperature and solar radiation [8]. Tomatoes are especially important for the human diet because of their content of vitamin C, carotenes, lycopene and phenolic compounds. Ascorbic acid, lycopene and phenolic compounds are a major source of antioxidants [14].
Freezing is one of the oldest and most widely used methods of food preservation, which allows preservation of taste, texture, and nutritional value in foods better than any other method [5].Freezing has been successfully employed for the long-term preservation of many foods. The process involves lowering the product temperature generally to -18°C or below [6]. Frozen tomatoes are best when used within 4-6 months, depending on quality of fruit at time of processing and how they are processed for the freezer, but have a freezer life of 8-12 months [18]. Tomatoes must be select firm, ripe tomatoes with a deep red color. Frozen tomatoes have a mushy texture when thawed and are suitable only for cooking, such as in soups, stews and spaghetti sauces [16].

Experimental
Tomatoes samples were collected on June-July at thoroughly fruit maturity. After harvesting tomato fruit were used for the analysis on fresh products and frozen immediately. Were used whole tomatoes, closed in the freezer bags, excess air removed, without blanching and kept in the Zanussi domestic freezer at -18^{0}C for 2-6 months. Before analysis, the tomato samples were thawed in refrigerator at 3-5^{0}C for 6 hours; tomatoes defrosted completely were using.

Tomatoes samples were homogenized and centrifuged for 10 min.
Moisture content was determined using the AOAC method (1990) [2]: tomato fruit were dried in the oven at 105 ± 1^0C; readings were taken hourly until constant weight was achieved. The results were reported as %fresh weight (FW).
Determination of sugar content:Tomatoes samples were homogenized and centrifuged for 10 min. The supernatant was used to measure the sugar content using a refractometer method by hand refractometer Carl Zeiss Jena. The results were reported as ^{0}Brix at 20^{0}C.
Determination of lycopene:Lycopene content in the tomatoes samples was extracted by hexane:ethanol:acetone (2:1:1, v:v:v) mixture following the method of Sharmaand Le Maguer (1996) [13]. The lycopene concentration were measured spectrophotometrically at 472 nm using its specific extinction coefficient (E1% 1cm) of 3450 in hexane at 472 nm by Spectrophotometer UV-VIS SPECORD 205 by Analytik Jena. The results were expressed as mg/100g FW.
The ascorbic acid content of samples was carried out based on AOAC method (1990) [2] by 2,6-Dichlorphenolindophenol Natrium. The results were expressed as mg ascorbic acid/100g FW.
Determination of phenolic compounds: The content of total polyphenolic compounds in tomatoes ethanol extracts diluted 1/10 was determined by Folin-Ciocalteu method (1927). The absorbance of blue-colored complex solution was then read at 725 nm using Spectrophotometer UV-VIS SPECORD 205 by Analytik Jena. Gallic acid was used as a standard, and results were calculated in gallic acid equivalents (GAE) per 100 g FW [11]. Correlation coefficient (r^2) for calibration curve was 0.9807.
Determination of total antioxidant capacity (TAC) by FRAP method: For determination phenolic compounds and total antioxidant capacitysample it was made the alcoholic extraction. FRAP method depend upon the reduction of ferric tripyridyltriazine complex to the ferrous tripyridyltriazine by a reductant at low pH. This ferrous tripyridyltriazine complex has an intensive blue color and can be monitored at 593 nm. TAC in tomatoes in Fe (II) equivalents was calculated [11]. Correlation coefficient (r^2) for calibration curve was 0.9891.
All determinations were repeated for three times.

Results and discussions

The consumers define quality. For tomatoes, the most important quality factors for consumers acceptance are that they look and taste good, are firm and have a good nutrient value. High sugar and high acid contents generally have a favorable effect on taste [9].
Cooking and freezing are generally regarded as destructive to antioxidants, so supporting the consumers' assumption that only fresh vegetables are healthy [10].
One of the main differences between home freezing and industrial deep-freezing is the blanching procedure, which is generally not used in home practice [4]. Tomatoes do not need to be blanched before freezing [17]. During freezing most of the liquid water changes into ice, which greatly reduces microbial and enzymatic activities? Oxidation and respiration are also weakened effectively by low temperature. However, freezing itself slightly decreases food quality [7]. Tomatoes were analyzed regarding moisture, sugar, lycopene content,ascorbic acid, phenolic compounds and total antioxidant capacity (Table 1).

Table 1. The nutritional compounds content in tomato fruit(fresh and freezing)

Freezing time	Compounds content					
	Moisture [%]	Sugar [^{0}Brix]	Lycopene [mg/100g]	Ascorbic acid [mg vit.C/100g]	Phenolic compounds [µM/100g]	TAC [µMFe/100g]
fresh	92.25	7.10	16.26	24.16	156.70	446.22
after 2 months	92.80	6.80	12.95	22.58	150.24	408.45
after 6 months	94.00	6.50	8.65	19.22	136.24	375.76

Water makes up over 90 percent of the weight of most fruits and vegetables. This water and other chemical substances are held within the fairly rigid cell walls which give support structure, and texture to the fruit or vegetable [15]. The freezing tomatoes were found to have the highest moisture content (94%) whilst fresh fruit has the lowest (92.25%) (Table1). When the water freezes, it expands and the ice crystals cause the cell walls to rupture. Consequently, the texture of the produce, when thawed, will be much softer than it was when raw. This textural difference is especially noticeable in products which are usually consumed raw: when a frozen tomato is thawed, it becomes mushy and watery [15].

The freezing process did not affect too much the level of sugars. However, differences between the fresh and freezing tomato fruit content are very small (8%)(Table1).

The freezing process had a significant decreasing effect on lycopene content. During the 2 months there were reduced to 21% up to 47% after 6 months freezing reported of fresh tomato fruit(Table1). Generally, the field grown tomatoes have been reported to contain higher levels of lycopene, ranging from 5.2 to 23.6 mg/100 g [1]. The main causes of tomato lycopene degradation during processing are isomerization and oxidation. Isomerization converts all-trans isomers to cis-isomers due to additional energy input and results in an unstable, energy-rich station. Determination of the degree of lycopene isomerization during processing would provide a measure of the potential health benefits of tomato-based foods. Thermal processing (bleaching, retorting, and freezing processes) generally cause some loss of lycopene in tomato-based foods [14].

The level of vitamin C was significantly higher in fresh tomato fruits (24.16 mg vit.C/100g FW) it decreased considerably after freezing(Table1). It is documented that vitamin C is lost during processing, but ascorbic acid represents only a minor part of the antioxidant activity, polyphenols being very important antioxidant compounds [10].

The content of phenolic compounds was slightly lower in the freezing months to fresh tomato fruit, the losses were between 4 - 13%.

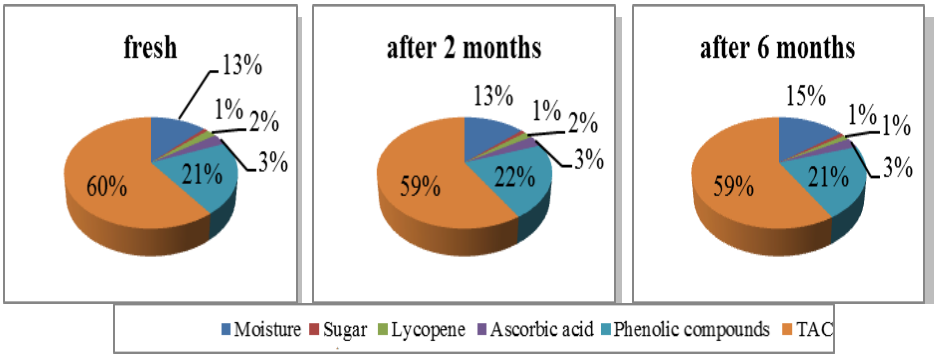

Figure 1. Changes in the nutritional compounds content in tomato fruit due to home-scale freezing

Also a decrease of the total antioxidant capacitylevel in fruits after freezing was not significant. This loss was higher in frozen tomatoes, possibly due to the alteration of the peel barrier. This decrease in total antioxidant capacityis in agreement with the recent study of Capanoglu and others [3], who showed that processing significantly affects the levels of antioxidants.From statistical terms, the sugar content and the ascorbic acid content it does not change during freezing. So, 1% respectively 3% of nutritional compounds in tomato fruit is insured by them. Other compounds were having a minor variation (Figure 1).

Conclusion

The home-scale freezing has no important changes of the level of sugars, ascorbic acid, phenolic compounds and total antioxidant capacity. Instead, were observed differences in the lycopene content and moisture level.

The decrease in the nutritional compounds content in tomato fruit occurring after home processing is relatively small.

For best quality, use the whole tomatoes without blanching, closed in the freezer bags, within six months.

References

[1] A.A. Abushita, H.G. Daood, P.A. Biacs, J Agric Food Chem. 48 (2000) 2075–2081.
[2] Association of Official Analytical Chemists (AOAC) Official Methods of Analysis. 15th ed. Association of Official Analytical Chemists Inc.; Arlington, VA, USA: 1990.
[3] E. Capanoglu, J. Beekwilder, D. Boyacioglu, R. Hall, R. de Vos, J Agric Food Chem. 56(3) (2008) 964–73.
[4] F. Danesi, A. Bordoni, J. Food Science. 73(6) (2008) 109-112.
[5] A.E. Delgado, D.W. Sun, J. Food Engineering. 47 (2000) 157-174.
[6]O.R. Fennema, W.D. Powrie, E.H. Marth, Eds, Plenum, New York, Ch.3, 1973.
[7]W. Haiying Z. Shaozhi, Ch. Guangming, LWT. 40 (2007) 1112-1116.
[8] E.M. Ionica, Review of Science and Scientometric Policy, Bucuresti, 2005.
[9] R.L. Mikkelsen, Better Crops. 89 (2) (2005)
[10]N.J. Miller, A.T. Diplock, C.A.Rice-Evans, J Agric Food Chem. 3(7) (1995)1794–1801.
[11] M.A. Poiana, M.F. Munteanu, D.M. Bordean, R. Gligor, E. Alexa, Chem Cent J. 7(1) (2013) 1-13.
[12] M.U. Sainju, D. Ramdane, S. Bharat, J. Food Agric. Environ. 1(2) (2003) 176-183.
[13] S.K Sharma, M. Le Maguer, Italian Journal of Food Science. 2 (1996) 107- 113.
[14] J. Shi, M. Le Maguer, Crit. Rev.Biotechnol. 20(4) (2000) 293-334.
[15]http://www.extension.umn.edu/food/food-safety/preserving/freezing/the-science-of-freezing-foods/
[16] http://extension.missouri.edu/p/GH1503
[17] http://food.unl.edu/freezing-raw-tomatoes-or-without-their-skins
[18] http://www.tomatodirt.com/freezing-tomatoes.html

THE CHARACTERIZATION OF RECYCLED POLY(STYRENE-CO-DIVINYLBENZENE) FUNCTIONALIZED WITH α-HYDROXYPHOSPHONIC ACIDS FOR NEW STUDY OF ANTIMICROBIAL TESTS

Ileana Nichita[1*], Adriana Popa[2*], Radu Valentin Gros[1], Smaranda Iliescu[2], Marcela Stoia[3], Monica Seres[1], Adriana Morar[1]

[1]„Banat" University of Agricultural Science and Veterinary Medicine, 119 Calea Aradului, 30465,Timisoara, Romani, [*]e-mail: nichita_ileana@yahoo.com
[2]Institute of Chemistry Timisoara of Romanian Academy, 24 Mihai Viteazu Blv., 300223 Timisoara, Romania
[3 c]Politehnica University of Timisoara, Faculty of Industrial Chemistry and Environmental Engineering, 6 Vasile Parvan Blv, 300223, Timisoara, Romania
e-mail: apopa@acad-icht.tm.edu.ro; apopa_ro@yahoo.com

Abstract
Antimicrobials are a wide variety of compounds with the attack for the destruction or inhibition of microorganisms.This article describes the using of recycled α-hydroxyphosphonic acids grafted on styrene-divinylbenzene copolymeras a recycled material for new study of antimicrobial tests.

Introduction
Antimicrobials are a wide variety of compounds with the attack for the destruction or inhibition of microorganisms. The development of the antimicrobial agents have extended with the acceptance germ theory in 1800s, with antibiosis, disinfection, preservation, sterilization and environmental control now an integrated aspect of modern infection control [1-3].
In water treatment, the most usual treatment method to disinfect and sterilize water is to use chlorine and other related chemicals. But, their residues can grow to be concentrated in the food chain and in the environment as well as the possible formation of halomethane analogues that are suspected of being carcinogenic should lead to the prevention of their use [3]. Due to the associated problems result from the use of conventional antimicrobial agents, the idea for using of polymeric antimicrobial agents appeared to be an attractive choice.
Biocide polymer is a polymeric material that has the ability to destroy microorganisms, by acting as a source of sterilizing ions or molecules [4].Polymers can act as matrix for the materials holding the antimicrobial agents [5].
This article describes the using of recycled α-hydroxyphosphonic acids grafted on styrene-divinylbenzene copolymer [1] as a recycled material for new study of antimicrobial tests.

Experimental
Recycled α-hydroxyphosphonic acids grafted on styrene-divinylbenzene copolymers was used as a study material. α-hydroxyphosphonic acids grafted on styrene-divinylbenzene copolymers were synthesized in our laboratory and the antimicrobial effects of the copolymers (S-12%DVB, %Cl= 10.32, G_F = 2.91 mmol Cl/g. copolymer; S-15%DVB, %Cl= 10.21, G_F = 2.88 mmol Cl/g. copolymer) functionalized with *α*-hydroxyphosphonic groups were tested on two species of Gram-negative bacteria (*Escherichia coli* and *Pseudomonas aeruginosa*) and two species of Gram-positive bacteria (*Staphylococcus aureus* and *Bacillus ceresus*) and a species of yeast (*Candida albicans*) [1].

The copolymers using in this work were recovered from previous antibacterial solutions [1] and they were used to new test of the antimicrobial activity. These samples were filtrated, autoclaved at 120 ° C and 1 atm pressure for 30 minutes and subsequent they re-use the antibacterial activity against one specie of Gram-negative bacteria (*Pseudomonas aeruginosa*) and one specie of Gram-positive bacteria (*Staphylococcus aureus*) and a specie of yeast (*Candida albicans*).
These recycled copolymers were characterized by IR, SEM and EDX and they are confirming the presence of active groups' pendant.
The obtained polymeric resins were characterized by Fourier transform infrared spectroscopy with a Jasco FTIR spectrophotometer.
The energy dispersive X-ray analysis (EDX) was performed using an Inspect S scanning electron microscope.
The antibacterial activity of the recycled copolymers were tested on standard strains of bacteria (obtained from MediMark Europe Company, France) as follows: gram-positive bacteria – *S.aureus* (ATCC 25923), gram-negative bacteria –*P.aeruginosa* (ATCC 27853), and on a strain of *C.albicans* (ATCC 10231). For experiments were used active cultures (24 h old for bacteria and, respectively, 48 h for yeasts) using Mueller-Hinton broth (Oxoid) for bacteria and Sabouraud dextrose agar for yeast.Each recycled α-hydroxyphosphonic acids grafted on styrene-divinylbenzene copolymers were mixed with each microbial bacterial culture. New study of antimicrobial tests was according to the method presented in our previous paper [1].

Results and discussion

Samples were analyzed after recovery: it is noted band at 3430 cm^{-1}, which is attributed to the OH group, also the band at ~2930 cm^{-1}, which is assigned to the group P-OH and also identifies the group P=O at ~1250 cm^{-1} [1] (see Figure 1 and 3). The morphology of the polymers grafted with α-hydroxyphosphonic groups can be directly visualized by SEM images (see Figure 2 and 4).The macrospores are presented among the agglomerations of microspheres, micropores being inside the agglomerations of microparticles [1].The phosphorus content was determined (see Table 1) and it has confirmed that the recovered poly(styrene-co-divinylbenzene) containing pendant groups with α-hydroxyl-phosphonic acid.
FTIR spectra, SEM images and phosphorus content confirm the presence of active groups (α-hydoxyphosphonic acid) for new study of antimicrobial tests.

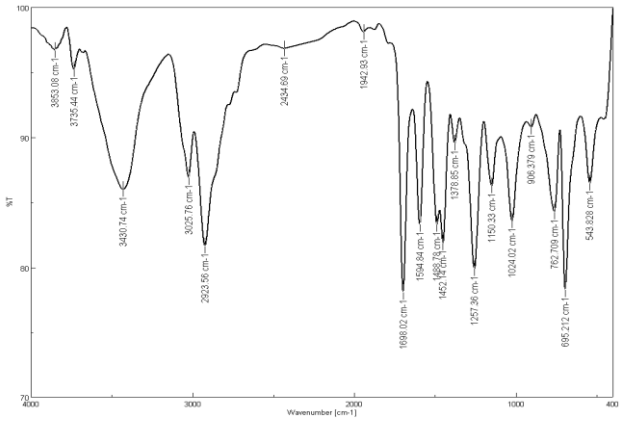

Figure 1. FTIR spectra for S-15%DVB P3 it was obtained after testing with *Pseudomonas aeruginosa*

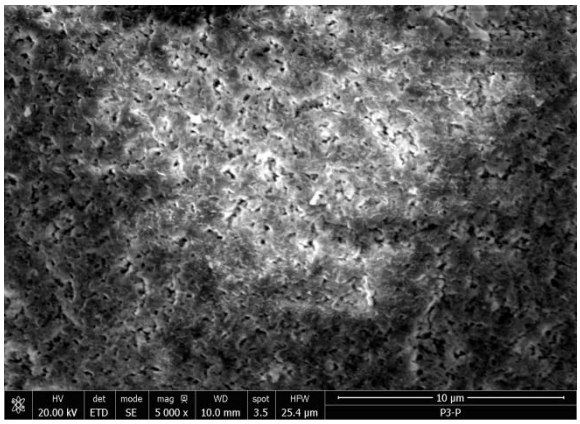

Figure 2. SEM image for S-15%DVB P3 it was obtained after testing with *Pseudomonas aeruginosa*

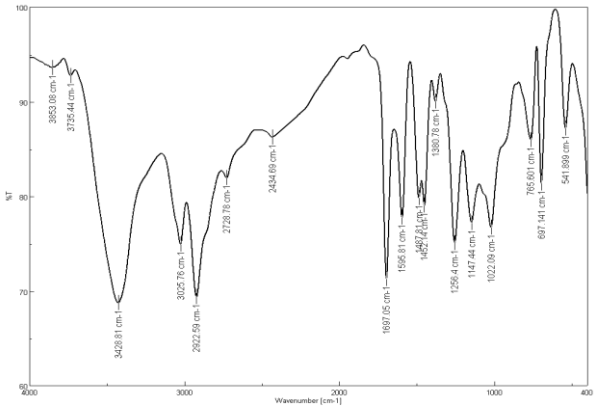

Figure 3. FTIR-spectra for S-12%DVB P2 it was obtained after testing with *Candida albicans*

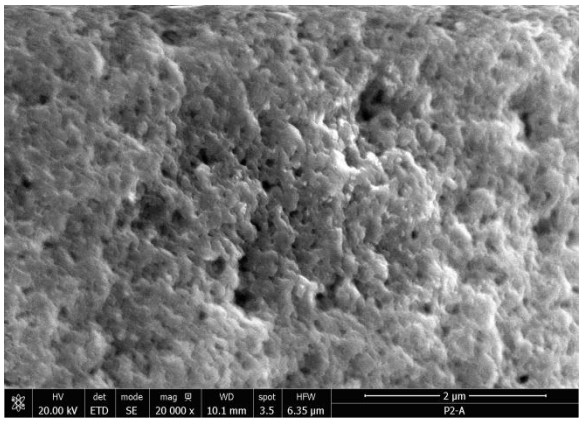

Figure 4. SEM image for S-12%DVB P2 it was obtained after testing with *Candida albicans*

Table 1. The phosphorus content of the recovered poly(styrene-co-divinylbenzene) with α-hydroxyl-phosphonic acid for using in new antimicrobial tests and the comparing with the phosphorus content the S-12%-(15%)DVBPHOS-presented in our previous paper.

Sample	P %	Sample	P %
S-12%DVBPHOS [1]	4.65	S-15%DVBPHOS [1]	5.14
S-12%DVB P2[1]	0.83	S-15%DVB P3[1]	1.19
S-12%DVB P2[2]	0.90	S-15%DVB P3[2]	1.07
S-12%DVB P2[3]	0.79	S-15%DVB P3[3]	0.96

Where:[1]it was recovered after testing with *Pseudomonas aeruginosa;* [2]it was recovered after testing with *Candida albicans;*[3]it was recovered after testing with *Staphylococcus aureus*

Antimicrobial activity

The results obtained from the testing of antimicrobial activity of the recycled α-hydroxyphosphonic acids grafted on styrene-divinylbenzene copolymers are presented in table 2.

Table 2. The antimicrobial activity of the recycled α-hydroxyphosphonic acids grafted on styrene-divinylbenzene copolymers

Microbial specie	RecycledS-12%DVB P2			Recycled S-15%DVB P3		
	CFU/mL in the start moment	**CFU/mL after 18 h of contact**	**Percentage of microbial reduction, %**	**CFU/mL in the start moment**	**CFU/mL after 18 h of contact**	**Percentage of microbial reduction, %**
S. aureus	2.05×10^8	0.19×10^8	90.73	7.06×10^8	4.68×10^8	33.71
P. aeruginosa	1.50×10^4	0.12×10^4	92	6.50×10^4	0.31×10^4	95.23
C. albicans	1.84×10^8	1.61×10^8	12.48	1.29×10^8	1.12×10^8	13.17

Both recycled copolymers still present antibacterial activity. The reduction in the number of bacteria (log CFU/mL) was found to be bigger in case of the recycle copolymer S-12%DVB comparatively with the copolymer S-15%DVB after 18 h of contact. In case of *Staphylococcus aureus* the recycle S-12%DVB had 90.73% reduction and the recycle copolymer S-15%DVB had 48.00% reduction. For the *Pseudomonas aeruginosa* specie were recorded 92 % of reduction in

case of recycle S-12%DVB and 95% reduction for copolymer S-15%DVB. None of two copolymer tested had antimicrobial effect for the yeast specie tested (*Candida albicans*).
The antimicrobial activity of the recicled copolymer comparatively with the first their form is presented in table 3. It coud be observed similar results. The antimicrobial activity of copolimers S-12%DVB was more pronounced than of the copolymer 15%DVBPHOS in case of the bacteria tested.

Table 3. The comparative antimicrobial activity of the α-hydroxyphosphonic acids grafted on styrene-divinylbenzene copolymers before and after recovery

Microbial specie	**Percent reduction, %**			
	recycled S-12%DVB P2	**S-12%DVBPHOS [1]**	**recycled S-15%DVB P3**	**S-15%DVBPHOS [1]**
S. aureus	90.73	100	33.71	48.00
P. aeruginosa	92	100	95.23	100
C. albicans	12.48	12.3	13.17	13.4

According to what was presented in our previous paper [1] we considered that the antibacterial activity is the result of hydrogen bonding between the organic groups (P=O) from α-hydroxyphosphonic acid groups and the OH groups in the cell walls of the bacteria. For the reason it is considered that the antimicrobial activity of the copolymers happened more quickly for the gram negative bacteria than the gram-positive bacteria. The copolymer S-15% DVB, even its recovery form, is more hydrophobe, comparatively with the copolymer S-12% DVB that is less hydrophobic and its α-hydroxyphosphonic functionalized groups from the interstitial copolymer S-12% DVB are more accessible for bonding through hydrogen bonding with the OH groups of the bacterial membrane.

Conclusion

The recycled copolymers were characterized by IR, SEM and EDX and they are confirming the presence of active groups' pendant.
The recycled α-hydroxyphosphonic acids grafted on styrene-divinylbenzene copolymersstill present antibacterial activity. The recycled S-12% DVB P2 copolymer had a better antimicrobial activity than the recycled S-15%DVB P3copolymer.
The antimicrobial activity of recycled copolymers is similar with those initially tested in our previous paper [1].

References

[1] I. Nichita, A. Popa, E.S. Dragan, S. Iliescu, G. Ilia, J. Biomater. Sci. Polym. Ed. 26(8) (2015) 483.
[2] Pendleton J. N., Gilmore B. F., Int. J. Antimicrob. Ag. 46 (2015) 131.
[3] Xue Yan, Xiao Huining, Zhang Yi, Int J Mol Sci. 16(2) (2015) 3626.
[4] Ahmed A.E.I., Hay J.N., Bushell M.E., Wardell J.N., Cavalli G., React. Funct. Polym. 68 (2008) 248.
[5]Munoz-Bonilla A., M Fernandez-Garcia., Prog Polym Sci. 37 (2012) 281.

PREPARATION, SURFACE AND POROUS CHARACTERIZATION OF ECO-FRIENDLY ACTIVATED CARBON PRODUCED FROM APRICOT STONES

Sabolč Pap[1*], Srđana Kolaković[1], Jelena Radonić[1], Dragan Adamović[1], Mirjana Vojinović-Miloradov[1], Miljana Prica[2], Maja Turk Sekulić[1]

[1]Faculty of Technical Sciences, Department of Environmental Engineering and Occupational Safety and Health, University of Novi Sad, Trg Dositeja Obradovića 6, 21 000 Novi Sad, Serbia
[2]Faculty of Technical Sciences, Department of Graphic Engineering and Design, University of Novi Sad, Trg Dositeja Obradovića 6, 21 000 Novi Sad, Serbia
e-mail: sabolcpap@uns.ac.rs

Abstract
This work presents a thermochemical approach toward controlled preparation of powdered activated carbons from lignocellulosic raw materials (apricot stones), as industrial byproducts and components of organic solid waste. The physicochemical changes of the biomass during thermochemical activation with H_3PO_4 obtained after carbonization at 500 C for 2 h have been investigated by means of Fourier Transform Infrared (FTIR) spectra, scanning electron microscopy (SEM) and Brunauer–Emmett–Teller (BET) technique. The BET surface area and total pore volume were as high as 1098.78 m^2/g and 0.5 cm^3/g, respectively. The experimental results indicated that the use of apricot stones as a precursor material for the preparation of activated carbon (AC) was feasible.

Introduction
Activated carbon is one of the most used and tested adsorbents in the removal of heavy metals, industrial organic compounds, pharmaceuticals and dyes. Different types of lignocellulosic materials was used as potential precursors in the production of low cost activated carbon, because these materials possess high carbon contents and are low in cost [1].
There are, two different processes for the preparation and production of activated carbon: physical and chemical. Chemical activation includes impregnating the lignocellulosic raw materials with chemical agents (H_3PO_4, HNO_3, H_2SO_4 and NaOH). After impregnation, the materials are carbonized and washed to eliminate the residues. The chemical activation, which was used in this study has two important advantages when compared to the physical activation. The first advantage is the lower temperature at which the process is conducted, and the second is that the yield (mass efficiency of activation) of the chemical activation tends to be greater [2].
In this study, AC was prepared from apricot stones, as industrial byproducts with H_3PO_4 as an activating agent in the complete absence of inert atmosphere. A detailed characterization of the obtained activated carbon was performed through various instrumental analyses, comprising of FTIR, SEM and BET.

Experimental
Apricot stones were obtained from fruit plantation located in Novi Becej, province of Vojvodina (Serbia). The stones were milled with a mechanical mill and < 3.0 mm fraction was chosen for the thermochemical conversion.
Preparation of activated carbon included the following steps: milled stones were washed with distilled water. Later, the fruit stones were impregnated with a solution of 50% H_3PO_4. After impregnation, the solution was filtered to remove the residual acid. Subsequently impregnated

samples were air dried at room temperature. The samples were placed in a furnace and heated (10 °C/min) to the final carbonization temperature of 500 °C for 2 h without the use of nitrogen. After cooling, the adsorbent was washed with distilled water to achieve acid free conditions and its pH was monitored until the filtrate pH value exceeded 4.

A detailed Fourier Transform Infrared spectra (FTIR) study of prepared activated carbon was carried out to identify qualitative characteristics of carbon material and the different functional groups responsible for the adsorption. FTIR spectra of AC were recorded with a FTIR/NIR spectrophotometer Nexus 670 (Thermo Nicolet, USA), at wavenumbers from 400 to 4,000 cm^{-1}.

The microstructures of the AC were determined by scanning electron microscope (SEM) JSM 6460LV instrument (JEOL, USA). Scanning electron micrographs were recorded without sample coating, with ×500 and ×5,000 magnification.

AC specific surface area determination was done by measurement of N_2 adsorption, applying Brunauer–Emmett–Teller technique (BET) and Autosorb iQ instrument (Quantachrome, USA).

Results and discussion

A review of the adsorption literature revealed that only materials with suitable physico-chemical characteristics are practical and cost effective for industrial scale applications [3]. The ideal properties to achieve the optimum adsorption performance include structural stability, porosity, large surface areas, hydrophilicity and appropriatefunctional groups [4].

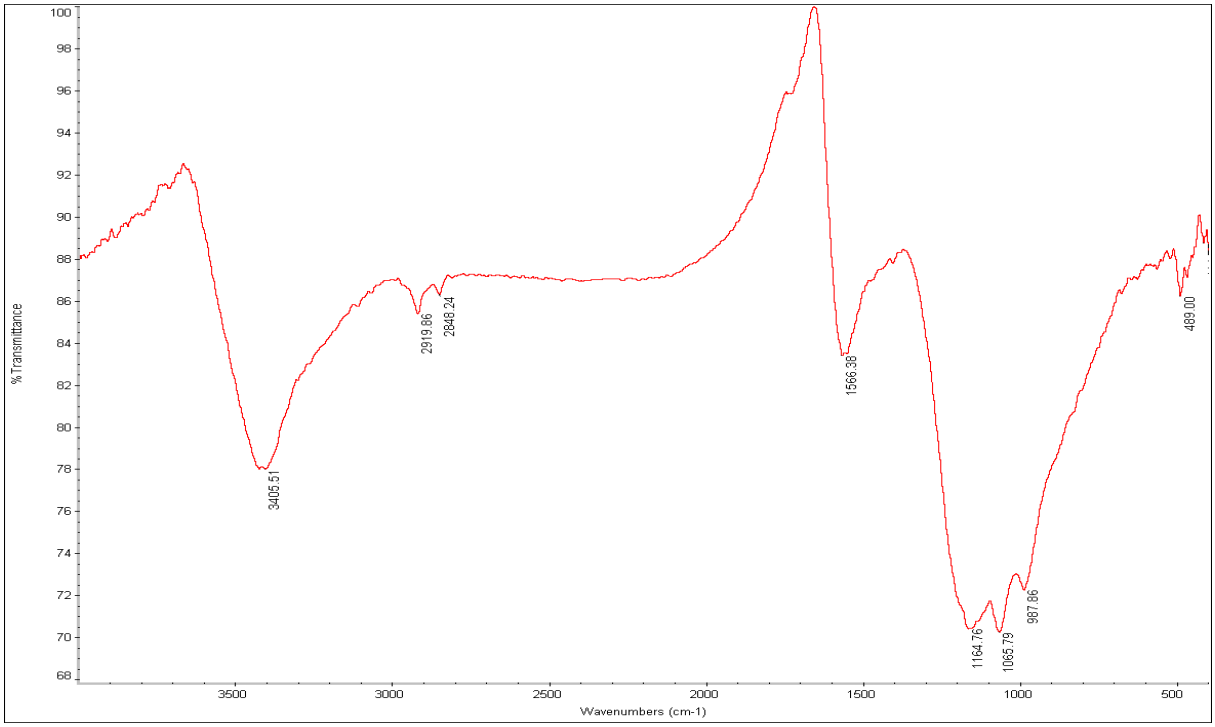

Figure 1.FTIR spectra of the activated carbon (AC)

The FTIR spectra of adsorbent (Figure 1) showed a broad band at 3405.91 cm^{-1} due to O–H stretching vibration and a peak at 489.00 cm^{-1} due to O–H bending vibration. Peaks between the range of 3700 and 3200 cm^{-1} represent the overlapping peaks of stretching vibrations of O–H and N–H groups. The distinct absorption peaks at 2919.86 cm^{-1} and 2848.24 cm^{-1} could be assigned to -CH stretching vibrations of $–CH_2$ and $–CH_3$ functional groups. The adsorption peak at 1566.38 cm^{-1} could be characterized by primary and secondary amide bands. The sharp bond

within 1164.76 – 987.86 cm^{-1} is attributed to the C–O groups, which confirms the lignin structure of the activated carbon.

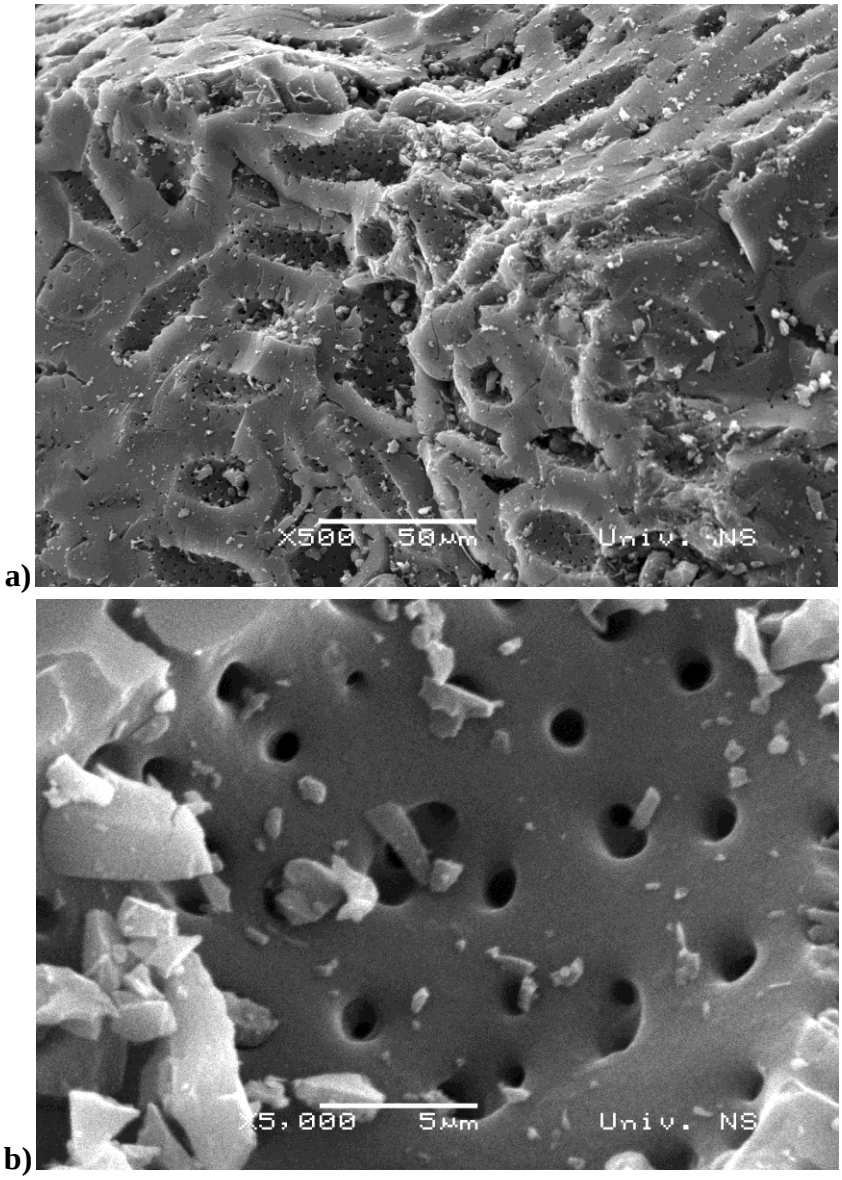

Figure 2.SEM images of the activated carbon (AC) with different magnification

Figure 2 display the SEM images of the surface structure for carbonized material at different magnification. The SEM micrographs of the activated carbon surface show homogenous and widely porous structure of AC after thermochemical activation by phosphoric acidmaking it suitable for trapping more species of pollutants with different sizes. In other words, the presence of various sizes of pores and large extent of surface area make the AC suitable for the adsorption of diverse species.

Surface area of the AC was determined byBrunauer–Emmett–Teller (BET) equation within the relative pressure range from 0.006 to 0.10. The micropore volume were obtainedby the Horvath–Kawazoe (HK) method. The total pore volume wascalculated from the amount of N_2 adsorbed at a relative pressure. Mesopore volume was calculated by subtracting the micropore volume from

the total pore volume. The textural properties of AC were summarized in Table 1. The BET surface area of AC was evaluated to be 1098.78 $m^2 g^{-1}$. The BJH adsorption cumulative volume of pores for AC was 0.022 $cm^3 g^{-1}$. The total pore volume and micropore volume of AC were determined to be 0.5 $cm^3 g^{-1}$ and 0.391 $cm^3 g^{-1}$, respectively. As can be seen from Table 1, both micropore (<2 nm) and mesopore (2– 50 nm) structures are present in the AC but the micropore volume occupies approximatelythe 80% of the total pore volume which is great larger than the mesopore volume. The smaller particle sizes of a porous carbon, the greater rate of diffusion and adsorption[5]. As seen from BET analysis, the AC has porous structure and this evidence supports the enhancement of the surface area representing a good sorption capacity of such materials.

Table 1
Textural properties of the synthesized activated carbon

	BET surface area ($m^2 g^{-1}$)	Total pore volume ($cm^3 g^{-1}$)	Micropore volume ($cm^3 g^{-1}$)	Mesopore volume ($cm^3 g^{-1}$)	Mesopore surface ($m^2 g^{-1}$)	Max. mesopore diameter (nm)
AC	1098.78	0.5	0.391	0.022	16.867	31.97

Conclusion

The activated carbon was synthesized from apricot stones by chemical activation with phosphoric acid.The present study has shown that the activated carbons prepared from apricot stone have a suitable surface characteristics, which can positively affect the adsorption properties with this material.

Acknowledgements

This study has been financially supported by Ministry of Education, Science and Technological Development, Republic of Serbia (III46009)

References

[1] H. Demiral, C. Gungor, J. Clean. Prod. 124 (2016) 103.
[2] V. Hernández Montoya and A. Bonilla Petriciolet, Lignocellulosic Precursors Used in the Synthesis of Activated Carbon**,**InTech,Rijeka, Croatia,2012.
[3] I.B. Rae, S.W. Gibb, S. Lu, J. Hazard. Mater. 164 (2009) 1601.
[4] B. Volesky, B. Volesky, Sorption and Biosorption, BV Sorbex Inc., Montreal-St., Lambert, Que., Canada, 2003.
[5]. J. Acharya, J.N. Sahu, B.K. Sahoo, C.R. Mohanty, B.C. Meikap, Chem. Eng. J. 150 (2009) 25.

DFT STUDY OF LONG BONDS IN RADICAL CATIONS OF SUGAR DERIVATIVES

Mihai-Cosmin Pascariu[1,2,3*], Madian Rafailă[4], Mihai Medeleanu[4], Ramona Curpan[5], Liliana Păcureanu[5], Nicolae Dincă[6], Eugen Sisu[1*]

[1] *"Victor Babeş" University of Medicine and Pharmacy of Timişoara, Faculty of Medicine, 2 Eftimie Murgu Sq., RO-300041, Timişoara, Romania*
[2] *National Institute of Research and Development for Electrochemistry and Condensed Matter – INCEMC Timişoara, 144 Dr. Aurel Păunescu Podeanu, RO-300569, Timişoara, Romania*
[3] *"Vasile Goldiş" Western University of Arad, Faculty of Pharmacy, 86 Liviu Rebreanu, RO-310045, Arad, Romania*
[4] *University Politehnica Timişoara, Faculty of Industrial Chemistry and Environmental Engineering, 6 Vasile Pârvan Blvd., RO-300223, Timişoara, Romania*
[5] *Institute of Chemistry Timişoara of Romanian Academy, 24 Mihai Viteazul Blvd., RO-300223, Timişoara, Romania*
[6] *"Aurel Vlaicu" University of Arad, Faculty of Food Engineering, Tourism and Environmental Protection, 2 Elena Drăgoi, RO-310330, Arad, Romania*
e-mail: mihai.cosmin.pascariu@gmail.com, sisueugen@umft.ro

Abstract
We have performed DFT computations on radical cations of several monosaccharide derivatives, using the STO-3G and 3-21G basis sets. The obtained long bond lengths were compared with the values we have previously obtained using the RM1 and PM7 semi-empirical methods. The applied DFT methods offered smaller values for the long bond lengths, attaining only 1.6÷1.7 Å. Also, in contrast with the simple STO-3G basis set, which shows some exceptions, the more advanced 3-21G basis set always places the long bond in the correct C4-C5 position, as suggested by the EI-MS analyses.

Introduction
Long bonds appear to be a ubiquitous feature in the molecular radical cations produced during the positive mode electron ionization mass spectrometry (EI-MS) analysis of compounds possessing vicinal electron donor substituents, like diols or diethers [1]. Carbohydrates are an example of such compounds. While semi-empirical methods [2,3] give long bond lengths for radical cations that are likely to be exaggerated, DFT computations are known to be more moderate in this respect. To verify this assumption we have performed DFT analyses on radical cations of five monosaccharide derivatives, which contain the furanose moiety (**Fig. 1**): 1,2:5,6-di-*O*-isopropylidene-α-D-glucofuranose (DAG), 1,2:5,6-di-*O*-isopropylidene-α-D-allofuranose (DAAlo), 1,2:5,6-di-*O*-isopropylidene-α-D-galactofuranose (DAGal), 2,3:5,6-di-*O*-isopropylidene-α-D-mannofuranose (α-DAM) and 2,3:5,6-di-*O*-isopropylidene-β-D-mannofuranose (β-DAM). All these species show, during the EI-MS analysis, a preference for the breaking of the C4-C5 bond, with the formation of the 2,2-dimethyl-1,3-dioxolan-4-ylium oxocarbenium ion, which exhibits a high intensity m/z = 101 peak [2,3].

Experimental
All structures were initially modeled using the HyperChem 8.0.10 software [4]. The starting neutral molecules, obtained after "MM+" pre-optimization, were optimized with the RM1 semi-empirical method [5]. The radical cations were obtained from these structures and were pre-

optimized with RM1. As for "Spin Pairing", RHF operators were used for neutral molecules, while UHF operators were employed for radical-cations. The SCF "Convergence limit" was set at 10^{-5}, without using the "Accelerate convergence" procedure. For geometry optimization, the "Polak-Ribière (conjugate gradient)" algorithm was selected with a RMS gradient of 0.01 kcal (Å mol)$^{-1}$, the molecules being considered in vacuum (conditions similar to those found in EI-MS detectors).

Theoretical calculations were finally performed using the Gaussian 09 software [6]. The equilibrium geometries of the radical cations were optimized using the density functional theory (DFT) method at the B3LYP/STO-3G or B3LYP/3-21G levels. The B3LYP hybrid functional was used for these studies because of convention and the successful use to model a range of gas-phase reactions.

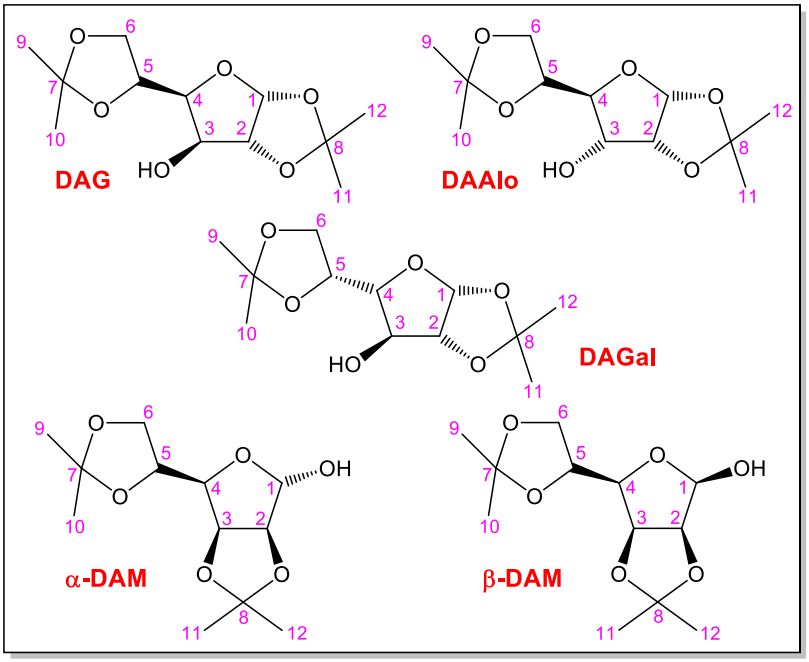

Figure 1. Structure of the studied compounds

Results and discussion

The DFT results regarding the enthalpy of formation ($\Delta_f H^0$) at 0 and 298.15 K, the Gibbs free energy ($\Delta_f G^0$) at 298.15 K and some bond lengths are given in **Tables 1** and **2**, while the O4-C4-C5, O5-C5-C4 and O4-C4-C5-O5 angle values are given in **Table 3**.

Table 1. Results obtained for the radical cations using the B3LYP/STO-3G level of theory

Compound	$\Delta_f H^0$ 0 K (kcal mol^{-1})	$\Delta_f H^0$ 298 K (kcal mol^{-1})	$\Delta_f G^0$ 298 K (kcal mol^{-1})	Bond length (Å)				
				C1-C2	C2-C3	C3-C4	C4-C5	C5-C6
DAG*	-1967.33	-1984.8	-2311.0	1.583	1.594	1.613	**1.637**	1.575
DAAlo	-1977.86	-1996.1	-2324.1	1.576	1.589	1.606	**1.628**	1.574
DAGal	-1961.96	-1979.3	-2305.4	1.586	**1.635**	1.585	1.617	1.580
α-DAM	-1969.30	-1987.0	-2314.2	1.586	1.575	1.592	**1.619**	1.573
β-DAM	-1972.65	-1990.7	-2319.0	1.595	1.581	1.585	**1.609**	1.566

*optimization was started from 3-21G geometry

Table 2. Results obtained for the radical cations using the B3LYP/3-21G level of theory

Compound	$\Delta_f H^0$ 0 K (kcal mol^{-1})	$\Delta_f H^0$ 298 K (kcal mol^{-1})	$\Delta_f G^0$ 298 K (kcal mol^{-1})	Bond length (Å)				
				C1-C2	C2-C3	C3-C4	C4-C5	C5-C6
DAG	-1250.31	-1267.4	-1592.9	1.536	1.529	1.538	**1.650**	1.531
DAAlo	-1254.74	-1272.5	-1599.7	1.542	1.553	1.572	**1.648**	1.541
DAGal	-1250.40	-1267.8	-1594.7	1.536	1.527	1.548	**1.712**	1.534
α-DAM	-1250.86	-1268.4	-1595.7	1.527	1.547	1.562	**1.562**	1.537
β-DAM	-1252.40	-1269.9	-1597.0	1.553	1.556	1.556	**1.597**	1.537

The molecular models for the considered radical cations (B3LYP/3-21G) are shown in **Fig. 2**.

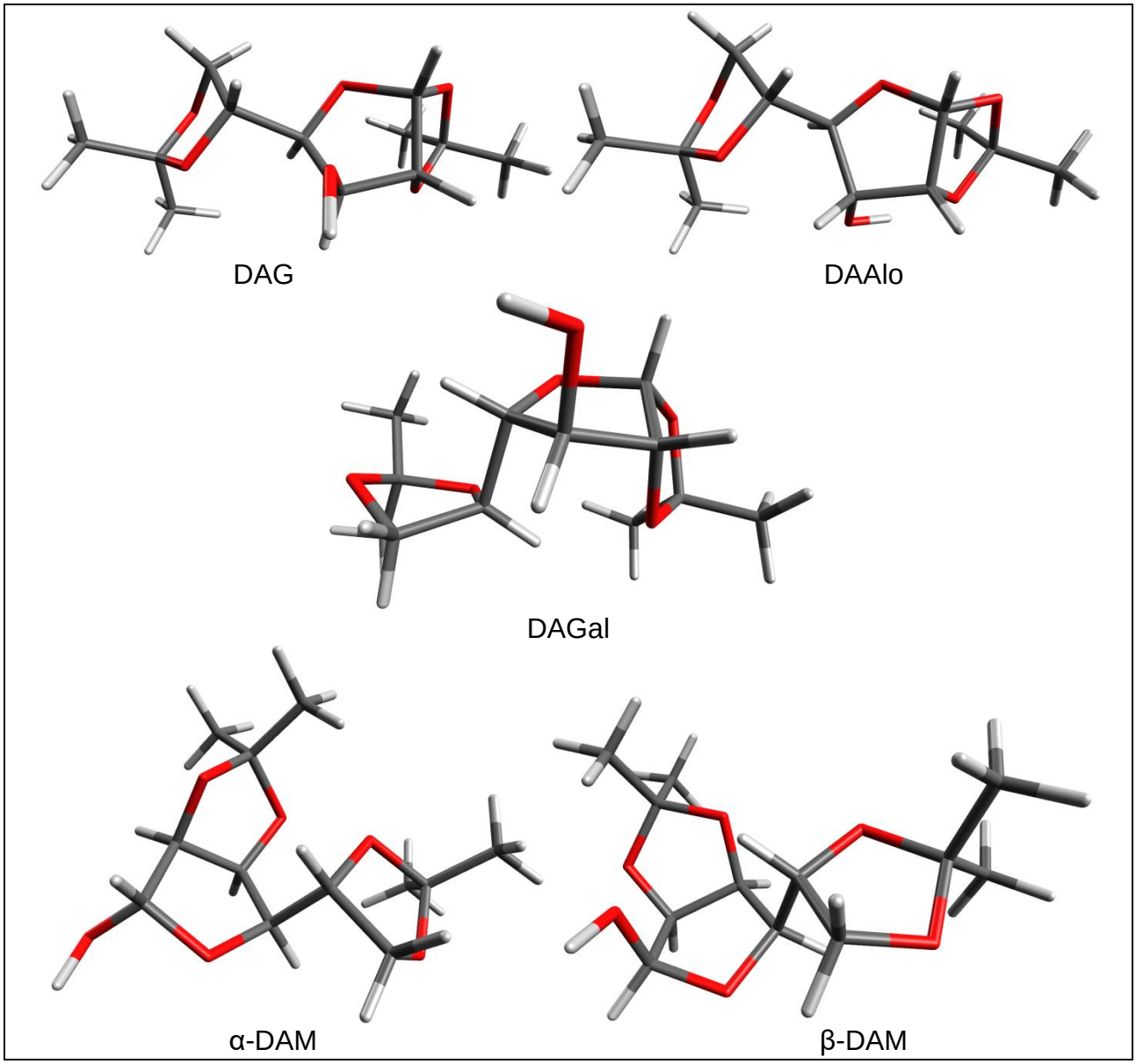

Figure 2. Molecular models obtained after running the B3LYP/3-21G optimization

The observed position of the long bond generally coincides with our previous results obtained using the RM1 and PM7 semi-empirical methods.

Table 3. Angle values (degrees) obtained for the studied radical cations

Compound	STO-3G			3-21G		
	O4-C4-C5	O5-C5-C4	O4-C4-C5-O5	O4-C4-C5	O5-C5-C4	O4-C4-C5-O5
DAG	113.4	108.1	117.6	105.8	105.3	176.2
DAAlo	115.8	108.2	-134.7	111.1	108.3	-162.1
DAGal	112.6	111.6	71.2	112.1	108.5	-42.7
α-DAM	112.5	110.7	-138.5	107.3	110.2	-161.5
β-DAM	110.7	110.2	-143.5	109.5	107.5	166.8

Conclusion

In contrast with our previous results [2,3] obtained using the RM1 and PM7 semi-empirical methods, which give long bonds of slightly over 2 Å, the DFT methods applied offered long bonds of maximum 1.712 Å. The 3-21G basis set seems to give better results with respect to the long bond location, when compared with the more simple STO-3G basis set.

Acknowledgements

This work was supported by the Romanian National Authority for Scientific Research (CNCS-UEFISCDI) through project PN-II-PCCA-2011-142. Part of the research was performed at the Center of Genomic Medicine of the "Victor Babeș" University of Medicine and Pharmacy of Timisoara, POSCCE 185/48749, contract 677/09.04.2015.

References

[1] D.J. Bellvile, R.A. Pabon, N.L. Bauld, J. Am. Chem. Soc. 107 (1985) 4978.
[2] M.C. Pascariu, M. Rafailă, M. Medeleanu, V. Badea, A.T. Gruia, V.L. Purcarea, M. Penescu, E. Sisu, Farmacia (Bucharest, Romania) 64 (2016) 553.
[3] M.C. Pascariu, L.A. Bozin, A. Șerb, N. Dincă, E. Șișu, Proceedings of The 21st International Symposium on Analytical and Environmental Problems, September 28, 2015, Szeged, Hungary, pp. 247.
[4] HyperChem™ Professional, Hypercube, Inc., 1115 NW 4th Street, Gainesville, Florida 32601, USA, version 8.0.10 for Windows.
[5] G.B. Rocha, R.O. Freire, A.M. Simas, J.J.P. Stewart, J. Comput. Chem. 27 (2006) 1101.
[6] M.J. Frisch, G.W. Trucks, H.B. Schlegel, G.E. Scuseria, M.A. Robb, J.R. Cheeseman, G. Scalmani, V. Barone, B. Mennucci, G.A. Petersson, H. Nakatsuji, M. Caricato, X. Li, H.P. Hratchian, A.F. Izmaylov, J. Bloino, G. Zheng, J.L. Sonnenberg, M. Hada, M. Ehara, K. Toyota, R. Fukuda, J. Hasegawa, M. Ishida, T. Nakajima, Y. Honda, O. Kitao, H. Nakai, T. Vreven, J.A. Montgomery, Jr., J.E. Peralta, F. Ogliaro, M. Bearpark, J.J. Heyd, E. Brothers, K.N. Kudin, V.N. Staroverov, T. Keith, R. Kobayashi, J. Normand, K. Raghavachari, A. Rendell, J.C. Burant, S.S. Iyengar, J. Tomasi, M. Cossi, N. Rega, J.M. Millam, M. Klene, J.E. Knox, J.B. Cross, V. Bakken, C. Adamo, J. Jaramillo, R. Gomperts, R.E. Stratmann, O. Yazyev, A.J. Austin, R. Cammi, C. Pomelli, J.W. Ochterski, R.L. Martin, K. Morokuma, V.G. Zakrzewski, G.A. Voth, P. Salvador, J.J. Dannenberg, S. Dapprich, A.D. Daniels, O. Farkas, J.B. Foresman, J.V. Ortiz, J. Cioslowski, D.J. Fox, Gaussian 09, Revision B.01, Gaussian, Inc., Wallingford CT, 2010.

TEM, EDX AND RAMAN STUDY OF NICKEL OXIDE MICRO- AND NANOPHASES OBTAINED BY THERMAL DECOMPOSITION OF AN ORGANOMETALLIC PRECURSOR

Mircea Niculescu[1,2*], Andrei Racu[3], Petrică Linul[3], Bogdan Tăranu[3], Mihai-Cosmin Pascariu[2,3,4*]

[1]University Politehnica Timişoara, Faculty of Industrial Chemistry and Environmental Engineering, Department of Applied Chemistry and Engineering of Inorganic Compounds and Environment, 6 Vasile Pârvan Blvd., RO-300223, Timișoara, Romania
[2]"Chemeia Semper" Association, 6 Giuseppe Verdi, RO-300493, Timişoara, Romania
[3]National Institute of Research and Development for Electrochemistry and Condensed Matter – INCEMC Timişoara, Renewable Energies - Photovoltaic Laboratory, 144 Dr. Aurel Păunescu Podeanu, RO-300569, Timişoara, Romania
[4]"Vasile Goldiş" Western University of Arad, Faculty of Pharmacy, Department of Pharmaceutical Sciences, 86 Liviu Rebreanu, RO-310045, Arad, Romania
e-mail: mniculescuro@yahoo.com, mihai.cosmin.pascariu@gmail.com

Abstract
Nickel(II) polyoxalate was thermally decomposed to nickel oxide in both oxidative and inert atmospheres and the products were investigated using TEM-EDX and Raman spectroscopy. The resulting micro- and nanoparticles were compared regarding their size, morphology and composition. In dynamic aerobic conditions, the product obtained at 1000 °C shows better crystallinity and presents more well defined shapes than the one obtained at 400 °C. The 1000 °C product obtained in argon is a mixture of NiO and metallic Ni.

Introduction
The thermal conversion of coordination compounds to metal oxides is a convenient way to produce micro- and nanoparticles with defined properties (degree of crystallinity, size, morphology and surface area), which make them useful for a variety of applications. For example, nanosized nickel oxide exhibits anomalous electronic and magnetic properties and can be used for catalysis, electrochromic windows and sensors. In this paper we have investigated the nickel oxide obtained through the thermal conversion of a complex compound, namely nickel(II) polyoxalate hydrate [1], in both aerobic (at 400 and 1000 °C) and inert (at 1000 °C) atmospheres.

Experimental
The nickel(II) polyoxalate hydrate was prepared starting from nickel(II) nitrate and ethylene glycol by using an original method, as described in a previous paper [1].
The Raman spectrum was measured at room temperature using a MultiView 1000 system (Nanonics Imaging, Israel), which incorporates the Shamrock 500i Spectrograph (Andor, UK). A laser wavelength of 514.5 nm was used as the excitation source, with a 20 s exposure time and a 300 l mm^{-1} grating.
For the TEM analyses, the material was deposited from ethanol on a 200 mesh TEM copper grid covered with lacey carbon film. We used a Titan G2 80-200 TEM/STEM (FEI Company, the Netherlands) instrument with image correction. The images were registered at 200 kV accelerating voltage. A Digital Micrograph v.2.12.1579.0 software was used for images recorded in TEM mode, while a TEM Imaging & Analysis v.4.7 software was used for recording the EDX

spectrum. The STEM-EDX elemental distribution maps were recorded with the Esprit v.1.9 software.

Results and discussion

The global decomposition process, which takes place during both aerobic (+ O_2) and inert (- CO) heating of the homopolynuclear coordination compound, can be illustrated as shown below:

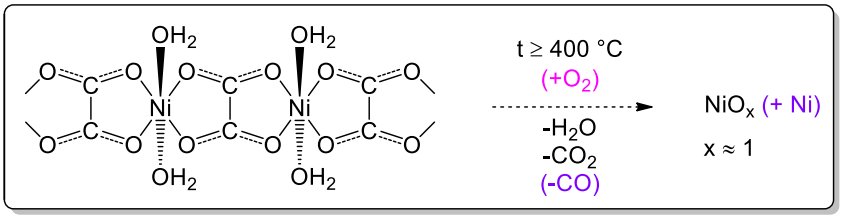

The particles obtained in aerobic conditions at 400 °C (**Fig. 1**) exhibit irregular shapes with microporous structure and with dimensions dispersed between 15 nm and 2.1 μm; the monocrystalline areas are rather small (14 nm at most) and have the crystalline planes distanced at about 2.27 Å, as seen using HRTEM. On the other hand, the aerobic samples produced at 1000 °C (**Fig. 2**) are composed of 50-750 nm polyhedrons, with extended monocrystalline areas composed of crystal planes distanced at about 2.15 Å. Lastly, the particles obtained at 1000 °C in argon (**Fig. 3**) consist of 60-220 nm parallelepipeds which present wide monocrystalline areas (2.47 Å between the crystalline planes) that are composed mostly of NiO, but also seem to contain metallic Ni particles as large as 2.6 μm in diameter (**Fig. 4**), as shown by EDX.

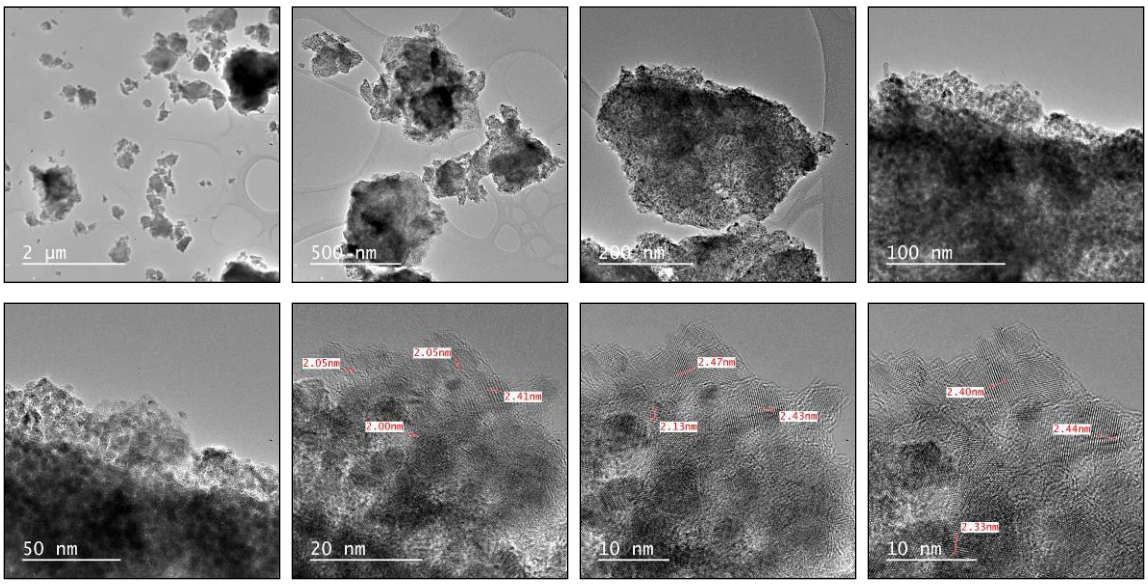

Figure 1. TEM images of the 400 °C aerobic decomposition product (mostly NiO)

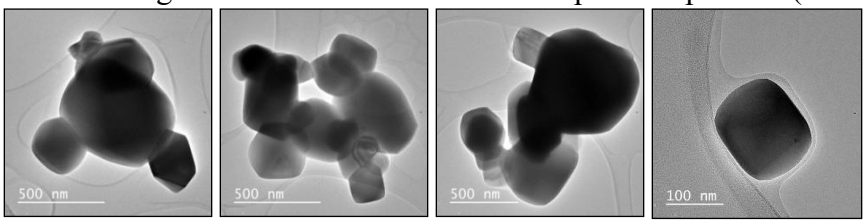

Figure 2. TEM images of the 1000 °C aerobic decomposition product (NiO)

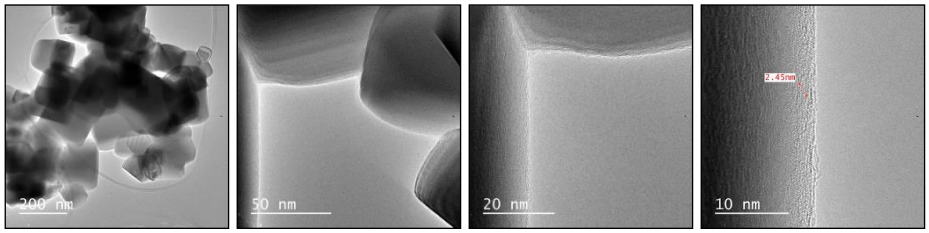

Figure 3. TEM images of the 1000 °C argon decomposition product, which show NiO nanocrystals

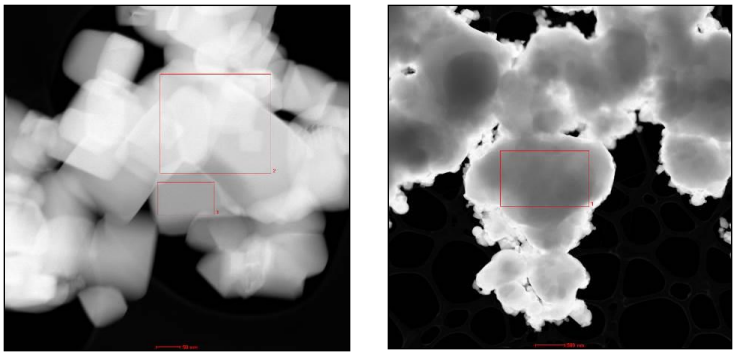

Figure 4. STEM images of the 1000 °C argon decomposition product; EDX analysis revealed mostly NiO in the two areas from the left image and mostly metallic Ni in the area from the right image

The EDX profile obtained for the aerobic 400 °C product is shown in **Fig. 5**, and is similar in shape to the one obtained in aerobic conditions at 1000 °C. The determined atomic ratios suggest a $NiO_{1.37}$ formula in the former case, and a $NiO_{0.82}$ formula in the latter.

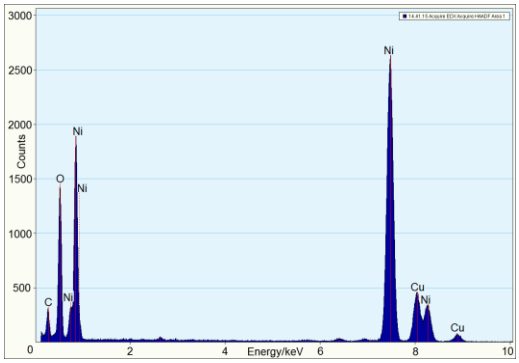

Figure 5. EDX profile in a surface area of the product obtained by aerobic thermal conversion of the complex compound at 400 °C (C and Cu peaks belong to the grid)

The EDX profiles for two distinct particles (**Fig. 4**) of the product obtained by the coordination compound's annealing in argon at1000°C are shown in **Fig. 6**. The analysis of the two selected surface areas reveals that this product is a mixture of NiO and metallic Ni.

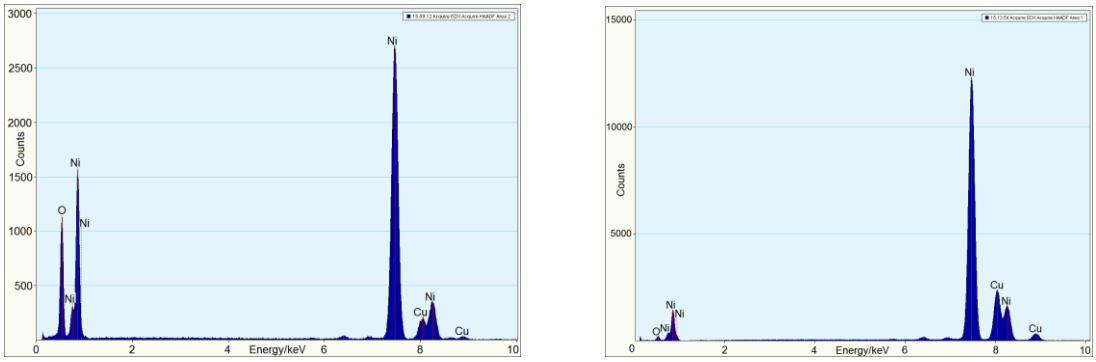

Figure 6. EDX profiles corresponding to the surface areas shown in **Fig. 4** (C and Cu peaks belong to the grid): left $NiO_{0.87}$, right metallic nickel (Ni > 97 atomic %)

The Raman spectrum of the final argon decomposition product is shown in **Fig. 7**. Peaks due to one-phonon (553 cm^{-1}), two-phonon (709, 892 and 1086 cm^{-1}) and two-magnon (1369 cm^{-1}) scattering for NiO [2] are all present.

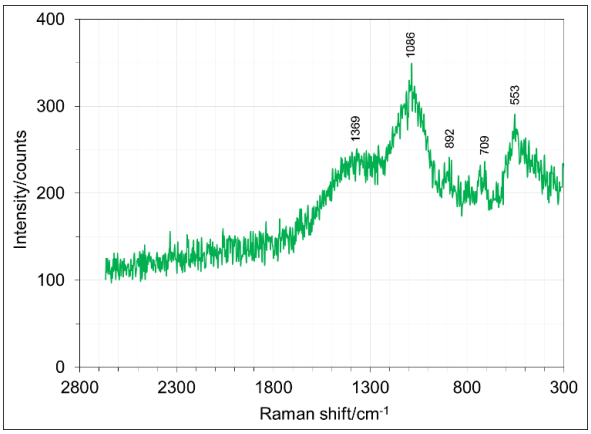

Figure 7. RAMAN spectrum of the 1000 °C argon decomposition product

Conclusions

The thermal conversion of the nickel(II) polyoxalate hydrate gave mostly NiO, which also contains some metallic Ni when inert (argon) dynamic atmosphere is used. The samples obtained at 1000 °C show more well defined edges and larger monocrystalline areas than the ones obtained at 400 °C.

Acknowledgements

Part of this research was done at the Center of Genomic Medicine of the "Victor Babeş" University of Medicine and Pharmacy of Timişoara, POSCCE 185/48749, contract 677/09.04.2015.

References

[1] M. Niculescu, M.C. Pascariu, C. Muntean, J. Therm. Anal. Calorim. (2016), *in press*.
[2] N. Mironova-Ulmane, A. Kuzmin, I. Steins, J. Grabis, I. Sildos, M. Pärs, J. Phys.: Conf. Ser. 93 (2007) 012039, doi:10.1088/1742-6596/93/1/012039.

ELECTROCHEMICAL DETECTION OF PARAQUAT FROM WATER USING PLATINUM MODIFIED BDD ELECTRODE

Aniela Pop[1*], Rodica Pode[1], Corina Orha[2], Florica Manea[1]

[1]Faculty of Industrial Chemistry and Environmental Engineering, Politehnica University of Timisoara, 6 V. Parvan Bd., 300223 Timisoara, Romania
[2]National Condensed Matter Department, Institute for Research and Development in Electrochemistry and Condensed Matter, Timisoara, 1 P. Andronescu Street, 300254 Timisoara, Romania
e-mail: aniela.pop@upt.ro

Abstract
Voltammetric and amperometric detection of paraquat (PQ) herbicide from aqueous solutions has been successfully achieved using a boron-doped diamond (BDD) electrode modified with platinum particles. Electrochemical deposition of platinum was performed by chronoamperometry technique operated at two potential levels, *i.e.*, -0.15 V for 1 s and 0.1 V for 6s. Operational parameters of electrochemical techniques tested in detection application were determined in order to achieve superior electroanalytical performances for quantitative assessment of paraquat concentration at trace level. Both cyclic voltammetry and multiple-pulsed amperometry exhibited best electroanalytical performances in terms of sensitivity and lowest detection limit, in comparison with the other applied voltammetric pulsed techniques.

Introduction
Paraquat (PQ) is a very toxic biquaternary ammonium compound usually synthesized as dichloride salt (Fig. 1). PQ is used as a quick-acting herbicide that destroy non-selectively the green plants by direct contact or by translocation within the plant [1]. PQ is adsorbed rapidly into soil, especially in the clay mineral lattice sheet, and then, it arrives into groundwater easily by leaching due to its high solubility of 620 g/L at 25 ^{o}C [1]. This compound have a long persistence into environment due to its non-biodegradability. Its toxicity affect all living organisms, and the accidental or deliberate ingestion could be lethal or cause acute poisoning [2].

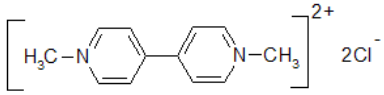

Figure 1. Structural formula of Paraquat

In European Union (EU) this pesticide was banned since 2007, but it is still used in nearly 90 countries all over the world in tobacco, apples, citric fruits, and other around 100 crops [3]. Several publications have been focused on the quantification of the organochlorine residue presence, including paraquat, in surface waters, sediments, biota and vegetation [4,5].
Electrochemical techniques could represent a simple, fast and sensitive alternative for the quantitative assessment of paraquat from water.
The aim of this paper is to modify a BDD electrode with platinum particles in order to obtain a sensitive sensor able to detect paraquat at very low concentration, up to 10^{-9} M. Cyclic voltammetry (CV), differential-pulsed voltammetry (DPV), square-wave voltammetry (SWV) and multiple pulse amperometry (MPA) were assessed in order to find the best operational condition for paraquat detection from water.

Experimental

A commercial BDD electrode, provided by Windsor Scientific has been modified with platinum particles by electrochemical deposition. Platinum electrodeposition was performed in galvanostatic regime, through chronoamperometry technique operated at two potential levels, the first of -0.15 V for 1 s and the second of 0.1 V for 6s and Pt-modified electrode was obtained, named BDD-Pt. All the electrochemical experiments were performed using an Autolab potentiostat/galvanostat PGSTAT 302 (EcoChemie, The Netherlands), with a standard three electrode cell with the BDD-Pt as working electrode, platinum sheet as counter electrode and saturated calomel electrode as reference electrode. Solution of 0.1 M sodium sulfate (Merck) and 1 mM PQ (Pestanal, Sigma-Aldrich) were freshly prepared with distillated water.

Results and discussion

Cyclic voltammetry

The first electrochemical technique used in order to characterize the behavior of BDD-Pt electrode in the presence of PQ and also, as electrochemical detection method was cycling voltammetry. The tests were performed in 0.1 M Na_2SO_4 supporting electrolyte, in the potential range between -1.25 V/SCE and 0 V/SCE. The reduction process of PQ occurred at the potential value of -0.72 V/SCE, and the useful cathodic signal increased with the PQ concentration from 0.2 µM to 1.2 µM. At higher concentration, a fouling of the electrode surface was noticed, probably due to the formation of an insulating layer on the electrode active surface.

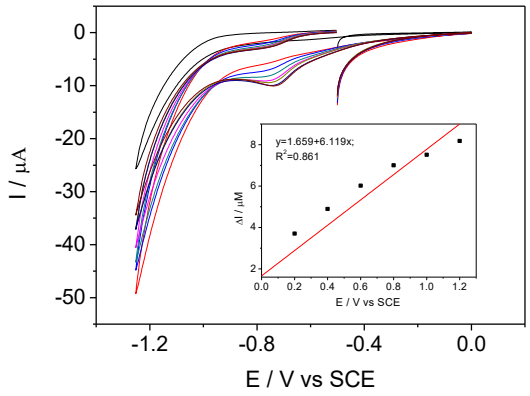

Figure 1. Cyclic voltammograms (CVs) recorded on BDD-Pt electrode in 0.1 M Na_2SO_4 supporting electrolyte (1) and in the presence of different PQ concentrations: 1-0 mM; 2-0.2 µM; 3-0.4 µM; 4-0.6 µM; 5-0.8 µM; 6-1.0 µM; 7-1.2 µM; 8-1.4 µM, scan rate: 50 $mV \cdot s^{-1}$. Inset: Calibration plot of dependence between cathodic peak current recorded at potential of-0.73 V vs SCE on BDD-Pt electrode and PQ concentration.

Pulsed Voltammetric Techniques

Taking into account the advantages of pulsed-voltammetric techniques, *e.g.*, rapid analyses time, , increased useful signal minimized effect of the background noise andgood reproducibility, differential-pulsed voltammetry (DPV) and square-wave voltammetry (SWV) were tested at different operational parameters in order to select the optimum conditions. The choosen operation parameters for DPV were: scan rate (v) of 50 $mV \cdot s^{-1}$, step potential (SP) of 10 mV, modulation time (Mt) of 0.1 s and modulation amplitude (MA) of 25 mV. Despite of the lower sensitivity value recorded by DPV on BDD-Pt electrode in comparison with the other tested techniques for PQ electrochemical quantification, no electrode fouling occured in the concentration range of

0.2µM - 5.0 µM, and a well-defined PQ reduction peak can be observed at the potential of -0.69 V/SCE (Fig. 2).

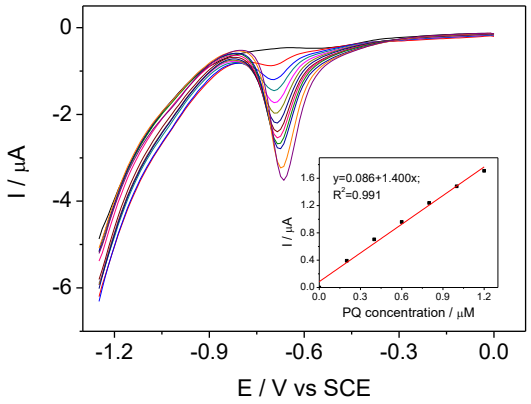

Figure 2. Differential-pulsed voltammograms recorded on BDD-Pt electrode in Na_2SO_4 0.1 M supporting electrolyte (1) and in the presence of different PQ concentrations: 2-0.2 µM; 3-0.4 µM; 4-0.6 µM; 5-0.8 µM; 6-1.0 µM; 7-1.2 µM; 8-1.4 µM; 9-1.8 µM; 10-2.0 µM; 11-3.0 µM; 12-4.0 µM; 13-5.0 µM. Inset: calibration plot of cathodic peak current vs PQ concentration.

SWV was performed in three different operational parameter conditions, and better electroanalitical performaces for this technique were recorded at a scan rate of 50 $mV \cdot s^{-1}$, a frequency of 25Hz, a step potential of 4mV and an amplitude of A=50mV (Table 1).

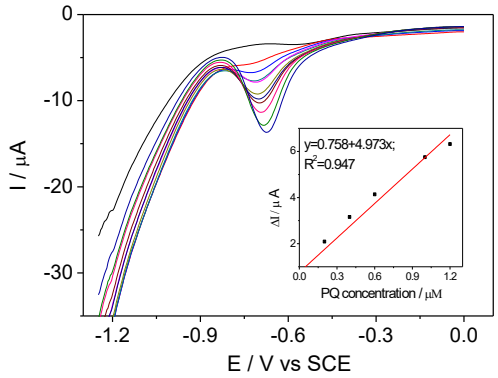

Figure 3. Square-wave voltammograms recorded recorded on BDD-Pt electrode in 0.1 M Na_2SO_4 supporting electrolyte (1) and in the presence of different PQ concentrations: 2-0.2 µM; 3-0.4 µM; 4-0.6 µM; 5-0.8 µM; 6-1.0 µM; 7-1.2 µM; 8-1.4 µM; 9-1.8 µM; 10-2.0 µM; 11-3.0 µM; 12-4.0 µM. Inset: calibration plot of cathodic peak current vs PQ concentration.

Among amperometric techniques, multiple-pulsed amperometry (MPA) was testedin this paper in order to achieve better electroanalytical performances for PQ detection. The lowest detection limit of 3.9 nM was achieved by this techniqueat an applied potential of -0.72 V/SCE. The electrode sensitivity was superior to the pulsed-voltametric techniques, but equal to the one recorded by cyclic voltammetry (Table 1). The role of *in-situ* cleaning step is envisaged by the recorded enhanced useful signal during continuous amperometric detection of PQ by MPA.

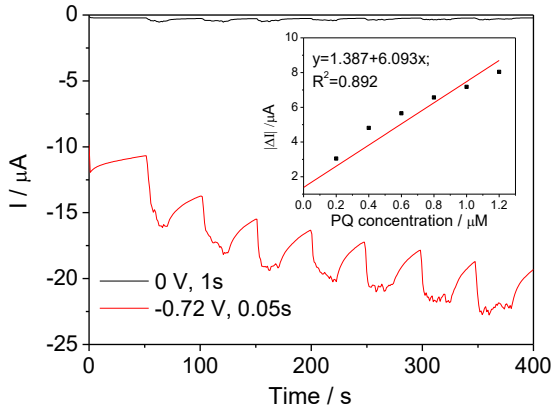

Figure 4. Multiple-pulse amperomgram recorded recorded on BDD-Pt electrode in 0.1 M Na_2SO_4 supporting electrolyte (1) and in the presence of different PQ concentrations: 2-0.2 µM; 3-0.4 µM; 4-0.6 µM; 5-0.8 µM; 6-1.0 µM; 7-1.2 µM; 8-1.4 µM. Inset: calibration plot of anodic peak current recorded at potential of -0.72 V/SCE vs PQ concentration.

Table 1. Electroanalytical performances recorded for PQ detection

Technique	Conc. range (µM)	Parameters	E / V	Sensitivity m (µA/µM)	LOD (µM)	LOQ (µM)	R^2
CV	0.2-1.2	0.05 V/s	-0.73	6.119	0.0041	0.0137	0.861
DPV	0.2-1.2	Mt=0.05s; It=0.1s; MA=25 mV; sp=10 mV	-0.69	1.400	0.0157	0.0523	0.991
SWV	0.02-1.22	F=50Hz, SP=4mV; A=85mV	-0.69	4.086	0.0144	0.0480	0.995
SWV	0.2-1.2	F=25Hz; SP=4mV; A=50mV	-0.71	4.973	0.0073	0.0244	0.947
MPA	0.2-1.2	0V, 1s; -0.72V, 0.05s	-0.72	6.093	0.0039	0.0128	0.892

Conclusion

BDD-Pt modified electrode was successfully applied for detection of trace amount of PQin aqueous solution. All voltammetric and amperometric techniques exhibited useful features for PQ detection from water, with very high sensitivity and lowlimits of detection (LOD) and quantification (LOQ) in the optimal determined conditions of CV and MPA technigue.

Acknowledgements

Funding for this study was provided by the Romanian National Research Programs PN-II-TE-123/2015 and WATUSER PN-II-PCCA-60/2012.

References

[1] K. Tyszczuk-Rotko, I. Bęczkowska, A. Nosal-Wiercińska, Diamond Relat. Mater. 50 (2014) 86.
[2] A. Farahi, M. Achak, L. El Gaini, M. A. El Mhammedi, M. Bakasse, J. Food Drug Anal. 23 (2015) 463.
[3] I.R. Pizzutti, G.M.E. Vela, A.de Kok, J.M. Scholten, J.V. Dias, C.D. Cardoso, G. Concenço, R. Vivian, Food Chemistry 209 (2016) 248.
[4] T.O. Ikpesu, Environ Sci Pollut Res 22 (2015) 8517.
[5] G.O. Olutona, S.O. Olatunji, J. F. Obisanya, SpringerPlus 5:67 (2016) 1.

BIOLOGICAL ACTIVITY OF CARUM CARVI ON TRIBOLIUM CONFUSUM (COLEOPTERA, TENEBRIONIDAE) ADULTS

Aleksandra Popović[1*], Miloš Petrović[1], Jovana Šućur[1], Milica Aćimović[2], Tijana Stojanović[1], Aleksandra Petrović[1], Vojislava Bursić[1], Dušan Marinković[1]

[1]*University of Novi Sad, Faculty of Agriculture, 21000 Novi Sad,Trg D. Obradovića 8, Serbia*
[2]*Institute of Field and Vegetable Crops, 21000 Novi Sad, Maksima Gorkog 30,Serbia*
popovica@polj.uns.ac.rs

Abstract

Tribolium confusum duVal, 1863 (Coleoptera: Tenebrionidae) is one of the most serious pests in stored grain and related products. *T. confusum* was reared on a diet of wheat flour. The colonies were maintained in a growth chamber (Witeg, Germany, Model: GC-450) at 25±1oC, 45-50% r.h. Only adults were used for the experiments. The aerial parts of *Carum carvi* L. plants were collected from the Mošorin village, Vojvodina region (N 45o 18' 21.5'' E 20o 10' 53.9'', 90 m above sea level) on the 15 May 2015. The bioassays were carried out using groups of ten adult insects of *T. confusum*.The experiment was set in four replicates and control. The 50µl of known concentrations (6,32µl/l, 5,17µl/l, 4,02µl/l, 2,87µl/l, 2,3µl/l) of *C.carvi* was applied on filter papers. Mortality was determined 24h, 48h and 72h after the treatment.The highest concentrations 6,32 µl/l and 5,17 µl/l led to death more than 50% of insect population, after 48h and 72h. Also, lower concentartion showed strong insecticidal effect, where the mortality rate was 52,5% after 48h at the concentration of 4,02 µl/l and 47,5% at the concentration of 2,87µl/l.

Introduction

Tribolium confusum duVal, 1863 (Coleoptera: Tenebrionidae) is one of the most serious pests in stored grain and related products. It is considered as a secondary pest, which can easily infest damaged or broken kernels, and apart from grain, it is particularly destructive to flour and other processed grain products [1].

Concerns over health and environmental problems associated with synthetic insecticides currently in use in agriculture have led to an intensification of efforts to find safe, effective and viable alternatives. In this regard plant-based insecticides (PBIs) as described by Rosenthal [2] can be less toxic to man, readily biodegradable, suitable for use by small scale farmers and yet capable of protecting crops from attack by a wide range of insect pests [3]. Essential oils (EO) are complex mixtures of volatile compounds isolated from a large number of plants [4]. Generally EOs are less toxic to mammals and the environment than conventional insecticides, they degrade rapidly and do not accumulate in the environment [5].

Experimental

Test insects

T. confusum colonies were maintained in the laboratory of the Department of Environment and Plant Protection, Factulty of Agriculture, University of Novi Sad, without exposure to any insecticide. Insects were reared in plastic container (22 cm length x 10 cm height) covered by fine mesh cloth for sufficient ventilation. *T. confusum* was reared on a diet of wheat flour. The colonies were maintained in a growth chamber (Witeg, Germany, Model: GC-450) at 25±1oC, 45-50% r.h. Only adults were used for the experiments.

Plant material and essential oil isolation

The aerial parts of *Carumcarvi* L. (caraway) plants were collected from the Mošorin village, Vojvodina region (N 45o 18' 21.5'' E 20o 10' 53.9'', 90 m above sea level) on the 15. May 2015. The air-dried plant material (30g) was submitted to hydro-distillation using a Clenger-type apparatus for 3h. The oils were dried over anhydrous sodium sulphate and stored in a sealed vial at -20oC before analysis. The yield of essential oils was 4.1%.

Toxicity test

The bioassays were carried out using groups of ten adult insects of *T. confusum*. All the insects were starved for 24h before tests.The experiment was set in four replicates and control. The 50µl of known concentrations (6,32µl/l, 5,17µl/l, 4,02µl/l, 2,87µl/l, 2,3µl/l) of *C.carvi* was applied on filter paper. Flour disks have been added to avoid insect starvation. The treated filter papers were left on the room temperature for 5 min to allow the n-hexane to evaporate and dry. After drying, the treated filter papers were introduced into petri dishes which contained insects. To compare the toxicity of tested EO, filter papers with 50µl n-hexane served as a control. After placing filter papers, in the petri dishes, petri dishes were sealed with the parafilm. Mortality was determined 24h, 48h and 72h after the treatment. Treated insects were held in dark at 25±1^{o}C, 45-50% r.h. Adults were considered dead if legs and antennae did not move when observed under stereo zoom microscope (Motic, SMZ 171).

Results and discussion

Table 1 shows mortality rate of *T. confusum* adults. Concentrations, which were used, caused mortality of tested insects. After 24h, the highest concentrations (6,32 µl/l and 5,17 µl/l) caused death of the largest number of insects 45% and 25% and the diference beatween these two mortality rates was significant. After 48h, again the highest concentrations (6,32 µl/l and 5,17 µl/l) affected mortality of 77,5% and 60%. The similar situation was after 72h, when the number of died insects was also in the range from 60% to 80%. Lower concentration 4,02 µl/l caused over 50% of moratlity after 48h and 72h. The death of insects was the lowest at the concentartions 2,87 µl/l and 2,3 µl/l and on the first day moratlity rates were 5% and 2,5% and the last day were 47,5% and 32,5% (Figure 1).

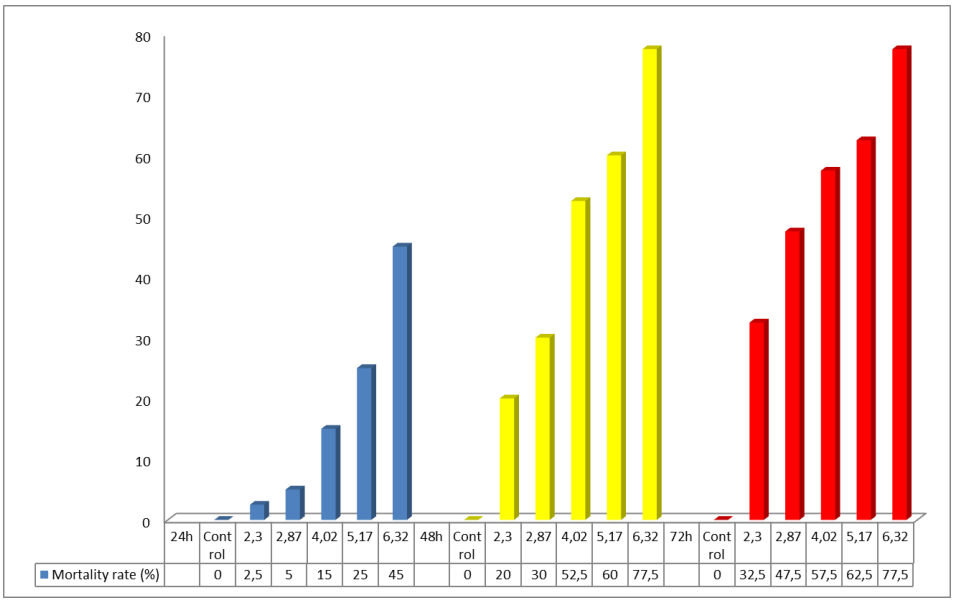

Figure 1. Moratlity of *T. confusum* after exposition of essential oil of *C. carvi*

Table 1. Number of died insects after applying essential oil of *C.carvi*

24h	Replicates				
Concentration (µL/L)	1.	2.	3.	4.	Mortality rate (%)
6,32	5	4	5	4	45,0
5,17	4	2	1	3	25,0
4,02	1	0	3	2	15,0
2,87	1	0	0	1	5,0
2,3	1	0	0	0	2,5
control	0	0	0	0	0
After 8h	Replicates				
Concentration (µL/L)	1.	2.	3.	4.	Mortality rate (%)
6,32	8	9	8	6	77,5
5,17	7	7	4	6	60,0
4,02	5	4	6	6	52,5
2,87	2	5	2	3	30,0
2,3	1	1	3	3	20,0
control	0	0	0	0	0
Nakon72h	Replicates				
Concentration (µL/L)	1.	2.	3.	4.	Mortality rate (%)
6,32	8	9	8	6	77,5
5,17	7	7	4	7	62,5
4,02	6	4	7	6	57,5
2,87	5	6	3	5	47,5
2,3	2	1	6	4	32,5
control	0	0	0	0	0

According to the [6] the essential oil of *Carumcarvi* fruits shows strong contact toxicity against *Sitophilus zeamais* and *Tribolium castaneum* adults with LD_{50} values of 3.07 and 3.39 µg/adult.

Furthermore, the essential oil of *C. carvi* has been demonstrated to possess strong contactand fumigant toxicity as well as repellency against several insects and mites, e.g. Japanese termite (*Reticulitermes speratus*), rice weevil (*S. oryzae*), sciarid fly *Lycoriella ingenua* larvae, the two-spotted spider mite *Tetranychus urticae* and its predator *Phytoseiulus persimilis*. The same authors mentioned that the insecticidal activity of the essential oil of caraway (*Carum carvi*) was investigated for the control of greenhouse whitefly (*Trialeurodes vaporariorum*). The results indicated that essential oil from caraway were the most effective at concentrations of 5 ppm (82. 95%) [7].

Conclusion

Different concentartions of essentail oil indicated very strong insecticidal activity. The highest concentartions (6,32µL/L and 5,17µL/L) caused mortality rate above 50% after 48h. Taking into account results of this experiment and other authors, it could be concluded that essential oil of caraway possesses strong insecticidal effect and it can be used as alternative method in the control of harmful insects.

References

[1] B. J. Vayias, C. G. Athanassious, D. N. Milonas, C. Mavrotas, Persistence and efficacy of

spinosad on wheat, maize and barley grains against four major stored product pests. Crop. Prot. 29, (2010)496-505.
[2] G.A Rosenthal, The chemical defense of higher plants. Scientific American Jan. (1986) 94–99.
[3] A.L.Tapondjou, C. Adler, D.A. Fontem, H.Bouda, C. Reichmuth, Bioactivities of cymol and essential oils of Cupressus sempervirens and Eucalyptus saligna against Sitophilus zeamais Motschulsky and Tribolium confusum du Val, Journal of Stored Products Research 41 (2005) 91–102
[4] D. Dussault, K. D. Vu, M. Lacroix: In vitro evaluation of antimicrobial activities of various commercial essential oils, oleoresin and pure compounds against food pathogens and application in ham. Meat Sci. 96, 514-520 (2014).
[5] V.Rozman, I. Kalinović, Z. Korunić:Toxicity of naturally occurring compounds of Lamiaceae and Lauraceae to three stored products insects. J. Stored Prod. Res. 43, 349-355 (2007).
[6] R. Fang, C. H. Jiang, X.Y. Wang, H. M. Zhang, Z. L. Liu, L. Zhou, S. S. Du, Z. W. Deng, Insecticidal Activity of Essential Oil of *Carum Carvi* Fruits from China and Its Main Components against Two Grain Storage Insects, Molecules, 15 (2010) 9391-9402
[7] P. Agrahari, D. K. Singh, A review on the pharmacological aspects of *Carum carvi*,J. Biologyand Earth Sci. 4(1), (2014),7

ANTIOXIDATIVE RESPONSE OF POPLAR TISSUE CULTURE EXPOSED TO PEG 6000

Popović M. Boris[1], Štajner Dubravka[1], Ždero Pavlović Ružica[1*], Blagojević Bojana[1], Galović Vladislava[2]

[1]Department of Field and Vegetable Crops, Faculty of Agriculture, University of Novi Sad, Trg Dositeja Obradovića 8, 21000 Novi Sad, Serbia
[2]Institute of Lowland Forestry and Environment, University of Novi Sad, Antona Čehova 13, 21000 Novi Sad, Serbia
e-mail: ruzica.zdero@polj.uns.ac.rs

Abstract
The aim of this work was to investigate the influence of the water deficit in poplar tissue culture (M-1 genotype) through proline content, level of lipid peroxidation and activities of antioxidative enzymes. Plants were exposed to PEG 6000 (100 and 200 mOsm) in *in vitro* conditions for 6 days. Malondialdehyde (MDA) content showed an increase only at 200 mOsm stress. Under the 100 mOsm stress, catalase and guaiacol peroxidase activities were induces indicating their important role in elimination of reactive oxygen species (ROS). Under the 200 mOsm stress, superoxide dismutase and guaiacol peroxidase activities were induced.

Introduction
During drought stress the production of ROS is dramatically elevated. Reactive oxygen species, including superoxide anion, hydroxyl radical and hydrogen peroxide, are derived from oxygen. As a response to ROS accumulation plants activate antioxidative enzymes such as catalase (CAT), non-specific peroxidase and superoxide dismutase (SOD) that cooperate together to mitigate cellular damages like unspecific oxidation of proteins, membrane lipids and nucleic acids [1]. Numerous studies have shown that proline content in higher plants increases under different abiotic stresses [2]. An osmoprotective function as well as antioxidant function of proline has been demonstrated [3].
The aim of this work was to study the variation in proline content, antioxidative enzymes activity (SOD, CAT, and guaoacol peroxidise (GPx)) and level of lipid peroxidation in poplar tissue culture imposed to different levels of PEG 6000.

Experimental
Culture tissue of *Populus canadensis* clone M-1 was obtained from the Institute of Lowland Forestry and Environment (Novi Sad). Calli were cultured on MS medium [4] containing 4 g/L MS, 10g/L sucrose, 3 g/L agar-agar and 0.5 g/L gerlit, pH 5.8 in the absence or presence of 100 and 200 g l^{-1} PEG 6000 (PEG 6000, Aldrich, Germany). After 6 days of treatment extracts were prepared for biochemical analyses.

Enzyme activity assays and soluble proteins
The SOD activity was assayed by measuring the ability of the enzyme extract to inhibit the photochemical reduction of nitro-blue tetrazolium [5]. One unit of SOD activity was defined as the amount of enzyme required to produce a 50% inhibition of reduction of NBT at 560 nm. GPx activity was analysed by measuring peroxidation of hydrogen peroxide with guaiacol as an electron donor at 436 nm [6]. Catalase activity was assayed according to Aebi [7]. The decomposition of H_2O_2 was followed spectrophotometrically by the decrease in A_{240}. One unit of

catalase activity corresponded to the amount of enzyme that decomposes 1 μmol of H_2O_2 per minute. The concentration of protein was measured according to Bradford [8].

Determination of proline content

Proline was extracted from frozen tissue with sulphoslicylic acid (3%) and mixture was centrifuged for 15 minutes at 3500 g. Following the method of Bates et al [9] proline was determinate from supernatant after reaction with ninhydrin. The proline concentration is determined from a standard curve using D-Prolin.

Determinations of contents of MDA

Lipid peroxidation (LP) was measured as the amount of MDA [10]. Fresh sample (100 mg) was homogenized using 0.3% (w/v) TBA in 10% (w/v) trichloroacetic acid (TCA), heated at 95°C for 20 min and cooled in an ice bath. After centrifugation (3500 g for 10 min) the absorbance of the supernatant was read at 532 nm and corrected for non-specific turbidity by subtracting the absorbance at 600 nm. As a blank 0.3% TBA in 10% TCA solution was used. The MDA content was calculated according to the molar extinction coefficient of 155 $mM^{-1}cm^{-1}$.

Statistical analysis

Results of the biochemical parameters represent data expressed as means of determinations made in triplicates and tested by ANOVA followed by comparisons of means by the Duncan test ($p<0.05$). Data were analyzed using STATISTICA for Windows version 11.

Results and discussion

Reactive oxygen species (ROS) are generated under stress conditions and antioxidant enzymes protect the cell structures against ROS. As shown in Figure 1, activity of GPx increased under both treatments, while SOD activity was significantly increased only at 200 mOsm stress conditions. CAT activity increased significantly at 100 mOsm stress, but at the highest level of stress it was at control level. Similar results were obtained by Turkan et al [11]where was observed high and significant induction of plant peroxidases to PEG 6000 induced osmotic stress, and lower sensitivity of CAT activity.

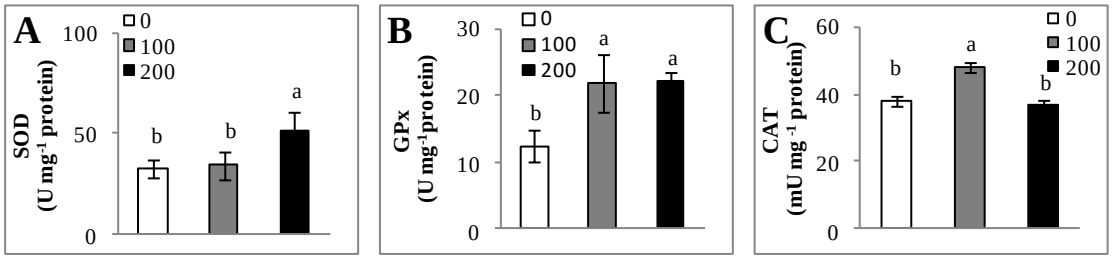

Figure 1. The effect of PEG 6000-induced stress (100 and 200 mOsm) on SOD (A), GPx (B) and CAT (C) activity in poplar tissue culture. Different letters (a, b, c) indicate statistically significant differences at ($P < 0.05$) according to Duncan test.

Abiotic stresses induced accumulation of many compounds such as ascorbate, glutathione, betaine, polyamines and proline in affected plant. In Table 1 are presented the results concerning proline accumulation in investigated tissue. The highest and significant increase of free proline was recorded by the highest stress (200 mOsm PEG 6000), by 199.34%. It is well known that proline metabolism is responsive to various environmental stresses such as drought, osmotic pressure, or ultraviolent irradiation leading to proline accumulation as a survival mechanism [3].

Results of our study agree with former finding that under NaCl treatment proline accumulation in *Populuseuphratica* callus was induced and was 5.6 times higher than in control [12].
The occurrence of MDA, a secondary end product of the oxidation of polyunsaturated fatty acids, is considered a useful index of general lipid peroxidation [13].As can be seen in Table 1 only the highest PEG 6000 concentration (200 mOsm) provoked the significant increase of MDA content (for 52.38%). Previous investigation on *Populuskangdingensis* drought affected many processes including increases in free proline, MDA and SOD activity [14].

Table 1. The effect of PEG 6000-induced stress (100 and 200 mOsm) on proline content and MDA levels in poplar tissue culture

	Proline content (µmol g^{-1} FW)	**MDA content (nmol g^{-1} FW)**
control	$422.37^{b} \pm 19.3$	$46.37^{b} \pm 4.7$
100 mOsm	$425.87^{b} \pm 34.7$	$50.00^{b} \pm 4.2$
200 mOsm	$1265.34^{a} \pm 35.4$	$70.66^{a} \pm 9.5$

*Values marked with same letter do not differ significantly at $p< 0.05$ (Duncan test)

Conclusion

Poplar tissue culture responded to 100 mOsm stress by enhanced CAT and GPX activities which could explain why stress did not cause increased level of lipid peroxidation. Under 200 mOsm conditions, stress provoked higher SOD and GPx enzyme activities and proline accumulation, but it was not enough to mitigate lipid peroxidation.

Acknowledgements

This research is part of Project no. III43002 which is financially supported by the Ministry of Science, Technologies and Development of the Republic of Serbia and IPA Planttrain project (ID: HUSBR/1203/221/173).

References

[1] D. Štajner, S. Orlović, B.M. Popović, M. Kebert, S. Stojnić, B. Klašnja, J. Chem.2013 (2012) Article ID 592695.
[2] W. Saibi, K. Feki, I. Yacoubi, F. Brini, Appl biochem biotech.176 (2015) 2107-2119.
[3] L. Szabados, A. Savoure, Trends Plant Sci. 15 (2010) 89–97.
[4] T. Murashige, F. Skoog, Physiologia plantarum, 15 (1962) 473-497.
[5] C.N. Giannopolitis, S.K. Ries, Plant physiol.59 (1977) 309-314.
[6] A. Polle, T. Otter, F. Seifert, Plant Physiol. 106 (1994) 53–60.
[7]. H. Aebi, Method enzymol.105 (1984) 121-126.
[8] M. M. Bradford, Anal. Biochem. 72 (1976) 248–253.
[9] L.S. Bates, R.P. Waldren, I.D. Teare, Plant soil.39 (1973) 205-207.
[10] R.L. Heath, L. Packer, Arch. Biochem Biophys. 25 (1968) 189–198.
[11] I. Türkan, M. Bor, F. Özdemir, H. Koca, Plant Sci.168 (2005) 223-231.
[12] F. Zhang, Y.L. Yang, W.L.He, X. Zhao, L.X. Zhang, In Vitro Cell. Dev. Biol.-Plant 40 (2004) 491-494.
[13] D.M. Hodges, J.M. DeLong, C.F. Forney, R.K. Prange,Planta. 207 (1999) 604-611.
[14] Y. Chunying, P. Youhong, Z. Runguo, Z. Yaping, L. Chunyang, Physiol. Plant. 123 (2005) 445–451.

THE IMMOBILIZATION OF COPPER FROM WASTE PRINTING DEVELOPER SLUDGE

Savka Adamović[1], Miljana Prica[1], Đurđa Kerkez[2], Jelena Tričković[2], Snežana Maletić[2], Dragan Adamović[1], Milica Velimirović[3]

[1]University of Novi Sad, Faculty of Technical Sciences, Trg Dositeja Obradovica 6, 21000 Novi Sad, Serbia
[2]University of Novi Sad, Faculty of Sciences, Trg Dositeja Obradovica 3, 21000 Novi Sad, Serbia
[3]University of Vienna, Department of Environmental Geosciences, Althanstrasse 14 UZAII,1090 Vienna, Austria
e-mail: miljana@uns.ac.rs

Abstract
The electrocoagulation (EC) treatment of the waste printing developer in laboratory conditions was produced the sludge with a high amount of copper. The solidification/stabilization (S/S) treatment of electrocoagulation sludge (ECS) has been conducted with four immobilization agents: Portland cement, calx, bentonite, and local clay. The efficiency of the S/S treatment was monitored by applying standard German (DIN 38414-4) leaching test. The characterization of ECS in terms of its toxicity was evaluated by comparing the copper concentration levels in the leaching solution with maximum allowed concentrations according to current regulations.

Key words:electrocoagulation, waste printing developer, sludge, copper, solidification/stabilization

Introduction
The term solidification/stabilization (S/S) is used for describing a wide specter of techniques for the transformation of waste into forms that are less harmful to the environment [1].
Stabilization refers to a procedure of applying different additives and/or binders, its principal goal being transforming the dangerous waste constituents into a less toxic, soluble and/or moveable form. This is achieved via chemical and/or physical processes. One of the more common stabilization methods implies adding a chemical agent that decreases the solubility of dangerous waste constituents, in that way significantly reducing their leaching into the environment [2].
Solidification implies the application of additives and binders that transform waste into a solid form that does not contain free liquid. Usually, the main goal of solidification is the transformation of waste into a form that is easier to manage and dispose of, while at the same time minimizing its harmful potential by reducing the surface of the waste that comes into contact with the environment. A chemical reaction is not implied. Besides that, a solidified waste lowers the risk of particle dissipation while managing, keeping, transporting, and disposing. Also, solidification contributes to the heightening of waste solidity and the lowering of permeability when compared to the untreated waste. The solid form gotten through solidification can be in the shape of a monolith block or solid pellets (balls) [3].
The amount and the composition of the printing waste depends on the the raw materials used, the process techniques applied and the properties to be achieved [4]. The waste printing materials are most often not geochemically stable and safe to the environment. It is generally thought that the highest potential risk comes exactly from the leaching of soluble waste pollutants when they come into contact with water. In order to successfully evaluate the potential risks of waste to

human health and the environment, it is necessary to conduct leaching tests. The main goals of the leaching tests are [5]: (i) classification of hazardous and non-hazardous waste; (ii) the assessment of the leaching potential of waste pollutants in environmental conditions; (iii) the simulation of conditions which facilitate leaching; (iv) getting samples that represent the quality of leaching water originating on landfills; (v) the assessment of the waste treatment efficacy; (vi) identification of a suitable scenario of waste management; (vii) determining the kinetic parameters for pollutant transport modeling.

During the EC treatment of the offset printing effluents the sludge with removed metals is formed as a byproduct. To solve the problem of the disposal of sludge formed after the EC treatment of the waste printing developer, the S/S treatment with Portland cement, calx, bentonite, and local clay as immobilization agents was applied.

Experimental

The electrocoagulation treatment of the waste printing developer

For the batch EC reactor, a borosilicate glass was used (250 ml in volume) with 220 ml of the waste printing developer. The EC treatment was conducted with four Fe electrodes placed at a distance of 0.5 cm. The external electrodes were connected to the DC power supply (DF 1730LCD) with constant current density of 8 mA/cm^2 during the operational time of 60 minutes [6]. A balanced stirring of the EC-treated waste printing developer was achieved by using a magnetic stirrer (IKA color squid). The sludge obtained was separated from the liquid phase by membrane filtration and dried to constant mass at 105^oC.

The characterization of the electrocoagulation sludge

The characterization of sludge of the EC-treated waste printing developer was conducted according to the pseudo-total content of heavy metals. The pseudo-total content of heavy metals in the sludge was determined by acidic digestion according to the ISO 11466:1995 method [7]. The samples obtained were analyzed by applying the AAS flame technique (Perkin Elmer AAnalyst™ 700) in accordance with the standard EPA 7000B procedure [8]. Also, the sludge characterization included the initial performance of the standard German leaching test on a raw sample of the EC-treated waste printing developer in order to determine its character.

The characterization of immobilization agents

The chemical composition of immobilization agents (Portland cement (PC), calx (C), bentonite (B), and local clay (LC)) for the S/S treatment of ECS is shown in Table 1.

Table 1. The chemical composition of immobilization agents

Compounds	Composition (%wt)			
	PC	C	B	LC
SiO_2	23.40	-	58.90	55.70
Al_2O_3	6.12	-	22.70	14.91
Fe_2O_3	3.21	-	4.83	5.78
MgO	1.01	-	1.40	2.86
CaO	63.20	99.00	1.85	5.90
K_2O	0.54	-	0.24	-
Na_2O	0.12	-	0.12	0.83
SO_3	1.18	-	-	0.22
TiO_2	-	-	-	0.80
Ignition loss	1.40	-	10.60	10.58

The S/S mixture

The S/S mixtures were created by mixing the dried ECS with immobilization agents in the ratio of 50 to 50. To the homogenized S/S mixtures an optimal content of deionized water was added according to the ASTM D1557-00 procedure [9]. Then, the S/S mixtures were placed into inert plastic bags to be stored in for 28 days at room temperature (23±2^{o}C).

Standard German leaching test

For the DIN 38414-4 leaching test, the samples of the S/S mixture was fragmented to particles smaller than 2 cm in size. Deionized water was used as an extraction fluid, and the leaching was conducted during 24 hours on a continuous stirrer. The ratio of liquid to solid was 10 to 1 (l kg^{-1}). DIN 38414-4 leaching test corresponds to the EN 12457/2 test, prescribed by the decision of the European Council [10] as a standard leaching test for determining general characteristics of waste materials and sludge. Also, DIN 38414-4 leaching test is used in Serbian Regulation on categories, evaluation and classification of waste [11].

Results and discussion

The results show the presence in ECS of iron and copper in mass concentrations of 455570 and 351 mg kg^{-1}, respectively. For the classification and characterization of the sludge of the EC-treated waste printing developer as waste, the iron and copper values were compared to the maximum allowed concentration values prescribed by the EPA 658/09 [12]. The iron value was not defined, whereas the value of copper exceeds the border value of 60 mg kg^{-1} prescribed by the EPA 658/09, which determines the tested sludge of EC-treated wasteprinting developer as hazardous waste that has to be treated before being disposed.

Table 2. The concentrations of copper leached from the S/S mixtures of ECS with immobilization agents according to the DIN 38414-4 test

Sample	Concentration 10^{-2}(mg kg)
ECS	772
ECS50B50	467
ECS50LC50	463
ECS50C50	236
ECS50PC50	79
A*	200
B*	5000 - 10000
LAGA Z2*	200
A* - Maximum allowed concentration of waste defined as **inert** L/S=10 (L/kg), [11]	
B* - Maximum allowed concentration of waste defined as **non-hazardous** L/S=10 (L/kg), [11]	
Z2* - The cupper recommended value of usage [13]	

The concentrations of copper leached from the ECS and the stabilized S/S mixtures (ECS50PC50, ECS50C50, ECS50B50, ECS50LC50) by DIN 38414-4 leaching tests are shown in Tables 2. The results of the DIN 38414-4 test of copper leaching from the ECS and the S/S mixture of the waste printing developer sludge and immobilization agents were interpreted by

using the national regulation on testing and classification of waste into inert, non-hazardous and hazardous [11] as well as based on the values prescribed for waste by the European Union [10]. The results obtained show that the ECS as well as the S/S mixture of the ECS and immobilization agents can be characterized as non-hazardous waste according to the national regulation on testing and classification of waste into inert, non-hazardous and hazardous. Only the S/S mixture of the ECF sludge and Portland cement (M50PC50) can be defined as inert waste. Also, M50PC50 mixture based on the LAGA criteria prescribed by the German state task-force for waste management [13] fulfills the prescribed value and may be used.

Conclusion

According to the DIN 38414-4 test it can be concluded that the ESC and S/S mixtures of the ECS and immobilization agents are not dangerous and can be safely disposed into the environment. If the S/S treatment is observed from the economic aspect, the fact is that it can be efficiently executed even with non-commercial clay.

References

[1] Q.Y. Chen, M. Tyrer, C.D. Hills, X.M. Yang, P. Carey, Waste Manage., 29 (2009) 390.
[2]M. Prica, Efekti primene razlicitih postupaka remedijacije na imobilizaciju teških metala u sedimentu, Prirodno-matematički fakultet, Univerzitet u Novom Sadu, Novi Sad, 2008 (In Serbian).
[3] Đ.Kerkez,Potencijal upotrebe piritne izgoretine u tretmanu otpadnih voda imogućnostnjenedaljesanacijeprimenomimobilizacionihagenasa, Prirodno-matematički fakultet, Univerzitet u Novom Sadu, NoviSad,2014 (In Serbian).
[5] M. Prica, M. Dalmacija, B. Dalmacija, J. Tricković, R. Milošević. R., Journal of Graphic Engineering and Design, 2(2011) 25.
[5] I. Twardowska, H.E. Allen, A.F. Kettrup, W.J. Lacy, Solid Waste: Assesment, Monitoring and Remediation, Elsevier, 2004.
[6] S. Adamovic, M. Prica, B. Dalmacija, S. Rapajic, D. Novakovic, Z. Pavlovic, S. Maletic, Arabian J. Chem., 9 (2016) 152.
[7] ISO 11466 Method,Soil quality – Extractionoftraceelementssolubleinaquaregia,1995.
[8] EPA 7000B Method, Flame Atomic Absorption Spectrophotometry, 2007.
[9] ASTM D1557-00 Method, Standard test method for laboratory compaction characteristics of soil using modified effort American Society for Testing Materials, Annual Book of ASTM standards: ASTM D1557-91, vol. 4.08. Philadelphia, P: ASTM, 2000.
[10] Official Journal of the European Communities, L11 (2003): Council Decision 2003/33/EC of 19 December 2002 establishing criteria and procedures for the acceptance of waste at landfills pursuant to Article 16 of and Annex II to Directive 1999/31/EC.
[11] Službeniglasnik („Sl. glasnik RS“, br. 56/2010): Pravilnik o kategorijama, ispitivanju i klasifikaciji otpada, 2010 (In Serbian).
[12] EPA 658/09, Supporting documentation for draft Guideline for solid waste: criteria for assessment, classification and disposal of waste, Environment Protection Authority GPO Box 2607Adelaide SA 5001, 2009.
[13] LAGA, Cooperation of the German federal authorities on waste, Anforderungen an die stoffliche Verwertung von mineralischen Reststoffen/Abfällen. 5th September 1995, Berlin, Erich Schmidt Verlag, 1996.

PORTFOLIO OPTIMIZATION IN INVESTMENTS: EMPIRICAL EVIDENCE FROM THE REPUBLIC OF SERBIA

Nebojsa M. Ralevic[1], Jelena S. Kiurski[2], Vladimir Dj. Djakovic[3], Goran B. Andjelic[4]

[1]University of Novi Sad, Faculty of Technical Sciences, Department of Fundamentals Sciences, Novi Sad, Serbia
[2]University of Novi Sad, Faculty of Technical Sciences, Department of Graphic Engineering and Design, Novi Sad, Serbia
[3]University of Novi Sad, Faculty of Technical Sciences, Department of Industrial Engineering and Management, Novi Sad, Serbia
[4]Educons University, Faculty of Business Economy, Sremska Kamenica, Serbia
e-mail: nralevic@uns.ac.rs, kiurski@uns.ac.rs, v_djakovic@uns.ac.rs, goran.andjelic@educons.edu.rs

Abstract
The main subject in this study is to test and analyze efficient portfolio optimization in investments with focus on the financial market of the Republic of Serbia. The basic objective of the research is to provide quantitative information about specific aspects of portfolio optimization in investments, especially having in mind the specificities of the financial market of the Republic of Serbia. The methodology used in the research includes quantitative methods in area of portfolio optimization. The results of the research point to the necessity of portfolio optimization in function of return maximization from the investment activities.
Keywords: portfolio, portfolio optimization, investments, risk, return.

Introduction
Modern aspects of portfolio investments understand an adequate approach regarding investment risk/return characteristics, especially having in mind the volatile business conditions. Namely, frequent occurrences of extreme events, which are enhanced by the global economic crisis, significantly affect the return from investment activities. This fact is particularly important for markets in transition, having in mind that these markets are “famous” for specific volatility and turbulent market conditions.
With that reason, the research is conducted on the financial market of the Republic of Serbia, as typical representative of transitional markets in general. The possibility of portfolio optimization in investments at these markets (for example, in the Republic of Serbia), opens a lot of questions about new ways in investment optimization.
This research is especially interesting regarding acquiring the specific knowledge about the investments assessment, that is, effects from investment activities, based on the empirical evidence from the transitional market of the Republic of Serbia. Hence, the significance lies in the fact that the research is conducted using concrete stocks historical data from the financial market of the Republic of Serbia.
Dynamic nature of investment return induces the necessity of testing the possibilities of portfolio optimization with special attention to investors risk preferences. Continuously changing environmental conditions significantly stress and change the investors risk aversion, in light of changing their attitude regarding the effect from investment activities. Previously mentioned is reflected in terms of adequate determination of portfolio weights, i.e. the shift in optimal balance of risk and risk free portfolio investment assets.

Research methodology

The methodology used in the research is contemporary oriented and takes into consideration the specific nature of the tested data. The applied portfolio optimization methods are based upon the following:

$$\sum_{j=1}^{n} \sigma_{ij}\omega_j - \lambda_1 \bar{r}_i^{\,p} - \lambda_2 = 0, \quad i = 1,2,...,k \tag{1}$$

$$\sum_{i=1}^{n} \omega_i \bar{r}_i^{\,p} = \bar{r}_\pi^{\,p} \tag{2}$$

$$\sum_{i=1}^{n} \omega_i = 1 \tag{3}$$

p takes the values: 1, 2 and 3.

The first approach is based on the following presumptions:

Objective: maximization of portfolio return for a given level of risk;

Changing variable: portfolio weight coefficient;

Constraints: The weight of every stock in the portfolio should not be less than zero;

The sum of all weights is: equal to 1;

The risk of the portfolio is: less than or equal 0.002 (or 0.2%).

The second approach is based on the following presumptions:

Objective: minimization of the portfolio variance;

Changing variable: portfolio weight coefficient;

Constraints: The weight of every stock in the portfolio should not be less than zero

The sum of all weights is: equal to 1;

The portfolio return: should be/used value is 5.04%

Results and discussion

The data used in the research comprises stock historical data from the Belgrade Stock Exchange. The stocks are selected with special focus on different segments of the stock market in the Republic of Serbia, with the objective to provide competent comparative data regarding the specific market conditions in the Republic of Serbia.

Calculation for the first approach: the research results for p=1 are shown in tables 1 and 2; for p=2 and p=3 only summarized data is given in tables 3 and 4.

Table 1. Portfolio optimization for the first calculation approach (p=1)

p=1						
	NIIS	AERO	ALFA	MTLC	BASB	AIKB
Weight	0.00000	0.46089	0.27440	0.26471	0.00000	0.00000
Expected return	-0.02140	0.07620	0.05040	-0.01020	-0.04240	0.00490
Covariation matrix	NIIS	AERO	ALFA	MTLC	BASB	AIKB
NIIS	0.00166	0.00109	-0.00015	-0.00011	0.0017	0.00072
AERO	0.00109	0.00468	0.00243	0.00046	0.00178	0.00113
ALFA	-0.00015	0.00243	0.00264	0.00027	0.00143	0.00027
MTLC	-0.00011	0.00046	0.00027	0.00054	-0.00001	0.00069
BASB	0.0017	0.00178	0.00143	-0.00001	0.00878	0.00164
AIKB	0.00072	0.00113	0.00027	0.00069	0.00164	0.00176
Variance	0	0.001357557	0.000525712	0.0001136	0	0
Return	0.00000	0.03512	0.01383	-0.00270	0.00000	0.00000

Source: the authors' calculations

Table 2. Portfolio optimization for the first calculation approach (p=1) – risk/return values

Portfolio variance	0.00199684
Standard deviation	0.044686011
Portfolio return	4.62%
Portfolio risk	0.002000997

Source: the authors' calculations

Table 3. Portfolio optimization for the first calculation approach (p=2) – risk/return values

Portfolio variance	0.002029924
Standard deviation	0.04505468
Portfolio return	0.37%
Portfolio risk	0.002000466

Source: the authors' calculations

Table 4. Portfolio optimization for the first calculation approach (p=3) – risk/return values

Portfolio variance	0.002029575
Standard deviation	0.045050799
Portfolio return	0.03%
Portfolio risk	0.001999656

Source: the authors' calculations

Calculation for the second approach: the research results for p=1 are shown in tables 5 and 6; for p=2 and p=3 only summarized data is given in tables 7 and 8.

Table 5. Portfolio optimization for the second calculation approach (p=1)

p=1						
Covariation matrix	NIIS	AERO	ALFA	MTLC	BASB	AIKB
NIIS	0.00166	0.00109	-0.00015	-0.00011	0.0017	0.00072
AERO	0.00109	0.00468	0.00243	0.00046	0.00178	0.00113
ALFA	-0.00015	0.00243	0.00264	0.00027	0.00143	0.00027
MTLC	-0.00011	0.00046	0.00027	0.00054	-0.00001	0.00069
BASB	0.0017	0.00178	0.00143	-0.00001	0.00878	0.00164
AIKB	0.00072	0.00113	0.00027	0.00069	0.00164	0.00176
Variance	0	0.000919491	0.001084091	0	0	0.000145061
Return	-0.0214	0.0762	0.0504	-0.0102	-0.0424	0.0049

Source: the authors' calculations

Table 6. Portfolio optimization for the second calculation approach (p=1) – risk/return values

Weight sum	1.00000
NIIS	0.00000
AERO	0.31616
ALFA	0.50454
MTLC	0.00000
BASB	0.00000
AIKB	0.17930
Portfolio variance	0.002148643
Portfolio return	0.050399

Source: the authors' calculations

Table 7. Portfolio optimization for the second calculation approach (p=2) – risk/return values

Weight sum	1.00000
NIIS	0.00000
AERO	1.00000
ALFA	0.00000
MTLC	0.00000
BASB	0.00000
AIKB	0.00000
Portfolio variance	0.00468
Portfolio return	0.005806440000000

Source: the authors' calculations

Table 8. Portfolio optimization for the second calculation approach (p=3) – risk/return values

Weight sum	1.00000
NIIS	0.00000
AERO	1.00000
ALFA	0.00000
MTLC	0.00000
BASB	0.00000
AIKB	0.00000
Portfolio variance	0.00468
Portfolio return	0.000000195762647

Source: the authors' calculations

Conclusions

Based on the conducted research, it can be concluded, that it is possible to achieve efficient portfolio optimization in investments at the specific financial market of the Republic of Serbia, but it is important to have in mind the fact that this market is highly volatile, with extreme return distribution tails, which point out to the significant level of investment risk. In this sentence lies both the importance of this research for academic and professional public and possible ways of further researches in the subject field.

Acknowledgements

The authors acknowledge the financial support of the Ministry of Education, Science and Technological Development of the Republic of Serbia, within the Project No. TR34014.

References

[1] V. Djakovic, I. Mladenovic, G. Andjelic, Acta Polytech Hung, 12(4), 2015, pp. 201-220.

[2] V. Djakovic, N. Ralevic, J. Kiurski, G. Andjelic, N. Glisovic, An empirical evidence of investment return prediction: the case of the Republic of Serbia, Proceedings / XVI InternationalScientific Conference on Industrial Systems - IS'14, Novi Sad, Serbia, October 15. – 17. 2014, pp. 233-236.

THE INFLUENCE *XANTHIUM STRUMARIUM* L. EXTRACTS ON MAIZE YIELD

Nataša Samardžić[1*], Bojan Konstantinović[1], Milena Popov[1], Milan Blagojević[1], Branimir Lukić[1], Branimir Pavlić[2]

[1]University of Novi Sad, Faculty of Agriculture,Department for Environmental and Plant Protection,Trg Dositeja Obradovića 8, 21000 Novi Sad, Serbia
[2]University of Novi Sad, Faculty of Technology, Bulevar Cara Lazara 1, 21000 Novi Sad, Serbia
e-mail: natasam@polj.uns.ac.rs

Abstract
In several years lasting period occur great numbers of harmful organisms that cause decrease in crops yield. The most frequently occurring weed species cause great damages in agricultural crops, with potential yield loss of 34% [5]. They compete with the crops for water, space, light and nutrients and are hosts to insects and pathogens [8].
During 2014 allelopathic influence of *Xanthium strumarium* L. on maize yield (*Zea mays* L.) was studied in field conditions. Beside water extract from plant dry weight of the studied weed species, extract of methanol was also used in different concentrations. Concentrations of 0.04, 0.02, 0.01 and 0.004 g of the plant dry weight per 1 ml of solution were used. The required material was made from weed species picked up in 3-4 leaves phenophases. The reduced maize yield was established in fields in which water extracts, as well as methanol extracts were used. In comparison to untreated control variants, the reduced yield of 10.53-30.3% was established in treatments in which water extracts were applied. In relation to control plots, methanol treatments reduced yield for 20.26-36.32%.

Introduction
Contemporary agriculture to a great extent relies on herbicide use as simple and the most efficient method for weed control. However, excessive and improper use of chemical products leads to a series of negative consequences such as the occurrence of weed resistance, the occurrence of herbicide residues in food, soil and water, i.e. environmental pollution with harmful effects to human and animal health [6] [1] [2]. In some kinds of productions, such as organic agriculture, use of chemical products is not possible and therefore different alternative and ecologically acceptable methods for weed control such as allelopathy have been studied. There are different manners for use of allelopathically active plants, for example as stubble crops that cover or suppress weeds, mulching, incorporation of plant residues, green fertilization, as united crops or in crop rotation, as well as the use of cultivars, i.e. genotypes with high allelopathic potential [7]. Weeds can be suppressed indirectly also by use of water extracts of allelopathic crops as natural herbicides or directly by use of purified allelochemicals or their derivates [10] [3].
Crop plants or crops with high allelopathic potential used for weed control include sorghum, Sudan grass, wheat, rye, rice, sunflower, buckwheat and species of the genus Brassica [9] [3].

Experimental
In the period 2012-2013, *Xanthium strumarium* L. plants were collected at localities Kać and Zmajevo near to Novi Sad.
Plants were collected in the phenophase of 2-4 leaves, and then dried at 60ºC for 5 days [11]. Extracts of *X. strumarium* L. were prepared according to Chon *et al*. (2003). Water extracts were obtained by extraction of 40g of dry material by 1l of distilled water. The samples were shaken

(GFL, Schuttelapparate Shakers, Germany, Model 3015) in the dark for 24 h at temperature of 24°C, and then filtered.

Methanol extracts were prepared by extraction of 40g of dry material by 1l of 95% methanol as extraction solvent. The samples were shaken (GFL, Schuttelapparate Shakers, Germany, Model 3015) in the dark for 24 h at temperature of 24°C, and then filtered. After filtration extraction solvent was evaporated under vacuum, and dry extracts were dissolved in distilled water, and then filtered. Water and methanol extracts of weed species *X. strumarium* L. were accurately diluted by sterile distilled water in order to obtain final concentrations of 0.02, 0.01 and 0.004 g/ml.

In 2014 the field trial was set up at locality Zmajevo, according to the randomized block design for both of the obtained extracts in maize crop phase according to BBCH scale 12-14. Measurements of 14 plants yield from each of treated plots were carried out in the phase of maize full ripening (BBCH 89). Subsequently, maize kernels were kept in paper bags (BBCH 99) for the purpose of further laboratory data processing.

Results and discussion

The influence of *Xanthium strumarium* L. water extracts on maize yield. During the studies on allelopathic influence of different concentrations of water extracts of weed species *X. strumarium* L. (0.04, 0.02, 0.01 and 0.004 g/ml), measurements and regular dating indicated a high allelopathic potential of this species to maize yield. The applied concentration of 0.04 g/ml resulted in the yield reduction of 30.3% in comparison to the control plot. The applied concentration of 0.02 g/ml resulted in the yield reduction of 25.26%, while in lower rates of 0.01 and 0.004 g/ml maize yield was lower for 23.69% and 10.53%, respectively.

Figure 1. The average weight of maize grain treated with water extract

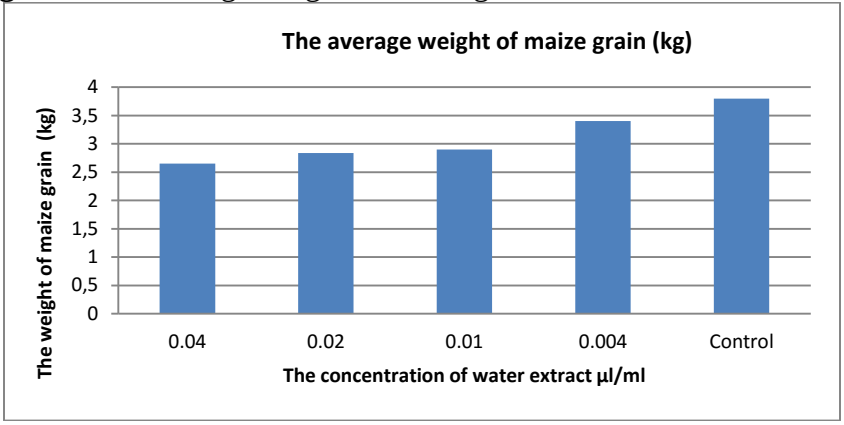

The influence of methanol extract of weed species *Xanthium strumarium* L. on maize yield

The studies and measurements of maize kernel after treatment by methanol extract in different concentrations showed that plants in the field treated by the highest concentration of 0.04 g/ml gave reduced yield of 36.32%. The applied concentration of 0.02 g/ml resulted in reduced yield percentage of 32.10%, while in lower concentrations 0.01 and 0.004 g/ml it was 30% and 20.26%, respectively. Significant yield reduction was established in relation to the untreated control variant.

Figure 2. The average weight of maize grain treated with methanol extract

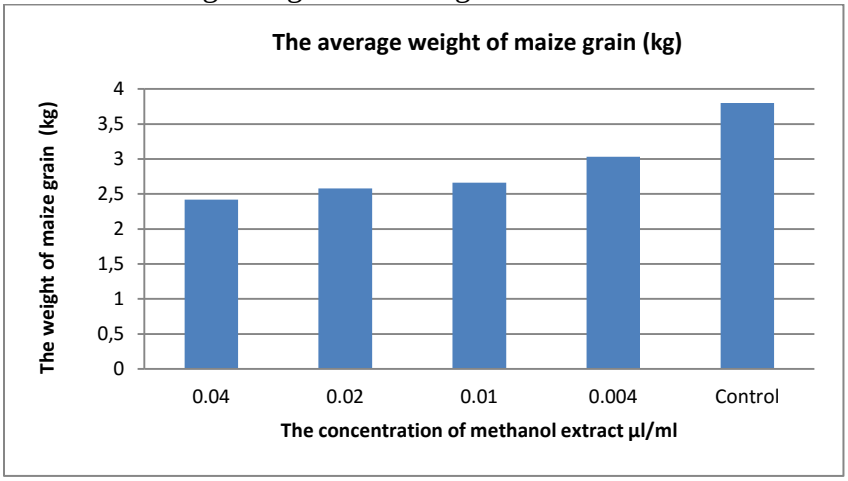

Conclusion

Based on these studies, data on the influence of *Xanthium strumarium* L. extract on maize yieldwere obtained. The influence of water and methanol extract made from *Xanthium strumarium* L. in studied concentrations of 0.04, 0.02, 0.01 and 0.004 g/ml was highly efficient in reduction in crop yield. Use of water extract in the highest concentration of 0.04 g/ml proved that it reduces crop yield even up to 30.3% in comparison to the control variant, while the lowest concentration of use resulted in crop yield reduction of 10.53% in relation to the control. Application of methanol extract provided similar data. The used methanol extract in the highest concentration resulted in the highest yield losses of 36.32% in comparison to the control, while the lowest used concentration provided crop yield reduction of 20.26% in relation to the control.

References

A. Khaliq, A. Matloob, Z.A. Cheema, M. Farooq. Chilean Journal of Agricultural Research, 71 (3) (2011) 418-423.

B. Konstantinović, N. Samardžić, M. Blagojević, M. Popov, S.Vidović, B. Pavlić. 26th International Scientific-Expert Conference of Agriculture and Food Industry (2015) 136.

[1] D. Soltys, U. Krasuska, R. Bogatek, A. Gniazdowska. Allelochemicals as Bioherbicides (Eds.), Herbicides – Current Research and Case Studies in Use. (2013) 517-542.

[2] E. C. Large. Growth stages in cereals illustration of the feekes scale". Plant Pathology. 3 (4) (1954) 128–129.

[3] E.C. Oerke. The Journal of Agricultural Science. 144(1) (2006) 31-43.

F.A. Macias, D. Marin, A. Oliveros-Bastidas, R.M. Varela, A.M. Simonet, C. Carrera, J.M.G. Molinilo. Biological Sciences in Space, 17 (1) (2003) 18-23.

[4] H.P. Singh, D.R. Batish, R.K. Kohli. Critical review in Plant Sciences. 22 (2003) 239-311. [5] J.R.Qasem, C.L. Foy. Journal of Crop Production. 4 (2001) 43-119.

[6] L. A. Weston. Agronomy Journal. 88 (1996) 860–866.

[7] M.J. Reigosa, L. Gonzáles, A. Sánchez-Moeriras, B. Durán, D. Puime, D. Fernández, J.C. Bolano. Allelopathy Journal. 8 (2001) 211-220.

[8] S.-U. Chon, C.J. Nelson. Communications in Soil Science and Plant Analysis. 32 (2001) 1607–1619.

[9] S.-U. Chon, Y.-M. Kim, J.-C. Lee. Weed Research. 43 (2003) 444–450.

ZORFLEX ADSORPTION OF ATRAZINE IN DRINKING WATER

Marjana Simonič

Faculty of Chemistry and Chemical Engineering, University of Maribor,
Smetanova 17, SI–2000 Maribor, Slovenia
e-mail: marjana.simonic@um.si

Abstract
Different types of carbon fibres cloths made of 100 % activated carbon were tested in water purification experiments. The atrazine removal efficiencies were studied on carbon cloths named Zorflex® ACC with a specific area of 1000-2000 m^2 /g. The experiments were performed in millipore water and real drinking water samples. The atrazine concentrations were chosen on two levels 1 μg/L and 1 mg/L. In order to improve the adsorption efficiency, the fibres were treated with different solutions. Some of the carbon cloths were regenerated with methanol and used again. A little less than 10 mg of atrazine per 1 g C-cloth was adsorbed. It could beattributed to the fact that in the real water some ions express higher binding affinity to the fibers. Since atrazine was in low concentrations, the removal of atrazine did not depend on methanol concentration.

Keywords: *Atrazine, carbon cloths, thermodynamics*

Introduction
Atrazine is a well-known persistent herbicide and endocrine disruptor for mammals [1]. According to the monitoring report [2] from our government the concentrations of atrazine are still above 0,1 μg/L in Slovene drinking water sources. Although, the adsorption of atrazine has been extensively studied, very little is known about adsorption onto activated carbon cloths. Different types were studied for nitrate removal. However, some studies of atrazine removal using carbon cloths were found. Activated carbon cloths were firstly used for pesticide removal [3] and later also for nitrate removal [4] The efficiency of pesticide removal was increased if the carbon cloths were modified with treatment in hot millipore water at 60°C. [3] The modification with acid solution turned to be more appropriate for nitrate removal [5]. Carbon clothes were successfully used for some pharmaceuticals removal [6].
To the best of our knowledge, thermodynamics of atrazine during the adsorption on carbon cloths was not studied yet. However, it was studied by using nanotubes for atrazine removal. The influence of oxygen was studied. Gibbs energy was negative which meant spontaneous reaction of atrazine on nanotubes [7].
In the present work the effects of functional groups on the adsorption efficiency of atrazine by carbon cloth was investigated. For the modification of surface functional groups and porous structures, the carbon cloths were chemically etched in different solutions, such as methanol and hot millipore water under inert conditions. The thermodynamic and kinetics of atrazine removal on carbon cloths were studied.

Experimental
ZORFLEX® ACC are microporous cloths, made of 100 % activated carbon and have large specific surface area of 1000-2000 m^2/g. They are available in knitted (FM30K) or woven fabric (FM70) as presented in Fig 1a and 1b, respectively.

1a 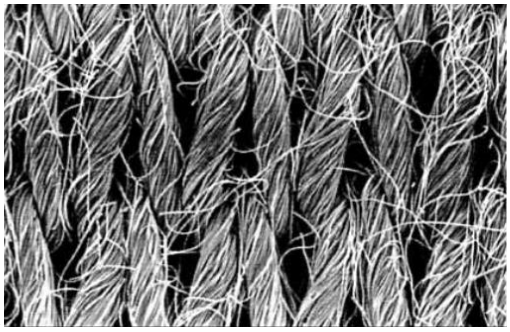 1b 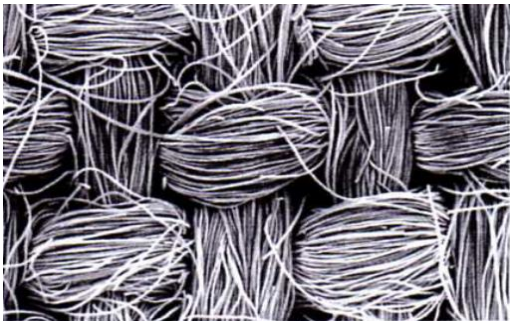

Figure 1 ACC fibres at 40x magnitude (knitted 1a) and wowen 1b)

Table 1 represents the surface area and thickness of the fibres used.

Table 1: The surface area and thickness of the fibres

Fibre	FM30K	FM70
Surface area (g/m^2)	110	160
Thickness (mm)	0,4	0,6

Initial carbon cloth treatment and modification

The cloth with the mass of 1 g was placed into a beaker with millipore water for 2 days. Nitrogen gas was bubbled into the cup to avoid possible CO_2 adsorption. The washed carbon cloth modules were then dried under vacuum at 120 ◦C and kept in a desiccator for further uses. For the modification of surface functional groups and porous structures, the carbon cloth was submersed in different solutions. Firstly, cloths were only wetted by water and atrazine adsorption was performed. Secondly, treatment using methanol solution was performed. Thirdly, acid treatment using 15 % H_2O_2 solution was performed. The carbon cloth was then washed with triply distilled deionized water and used. Initial concentration of atrazine was always the same, determined at 1 mg/L and after 2, 5, 20, 40, 60 and 120 mins the concentrations were measured again.

Analyses

Atrazine concentration in water samples was determined following SIST ISO 10695/2000, using LC/MS/MS. Solid phase extraction (SPE) was performed with using cartridges as well as methanol and ethyl acetate as solvents. Bod elute SPE was used which is made of C8 (non-polar).

Adsorption capacity N_f (mg/g) was determined according to Eq. 1:

$$N_f = \frac{V(\gamma_0 - \gamma_s)}{m} \qquad \text{Eq.1}$$

where

γ_0 initial mass concentration (mg/L)
γ_s equilibrium mass concentration (mg/L)
m activated carbon cloth fibre mass (g)
V volume of water solution (L)

To analyse the adsorption rate of atrazine onto carbon cloths, the pseudo second order was evaluated based on experimental results according to Eq.2:

$t/q_t = 1/(k_2.q_{c2}) + t/q_e$ Eq.2

where q_e (mg/g) and q_t (mg/g) are the concentrations of atrazine adsorbed on cloth at equilibrium and at time t, k_2 (g/mg.min) is the rate constant.

Results and discussion

Sorption capacity of atrazine

The results obtained are presented in Fig. 1. The concentrations of atrazine in time dependence for water were done with FM30K cloth. It is seen that already after 40 mins the total removal of atrazine was noticed. The concentrations of atrazine decreased in water for up to 97 %. Desorption of adsorbed atrazine and other ions was performed, however, after the desorption no noticeable differences in atrazine adsorption were noticed.

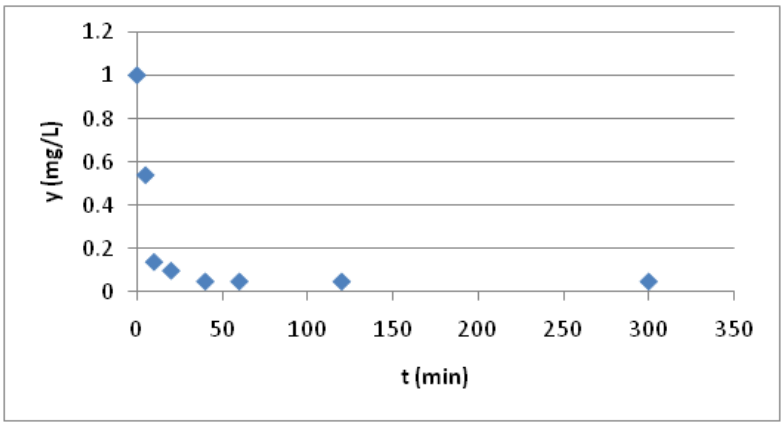

Figure 1. Atrazine removal in dependence of time

The linear regression of the sorption is shown in Fig. 2. The R^2 value close to 1 clearly shows the pseudo second order of reaction.

Effect of temperature was studied on atrazine removal. The standard energy change ΔG^o was calculated as negative value of product of R, T and ln K_o, where constant K_o was determined using a method described by equation 3:

$K_o = a_s/a_e = v_s.c_s/(v_e.c_e)$ Eq. 3

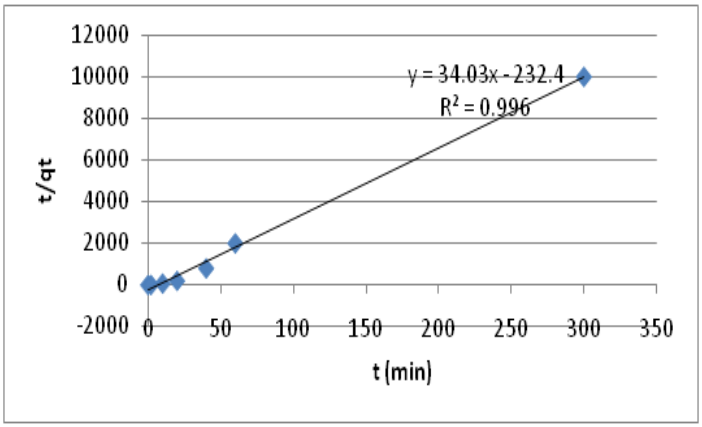

Figure 2. Pseudo second order kinetics of atrazine

Average enthalpy change ΔH^o was obtained by Van't Hoff equation:

$$\text{Ln } K_o(T_3) - \ln K_o(T_1) = -\Delta H^o/R.(1/T_3 - 1/T_1) \qquad \text{Eq. 4}$$

The values ΔG^o determined at 295, 303 and 323 C were -0.90 kJ/mol, -1.67 kJ/mol and -1.83 kJ/mol, respectively. All three values are negative, therefore, the adsorption of atrazine is spontaneous. ΔH^o was calculated at -11,58 kJ/mol and is negative, which is supported by the observation that the adsorption decreased with increasing temperature.

Conclusions

Carbon cloths designed as "Chemviron Zorflex® ACC" were tested for their adsorption of atrazine in millipore water. Modification with acid or methanol did not affect the removal efficiency. The results showed that atrazine adsorpction follows the pseudo second order kinetics. Gibbs energy was determined to be negative, therefore, the adsorption of atrazine is spontaneous. Average enthalpy was determined at the value of -11,58 kJ/mol.

References

[1] Chu W., Chan . H., Graham N. J. D. (2006) Chemosfere, 64, 931-936.
[2] Report (2015) Drinking water monitoring 2014, Annual report of drinking water quality for year 2014, Ministry of Health, Slovenia, available:
[3] Ayranci E. and Hoda N. (2005) Chemosphere 60, 1600-1607.
[4] Ayranci E. and Duman O.(2006) J. Hazard. Mater., B136 542–552
[5] Afkhami A., Madrakian T., Karimi Z. (2007) Journal of Hazardous Materials 144, 427–431.
[6] Hanen Guedidi, L Reinert, Y. Soneda, N. Bellakhal, L. Duclaux (2014)Arabian Journal of Chemistry, In Press, Corrected Proof, Available online 20 March 2014
[7] Chen GC., Shan X.Q., Zhou Y. Q., Shen X., Huang H. L., Khan S.U. (2009) J Hazard Mater. 169, 912-918.

USE OF SOME NATURAL SUPPORTS FOR THE ADSORPTION OF THEOPHYLLINE FROM AQUEOUS SOLUTIONS

Georgeta-Maria Simu[1*], Anca Octavia Dragomirescu[1], Mihaiela Andoni[1], Loreta-Andrea Bozin[2], Eugen Sisu[2]

[1]University of Medicine and Pharmacy „Victor Babeş" Timişoara, Faculty of Pharmacy, 2 Eftimie Murgu, 300041, Timişoara, Romania
[2]University of Medicine and Pharmacy „Victor Babeş" Timişoara, Faculty of Medicine, 2 Eftimie Murgu, 300041, Timişoara, Romania
e-mail: simu.georgeta@umft.ro

Abstract
In this work, the interaction of Theophylline with lemon peel and olive leaves (two natural solid supports) was studied at 25, 35 and 45 ^{o}C in order to identify the most appropriate theoretical adsorption model, as well as the corresponding thermodynamic parameters (free energy of Gibbs, enthalpy and entropy) of the adsorption process. In the first stage, the time necessary for attaining the equilibrium was established in a series of preliminary experiments, which indicated periods of time ranging from 182 to 356 minutes. The experimental data obtained from the adsorption process was fitted to the Freundlich and Langmuir classical adsorption models by linear regression analysis. The obtained results indicate that for both studied systems, the Langmuir model described better the interaction of Theophylline with the solid supports taken in work.

Introduction

Adsorption of pharmaceutical substances on different solid supports influences the bioavailability as well as other characteristics of the active substances. Despite this, the number of studies on the adsorption of pharmaceutical substances on different solid supports or excipients is quite limited in the speciality literature. The study of the adsorption process of drugs on some natural supports (peel of citrus fruits and other plant waste, different species of wood, cotton, jute, etc) is even more poorly represented in the literature of specialty, despite its rich potential application in the pharmaceutical field, and its implications on the health of the environment, especially with regard to the purification of residual waters [1-4].
Citrus (oranges, lemons, etc) are known for their antioxidant activity, which results from their rich composition in phytochemical components. The peel of these fruits is particularly rich in nutrients, presenting also an important antimicrobial activity. For this reason, one could use them both as drugs and dietary supplements. Since the number of antibiotic-resistant pathogens becomes increasingly large, in-depth research on such compounds becomes highly topical [5-11].
In the last years, olive leave extracts have been found to preserve the immune system, also acting against viral bacterial and fungal infections. It was also found that this vegetal material improves blood circulation, prevents and treats hypertension and arteriosclerosis. [12-17].
Theophylline is a methylxanthine type alkaloid, acting as a diuretic, stimulant, bronchodilator and as lipolytic agent. Theophylline acts at the level of intracellular calcium movements. It has a broncho-dilatatrice action, strengthening the respiratory muscles and with inotropic cardiac positive action. Theophylline is also a phosphodiesterase inhibitor [18].
The aim of this present work is to study the adsorption process of some aqueous solutions of Theophylline on two natural supports: the lemon peel and the olive leaves, at different temperatures, in order to obtain original experimental data whose analysis could provide

information of great interest onto the interaction of this active substance with the specified solid supports.

Experimental

Theophylline (1,3-Dimethyl-7H-purine-2,6-dione) was supplied by Aldrich Sigma as a reagent of high purity (99%). The solid supports used as adsorbents were the lemon peel originating from Eureka lemon variety (*Citrus lemon L.)*and olive leefs *(Olea europaea)*. Lemons were purchased from a local market (Timișoara, Romania) and the olive leefs were collected from Tunisia in march 2016. The vegetal materials were washed with tap water, then with de-ionized water, and dried in the shade at constant temperature for several days. Thereafter, they were dried in an incubator at 60^{o} ($\pm 5°C$) for 10 hours. The dried materials were grounded into powder (mesh size of about 120 ± 5 micron) with an electrical sieve shaker. The adsorbents thus prepared were analysed by microscopy (Olympus microscope, 400x magnifier) as well as by FTIR spectroscopy, by means of IR JASCO FT-IR 4200 spectrometer, in the wavelengh range of 4000 – 400 cm^{-1}.

The adsorption experimental study was carried out in a similar mode as it was described in previous work [4,19]. The measurement of the optical density of the drug solutions at 270 nm was performed on a Perkin-Elmer-Lambda-950 spectrophotometer. The calibration curve was obtained, according to Lambert-Beer law. The adsorption experiments were carried out in a Julabo ED 5M bath, at 25, 35 and $40^{o}C$ ($\pm 1^{o}C$)). The amount of the adsorbed drug on the solid support was calculed according to equation (1):

$$[D]_{ad} = ([D]_i - [D]_s) \cdot V/1000 \cdot m \qquad (1)$$

where $[D]_{ad}$ is the equilibrium drug concentration on the solid supports (mmol/g), $[D]_i$ the initial concentration, $[D]_s$ the equilibrium concentration of the drug solution (both in mmol/L), V the volume of drug solution (L), and m the amount of the solid support (g).

Results and discussion

In this work, the study of the interaction of Theophylline with two natural solid supports, e.g. lemon peel and olive leaves powder was carried-on at 25, 35 and $40^{o}C$ ($\pm 1^{o}C$).

The main criteria in the choice of the solid supports were their natural origin, as well as their great potential for pharmaceutical and/or environmental protection applications. The FT-IR spectra of the two adsorbents indicate the complex structure of these adsorbents. The spectra display broad, intense peaks around 3400 cm^{-1} (lemon peel) and 3423,03 cm^{-1} (olive leaves) which could result from the O-H stretching mode of hydroxyl groups, while the bands at 1700-1200 cm^{-1} can be attributed to the aromatic C-C bond. The peaks situated at 1104,05 and 1053,91 1080 cm^{-1} in the case of the lemon peel, or at 1158,04, 1099,23 et 1028,84 cm^{-1} (olive leaves) can be attributed to C-O symmetric or –C-O-C- ring asymmetric stretching vibration. The peaks from the 2000-2400 cm^{-1} region: 2105,89 and 2366,23 cm^{-1} for lemon peel; 2344,05 cm^{-1} in the case of olive leaves could indicate the carbon dioxide from normal air [20].

Generally, the results of adsorption processes can be reported as sorption isotherms, the most used in the case of drugs being the Freundlich and Langmuir classical models described by equations (2) and (3):

$$[D]_s = K_F \cdot [D]_{sol}^{x} \qquad (2) \qquad \frac{1}{[D]_s} = \frac{K_L}{S_f \cdot [D]_{sol}} + \frac{1}{S_f} \qquad (3)$$

where $[D]_s$ represents the drug concentration in the support at equilibrium, in mol/kg dry support, $[D]_{sol}$ represents the drug concentration in solution at equilibrium, in mol/L, K_F is the Freundlich

equilibrium constant and x is a sub-unitary power; S_f is the saturation value in mol/kg fibre and K is the equilibrium constant.

The sorption isotherms of Theophylline on the two natural supports (lemon peel and olive leaves) were obtained at the three mentioned temperatures, at the corresponding times established through the preliminary experiments, which are presented in Table 1.

Table 1. Equilibrium time for the adsorption of Theophylline on lemon peel and olive leaves at 25, 35 and 40°C

Solid support	Time [min]	Time [min]	Time [min]
	T= 25 °C	T= 35 °C	T= 45 °C
Lemon peel	356	310	254
Olive leaves	321	245	182

In order to find out the classical model which fitts better to the adsorption of Theophylline on lemon peel and olive leaves respectively, the experimental data resulted from this study were fitted by linear regression analysis to the general equations (4) and (5), corresponding to the Freundlich and Langmuir models:

$$\ln y = b_o + b \cdot \ln x \qquad (4)$$

$$y^{-1} = b_o + \frac{b}{x} \qquad (5)$$

where y represents the drug concentration in the support at equilibrium, x the drug concentration in solution at equilibrium, b_o the logarithm of the equilibrium constant (K_F), b a sub-unitary power; b_o is $1/S_f$ and b represents K_L/ S_f.

The linear regression analysis was performed by means of the STATISTICA package [21].The main statistical criteria were the squared multiple regression coefficient (r^2), the standard deviation (SE) and the Fischer test (F). The obtained results are shown in Tables 2 and 3.

Table 2. Statistical parameters for the adsorption process of Theophylline (THP) on lemon peel (LEP) and olive leaves (OLL) at 25, 35 and 40°C , according to equation (4)

System	Temp. [°C]	b_o	b	r^{2*}	SE*	F*
THP-LEP	25	3,036±0,0429	0,591±0,049	0.968	0.178	139.81
	35	3,021±0,0431	0,589±0,063	0,972	0,206	116,24
	45	3,014±0,424	0,595±0,053	0,969	0,114	198,47
THP-OLL	25	2,651±0,028	0,498±0,038	0,971	0,119	176,67
	35	2,751±0,345	0,506±0,041	0,965	0,311	103,12
	45	2,552±0,332	0,499±0,039	0,972	0,138	164,47

Table 3. Statistical parameters for the adsorption process of Theophylline (THP) on lemon peel (LEP) and olive leaves (OLL) at 25, 35 and 40°C , according to equation (5)

System	Temp. [°C]	b_o	b	r^{2*}	SE*	F*
THP-LEP	25	2,440±0,0703	$0{,}010.10^{-3}\pm0{,}021.10^{-6}$	0,999	0,182	16392,18
	35	2,312±0,0661	$0{,}011.10^{-3}\pm0{,}029.10^{-6}$	0,998	0,296	10820,12
	45	2,319±0,0597	$0{,}012.10^{-3}\pm0{,}048.10^{-6}$	0,997	0,232	13969,48
THP-OLL	25	1,621±0,0482	$0{,}011.10^{-3}\pm0{,}011.10^{-6}$	0,996	0,291	9875,45
	35	1,5312±0,0454	$0{,}009.10^{-3}\pm0{,}007.10^{-6}$	0,998	0,224	143959,42
	45	1,543±0,446	$0{,}011.10^{-3}\pm0{,}010.10^{-6}$	0,997	0,251	11784,62

The values of the thermodynamic parameters: the Gibb's free energy (ΔG^0), the enthalpy (ΔH^0) and the entropy (ΔS^0) are presented in Table 4.

Table 4. Caracteristic thermodynamic parameters for the adsorption process of Theophylline on lemon peel and olive leaves

Solid support	Temperature [K]	ΔG^o [kJ/mole]	ΔH^o [kJ/mole]	ΔS^o [J/mole.K]
Lemon peel	298,15	-20,43	-9,235	80,23
	308,15	-21,07		
	318,15	-21,7		
Olive leaves	298,15	-19,97	-8,172	67,36
	308,15	-20,61		
	318,15	-21,15		

Conclusion

The adsorption isotherms of Theophylline on lemon peel and olive leaves were studied using Freundlich and Langmuir isotherm models.

The statistical analysis of the experimental results indicates that the Langmuir model describes better the adsorption of Theophylline on lemon peel and olive leaves.

The corresponding thermodynamics parameters of the adsorption process were calculated and their values show the spontaneity and the exothermicity of the studied processes.

References

[1] S. Al-Nimry, S. Assaf, I. Jalal, N. Najib, Int. J. Pharm. 149 (1997), 115.
[2] S. Okada, H. Nakahara, H. Isaka, Chem.Pharm.Bull. 35 (1987) 761.
[3] A. Reem, Eur. J. Sci. Res. 40(4) (2010) 580.
[4] G.M. Simu, I.V. Ledeti, S.G. Muntean, A. Fuliaş, I.M. Cîtu, C. Şoica, D. Onisei, G. Săvoiu–Balint, Rev. Chim. (Bucharest) 65(6) (2014), 664.
[5] A. Mamta, K. Parminder, IJRET 2(12) (2013) 517.
[6] U. Suryavanshi, S.R.Shukla, Ind. Eng. Chem. Res.49 (22) (2010) 11682.
[7] J. Sirajudeen, J. Naveen, S.A. Manikandan, M.M.M. Mubashir, Der Chemica Sinica 4(2) (2013) 133.
[8] Y.R.M. Rao, S.S. Malkhede, IJRESTs 1(8) (2015), 55.
[9] R. Rajoriya, B. Kaur, IJESI 3(6) (2014) 60.
[10] A.R. Tembhurkar, R. Deshpande, J. Haz. Tox. Radioact. Waste 16(4) (2012) 311.
[11] M.J. Dhanavade, C.B. Jalkute, J.S. Ghosh, K.D. Sonawane, Brit. J. Pharmacol. Toxicol. 2(3) (2011) 119.
[12] J. Fonolla, P. Diaz-Ropero, E. de la Fuente, J. Quintela, Atheroscler Suppl. 11 (2010), 182 (MS358).
[13] T. Perrinjaquet - Moccetti, A. Busjahn, C. Schmidlin, A. Schmidt, B . Bradl, Phytother. Res.22 (2008) 1239.
[14] S. Prabuseenivasan, M. Jayakumar, S. Ignacimuthu, Complem. Altern. Med. 6 (2006), 39.
[15] E. Susalit, N. Agus, I. Effendi, R.R. Tjandrawinata, D. Nofiarny, Phytomedicine 18 (2011) 251.
[16] M. de Bock, J.G.B. Derraik, C.M. Brennan, J.B. Biggs, P.E. Morgan, S.C. Hodgkinson, P.L. Hofman, W.S. Cutfield, PLoS One 8(3) (2013) e57622.
[17] H.A. El-Shemy, Pharmacology, Toxicology and Pharmaceutical Science "Drug Discovery", 2013.
[18] A. Markham, D. Faulds, Drugs 56 (1998), 1081.
[19] G. Simu, S. Funar-Timofei, S. Hora, L. Kurunczi, Mol. Cryst. Liq. Cryst. 416 (2004), 97/353.
[20] P.S. Kalsi, Spectroscopy of Organic Compounds. Sixth Edition, New Delhi: New Age International (P) Ltda, 2004, pp. 163.
[21] STATISTICA 7.1 software (STATSOFT Inc., USA).

PHOTOCATALYTIC DEGRADATION OF SOME AQUEOUS SUSPENSIONS OF PROPRANOLOL

Georgeta-Maria Simu[1*], Codruta Soica[1], Cristina Trandafirescu[1], Savoiu-Balint Germaine[1], Cristina Dehelean[1]

[1]University of Medicine and Pharmacy „Victor Babeş" Timişoara, Faculty of Pharmacy, 2 Eftimie Murgu, 300041, Timişoara, Romania
e-mail: simu.georgeta@umft.ro

Abstract
In this work, the photocatalytic degradation of Propranolol aqueous solutions of different concentrations was investigated in the presence of TiO_2 and TiO_2-MoO_3 catalysts. Among the two photocatalysts used, the best performance can be attributed to the TiO_2-MoO_3 catalyst. Optimal reaction conditions were established: $C_{cat.}$ = 2 g/L; $C_{Propranolol.}$ = 0,25 mM; V = 20 mL, lampe – sample distance = 10 cm, when the UV-A-induced photocatalytic oxidation over the Propranolol suspensions was able to degradate almost completely the studied drug. The speed of decomposition of Propranolol was accelerated when the process was carried out at a temperature of 50°C.

Introduction
One of the major problems that arise at global level since the end of the last century is the scarcity of fresh water. It was stated that global water consumption has increased substantially, 32% of the total taken being attributed to industries [1].
Among the great number of chemicals which can penetrate into the aquatic and terrestrial environment, the pharmaceutical active substances constitute a growing environmental concern [2,3]. These compounds play an important role in the life expectancy of the population over the past centuries, and this matter of fact explains their increasingly growing consumption in human and veterinary medicine. A major issue raised by these compounds is that the drug residues present in the (residual) waste water more often leave the STEP (cleansing stations) almost unchanged.
Studies conducted in several countries noted the presence of more than 80 pharmaceutical products in urban sewage at concentrations ranging from ng L^{-1} to μg L^{-1} [3,4]. Time of residence of drugs in the environment varies, being depend by their physicochemical characteristics. On the other hand, the increasing use of drugs, as well as their inadequate disposal constitutes two factors which are responsible for their presence and their "persistence" in the environment. Thus, these substances could be considered to contribute to the phenomenon of the emergence and dissemination of resistant germs, as well as failures of antibiotic therapy [5].
This complex problem, reveal the need for the development of new methods, more effective for the treatment of wastewater. From this point of view, during the last decade, much research have been focused onto the advanced oxidation processes (AOP), which have already shown their potential in the treatment of toxic and biologically refractory organic pollutants [6-11].
Propranolol ((RS)-1-(isopropylamino)-3-(naphthalen-1-yloxy)propan-2-ol) is a beta blocking not selective sympatholytique drug, used in the treatment of hypertension, states of anxiety and panic. This drug is available in the generic form of Propranolol hydrochloride under different trade names. Propranolol has been studied in the treatment of diseases of post-traumatic stress, because this drug inhibits the action of the norepinefrine, a neurotransmitter that contributes to

the consolidation of memory [12-15]. In addition, Propranolol (in combination with etodolac), has been studied as a potential therapeutic agent in the recurrence of colorectal cancer [13].
The aim of this present work, was to carry on an experimental study regarding the purification of residual waters contaminated with pharmaceuticals. In this context, the study focused on the development of an advanced oxidation process, specifically the heterogeneous photocatalysis and its application to the degradation of Propranolol from aqueous solutions.

Experimental

The reagents used in this work were of analytical purity and were used as such. Propranolol, of 99% purity was obtained from Sigma - Aldrich. In this work, we used the following catalysts: TiO_2 and TiO_2-MoO_3, which were prepared and characterized according to previous work, as well as literature data [16-20]. The photocatalytic activity of these two catalysts has been evaluated by following the kinetics of photodegradation of a series of azo compounds [19].
The heterogeneous photocatalysis process was conducted in a photochemical reactor in Pyrex glass whose dimensions were 3 cm in diameter and 5 cm high. The reactor was initially loaded with 20 ml of Propranolol solution. During the experiment, the mixture was held under continuous stirring (100 rpm) using a magnetic stirrer, placed underneath the photoreacteur. The source of irradiation was a UV Bioblock VL-4LC lamp; 8 W; 230V; 50Hz; 4W-365nm Tube and 4W-254nm Tube. The reactor had also a spring system that enabled us to vary lamp UV-sample distances. The catalyst was added in the reaction medium prior to photodegradation and the irradiation began after 30 minutes, in order to achieve the equilibrium of absorption. A sample was taken every 5 minutes, the catalyst being eliminated by filtration on Whatman filter 0, 45 µm. The degradation process of Propranolol was monitored by means of UV-Vis spectroscopy, au cours de la photodégradation a été suivie qualitativement et quantitativement par spectroscopie UV-visible, using a Perkin-Elmer-Lambda -950 spectrophotometer.
The Propranolol solutions were prepared by dissolution in an aqueous medium (distilled water) at 50°C, at the limit of solubility of the compound. Sulfuric acid has been added directly in the solution of Propranolol in order to adjust the pH to the desired value. Catalyst concentrations ranged from 1 to 6 g/L.

Results and discussion

According to literature data, the TiO_2 catalyst is the most frequently used, while TiO_2-MoO_3 is a newer compound, used most of the time as a catalyst for the oxidation of propylene in acetone.
In order to study the influence of experimental parameters on the photodegradation process, we conducted a series of measures on Propranolol solutions, in order to establish the optimal conditions of degradation by heterogeneous photocatalysis. This study focused on the following experimental parameters: distance of irradiation, type of catalyst, concentration of the solution of Propranolol, the initial concentration of the catalyst, the pH and the temperature of the reaction medium.
Propranolol (initial concentration of 0.25 mM) has been degraded in acidic medium (pH = 3) in the presence of different amounts of catalysts (TiO_2 and TiO_2-MoO_3) in order to determine the optimal lamp-sample distance necessary for the most suitable degradation of Propranolol. It was found that the speed of degradation of Propranolol at 30 cm lamp-sample distance is less important than that of solutions situated at 25 cm, 20 cm, 15 cm and 10 cm. In fact, more the lamp-sample distance is lower, most the degradation occurs faster. After 8 min of treatment, we managed to degrade with a rate of 45, 95, 97 and 99% the solutions situated at 15 cm, 10 cm and 30 cm distance from the lamp.

In another series of experiments, it was noticed that the nature of the catalyst (TiO_2 and TiO_2-MoO_3) influence in a great extent the kinetics of degradation of Propranolol, e.g. the photodegradation of Propranolol was faster when the TiO_2-MoO_3 catalyst was used.
In order to study the influence of the initial concentration of Propranolol, four aqueous solutions of Propranolol with concentrations ranging from 0.25 x 10^{-3} to 1 x 10^{-2} M were submitted to degradation process. The obtained results revealed that the heterogeneous photocatalysis remains applicable in a wide range of concentrations; the speed of degradation of a 1.10^{-2} M Propranolol solution was less important than in the case of the solutions whose concentrations ranged from $0,75.10^{-2}$M to $0,25.10^{-2}$ M. After 10 min of treatment, we managed to degrade with a rate of 45, 95, 97 and 99% the solutions of 1.10^{-2}M, $0,75.10^{-2}$ M, $0,50.10^{-2}$ M and $0,25.10^{-2}$ M concentrations.
Further, equal volumes of Propranolol solutions (100 mL) were degraded in acidic medium (pH = 3) in the presence of different TiO_2-MoO_3 concentrations (ranging from 1 to 6g/L), in order to establish the optimal catalyst concentration for the complete degradation of Propranolol. It was noticed that the degradation was more effective for a 2 g/L TiO_2-MoO_3 concentration then at 6g/L, but in all cases the Propranolol was completely degraded in 30 min for an initial concentration of 0.25 mM.
Under our experimental conditions thus determined ($C_{cat.}$ = 40 mg; $C_{Propranolol.}$ = 0,25 mM; V = 20 mL, lampe – sample distance = 10 cm), the evolution of the solution of Propranolol during the heterogeneous photocatalytic degradation process was qualitatively and quantitatively monitorised by UV-visible spectroscopy, as it can be seen in Figure 1.

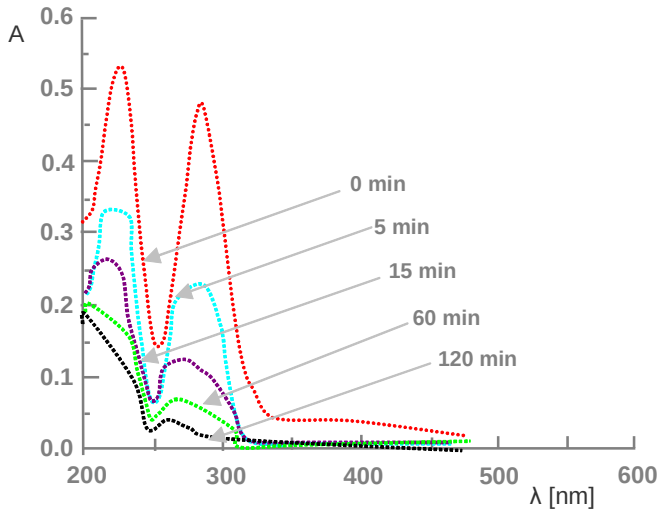

Figure 1. UV-Vis spectra of Propranolol during the heterogeneous photocatalytic treatment. [Propranolol] = 0,25 mM, V = 20 ml [TiO_2-MoO_3] = 40 mg, pH = 3

This figure shows that the disappearance of Propranolol during the heterogeneous photocatalysis process occurs fast. The absorbance peak located at λ = 225 nm decreases gradually and then completely disappears after 15 min. The peak located at λ = 288 shows a similar evolution.

Conclusion

The obtained results revealed that among the two photocatalysts used, the best performance can be attributed to the TiO_2-MoO_3catalyst.

The optimal concentration of this photocatalyst was of 2 g/L TiO_2-MoO_3. This concentration increases the efficiency of the method to treat aqueous solutions of Propranolol.
The speed of decomposition of Propranolol is accelerated if the process is carried out at a temperature of 50°C.
From ecological point of view, as well as economic, heterogeneous photocatalysis process presents a significant advantage as compared to conventional methods of wastewater treatment.
This method proved effective for the clean-up of contaminated water by Propranolol, with rates of mineralization above 95% in the adopted working conditions.

References

[1] J.L. Acero, F.J. Benítez, F.J. Real, M. González, J. Haz. Mat. 153 (2008) 320.
[2] G. Agrios, P. Pichat, J. Appl. Electrochem. 35 (2005) 655.
[3] A.B.C. Alvares, C.Dlaper, S.A. Parsons, Env. Techn. 22 (2001) 409.
[4] C. Anselme,E.P. Jacobs,Watertreatmentmembraneprocesses,NewYork:McGrawHill Mallevialle, 1996, pp. 401.
[5] R. Atkinson, Kinetics and Mechanisms of the gas phase reactions of the hydroxyl radical with organic compounds, American Institute of Physics, New York, 1989.
[6] C. Blieffert,R. Perraud,Chimie de l'environnement, air, eau, sols, déchets,Paris: DeBoeck Université,2001, pp. 102.
[7] E. Brillas, B. Boye, M.M. Dieng, J. Electrochem. Soc. 150 (2003) 148.
[8] R.D. Combes, R.B. Haveland-Smith,Mut. Res./Rev. Gen. Tox. 98(2) (1982) 101.
[9] M. Diagne, N. Oturan, M.A. Oturan, Chemosphere. 66 (2007) 841.
[10] L. Diez,M.H. Livertoux,A.A. Stark,J. ChromatographyB. 763 (2001) 185.
[11] M. Farhadian, D. Duchez, C. Vachelard, C. Larroche, Water Res. 42 (2008) 1325.
[12] A. Brunet, S.P. Orr, J. Tremblay, K. Robertson, K. Nader, R.K. Pitman, J. Psych. Res. 42(6) (2008) 503.
[13] A.J. Kolber, Vanderbilt Law Rev. 59 (2006) 1561.
[14] K.G. Shields, P.J. Goadsby, Brain. 128(1) (2005) 86.
[15] G. Vaiva, F. Ducrocq, K. Jezequel, B. Averland, P. Lestavel, A. Brunet, C.R. Marmar, Biol. Psychiatry. 54(9) (2003) 947.
[16] A. Fujishima, X.T. Zhang, D.A. Tryk, Surf. Sci. Rep. 63 (2008) 515.
[17] X. Zhang, H. Yang, F. Zhang, K.Y. Chan, Mat. Lett. 61 (2006) 2231.
[18] L. Gomathi Devi, G.M. Krishnaiah, J. Photochem. Photobiol. A: Chem. 121 (1999), 141.
[19] J. Atchana, G.M. Simu, S.G. Hora, M.E. Grad, J.B. Tchatchueng, B.L. Benguellah, R. Kamga, JFAE 9(1) (2011) 457.
[20] J.B. Tchatchueng, B.B Loura., J. Atchana, R. Kamga, J. Environ. Sci. 2(1) (2009) 31.

QUALITATIVE DETERMINATION OF KEY EMERGING XENOBIOTICS IN MIXED WASTEWATER DISCHARGE

Maja Sremački[1*], Ivan Špánik[2], Ivana Mihajlović[1], Maja Turk Sekulić[1], Jelena Radonić[1], Mirjana Vojinović Miloradov[1]

[1]University of Novi Sad, Faculty of Technical Sciences, Department of Environmental Engineering and Occupational Safety and Health, Trg Dositeja Obradovića 6, 21000 Novi Sad, Serbia
[2]Slovak University of Technology, Faculty of Chemical and Food Technology, Institute of Analytical Chemistry, Radlinskeho 9, Bratislava, Slovakia
e-mail: majasremacki@uns.ac.rs

Abstract
Nowdays, it is unattainable to follow, detect or identify all the chemicals that are excreted into the environmental aquatic bodies. The number of chemicals introduced into the environment in modified structures, as metabolites or as mixtures of chemical cocktails, is growing progressively. Illicit drugs and endocrine disruptive substances (EDCs) (emerging xenobiotics) are not excluded from this fate. Illicit drugs are xenobiotics with psychoactive effects and influences onto the human body and mind, and are excreted into the environment mostly in forms of metabolites. In sense of these facts, a high level off importance is appointed on an optimal and effective analytical practices and high performing equipment, but far more important is a good detection model for emerging substances, especially for detection of emerging xenobiotics in a highly polluted sample, as wastewater. This paper will show the results of qualitativeanalyses for complex sample matrix of mixed wastewater and results of detection for selected xenobiotics with endocrine disruptive and psychoactive effects.

Introduction
The safety and quality of surface water that is used as a source for drinking water production and for the significant number of human activities have to be an important topic for society, since the pollution can cause serious effects on human health [1, 2]. Newly recognized environmental contaminantsidentified as emerging substances are perceived as globally unregulated substances [3]. The emerging substances include organic and inorganic pollutants, such as pharmaceuticals, personal care products, flame retardants, endocrine disruptive compounds, industrial chemicals, biological metabolites, hormones, toxins and other chemicals [4, 5].
The sewerage system in Novi Sad is designed and constructed as a mixed wastewater channelling system that collects domestic and industrial wastewater mixed with the urban, sub-urban and rural runoff, making maintenance of regular water quality very difficult. The system does not incorporate treatment of wastewater before discharge.
Xenobiotic is a chemicalcompoundforeign to a givenbiologicalsystem.Withrespect to animalsandhumans,xenobioticsincludedrugs,drugmetabolites,andenvironmentalcompoundssuch as pollutantsthatarenotproduced by thebody. In theenvironment,xenobioticsincludesyntheticpesticides,herbicides,hormones, illicit and licit drugs and medication, agricultural andindustrialpollutantsthatwouldnot be found in nature [6].
The illicit use of substance makes it more difficult to research and observe, especially when excreted levels are in nano levels or less. Illicit drugs are the latest group of emerging compounds

identified in the aquatic environment [7].Mixed wastewater from urban areas are the dominant source of illicit drugs and their metabolites in surface water. The results represent an introduction to a new approach to organic contamination monitoring of waste and surface water. 24h composite samples of mixed urban wastewater were collected over a period of 7 days from selected location in the city of Novi Sad in order to determine concentration levels of cocaine, benzoylecgonine, amphetamines, ecstasy, methamphetamine and cannabis metabolite THC – COOH, caffeine, antibiotics, pesticides and other. For the target determination 41 analytes in total were selected - 16 pesticides, 9 hormones, 11 sterols and 5 illicit drugs.

Exerimental

In order to identify the list of compounds that could be expected in aquatic environment in Novi Sad and it's vicinity, screening analyses of waste (four samples per cycle) and surface water (six samples per cycle) were performed during the three cycles of sampling in 2011 [8]. Detailed description of the sampling, sample preparation and analysis is available in Milić et al., 2013.

The samples were collected from collectors GC1 and GC2 in glass bottles and stored at 4 °C. For screening analyses a 1000 ml aliquot of water sample were spiked with internal standard to achieve final concentration of 1μg/L and extracted with two 50 ml portions of DCM for 30 minutes. Extract was dried with anhydrous sodium sulfate. Kuderna-Danish apparatus was used to evaporate to final volume of 1 ml. A 50 μl of extract was injected into Agilent 6890 GC Agilent 5973 MSD system equipped with PTV injector that was programmed from 60 ˚C to 260 ˚C. Capillary GC analysis was performed on a 30 m x 250 mm I.D., 0.25 mm df DB-XLB and HP-5MS column. Helium was used as carrier gas. The MSD was used in SIM mode for all samples.

Each target compound during target analyses was qualified by two qualifier ions. The group of pesticides were analyzed using GC-MS according to modified ISO 6468 procedure, VOCsby GC-MS according to ISO 10301 procedure. Pesticides and hormones were analyzed using SPE-HPLC-DAD according to modified ISO 11369 procedure [9]. During the screening analyses a high number of substances were identified, from which 41 were selected as key substances for the target analyses according to lists of priority and hazardous priority and emerging substances.

For quantification of selected analytes validated target methods - liquid chromatography tandem mass spectrometry (HPLC-MS^2) or high-resolution mass spectrometry (HPLC-HRMS) are used.

Results and discussion

In the samples of wastewater collected from two main discharges of wastewater (GC1 and GC2), the presence of all monitored analytes was confirmed in concentration levels of ng/L. [10, 11]

Pesticides were detected in the highest concentrations, especially in the wastewater. According to the concentration ratio of p,p′-DDD and p,p′-DDT at sampling point with the highest concentrations, GC1, the value of 1.29 indicated historical contamination with these chemicals. p,p`-DDD, p,p`-DDE and p,p`-DDT at sampling site GC1 were determined in concentrations more than eight times higher than annual average values in EU countries. Hexachlorobenzene (Lindane) was found in concentrations three to five times higher than AA EQS at GC1 and GC2. The significant quantity of the hormones androstane-17-one, -cholestan-3-ol, cholest-5-en-3-ol, cholestan-3-one, cholestane, 3- hydroxy-, (3.beta,5.alpha)-, stigmast-5-en-3-ol and coprostanol were detected in urban effluent at the sampling points of GC1 and GC2. The presence of hormones is mainly highlighting the impact of faecal pollution, due to the lack of the WWTP. The hormones were only detected above the LOD, but it was not possible to quantify them. In sampling point GC2, estriol has been detected in concentration of 4.1±0.5 ng/mL.

During the determination of the 5 selected analytes from the group of illicit drugs, THC-COOH singled out as very interesting for the site of Novi Sad.THC-COOH was recorded in significantly higher concentration in all samples from the city of Novi Sad, compared to the region, but also to all selected sites in Europe that were also involved in this research. The concentration levels of all 5 analytes from the group of illicit drugs are presented in Table 1.

Table 1. Measured concentration levels of selected illicit drugs in Novi Sad

Illicit drug	Measured concentrations in [ng/L] for Novi Sad						LOQ
	Thursday	Friday	Saturday	Sunday	Monday	Tuesday	
Cocaine	4.40	17.00	14.00	5.30	n.d.	16.00	12.00
Benzoylecgonine	14.00	25.00	60.00	43.00	43.00	39.00	10.00
Amphetamine	31.00	50.00	61.00	60.00	52.00	95.00	25.00
MDMA	n.d.	n.d	16.00	24.00	14.00	22.00	20.00
THC-COOH	442.00	368.00	435.00	500.00	345.00	284.00	10.00

Up to 4 times higher concentrations of all selected analytes were detected during the weekend(from Friday till Sunday). According to the results shown in Table 1. and Figure 1, THC-COOH has a significantly higher concentrations in regard to other illicit drugs, as well as to other cities in the region.

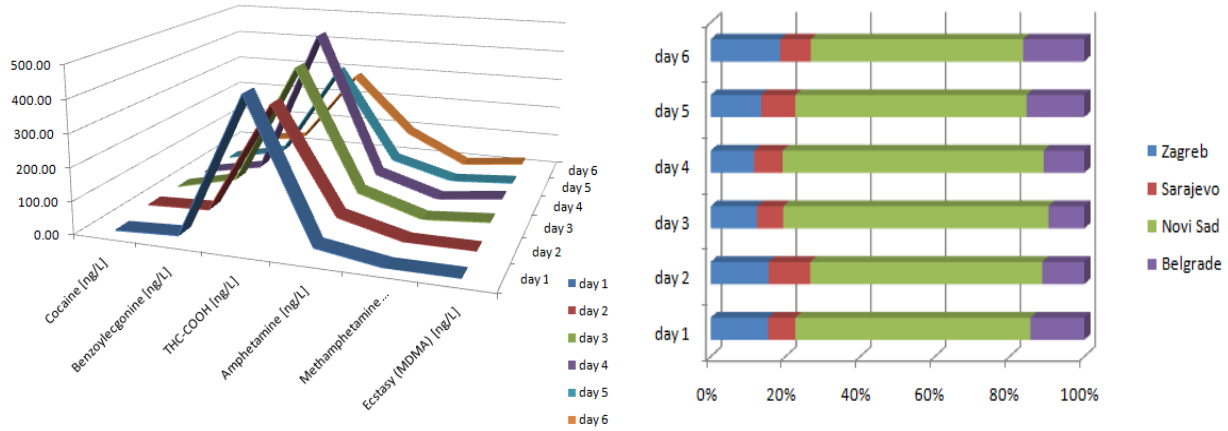

Figure 1. Concentration levels of selected compounds and contribution of Novi Sad in THC-COOH excretions to surface water in Balkan region

Conclusion

In recent years a new problem has emerged in our water environment, namely, the presence of endocrine disruptive compounds (EDCs) that may affect the reproductive functions of human beings and wild life. Most potent EDCs are pesticides, hormones and illicit drugs. In our research, it is shown that all three groups of emerging xenobiotics from the group of EDCs are present in the mixed wastewater of city of Novi Sad, as a result of discharging of wastewater into the Danube without any treatment. Out of 41 selected endocrine disruptive compounds, 20 were detected, with pesticides in the highest concentrations. From the group of illicit drugs, THC-COOH was detectedin the highest concentrations. Republic of Serbia is in the midst of planning efforts that will lead to selection of a water plan and wastewater treatment facilities that should serve for decades. Wastewater reclamation and reuse will be a major part of both water supply and wastewater treatment planning. City of Novi Sad is in the planning and design stage of

WWTP which means that is of essential importance to have and obtain up-to-date specific data on wastewater quality and quantity.

Acknowledgements
This research was supported by NATO Science for Peace Project (ESP.EAP.SFP 984087) and NIVA Institute collaboration for investigation of illicit drugs – TheEuropean Centre for Drugs and Drug Addiction (EMCDDA); European Union's Seventh Framework Programme for research, technological development and demonstration. Special thanks to Dr. Jaroslav Slobodnik, Environmental Institute, Kos, Slovak Republic.

References

[1] K. Kümmerer (2011) Clean – Soil Air Water, *39 (10)*, 889–890.
[2] J. R. Dominguez-Vargas, T. Gonzalez, P. Palo, E. M. Cuerda-Correa (2013) Clean – Soil Air Water, 41 (11), 1052--1061.
[3] S. M. Rodrigues, G. A. Glegg, M. E. Pereira, A. C. Duarte (2009) Pollution Problems in the NE Atlantic: Lessons Learned for Emerging Pollutants such as the Platinum Group Elements, Ambio, *38 (1)*, 17--23.
[4] D. Calamari, E. Zuccato, S. Castiglioni, R. Bagnati, R. Fanelli (2003) Environ. Sci. Technol. *37*, 1241--1248.
[5] S. Grujic, T. Vasiljevic, M. Lauševic (2009) J. Chromatogr. A, *1216 (25)*, 4989--5000.
[6] Miller-Keane (2003) Encyclopedia and Dictionary of Medicine, Nursing, and Allied Health, Seventh Edition, © by Saunders, an imprint of Elsevier, Inc.
[7] C.G. Daughton, (**2001)** Illicit Drugs in Municipal Sewage: Proposed New Non-Intrusive Tool to Heighten Public Awareness of Societal Use of Illicit/Abused Drugs and Their Potential for Ecological Consequences, Pharmaceuticals and Personal Care Products in the Environment: Scientific and Regulatory Issues, *Symposium Series 791*; ACS, Washington, D.C., , pp. 348-364.
[8] N. Milić, I. Spanik, J. Radonić, M. Turk Sekulić, N. Grujić, O. Vyviurska, M. Milanović, M. Sremački, M. Vojinović Miloradov (2013) Fresenius Environmental Bulletin, 23 (2), p.p. 372-377
[9] M. Vojinovic-Miloradov, I. Mihajlovic, O. Vyviurska, F. Cacho, J. Radonic, N. Milic, I. Spanik (2014) Fresenius Environmental Bulletin 23 (9), p.p. 2137-2145
[10] C. Ort, A.L N. van Nuijs, J.D. Berset, L. Bijlsma, S. Castiglioni, A. Covaci, P. de Voogt, E. Emke, D. Fatta-Kassinos, P. Griffiths, F. Hernández, I. González-Mariño, Roman Grabic, B. Kasprzyk-Hordern, N. Mastroianni, A. Meierjohann, T. Nefau,M. Östman, Yolanda Pico, I. Racamonde, M. Reid, J. Slobodnik, S. Terzic, N. Thomaidis, K.V. Thoma (2014) Spatial differences and temporal changes in illicit drug use in Europe quantified by wastewater analysis, Addiction, Society for the study of Addiction research raport, 109, p.p. 1338-1353, doi: 10.1111/add.12570, John Wiley & Sons Ltd
[11] M. Sremački, M. Stošić, J. Simić, I. Mihajlović, M. Vojinovic Miloradov "Detection of organochlorine pesticides and estrogen in mixed municipal waste water of Novi Sad" International Conference "Waste waters, municipal solid waste and hazardous waste" ISBN 978-86-82931-68-3, p. 133-137, 21-23.04.2015. Budva

CHEMICAL ANALYSIS AND BIOTEST IN THE ASSESSMENT OF NICOSULFURON SOIL POLLUTION

Sanja Lazić, Bojan Konstantinović, Dragana Šunjka, Nataša Samardžić, Mirjana Kojić, Slavica Vuković, Milena Popov, Milan Blagojević

Department of Environmental and Plant Protection, Faculty of Agriculture, University of Novi Sad, 21000 Novi Sad, Trg Dositeja Obradovića 8,Serbia
e-mail: draganas@polj.uns.ac.rs

Abstract
The assessment of soil pollution exposed to nicosulfuron can be conducted through chemical analysis, by determination of residue quantity, and biotests. In this research, the field dissipation study of nicosulfuron herbicide in soil under maize, was conducted in controled conditions. Nicosulfuron residue in top soil layers were determined by HPLC-DAD, while nicosulfuron extraction was performed by modified QuEChERS method. In five months period, from the first application at the manufacturer's recommended concentration, until harvest, nicosulfuron concentration decreased over time from 0.95 mg/kg to 0.12 mg/kg. In order to evaluate phytotoxicity of nicosulfuron on susceptible crops, *Triticum vulgare* L.and *Beta vulgaris* L.were used as test plants. Inhibitory action of nicosulfuron on the studied species was proved on the basis of the obtained results, by studying the morphological parameters, roots and above-ground seedlings lengths (mm), i.e. length of shoot.

Introduction
After herbicide application its remainings in the soil can prove beneficial during the season for control of later flushes of target weeds. However, their residues, found in the soil during the following year, can reduce yields of susceptible crops grown in rotation. The amount of herbicide that sorbs to the soil and the rate it can desorb back into the soil solution determines the overall phytotoxicity of the herbicide [1].
Sulfonylurea herbicides are used to control a variety of broad-leafed weeds and grasses in cereals and other row crops and for industrial weed control. They can be considered such "as new formulation pesticides" because of their high selectivity and low persistence in the environment [2]. These characteristics significantly reduce the amount of the applied chemicals to the field in comparison with conventional ones [3]. However, the application of low levels of these herbicides does not guarantee high levels of environmental tolerance. In some cases, sensitive plants suffer damage by dosages lower than 1% of the initial application rate [4]. Sulfonylurea herbicides, such as nicosulfuron, are more mobile in alkaline soils and in soils with lower organic matter content. Nicosulfuron is the most applicable sulfonylurea herbicide in maize for successful control of annual and perennial weeds.
The phytotoxic effect of nicosulfuron and its metabolites on dicotyledonous plants leads to a self-limitation in the re-planting period. After sowing, in 27-30 days interval since pesticide application, phytotoxic effects are obvious on cereals, sugar beet, canola and clover. The listed crops should not be sown on land previously treated by nicosulfuron before next spring, when the expected level of herbicide residues and their degradation products is <0.001 mg/kg [5].
Quality evaluation and the level of environmental pollution are established by application of different physical, chemical and biological methods. Usually, the assessment of soil contamination is based on the chemical analysis. These methods imply the use of corresponding

extraction and purification methods, as well as sensitive methods of pesticide residues determination, such as gas and liquid chromatography.
However, world wide, there is an increase in the use of biological methods that imply use of cultivated plants as test organisms, i.e. phytoindicators. Biological methods and tests by which soil quality is evaluated, have a great importance for agricultural production as they indicate potentialphytotoxical action of the applied pesticides. Use of cultivated plants as tests organisms is especially significant for biological tests in agricultural production.

Experimental

Field trial

The monitored field trial was carried out on a chernozem soil, according to OEPP standard methods for experimental design and data analysis. In mazie field, nicosulfuron (OD, 40 g/l) was applied at the recommended dose, at the corn growth stage of BBCH 12-18. Soil samples were collected before and immediately after the pesticide application, and every two weeks until harvest, from surface soil layer, of 0-30 cm.

Chemical analysis

For the chromatographic analysis, an Agilent 1100 Series system with DAD detector and Zorbax SB-C18 column (5 μm, 250mm ×3 mm internal diameter) were used. The mobile phases were composed of acetonitrile (A) and 0.1% (V/V) acetic acid in water (B), at a flow rate of 1.0 ml/min, using following gradient profile: 0–10 min linear from 52% to 47% (A).
For nicosulfuron extraction of 10.0 g of previously dried, milled and sieved soil samples were weighted and transferred into 50 ml polypropylene tube. Afterwards, 3 ml of deionized water and 10 ml of acidified acetonitrile were added. The tube was shaken and vortexed for a 1 min. A mix of buffered salts from separate pouches was added, shaken for 1 min and vortexed 1 min. The tube was placed in an ultrasonic bath for 10 min and centrifuged at 4000 rpm for 5 min. The supernatant was filtered through a 0.45 μm membrane filter and transferred into an autosampler vial for HPLC-DAD analyses [6].

Biotest

The method prescribed by ISTA rules (International rules for seed testing) for 2013 and the Regulations on the quality of seeds of agricultural plants [7] was used for the biotests. In laboratory bioassays, in controlled conditions the impact of different, previously by chemical analysis determined nicosulfuron doses, was studied on seed germination and the initial growth of wheat and sugar beet. On filter paper in Petri dishes 10 ml of nicosulfuron working liquid was added in doses close to those previously obtained by chemical analysis (0.96-0.07 μg/ml), and each Petri dish was filled with 10 seeds of wheat (*Triticum vulgare* L.) and sugar beet (*Beta vulgaris* L.). The trial was set up in four replications. Seeds were germinated for 10 days in thermostat at a temperature of 25±2 °C in dark. Morphological parameters, root length and seedlings above-ground parts (mm), i.e. length of seedlings of the above mentioned cultures were measured after incubation.

Results and discussion

The results for determination of nicosulfuron in trace amount were presented in our previous paper [6]. The validation study performed according to SANCO/825/00 rev. 8.1 16/11/2010 [8], has fully met the criteria mentioned in the document.
The results of dissipation demonstrated a gradual and continuous decrease of nicosulfuron content in the soil. Herbicide concentration decreased over time from 0.95 mg/kg to 0.12 mg/kg,

in five months period. The half-life ($t_{1/2}$) of nicosulfuron in soil, calculated using results obtained in this study, was 6.93 days.

The amount of nicosulfuron residue obtained in the field dissipation study were used in biotests.Ten days after the treatment, wheat and sugar beet seedlings exhibited different levels of inhibition depending on the applied dose of nicosulfuron.

It was established that all studied doses of nicosulfuron applied in wheat significantly inhibit seedlings length in comparison to the control. In regard to the control, seedlings length was reduced by 86.89-91.37%(Table 1, Figure 1). In sugar beet, more significant inhibition in seedlings growth was recorded in the use of the highest dose of nicosulfuron, while the results of the remaining variants were statistically at the same significance level in comparison to the control, for shoot length (Table 1). Inhibition of growth of seedlings treated by different nicosulfuron doses was from 6.23 do 85.04%.

Table 1. The effect of nicosulfuron on seedling length *T. vulgare* L. and *B. vulgaris* L. after 10 days under laboratory conditions

nicosulfuron (a.i. µg/ml)	*Triticum vulgare* L. (cm)		*Beta vulgaris* L. (cm)	
	root	shoot	root	shoot
0.96	8.35[a]	12.97[a]	0.03[a]	0.09[a]
0.52	11.80[a]	18.25[a]	0.08[a]	0.17[a]
0.34	7.37[a]	13.35[a]	0.05[a]	0.11[a]
0.22	8.97[a]	14.02[a]	0.12[ab]	0.15[a]
0.07	13.10[a]	17.35[a]	0.04[a]	0.21[a]
Control	**116.00[b]**	**116.40[b]**	**0.18[b]**	**0.13[a]**

*Values followed by the same letter at the same significance level (95% confidence interval)

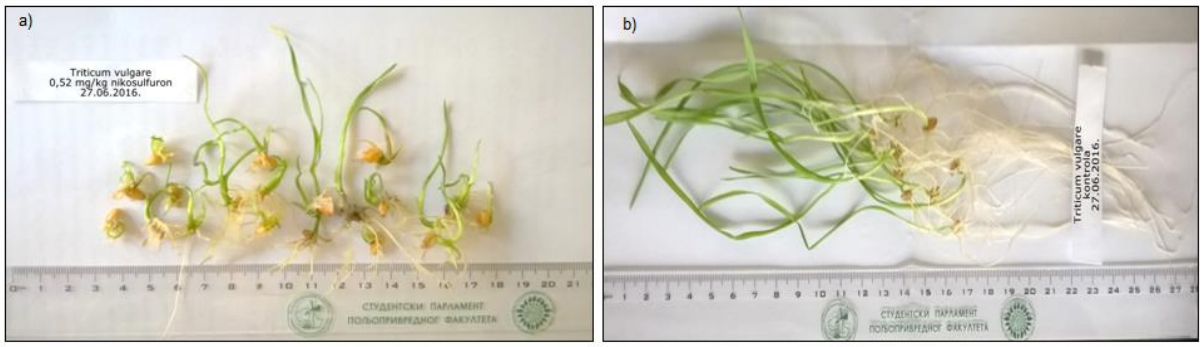

Figure 1. Effect of nicosulfuron from 0.52 µg/ml of the length of root and shoot *T. vulgare* L. after ten days (a); Length of root and shoot *T. vulgare* L. in control after ten days (b)

According to the results obtained in biotests, it can be concluded that the lowest amount of nicosulfuron remained in soil five months after application, determined by chemical analysis, can cause inhibitory effect on seedlings length *T. vulgare* L. (86.9%). However, the same concentration of nicosulfuron was significantly reduced only root length *Beta vulgaris* L. (77.8%), without influence on shoot length, in comparison to the control.

Conclusion

Based on the obtained results it can be concluded that there exists an inhibitory effect of the herbicide nicosulfuron residues on growth of wheat (*Triticum vulgare* L.) seedlings, compared to the control treated with distilled water. Wheat shows significant susceptibility to nicosulfuron residues in soil, and they can have negative effect on this culture. Moreover, the conducted laboratory assays showed that inhibitory action of nicosulfuron increase sugar beet root length. In relation to roots and seedlings length, seedlings of *T.vulgare* L., and smaller seedlings of *B. vulgaris* L. exibited higher susceptibility to the tested concentrations of nicosulfuron. In relation to roots and shoots length, seedlings of *T.vulgare* L., and smaller seedlings of *B. vulgaris* L., exibited higher susceptibility to the tested concentrations of nicosulfuron.

Acknowledgements

The authors appreciate funding from the Ministry of Education and Science of the Republic of Serbia (Project No. III43005) for supporting this study.

References

[1] B.G.L. Geisel Thesis for the Degree of Master of Science, University of Saskatchewan, Saskatoon, Saskatchewan, Canada, 2007.
[2] M. Benzi, E. Robotti, V. Gianotti, Giornate Italo-Francesi di Chimica, GIFC 2010, 26-27 Aprile 2010, Genova, Italy.
[3] H.M. Brown, Pesticide Science, 29 (1990) 263.
[4] E.M. Beyer, M.J. Duffy, J.V. Hay, D.D. Schlueter, in: P.C. Kearney, D.D. Kaufman (Eds.), Chemistry, Degradation and Mode of Action, Marcel Dekker Inc., New York, 1987.
[5] S. Lazić, D. Šunjka, I. Stojanović, S. Vuković, B. Konstantinović, M. Popov, 6th International Scientific Agricultural Symposium "Agrosym 2015", October 15 - 18, Jahorina, Bosnia and Hernzegovina, Proceedings, pp. 959 (2015).
[6] S. Lazić,D.Šunjka, N. Grahovac, 20th International Symposium on Analytical and Environmental Problems, SZAB Kémiai Szakbizottság Analitikai és Környezetvédelmi Munkabizottsága, 22 September 2014, Szeged, Hungary, (2014) Proceedings, pp. 143.
[7] Official Gazette of SFRY", No. 47/87, 60/87, 55/88 and 81/89 and "Official Gazette of SRY", No. 16/92, 8/93, 21/93, 30/94, 43/96, 10/98, 15/2001 and 58/2002, ''Official Gazzete of RS", No. 23/2009, 64/2010, 72/2010 and 34/2013.
[8] EU COMMISSION, Directorate General Health and Consumer Protection, SANCO/825/00 rev. 8.1 16/11/2010, Guidance document on pesticide residue analytical methods.

THE INFLUENCE OF CADMIUM PRECURSORS UPON PdS/$Zn_{1-X}C_XS$ PHOTOCATALYSTS EFFICIENCY IN WATERSPLITTING REACTION

Paula Svera[1,2], Cristina Mosoarca[1], Radu Banica[1]

[1]National Institute for Research and Development in Electrochemistry and Condensed Matter, no 144 A. PaunescuPodeanu Street, Timisoara 300569
[2]PolitehnicaUniversity Timisoara, PiataVictoriei, no. 2, 300006 Timisoara, Romania;
e-mail: mosoarca.c@gmail.com

Abstract
Photocatalysts based on hexagonal cadmium sulfide have been hydrothermally synthesized using crystalline zinc sulfide as sulfide source, and metal nitrates, acetates, chlorides and sulfatesas cadmium sources. The powders have been characterized by X-Ray Diffraction (XRD), UV-VIS Diffuse Reflectance Spectroscopy (DSR)and Energy-Dispersive X-ray Spectroscopy (EDX). Further experiments of photocatalysis in aqueous solution of sulfide and sulfite for hydrogen evolution, were conducted. The samples were irradiated by monochromatic blue light, generated by an LED. From these experiments it was concluded that the presence of sulfate and acetate anions in the system results in more performantphotocatalysts than the presence of nitrate and especially chlorideanions.

Introduction
The increasing demand for new, environment friendly energy sources opens the opportunity for hydrogen production by photocatalytic water splitting. Currently scientific and industrial interest is focused on the capability of materials (photocatalysts) to absorb light especially in the visible range, which represents about 43% of the solar spectrum [1]. The highly negative potential of excited electrons in the conduction band and the rapid generation of electron-hole pairs by incident photon providesa high photocatalytic activity to the zinc sulfide based compounds [2]. Using dual/coupled systems such as ZnS-CuS, ZnS-WS_2, ZnS-CdS [2] composites or doping with Cd [3], represents a common way for shifting the wide band gap energy of ZnS (3.35 eV) to visible region. In the case of dual semiconductor photocatalysts the charge separation mechanism consists in the injection of electrons from one of the semiconductors into the conduction band of the second semiconductor [4].

The aim of this study was the comparison of the photocatalytic efficiency of PdS/CdS-ZnS composite compounds obtained from different cadmium salts.

Experimental
ZnS precursor synthesis
ZnS is precipitated by the addition of a Na_2S solution in an acidified aqueous solution of $ZnSO_4$. The S^{2-}:Zn^{2+}molar ratio used in the precipitation was 0.9. Due to the acid environment, the $Zn(OH)_2$ precipitation is excluded. ZnS was then washed with distilled water and placed in an autoclave which was heated for 20 hours at a temperature of 200°C to improve the crystallinity. Crystallized Zn sulfide was washed twice with water and the last time with ethanol, then dried in vacuum at 60ºC. XRD spectra revealed the existence of cubic ZnS phase.

Photocatalysts synthesisusing different Cd^{2+} salts as precursors
290 mg of crystallized ZnS was dispersed by 30 minutes sonication in 30 ml of bidistilled water. In the resulted suspension, 1 ml of glacial acetic acid was added, under constant stirring. After 5

minutes,4 mL K_2PdCl_4 with a concentration of 0.6 mg/mL Pd^{2+}, was added. After 2 minutes of stirring, 2 mmols of cadmium salt were added in each autoclave, to achieve the same Zn : Cdatomic ratio. The suspensions were subjected to hydrothermal treatment at 200°C for 70 hours. After the hydrothermal treatment, the powders were separated by filtration, washed with distilled water and were kept in Na_2S 0.2 M solution.

Photocatalysis

For the conductedphotocatalysis experiments, in each particular case, a variable volume of photocatalyst suspension was takenin order obtain a final mass of 25 mg photocatalyst. The reaction volume was brought to 25 mL and the S^{2-} ion concentration to 0.2 M. By adding sodium sulfite the SO_3^{2-} concentration was brought to 0.1 M. The reactions were conducted at 25°C andthe suspension was irradiatedwith400 nm blue light. The determination of the amount of released hydrogen was done volumetrically.

Results and discussions

The main reactions that occurred during the hydrothermal treatment are the following:

$$ZnS + x\ Cd^{2+} \rightarrow Zn_{1-x}Cd_xS + x\ Zn^{2+} \quad (r1)$$

$$Pd^{2+} + ZnS \rightarrow PdS + Zn^{2+} \quad (r2)$$

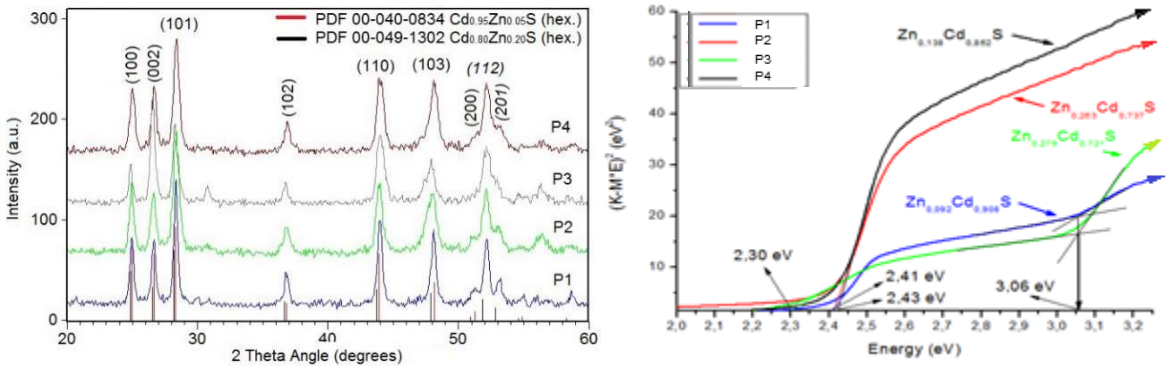

a) b)

Fig. 1. The XRD spectraof P1-P4 samples (a) and the band gap values for various photocatalysts(b).

It was observed that r2 reaction takes place at high speed even at room temperature, leading to immediate changes in color of ZnS suspension from white to brown.This change takes place in the presence of Pd^{2+} ions, which also highlights the formation of PdS. The process takes place due to lower solubility of the PdS in comparison to CdS and ZnS. Stoichiometry of the compounds was determined from EDX analysis and is presented in Table 1. Both XRD (Fig. 1a) and UV-VIS spectra (not shown here) demonstrates the presence of dual phases in P3 which are a mixture of ZnScubic phase and hexagonal $Zn_{1-x}Cd_xS$ solid solution. In conclusion, the reaction product is a mixture of $Zn_{1-x}Cd_xS$ and unreacted ZnS, the amount of unreacted ZnSbeing dependent on the used cadmium salt. In comparison to other samples which are preferentially oriented to 101 direction, P3 shows a preferential growth to 002 direction. Regarding the photocatalytic performance, P3 shows the lowest activity.

Table 1

No.	Cd precursor	Zn precursor	Composition obtainedby the EDX analysis	Photocatalyst code
1	$Cd(NO_3)_2*4H_2O$	ZnS	$Zn_{0.092}Cd_{0.908}S$	P1
2	$Cd(CH_3COO)_2*2H_2O$	ZnS	$Zn_{0.263}Cd_{0.737}S$	P2
3	$CdCl_2*2.5H_2O$	ZnS	$Zn_{0.279}Cd_{0.721}S$	P3
4	$CdSO_4*8/3$	ZnS	$Zn_{0.138}Cd_{0.862}S$	P4

The band gap values, Eg, were determined from DSR spectra. As shown in figure 1b, the P1 and P3 samples have two band gap values indicating two different compounds. Regarding P1sample, the band gap value of $Cd_{1-x}Zn_xS$ compound is around 2.41 eV. Also a small amount of ZnS is visible in diffuse reflectance spectra (not shown here); however, in case of sample P3 a larger amount of ZnS was detected. Eg value of unreacted ZnS, which was probably Cd-doped, was about 3.06 eV in both cases, with slightly decreased value compared to the pure cubic crystalizedZnS which is about 3.55 eV.

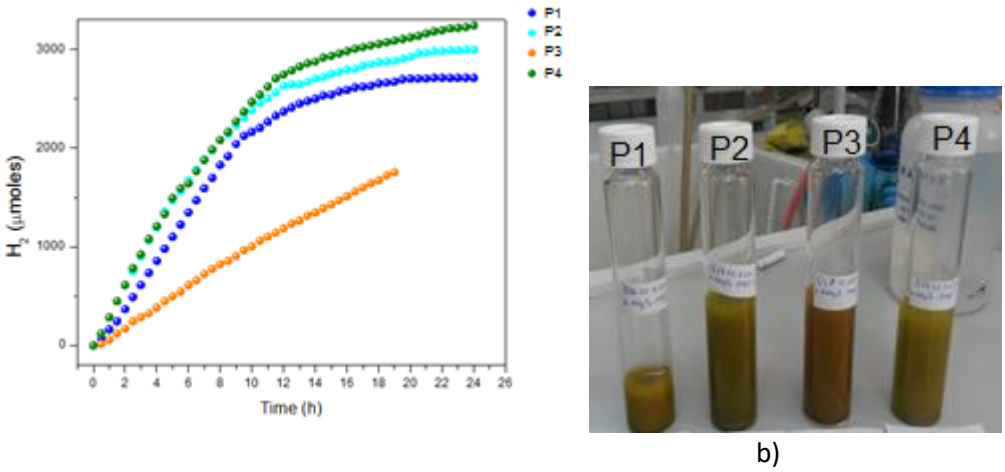

b)

Fig. 2. Hydrogen evolution curve for various environments synthesized photocatalysts (P1 – NO_3^-, P2- CH_3COO^-, P3 – Cl^-, P4-SO_4^{2-}) – a) and the image showing the suspensions of the used photocatalysts – b)

As shown in the figure 2a, in the first two hours of illumination, the evolution rate of hydrogen increases progressively. Between 2 and 8 hours, the hydrogen evolution rate is relatively constant, with a decline after more than 8 hours of illumination. The decreasing rate of hydrogen production is due to the decrease of sodium sulfite concentration in the solution. In the absence of sodium sulfite, the sulfide ion is oxidized to sulfur. It reacts with excess of sodium sulfide producing polysulfide ions. The polysulfide solutionis yellow, which means that it absorbs blue light emitted by the LED. The main reactions that take place are:

$$\text{Photocatalyst} + h\nu \rightarrow \text{Photocatalyst}\ (e^- + h^+)$$
$$2H_3O^+ + 2e^- \rightarrow 2H_2O + H_2$$
$$S^{2-} + 2\ h^+ \rightarrow S$$
$$S + SO_3^{2-} \rightarrow S_2O_3^{2-}$$

As seen from the above reactions, in order to obtain one millimole of hydrogenit is required to use 1 mmolof sodium sulfite before the beginning of the sodium polysulfide formation. Because 2.5 mmol sulfite was introduced in the reaction, we can expect to observe reaction speed reduction after the 2.5 mmol of hydrogen production. Indeed, in figure 2a we can see that after the release of 2-2.5 mmol hydrogen, the hydrogen production rate drops steeply due to the formation of polysulfide which can be observed visually (yellow solution) as well, after the photocatalyst filtration.

Conclusion

The obtained photocatalysts are mixtures of ZnS and $Zn_{1-x}Cd_xS$ (where x is close to 1) the amount of unreacted ZnS salt depending on the nature of the used cadmium salt. The photocatalytic experiments were conducted under monochromatic light (400 nm).According to the XRD, DSR and EDX analyses, in the presence of chloride ions, the ZnS reactivity is minimal leading to the formation of the lowest performantphotocatalyst. The presence of sulfate and acetate anions in the system,may be the reason for obtaininghigher performance photocatalysts.

Acknowledgements

This work was carried out through the Partnerships in priority areas - PN II program, developed with the support of MEN - UEFISCDI, project no. PN II PT PCCA-2013-4-1708.

References

[1] Z. Xiong, M. Zheng, C. Zhu, B. Zhang, L. Ma, W. Shen, Nanoscale Res. Lett. 334 (2013) 1.
[2] E. Hong, D. Kim, J.H. Kim, J. Ind. Eng. Chem. 20(2014) 3869.
[3] K. Zhang, D. Jing, C. Xing, L. Guo, Int. J. Hydrogen Energy 32(2007) 4685.
[4] C.H. Liao, C.W. Huang, J.C.S. Wu, Catalysts 2(2012) 490.

pH STABILITY AND PHOTODEGRADATION OF SUNSCREEN UV-A FILTER'S (AVOBENZONE) CHLORINATION PRODUCTS

Cheng Wang[1], Mojca Bavcon Kralj[2], Suzana Košenina[2], Polonca Trebše[2], Vojislava Bursić[3]

[1]Faculty of Energy, Environmental Science and Engineering, University of Science and technology Beijing, Xueyuan Road 30, Haidian strict, Beijing, China
[2]Faculty of Health Sciences, University of Ljubljana, Zdravstvena pot 5, 1000 Ljubljana, Slovenia
[3]Faculty of Agriculture, University of Novi Sad, Trg D. Obradovića 8, Novi Sad, Serbia

Introduction

UV filters are a group of chemicals, which are used in sunscreen products to prevent sunburns on human skin. They represent an important group of anthropogenic organic compounds introduced in swimming pools and marine bath waters and are nowadays treated as emerging contaminants [1]. Under chlorination and photolytic conditions, they easily decompose and several degradation products are formed [2, 3, 4]. The degradation products are rarely, or even in most countries never analysed or monitored.

The advantage of chlorination lies in the fact that still nowadays is one of the most efficient pathways of pathogens inactivation. On the other hand, it has some drawbacks. One of them represents the reactions of chlorine with organic matter and other human outputs and the formation of different disinfection by-products (DBPs) [5]. The additional use of advanced oxidation processes (like UV-irradiation, photocatalysis, oxidation) generally lead to the formation of different DBPs as in case of disinfection. Since the toxicity of the transformation products may be higher than that of the parent compound, it is important to take into account not only the initial compounds, but their transformation products as well.

There are several studies dealing with the chlorination of avobenzone - AV, one of the most common UV-A filter [6,7]. The chlorination and UV-irradiation of avobenzone has proved the formation of twenty five compounds, which were identified by GC/MS [3]. The identification of the two primary chlorination products AV-Cl1 - (2-chloro-1-(4-tert-butylphenyl)-3-(4-methoxyphenyl)-1,3-propanedione and AV-Cl2 - 2,2-dichloro-1-(4-tert-butylphenyl)-3-(4-methoxyphenyl)-1,3-propanedione) led our research in investigation of their pH stability and photostability. Additionally our focus was on the investigation of the possibility of application of TiO_2 photocatalysis as a method for the removal of these persistent chlorinated compounds.

2. Materials and methods

2.1. Materials

The analytical standard of avobenzone (95.0% purity) has been provided by TCI Europe. For stability experiments, avobenzone, chloro-avobenzone and dichloro-avobenzone have been synthesized and characterized according to the literature [3]. Dichloromethane, diethyl ether, petroleum ether, acetonitrile (Chlomasolv gradient grade, for HPLC), acetone, acetic acid have been provided from Sigma Aldrich company, whereas sodium sulfite, sodium sulfate, sodium hydrogen carbonate, from Fluka. The tert-butyl hyprochlorite was prepared in our lab, according to the procedure [8].

Experimental

Stability studies

pH stability: 12,5 mL of AV solution in acetone (1000 mg/L) was dilluted with buffers pH 4 and pH 7 up to to 250 mL, and left at room temperature. Everyday up to 10 days 1 mL of solutions have been withdrawed for HPLC analyses. The procedure was same for AV-Cl1 and AV-Cl2.

Photostability: 50 mL of AV solution in acetone (1000 mg/L) was dilluted with deionised water up to 1 L, and the solution was transfer into the UVA reactor, which consisted of a glass tube (280 mm, inner diameter 87 mm) with 1 L of effective volume. The reaction time was set 6 h, and every hour the sample was withdrawed 1 mL for HPLC detection. The procedure was same for AV-Cl1 and AV-Cl2.

TiO_2 photocatalytical study: Photocatalytic experiments with AV, AV-Cl1 and AV-Cl2 were done in UVA photoreactor, which consisted of a glass tube (280 mm, inner diameter 87 mm) with 1 L of effective volume. Twelve glass slides with immobilised TiO_2 catalyst were fastened around the axis of a spinning basket and immersed into the photocatalytic glass tube [9]. The reaction time was set to 3 h. At different time intervals (5, 15, 30, 45, 60, 90, 120, and 180), samples of 1 mL were taken for HPLC analyses.

	pH=4			pH=7		
	AV	**AV-Cl1**	**AV-Cl2**	**AV**	**AV-Cl1**	**AV-Cl2**
Rate constant (day^{-1})	0.71±0.04	1.19±0.05	1.63±0.04	0.20±0.01	0.85±0.09	5.67±0.47
$t_{1/2}$ (day)	1.44±0.14	0.85±0.06	0.60±0.02	3.54±0.31	1.22±0.15	0.20±0.01

Table 1: Stability of avobenzone, chloro and dichloro-avobenzone at different pHs

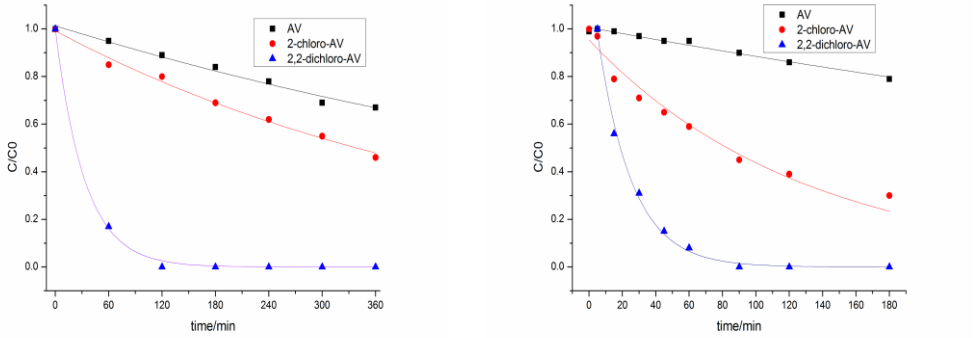

Figure 1: Disappearance curves of avobenzone, chloro-avobenzone and dichloro-avobenzone aqueous solutions via (a): UV A photolysis and (b) UV A photocatalysis with TiO_2

Analytical methods: Aqueous solutions of AV, AV-Cl1 and AV-Cl2 were analysed by Agilent 1000 HPLC - UV-Vis chromatograph. The separation was done using C18 column (150 mm × 4.6 mm), the mobile phase consisted of 70% acetonitrile and 30% distilled water with the flow rate of 1.0 mL/min and the wavelength was set at 330 nm. The retention time for avobenzone was 16.0 min, for chloro-avobenzone 5.34 min, and for the dichloro-avobenzone 10.48 min. For the quantification purposes, the calibration curve was ranged from 1.0 mg/L to 200 mg/L with 9

different concentrations; all the coefficient of determination (r^2) was above 0.99. To decrease the error, all the experiments were repeated twice.

Results and discussion

pH stability: The differences in stability of all three studied compounds in relation of the pH value are presented in Table1. At acidic conditions, all three compounds degraded fast with half-lives from 0.60±0.02 day (AV-Cl2) and 0.85±0.06 day (AV-Cl1) for chlorinated products, to 1.44±0.14 day in the case of parent one. At neutral conditions, only AV-Cl2 degraded fast (half-life 0.20±0.01 day), while AV and AV-Cl1 expressed higher stability (up to 3.54±0.31day in the case of AV).

Photolysis and photocatalysis: The differences in stability of all three studied compounds under photolytic and photocatalytic conditions are presented in Figure 1. In the case of photolysis under UV-A light, AV-Cl2 expressed the lowest UV-A stability (half-life 33.5 ± 1.6min), followed by AV-Cl1 and AV. In case of photocatalysis the expressed tendency of faster degradation was again achieved in case of AV-Cl2 (half-life 20.3 ±1.3 min), while AV-Cl1 had an average half-live of 68.6 ± 10.7 min.

Conclusions

The study of avobenzone, one of the most used UV-A filter in sunscreen products and its two most common DBPs, AV-Cl1 and AV-Cl2, indicates, that contrarily to avobenzone, which is a relatively stable compound, AV-Cl1 and AV-Cl2 are more polar and they both degrade faster under photolytic and under photocatalytic experiments. Besides, AV-Cl1 and AV-Cl2 are both more susceptible to acidic hydrolysis. Our findings are positive in relation with the fact that avobenzone is widely used, non-polar and environmently stable compound, its two DBS are less stable and degrades more easily then the parent compound.

References

[1] Lebedev, A.T., 2013. Environmental mass spectrometry. Annu. Rev. Anal. Chem. 6, 163-189
[2] Santos, A.J.M., Crista, D.M.A., Miranda, M.S., Almeida, I.F., de Silva, J.P.S., Costa, P.C., Amaral, M.H., Lobao, P.A.L., Lobo, J.M.S., da Silva, J.C.G.E., 2013. Environ. Chem. 10 (2), 127-134
[3] Trebse, P., Polyakova, O.V., Baranova, M., Bavcon Kralj, M., Dolenc, D., Sarakha, M., Kutin, A., Lebedev, A.T. Water Research 101 (2016) 95-102
[4] Shujuan Zhang, Xiaomao Wang, Hongwei Yang, Yuefeng F. Xie, Chemosphere 154 (2016) 521-527
[5] Chowdhury, S., Alhooshani, K., Karanfil, T., 2014. Water Res. 53, 68-109
[6] A. J. M. Santos, D. M. A. Crista, M. S. Miranda, I. F. Almeida, J. P. S. de Silva, P. C. Costa, M. H. Amaral, P. A. L. Lobão, J. M. S. Lobo, J. C. G. E. da Silva. Environ. Chem. 2013,10 (2), 127-134;
[7] D. M. A. Crista, M. S. Miranda, J. C. G. Esteves da Silva. Environmental Technology 2015, 36 (10), 1319-1326
[8] A. Vogel, Vogel's Textbook of Practical Organic Chemistry, 4th ed. Longman: London, 1978, P. 405.
[9] M. Kete, E. Pavlica, F. Fresno, G. Bratina, U. Lavrenčič Štangar. Environmental Science and Pollution Research 2014, 21 (19), 11238-11249.

ENHANCED COAGULATION WITH PRE-OXIDATION FOR THE REMOVAL OF ARSENIC FROM GROUNDWATER

Aleksandra Tubić[1*], Jasmina Agbaba [1], Malcolm Watson[1], Jelena Molnar Jazić[1], Snežana Maletić[1], Marijana Kragulj Isakovski[1], Božo Dalmacija[1]

[1]University of Novi Sad, Faculty of Sciences, Department of Chemistry, Biochemistry and Environmental Protection, Trg Dositeja Obradovića 3, 21000 Novi Sad
e-mail: aleksandra.tubic@dh.uns.ac.rs

Abstract
One of the most wide-spread problems with current drinking water resources globally is the natural presence of arsenic in groundwaters. The aim of this work was to investigate the removal of arsenic by a variety of combined oxidation/coagulation processes, in order to identify and optimise the most critical process parameters. The most significant gains made by both preoxidation steps were observed in the techniques which combined aluminum and ferric chloride based coagulation. The most efficient coagulation treatment investigated involved application of preozonation at a dose of 7.5 mg O_3/l with subsequent combined coagulation with PACl–$FeCl_3$ (30 mg Al/l and 10 mg $FeCl_3$/l).

Introduction
Throughout South-East Europe, groundwaters are commonly used as sources for drinking water. Within the Pannonian Basin, the groundwaters are naturally contaminated with particularly high concentrations of arsenic, which poses a severe challenge for public water utilities. The extremely negative impact of chronic arsenic exposure on human health led the World Health Organisation to recommend a maximum allowable concentration (MAC) of 10 µg As/l for drinking water (WHO, 2011). Meanwhile, in parts of Vojvodina, the groundwaters can contain as much as 250 µg As/l, and it is estimated that almost 1 million people in Vojvodina are currently supplied with drinking water which contains arsenic concentrations which exceed 10 µg/l (Agbaba et al., 2015). Given the negative health effects of chronic arsenic exposure, there is thus not just a legal, but also a social imperative to reduce the As concentrations to acceptable legally defined levels. The process of removing As from water is made more complicated by the other water constituents present, which may either indirectly reduce effectiveness of removal mechanisms, or compete directly for adsorption sites. NOM is particularly significant here, as it is known to play a key role in the mobility of As from the mineral layers surrounding aquifers into the water phase. In this context, there is a critical need for research relating to new drinking water treatment technologies, capable of sustainably treating a wide variety of source waters, and providing chemically and microbiologically safe drinking water.
The aim of this work was to investigate the removal of arsenic by a variety of combined oxidation/coagulation processes, in order to identify and optimise the most critical process parameters.

Experimental
For these experiments, groundwater from Zrenjanin was used which contains average As concentration of 134±4.5 µg/l, as well as high NOM (DOC=9.85±0.99 mg C/l) and alkalinity (745±12 mg $CaCO_3$/l). All coagulation experiments were carried out by jar tests. Coagulation was carried out with rapid stirring at 120 rpm for 2 min, after which flocculation was conducted

with slow mixing at 30 rpm for 30 minutes. MagnaflokLT27 flocculantwas dosed at 0.2mg/l. After the mixing was finished, samples were settled for 60 minutes, after which the supernatant was separated. Water samples were filtered through a 0.45 µm membrane filter and analyzed for total arsenic concentrations. The following coagulants were used: a 4% solution of iron (III) chloride in doses of 50–200 mg $FeCl_3$/l (0.1–2.0 mmol/l); a 1% solution of polyaluminium-chloride (PACl) in doses from 2.5 to 30 mg Al/l (0.1–2.0 mmol/l); and 1% $Al_2(SO_4)_3$ in doses from 2.5 to 30 mg Al/l (0.1–2.0 mmol/l). Possible improvements to the coagulation process using different coagulant and oxidant combinations were investigated. The following doses of hydrogen peroxide or ozone were investigated with the coagulant combinations in Table 1 below: H_2O_2 doses: 2.5, 5.0, 7.5, 10.0 mg H_2O_2/l; O_3 doses: 2.5. 5.0, 7.5, 10.0 mg O_3/l. Arsenic concentrations were determined either by inductively coupled plasma mass spectrometry (ELAN 5000, PerkinElmer-SCIEX) or graphite furnace atomic adsoprtion spectroscopy (AAnalyst 700, PerkinElmer). The PQL was 0.5 µg As/l.

Results and discussion

Enhanced coagulation with preoxidation using hydrogen peroxide: Hydrogen peroxide doses of 2.0–10 mg H_2O_2/l were applied prior to coagulation with $FeCl_3$, PACl, $Al(SO_4)_3$ and their combinations (PACl/$FeCl_3$ and $Al(SO_4)_3$/$FeCl_3$). The arsenic removal results for the coagulants are shown in Figure 1.

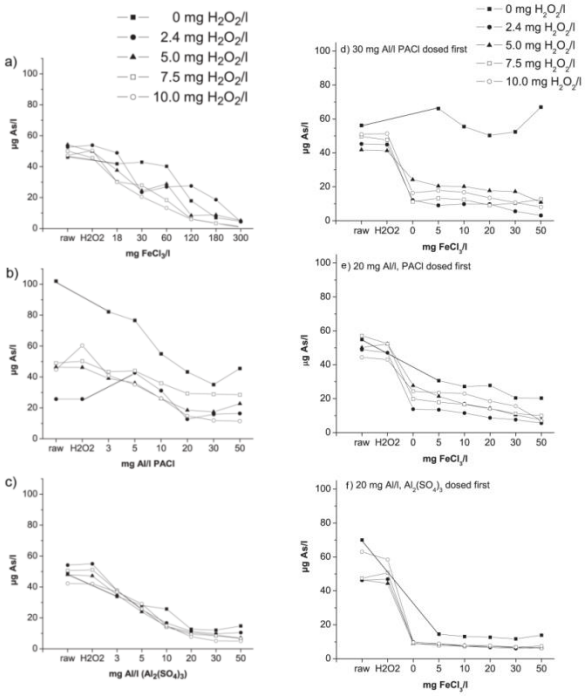

Figure 1. Effect of hydrogen peroxide oxidation on the removal of As by coagulation

The preoxidation step with hydrogen peroxide did not overcome the weak affinity of PACl for arsenic sufficiently enough for this technique to be a practical solution for arsenic removal, as the MAC for As was not satisfied. However, significant gains were made in the As removal efficacy of $FeCl_3$, while coagulation by $Al_2(SO_4)_3$ was also improved. These gains were expected, as the results of the speciation study show that As(V) is more readily removed by coagulation then As(III), a conclusion supported by many authors (Cui et al., 2015). The PACl–$FeCl_3$ combination which applied 30 mg Al/l needs doses of 5 mg $FeCl_3$/l and 2.4 mg H_2O_2/l in order to achieve As

levels below the 10 µg As/l MAC. The best removal was achieved with the same conditions but with a 30 mg $FeCl_3$/l dose. However, the As removal gains made in comparison to the 5 mg $FeCl_3$/l dose are not significant enough to justify application of the increased dose from an economic standpoint, especially considering the considerably larger volume of waste sludge that would be produced.As could be expected, the PACl–$FeCl_3$ combination with the lower Al dose (20 mg Al/l) was less effective than the 30 mg Al/l dose. Reducing the PACl dose from 30 mg Al/l to 20 mg Al/l meant that 4 times more $FeCl_3$ was required, with the same 2.4 mg H_2O_2/l dose, to reduce As below 10 µg/l. Finally, none of the $Al_2(SO_4)_3$–$FeCl_3$ doses investigated were able to achieve arsenic concentrations of less than 10 µg/l without preoxidation (Figure 1b). However, 2.4 mg H_2O_2/l sufficiently enhanced coagulation with 20 mg Al/l and 5 mg $FeCl_3$ to achieve satisfactory water quality, with the preoxidation step increasing coagulation efficacy by almost 10%. Further increasing the $FeCl_3$ and H_2O_2 doses did not result in improvements in the arsenic removal.

Enhanced coagulation with preoxidation using ozone: Ozone doses of 2.0–10 mg O_3/l (0.2-1.0 mg O_3/mg DOC) were chosen for investigation, based on previous research (Tubić et al., 2010). The results of the experiments with preozonation prior to coagulation with PACl, $Al_2(SO_4)_3$ and $FeCl_3$, as well as the PACl–$FeCl_3$ combination, are shown in Figure 2.

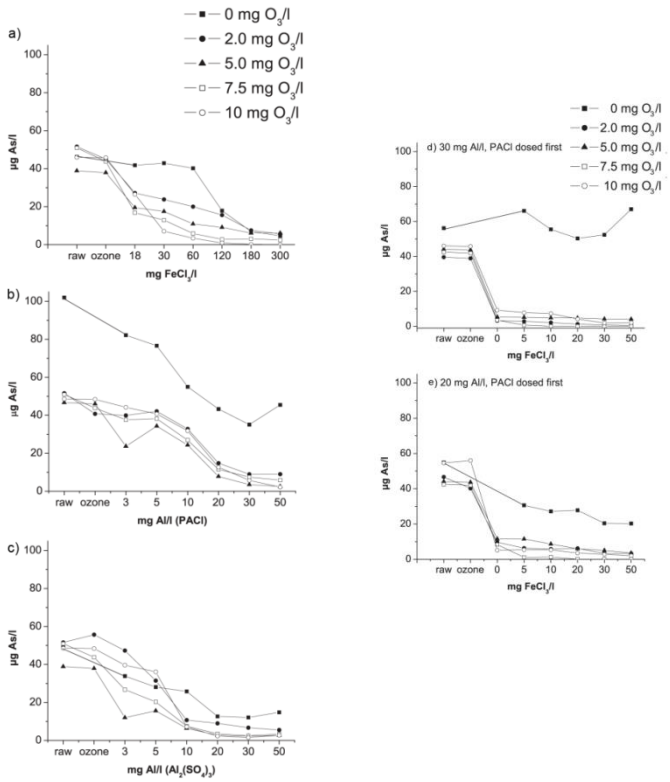

Figure 2. Effect of pre-ozonation on the removal of As by coagulation: (a-c) single coagulants (d-e) combined coagulants

Without preozonation, a 180 mg $FeCl_3$ dose is required to satisfy the MAC for arsenic. With preozonation, arsenic concentrations of less than 10 µg/l were obtained by either i) dosing 10 mg O_3/l prior to just 30 mg $FeCl_3$/l, or ii) dosing 5 mg O_3/l with 120 mg $FeCl_3$ (Figure 2a). Aalthough it is unlikely to be economically viable, preozonation with 10 mg O_3/l prior to 180 mg $FeCl_3$/l coagulant dose resulted in complete arsenic removal (<0.5 µg/l).In the case of

PACl, preozonation with a dose of 5 mg O_3/l increased the percentage removal of As at a dose of 20 mg Al/l by 25%, sufficient to bring the concentration to less than 10 µg As/l. Preozonation dramatically improved the performance of $Al_2(SO_4)_3$ coagulation for As removal. With the preoxidation step, applying a 5 mg O_3/l dose together with 10 mg $Al_2(SO_4)_3$/l was sufficient to remove As down to 6.4 from 38.9 µg/l.Given its superior impact on the removal of arsenic, it can be concluded that ozone, which is a strong oxidising agent which reacts faster than H_2O_2, is the most effective agent for oxidising arsenic containing molecules, and is therefore a very good choice for implementation together with single-coagulant coagulation during the water treatment process. This conclusion is supported by the literature (Sharma and Sohn, 2009).The final set of treatments investigated was preozonation prior to different PACl–$FeCl_3$ combined coagulant doses (30 and 20 mg Al/l). At 30 mg Al/l, preozonation at 2 mg O_3/l already reduces As concentrations below 10 µg/l without the addition of $FeCl_3$ (Figure 2b). At the lower 20mgAl/l dose, a higher dose of 10 mg O_3/l was required to achieve satisfactory drinking water quality without the addition of $FeCl_3$. Addition of 5 mg $FeCl_3$/l allows the ozone dose to be reduced to 2 mg O_3/l, whist still maintaining satisfactory water quality.Of the combined coagulation treatments investigated, the most effective coagulation treatment for the removal of arsenic applied preozonation at a dose of 7.5 mg O_3/l, with subsequent combined coagulation with PACl–$FeCl_3$ at doses of 30 mg Al/l and 10 mg $FeCl_3$/l.

Conclusion

Preoxidation with hydrogen peroxide or ozone before combined coagulation increased the efficiency of the coagulation processes sufficiently that lower coagulant doses could be applied to reduce residual As concentrations below the analytical limits of detection. Preoxidation with hydrogen peroxide was capable of reducing the coagulant demand of the already very effective $FeCl_3$ process, and also improved the efficacy of$Al_2S(O_4)_3$ coagulation. However, it was not able to overcome the poor affinity of PACl for As to achieve As concentrations below 10 µg/l. In contrast, ozone proved to be a much more effective arsenic-oxidising agent. The most significant gains made by both preoxidation steps were observed in the techniques which combined aluminum and ferric chloride based coagulation. As such the most efficient coagulation treatment investigated for removing As below the MAC involved application of preozonation at a dose of 7.5 mg O_3/l with subsequent combined coagulation with PACl–$FeCl_3$ at doses of 30 mg Al/l and 10 mg $FeCl_3$/l. This $FeCl_3$ dose is an order of magnitude lower than the doses required by coagulation alone, resulting in not just a more economic treatment process, but also in the generation of much smaller amounts of more concentrated arsenic–bearing sludge.

Acknowledgements

The authors gratefully acknowledge the support of the Ministry of Education, Science and Technological Development of the Republic of Serbia (project No. III43005).

References

[1] J.Agbaba, E. Fleit, B. Dalmacija, Z. Melicz, A. Szabó, M. Vasiljević, et al. in: M. Pavkov Hrvojević, J. Agbaba, E. Fleit, B. Dalmacija (Eds.) Possibilities for Using Bank Filtration for Sustainable Water Supply in AP Vojvodina. UNS, Faculty of Sciences, 2015.
[2] J. Cui, C. Jing, D. Che, J. Zhang, S. Duan, J. Environ. Sci. (China) 32 (2015) 42.
[3] B.Y.G. Ghurye, D. Clifford, J Amer Water Works Assoc. 96 (2004) 84.
[4] V.K. Sharma, M. Sohn, Environ. Int. 35 (2009) 743.
[5] A. Tubić, B. Dalmacija, J. Agbaba, I. Ivančev-Tumbas, M. Klašnja, M. Dalmacija, Wate. Sci. Tech. 61 (2010) 3169.
[7] WHO Guidelines for Drinking-Water Quality, 4th ed. (2011) World Health Organization.

PRELIMINARY INVESTIGATION OF COMMON GSK3, PPARγ AND DPP IV CHEMICAL SPACE

Daniela Maria Varga, Luminita Crisan, Liliana Pacureanu

Department of Computational Chemistry, Institute of Chemistry of Rumanian Academy, Timişoara, Mihai Viteazul Avenue, 24, 300223 Timişoara, Romania
e-mail: pacureanu@acad-icht.tm.edu.ro

Abstract

Cross-target biochemical experiments demonstrated that some molecules display an ample spectrum of biological activities which are therapeutically effective. In this regard we investigated the chemical space of the following targets GSK3, DPP IV and PPAR gamma since the DPP IV inhibitors, and PPAR gamma agonists are used to treat diabetes miellitus of type 2. Nevertheless, GSK-3 inhibitors have shown therapeutic potential for insulin resistant type-2 diabetes, the drug market does not register yet an inhibitor of GSK-2 for therapeutical use. The ChEMBL homo sapiens assay data for GSK-3, DPP IV and PPAR gamma were assembled into are database including 7599 compounds. GSK-3 assay comprise 2497 compounds, from which 1889 are unique divided into 428 chemotypes. DPP IV register 3482 compounds and 3026 were unique sharing 510 chemotypes. PPAR gamma incldes 1620 agonists from which 1333 are unique partitioned into 264 chemotypes. The chemical space of GSK3, DPP IV and PPAR gamma share 12 chemotypes, GSK3 and DPP IV share 30 chemotypes, DPP IV and PPAR gamma share 13 chemotypes, whereas GSK3 and PPAR gamma share 17 chemotypes. The 12 chemotypes active on all three proteins were superposed to develop a common pharmacophore which will be further used to identify novel chemotyes with potential biological activity.

Introduction

In this study we investigated the chemical space of the following targets: Glycogen Synthase Kinase-3 (GSK-3)[1] and Dipeptidyl Peptidase IV (DPP IV) inhibitors [2] and Peroxisome Proliferator-Activated Receptor Gamma (PPARγ) [3] agonists which are used to treat diabetes miellitus of type 2.

Sitagliptin (original brand name Januvia) is a highly selective DPP IV inhibitor, used in patients with type 2 diabetes mellitus to improve glycemic control in combination with metformin or a PPARγ agonist (e.g., thiazolidinediones)[2].

Our goal was to detect shape similar compounds with Sitagliptin (2R)-4-oxo-4-[3-(trifluoromethyl)-5,6-dihidro[1,2,4]triazolo[4,3-A]pirazin-7(8H)-yl]-1-(2,4,5-trifluorophenyl)butan-2-amine (PDB code: 4FFW_715) conformer cocrystallized with DPP IV. To accomplish our goal aRapid Overlay of Chemical Structures(ROCS) search was performed using the above mentioned sitagliptin conformation.Further we investigate the commom pharmacophore point to identify a possible common interaction pattern.

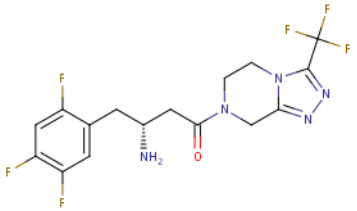

Figure 1.The structure of sitagliptin DPP IV inhibitor used as query

Methodology

The dataset used in our study was downloaded from the ChEMBL [4] database, to obtain bioactive compounds on GSK-3, DPP IV and PPAR gamma, whch asseembled resulted in 7599 compounds.
In the fisrt step the active compounds were filtered for duplicates using InstantJChem [5] software resulting 6248 unique compounds from which 1889 active compounds were for GSK-3, 3026 active compounds for DPP IV, and 1333 active compounds for PPAR gamma.
In the second step these unique compounds were divided into 428 chemotypes for GSK-3, 510 chemotypes for DPP IV and 264 chemotypes for PPAR gamma using Bemis Murko frameworks from InstantJChem [5] software.
In the third step were found 12 common chemotypes for the all proteins from where we extracted 12 active compounds with the highestIC_{50}.
Thesitagliptin conformation was downloaded from the RCSB Protein Data Bank [6] and the bond orders were checked.
The input for ROCS [7] analysis were the conformers of the 12 compoundswhose affinities were measured against all hereby investigated proteins which were generated with Omega version 2.3.2 from OpenEye [8] package using by default settings (RMSD = 0.8 Å, a energy window of 10 kcal, maximum output conformers 400.

Results and Discussions

The shape similarity search with ROCS has been proved to produce fast and reliable results that guarante good quality alignment.
All the conformes were overlaid, over the X-ray structure (4FFW_715) [4]) and thirteen similarity functions TanimotoCombo, ShapeTanimoto, ColorTanimoto, FitTverskyCombo, FitTversky, FitColorTversky, RefTverskyCombo, RefTversky, RefColorTversky, ScaledColor, ComboScore, ColorScore, Overlap implemented in ROCS were calculated [7-10].
The minimal, maximal and mean values of the most important similarity coefficients resulted from the similarity searches against the query (Figure 1) are listed in Table 1.

Table 1. The minimal, maximal and mean values of Tanimoto coefficients

Query (4FFW_715)	TC*	ST*	SC*	CS*
min	0.479	0.338	0.13	0.6
max	1.531	0.848	0.71	1.558
average	0.72051	0.485677	0.316521	0.818698

*TC-TanimotoCombo, ST-ShapeTanimoto, SC-ScaledColor, CS-ComboScore

The distributions of the minimal, maximal and mean values of important tanimoto similarity functions are shown in Figure 2

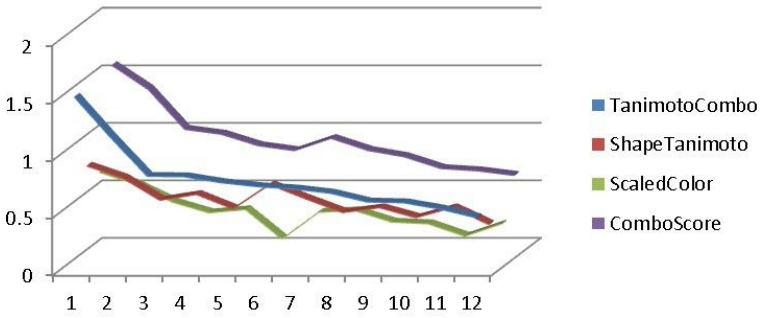

Figure 2. The distribution of the Tanimoto Combo, Shape Tanimoto, Scaled Color and Combo Score

The first 10 molecules ranked by ROCS were DPP IV inhibitors bearing different substituents (Figure 3). As expected, it can be observed (Figure 3) that these compounds align very well to the sitagliptin conformation.

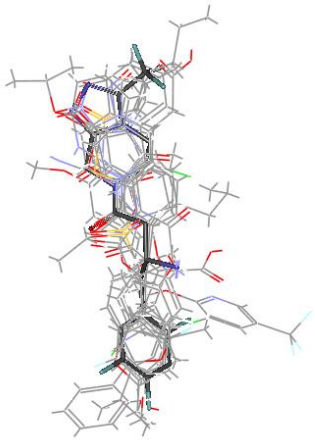

Figure 3. Alignment of the top 10 hits (line) to the RX ligand (stick) [11].

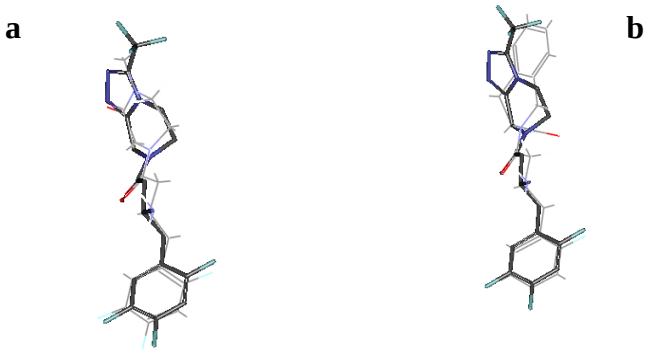

Figure 4. Superposition of the X-ray structure of the ligand (stik) and the corresponding best overlayed conformation for CHEMBL1779688 (line) (a) and CHEMBL381806 (line)(b)[11].

The best superposition compounds whose corresponding shape TanimotoCombo is of 1.531 CHEMBL1779688 (Figure 4a) and ComboScore (including Shape + ColorScore) values (1.347)

corresponds CHEMBL381806 (Figure 4b) [11].These values are good enough to suggests structural similarity, but also a certain degree of scaffold hopping.

Conclusions

The 7599 compounds downoladed from ChEMBL database with experimentally determined IC_{50} were involved in our final study.The ROCS analysis provided 12 active compounds for all tree protein with common chemical space.The 12 compounds active on all three proteins were superposed to develop a common pharmacophore which will be further used to identify novel chemotyes with potential biological activity.

Aknowledgment: The authors thanks for provinding the academic free license to OpenEye Scientific Software, Inc.(Simona Funar- Timofei laboratory), Accelrys Inc. for Discovery Studio Visualizer v. 2.5 and ChemAxon for InstantJchem v. 5.12.4. This work was supported by the Project 1.2 of the Institute of Chemistry Timisoara of the Romanian Academy.

References

[1]Bertrand JA, Thieffine S, Vulpetti A, Cristiani C, Valsasina B, Knapp S, Kalisz HM, Flocco M., J Mol Biol.2003 Oct 17;333(2):393-407.
[2]Heung Jae Kim , Woo Young Kwak , Jong Pil Min , Jae Young Lee , Tae Hyun Yoon , Ha Dong Kim ,Chang Yell Shin , Mi Kyung Kim , Song Hyen Choi , Hae Sun Kim , Eun Kyoung Yang , Ye Hwang Cheong ,Yu Na Chae , Kyung Jin Park , Ji Myun Jang , Soo Jung Choi , Moon Ho Son , Soon Hoe Kim , Moohi Yoo ,Bong Jin Lee, Bioorganic & Medicinal Chemistry Letters 21 (2011) 3809–3812.
[3]Kuhn B, Hilpert H, Benz J, Binggeli A, Grether U, Humm R, Marki HP, Meyer M, Mohr P, Bioorg Med Chem Lett. 2006 Aug 1;16(15):4016-20.
[4]ChEMBL Database via https://www.ebi.ac.uk/chembl/index.php/compound/results/true
[5]InstantJChem version 5.12.4 (2011) ChemAxon. Available at: http://www.chemaxon.com.
[6]RCSBProteinDataBank.http://www.rcsb.org
[7]OpenEye Scientific Software (2010) ROCS version 3.1.0 Santa Fe NM 87508; http://www.eyesopen.com
[8]OpenEye Scientific Software (2008) OMEGA, version 2.3.2 Santa Fe NM 87508; http://www.eyesopen.com
[9] P.C.D. Hawkins, A. Nicholls, J. Chem. Inf. Model. 52 (2012) 2919–2936.
[10]T.S. Rush, J.A. Grant, L. Mosyak, A. Nicholls, J. Med. Chem. 48 (2005) 1489–1495.
[11]Discovery Studio Visualizer-Accelrys, version 2.5, 2009, San Diego, CA.

RESVERATROL AS CORROSION INHIBITOR FOR METALS IN WINE AND FOOD INDUSTRIES

[1]Cristian George Vaszilcsin, [2]Mircea Laurentiu Dan, [2]Delia Andrada Duca, [2]Mihaela Alexandra Labosel

[1]INCEMC Timişoara, Dr. A. Paunescu Podeanu 144, 300569,Timisoara, Romania
[2]University Politehnica Timişoara, Faculty of Industrial Chemistry and Environmental Engineering, 300223, Parvan 6, Timisoara, Romania
e-mail: cristi_vasz@yahoo.com

Abstract
This paper presents preliminary results obtained in the case of Resveratrol used as corrosion inhibitor for stainless steel, carbon steel, polished and brushed aluminum in ethanol solutions. Electrochemical behavior of Resveratrol in ethanol solutions has been studied by cyclic voltammetry on platinum electrode. Information about the inhibitory effect mechanism was provided by kinetic parameters calculated with Tafel method from linear polarization curves. Corrosion rate diminution of studied electrodes in the presence of Resveratrol can be assigned to the adsorption of inhibitor molecules on the sample surface, or depositing corrosion products onto metal surface, blocking the active sites.

Introduction
Wine industry contributes to the food position of industry as one of the three largest markets worldwide, which also includes the energy and water industries based on production, number of consumers, and economic and social significance [1]. As above mentioned industries, the wine industry is subject of corrosion.
High quality materials represent a key factor for whole food industry, especially wine production [2]. Corrosion resistance is the main property to be considered when choosing materials for winery equipment. Preserving of the organoleptic characteristics: taste, fragrance and color is the crucial element in order to achieve high quality wines [2]. Industrial alcoholic fermentation containers are made of stainless steel. Aluminum is used in wine industry as material component for cans and screw caps [3].
The wine quality is dependent on approximately eight hundred components [2]. It can be expected the change of percentage of any one of these components to affect the quality of wines.
Resveratrol (3,5,4′-trihydroxy-trans-stilbene) is a stilbenoid, a natural phenol, and at the same time a naturally produced phytoalexin by several plantsas response to the injuries or attacks of pathogens such as bacteria or fungi [4].
Resveratrol is also found in the skin of grapes, blueberries, raspberries and mulberries. Considerably higher amounts of Resveratrol is contained in red wines than in white wines because, although it is present in ripe grapes of both red and white varieties, the concentration is higher in the red berries [5,6].
The inhibitory properties of Resveratrol on the corrosion process of stainless steel, carbon steel, polished and brushed aluminum in ethanol solutions offers considerable prospects for the wine industry, also being defined as a natural, eco-friendly corrosion inhibitor in alcoholic media.

Experimental
Electrochemical measurements were carried out using BioLogic SP150 potentiostat/ galvanostat

in a conventional three-electrode cell systems. Stainless steel, carbon steel polished and brushed aluminum samples were used as working electrode. The counter electrode was graphite, and Ag/AgCl acted as reference electrode. Electrochemical experiments were performed in 12% ethanol added in 0.25 M Na_2SO_4 solution, in order to determine the corrosion potential and corrosion current. Electrochemical behavior of Resveratrol in test solutions was studied by cyclic voltammetry on platinum electrode.

To determine the inhibitor effect of Resveratrol on the corrosion rate of the four samples in test solution, 10^{-5} mol L^{-1} concentration has been used in preliminary studies. Resveratrol ($C_{14}H_{12}O_3$) exists in two isomeric forms, as trans- and cis-resveratrol. Both chemical structures are presented in figure 1 [6].

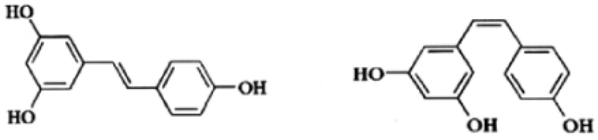

Figure 1. Chemical structures of *trans*- and *cis*- resveratrol [6].

Results and discussion

Preliminary information about how Resveratrol can influence the corrosion process of test electrodes are provided by its electrochemical behavior on platinum electrode in alcoholic solution, emphasised by cyclic voltammetry.

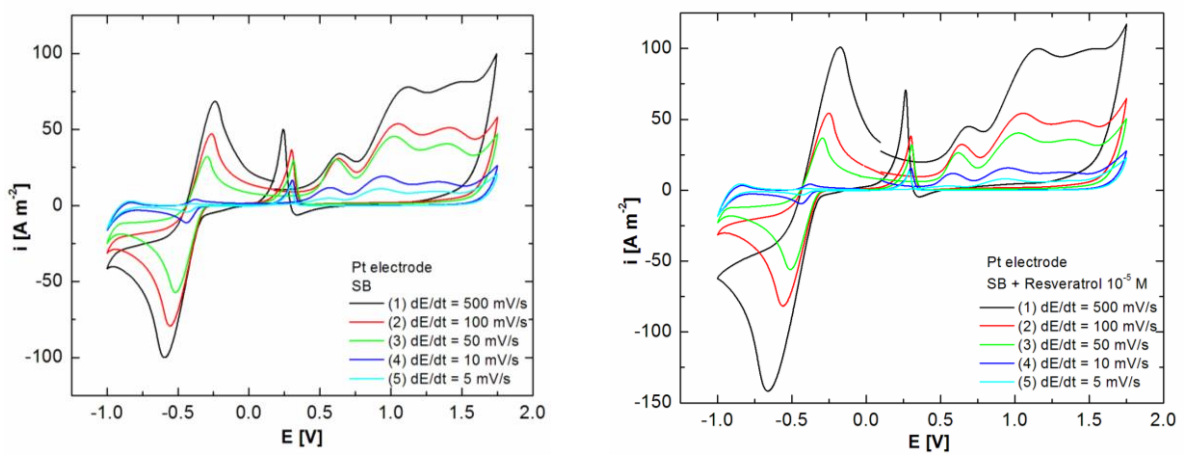

a) b)

Figure 2. Cyclic voltammograms on Pt electrode in 0.25 mol $L^{-1}Na_2SO_4$ + 12% ethanol (SB) in the absence (a) and presence of 10^{-5} mol L^{-1} Resveratrol (b), at different scan rates.

In figure 2, cyclic voltammograms recorded at different scan rates, between 500 and 5 mV s^{-1}, on Pt electrode, in 0.25 mol $L^{-1}Na_2SO_4$ + 12% ethanol solution without (Fig.2a) and with Resveratrol (Fig.2b) are shown. The base curve obtained in blank solution has the characteristic polarization curve drawn in ethanol solutions.

In order to identify how Resveratrol influences the electrode processes, cyclic curves without and with Resveratrol (dE/dt = 10 mV s^{-1}) are presented comparative in figure 3.

The way Resveratrol acts as corrosion inhibitor for test electrodes in alcoholic solution and its effect on the corrosion rate can be estimated by Tafel polarization method. The potentiodynamic polarization curves recorded without and with 10^{-5}mol L^{-1} Resveratrol are shown in figure 4 for

stainless steel and carbon steel electrodes and in figure 5 for polished and brushed aluminum electrodes.

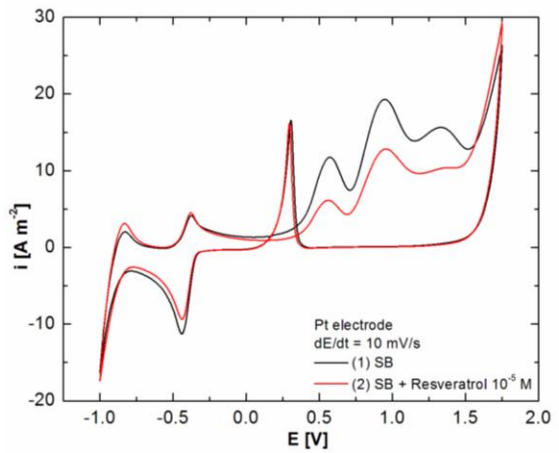

Figure 3. Cyclic voltammograms on Pt electrode in 0.25 mol $L^{-1}Na_2SO_4$+ 12% ethanol (SB) in the absence/presence of 10^{-5}mol L^{-1} Resveratrol at 10 mV s^{-1} scan rate.

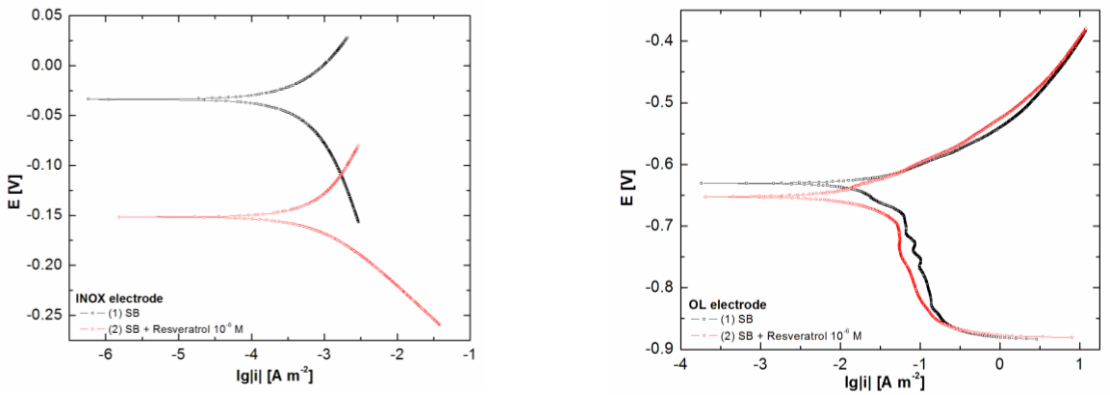

a) b)

Figure 4. Linear polarization curves on stainless steel (a) and carbon steel electrode (b) in test solutions in the absence/presence of 10^{-5}mol L^{-1} Resveratrol, scan rate: 1 mV s^{-1}.

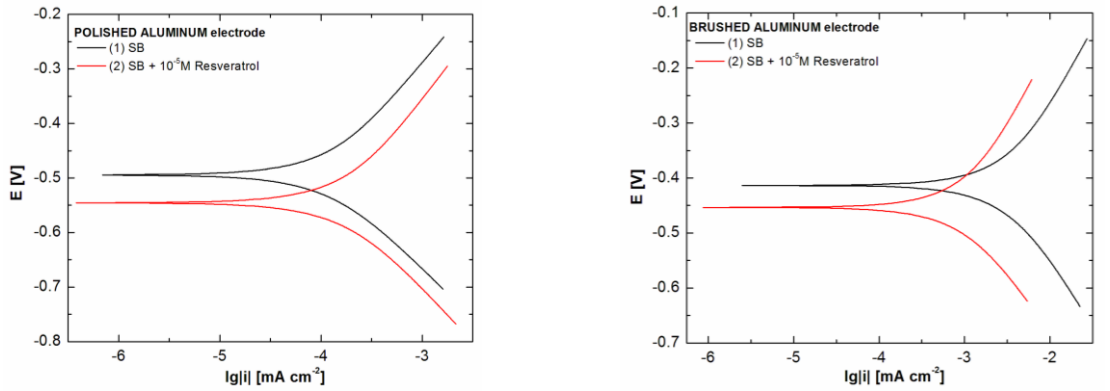

a) b)

Figure 5. Linear polarization curves on polished (a) and brushed aluminumelectrodes (b) in test solutions in the absence/presence of 10^{-5}mol L^{-1} Resveratrol, scan rate: 1 mV s^{-1}.

Numerical values of corrosion current density (i_{corr}), corrosion potential (E_{corr}), anodic Tafel slope (b_a), cathodic Tafel slope (b_c) and polarization resistance (R_p) were obtained from polarization profiles extrapolating potentiodynamic curves from figures 4 and 5 using BioLogics software.The inhibition efficiency (*IE*) has been calculated using equation (1). All obtained values are given in Table 1.

$$IE(\%) = \left(\frac{i^{o}_{corr} - i^{inh}_{corr}}{i^{o}_{corr}}\right) \times 100 \qquad (1)$$

where i^{0}_{corr} and i^{inh}_{corr} are the uninhibited and inhibited corrosion current densities, respectively.

Table 1. Polarization parameters for test electrodes corrosion process in 0.25 mol L^{-1} Na_2SO_4 + 12% ethanol solution in the absence/presence of Resveratrol, at 25°C.

Electrode	Inh.conc. [M]	i_{corr}, [μA cm^{-2}]	E_{corr}, [mV]	$-b_c$, [mV dec^{-1}]	b_a, [mV dec^{-1}]	R_p, [kΩ]	v_{corr}, [mm an^{-1}] · 10^3	*IE*, %
Stainless steel	0	0.148	-33.7	253	108	187	3.3	-
	10^{-5}	0.078	-151.7	68	154	314	2	47.3
Carbon steel	0	5.22	-630	369	69	2.1	132	-
	10^{-5}	2.49	-653	243	82.3	3.4	58	52.3
Polished Al	0	0.162	-494	205	242	223	4.5	-
	10^{-5}	0.067	-545	201	236	654	1.8	58.6
Brushed Al	0	1.112	-413	259	288	22	37	-
	10^{-5}	0.404	-453	229	298	50	16	63.7

Conclusion

Preliminary studies confirm that Resveratrol has promising corrosion inhibition properties for stainless steel, carbon steel, polished and brushed aluminum in alcoholic solutions. Resveratrol can be added to the list of non-toxic and effective green corrosion inhibitors in wine industry from renewable sources.

Acknowledgements

This work was partially supported by *INCEMC Timisoara* in the frame of *PN 16 14 02 01Research Program* andbyUniversity *Politehnica* Timisoara in the frame of *PhD studies*.

References

[1] http://www.materialsperformance.com/articles/material-selection-design/2015/09/wineries - equipment-materials-and-corrosion
[2] V. Alar, B. Runje, F. Ivušić, A. Horvatić, M. Mihaljević, METABK. 55(3) (2016) 437.
[3] M. Ramos, A.Valdés, A.C.Mellinas, M.C.Garrigós, Beverages. 1 (2015) 248.
[4] L. Fremont, Life Sciences 66 (2000) 663.
[4] P. Gatto, U.Vrhovsek, J. Muth, C. Segala, C. Romualdi, P. Fontana, D. Pruefer, M. Stefanini, C. Moser, F. Mattivi, J. Agric. Food Chem., 56 (2008) 11773.
[5] L. Bavaresco, L. Lucini, M. Busconi, R. Flamini, M. De Rosso, Nutrients 8(222) (2016) 1.
[6] https://en.wikipedia.org/wiki/Resveratrol.

TREATMENT OF BIODEGRADABLE WASTE – CASE OF NOVI SAD REGION

Višnja Mihajlović

Department of Environmental Engineering and Occupational Safety, Faculty of Technical Sciences, University of Novi Sad, 21000 Novi Sad,, Trg Dositeja Obradovica 6, Serbia
e-mail: visnjamihajlovic@uns.ac.rs

Abstract
Main driver for the development of waste management system in waste management regions in Serbia, will be transposition of the European waste management directives. Implementation of Landfill Directive will have a great impact on management of biodegradable waste and reducing the waste disposed at landfill. Composting and anaerobic digestion are proven technologies for treatment of biodegradable waste. Selection of treatment of biodegradable waste will depend on many factors, but must be tailored to local conditions.

Introduction
The municipal waste management landscape in Serbia will go through the changes, especially with regard to its waste policies and legislation. Serbia is a candidate country for European Union membership (EU), and so will have to transpose and implement the total body of EU legislation. The directive regulating management of biodegradable municipal solid waste in the European Union is the Landfill Directive. The Landfill Directive propose the targets for reduction of biodegradable waste which is sent to the landfill from 75% of 1995 baseline levels by 2010, 50% of 1995 baseline levels by 2013 and 35% of 1995 baseline levels by 2020 [1]
The Landfill Ordinance [2] is actually a transposition of the Landfill Directive and require the reduction of biodegradable municipal waste (BMW) sent to landfill by 25%, 50% and 65% in the year 2016, 2019 and 2026 respectively.
Waste management in Serbia, is still focused on waste collection and protection of public health. Main deficiencies in solid waste management are weak and inefficient law enforcement mechanism, lack or weak capacity or motivation of staff, lack of finances for investments, lack of incentives for both local community and for the citizens. Dominant waste treatment method is still landfilling with high share of biodegradable municipal waste (BMW) going to landfill, like in South Eastern Europe countries [3][4]. Regarding the packaging waste, almost all waste from the household which is sent to recycling is collected by an informal sector. Separate collection is not established in Serbia as well.
Based on experience of EU Member States where the disposal of waste remained cheap, and where there are no fees and charges for waste disposal, diversification of biodegradable waste from landfills and implementation of waste treatment technologies has been more slowly, unlike in countries where fee for waste disposal was introduced prior to LD implementation, and thus gradually started to build the necessary infrastructure for waste management [5]. In addition, new member states e.g. Poland, Bulgaria, Romania, Croatia, still depend on landfilling, and treatment options are rarely in place. Therefore still a large amount of biodegradable waste is disposed of in landfills
The transposition and implementation of the Directive provisions legislation will be an extremely challenging task for the country. The aim of this paper is to identify the amount of BMW and the treatment process in order to fulfill the LD provisions and divert the BMW from landfill in Novi Sad Waste Management Centre (NSWMC).

Experimental

The input for the analysis is morphological composition of MSW in NSWMR and generated MSW waste. In 2009. total amount of generated waste was 189.000 tonnes [6]. Out of this, 44% is biodegradable waste (see Figure 1).

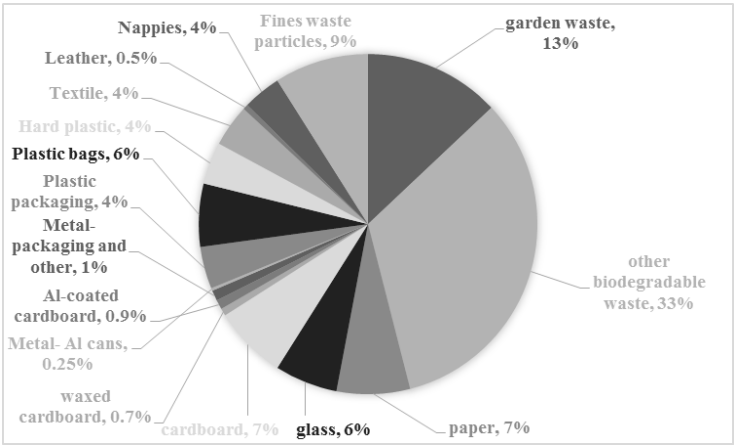

Figure 1: Morphological composition of MWS in NSWMR [6]

For the projected waste generation growth rate we have used GDP in Serbia, which was around 2% [7].Due to the Landfill Directives requirements, composting and anaerobic digestion are used for the treatment of the biodegradable fraction. Composting considers open-air process in a box, which include composting and the stage of maturation. Compost, wastewater and residues are produced during the process. Biogas, wastewater and a digestion residue are produced during the anaerobic digestion. The biogas is combusted to produce electricity and heat; the residues are further treated in the aerobic maturation process stage, producing compost.

Table 1: Analzsed technologies for the BMW treatment [8,9,10]

Technology	Mass balance	
Composting	Compost	35%
	Residues	7%
	Wastewater	43%
	Off'-gases	15%
Anaerobic digestion CHP	Biogas	15%
	Compost	30%
	Residues	7%
	Wastewater	48%

Results and discussion

In 2035. total amount of generated municipal waste will be 322,769 tonnes with 2% increased rate. In order to comply with Landfill Directive, it would be necessary to treat 96,506 tonnes of biodegradable waste in composting plant or anaerobic digestion plant. Outputs of the analysed technologies are given in Table 2. Both treament technologies produce compost which can be sold and wastewater which need to be treated. In addition, during the anaerobic digestion process biogas is generated, which is used for production of electricity and heat. Production of energy,

could contribute to increase of revenues for the plant.

Table 2: Biodegradable waste treatment output's

	Anaerobic digestion	Composting
From treatment plant (tonnes year^{-1})		
Biogas	14,476	-
Compost	28,952	33,778
Wastewater	46,324	55,972
Residues for landfill	6,756	6,756

Selection of waste treatment plant will depend on many factors. One of the important factors will be the investment cost of the plant and economic sustainability of the plant. However, treatment of biodegradable waste must tailored to local conditions.

Conclusion

Anaerobic digestion and composting are proven waste treatment technologies for BMW. Implementation of those technologies will be challenging task for the region. Decision makers will have to implement and introduce different mechanisms e.g. landfill ban, landfill taxes in order to divert BMW from the landfill and fulfill the Landfill Directive goals.

References

[1] EC (1999) Directive 1999/31/EC on the landfill of waste, European Parliament and of the Council, Official Journal L 182, 16/07/1999, p 1-19, Luxembourg.
[2] Official Gazette of Republic of Serbia , Decree on landfilling. Official Gazette of RS 69/10 (2010)
[3] I.STANIC-MARUNA, J. FELLNER: Solid waste management in Croatia in response to European Landfill Directive. Waste Management and Research, 30(8), 825 (2012)
[4] K. LASARIDI : Implementing the Landfill Directive in Greece: problems, perspectives and lessons to be learned, The Geographical Journal, 175 (4): 261 (2009)
[5]BiPRO, Support to member states in improving waste management based on assessment of member states' performance 070307/2011/606502/SER/C2. Final report to the European Commission, Beratungsgesellschaft für integrierte Problemlösungen (BiPRO), Brussells, Belgium, (2013)
[6]Vujić G, Jovičić N, Redžić N et al., A fast method for the analysis of municipal solid waste in developing countries – case study of Serbia. Environmental Engineering and Management Journal 9:1021–1029 (2010).
[7] World Bank (2015) Economic indicator database http://data.worldbank.org/indicator/NY.GDP.MKTP.PP.KD (Accessed 10 July 2015)
[8]Alevridou A, Venetis C, Mallini D et al. Guidelines for development of alternative waste management, Project: Waste Network for sustainable solid waste management planning and promotion of integrated decision tools in the Balkan Region (2011)
[9]IPPC, Reference Document on Best Available Techniques for the Waste Treatments Industries, European Commission - Integrated Pollution Prevention and Control (2006)
[10] Le Bozec A, Costs models for each municipal solid waste process, Deliverables 5 & 7. Aid in the Management and European Comparison of Municipal Solid Waste Treatment methods for a Global and Sustainable Approach (AWAST) (2004)

POLAR PESTICIDE ANALYSES: VALIDATION OF GLYPHOSATE DETERMINATION IN SOIL BY LC-MS/MS

Vuković Gorica[1], Bursić Vojislava[2], Agarski Miroslav[2], Zeremski Tijana[3], Rada Đurović-Pejčev[4]

[1]Institute of Public Health, Bul. despota Stefana 54a, 11000 Belgrade, Serbia,
[2]University of Novi Sad,Faculty of Agriculture, Trg Dositeja Obradovića 8, Novi Sad, Serbia,
[3]Institute of Field and Vegetable Crops, Maksima Gorkog 30, 21000 Novi Sad, Serbia
[4]Institute of Pesticides and Environmental Protection, Banatska 33, Zemun, Serbia
e-mail: goricavukovic@yahoo.com

Abstract

Although glyphosate is a heavily applied herbicide worldwide, the risk of environmental contamination through transport mechanisms of this substance is still not well documented and the methods for its analysis are usually very complex and nor sensitive enough. In the measurement procedure with LC-MS/MS, a negative mode was used. FMOC-Cl derivatized glyphosate ions were identified by the precise determination of their ion mass. The LOQ was 0.01 mg/kg, with recovery of 101.4±4.49% and linearity over 0.99. The obtain method demonstrates the sensitivity, which enables measurements of glyphosate soil as a matrix. The success of the new extraction method was confirmed by measuring spiked soil samples to control recovery, linearity, LOD and LOQ.

Introdustion

Glyphosate (n-phosphonomethyl glycine) is a polar herbicide widely used in agriculture, horticulture, and silviculture applications but also commonly used around homes and gardens [1]. Its usage was approved by European Commision in 2002. This herbicide is among the largest-selling single crop-protection chemical products on the market [2]. Commercial glyphosate formulations are frequently used as herbicides in agriculture, due to their good efficacy on most weed species and their relatively low cost but recently discussed due to the re-evaluation process by the European Union. As a most frequently used herbicide, it is the one of several hundred active substances that have been assessed by Member States and the European Food Safety Authority (EFSA) in recent years.

The Member States – in the Standing Committee on Plants, Animals, Food and Feed during the meeting of national experts, recently, voted in favor of a proposal by the European Commission to restrict the conditions of use of glyphosate in the EU. These conditions include a ban of a co-formulant (POE-tallowamine) from glyphosate-based products, obligations to reinforce scrutiny of pre-harvest use of glyphosate as well as to minimise the use in specific areas (public parks and playgrounds). The proposal was made in parallel with the extension of the approval of the active substance for the limited time. The measures will apply for the duration of the extension untilEuropean Chemical Agency (ECHA) issues its opinion. The Commission adopted the extension of the current approval of glyphosate for a limited period until the ECHA has concluded its review - since Member States failed to take responsibility (no qualified majority was reached at either the Standing Committee or the Appeal Committee) [3].

For a long time many polar pesticides like glyphosate has been excluded from the routine scope of laboratories due to the lack of sample methods[4].Direct analyses usually show low sensitivity, high method detection limits, poor chromatographyc separation, etc. Derivatization with FOMC-Cl (fluorenylmethyloxycarbonyl chloride), represents a solution of some drawbacks of direct

methods; however this step makes the determination more expensive and time consuming [4]. Polar pesticides represents compounds of middle or high polarity and low molecular mass which makes glyphosate is analytically called as "SRM (single residue method) analyte" and is not possible to analyse with pesticide multiresidues method. Variety of SRMs are published for glyphosate.

In this work derivatization with FMOC-Cl purification step followed by liquid chromatography tandem-mass spectrometry (LC-MS/MS) were optimizes in order to decrease detection limit for residue analyses of glyphosate in soil. Method was validated according to SANTE/11945/2015.

Experimental

Chemicals and apparatus

The acetonitrile and methanol were of HPLC quality.The KOH, H_3BO_3, KCl, NaOH, H_3PO_4, FOMC-Cl, NH_4HCOOH and EDTA were analytical grade and obtained from Merck (Darmstadt, Germany). The water was deionized and formic acid was concentrated (>95%). The certified pesticide analytical standard of glyphosate (99.0%) was purchased from Dr. Ehrenstorfer (Augsburg, Germany). Glyphosate-D3 was used as an internal standard (ISTD, c=1 µg/mL).

For LC analysis, an Agilent 1200 (Agilent Technologies, USA) HPLC system with a binary pump was used. This was equipped with a Zorbex Eclipse Plus C18 (3.5 µm, 2.1×100 mm) (Agilent Technology). The mobile phase was 10 mM NH_4HCOOH (pH 9, solvent A in methanol) and 10 mM NH_4HCOOH (pH 9, solvent B in water) in gradient mode, with the flow rate of 0.2 mL/min. The elution program was started with 70% B. It was linearly decreased to 10% B in 15 min. The stop time was 15 min with the post run of 5 min. The 5 µL of sample was injected.

For the mass spectrometric analysis, an Agilent 6460 Triple-Quad LC/MS system was applied. Agilent MassHunter B.04.00 software was used for the data acquisition and processing. The analysis was performed in the negative ion mode. The ESI source values were as follows:drying gas (nitrogen) temperature 325 °C, drying gas flow rate 5 L/min, nebulizer pressure 45 psi and capillary voltage 2000 V. The detection was performed using the multiple reactions monitoring mode (MRM).

Validation parameters

The evaluation of the calibration curve`s linearity was done based on the injections of standard solutions prepared in the mobile phase and also in the extract of blank soil samples, at the concentrations of 0.01, 0.025, 0.05 and 0.1 µg/mL.

The LOD was estimated from the chromatogram of the lowest level of calibration using the Agilent MassHunter software (Agilent Technologies, Data Acquisition for Triple Quad B.04.00) for those concentrations that provide a signal to noise ratio of 3:1. The LOQ was based on the accuracy and precision data, obtained via the recovery determinations and was defined as the lowest validated spike level which meets the requirements of a recovery within the range of 70 – 120% and a RSD ≤ 20 % (SANTE/11945/2015). The LOQ was determined at 0.01 mg/kg.

The main goal of the recovery experiments was to determine the method accuracy via the comparison of the real concentration of a glyphosate, measured by performing the complete procedure, with the known pesticide concentration initially added to the matrix [4]. The method precision is expressed as the repeatability (RSD, 4.49 %) of the recovery determinations at three different spiking levels (0.025, 0.05 and 0.10 mg/kg).

Glyphosate extraction

10 g sample + 9mL d. H_2O + 1mL KOH
↓ Shake vigorously for 5 min and centrifuge for 5 min at 4000 rpm
1 mL of aliquot + 100 µL ISTD + 1 mL botate buffer + 0.5 mL FMOC-Cl Shake immediately for 1 min
↓ Storage in dark for 2 hours
100 µL 2% H_3PO_4 + 0.1 M EDTA
↓Shake vigorously for 1 min
LC-MS/MS

Results and discussion

Basic acquisition parameters (precursor ion – prec ion, product ion – prod ion, fragmentation energy – Frag, collision energy – CE and polarity) for glyphosate and glyphosate-D3 as an internal standard, were given below.

Compound	Prec Ion	Prod Ion	Frag (V)	CE (V)	Polarity
Glyphosate	390.2	168	100	5	Negative
	390.2	150	100	15	Negative
Glyphosate-D3	393.2	170.8	100	15	Negative

The calibration curves based on matrix-matched standards were obtained at the concentration levels from 0.01-0.10 µg/mL. The good linearity was achieved, with the coefficient of determination (R^2) better than 0.99 (Figure 1).

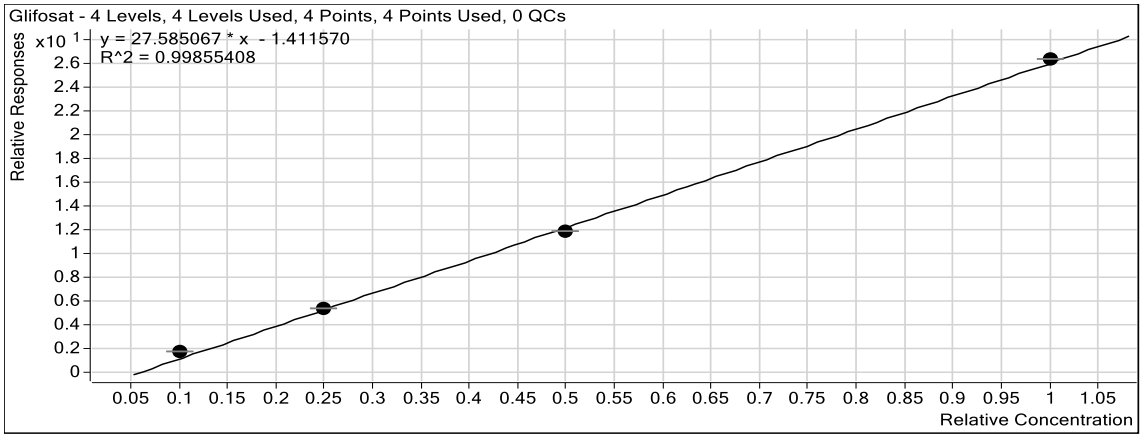

Figure 1. Calibration curve

The recovery studies were performed with the fortification experiments at the final mass concentrations of 0.025 to 0.10 mg/kg in three replicates. The average recovery was 101.4±4.49%. The precision was assessed in terms of repeatability at 0.10 mg/kg. A good repeatability (n = 6), with RSDs of 4.49% was obtained and it was calculated through the recovery.

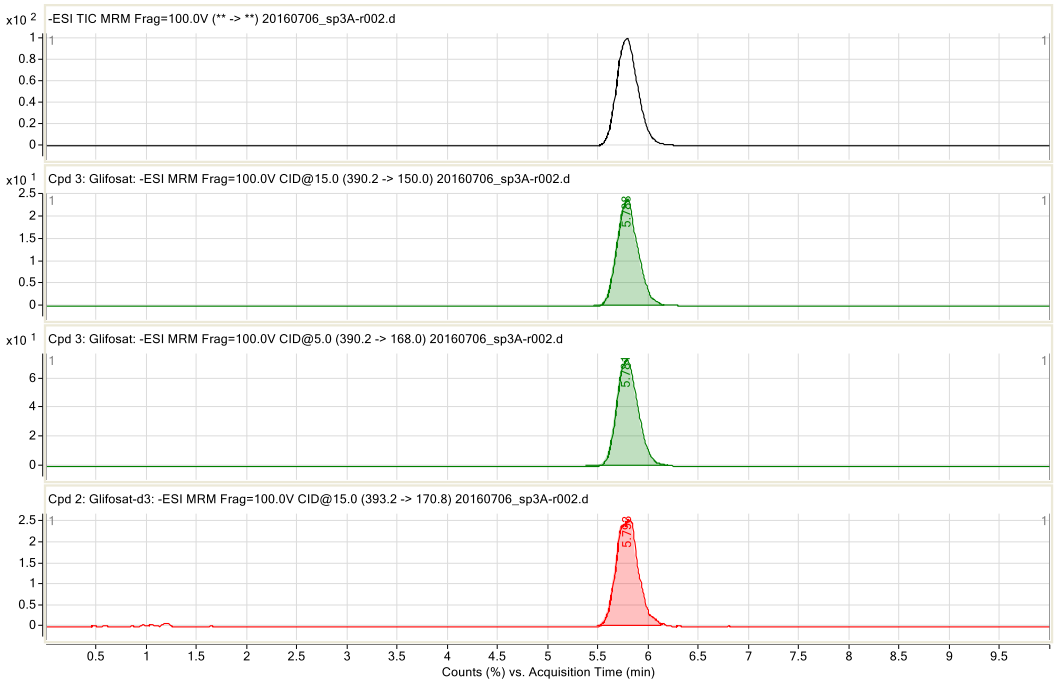

Figure 2. Chromatogram of spiked soil sample (level0.1 mg/kg)

Conclusion

The LC-MS/MS method is robust, can be applied to determine the glyhosate residues from soil as a matrix without any loss of sensitivity and assures a LOQ of 0.01 mg/kg. One sample can be processed with less than 2.5 hours. Quantifies man power is necessary to maintain very complex instrumentation in a good working condition.

Acknowledgments

The authors acknowledge the financial support of the Ministry of Science and Technological Development, Republic of Serbia for Projects Ref. III43005, TR31072and TR31043.

References

[1] M. Agarski, T. Stojanović, V. Bursić, M. Meseldžija, G. Vuković, B. Špirović Trifunović, T. Zeremski, Politehna, Belgrade, Serbia, Proceedings, (2015) 106.
[2]S. Goscinny, H. Unterluggauer, J. Aldrian, V. Hanot, S. Masselter, Food Anal. Methods. 5 (2012)1177.
[3] Europan Commicion in Press Release Databese (2016)
[4] G. Vuković, V. Bursić, J. Vlajković, B. Špirović, M. Cara, The 20th Symposium on analytical and environmental problems, Szeged, Hungary, Proceedings, (2014) 193.
[5] K. Kantošova, P. Kosubova, J. Časlavsky, 11thEPRW, Programme & Book of Abstracts, (2016) 140.
[6]SANTE/11945/2015, Guidance document on analytical quality control and method validation procedures for pesticides residues analysis in food and feed.

THE USE OF CULTIVATED PLANTS IN WATER QUALITY MONITORING

Antonije Žunić[1], Slavica Vuković[1], Sanja Lazić[1], Maria Fátima Alpendurada[2], Dragana Šunjka[1]

[1]*Department of plant medicine and environmental protection, University of Novi Sad, Faculty of Agriculture, Trg Dositeja Obradovića 8,Novi Sad, Serbia*
[2]*Water Institute of the Northern Region,Rua de Dr. Eduardo Torres 229, Porto, Portugal*
e-mail: zunictoni@gmail.com

Abstract

Water contamination is the most complex global environmental problem. Any pollution that is emitted into the environment at a certain time reaches the groundwater, rivers, lakes and seas. Nowadays aquatic ecosystems around the world are increasingly threatened by different pollutants. Rivers and lakes are under constant pressure from urban wastewater pollution, chemical waste from industry and transport, pesticides from agricultural areas, etc. By applying various methods in the laboratory were tested quality and impact of the water, characteristic for its high content of certain pollutants, to the test plants: buckwheat (*Fagopyrum esculentum*) and cabbage (*Brassica oleracea*). The analyzed water was taken from two locations of the River Lesa in Portugal. Physico-chemical analysis of water indicates that nitrates, nitrites and ammonium were detected in values exceeding maximum allowable concentration, according to Portuguese regulations of water quality. Also, in the analyzed water samples cadmium (Cd), magnesium (Mg) and iron (Fe) were found in quantities that exceed the MAC values, as well as some pesticidal substances (MCPA, fonofos). In the tested samples, long list of pharmaceuticals were detected. The obtained results indicate differences in tolerance of the test plants according to the parameters which have been detected in the water. Physiological parameters (germination energy and germination) have not been proven to be good indicators of water quality, while the more reliable may be considered some morphological parameters (length of shoot), that reacted by stimulation of the shoot.

Introduction

Water pollution is a problem of global proportions which refers both to drinking and water used for irrigation of agricultural crops. The biggest polluter of the environment, in addition to industry, is agriculture. Pesticidal residues carried by water from agricultural areas pose an environmental threat as a result of intensive agricultural production and irrigation. In order to prevent and reduce environmental pollution, it is essential to carry out the continuous monitoring of water quality. Methods that involve the use of cultivated plants as test organisms are extremely important for assessing the contamination of water used in agricultural production, because its results reflect the benefits of the area for cultivation of plants and the use of water for irrigation. The aim of the study was to by using test plants buckwheat (*Fagopyrum esculentum*) and cabbage (*Brassica oleracea*) determine the degree of water pollution through morphological (germination energy, germination) and physiological parameters (length of roots and shoots, fresh and dry weight of roots and shoots).

Experimental

Water sampling was conducted in 2014, by experts from "Northern Region Water Institute"-IAREN (Instituto da Água da Região do Norte) from Portugal. Water was sampled from two sites along the River Lesa in Portugal. Physico-chemical analysis of water was also conducted in Portugal and includes the following parameters: general parameters of water quality, organic

compounds, heavy metals, pesticides, pharmaceuticals. For chemical analysis, the following techniques were used: Atomic Adsorption Spectrometry-Flame Technique (EPA Method 7000B), Liquid Chromatography-Tandem Mass Spectrometry (LC-MS-MS), Gas Chromatography Mass Spectrometry (GC-MS) and Inductively Coupled plasma Mass spectrometry (ICP-MS). For the extraction that preceded detection of the presence of pollutants Solid Phase Extraction (SPE) and Accelerated Solvent Extraction (ASE) were used. The maximum allowable quantities (MAC) used in this experiment are stipulated by Portuguese regulations Decreto-Lei nº 103/2010, D.-Lei nº 236/1998 and the EU Directive 2008/105/EC. Water quality was evaluated using physiological (germination energy and germination /%/) and morphological parameters (length of roots and shoots of seedlings /cm/, fresh and dry weight of roots and shoots of seedlings /g/) of the test plants. A filter-paper method by ISTA (International rules for seed testing) for 2013 was used. Results for physiological parameters are expressed in percentages. The values of morphological parameters are shown as average values and are processed using the Analysis of Variance and Duncan's multiple comparison test, in the statistical software R ver. 3.2.2.

Results and discussion

According to the results of the physico-chemical analysis (Tab. 1.), in water sample Lesa I a high concentration of ammonia nitrogen (exceeding maximum allowable concentration for 126x) and nitrite (3x) was established, while the other test parameters were in allowable limits. In water sample Lesa II was found that nitrate values exceed the MAC for 2.5x and ammonia nitrogen (184x), so this water sample is also polluted and does not meet the required quality for irrigation. Water containing a high concentration of nitrogen and nitrogen compounds can adversely affect the yield and quality of barley, sugar beet and some vegetable crops, causing excessive growth of vegetative organs (Bauder et al., 2014). The results indicate that the shoot length of cabbage was significantly stimulated by water from the sample Lesa I and Lesa II (found to have a high concentration of nitrate, nitrite and ammonia) which is consistent with the allegations of Bauder et al. (2014).

Table 1. Physico-chemical analysis of the general parameters in analyzed water samples

Location	Detected values of general parameters							
	pH	EC (mS/cm) at 20˚C	t°C	NO_3^- mgN/l	NO_2^- mgN/l	NH_3 mgN/l	P mgP/l	B mgB/l
Lesa I	7.5	463	21.4	0.6	**3.0**	**6.3**	<0.1	<0.1
Lesa II	7.3	423	22.3	**25.0**	0.7	**9.2**	0.9	<0.1
MAC*	**5-9**	**≤1000**	**30.0**	**10.0**	**1.0**	**0.05**	**1.0**	**1.0**

The results from analysis of heavy metals and other elements from the list of priority pollutants indicate an extremely high amount of cadmium (Cd), three times higher than the MAC and also the increased amount of molybdenum (Mo) and magnesium (Mg) in the water sample Lesa I. Iron (Fe) is found in high quantities in a water sample Lesa II (2.5x more than the MAC). In the sample Lesa II a higher concentration of manganese (Mn) was also detected, but values were below the MAC (Tab. 2). Heavy metals are very harmful because of their non-biodegradable nature, long biological half-lives and their potential to accumulate in different body parts. Cadmium is toxic to many plant species. High concentrations of cadmium cause the inhibition of plant growth, development and to the occurrence of deformities. The shoots are shortened, the root is reduced and becomes brown, stiff (Rascio & Navarre-Izzo, 2011). Iron is one of 16 essential elements for plant growth and reproduction. Although required by plants in small amounts, Fe is involved in many important compounds and physiological processes in plants.

Toxicity of iron has not been reported under most aerobic plant production systems (Hochmuth, 2011).

Table 2. The content of heavy metals and elements from the list of priority pollutants in water

Location	Detected values of heavy metals and other elements									
	Cd (µg/l)	Se (µg/l)	As (µg/l)	Mo (µg/l)	Cr (µg/l)	Pb (µg/l)	Mn (µg/l)	Fe (µg/l)	Zn (µg/l)	Mg (mg/l)
Lesa I	**16**	<2.5	<1.0	33	<0.5	<0.2	<1.0	<0.1	<10.0	**75**
Lesa II	<0.5	<2.5	<1.0	<0.01	5	<0.2	72	**250**	24	9,6
MAC	**5**	**10**	**10**	**50**	**50**	**50**	**100**	**100**	**500**	**50**

Chemical analysis of pesticide content in the tested waters showed the presence of pesticide substances MCPA and fonofos. The highest concentration of these substances was found in water sample Lesa I. In the sample Lesa II listed pesticides were below the limit of detection (Tab. 3.). Fonofos represents a highly toxic organophosphate insecticide. In plant tissues it is rapidly metabolized to non-toxic compounds. It is extremely dangerous and toxic to bees, birds, fish and other aquatic organisms (Wagner, 1983). MCPA is a selective herbicide for control of broadleaf weeds. Applied in small quantities, it stimulate growth like natural hormones. Moderate amounts stimulate cell division and elongation, while large amounts inhibit grow (Konstantinović, 2008). The research results are consistent with this these, as the test plant cabbage had a growth stimulation in the treatment with water from sample Lesa I, where it is detected an increased amount of MCPA.

Table 3. The content of pesticides and organic compounds in water samples

Location	Parameters (µg /l)						
	Endosulfan	MCPA	Alachlor	Simazin	Fonofos	Aldrin	Benzene
Lesa I	<0.009	**5.9**	<0.01	<0.05	**670.0**	<0.01	<0.28
Lesa II	<0.009	<0.05	<0.01	<0.05	<0.01	<0.01	<0.28
MAC	**0.01**	**0.5**	**0.7**	**4.0**	**10.0**	**30.0**	**50.0**

Chemical analysis of the content of pharmaceuticals in tested water samples showed that the drugs, such as paracetamol, naproxen, ibuprofen, hydrochlorothiazide, azithromycin, diclofenac, furosemide and ciprofloxacin, were over the limit of detection. Water sample Lesa II contained the highest concentrations of these drugs, so it can be considered more polluted compared to Lesa I. The main sources of pollution of surface and ground-waters with these compounds are urban and agricultural waste waters or households, hospitals and agricultural lands. Also, the significant source of pollution are wastewaters from the pharmaceutical industry.

*Bioassay results - test plants buckwheat and cabbage:*The obtained results indicate differences in tolerance of the test plants according to the parameters which have been detected in the water. Physiological parameters (germination energy and germination), in both cases, have not been proven to be good indicators of water quality, while the more reliable may be considered some morphological parameters of cabbage (length of shoot), that reacted by stimulation (Tab. 4.). Shoot length of cabbage was significantly stimulated by water from Lesa I (by 22%) as compared to control, and from Lesa II by 14%. Differences between the treatments are statistically significant ($F=11.78^*$, $p < 0.05$). Other morphological parameters (length of root, fresh and dry weight of root and shoot), were not affected by water quality and all values are on the same level of significance, compared to the control. Buckwheat has not proved to be a good indicator of

water quality, which is contaminated with specified pollutants. More reliable can be considered the results obtained from the test plant cabbage.

Table 4. Impact of water quality on morphological parameters – Root and Shoot

Root				Shoot			
Parameters	Water sample	Buckwheat Values	Cabbage Values	Parameters	Water sample	Buckwheat Values	Cabbage Values
Length of root (cm)	Lesa I	6,82 ±0,95 a	4,62 ±0,81 a	Length of shoot (cm)	Lesa I	5,77 ±0,70 a	6,05 ±0,06 a
	Lesa II	6,10 ±1,26 a	4,20 ±0,51 a		Lesa II	5,95 ±1,15 a	5,65 ±0,49 a
	Control	5,87 ±0,96 a	3,80 ±0,53 a		Control	4,87 ±0,17 ab	4,97 ±0,33 b
	F value	0.87 ns	1.71 ns		F value	2.176 ns	9.96 *
Fresh weight of root (g)	Lesa I	0,32 ±0,07 a	0,08 ±0,04 a	Fresh weight of shoot (g)	Lesa I	2,50 ±0,20 a	0,99 ±0,10 a
	Lesa II	0,33 ±0,11 a	0,07 ±0,04 a		Lesa II	2,55 ±0,34 a	0,95 ±0,27 a
	Control	0,22 ±0,08 a	0,06 ±0,03 a		Control	2,14 ±0,11 ab	0,77 ±0,10 a
	F value	1.98 ns	0.34 ns		F value	3.47 ns	1.84 ns
Dry weight of root (g)	Lesa I	0,03 ±0,005 a	0,011 ±0,001 a	Dry weight of shoot (g)	Lesa I	0,23 ±0,029 a	0,054 ±0,007 a
	Lesa II	0,02 ±0,008 a	0,010 ±0,003 a		Lesa II	0,24 ±0,026 a	0,051 ±0,016 a
	Control	0,03 ±0,005 a	0,009 ±0,001 a		Control	0,24 ±0,024 a	0,048 ±0,004 a
	F value	1.24 ns	2.29 ns		F value	0.30 ns	0.39 ns

Conclusion

Based on the conducted tests and the results achieved on the impact of water quality (Lesa I, Lesa II) on the test plants (buckwheat, cabbage) the following can be concluded:

• In water sample from Lesa river site I, detected pollutants, in the quantities exceeding MAC according to the Regulations, are: nitrites, ammonia, cadmium, magnesium, fonofos, MCPA and none of the tested pharmaceuticals. Based on the biological test of water quality on phyto-indicators, cabbage reacted in a significant stimulation of the length of shoot, which can be attributed to the presence of ammonia, nitrites and MCPA;

• In a sample of water from the site Lesa II in quantities exceeding MAC, nitrates, ammonia and iron were detected. The pharmaceuticals such as: paracetamol, naproxen, ibuprofen, hydrochlorothiazide, azithromycin, diclofenac, furosemide and ciprofloxacin, were alsoregistered. Water significantly stimulated shoot length of cabbage. These effects can be attributed to the presence of ammonia, nitrates and iron in a greater amount in this sample;

Bioassay test results indicate the different susceptibility of tested plant species and parameters as well as their validity in assessing water contamination. Different plant species and parameters responded in dissimilar manner to the quality of the sampled water.An expressed variability of parameters indicates their potential as possible bioindicators.

Acknowledgements

This study was part of the project III43005, funded by the Ministry of Education, Science and Technological Development of the Republic of Serbia.

References

[1] Bauder, T.A., Waskom, R.M., Sutherland, P.L and Davis, J.G. (2014): Irrigation Water Quality Criteria. Colorado State University, 1-5.

[2] Hochmuth, G. (2011): Iron Nutrition of Plants. University of Florida, IFAS Exst.,1-7.

[3] Konstantinović, B. (2008): Weeds and their control. Faculty of Agriculture, Novi Sad, 220-226.

[4] Rascio N. & Navari-Izzo F. (2011): Heavy metal hyperaccumulating plants: How and why do they do it? Plant Science 180, 169–181.

[5] Wagner, S.L. (1983): Clinical Toxicology of Agricultural Chemicals. Noyes Data Corp. 1983., 205-246.

EFFECT OF SYNTHESIS METHOD ON THE STRUCTURE AND PROPERTIES OF PEROVSKITE $NaNbO_3$ TYPE NANOMATERIALS

P. Vlazan, M. Poienar, P. Sfirloaga

National Institute for Research and Development in Electrochemistry and Condensed Matter, Department of Condensed Matter, 1 Plautius Andronescu St., 300224 Timisoara, Romania
vlazanp@yahoo.com

Abstract

Ferroelectric nanostructures have attracted much attention recently due to the ongoing demand for miniaturization of devices and discover new phenomena. One of the materials studied intensively in recent years is potassium niobates with perovskite structure is a promising material for electro-optic, nonlinear optical, and photorefractive applications such as frequency doubling, wave guiding, and holographic storage.

The structure and morphology of $NaNbO_3$ perovskites are studied in the context of their possible use for sensors application. Materials are prepared by hydrothermal, sol-gel and ultrasonic method using different thermal treatments. Powders obtained were characterized by X-Ray diffraction (XRD), scanning electron microscopy (SEM) and Fourier Transform Infrared Spectroscopy (FTIR).

Acknowledgement

The authors wish to acknowledge the financial support of Partnerships Program - (PCCA 2013) – Project nr. 177/2014

SUBSTITUTION EFFECT ON THE PHYSICO-CHEMICAL PROPERTIES IN CREDNERITE $CuMnO_2$ TYPE MATERIALS

Maria Poienar, **Paula Sfirloaga**, **Paulina Vlazan**

National Institute for Research and Development in Electrochemistry and Condensed Matter, Plautius Andronescu Str Nr.1, 300224 Timisoara, Romania
maria_poienar@yahoo.com

Abstract

Recently, the ABO_2 delafossite-type class of materials, B being a transition element, has attracted a lot of interest. First of all in the field of transparent conducting oxides, thin films of $CuAlO_2$ show the unusual combination of high transparency and rather high p-type semi-conductivity [1]. On the other hand, in the field of the exotic magnetic and structural properties, a good example is the $CuFeO_2$ delafossite, a triangular lattice antiferromagnet which has been extensively studied over the last years for its multiferroïcity [2,3].

The ABO_2 delafossite structure, where A=Cu and Ag, and B a transition element, belongs to the R-3m space group and is characterised by O-Cu-O dumbells linking layers of edge sharing BO_6 octahedra. However, in this class of materials,crednerite $CuMnO_2$occupies a unique placedue to the Jahn-Teller (JT) distortion of the Mn^{3+} ($t_{2g}^3e_g$) which leads to a monoclinic structure (C2/m space group at room temperature) and to a different topology of the magnetic triangular lattice and out-of-plane stacking sequence compared to delafossite structure.

In this work, we investigated the physico-chemical properties of $CuMn_{1-X}B_XO_2$ (B=Al, Mg; x=0 - 0.08) type materials by X-Ray diffraction, SEM-EDAX, thermal analysis, UV-VIS and infrared spectroscopy. The effect of the substitution on the lattice parameter in $CuMnO_2$is significant in order to understand the correlation between the structure and the properties in this compound.The crednerite nanoparticles were synthesized at low temperature by hydrothermal method in teflon-lined steel autoclave.

Acknowledgment: This work was supported by a grant of the Romanian National Authority for Scientific Research and Innovation, CNCS – UEFISCDI, project number PN-II-RU-TE-2014-4-2179.

References

[1] Kawazoe, H.; Yasukawa, M.; Hyodo H.; Kurita, M.; Yanagi, H.; Hosono, H. Nature (London) 1997, 389, 939.
[2] Kimura, T.; Lashley, J. C.; Ramirez; A. P. Physical Review B 73(22), 220401 June (2006).
[3]Ye, F.; Ren, Y.; Huang, Q.; Fernandez-Baca, J. A.; Dai, P. C.; Lynn, J. W.; Kimura, T. Physical Review B 2006, 73, 220404.

IMPACT OF DOPANTS ON THE ELECTRICAL PROPERTIES IN ABO_3 PEROVSKITE TYPE MATERIALS

P. Sfirloaga[a], **I. Malaescu**[b], **M. Poienar**[a], **C. N. Marin**[b], **P. Vlazan**[a]

[a]*National Institute for Research and Development in Electrochemistry and Condensed Matter, Timisoara, P. Andronescu no. 1, 300254 Romania*
[b] *West University of Timisoara, Vasile Parvan no. 4, Timisoara, 300223 Romania*
paulasfirloaga@gmail.com

Abstract

The ceramics materials with ABO_3 structure based on iron or silver doped sodium tantalate, were successfully synthesized using the ultrasonically method with immersed sonotrode in the reaction medium followed by heat treatment at 600°C. Samples were doped with silver for the A site of the perovskite lattice and with iron for the B site. The doping was performed in order to improve the electrical properties through change the crystalline structure and prevent ordering of the oxygen vacancies in these materials. The obtained materials were characterized by X-ray diffraction (XRD), transmission electron microscopy (TEM), BET analysis, energy-dispersive X-ray spectroscopy (EDX) and electrical measurements. Structural analysis shows that the obtained materials have cubic structure and a homogeneous composition, without secondary compounds. Electrical measurements indicate that the presence of metal ions of iron or silver in the structure of $NaTaO_3$ lead to decreases of the gap band energy, resulting in increase of electric conductivity.

Acknowledgment

This work was supported by Collaborative applied research project **49/2012 BIOSIM**.

OBTAINING OF $FeCO_3$ MICROPARTICLES

Marius Chirita[1], Mihaela Luminita Kiss[1], Adrian Ieta[2]

[1]*Department of Nanocrystal Synthesis, National Institute for Research and Development in Electrochemistry and Condensed Matter, Timisoara, Plautius Andronescu Str. No. 1, RO-300224, Timisoara, Romania; tel. 0040256494413*
[2]*Department of Physics, State University of New York at Oswego, Oswego, NY*
e-mail: chirifiz@yahoo.com

Abstract
Usinghydrothermal decomposition of the Fe(III)-EDTA complex in the presence of urea, we developed a new procedure for synthesizing highly crystalline $FeCO_3$ starting from Ferric Ammonium Sulfate and Na_4EDTA as main precursors. Single phase $FeCO_3$ microcrystals with size in the range of 50µm-200µm have been obtained after high pressure-temperature treatment time between 15 hours and 26 hours at 230ºC and 250ºC.

Keywords: $FeCO_3$, iron carbonate, hydrothermal decomposition, Fe-EDTA complex.

Introduction
Due to its implications upon the geological sequestration of CO_2[1], the thermodynamics of iron carbonate ($FeCO_3$) has been studied in many research fields, such as geology [2, 3], oceanography [4, 5] and sedimentology [6, 7]. A very interesting application in crystallography is the potential of the iron carbonate to be used as precursor to prepare Fe_3O_4 and Fe_2O_3 crystals [8] by partial or total oxidation of Fe^{2+} ions to Fe^{3+} ions, respectively.
Continuing our previous studies [9], the present experimental procedure is focused on the hydrothermal synthesis of iron carbonate microparticles in a pure crystalline structure, by hydrothermal decomposition of the Fe(III)-EDTA complex in the presence of urea, starting from Fe(III)-Ferric Ammonium Sulfate (FAS) and Na_4EDTA as main precursors.

Experimental methods
Synthesis
The following procedure of chemical preparation was followed:
An aqueous solution of $1.05x10^{-1}$M of FAS, an aqueous solution of $1.05x10^{-1}$M Na_4EDTA, and an aqueous solution of $9.71 \cdot 10^{-1}$ M of urea were mixed under continuous stirring. This solution was transferred into a number of Teflon-lined stainless-steel autoclaves and was heated up to 230°C and 250ºC by a rate of 1.7ºC/min. The autoclaves were removed, one by one, every two hours in the range between 15 and 26 hours. All the pH measurements indicated a value between 9.4 and 9.5 for the final solutions. The obtained microparticles were filtrated, washed with bidistilled water and dried at 60°C in air.

Results
The crystalline structure of the $FeCO_3$ microparticles synthesized between 15 and 26 hours of high pressure-temperature treatment time is confirmed by XRD analysis spectra (Figures 1.a) in agreement with the respective ICSD (Inorganic Crystal Structure Database) reference code: 01-083-1764. The high purity of FeCO3 microcrystals synthesized between 16 and 24 hours of high

pressure-temperature treatment time is confirmed by EDAX analysis. All the spectra collected in this interval have the same characteristics as the presented spectra (Figure 1.b), which indicates the presence of iron and oxygen only, without any traces of Na, S, C and N, which could result from EDTA and FAS decomposition.

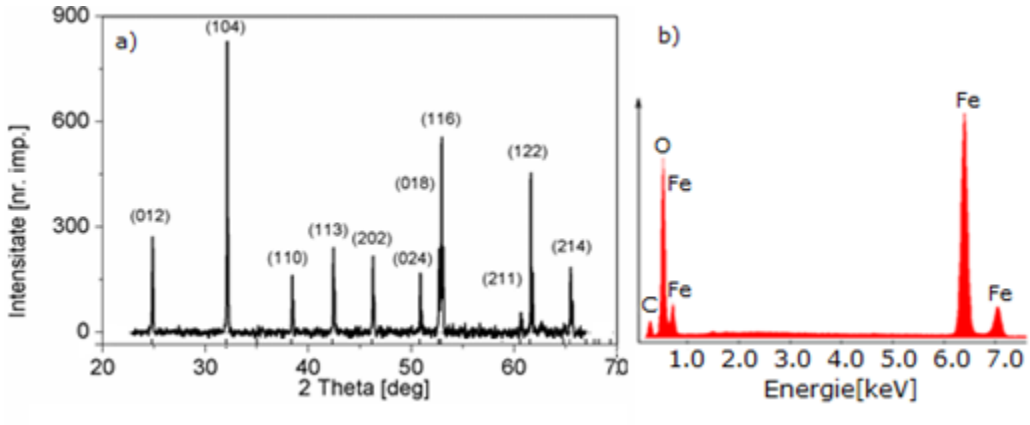

Figure 1. XRD (a) and EDAX (b) spectra.

The SEM images reveal the rhombohedral morphology of the $FeCO_3$ microcrystals synthesized after 22 hours of high pressure-temperature treatment time. The sizes of the $FeCO_3$ microcrystals are in the range of 50 - 200 μm and were evaluated following the SEM image (Figures 2).

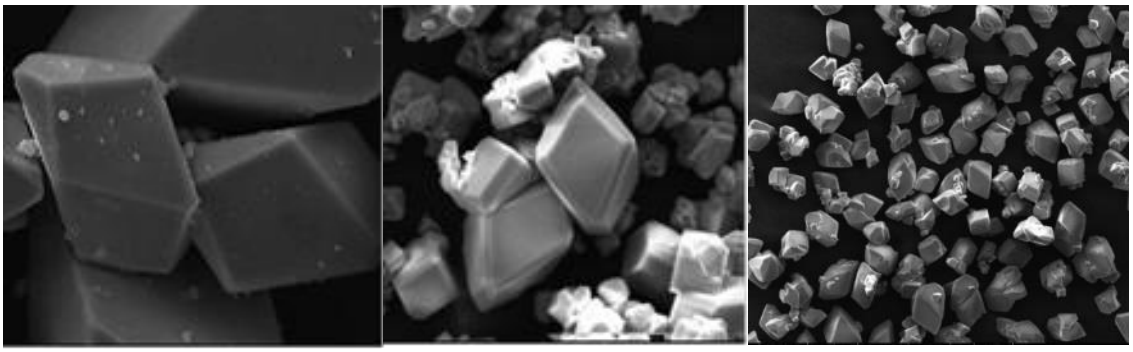

Figure 2. SEM images of the $FeCO_3$ microcrystals

Our preliminary research has shown that by changing some synthesis conditions, e.g. autoclavation time between 15h and 26h and synthesis temperature between 230ºC and 250ºC, particle size may be controlled within the range of 10μm-200μm. For a precise control of the particle's dimension, additional experiments have to be done. An extension of these results has been presented by as in [9].

Conclusion

We developed a new procedure for synthesizing highly crystalline $FeCO_3$ microparticles by hydrothermal decomposition of the Fe(III)-EDTA complex in the presence of urea, starting from Ferric Ammonium Sulfate and Na_4EDTA as main precursors. Single phase $FeCO_3$ microcrystals with sizes in the range of 50μm-200μm were obtained after high pressure-temperature treatment time between 15 hours and 26 hours at 230ºC - 250ºC. The synthesis of pure iron carbonate

microparticles was confirmed using X-ray powder diffraction and EDAX investigation. The present investigation has demonstrated the possibility of synthesizing microsize iron carbonate particles, having rhombohedral morphology, starting from Fe^{3+} ions only and using the hydrothermal decomposition of the Fe(III)-EDTA complex in the presence of urea.

Acknowledgments

The authors would like to thank Dr. Radu Banica, Dr. Aurel Ercuta, Dr. Cecilia Savii, Dr. Zoltan Szabadai, Dr. Alexandra Bucur, Dr. Paula Sfarloaga, and Dr. Ioan Grozescu for helpful discussions and technical support.

This work was supported by project PN 09 34 01 01 and PN 16-14-03-07 of the Ministry of Research and Education in Romania.

References

[1]. D. Testemale, F. Dufaud, I. Martinez, P. Bénezeth, J.-L. Hazemann, J. Schott, and F. Guyot, Chemical Geology DOI:10.1016/j.chemgeo.2008.08.019, 2008.

[2]. C. A. R. Silva, X. Liu, and F. J. Millero, J. Solution Chem. 31 (2002): 97–108.

[3]. Q. J. Fisher, R. Raiswell, and J. D. Marshall, J. Sediment. Res. 68 (1998): 1034–1045.

[4]. L. Jensen, J. K. Boddum, J. C. Tjell, and T. H. Christensen, Appl. Geochem. 17 (2002): 503–511.

[5]. C. J. Ptacek and E. J. Reardon, Water–Rock Interaction (1992): 181–183.

[6]. H. L. James, "Chemistry of the iron-rich sedimentary rocks." US Geol. Surv. Prof. Paper 440-W, 1966.

[7]. H. J. Smith, J. Am. Chem. Soc. 40 (1918): 879–883.

[8]. Shouhu Xuana, Mingwei Chen, Lingyun Hao, Wanquan Jiang, Xinglong Gong, Yuan Hu, and Zuyao Chen, Journal of Magnetism and Magnetic Materials 320 (2008): 164–170.

[9]. M. Chirita, A. Ieta, Crystal Growth & Design, 12 (2) (2012): 883–886.

CORROSION OF CONCRETE

Bálint Augusztin[1,2], Imre Kovács[1]

[1]*Department of Natural Sciences and Environmental Protection, Institute of Technology. University of Dunaújváros, H-2401 Dunaújváros, Táncsics M. u. 1/a, Hungary*
[2]*Augusztin Kft. H-8200 Veszprém, Batthyány út 17/D, Hungary*
e-mail: kovacsimre@uniduna.hu

Abstract
Studies on corrosion of concrete are both of technical and theoretical interest. In this work we studied the effect of CO_2 absorption on concrete. We investigated blocks of concrete of different compositions and treatments. These blocks were put into a chamber where we simulated the long time effect of CO_2 on the mechanical properties of concrete by high concentrations of CO_2. In this publication we show our preliminary results on this system. The detection of the corrosion was carried out by phenolphthalein indication.

Bevezetés

A beton egy többszörösen összetett építőanyag [1]. A beton adalékanyag (sóder), cement és vízen kívül egyéb vegyszerek hozzáadásával készül. Vasbeton esetén acél szálakat, betéteket tartalmaz. Megfelelő homogenizálás után általában a helyszínen dolgozzák be a zsaluzatba amelyben a megfelelően elhelyezett betonacél található. A cement több fázisából különböző reakciótermékek jönnek létre. A kialakuló un. C-S-H gél „ragasztja" össze a különböző komponenseket. Kristályosodó fázisok is keletkeznek a kötés során, de ezek nem alkotnak összefüggő szerkezetet. Acélszálak alkalmazásával pótoljuk a beton azon hiányosságát, hogy a hajlító és húzószilárdsága a nyomószilárdságához képest kicsi. A megkötő beton pH-ja 12-13-as érték körül van. A betonban a kötés közben a nem eléggé tökéletes tömörödés, valamint a reakciótermékek és a kiinduló komponensek térfogatának különbsége miatt pórusszerkezet jön létre. Ezek lehetnek i. légbuborékok (mm – μm-es tartományban) ii. kapillárisok (jellemzően mikro- és nanométeres nagyságrendben) és iii. nanométeres pórusok a gélben. A pórusrendszer zártságához egy elméletileg 0,55 víz/cement arány tartozik, de a pórusok kialakulásával mindig kell számolni [2].

A beton környezeti károsodásai többfélék, lehetnek fizikai vagy kémiai jellegűek. A fizikai hatások szélsőséges hőmérséklet, zsugorodás, vagy kopás miatt alakulnak ki. Kémiai hatások elsősorban szulfátok, kloridok, vagy savak jelenléte, amik a pórusokon keresztül jutnak a betonba. Ezen tényezők jelenléte a cementkő mállásán kívül előidézhetik a passziált acélszálak rozsdásodását is ha a pH<10,5 alá csökken. A CO_2 a levegőben és páratartalom a pórusokban karbonát sókat képez, amik a cement CaO tartalmával $CaCO_3$-ttá alakulnak, valamint víz is keletkezik és a pH lecsökken. Ha az így kialakuló karbonátosodási front eléri az acélszálakat, a korrózió elindul. A fenti mechanizmusból következik, hogy a CO_2 diffúziója lehet a sebességmeghatározó lépés. Hosszú idő kell a diffúzióhoz is, de mivel a beton épületek hosszú időre készülnek, a tervezett élettartam közben a lassú károsodás jelentősége nem elhanyagolható. Az összetevők helyes megválasztásával azonban a fenti folyamatok jelentősen lassíthatók. Az ilyen rendszereken az öregedési folyamatot célszerű mesterséges körülmények között, a vizsgálati idő jelentős, több nagyságrenddel rövidítése mellett lehet vizsgálni. A bemutatott kísérleti munkában csak a CO_2 hatást igyekeztünk követni, ennek érdekében a légköri CO_2 koncentráció helyett annál jóval nagyobb, legalább 80% koncentrációjú CO_2

atmoszférába tettük a mintákat, így a vizsgálatok idejét le tudtuk rövidíteni kb. 2 hétre. A karbonátosodási front előrehaladását fenolftaleines vizsgálattal követtük.

Kísérleti eszközök és módszerek

Kísérleteinkhez Lafarge Cement Kft. gyártású, CEM II A-S 42,5 R típusú cementet, különböző frackciókból összekevert adalékanyagot és desztillált vizet használtunk. A kísérletekben használt légpórusképző anyag és képlékenyítőszer a Mapei Kft-tól származott. A 10x10x10 cm-es mintákat az MSZ 4798-1:2004 szabvány előírásait betartva gyártottuk le.

A vizsgálati kamra egy 200 liter térfogatú műanyaghordó volt, melybe háztartási páramentesítőt és egy elektromos ventillátoros fűtőtestet állítottunk be. Ezek az eszközök egy kapcsolóüzemű pára- és hőmérséklet szabályzóra vannak kötve, ezzel biztosítva az egyenletes környezeti feltételeket. A páratartalmat és a hőmérsékletet egy adatrögzítőn tároltuk. A vizsgálati mintákat egy vas állványon helyeztük el. A CO_2-ot egy gázpalackból vezettük a tartályba amit naponta rendszeresen átöblítettünk. A frissbeton mintákat készítésük után 1 napig levegőn tároltuk, majd 27 napra víz alá tettük. Ezen érlelési fázis után kerületek a CO_2 kamrába.

A karbonátosodás mértékét a betonkocka kettéhasítása után fenolftalein indikátorral mutattuk ki.

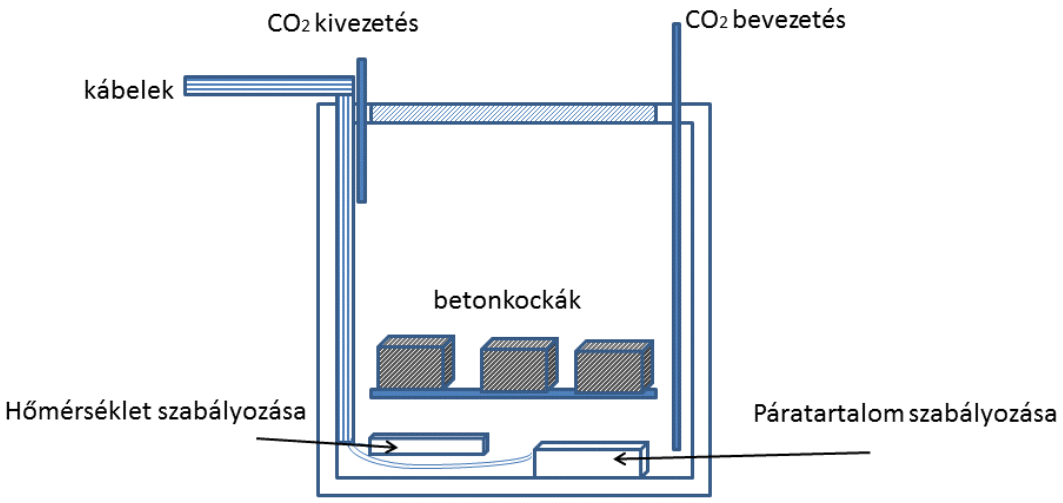

1. Ábra A kísérletekhez használt kamra melyben CO2-atmoszférát, állandó hőmérsékletet és páratartalmat biztosítottunk.

Eredmények és értelmezésük

Az első vizsgálatnál egy C25-ös és egy C10-es szilárdsági jelű betont készítettünk. A mintákat együtt tettük a kezelő kamrába. Két hétig folyamatosan több mint 80 % CO_2 atmoszférában tartottuk őket. A relatív páratartalom 60-70 %rH és a hőmérséklet 22 C° volt. A fenolftaleines kezelés után a 2. ábrán látható képeket kaptuk a C25-ös cementkockáról. A 3. ábrán a C10-es

betonról készült hasonló felvételt látjuk.

2. ábra A C25-ös betont a CO_2 kezelés után elhasítva és az indikátorral ecsetelve. A minta épen maradt éle megfele 10 cm-es élhosszúságnak

3. ábra A C10-es betonkockát a CO_2-os kezelés után elhasítva és indikátorral ecsetelve A minta élhosszúsága 10 cm.

A mintákon látható, hogy a kéreg pH értéke, amelybe a CO_2 bediffundált, kisebb mint a fenolftalein átcsapási tartománya. A C25-ös mintán ez nem haladja meg az 1 cm-t. A C10-es

mintában a karbonátosodás sokkal gyorsabban haladt előre.
Következő lépésként a cementpéphez légpórusképző anyagot is adagoltunk a C25-ösnek megfelelő összetételhez. Ez esetben henger alakú mintákat készítettünk. Jól látszik, hogy a pórusok méretének növekedésével a karbonátos réteg vastagabb lett, hasonló körülmények mellett.

4. ábra A C25-ös betonból készült minták azonos körülmények között voltak a széndioxidban 2 hétig. Majd törés után fenolftalein oldattal kezeltük őket.

Következtetések
A beton korrózióállóságának tanulmányozásában a fenolftaleines indikálás jól használható. Hátránya viszont, hogy a mintáról csak törés után kapunk eredményt. Az ugyanolyan összetételű, de tömörebb minta nagyobb szilárdságú és a karbonátosodással szemben is ellenállóbb.
A mintákat a pépes állapottól kezdve is igyekszünk a jövőben mérni és erre módszert kialakítani és a karbonátosodási front előrehaladását roncsolásmentes vizsgálattal kimutatni. Továbbá a minták utókezelésének hatását is meg kívánjuk vizsgálni.
Más indikátorok használatával igyekszünk a vizsgálatokat finomabbá tenni. Ez a szakirodalomban eddig még nem volt ismert.

Szakirodalom:
[1] Bonded Cement-Based Material Overlays for the Repair, the Lining or the Strengthening of Slabs or Pavements; Benoît Bissonnette, Luc Courard, David W. Fowler, Jean-Louis Granju (Eds), Springer, 2011
[2] Fehérvári Sándor ; Betonösszetevők hatása az alagútfalazatok hőtűrésére, PhD értekezés, Budapest, 2009

WO_3-TiO_2/MWCNT NANOKOMPOZITOK ELŐÁLLÍTÁSA ÉS FOTOKATALITIKUS VIZSGÁLATA

Bárdos Enikő[1], Kovács Gábor[1,2,3], Gyulavári Tamás[1], Németh Krisztián[1], Kecsenovity Egon[1], Berki Péter[1], Baia Lucian[2,3], Pap Zsolt[2,3,4], Hernádi Klára[1]

[1] Department of Applied and Environmental Chemistry,University of Szeged, Rerrich Béla tér 1, HU-6720, Szeged, Hungary;
[2]Faculty of Physics, Babeș–Bolyai University, M. Kogălniceanu 1, RO–400084 Cluj-Napoca, Romania;
[3] Institute for Interdisciplinary Research on Bio-Nano-Sciences, Treboniu Laurian 42, RO–400271 Cluj-Napoca, Romania
[4]Institute of Environmental Science and Technology, Tisza Lajos krt. 103, Szeged HU-6720, Hungary

Abstract

The "build-up" methodology, the importance of the order of the semiconductor layers in WO_3-TiO_2/MWCNT composite materials was studied in terms of the applied synthesis pathway, morpho-structural parameters (mean crystallite size, crystal phase composition, morphology) and photocatalytic efficiency (using oxalic acid as model pollutant). The appearance of $TiWO_x$ phase in the composites contributed to the enhancement of the photocatalytic efficiencies, as different synthesis methods led to different crystal phasecompositions. Although, it was proven that a beneficial phase's presence can be hindered if an excess of MWCNT or WO_3 was applied. As the ratio of the mentioned materials was reduced, active composites were obtained, but the previously noticed $TiWO_x$ disappeared. Therefore, in the case of WO_3-TiO_2/MWCNT nanocomposite system several photocatalytic activity enhancement factors can be introduced, but not simultaneously (the disappearance of $TiWO_x$ at low MWCNT and WO_3 contents and the appearance of highly crystalline anatase).

Bevezetés

A szén nanocsövekről (CNT) 1991-ben publikáltak először és mára már számos alkalmazásuk ismert. Kiváló mechanikai sajátságaik, elektromos és hővezető képességük miatt már évek óta a kutatások középpontjában állnak, kompozitjaik létrehozásával pedig további előnyös tulajdonságokkal rendelkező anyagokra tehetünk szert. A mindennapi életben és az anyagtudomány kutatási területein is egyre jobban előtérbe kerül a kompozit anyagok felhasználása és előállítása. Ennek oka, hogy különböző kémiai tulajdonságú és szerkezetű anyagokat kombinálva, egymás előnyös tulajdonságait fokozhatják.

A többfalú szén nanocsövek (MWCNT) alkalmazhatók a kompozitokban diszperz fázisként a kiváló rugalmassági modulusuk és a hosszúság/átmérő arányuk miatt, és emellett kiváló elektromos tulajdonságokkal is rendelkeznek. A szén nanocső alapú kompozitokat alkalmazhatjuk gázszenzorként és fotokatalizátorként is.

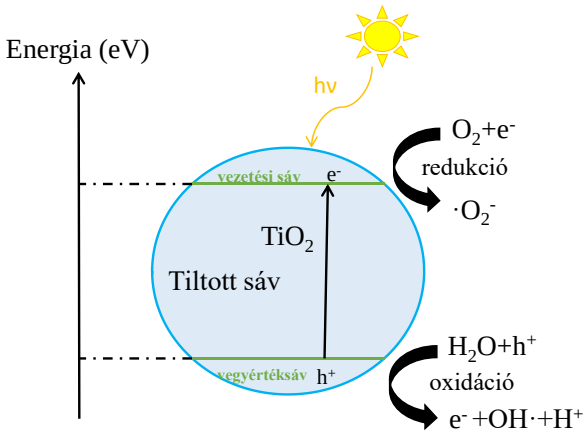

1.ábra A fotokatalitikus folyamatok sematikus ábrázolása

A fotokatalízis olyan nagyhatékonyságú oxidációs eljárás, amely során a pozitív töltésű lyukak (h^+) a vízmolekulát hidroxilgyökké (•OH) alakítják, azelektronok (e^-) az oxigént (O_2) pedig szuperoxidgyök anionná (•O_2^-). Ezek segítségével szerves mikroszennyezőket (fenol, oxálsav és szalicilsav) vagy festékeket (metilnarancs, metilénkék) oxidálhatunk szén-dioxiddá és vízzé, vagy éppen energiahordozó hidrogéngázt fejleszthetünk oxigénmentes környezetben. A teljes folyamat az *1.ábrán*található. Napjaink egyik legígéretesebb fotokatalizátora a titán-dioxid (TiO_2).Előnyös tulajdonságai, hogy fotostabilis, könnyen és nagy mennyiségben hozzáférhető, hosszútávon aktív, olcsó,nem mérgező ésUV fénnyel való gerjesztés során is stabilis[1].Legnagyobb hátránya azonban, hogy nagy a tiltottsávszélessége 3,0-3,2 eV (380-410 nm), miatt kevesebb fényt tud hasznosítani (4-5%). Erre a problémára megoldást nyújthat egy másik félvezető oxiddal való kompozitképzés, amelynek tiltott sávszélessége kisebb. Emiatt alkalmazzák a TiO_2 mellett a volfrám-trioxidot (WO_3). A WO_3 tiltott sávszélessége 2,4-2,8 eV körüli (440-510 nm), így már látható fényben isgerjeszthetőa katalizátor[2], illetve a WO_3 és a TiO_2együttes alkalmazása növeli a fotokatalitikus hatékonyságot[3, 4].

Kísérleti rész

Munkánk során a titán-dioxidnál lassú hidrolízises (LH) és egy módosított lassú hidrolízises eljárással (MLH) (más oldószer, más prekurzor, mint a LH esetén), amíg a volfrám-trioxidnálaz impregnálás (I) módszerével folytattuk kísérleteinket. Oldószerként acetont és etanolt, prekurzorként pedig titán-izopropoxidot, titán-etoxidot és volfrám-hexakloridot használtunk. Az oxidokat egyenként is felvittük a szén nanocsövek felületére (először a TiO_2-ot, utána a WO_3-ot, azután fordítva is) úgy, hogy az első oxid felvitele után alkalmaztunk hőkezelést a felvitt oxid kristályosodási hőmérsékletén, de alkalmaztunk olyan eljárást is, amikor előzetesen nem hőkezeltük a kompozitot. Ezek mellett volt olyan kísérleti megközelítésis, hogy a prekurzorokat egyszerre adagoltuk (PE) a szén nanocső szuszpenzióhoz. Alkalmazott rövidítések:

1. Lassú hidrolízissel és impregnálással készült minták:Nem hőkezelt TiO_2/MWCNT-ből kiindulva: **LHI-TiO_2-0-WO_3-450;** Hőkezelt TiO_2/MWCNT-ből kiindulva: **LHI-TiO_2-400-WO_3-450;**Nem hőkezelt WO_3/MWCNT-ből kiindulva: **LHI-WO_3-0-TiO_2-400;** Hőkezelt WO_3/MWCNT-ből kiindulva: **LHI-WO_3-450-TiO_2-400**
2. Módosított lassú hidrolízissel és impregnálással készült minták: **MLHI-TiO_2-400-WO_3-700**
3. Prekurzorok együttes adagolásával előállított kompozitok: **PE-TiO_2-WO_3-700**

Az oxidok és a szén nanocsövek aránya először 1:10:15 (MWCNT:TiO_2:WO_3) volt, majd előzetes fotokatalitikus aktivitás felmérés során rangsoroltuk a kompozitokat,és módosítottuk a fenti arányt (a legjobb hatékonyságot mutató módszer alapján készült kompozitok esetén) 1:16:3-ra és 1:18:1-re, hogy a fotokatalitikus aktivitásukat növeljük. A szintézist lezáró hőkezelést 400 °C-on, 450 °C-on és 700 °C-on végeztük.

A módszerek rangsorolásához un. gyorsteszteket végeztünk: a mintáinkat Evonik Aeroxide P25-el kevertük (70% P25 és 30% kompozit), majd fotokatalitikus aktivitásukat vizsgáltuk oxálsav bontásával. Miután kiválasztottuk a 2 legaktívabb kompozitot, és módosítottuk az összetevők arányát, már önmagukban is volt aktivitásuk, így a P25-el való keverést elhagytuk. Az oxálsav koncentrációjának változását nagyhatékonyságú folyadékkromatográfiával (HPLC) követtük nyomon.
Az elkészített kompozit anyagokat többféle módszerrel is vizsgáltuk: röntgendiffrakcióval (XRD), pásztázó és transzmissziós elektronmikroszkóppal (SEM és TEM) a szerkezetükről és morfológiájukról nyertünk információt, emellett Raman spektroszkópiát is alkalmaztunk és az optikai tulajdonságait is vizsgáltuk diffúz reflexiós spektrometriával (DRS).

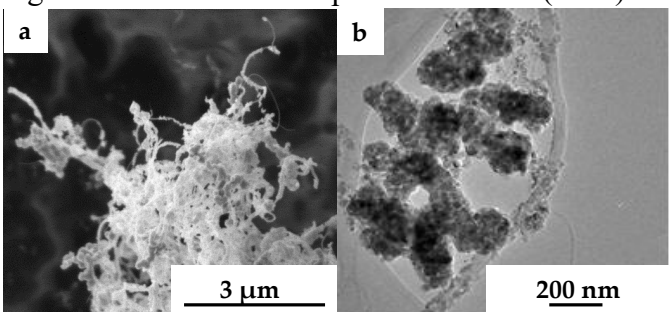

2. ábra Az PE-TiO_2-WO_3-700 1:18:1 arányú kompozit SEM (a) és TEM (b) felvétele

Eredmények

A TEM és SEM felvételekből megállapítható, hogy a különböző módszerekkel előállított kompozitoknál különböző szerkezetek alakultak ki: bizonyos esetekben a szén nanocsöveket homogén módon befedi a két oxid (például: MLHI-TiO_2-400-WO_3-700), míg más mintáknál nagyobb aggregátumok képződtek a nanocsöveken (LHI-WO_3-0-TiO_2-450) és megfigyeltünkolyat is, hogy bevonat és aggregátum is képződött egyszerre(PE-TiO_2-WO_3-700) (*2. ábra*).Az XRD, Raman vizsgálatokból arra tudtunk következtetni, hogy minden esetben megjelentek a TiO_2-ra, a WO_3-ra és az MWCNT-re jellemző reflexiók. A lassú hidrolízis során megállapítottuk, hogy amikor előzetes hőkezelés nélkül vittük fel a második oxidot, majdegyütt hőkezeltünk, sem alacsonyabb (400 °C és 450 °C), sem magasabb hőmérsékleten (700 °C)nem kristályosodott ki teljesen a két oxid. Abban az esetben, amikor a kiindulási anyagot előzetesen hőkezeltük, a két oxid kikristályosodása nem akadályozta egymást. Atitán-dioxid legtöbb esetben anatáz, a volfrám-trioxid pedig monoklin kristályszerkezettel fordul elő a kompozitokban. A módosított lassú hidrolízises módszer esetében, már csak hőkezelt TiO_2/MWCNT kompozitra vittük fel a volfrám-trioxidot, és 700°C-on hőkezeltük annak érdekében, hogy mindkét anyag teljesen kikristályosodjon. Érdekesség az is, hogy ennél a módszernél a volfrám-trioxid nem monoklin szerkezetű lesz, hanem hexagonális parciális hidrát ($WO_3 \cdot 0{,}33H_2O$) alakul ki. Abban az esetben, amikor a prekurzorokat egyszerre vittük fel, a 700°C-os hőkezelésnek köszönhetően mindkét anyag kristályos formában van jelen, de ezek mellett egy amorf fázis is megfigyelhető. Ebben az esetben a titán-dioxid anatáz és rutil formában is megjelenik, és ezek mellett a megjelenik a titán-volframát ($TiWO_x$).
A fotokatalitikus teszteknélaz elkészített kompozitoknak önállóan nem volt fotokatalitikus aktivitása, valószínűleg a volfrám-trioxid nagy mennyisége miatt, ezért kevertük Evonik Aeroxide P25-tel.A fenti mérésekből megállapítottuk, hogy a P25 mellett az LHI-TiO_2-0-WO_3-450 (83,3%) és a PE-TiO_2-WO_3-700 (75,1%) módszerrel készült katalizátorok bontottak leghatékonyabban (*3. ábra*, kék oszlopok).A két leghatásosabbnak bizonyuló módszerrel készített

kompozitok arányát módosítottuk 1:10:15-ről (MWCNT:TiO_2:WO_3)1:16:3-ra és 1:18:1-re. Ezeknek a katalizátoroknak már önmagukban is volt fotokatalitikusaktivitásuk, és ezek közül is kiemelkedett az 1:18:1 arányú PE-TiO_2-WO_3-700 kompozitanyag (*3. ábra,* piros oszlopok).

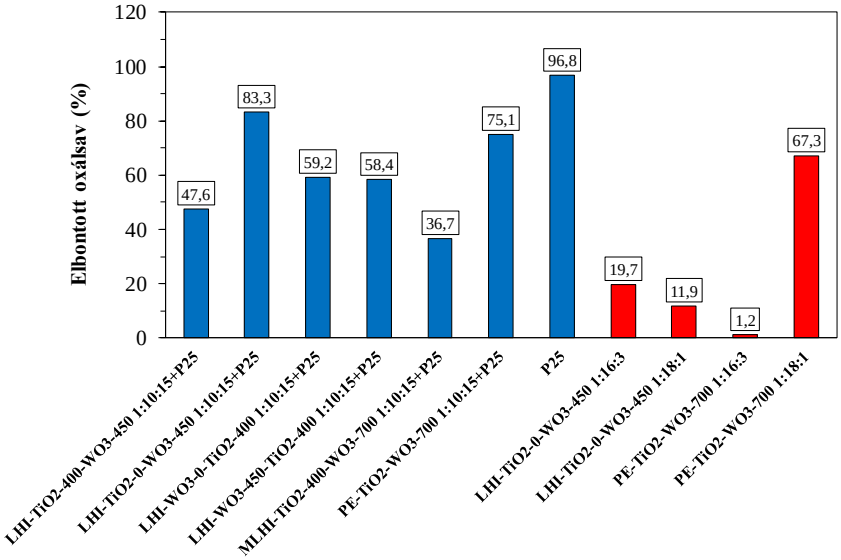

3.ábraA módszerek rangsorolásához használt (kék) és a módosított arányú katalizátorok (piros) fotokatalitikus hatékonysága

Összefoglalás

Sikeresen állítottunk elő többféle módszerrel WO_3-TiO_2/MWCNTkompozitot, amelynek morfológiája (bevonat vagy aggregátum, esetleg egyidejűleg mindkettő), szerkezete(anatáz, rutil, monoklin, parciális hidrát vagy $TiWO_x$) és fotokatalitikus aktivitása nagymértékben függött az alkalmazott szintézis oldószerétől, prekurzorainak szerkezetétől és kalcinálási hőmérsékletétől. Az XRD, Raman és DRS vizsgálatok egyértelműen alátámasztották, hogy TiO_2, WO_3 és többfalú szén nanocső is megtalálható az előállított mintákban. A fotokatalitikus tesztekből pedig megállapíthattuk, hogy a PE-TiO_2-WO_3-700 eljárással készült 1:18:1 arányú anyagbizonyultak a legaktívabbnak.

Köszönetnyilvánítás

Szeretnénk megköszönni az anyagi támogatást a Svájci hozzájárulásnak (SH/7/2/20), a Magyar-Indiai TÉT(TÉT_15_IN-1-2016-0013) és a GINOP pályázatnak (GINOP-2.3.2-15-2016-00013).

Irodalom

[1] B. Réti, Z. Major, D. Szarka, T. Boldizsár, E. Horváth, A. Magrez, L. Forró, A. Dombi, K. Hernádi, Journal of Molecular Catalysis A: Chemical 414 (2016) 140-147.

[2] L. Baia, E. Orbán, S. Fodor, B. Hampel, E.Z. Kedves, K. Saszet, I. Székely, É. Karácsonyi, B. Réti, P. Berki, A. Vulpoi, K. Magyari, A. Csavdári, C. Bolla, V. Coşoveanu, K. Hernádi, M. Baia, A. Dombi, V. Danciu, G. Kovács, Z. Pap, Materials Science in Semiconductor Processing 42 (2016) 66-71.

[3] D. Ke, H. Liu, T. Peng, X. Liu, K. Dai, Materials Letters 62 (2008) 447-450.

[4] L. Baia, A. Vulpoi, T. Radu, É. Karácsonyi, A. Dombi, K. Hernádi, V. Danciu, S. Simon, K. Norén, S.E. Canton, G. Kovács, Z. Pap, Applied Catalysis B: Environmental 148-149 (2014) 589-600.

SYNTHESIS AND CHARACTERIZATION OF Pt-CoO JANUS NANOSTRUCTURES

Dániel S. Berkesi[1,2], Roland Bálint[1], András Sápi[1], Ákos Kukovecz[1,2], Zoltán Kónya[1,3]

[1]University of Szeged, Department of Applied and Environmental Chemistry, Szeged, H-6720 Szeged, Dóm tér 7, Hungary
[2]MTA-SZTE "Lendület" Porous Nanocomposites Research Group, Szeged
[3]MTA-SZTE Reaction Kinetics and Surface Chemistry Research Group, Szeged
email: sapia@chem.u-szeged.hu

Abstract

Janus nanoparticles, nano-sized particles with two regions of different surface and different chemical composition, possess energetic interactions that depend not only on their separation but also on their orientation. Since it is known that the metal-metal oxide interfaces take important part in catalytical reactions[1], we are focusing our researches to this field.

Various Pt-CoO nanostructures were synthesized using Pt seeds made with polyol[2] method. Not only Janus nanoparticles but other nano-sized structures were synthesized. During the experiments an universal experimental system was built and used to produce monodisperse noble metal nanoparticles in different sizes. The results were investigated with X-ray Diffractometry and with Transmission Electron Microscopy. The future aims are to use these particles as a supported catalyst on solid-liquid and solid-gas phase interfaces, and determine the turnover rates and selectivity based on the experiments in different catalytic reactions.

References

[1] Yusuke Yamada, Chia-Kuang Tsung, Wenyu Huang, Ziyang Huo, Susan E. Habas, Tetsuro Soejima, Cesar E Aliaga, Gabor A. Somorjai ,Peidong Yang: Nanocrystal Bilayer for Tandem Catalysis, Nature Chemistry 3, 372–376 (2011)

[2] Hailiang Wang, Andras Sapi, Christopher M. Thompson, Fudong Liu, Danylo Zherebetskyy, James M. Krier, Lindsay M. Carl, Xiaojun Cai, Lin-Wang Wang, Gabor A. Somorjai: Dramatically Different Kinetics and Mechanism at Solid/Liquid and Solid/Gas Interfaces for Catalytic Isopropanol Oxidation over Size-Controlled Platinum Nanoparticles J. Am. Chem. Soc., 2014, 136 (29), Pp 10515–10520

STUDY OF 1.8 NM Pt NANOPARTICLES ANCHORED ON DIFFERENT AMORPHOUS SILICA SUPPORTS IN ETHANOL DECOMPOSITION REACTION

Dorina G. Dobó[1,5], András Sápi[1], Gyula Halasi[2], Dániel Sebők[3], Koppány L. Juhász[1], Ákos Kukovecz[1,5], Zoltán Kónya[1,2]

[1]*Department of Applied and Environmental Chemistry, University of Szeged, 1 Rerrich square, H-6720 Szeged, Hungary*
[2]*MTA-SZTE Reaction Kinetics and Surface Chemistry Research Group, University of Szeged, 1 Rerrich square, H-6720 Szeged, Hungary*
[3]*Department of Physical Chemistry and Material Science, University of Szeged, 7 Dóm square, H-6720 Szeged, Hungary*
[4]*Department of Inorganic and Analytical Chemistry, University of Szeged, 1 Rerrich square, H-6720 Szeged, Hungary*
[5]*MTA-SZTE "Lendület" Porous Nanocomposites Research Group, University of Szeged, 1 Rerrich square, H-6720 Szeged, Hungary*

Abstract
1.8 nm Pt nanoparticles with narrow size distribution were anchored on mostly identical, amorphous silica supports (SBA-15 [1], MCF-17 [2], Silica Foam [3]) and were tested in ethanol decomposition reactions at < 573 K. The reaction on the Pt/SF (0.117 molecules·site^{-1}·s^{-1}) was ~2 times faster compared to Pt/MCF-17 (0.055 molecules·site^{-1}·s^{-1}) and Pt/SBA-15 (0.063 molecules·site^{-1}·s^{-1}) at 573 K. In the case of Pt/SBA-15, selectivity towards acetaldehyde was ~4

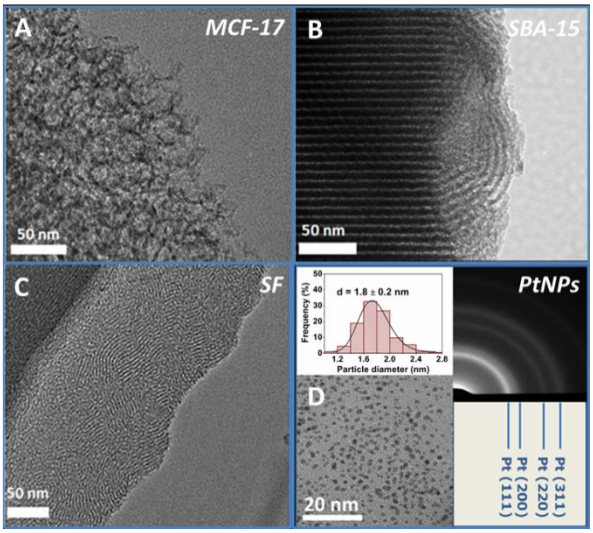

Fig. 1. Typical TEM images of MCF-17 (A), SBA-15 (B) and SF (C) silica supports as well as 1.8±0.2 nm metallic Pt nanoparticles with narrow size distribution (D).

times higher (68%) compared to the Pt/MCF-17 (18%) and Pt/SF (16%) catalysts. In the case of Pt/MCF-17 and Pt/SF, the methane to acetaldehyde ratio was 0.27 and 0.24, respectively, while it was ~ 10 times higher (1.97) for Pt/SBA-15 catalyst. The ethene selectivity was ~2 times higher

in the case of Pt/MCF-17 (0.99%) and Pt/SF (0.93%) compared to Pt/SBA-15 (0.41%). Pt/MCF-17 and Pt/SBA-15 produces ~ 50% more hydrogen (~27%) compared to Pt/SF catalyst (21 %). Small Angle X-ray Scattering (SAXS) and Transmission Electron Microscopy (TEM) studies showed striking differences in the porosity, pore- and mesostructure, sintering and Pt-SiO_2 interface altering effect of the silica supports as well as the Pt nanoparticles decorated catalysts which may have significant effect on the catalytic activity.

References

[1] D. Y. Zhao, Q. S. Huo, J. L. Feng, B. F. Chmelka, G. D. Stucky*J. Am. Chem. Soc.* 120 (1998) 6024.
[2] P. Schmidt-Winkel, W. W. Lukens, P. D. Yang, D. I. Margolese, J. S. Lettow, J. Y. Ying, G. D. Stucky*Chem. Mater.* 12 (2000) 686.
[3] S. A. Bagshaw, *Chem. Comm.* (1999) 767-768.

EXTRACTION OF ANTIOXIDANT AND POLYPHENOL COMPOUNDS FROM TOKAJI ASZÚ MARC

Eszter Dusza[1]*, Szilvia Bánvölgyi[1], István Kiss[2], Éva Stefanovits-Bányai[3], Gyula Vatai[1]

[1]Department of Food Engineering,Szent István University, H-1118 Budapest, Ménesi str 44., Hungary
[2]Fitomark 94 Kft., H-3934 Tolcsva, Arany János utca 16/a
[3]Department of Applied Chemistry,Szent István University, H-1118 Budapest, Villányi str 29-43., Hungary
e-mail:du.eszter@gmail.com

Abstract
Grapes and even wine-making wastes such as marc and stalks, are rich in phenols. The polyphenolic content has many favourable effects on human health,such as the anti-carcinogenic effects and the inhibition of the oxidization of low-density lipoproteins. An antioxidant is a molecule that hinder the oxidation of unlike molecules. Ouraim was to find the optimal conditions of the extraction of the antioxidant and phenolic compounds from Tokaji aszú marc. Absolute ethanol and deionized water were used to prepare the solvent, 4:1 solvent-to-sample ratio was choosen. The solvent contains different volumes of ethanol (0 – 25 – 50 – 75 – 100%). The temperature was 30 °C and 60 °C.The time of the extraction was half-, one-, two-, three-, four- and five-hours long. The extractions were more efficiency using ethanol solvent compared with the water solvent. In all casesthe phenol concentration and antioxidant capacity were two and three times higher at higher temperature (60 °C) than at lower temperature (30 °C).The maximum value of total phenol content (67830±509 μM GS/L) was reached at 60 °C temperature, 25% ethanol solvent after 3 hours.The maximum value of antioxidant capacity (11126±145 μM AS/L) was reached at 60 °C temperature, 50% ethanol solvent after 5 hours.

Introduction
Grapes are one of the world's largest fruit crops, and even wine-making wastes such as marc (theremainsofgrapesorotherfruitthathavebeenpressedforwine-making) and stalks, are rich in phenols. Grapes, wine, grape seeds and skins extracts have many favourable effects on human health due to their polyphenol content,such as the anti-carcinogenic effects and the inhibition of the oxidization of low-density lipoproteins, thereby decreasing the risk ofcardiovascular diseases.Therefore, phenolic compounds can be considered to be added-value by products,corroborating their isolation from the industrial waste [1, 2].
Furthermore, the activity of these compounds as food lipid antioxidants is well known. By adding antioxidants is a method which is increase the shelf life, especially of fats, oil and fat containing food products. Since synthetic antioxidants, such as BHA and BHT have restricted use in foods because their toxicological effects on different species and suspected carcinogenic potential, the search of natural and safe antioxidants, especially of plant origin, has increased latterly [1].
The goalof an extraction process is to provide the maximum yield of substances and of the highest quality (concentration of phenolic compoundsand antioxidant power of the extracts).

Experimental
The marc of Tokaji aszú was provided by theFitomark Ltd. (Tolcsva). The marc wasstored in freezer till the experiments.

Extraction measurements

Our aim was to find the optimal conditions of the extraction from Tokaji aszú marc. Absolute ethanol and deionized water were used to prepare the solvent,4:1 solvent-to-sample ratio was choosen. Continuous stirring was ensured during all experiments. The picture and flow sheet of the equipment can be seen at Figure 1.

In the experiments three parameters of the extraction were changed: the temperature, the solvent concentration and the time of the extraction. The temperature was 30 °C and 60 °C. To keep the temperature at constant value a Lauda Ecoline E100 Immersion Thermostat was used. The solvent contains different volumes of ethanol (0 – 25 – 50 – 75 – 100%). The time of the extraction was half-, one-, two-, three-, four- and five-hours long.

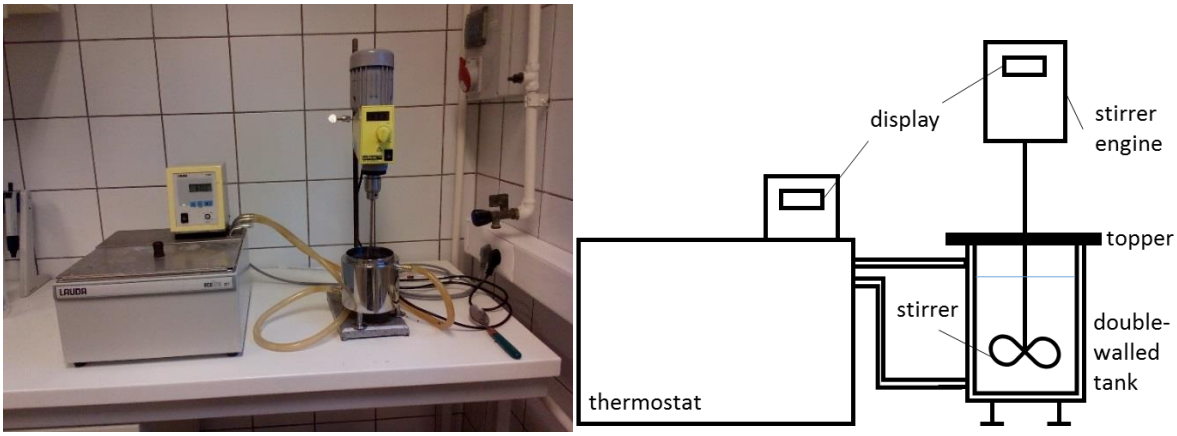

Figure 1. (a) picture of the experimental equipment and (b) flow sheetof the experimental equipment

Analitical measurements

The TPC, FRAP assays were run with a Nicolet Evolution 300 BB type spectrophotometer (Thermo Electron Corporation, Cambridge, UK) at the respective wavelengths. Measurements were run triplicate.

Analysis of total phenol content (TPC)

Total phenol content was determined by the Folin-Ciocalteu assay [3] applying gallic acid as the standard at 760 nm. Total phenol content was expressed in µmol equivalents of gallic acid (GS)/L.

Antioxidant capacity measurements (FRAP)

The FRAP antioxidant capacity assay was run as described by Benzie and Strain [4] using ascorbic acid as standard. The absorbance was measured at 593 nm and results were determined in µmol equivalents of ascorbic acid (AS)/L.

Results and discussion

Figure 2. shows the phenol concentration (a) and antioxidant capacity (b) of the extracts in case of water solvent at different temperatures versus extraction time. At higher temperature (60 °C) the phenol concentration and antioxidant capacity were two and three times higher than at lower

temperature (30 °C). The extraction time generally increased the total phenol content and the antioxidant capacity. In case of water solvent the maximum values of polyphenol concentration was 3000±17 µM GS/L (after 5 hours), and the maximum of antioxidant capacity was 1575±33 µM AS/L (after 5 hours).

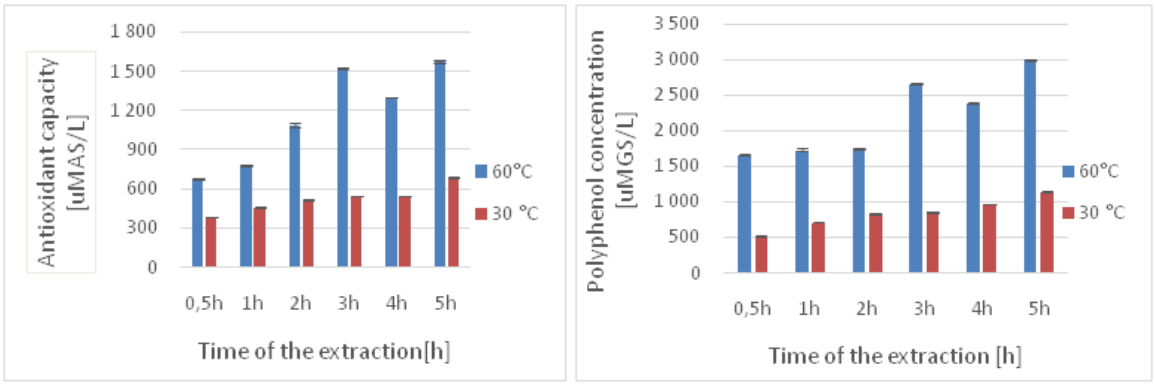

a) b)

Figure 2. (a) Polyphenol concentration incase of water solvent and b) Antioxidant capacity incase of water solvent

In our experiments the phenol content and the antioxidant capacity of the extracts were much higher at 60 °C temperature than at 30 °C temperature, therefore we only represent the results at 60 °C temperature comparing the various solvent concentrations.

The total phenol content of the extracts can be seen in Figure 3. in case of 25% – 50% (a) and 75% – 100% (b) ethanol solvent versus extraction time. The different volumes of ethanol in the solvent reached a more varied result than the water solvent. In case of 25% ethanol solvent the total phenol content was increased in the first 3 hours and after that it was decreased. In case of 50%, 75% and 100% ethanol solvent a continuously raise was observed in total phenol content during the five hours. The maximum value of total phenol content (67830±509 µM GS/L) was reached at 60 °C temperature, 25% ethanol solvent after 3 hours.

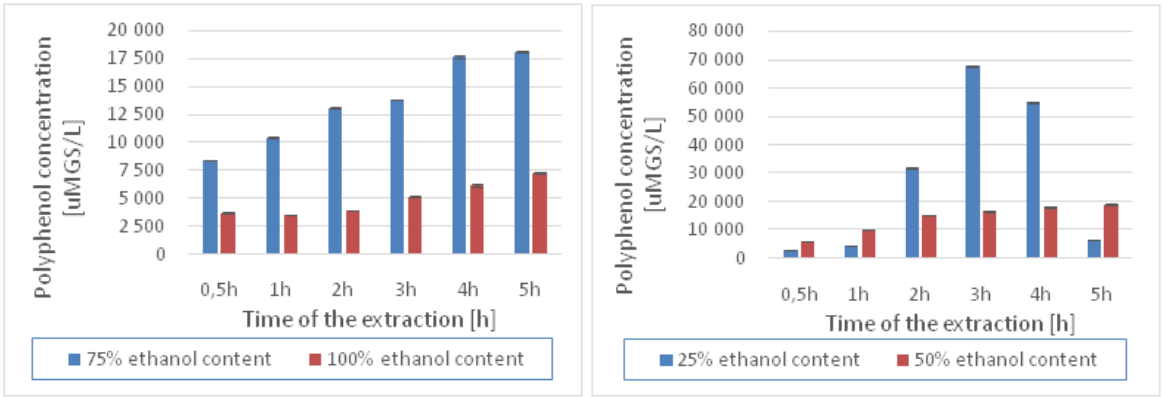

a) b)

Figure 3. (a) Polyphenol concentration incase of 25% and 50% ethanol solvent (b) Polyphenol concentration incase of 75% and 100% ethanol solventat 60 °C temperature

The antioxidant capacity of the extracts can be seen in Figure 3. in case of 25% – 50% (a) and 75% – 100% (b) ethanol solvent versus extraction time.The same trend was observed in antioxidant capacity with 75% ethanol solvent than the total phenol content with 25% ethanol: the antioxidant capacity of the extracts was increased in the first 3 hours and after that it was decreased. In other cases the antioxidant capacity was increased with the extraction time. The maximum value of antioxidant capacity (11126±145µM AS/L) was reached at 60 °C temperature, 50% ethanol solvent after 5 hours.

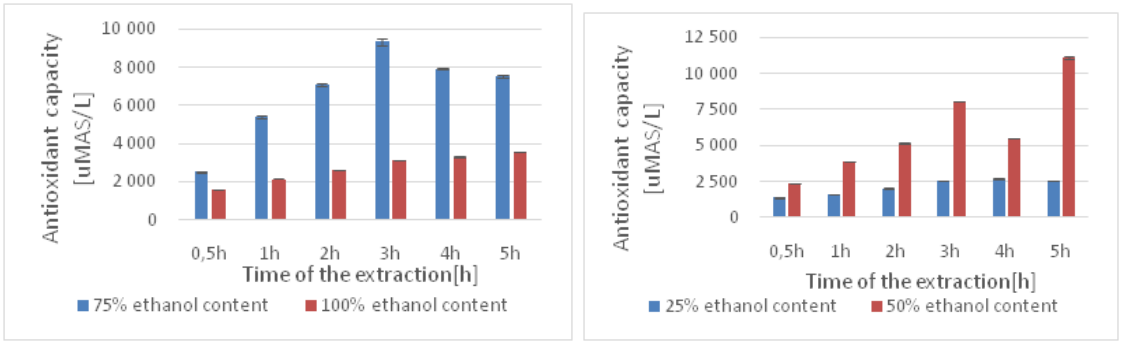

a) b)

Figure 4. (a) Antioxidant capacity incase of 25% and 50% ethanol solvent (b) Antioxidant capacity incase of 75% and 100% ethanol solventat 60 °C temperature

Conclusion

The extraction experiments were achieved successfully. In all cases the concentration of total phenol content and antioxidant capacity was higher at higher temperature. The extractions were more efficiency using ethanol solvent compared with the water solvent. Determine the optimal parameters of the extraction (temperature, solvent concentration and extraction time) is not easy because of the different optimum of the total phenol content and antioxidant capacity.Comparing the proportions we can summarize that the total phenol content is about quarters of it's maximum value at the optimal parameters of antioxidant capacity (T = 60 °C, c_s= 50%, t = 5 hrs).The antioxidant capacity is about quarters of it's maximum value at the optimal parameters of total phenol content (T = 60 °C, c_s= 25%, t = 3 hrs). Our suggestion to choose the optimal operating parameters according to the more important component.

References

[1] G. Spigno, D. M. De Faveri, J. Food Eng.78(3) (2007) 793-801.
[2] F. Bonilla, M. Mayen, J. Merida, M. Medina, Food Chemistry 66(2) (1999) 209-215.
[3] V.L. Singleton, J.A. Rossi, Am. J. Enol. Vitic. 16 (1965) 144-158.
[4] F.F. Benzie, J.J. Strain, Anal. Biochem 239 (1996) 70-76.

ADSORPTION OF ASYMMETRIC POLAR COMPOUNDS ON OIL SHALE AND ITS SPECIAL FORM

Miklós Molnár[1], Ottó Horváth[2], Rita Földényi[1*]

[1]*Institute of Environmental Sciences, University of Pannonia, Veszprém, Hungary*
[2]*Institute of Chemistry, University of Pannonia, Veszprém, Hungary*
e-mail: foldenyi@almos.uni-pannon.hu

Abstract

Adsorption of two different asymmetric polar organic compounds - TEBA (benzyltriethylammonium chloride) and Supragil WP (sodium diisopropyl naphthyl sulfonate)- on oil shale andits composite was investigated. These anthropogenic pollutants are similar to surfactants therefore they are frequently used in different products and could be transformed into environmental contaminants. In order to find more efficientandmanageable form of oil shale, we compared the adsorption of oil shale powder to oil shale ina composite form (oil shale-alginate). According to the comparison, the amount of TEBA adsorbedon oil shale in composite form was lessthan on powder, while that of Supragil WP was higher. These results could be explained by the differentliquid-solid ratioand by the different diffusion rate through the alginate.

Introduction

In Hungary, the oil shale is a unique rock, which is present in a large amount. Oil shale originatesfrom the biomass of algae accumulated in the volcanic craters over 4 to 5 million years.This oil shale is widely used as a soil-ameliorating agent because of its special microelement and organic contents and low price. The organic material content is between 5 to 50 % and consists of mainly kerogen [1]. Recently, usage of oil shale to eliminate chemical pollutants is an emerging topic [1-3]. This oil shale is easily crumbling, which hindersits easy and routine applicability.

Alginate is an anionic polysaccharide copolymer, it derives from cell wall of brown algae, consists of β-D-mannuronate and α-L-guluronate. In the literature, alginate is a new material as a forming, immobilizing agent [4-5]. Alginate has also been used as an environmental pollutant removal agent [6]. The disadvantage of application of alginate is its relatively high price. The combination with a lower-cost adsorbent can result in a new material, which might be useful to eliminate hazardous chemicals.

Supragil WP (Figure 1, left) is an anionic chemical, which is widely used as a dispersant, especially in pesticides.TEBA is a popular cationic phase transfer catalyst at organic chemical syntheses (Figure 1,right).The structure of both chemicals is similar to surfactants, therefore they can be considered as asymmetric polar compounds[7].

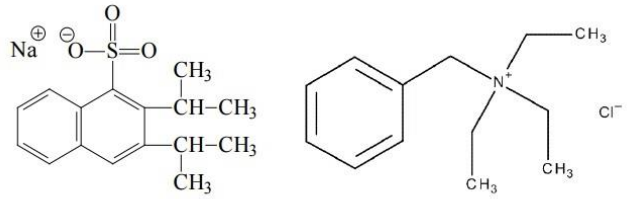

Figure 1. Chemical structures of Supragil WP (left) and TEBA (right)

Due to these facts, these two asymmetric polar compounds (Supragil WP and TEBA) might be potential environmental pollutants when they get into the soil or natural waters.
The aim of this present work is to form the oil shale in a practical form, whose adsorption is similarly efficient as the oil shale powder.In order to achieve our aim,we performedadsorption experiments on oil shale powder and oil shale composite, and compared their adsorption capacities.

Experimental

Oil shale sample originated from Pula (Hungary) and was milled: ∅<0.8 mm.
Sodium alginate was purchased from Sigma-Aldrich Co., Supragil WP was obtained from Rhodia Geronazzo Spa., TEBA originated from Merck KGaA. and calcium chloride was purchased from Lach-Ner, s.r.o. All chemicals were used without further purification.
UV-VIS measurements were performed on a Varian Cary 50 UV-VIS spectrophotometer,pH was determined with a Radelkis combination pH electrode.
The nonlinear least square fitting procedure of the Origin scientific graphing and analysis software was utilized, using Levenberg-Marquardt algorithm.

Preparation of alginate beads

Alginate beads were prepared according to the literature [4]. A solution of 2.5 % (w/v)concentration was prepared by dissolution of sodium alginate in deionized water. The obtained mixture was dropped into 0.2 mol/L $CaCl_2$ solution and alginate beads were formed (∅: ~ 5 – 6 mm). After standing in the gelation media overnight, the beads were filtered out and washed with deionized water.

Preparation of oil shale composite beads

According to the above described procedure, sodium alginate mixture was prepared. This solution was mixed with the swollen oil shale,using 8 : 1 mass ratio of oil shale and sodium alginate. This suspension was added dropwise into 0.2 mol/L $CaCl_2$ solution and oil shale composite beads were formed (∅: ~ 5 – 8 mm). The post-treatment is identical with that applied in the case of alginate beads.

Adsorption on oil shale powder

The adsorption experiments were performed in 250 mL stoppered Erlenmeyer flasks. 5 g of oil shale powder was weighed into the flask and was left to swell in 5 mL water overnight at 25 °C. Different concentrations of Supragil WP (from 50 to 500 μmol/L) or TEBA (from 2 to 20 mmol/L) solutions were prepared with 0.01 mol/L $CaCl_2$(pH=7.4).50-50 mL of these solutions were transferred to the swollen oil shale samples. The suspension was then shaken and left to stand for 24 hours for equilibration at 25 °C. Then approximately 2 mL of the supernatant was transferred into an Eppendorf tube and was centrifuged at rpm = 15000 for 20 minutes for perfect separation of the supernatant and oil shale powder. After the centrifugation, the supernatant was measured by UV-VIS spectrophotometer and the concentration was determined.

Adsorption on alginate beads and oil shale composite beads

The procedure to measure the adsorption on alginate and oil shale composite was almost the same

as in the case of the adsorption on oil shale powder. In this case,instead of oil shale powder,the alginate beads or oil shale composite beads were weighed. Everyoil shale composite bead contained 5 g of oil shale powder. The alginate content of the weighed oil shale composite beads was equal to the weighed alginate beads at these adsorption experiments.

All samples were in triplicate. The UV-VIS absorbance of the blank sample (c_0= 0 mol/L) was subtracted.

Results and discussion

The adsorption isotherms for Supragil WP and TEBA on oil shale powder and oil shale composite were analyzed in terms of Freundlich isotherm equation well:

$$q_e = K_F \cdot c_e^n$$

where q_e is the adsorption capacity at equilibrium, mol of solute adsorbed per gram of adsorbent (mol/g);c_e is the equilibrium solution concentration (mol/L);K_F(L^n/($mol^{(n-1)}$·g)) and$n$ are constants that characterize the adsorption capacity of adsorbent of solute.

The equations were fitted to the obtained data, the calculated parameters and the statistical indicators of the overall goodness of fitting (R^2) were between 0.98144 and 1.

The adsorbed amount of the solute was calculated according to the following equation:

$$q = \frac{V \cdot (c_0 - c)}{m}$$

where q is adsorption capacity at equilibrium (mol/g); V is the volume of the equilibriumsolution (0.05 L); c_0 and c are the initial and the equilibrium concentrations of the solute (mol/L); m is the weighed amount of the dry adsorbent (g).

The obtained adsorption isotherms are shown in Figure 2.

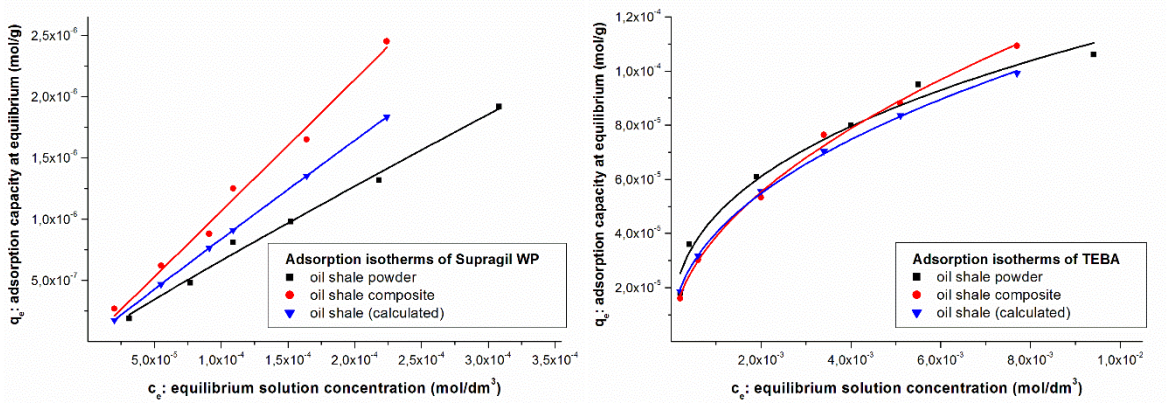

Figure 2. Adsorption isotherms of Supragil WP (left) and TEBA (right)

As can be seen on Figure 2,the adsorbedamount of Supragil WP on oil shale in composite (left, blue line) is higher than that on oil shale powder (left, black line). It can be explained by the difference of liquid-solidratio compared the powder to the composite. Thus, the repulsion between the anionic Supragil WP and the anionic surface-charged oil shale powder is more significant.

In the case of TEBA, the adsorbedamounton oil shale in composite (right, blue line) is lower thanon the powder (right, black line). It can be caused bythe hindered diffusion of cationic TEBA through the negatively charged alginate tothe oil shale.

Conclusion

The adsorption of two widely used asymmetric polar compounds was investigated on Hungarian oil shale powder and its newly synthesized composite form. The extent of adsorptionof anionic Supragil WP as adsorbate on oil shale in the new composite, wasgreater. This result is attributed to the different liquid-solid ratio. Thesame experimentcarried out with cationic TEBA as adsorbate resulted in less adsorbed amount on oil shale than on its composite form. This can be explained by the hindered diffusion of the compound through the alginate adhesive. The results of the present work suggest that the alginate could be a promising material to form a manageable composite for eliminating chemical pollutants efficiently.

References

[1] R. Rauch, R. Földényi, Journal ofEnvironmental Science and Health, Part B 47 (2012) 670.
[2] E. T. Acar, S. Ortaboy, G. Atun, Chemical Engineering Journal 276 (2015) 340.
[3] N. Ayar, B. Bilgin, G. Atun, Chemical Engineering Journal 138 (2008) 239.
[4] J. Li, Z. Jiang, H. Wu, L. Long, Y. Jiang, L. Zhang, Composites Science and Technology 69 (2009) 539.
[5] S.-W. Xu, Y. Lu, J. Li, Y.-F. Zhang, Z.-Y. Jiang, J, Journal of Biomaterial Science, Polymer Edition 18 (2007) 71.
[6] S. Peretz, O. Cinteza, Colloids and Surfaces A: Physicochem. Eng. Aspects 319 (2008) 165.
[7] F. Szántó (Ed.), A kolloidkémia alapjai, Gondolat Könyvkiadó, Budapest, 1987.

THE EFFECT OF DIFFERENT DRYING AND EXTRACTION CONDITIONS ON THE ANTIOXIDANT CONTENT OF ELDERBERRY POMACE

Diána Furulyás[1*], Lilla Anna Jankó[1], Mónika Stégerné-Máté[1], Éva Stefanovits-Bányai[2]

[1]Department of Food Preservation,Szent István University, H-1118Budapest, Villányi street 29-43., Hungary
[2]Department of Applied Chemistry, Szent István University, H-1118 Budapest, Villányi street 29-43., Hungary
e-mail: Furulyas.Diana@phd.uni-szie.hu

Abstract
Nowadays waste is a critical subject in every industry, in every household; but in many cases by-products should not be considered as waste. The aim of this study is to explore the best combination of drying and extraction, to achieve the highest antioxidant content in elderberry pomace, which appears as a by-product when making use of the berry. The chosen cultivar, Haschberg is from a pen in Hungary, these elderberries contain high biological activity components, primarily polyphenols, anthocyanins, flavonols which compounds are known to have potential antioxidant properties. In this study, the antioxidant capacity was determined by FRAP (Ferric Reducing Ability of Plasma), Total Polyphenol Content (TPC) and Total Anthocyanin Content (TAC) assays. The optimal drying conditions were previously tested, relying on the results atmospheric drying was executed at 60 and 80 °C. When extracting the antioxidant compounds, ethanol and acetone were used as solvents, applied in different proportions: 1:10, 1:20, 1:30. Based on our result, the highest antioxidant capacity was registered using 20 V/V % acetone in 1:30 ratio, extracted from the pomace, dried at 60°C. Further examination could reveal whether the extracted antioxidant content of the elderberries could be used as bio-preservatives in the food industry.

Introduction
Black elderberry (*Sambucus nigra* L.) is from Adoxaceae family, its shrubs are multi stemmed, they have weak, grey coloured branches on which fruit clusters develop with 5-9 mm (d) glossy, dark purple berries [1, 2]. Anthocyanins (specifically cyanidin-3-sambubioside) are responsible for the colour of the berries, as they are the most widespread water-soluble plant pigments [3]. The berries are a good source of protein, amino acids, vitamins and minerals, and contains compounds that show antioxidant effects. Anthocyanins, flavonols, and phenolic acids are bioactive compounds present in the elderberry, which can safely interact with free radicals and even terminate molecule damaging chain reactions [4, 5]. Almost every part of the plant is used somehow, that is why elderberry is known as one of the oldest medical plants [6]. Elderberry's medical properties are associated with polyphenols, antioxidants that play an essential role in preventing several diseases (cardio-vascular, neurodegenerative, etc.) [7]. In the 21st century, industries try to benefit from this plant in many ways. For instance, berries can be utilized as colouring food, jam, or, because of its favorable composition, as dietary supplements [8]. Pomace, which is left when elderberry is processed, could be beneficial to use as animal feed, or to make alcoholic beverages from it. However, when it is well known, that 75-98% of total anthocyanin content can be found in this byproduct, the question arises: shouldn't we take advantage of what we already have, rather than causing more environmental issues? [9]

Our goal, when conducting this experiment, was to find the right extraction method for extracting the antioxidant compounds from black elderberry pomace, which allows further usage in the food industry.

Experimental

The raw material of the study was collected from Nagyenyed, where Haschberg cultivar is grown by a co-operative society called BOTÉSZ. Chemicals used for extraction and antioxidant measurements were provided by Sigma-Aldrich Chemie Ltd.

Elderberries were destemmed, mashed, and then heated to 80°C, to inactivate enzymes. When it was cooled to 35 °C, pectolytic enzyme, Fructozym P was given as a treatment. After an hour, the material was pressed, resulting in juice and pomace. Drying was the next step, using atmospheric dryer at 60°C and 80°C, then the pomace was grinded. It was time, for the extraction, which was performed at room temperature, using two different solvents, acetone and ethanol at different concentrations 20 V/V % and 40 V/V%. We differed one more parameter, the ratio between pomace and extraction solvent, using 1:10, 1:20 and 1:30 proportions. After half-an-hour of extraction, supersonic bath was used for another 30 minutes, to intensify the process. Centrifugation made the phases separate, extracts were further analysed using three methods:

- Antioxidant capacity was determined based on Ferric Reducing Ability of Plasma (FRAP) method, by Benzie and Strain [10]. Antioxidant capacity was defined in ascorbic acid equivalent (mg ascorbic acid equivalent/ 100 g DW).
- Total Polyphenol Content (TPC) was evaluated using a method by Singleton and Rossi [11]. Results were specified in mg gallic acid equivalent/ 100 g DW
- Total Anthocyanin Content (TAC) measurement was based on Lee's pH differential method [12], result are given in mg/ 100 g DW.

Results were calculated, statistical evaluations were performed using Microsoft Excel. Difference between drying at 60°C and 80°C was evaluated by Student t-test at 95% confidence. One-way ANOVA was used for testing the effect of extraction solvents. Data were also evaluated using Pearson's correlation coefficients to identify relationships between phenolic contents, anthocyanin contents and antioxidant activities of elderberry pomace extract.

Results and discussion

Samples, dried at different temperatures, and extracted with two solvents, were measured to define total anthocyanin and polyphenol content, as well as their antioxidant capacity, in order to find the most effective method of extraction to achieve an extract rich in biological activity components.

Figures 1-3. show the average results of the measurements. Elderberry pomace dried at 60 °C showed significantly higher ($p>0.05$) outcome, consequently, lower drying temperature affected the antioxidant compounds in a positive way. Regarding the solvents applied, 20 V/V% concentrated acetone extracted the analyzed components with the best results. More concentrated solvents effected the process negatively, in all cases. Figure 1. draws the attention to the measured FRAP values, which varied between 824.57 and 3529.98 mg ascorbic acid equivalent/ 100 g DW. The highest antioxidant capacity was registered using 20 V/V % acetone in 1:30 ratio with pomace made at 60°C.

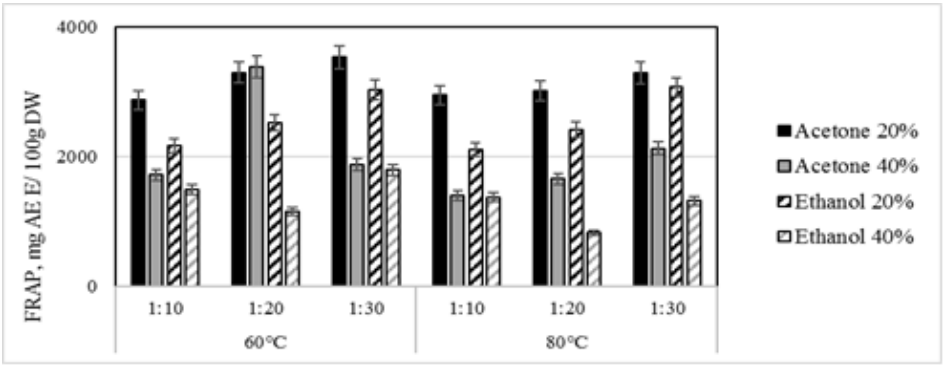

Figure 1. Average values of antioxidant capacities, evaluated using the method relying on Ferric Reducing Ability of Plasma, mg ascorbic acid equivalent/ 100g DW

In Figure 2., total antioxidant content concentrations in mg/ 100 g DW are shown. The highest value (2128.99 mg/ 100 g DW) was reached by the sample which was dried at 60°C, extracted with 20 V/V % acetone, and dosed in 1:30 ratio. This result corresponds with the conclusion of the FRAP method. The sample dried at the same temperature, but treated with 40 V/V% ethanol in 1:20 ratio led to the lowest TAC detected (548.68 mg/ 100 g DW).

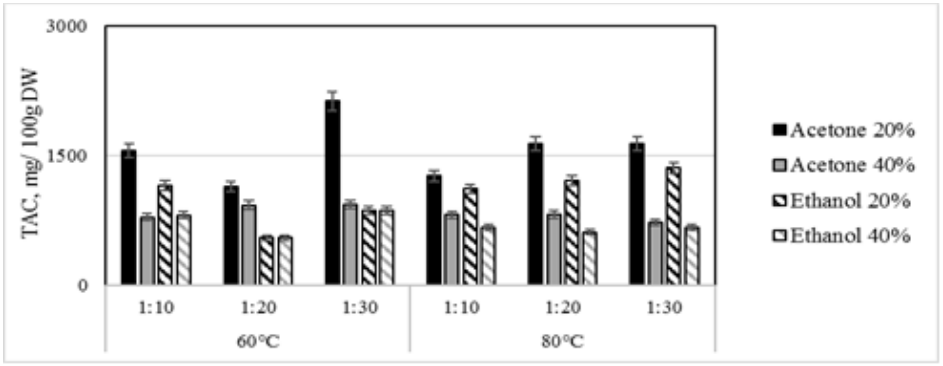

Figure 2. Average values of Total Anthocyanin Content, mg/ 100 g DW

Avarage results, regarding the total polyphenol content of the pomace samples, are presented in Figure 3. All measured polyphenol contents were between 1304.98 and 4318.40 mg gallic acid equivalent/ 100 g DW. Unlike the previous methods, TPC experiment showed the highest value using 20 V/V% ethanol, whereas the second highest was achieved via 20 V/V% acetone (3961.39 mg GAE / 100 g DW, $p>0.05$).

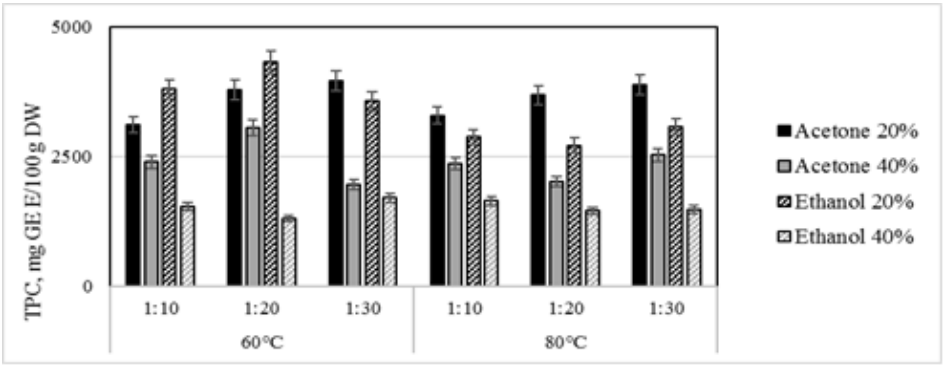

Figure 3. Total polyphenol content (TPC) average results, mg gallic acid equivalent/100g DW

It is well known, that antioxidant potential in plants often correlates with phenolic or anthocyanin compounds [13]. In order to find out which components correlate with antioxidant capacity, Pearson Product Moment Correlation was conducted. We present Person correlation coefficients in Table 1. The highest positive correlation was registered between polyphenol content and antioxidant capacity (R=0.855), there is a weaker correlation (R=0.74) between anthocyanin content and antioxidant capacity.

	FRAP	*TPC*	*TAC*
FRAP	1		
TPC	0.86	1	
TAC	0.74	0.62	1

Table 1. Pearson's correlations among total phenolic content (TPC), total antocianin content (TAC) and antioxidant capacity (FRAP) of elderberry pomace

Conclusion

In the past few years, treating waste coming from the food industry, has become a remarkably important issue, due to environmental and economic reasons. Recycling waste should mean a satisfactory alternative, particularly, if we consider the amount of valuable components remaining in the waste of certain plants. On one hand, these could be retrieved using the proper method, and used again by the food industry. On the other hand, the adequate method widely depends on the treatments applied during the preparation of the samples.

The aim of this study was to extract bioactive compounds from black elderberry pomace, using the optimal extraction-method. According to our results, the most efficient technique is drying at 60°C, using 20% concentrated acetone solvent in 1:30 proportion, for an hour. This combination resulted in outstanding yield, regarding the antioxidant capacity, and the content of both anthocyanins and polyphenols.

AcknowledgementsThe authors would like to acknowledge to support of the BOTÉSZ.

References

[1] D. Topolska, K. Valachova, P. Rapta S. Silhár, E. Panghyová, A. Horváth, L. Soltés, Chemical Papers 69 (2015) 1202-1210.
[2] E. Mudge, W.L.Applequist, J. Finley, P. Lister, A.K. Townesmith, K.M. Walker, P.N. Brown, Journal of Food Composition and Analysis 47 (2016) 52-59.
[3] I. Ochmian, J. Oszmianski, K. Skupien, Journal of Applied Botany and Food Quality 83 (2009) 64-69.
[4] A. Sidor, A. Gramza-Michalowska, Journal of Functional Foods (2014) 941-958.
[5] M. Oroian, I. Escriche, Food Research International, 74 (2015) 10-36.
[6] A. Simonyi, Z. Chen, J. Jiang, Y. Zong, D.Y. Chuang, Z. Gu, C. Lu, K.L. Fritsche, C.M. Greenlief, G. E. Rottinghaus, A. L. Thomas, D. B. Lubahn, G. Y. Sun, Life Sciences 128 (2015) 30-38.
[7] H.G. Duymus, F. Göger, K. H. C. Baser, Food Chemistry 155 (2014) 112-119
[8]M. M. Stégerné, in B. Sipos, A fekete bodza termesztése, Mezőgazda Kiadó, Budapest, 2010, pp. 82-86.
[9] K. Brønnum-Hansen, F. Jacobsen, J. Flink, International Journal of Food Science & Technology 20, (1985) 703–711.
[10] F. Benzie, J. Strain, Analytical Biochemisrty 239, (1996) 70–76.
[11] V.L. Singleton, J.A. Rossi,American Journal of Enology and Viticulture 16, (1965) 144–158.
[12] J. Lee, R. Durst, R. Wrolstad, Journal of AOAC International, 88, (2005) 1269-1278.
[13] S. Dudonné, X. Vitrac, P.Coutiere, M. Woillez, J.M. Mérillon, Journal of Agricultural and Food Chemistry, 57 (2009), 1768-1774.

HIDROGÉN-PEROXID ALKALMAZÁSA LÁTHATÓ FÉNNYEL GERJESZTHETŐ ANATÁZ FÁZISÚ TITÁN-DIOXIDOK ELŐÁLLÍTÁSÁRA

Tamás Gyulavári[1,2], Gábor Veréb[2,3], Zsolt Pap[2,4,5], András Dombi[2], Klára Hernádi[1,2]

[1]Szegedi Tudományegyetem, Természettudományi és Informatikai Kar, Alkalmazott és Környezeti Kémiai Tanszék, Magyarország, HU-6720 Szeged, Rerrich Béla tér 1.
[2]Szegedi Tudományegyetem, Természettudományi és Informatikai Kar, Környezettudományi és Műszaki Intézet, Környezetkémiai Kutatócsoport, Magyaroroszág, HU-6720 Szeged, Tisza Lajos krt. 103.
[3]Szegedi Tudományegyetem, Mérnöki Kar, Folyamatmérnöki Intézet, Magyarország, HU-6725 Szeged, Moszkvai krt. 9.
[4]Babeş-Bolyai Tudományegyetem, Interdiszciplináris Bio-Nano Tudományok Intézete, Románia, RO-400271 Kolozsvár, Treboniu Laurian 42.
[5]Babeş-Bolyai Tudományegyetem, Fizika Kar, Románia, RO-400084 Kolozsvár, M. Kogalniceanu 1.
e-mail: gyulavarit@chem.u-szeged.hu

Abstract

In the present study anatase phase titanium dioxide was fabricatedusing hydrogen peroxide during the synthesis method, to facilitate the visible light excitability of the titania. The photocatalysts were characterized by XRD, DRS, and IR measurements, and the photocatalytic activity was determined by the degradation of phenol under visible light irradiation.
Self-made anatase TiO_2 (denoted as 'TiO_2_pH3_70°C') possessed superior photocatalytic efficiency compared to commercial Aeroxide P25 and Aldrich Anatase. The DRS spectra indicated that the light absorption was shifted into the visible region in case of our self-made TiO_2which corresponds well with the resulted high photocatalytic efficiency.

Bevezetés

Napjaink ígéretes alternatív vízkezelési módszerei a nagyhatékonyságú oxidációs eljárások, melynek egyik típusa a heterogén fotokatalízis. Lényege, hogy félvezető fotokatalizátorok fénnyel történő gerjesztése következtében egy elektron a vegyértéksávból a vezetési sávba lép át miközben a vegyértéksávban egy pozitív töltésű lyukat hagy maga után. A gerjesztettfotokatalizátor felületén, összetett gyökös folyamatok révén a szervesszennyező anyagok lebonthatók. Fotokatalizátorként az esetek döntő többségében titán-dioxidot alkalmaznak számos előnyös tulajdonsága miatt.
Korábbi publikációnkban [1] egy rutil fázisú titán-dioxid kiemelkedő fotokatalitikus aktivitása a felületén lévő Ti-O-O-Ti (peroxo) csoportok jelenlétének,vagyis a „peroxidált" felületnek volt tulajdonítható.Vizsgálataink alapján a peroxidált felület a fényelnyelés vöröseltolódását is eredményezi. Mivel általánosan elfogadott tény, hogy az anatáz fázis nagyobb fotokatalitikus aktivitással rendelkezik mint a rutil fázis [2, 3], ugyanakkor nem gerjeszthető látható fénnyel, így jelen munkában akorábbi, hidrogén-peroxidot isalkalmazó szintézismódszerünkmódosításával (magasabb pH érték beállításával) kívánunkelőállítani látható fénnyel is hatékonyan gerjeszthetőanatáz fázisú titán-dioxidot.

Alkalmazott anyagok és módszerek

A fotokatalizátor előállításáhozvizet, sósavat, hidrogén-peroxidot és titán-tetrabutoxidot mértünk össze a következő anyagmennyiség-arányban: $Ti(OC_4H_9)_4$:H_2O_2:HCl:H_2O = 1:2:3:50.Tang és munkatársainak publikációja alapján [4] a kevésbé savas körülmény már anatáz fázis kialakításának kedvez. Ennek megfelelően a pH-t NaOH oldattal 3-as értékre emeltük, majd24 óra 40 °C-on és 24 óra 70 °C-on történő kristályosítás után az előállított fotokatalizátort(TiO_2_pH3_70°C) Milli-Q vizes centrifugálásos mosással tisztítottuk, ezt követően szárítottuk, majd a keletkező sárga TiO_2-ot achát mozsárban porítottuk.

Referencia fotokatalizátorként az Evonik Industries által gyártott Aeroxide P25 titán-dioxidot és Aldrich anatáz TiO_2-ot is vizsgáltunk.

A részecskeméretet és kristályos összetételt egy Rigaku Miniflex II típusú röntgendiffraktométerrel határoztuk meg. A diffúz reflexiós spektrumokat egy ILV-724 jelűdiffúz reflexiós modullal ellátott Jasco-V650 diódasoros spektrofotométerrel, míg az infravörös spektrumokat egy „FRA 106 Raman" modullal kiegészített „Bruker Equinox 55"típusú spektrométerrel rögzítettük.

A fotokatalitikus aktivitást fenol ($c=10^{-4}M$) bontásávaljellemeztük. A látható fényt sugárzó lámpákkal felszerelt fotoreaktorból vett minták fenol koncentrációját egy Agilent 1100 series típusú HPLC berendezéssel határoztuk meg.

Eredmények és kiértékelésük

A röntgen diffraktométerrel végzett vizsgálatok eredményei az **1. ábrán** láthatóak. Megállapítottuk, hogy azelőállított titán-dioxid kristályos fázisa nagyrészt anatáz (d=8,0 nm), azonban csekély, de kimutatható mennyiségű rutilt és brookitot is tartalmaz.

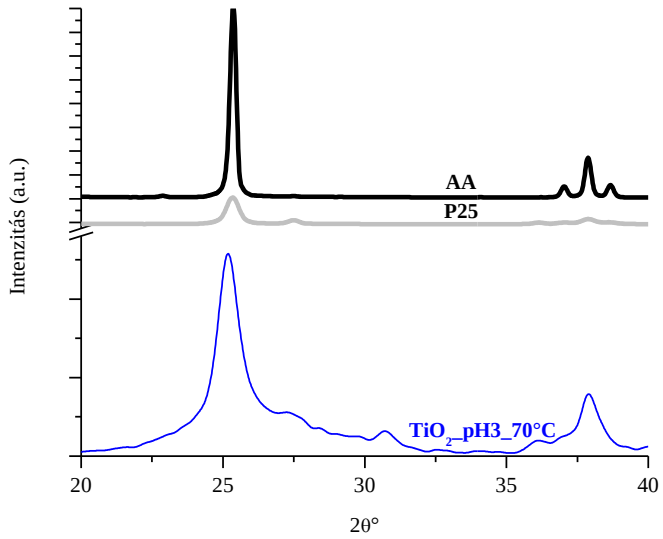

1.ábra:A vizsgált fotokatalizátorok röntgendiffraktogramja

Afotokatalitikus aktivitásokat bemutató **2. ábra** alapján az általunk előállított TiO_2_pH3_70°C fotokatalizátor jelentős mértékben meghaladta mind az Aldrich anatáz (AA), mind az Aeroxide P25referencia titán-dioxidok fotokatalitikus aktivitását.

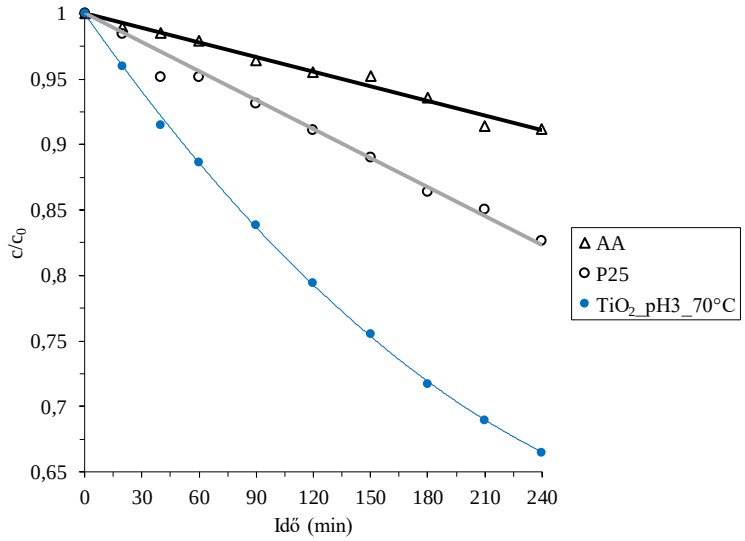

2.ábra: Fenol (c=10^{-4} M) fotokatalitikus oxidációja látható fénnyel történő gerjesztéskor

A3. ábrán láthatóak a fotokatalizátorokdiffúz reflexiós spektrumai, melyek alapján az Aldrich anatáz és az Aeroxide P25 csekély mennyiségű látható fényt (λ>400nm) nyel el, míg az általunk előállított TiO_2_pH3_70°C fotokatalizátor fényelnyelése a látható hullámhossztartományban is jelentős, ami jó összhangban van a katalizátor sárga színével.

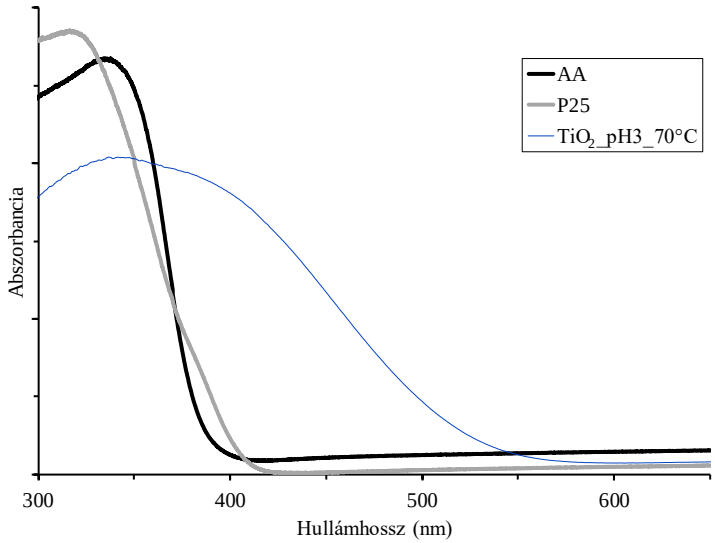

3.ábra: A vizsgált fotokatalizátorok DRS spektruma

Flak és társai [5] munkája alapján a fotokatalizátorok hullámhossz szerinti reflexiójának elsőrendűderiváltját ábrázolva **(4. ábra)** vizsgálható az egyes fotokatalizátorok gerjeszthetőségének hullámhossz szerinti függése.Az ábrán jól látható, hogy a TiO_2_pH3_70°C TiO_2gerjeszthetősége egészen 600 nm-ig kiterjed.

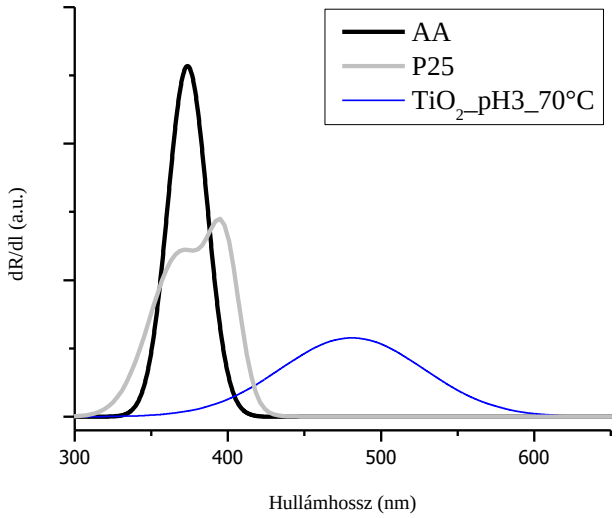

4.ábra: A vizsgált fotokatalizátorok DRS-ének első rendű deriváltja

Várakozásainkkal ellentétben a saját készítésű TiO_2_pH3_70°Cfotokatalizátorbaninfravörös spektroszkópiávalnem mutatható ki a peroxo-csoportok jelenléte (667 cm^{-1} hullámszámnál). Ezért a peroxo csoportok kimutatása szempontjából érzékenyebb röntgen fotoelektron spektroszkópiai (XPS) méréseket fogunk végezni.

Következtetések

Jelen tanulmánybana szintézismódszerünk során alkalmazott hidrogén-peroxid segítségével 3-as pH érték beállításával sikeresen állítottunk elő nem adalékolt, de sárga színű anatáz fázisú titán-dioxidot, amely a DRS spektrum alapján jelentős mennyiségű látható fényt nyel el. A DRS spektrumok deriválásával kapott görbék alapján a fotokatalizátor nem csak elnyeli a látható fényt, de hatékonyan gerjeszthető is vele, amit a fenol modellszennyezővel kivitelezett fotokatalitikus oxidációs kísérletek is igazoltak: A saját készítésű fotokatalizátor a referenciaként használt Aldrich anatáz, és Aeroxide P25 aktivitását is jelentősen meghaladta.

Köszönetnyilvánítás

A munka a Bolyai János Kutatási Ösztöndíj támogatásával készült. A kutatás előzményét a TÁMOP 4.2.4.A/2-11-1-2012-0001 Nemzeti Kiválóság Program című kiemelt projekt támogatta. A kutatócsoport infrastruktúrájának beszerzését a Svájci Alap (SH/7/2/20) biztosította. A szerzők köszönetet mondanak a GINOP-2.3.2-15-2016-00013 azonosító számú projektnek.

Irodalomjegyzék

[1] G. Veréb, T. Gyulavári, Zs. Pap, L. Baia, K. Mogyorósi, A. Dombi, K. Hernádi, RSC Adv., 82 (2015) 66636-66643
[2] M.A. Fox, M.T. Dulay, Chem. Rev., 93 (1993) 341-357
[3] H.P. Boehm, Disc. Faraday Soc., 52 (1971) 264-275
[4] Z. Tang, J. Zhang, Z. Cheng, Z. Zhang, Mater. Chem. Phys., 77 (2002) 314-317
[5] D. Flak, A. Braun, B. S. Mun, J. B. Park, M. P. Wojtan, T. Graule, M. Rekas, Phys. Chem. Chem. Phys. 15 (2013) 1417-1430

INDICATORS FOR ESTIMATING CORROSION OF CONCRETE AND CONSTRUCTION MATERIALS

Anna Honfi[1], Bálint Augusztin[1,2], Imre Kovács[1]

[1]*Department of Natural Sciences and Environmental Protection, Institute of Technology. University of Dunaújváros, H-2401 Dunaújváros, Táncsics M. u. 1/a, Hungary*
[2]*Augusztin Kft. H-8200 Veszprém, Batthyány út 17/D, Hungary*
e-mail: kovacsimre@uniduna.hu

Abstract
Detecting and monitoring the destruction of some building materials may require sophisticated equipment and personal skills. In case of reinforced concrete one the important parameter influencing the stability is alkalinity. It can influence both the stability of concrete and the protection steel against corrosion. A simple but very effective method is the application of phenolphthalein indicator to determine the alkalinity. In this work we investigate the applicability of acid-base indicators on the surface of construction materials. We will confirm our idea that - by combination of some selected indicators - the determination of acid-base properties of the construction materials as well as any changes in this character after possible environmental reaction is extensible.

Bevezetés
Környezeti károsító anyagok, gázok és folyadékok az építőanyagok állapotát nagymértékben befolyásolhatják. Az ilyen károsodások észlelése, illetve előrehaladásuk követése katasztrófák megelőzésében, a műtárgyak állapotának megőrzésében fontos szempont. Mint azt más munkánkban bemutattuk [1], vasbeton korrózió vizsgálatában a CO_2 gáz diffúziójának előrehaladását fenolftalein indikátorral ki lehet mutatni. Amennyiben a CO_2 gáz be tud diffundálni a beton mélyebb rétegeibe, ott az egyébként uralkodó bázikus kémhatást a savas tartomány felé mozdítja el. A vasbetonban uralkodó lúgos kémhatás az acélszerkezetek rozsdásodásának nem kedvez, de a pH csökkenése a vas korróziója felé hat [2]. Ahol a savasodás még nem következett be, a fenolftalein jellemző lila színe fog látszódni. A szilárd, pórusos szerkezetű anyagok esetében hagyományos elektródákkal a pH-mérés nem kivitelezhető. A felületeken adszobeált vízrétegekben uralkodó sav-bázis kölcsönhatások megértése, felderítése és vizsgálata szükségszerű. Az eddig idézett kémiailag többszörösen összetett vasbetonon kívül más építőanyagok esetében is felléphetnek környezeti hatásra roncsolódások. Az eredeti anyag sav-bázis tulajdonságainak megváltozása ekkor sem követhető pH-mérővel. Ilyenek lehetnek gipsz, vagy gipsz tartalmú vakolatok, téglafalak, homokkő építmények, vagy akár márványszobrok is. Illusztrációul szolgáljon néhány lehetőség. Ilyen esetek lehetnek pl. szivárgó vízvezetékek mentén, felszívódó talajnedvesség, a vakolat nem megfelelő összetétele (pl. gipszet kevertek a habarcsba), savas eső, avagy ipari, esetleg kommunális szennyvíz következtében.
Az itt bemutatandó munkánkban sav-bázis indikátorok alkalmazásával teszünk javaslatot az ilyen jellegű, az anyagok sav-bázis tulajdonságait megváltoztató környezeti károsodások mérésének kivitelezésére, illetve a lehetőségek és korlátok bemutatására. Ebből a célból egyszerű modellrendszert választottunk: gipszet, amihez adalékul kis mennyiségű vízüveget kevertünk.

Kísérleti körülmények

Felhasznált anyagok: Kísérleteinkhez használt indikátorok a következők voltak:

A „MODELLGIPSZ”-et kereskedelmi forgalomban vásároltuk. A lapok előállításához desztillált vizet használtunk. Az adalékolt mintákat a Kemikál gyártótól szintén kereskelmi úton beszerzett vízüveggel módosítottuk. A 36 tömeg%-os nátrium-szilikát oldatot desztilláltvízzel hígítottuk A vizsgálatainkhoz készített mintákat száraz levegőn a vizsgálataink előtt legalább egy hétig tároltuk.

Az indikátor oldatokat az analitikában szokásos módon készítettük el [3]. Előzetesen megállapítottuk, hogy az indikátorok felhordása nemcsak permetezéssel, hanem ecseteléssel is felvihető a felületre. Az 1. ábrán mutatjuk be a választott négy indikátor és átcsapási tartományuk skáláját. Különböző pH-jú vizes oldatban az indikátorok szinét összehasonlítás kedvéért is elkészíthetjük [4]. Az indikátorok a vizsgált felületeken nem terjedtek szét, ennek következtében egymástól kb. 5-6 mm-es távolságban is felvihetők. A módszernek korlátot szab, ha a felületen összefüggő folyadékréteg alakul ki, vagy a minta a vizes oldattal közvetlenül érintkezik. Ez esetben az indikátorok leoldódnak a felületről, de az indikátor, vagy indikátorok újabb ecsetelésével a vizsgálat folytatható.

Módszer: Az indikátorok alkalmazásával a pórusos szerkezetű, szilárd, anyagok hidrofil felületén több pontos pH változási értékeket határozunk meg. A beton vizsgálatára alkalmazott fenolftalein esetén azt tudjuk megállapítani, hogy a pH egy küszöbérték felett, vagy alatt van. Az általunk használt négy indikátor esetében 4 átcsapási értékhez képest tudjuk megadni a felület hozzávetőleges pH-értékét. Elkészítettük az indikátorok saját színskáláját különböző pH-ra beállított vizes oldatokkal is, de ezt a színskálát a felületen tapasztalható színekkel összevetni nem érdemes, ugyanis a szilád felület színe is befolyásolja, valamint kalibrált felületi pH értékű felületek készítésére nem találtunk lehetőséget.

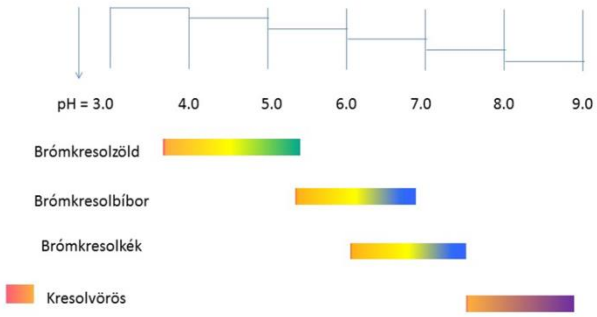

1. ábra A felhasznált négy indikátor és az átcsapási tartományuk skálája

Eredmények és értelmezésük

Az adalékolatlan gipsz felületének sav-bázis tulajdonságait a 2. ábra első mintája mutatja, amin látható színe ezen a felületen. Ebből arra a következtetésre jutottunk, hogy a felület pH értéke 7,5. A második minta készítésekor desztillált víz helyett egy 1g/100 cm^3, a harmadik mintához pedig 2g/100 cm^3 koncentrációjú vízüveg (Na_2SiO_3) oldatot használtunk. Az így előállított minták felülete pH ~ 8, illetve pH ~ 8,6 volt.

Mint várható volt, a lúgosság a felhasznált lúgos oldat koncentrációjával együtt változott. Az első és második mintán a két alsó indikátor színe eltér, a 3. mintán pedig a csak a 4. indikátor színárnyalata különbözik az előzőtől. Ezt összevetve az első ábra trendjével állapítottuk meg a

pH értékeket.

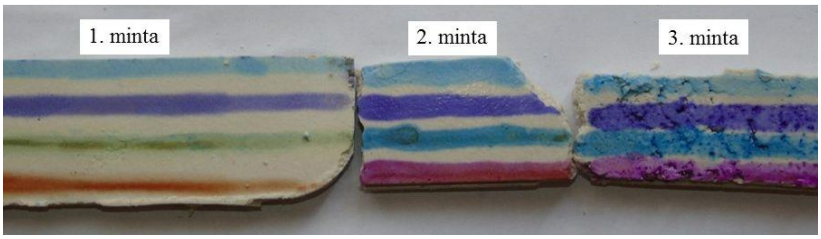

2. ábra A felhasznált négy indikátor és az átcsapási tartományuk skálája
Az indikátorok sorrendje megegyezik az első ábrán bemutatott sorrenddel.

Ecetsavval érintkezett felületeken alkalmazva a fenti módszert, a gipszlapok egyik végét 1g/100 cm^3 töménységű ecetsav oldatba mártottuk, majd felvittük az indikátorokat. Az eredmény a 3. ábrán látható. A nyilak jelzik azokat a helyeket ahol a savasabb felületen az indikátorok színe megváltozott:

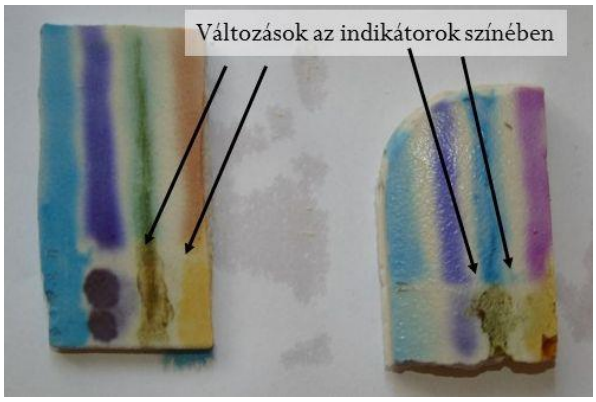

3. ábra Az előző ábra 1. és 2. mintáját mutatja miután az ecetsavval reagáltak.

A nyilakkal jelzett helyeken a brómkrezolkék és krezolvörös indikátorok sárgák lettek, azaz a felületek ezen részén a pH ~ 6-os érték lett.

Következtetések

Megállapíthatjuk, hogy az indikátorok alkalmazása környezeti hatások kimutatására nem cask oldatban lehetséges. Az általunk alkalmazott anyagok a tesztelésben a fehér vagy világos, márvány, esetleg szürke háttéren a színek megkülönböztetését lehetővé teszik. Az indikátorok átcsapási pH tartományát befolyásolhatja az adszorpció a felületen, a protonálódott vagy anionos forma adszorpciója is eltérő lehet. Mint kísérleteink mutatják bizonyos mértékig használhatók az indikátorok, hasonlóan mint a betonkorróziós vizsgálatokban a fenolftalein. A módszernek további korlátot szabhat a sötétebb színű mátrixok is, pl. a vörös tégla színe.

Szakirodalom

[1] Bálint Augusztin, Imre Kovács; Proceedings of the 22nd International Symposium on Analytical and Environmental Problems Szeged, Hungary, October 10, 2016
[2]Nataliya Turova; Inorganic Chemistry in Tables; Springer, Berlin Heidelberg 2011

[3] Burger Kálmán, A mennyiségi kémiai analízis alapjai, Medicina, Budapest, 1981
[4] Darrel D.Ebbing and Mark S. Wrighton (Eds) General Chemistry, 1984, Houghton Mifflin Company

ANALYSIS OF SPELEOTHEM AND ZIRCON SAMPLES BY LA-ICP-MS

Patrick Martin Janovszky[1], Mihály Braun[2], Előd Mészáros[3], Gábor Galbács[1]

[1]Dept. of Inorg. and Anal. Chem., Univ. of Szeged, 6720 Szeged, Hungary
[2]Hung. Acad. Sci., Inst. of Nuclear Sci., Hertelendi Lab., 4026 Debrecen, Hungary
[3]Dept. of Mineralogy, Geochem. and Petrology, Univ. of Szeged, 6722 Szeged, Hungary
e-mail: janovszkyp@gmail.com

Abstract
An inductively coupled plasma mass spectrometer (ICP-MS) equipped with a laser ablation (LA) sample introduction device was used to study the element and isotope distribution in a speleothem sample from the Hajnóczy cave (Hungary) and to perform U-Pb zircon geochronology of a drill sample taken from in the Szalatnak area (Hungary). The purpose of the study was to assess the analytical capabilities of the LA-ICP-MS combination in these applications and to obtain data relevant to geochemical research.

Introduction
It was in the mid-1980s that the analytical potential of LA-ICP-MS was first shown by Gray [1]. Subsequent studies by Jackson et al. [2] and Longerich et al. [3] in the 1990s demonstrated that entirely new calibration strategies would have to be developed and significant improvements made in laser technology and ICP mass spectrometry in order to achieve the precision and accuracy required for applications such as isotopic dating of geological samples. The key paper on the application of laser ablation in the Earth sciences came from Jackson et al. [2], who published the first comprehensive work on the use of LA- ICP-MS for analysis of trace elements in minerals. Since then, this analytical methodology is continuously developing, largely determined by the technological advancements made available to the public both in the areas of pulsed lasers and ICP-MS instrumentation. A relatively widespread application of LA-ICP-MS in Earth sciences only started at around the end of 1990s, when suitable calibration standards also became available [4].
The main advantage of LA-ICP-MS geochemical analysis is that the *in-situ* study of minerals and accessory minerals is possible, without separating them from the rock and also without any significant sample preparation for that matter. The elemental or isotopic analyis, as well as dating based on the measurement of isotope ratios by LA-ICP-MS is therefore fast and cheap. The lateral resolution achievable is 5-25 microns.
In Hungary, LA-ICP-MS technology is only available in a couple of research laboratories all located in Budapest (MFGI, ELTE, MTA EK, etc.). Recently, a new, very capable LA-ICP-MS instrument combination was purchased by the Hertelendi Laboratory of the Institute of Nuclear Sciences of the Hungarian Academy of Sciences (Debrecen, Hungary), thus the possibility presented itself to test its performance in some geochemical samples. The present study can be considered as a pilot study.

Experimental
A 8800-type Triple Quadrupole ICP-MS (ICP-QQQ) by Agilent Technologies was coupled to an NWR 213 laser ablation system from ESI & New Wave Research. The Nd:YAG laser was operated at the 213 nm frequency quintupled wavelength. The speleothem sample was from the Hajnóczy cave. The laser operating parameters for the speleothem sample were set to a repetition

frequency of 20 Hz, 15 J/cm^2 fluence, spot size 100 µm. Surface scans of the sample were recorded for ^{27}Al, ^{137}Ba, ^{43}Ca, ^{24}Mg, ^{55}Mn, ^{88}Sr, ^{208}Pb, ^{13}C, ^{29}Si and ^{56}Fe isotopes with a spatial resolution of 100 µm. The zircon minerals were presented to the instrument in the form of a thin, micro-polished section (30 µm thickness) affixed to a microscope slide. The sample was a section of a drilled rock sample taken in the Szalatnak area. The section contained 8-10 small (max. ca. 100 µm length) zircon minerals, which were located using optical and catohodoluminescence microscopy. Because of the small size of the zircon particles, we used more gentle conditions in the laser ablation exprirments: 40 µm spot size, 10 Hz repetition frequency and 10 J/cm^2 the energy density. We measured the ^{206}Pb, ^{207}Pb, ^{235}U and the ^{238}U isotopes for the purpose of U-Pb dating [5]. A NIST No. 612 glass LA standard was used for the U and Pb calibration os the system.

Results and discussion

As it can be seen in the exemplary data in **Figure 1.**, the Ca content of the speleothem sample was uniformly high (due to the essentially $CaCO_3$ composition of speleothem formations). The increase of the Mg concentration in certain areas indicates that the calcite form is dominant (over the aragonite form) at these places. In accordance with our expectations, the elemental (isotopic) maps for Fe and Mn recoded on the speleothem sample correlated well with the visually observable colored bands and microscopic features of the sample. A further correlation with the Al content was also revealed, therefore these localized formations are though to be rich in iron alumino silicates.

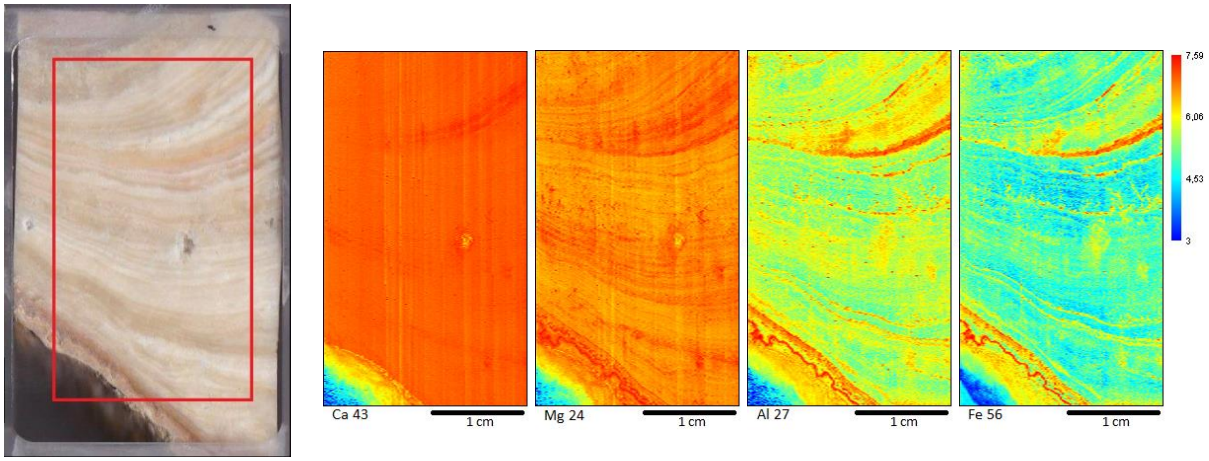

Figure 1. Optical microscopy image (on the left, with the mapped area indicated) and LA-ICP-MS surface maps for ^{40}Ca, ^{24}Mg, ^{56}Fe and ^{27}Al isotopes of the speleothem sample

Seven zircon mineral particles (grains) were ablated in order to determine the average age of the rock sample (a zircon mineral grain and the effect of laser ablation on it can be seen in **Figure 2.**). As the calculation is based on the concentration ratios of U and Pb (we asssessed both the ^{207}Pb/^{235}U and ^{206}Pb/^{238}U ages), thus a calibration was performed with the matrix similar NIST 612 sample certified for the U and Pb isotope composition. The laser ablation signal time profiles had to be processed for the calibration and also for the age measurements. The initial part (up to 28 sec) and the tailing part (after 33 sec) of the time-resolved signal profile was discarded identified as transitional, so only the data between 28 and 33 seconds was processed. The result

of the age calculations was 313 Ma (million years) with 16 Ma uncertainty based on the $^{207}Pb/^{235}U$ data whereas it was 322 Ma with 29 Ma uncertainty based on the $^{206}Pb/^{238}U$ data. As the the sample was previously determined by the Rb-Sr method to be 330-320 Ma [6], it can be concluded that the quick and convenient LA-ICP-MS measurement provided well matching results.

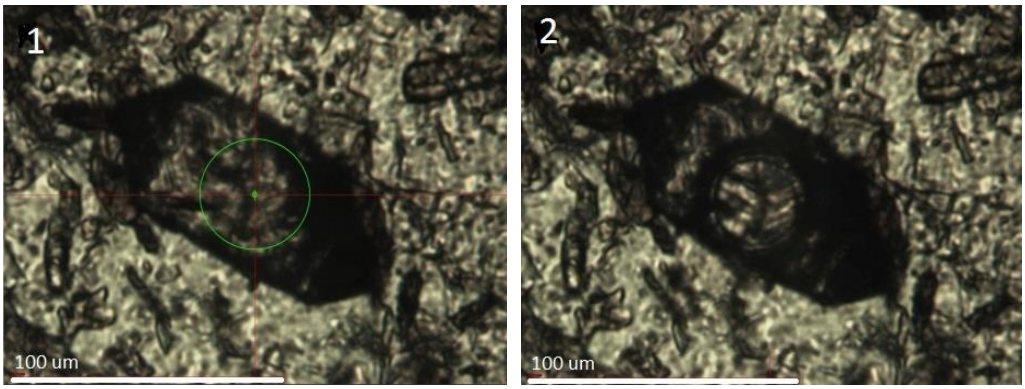

Figure 2. A zircon mineral grain (about 100 μm in length) before (on the left) and after (on the right) of the laser ablation process.

Conclusion

Laser ablation ICP-MS was found to a reliable and convenient method for the recording of element distribution maps and for U-Pb dating of geochemical samples. The achieved U-Pb age result shows a good agreement with the previous Rb-Sr dating result.

References

[1] A.L. Gray, Analyst, 551 (1985) 556.
[2] H.P. Longerich, S.E. Jackson, D. Günther, Journal of Analytical Atomic Spectrometry, 899 (1996) 904.
[3] S.E. Jackson, H.P. Longerich, R. Dunning, BJ. Fryer, Canadian Mineralogist, 1049 (1992) 1064.
[4] J. Kosler, Proceedings of the Geologists' Association, 19 (2007) 24.
[5]U-Th-PbGeochronology, https://www.princeton.edu/geosciences/people/schoene/pdf/4_10_Schoene_UThPb_geochronology.pdf
[6] L. Gyalog, A földtani térképek jelkulcsa és a rétegtani egységek rövid leírása. MÁFI, Budapest, 1996, pp. 171.

KÜLÖNBÖZŐ POLARITÁSÚ ADALÉKANYAGGAL ELŐÁLLÍTOTT NAGY FOTOKATALITIKUS AKTIVITÁSÚ BIZMUT-VOLFRAMÁT ELŐÁLLÍTÁSA ÉS VIZSGÁLATA

Zsolt Kása[1*], Kata Saszet[2], Zsolt Pap[1, 3], Gábor Kovács[2, 3], András Dombi[1], Klára Hernádi[1, 4], Lucian Baia[3], Virginia Danciu[2]

[1]Research Group of Environmental Chemistry, Institute of Environmental Science and Technology, University of Szeged, Szeged, HUNGARY
[2]Faculty of Chemistry and Chemical Engineering, Babeş-Bolyai University, Cluj-Napoca, ROMANIA
[3]Faculty of Physics, Babeş-Bolyai University, Cluj-Napoca, ROMANIA
[4]Department of Applied and Environmental Chemistry, University of Szeged, Szeged, HUNGARY
e-mail: kasa.zsolt@chem.u-szeged.hu

Abstract
In this study, Bi_2WO_6 photocatalysts with different morphologies were obtained by a one-step hydrothermal method. The resulted 3D structures consisted from individual nanoplates. The synthesis procedure involved acetic acid, a surfactant (Triton X-100) and a shaping agent, such as urea, thiourea acetamide and thioacetamide. The effect of these compounds were also investigated in-detail. The above mentioned morphological changes significantly influenced the photocatalytic activity, which was evaluated successfully by the degradation of Rhodamine B (RhB) under visible lightirradiation.

Bevezetés
A fotokatalízis, mint egyalternatív víztisztítási folyamat lényege, hogy ha egy félvezető részecskét a megfelelő elektromágneses sugárzással gerjesztünk, akkor a vegyérték sávból a vezetési sávba „kényszerítünk” egy elektront, ez által hátramarad egy pozitív töltésű „lyuk”, akkor a felület közelében lévő szerves szennyezők sora gyökös folyamatok által oxidálható, egyes esetekben mineralizálhatók (szén-dioxiddá, vízzé és szervetlen ionokká). Fontos, hogy ha megfelelően megválasztott félvezetőt alkalmazunk (például titán-dioxid, volfrám-trioxid, bizmut oxid tartalmú vegyesoxidok), akkor a folyamat elindításához kizárólag csak napfényre van szükség[1]. Fontos paraméterek a kiválasztott fotokatalizátor esetében a fizikai-kémiai, optikai, morfológiai és egyéb tulajdonságok, amelyek nagyban befolyásolják az adott félvezető fotokatalitikus aktivitását is.Így a katalizátorok paramétereinek finomhangolásávalmegnövelhető a fotokatalitikus oxidációs képesség.Ez szorosan összefügg a félvezető kristály méretével, alakjával és morfológiájával[2]. Ezek adalékanyagok hozzáadásával, vagy éppen utólagos hőkezeléssel befolyásolhatók, ezáltal a fotokatalitikus aktivitás nagymértékben megnövelhető. Az irányított kristályosítás lényege az, hogy adott előállítási/kristályosítási körülmények optimalizálásával a fotokatalitikusan aktívabb kristályoldalak felületét megnöveljük (TiO_2 esetében jellemzően a [001]-es felületet [3]). Ez esetben kvázi egykristályokat állítunk elő, de lehetőség van a kristályok kétszintű rendezésére, úgy, hogy a nanoméretű egykristályokat alakformált aggregátumokba tömörítjük.Bizmut-volframát esetében a kétszintű szerveződés spontán is megtörténhet, amely során egy egyedi kristálylapokból felépülő speciális „rózsaforma” alakul ki. Kulcsfontosságú paraméter a kristálylapok által bezárt szög, a feltekeredés és annak mértéke, tehát a rózsaforma kialakulása, illetve annak fejlettségi szintje, ami az előállítás során nagymértékben befolyásolható[4]. A determinizmus elve szerint már a szintézis során előre

meghatározható a keletkező katalizátor tulajdonságai, mint például a morfológia. Az előzetes kísérleteinkalapján az egyik ilyen paraméter lehet, ha a szintézis során hasonló, ám mégis kicsit eltérő adalékanyagokkal megváltoztatjuk a szintéziselegy polaritását, ionerősségét. Így a változó polaritás (hasonló szénlánc vázú, de különböző funkciós csoport tartalmú) miatt más-más szerkezetű anyag keletkezik.

Kísérleti rész

Munkám során hidrotermálisan állítottam elő bizmut-volframát mikrorészecskéket, ami alatt eltérő funkciós csoportú, és polaritású adalékanyagokat használtam. A szintézisek a következőképpen zajlottak:

5 mmol bizmut-nitrát pentahidrátot ($Bi_2(NO_3)_3 \cdot 5\ H_2O$) feloldottam 43 mL 36%-os ecetsavban (A oldat). Ezalatt egy másik edényben 2,5 mmol nátrium-volframátot ($Na_2WO_4 \cdot 2\ H_2O$) oldottam fel 69mLnagy tisztaságú Milli-Q vízben, majd 30 perc kevertetés után hozzácsepegtettem 1,25 mmol felületaktív anyagot, ami a Triton X-100 volt (oktil-fenol-etoxilát). Újabb 5 perc kevertetés után hozzáadtam 1,25 mmol változó funkciós csoportú és polaritású adalékanyagot (B oldat). Az adalékanyagok és a későbbi jelölésük a következők: acetamid (AcA), tioacetamid (TAA), karbamid (U) és tiokarbamid (TU).Ezt követően a B oldatot választótölcsér segítségével hozzácsepegtettem az A oldathoz, majd a kicsapódó fehér, amorf bizmut-volframát szuszpenziót egy acél köpenyes teflon autoklávba töltöttem, majd 15 órára 180 °C-ra programozható szárítószekrénybe tettem. A hidrotermális kezelést követően az autoklávot szobahőmérsékletre hűtöttem ésa kristályos bizmut-volframátot abszolút etanollal és Milli-Q vízzel mostam és 40 °C-on 12 órán át szárítottam.

Fotokatalizátorok jellemzése

A kristályos anyagokat számos anyagvizsgálati módszerrel jellemeztük: pásztázó elektronmikroszkópia (SEM), röntgendiffraktometria (XRD), diffúz reflexiós spektroszkópia (DRS), valamint infravörös spektroszkópia (IR).

A létrehozott anyagok fotokatalitikus aktivitását látható fény megvilágítása mellett teszteltem 25 °C-on. A fényforrás 4 darab 24 W-os hagyományos energiatakarékos izzó volt (λ_{max}> 400 nm). A modellszennyező egy festékanyag, a rhodamin B volt. A tesztek során 100 mg fotokatalizátort szuszpendáltam 100 mL, $5 \cdot 10^{-5}$M-os rhodamin B oldatban, majd 30 percig sötétben kevertettem, hogy a szorpciós folyamatok egyensúlyba kerüljenek. A lámpák felkapcsolását követően 30 percenként mintát vettem, amelyet lecentrifugáltam. A rhodamin B mennyiségének változását UV-vis spektrofotométerrel követtem nyomon (detektálási hullámhossz = 553 nm).

Eredmények és értékelésük

A fent felsorolt méréstechnikákkal vizsgáltuk meg a létrehozott részecskéket, hogy többet megtudjunk a morfológiáról, a kristálytani és optikai tulajdonságairól, valamint az anyagok fotokatalitikus tulajdonságairól.A SEM felvételekből egyértelműen látszik, hogy a legtöbb minta esetében lapokból álló mikrokristályok jöttek létre, amelyeknek a másodlagos szerveződése igencsak eltérő. Egyértelmű tehát, hogy csupán a szintéziselegy polaritásának változtatásával nagymértékben befolyásolható a keletkező részecskék morfológiája. A minták SEM felvételei az *1. ábrán* látható.

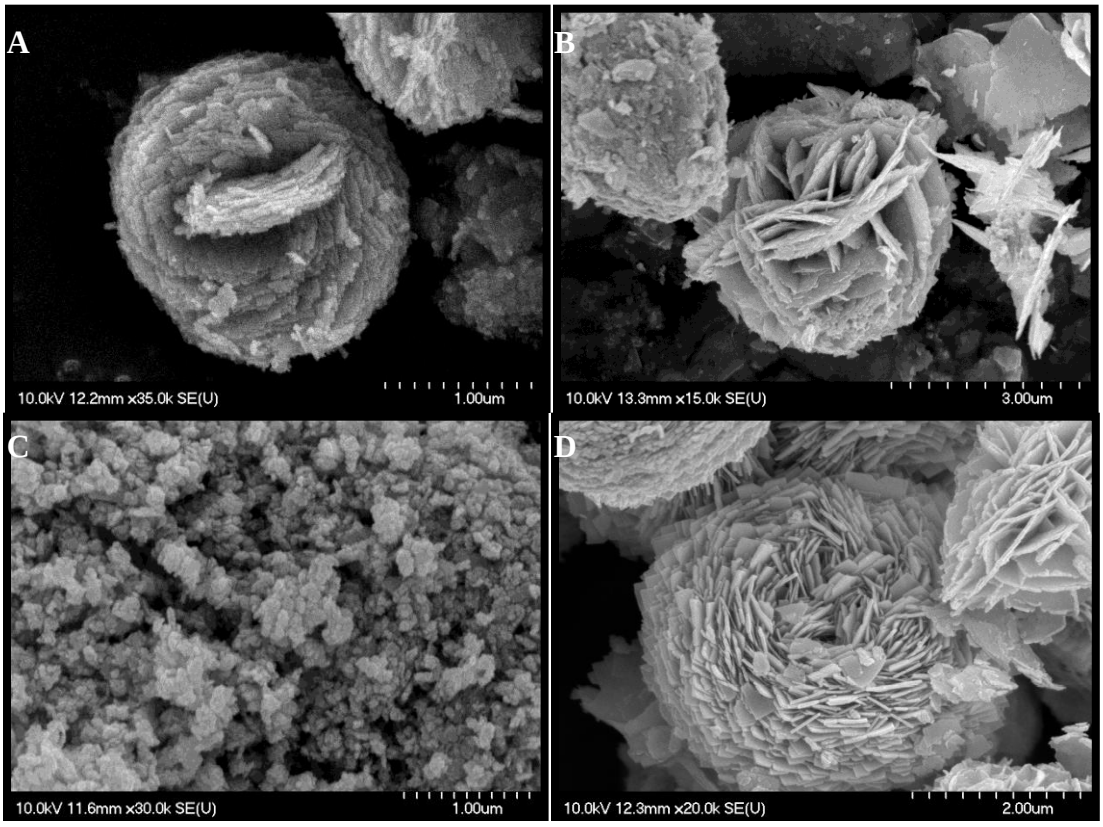

1. ábra: SEM felvételek ***A***:TU, ***B***:U, ***C***: TAA,***D***: AcA

Felvettük a minták diffúz reflexiós spektrumait is. Azt tapasztaltuk, hogy a TAA jelű minta esetében, ha a DRS spektrumot deriváljuk, akkor úgynevezett kettős reflektanciaváltozás maximum figyelhető meg*(2/A ábra,)*, ami arra enged következtetni, hogy ezek a minták a fény spektrumának nagyobb hányadát és hatékonyabban képesek hasznosítani, mint más félvezető fotokatalizátorok.

Az előállított bizmut-volframát minták fotokatalitikus aktivitását is teszteltük látható fény megvilágítása mellett, ami során a modellszennyező a rhodamin B festékanyag volt. Jól látható, hogy mindegyik minta nagyobb degradációs kapacitással rendelkezett, mint a referenciaként használt P25 fotokatalizátor. A bomlásgörbék a *2/B ábrán*láthatók.

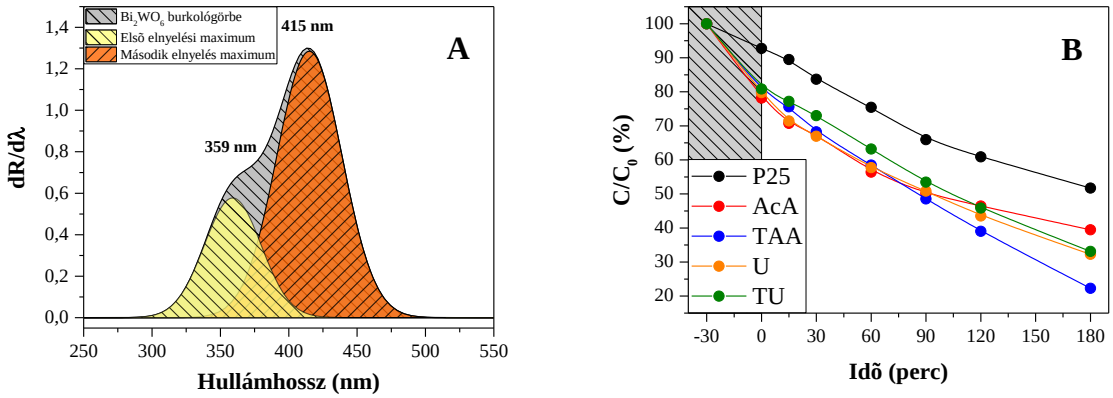

2. ábra: ***A:***TAA derivált DRS spektrum, ***B:*** fotokatalitikus bomlásgörbék

Észrevehető, hogy a TAA jelű minta derivált DRS spektruma jól korrelál a fotokatalitikus bontás során kapott eredményekkel, azaz a kettős reflektanciaváltozás egy lehetséges magyarázat lehet a kiemelkedően jó fotokatalitikus aktivitásra.

Végezetül infravörös spektroszkópiával megvizsgáltuk, hogy a szintézis során használt adalékanyagok a felületen maradnak-e, illetve befolyásolják-e a fotokatalitikus aktivitást. A korábban előállított minták esetében detektálhatóak voltak az adalékanyagoktól származó elnyelési sávok, amelyek egy plusz tisztítási folyamat végén már nem voltak jelen. Ezek a felületi reziduális szennyeződések egyetlen esetben sem rontottak, s nem is javítottak a fotokatalitikus aktivitáson, de annak érdekében, hogy a felületet teljes egészében megtisztítsuk, a korábban alkalmazott tisztítási eljárást alkalmaztuk, ami többszöri mosást, és UV fénnyel végzett tisztítást jelentett. Így a jelenlegi mintasorozaton egyértelműen látszik, hogy kizárólag a bizmut-volframáthoz tartozó elnyelési sávok figyelhetők meg. A minták IR spektruma a *3. ábrán* látható.

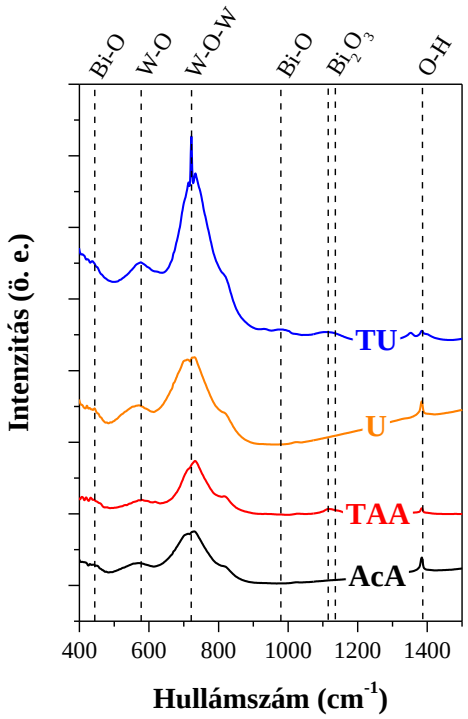

3. ábra: A Bi_2WO_6 infravörös spektrumai

Következtetés

Munkám során sikeresen állítottamelő azonos kristályfázisú, de eltérő hierarchikus szerkezetű és tulajdonságú bizmut-volframát részecskéket. A keletkező részecskék finomhangolását kizárólag a szintézis során használt változó polaritású adalékanyaggal értem el. Ezzel nagymértékben meg tudtam növelni a fotokatalitikus aktivitást látható fény megvilágítása mellett. A használt adalékanyagok a tisztítást követően nem maradnak a felületen, kizárólag csak a keletkező részecske tulajdonságainak befolyásolásában vesznek részt.

Köszönetnyilvánítás

Kása Zsolt köszönia támogatást a Campus Hungary Programnak (TÁMOP-4.2.4.A/2-11/1-2012-0001). A szerzők köszönik az anyagi támogatást a Svájci Hozzájárulásnak (SH/7/2/20) és a GINOP (GINOP-2.3.2-15-2016-00013) valamint a GTC-31805/2016 jelű pályázatnak. Pap Zsolt köszönetet mond a Magyar Tudományos Akadémia Prémium Posztdoktori pályázatának az anyagi támogatásért.

Hivatkozások

[1] Fox, M.A. and M.T. Dulay, Chem. Rev., 1993. 93(1): p. 341
[2] He, J.Y., W.M. Wang, L.L. Zhang, Z.G. Zou, Z.Y. Fu, and Z. Xu, J. of W. U. of Tech.-Mat. Sci. Ed., 2013. 28(2): p. 231
[3] Vajda, K., Z. Kasa, A. Dombi, Z. Nemeth, G. Kovacs, V. Danciu, T. Radu, C. Ghica, L. Baia, K. Hernadi, and Z. Pap, Nanos., 2015. 7(13): p. 5776

[4] Wang, J., J. Li, N. Zhao, J. Sha, S. Hao, E. Liu, C. Shi, C. He, and D. Wang, App. Surf. Sci., 2015. 324: p. 698

INVESTIGATION OF Pt/SiO_2NANOPARTICLES BY SOLUTION AND SINGLE PARTICLE MODE ICP-MS

Albert Kéri[1*] – Ildikó Kálomista[1] – Ákos Szamosvölgyi[2] – Dorina Dobó[2] – Koppány Juhász[2] - András Sápi[2]– Ákos Kukovecz[2] - Zoltán Kónya[2] – Gábor Galbács[1]

[1]Dept. of Inorg. and Anal. Chem.,University of Szeged,H-6720 Szeged, Dóm sq. 7, Hungary, e-mail: galbx@chem.u-szeged.hu
[2]Dept. of Appl. and Environ. Chem., University of Szeged, H-6720 Szeged, Rerrich B. sq. 1, Hungary
e-mail: sapia@chem.u-szeged.hu

Abstract
Pt/SiO_2 nanocomposites (Stöber SiO_2 support particles surface coated with 1.6 nm Pt nanoparticles) were analysed utilizing inductively coupled plasma mass spectrometry (ICP-MS) in the solution and single particle modes. Both analytical approaches were optimized and their performance compared in detail. The single particle ICP-MS approach proposed in this study is a novel approach for the determination of the surface concentration nanoparticles in nanocomposites.

Introduction
In the last decades, the advancement of material science has been fast, and nanotechnology has become one of the most significant and innovative fields of this research direction. The application of nanoparticles (NPs) and nanocomposites in catalysis is particularly desirable due to their specific capabilities. It is important to be noted that the attributes of NPs (size distribution, composition,, structure, etc.) can greatly influence the characteristics (selectivity, activity) of the catalytic processes, as well as the lifetime of the catalyst [1]. Therefore, the thorough characterization of NPs is essential in these studies.
Solution mode ICP-MS has already been used for the characterization of the composition of NPs following acid digestion of the particles in recent years. This process is relatively time-consuming and also has the drawback that the determined concentrations (e.g. of surface concentrations) can potentially carry a positive error, as the dissolved analyte content of the original dispersion and the concentration originating from NPs add up. A significant advantage of the novel single particle approach is that it can directly provide information separately about the dissolved analyte content of the dispersion and about the NPs, as well as the size distribution and number concentration of the latter. A small dispersion volume (e.g. a few mL) and as little as 10^3 – 10^5 /mL particle concentration is adequate for the measurement, which requires almost no sample preparation and gives statistically relevant size distribution histograms, which are based on the measurement of tens of thousands of particles. The measurement is also fast, as it takes only about 5-10 minutes per sample. Thus nowadays spICP-MS offers a viable technique for the investigation of individual nano and micro particles of colloidal systems [2], alternative to such widely spread NP characterization methods such as Dynamic Light Scattering (DLS), Scanning Electron Microscopy (SEM), Transmission Electron Microscopy (TEM) and Atomic Force Microscopy (AFM).
The aim of the present study was to develop accurate analytical methods for the determination of the Pt surface concentration in Pt/SiO_2 nanocomposites by ICP-MS both in the solution and single particle modes.

Experimental

Silica support particles, with a typical diameter of 449 nm as determined by TEM, were prepared through a process based on the Stöber method [3]. The 1.6 nm Pt particles used as loading were synthesized by the reduction of $PtCl_4$ and characterized also by TEM. The Pt nanoparticles were anchored on the surface of SiO_2 support particles by ultrasonic treatment in a nominal concentration of 1 m/m% [4]. TEM images of the Pt/SiO_2 particles are shown in Fig. 1.

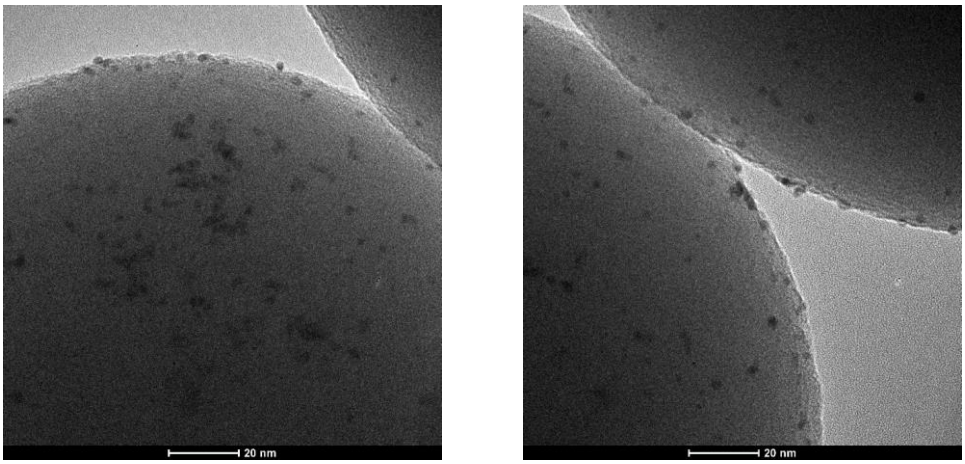

Figure 1. TEM images of the Pt/SiO_2 nanocomposite particles

An Agilent Technologies 7700 X ICP-MS instrument was used throughout the experiments. Sample introduction was performed by an Agilent I-AS autosampler and a Micro Mist type nebulizer equipped with a Peltier-cooled spray chamber. The sample uptake rate was 400 µL/min. The data acquisition software was used in Time Resolved Analysis (TRA) mode. The integration time of TRA measurement was set to 6 ms. Plasma and interface parameters were optimized prior to the analysis searching for the most resolved and maximum intensity NP signals.

An Agilent Technologies Multi-Element Calibration Standard-3 was used for solution-based calibration. For particle-based calibration, Pt nanosol calibration suspensions were synthetized by the method reported by Bigall et. al. [5], with typical spherical nanoparticle diameters of 21.8 nm, 39.2 nm, 51.0 nm and 81.5 nm.

For solution mode ICP-MS measurements, an acid digestion procedure was optimized for the complete dissolution of the Pt content of the nanocomposite. During the execution of this procedure, we used ultratrace analytical quality nitric acid and hydrochloric acid. Dilution of all solutions and dispersions was carried out by Class I (trace analytical) quality deionized water from a VWR Puranity TU 6 UV/UF device. In order to ensure the homogeneity of the suspensions and to avoid the aggregation of the nano particles, we applied ultrasonic treatment performed by a NEY Ultrasonik 300 instrument.

Results and discussion

Solution Mode ICP-MS measurements were performed by using a mixture of nitric acid and hydrochloric acid (1:3 molar ratio) for digestion. The analysis resulted in 0.281 m/m% Pt content in contrast to the nominal 1%. This indicates that the nominal concentration is a strong

overestimation, which is, of course, not a surprise. That is exactly why the post-synthesis elemental analysis is needed in the first place.
The size of the anchored Pt NPs in the studied nanocomposite presented a challenge for spICP-MS measurements, as the size detection limit of this method for Pt is actually about 18 nm, thus the direct (individual) measurement of particles of 1.6 nm diameter was not possible. The measurement was made possible by the relatively high surface coverage (loading), since the spICP-MS detects the cumulative signal from Pt NPs attached to the silica surface. Hence, the ensemble of Pt NPs on the surface generate a signal which is equivalent to a (virtual) Pt NP larger than the size detection limit.
The first step of spICP-MS measurements to determine the surface concentration of Pt NPs was the particle calibration. As it can be seen in Fig. 2, the calibration plot had a good linearity.

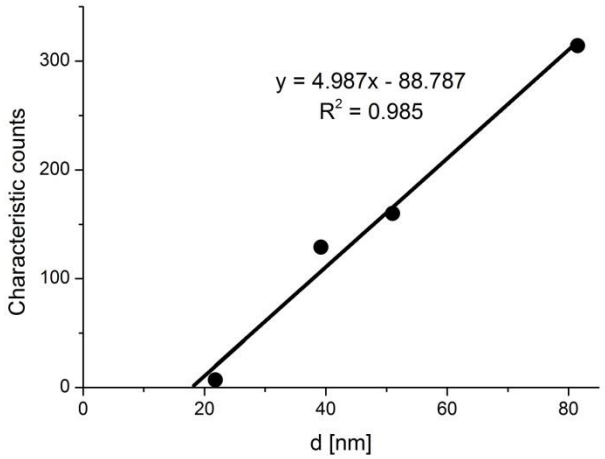

Figure 2. Platinum spICP-MS size calibration curve

The measurement of the nanocomposite samples was performed with an extended 10 ms integration time, and maintaining a low particle concentration in the dispersion, so to ensure an accurate measurement. The histogram of the investigated particles is shown in Fig. 3. As it can be observed, the Pt NP peak is nicely resolved from the background peak. The mode of the peak (the characteristic count) was found to be 11.1, which is equivalent to the signal of a 20.0 nm diameter "hypothetic", spherical Pt particle according to the above calibration curve.

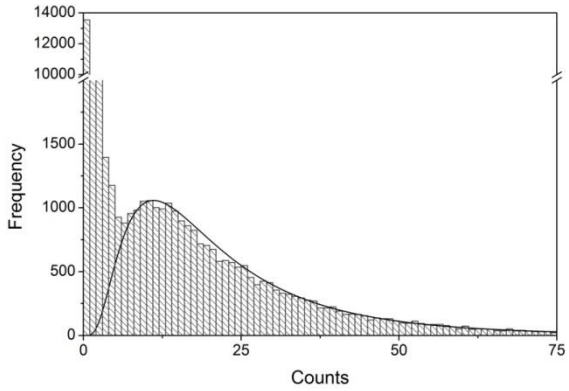

Figure 3. spICP-MS histogram of the nanocomposite particles

(the fitted part originates from the Pt NPs).

Consequently, the Pt surface concentration on a support particle is also equivalent to the mass of this 20.0 nm virtual nanoparticle. This results in a 0.0918 m/m% surface concentration. The result was also confirmed by TEM statistical analysis, during which the surface concentration was determined by the time-consuming counting the Pt NPs on the surface of the silica support in the TEM images. Knowing the size of both the support and the load particles, as well as their specific gravity, the surface concentration could be calculated. This calculation gave a value of 0.0838 m/m%. The good agreement between the spICP-MS and TEM results indicates that spICP-MS can indeed be an accurate and convenient tool in nanocomposite characterization. The fact that both of these results is significantly smaller than the solution mode ICP-MS result indicates that the latter was indeed affected by either the dissolved Pt content (e.g. remnants of precursors) or released Pt NPs from the nanocomposite.

Conclusion

In this study we analysed Stöber SiO_2 support particles surface coated with 1.6 nm Pt nanoparticles utilizing solution and single particle mode ICP-MS. We proved that accurate surface concentration values can be determined by spICP-MS even in cases when the size of the anchored particles are below the size limit of the detection of individual particles. The new technique was less complicated and time-consuming, needed less chemicals and was more accurate than the classical solution-based approach.

References

[1] J.E. Mondloch, E. Bayram, R.G. Finke, *J. Mol. Catal. A: Chem.*355(2012) 1-38.
[2] C. Degueldre, P.-Y. Favarger, *Coll. Surf.*217 (2003) 137-142.
[3] W. Stöber, A. Fink, *J. Coll. Interf. Sci.* 26 (1968) 62-69.
[4] A. Kéri, Összetett nanorészecskék vizsgálata ICP-MS spektrometriával, MSc Thesis, SZTE, 2016
[5] N. C. Bigall, A. Eychmüller, *Phil. Trans. Roy. Soc.*368 (2010) 1385-1404.

PESTICIDE RESIDUES IN ENVIRONMENTAL AND PRODUCE SAMPLES FROM ECOLOGICAL AND CONVENTIONAL PAPRIKA CULTIVATION FIELDS

Marianna Ottucsák, Szandra Klátyik, Mária Mörtl, András Székács

Agro-Environmental Research Institute, National Agricultural Research and Innovation Centre, Herman Ottó u. 15, H-1022 Budapest, Hungary
e-mail: m.ottucsak@cfri.hu

Abstract
To support environmental and food safety of spice paprika production, paprika growing sites in intensive and ecological cultivation have been sampled and analyzed for pesticide residues in Hungary. Two sites of three producers in each cultivation mode were sampled in early summer. Soil samples have been collected at three different points from two or three depth levels, thus, altogether 42 soil samples have been collected at six intensive cultivation fields (ICFs) and 23 soil samples from ecological cultivation fields (ECFs). Pesticide residues in soil extracts have been determined by gas chromatography coupled with mass spectrometry (GC-MS). In soils from ICF sampling sites pesticide active ingredients trifluralin, tefluthrin, chlorpyrifos and DDT were detected together with certain decomposition products (DDE, DDD). Harvested paprika samples were collected in September from four ICFs and from one ECF. Biological samples, prepared by a modified QuEChERS extraction method and analyzed for pesticide residues by GC-MS, contained no detectable amounts of pesticide active ingredients and metabolites, even when plants were grown in ICF on soil containing pesticide residues.

Introduction
Spices used for flavoring in food industry and households are often contaminated with organic microcontaminants [1, 2] or microorganisms [3] of agricultural origin. As a result, production and trade of spices deserve special attention in the assurance of environmental and food safety. Traceability of spice contamination cases is difficult as possible occurrence patterns are very complex. In case of spice paprika mycotoxins, illegal dye utilization, pesticide residues, non-pathogenic microorganisms and heavy metals are the main risk sources. The third biggest hazard factor has been pesticide residues [4], being the reason for 27 various pesticide active ingredients and one metabolite notifications between 2005 and 2015 [2] within the Rapid Alert System for Food and Feed (RASFF) of the European Union [5]. In the present work, our aim was to find out if there are quantitative pesticide residue differences between intensive cultivation mode and organic farming method among different paprika growers in Hungary.

Experimental
In field studies six sites of three paprika producers practicing intensive cultivation mode and two organic farmers in the Southern region of Hungary have been involved (Figure 1). Soil and surface water contamination has been studied in two sampling regimes in June/July and in September. Altogether 42 soil samples have been collected at six intensively cultivated sampling sites (two sites of each producer, three different points from two or three depths). Soil samples from organic farmers have been collected also at three different points from two or three depths (0-20, 20-40, 40-60 cm) and one additional point was sampled (23 samples). Soils of all intensively cultivated fields and a single organic field were sampled in the same way in September, thus, 49 soil samples were collected in this regime. In addition, 6 samples from

surface water in these fields, partly used for irrigation purposes, were also obtained, in each sampling regime. Harvested paprika samples were collected in September from four intensive cultivation fields and from two organic cultivation fields as well.

Water samples were prepared and determined by GC-MS by the multiresidue pesticide analysis method applied by survey authorities in Hungary [6] and modified and validated in our laboratory [7, 8]. Acidic ingredients, including chlorophenoxy acid type herbicides, were eluted from graphitized carbon black solid phase extraction cartridges in a second fraction and were then subjected to derivatization to silyl esters using *t*-butyldimethylsilyl *N*,*N*-dimethylcarbamate as a derivatizing agent [9]. GC-MS analysis was performed on a Varian Saturn 2000 workstation equipped with a Varian CP 8200 autosampler (Varian Inc., Walnut Creek, CA, USA). Quantification of the selected pesticides was performed using matrix-matched calibration. The estimated values of the limits of detection (LODs) were in the range 0.4–5.5 ng/L. Pesticide residues in soil and plant extracts were also determined by GC-MS, paprika samples were prepared by a modified QuEChERS extraction method.

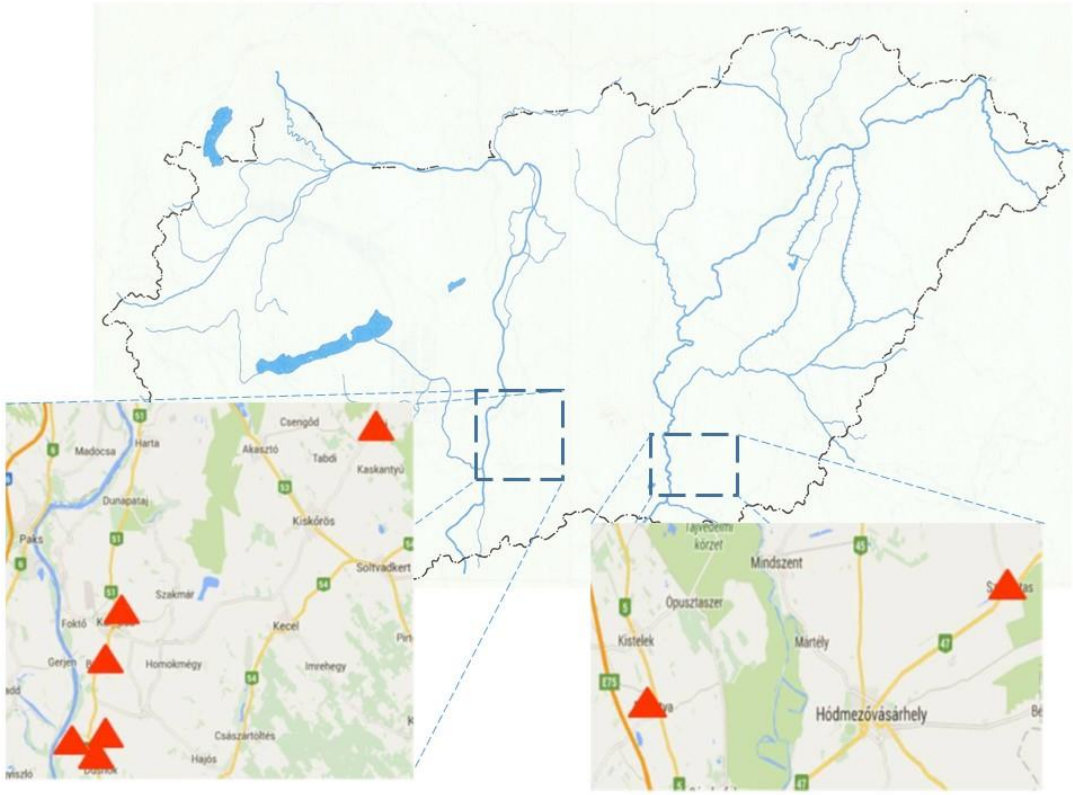

Figure 1. Sampling sites at intensive (6) and ecological (2) cultivation fields

Results and discussion

In soils from intensive cultivation fields as sampling sites pesticide active ingredients trifluralin, tefluthrin, chlorpyrifos and DDT together with their decomposition products (DDE and DDD) have been identified, whereas in some cases traces of diazinon and atrazine, and in a single case metolachlor have been detected, but not quantified. Trifluralin has been measured in soil samples collected at five sites. Although not always occurring, most of the samples contained this pollutant. Contamination levels detected in soils in the Summer and Autumn sampling regimes are listed in Table 1, the chemical structures of the contaminating pesticide active ingredients

detected are depicted in Figure 2.

Table 1. Concentration of pesticides (µg/g soil) found in soil samples collected in June (upper row, normal font) and September (bottom row, *Italics font*) from intensively cultivated fields.

Sampling site	Pesticide/metabolite/residue					
	trifluralin	tefluthrin	chlorpyrifos	DDT	DDE	DDD
1	0.021-0.072	–	–	–	–	–
	0.002-0.049	–	–	–	–	–
2	0.027-3.201	0.106-0.277	–	–	–	–
	0.038-0.358	*0.037-0.195*	–	–	–	–
3	0.013-0.029	–	–	–	–	–
	–	–	–	–	–	–
4		–	0.595-16.610	–	–	–
		–	–	–	–	–
5	–	0.071-0.441	–	0.040-0.865	0.030-0.051	0.044-0.572
	0.011-0.019	*0.027-0.306*	–	*0.057-0.756*	*0.007-0.040*	*0.007-0.031*
6	0.024-0.057	0.188-0.864	–	1.353-4.805	0.046-0.471	1.141-8.351
	–	*0.007-0.154*	–	*0.488-5.699*	*0.028-0.449*	*0.208-1.594*

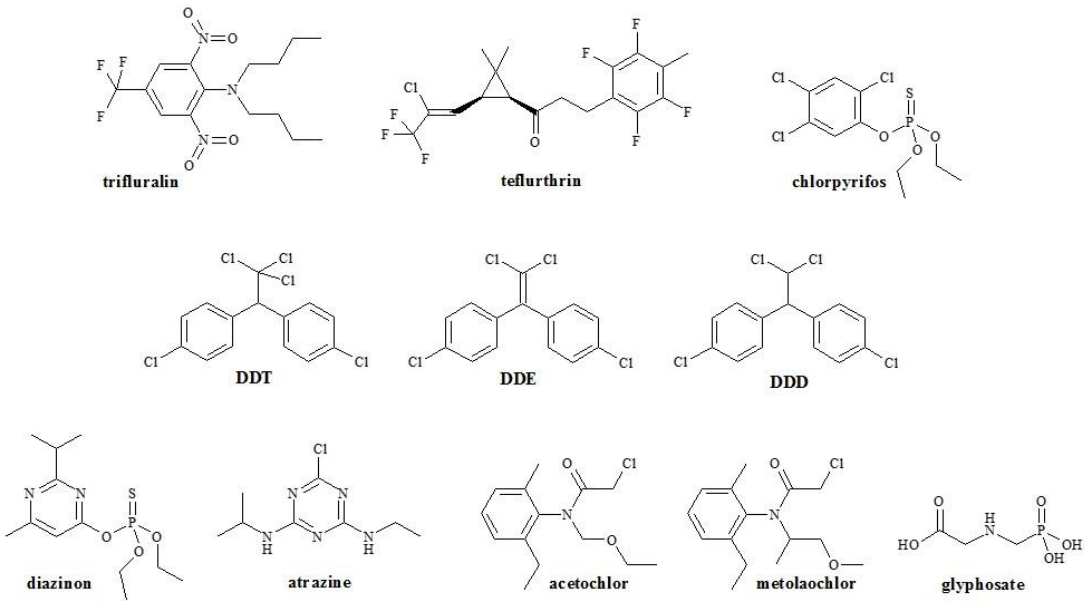

Figure 2. Soil contaminants identified in intensive cultivation fields of spice paprika or of concern in surface water in Hungary

The most common surface water contaminant has been the herbicide active ingredient trifluralin,detected in 50% of the water samples tested at levels of 11-34 ng/L.Although the long banned chlorinated hydrocarbon insecticide active ingredient DDT and its metabolite (DDE) ordegradation product (DDD) appeared at high levels in soilsamples collected at two sites, due to

their low water solubilitythey have not occurred in surface water nearby and or inpaprika harvested from these intensively cultivated fields. Therefore, common reported pesticide contaminants in surface water (e.g. atrazine or acetochlor) [6, 7] have not been detected in the surface water samples collected from paprika cultivation fields, yet currently emerging pollutants, e.g. glyphosate or neonicotinoids [8] (not analyzed in the current study) are expected to become more frequent.

No pesticide residues were detected in paprika extracts, even when plants were grown in polluted soil. This is partially explained by the fact that matrix effects are more substantial in biological (paprika) than in soil samples, but also indicate low absorption/penetration of pesticide active ingredient into paprika fruit, an obvious advantage in food safety. It has to be noted, however, that in contrast to the cultivation field study, pesticide residues occurred in the harvested paprika fruits in a highly intensive cultivation model experiment. Result of this model indicated that the higher the amounts of applied pesticides were, the higher residue levels in soil and in paprika fruits were measured.

Conclusion

The current study allowed, proportionally to its limited scope, a comparative evaluation of spice paprika cultivation under intensive and ecological agronomical conditions in Hungary. Pesticide residues in intensive cultivation fields (ICFs)indicated four major (trifluralin, tefluthrin, chlorpyrifos and DDT) and several minor (diazinon, atrazine, metolachlor, as well as DDT decomposition products DDE and DDD) as soil contaminants, and trifluralin as surface water contaminant. This indicates that mostly past treatments with pesticide active ingredients with more or less persistent characteristics pose hazard of contamination with pesticide residues in environmental matrices. Nonetheless, pesticide residues were not identified (above their limits of detection) in paprika fruit, even if grown under ICF conditions on soil containing pesticideresidues.

Acknowledgements

This research was executed in the framework of the EU-project SPICED (Grant Agreement: 312631) [10] with the financial support from the 7th Framework Programme of the European Union. This publication reflects the views only of the authors, and the European Commission cannot be held responsible for any use, which may be made of the information contained therein.

References

[1] I. Reinholds, I. Pugajeva, V. Bartkevics, Food Control 60 (2016) 683-689.
[2] Sz. Klátyik, B. Darvas, M. Mörtl, M. Ottucsák, E. Takács, H. Bánáti, L. Simon, G. Gyurcsó, A. Székács, Intl. J. Biol. Biomol. Agric. Food Biotech. Engineer., 10 (3)(2016) 156-159.
[3] L. Eliasson, S. Isaksson, M. Lövenklev, L. Ahrné, Front. Microbiol., 6 (2015)1071.
[4] É. Kónya, E. Szabó, I. Bata-Vidács, T. Deák, M. Ottucsák, N. Adányi, A. Székács, Intl. J. Biol. Biomol. Agric. Food Biotech. Engineer., 10 (3)(2016) 160-166.
[5] European Commission, "The Rapid Alert System for Food and Feed. Annual Reports," 2005-2015, Brussels, Belgium: European Commission, Health and Food Safety Directorate General. *http://ec.europa.eu/food/safety/rasff*
[6] E. Majzik-Solymos, É. Visi, G. Károly, B. Beke-Berczi, L. Győrfi, J. Chromatogr. Sci. 39 (8) (2001) 325-331.
[7] E.Maloschik, A. Ernst, G. Hegedűs, B. Darvas, A. Székács, Microchem. J. 85 (1) (2007) 88-97.

[8] A. Székács, M. Mörtl, B. Darvas, J. Chem. 2015, Article ID 717948, 15 pages
[9] E. Maloschik, M. Mörtl, A. Székács, Anal. Bioanal. Chem. 397 (2) (2010) 537-548.
[10] SPICED Consortium, "Securing the spices and herbs commodity chain," EU-FP7-SEC-2012-1-312631, 2013 *http://www.spiced.eu*

TÖBBVÁLTOZÓS FOLYAMATSZABÁLYOZÁS ALKALMAZÁSÁNAK ELŐNYEI ÉS HÁTRÁNYAI AZ ÉLELMISZERIPARBAN

Mihalkó József, Rajkó Róbert

Szegedi Tudományegyetem, Mérnöki Kar, Folyamatmérnöki Intézezet, 6725 Szeged, Moszkvai krt. 5-7.
Institute of Process Engineering, Faculty of Engineering, University of Szeged, 5-7. Moszkvai krt., Szeged, Hungary, H-6725

Abstract
In the first phase of our work, the theoretical knowledge needed to use the multivariate statistical process control (MSPC) was explored. We have clarified the sometimes confused concepts, equations and formulas. In the second phase, R project simulation studies and some food industrial practical model researches will be carried out for confirming the MSPC advantages compared with the univariate one, e.g. to avoid false negative errors in decisions.

Bevezetés
A statisztikai folyamatszabályozás (Statistical Process Control, SPC) során akkor történik beavatkozás a termékgyártás adott folyamatába (azaz akkor lesz instabil), ha ismerünk olyan okot, amelynek hatására a minőségjellemző (pl. tömeg, selejtarány) értéke megváltozik. Ha csak a véletlen miatt következik be az eltérés, akkor is szükséges beavatkozni a folyamatba, annak ellenére, hogy stabilnak tekinthető (Kemény et al., 1998).
Az SPC fő eszközei közé az ellenőrző (más néven szabályozó) kártyák (control charts) sorolhatók, amelyeknek két nagyobb csoportjuk van az adott értékelési skála alapján (Kemény et al., 1998):

- méréses ellenőrző kártyák (pl. tömeg)
- minősítéses ellenőrző kártyák (pl. selejtarány).

Ha az adott folyamat nem stabil, akkor megnő az első-, és másodfajú hiba valószínűsége. Az elsőfajú hibánál nem fogadjuk el a nullhipotézist, miközben az igaz. A másodfajúnál viszont elfogadjuk a nullhipotézist, amely nem igaz (Kemény et al., 1998; Kosztyán et al., 2014).

Módszerek
A statisztikai folyamatszabályozáson belül elkülöníthetőek az egy-, illetve a többváltozós folyamatszabályozási módszerek. A két módszer közötti fő különbség, hogy az egyváltozós módszereknél (Univariate SPC, USPC) egy ismert változónak az értelmezése történik egy vagy több ismert – nem mesterséges – változóval, míg a többváltozós módszereknél(Multivariate SPC, MSPC) a több ismert változót kevesebb számú mesterséges változóval értelmezzük (Sváb, 1979).
Az egyváltozós folyamatszabályozási ellenőrző kártyákra példa a Shewhart-kártyák, a többváltozósokra pedig a Hotelling-féle T^2-kártya.
Több ismert egymástól független változók esetén lehet külön-külön szabályozókártyával vizsgálni az egyes jellemzőket, azonban ha együtt szeretnénk használni, akkor jelentősen nőhet a téves riasztás valószínűsége. Vannak olyan esetek, amikor a változók egymástól függőek, ekkor csakis a többváltozós folyamatszabályozást lehet alkalmazni, mivel szükségünk van a kovarianciák meghatározására (Ittzés, 1999).
A T^2-eloszlás esetén a változók – előre nem ismert - kovarianciamátrixának becslését kell használnunk. A T^2-kártya ellenőrzési területe két változó esetén egy ellipszis, több dimenzióban

pedig egy hiperellipszoid lesz, míg ha a két korrelálatlan változót külön-külön vizsgáljuk, akkor egy téglalap felel meg kontrollrégiónak. A kártya akkor fog riasztani, ha a téglalapon vagy az ellipszisen kívül van az adott pont. Korrelálatlan változók esetén az ellipszis tengelyei párhuzamosak a koordinátatengellyel, korrelált változóknál pedig a főkomponensekkel (Ittzés, 1999).
Az ellipszis középpontjával megegyező középpontú, és az ellipszis elforgatásával azonos elforgású téglalappal pontosabb eredményt kaphatunk, mint a külön-külön való vizsgálat alapján kapott téglalappal (1. ábra).

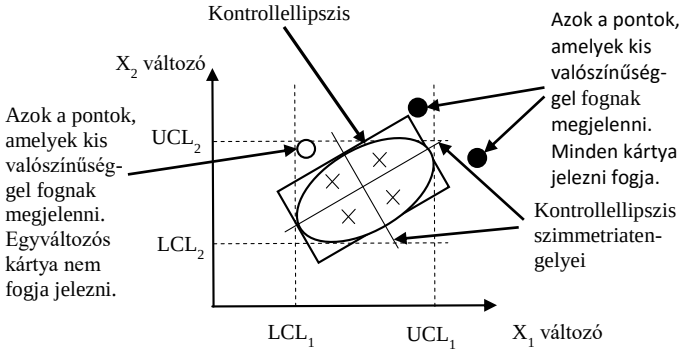

1. ábra: Egy- és többváltozós módszerek összehasonlítása

A T^2-statisztika pontos eloszlása két szemponttól függ (Ittzés, 1999):

- egyrészt attól, hogy egyedi vagy csoportosított (ún. „kisminták”-ba sorolható) adatokkal dolgozunk;
- másrészt attól, hogy visszatekintő (retrospektív) elemzést végzünk vagy az aktuális folyamatot felügyeljük: azaz a folyamat korábbi szakaszáról vizsgáljuk meg, hogy szabályozottnak tekinthető-e (I. fázis), vagy a jelenleg működő folyamatról akarjuk megállapítani, hogy fennmaradt-e a szabályozott állapota (II. fázis).

A T^2-statisztika pontos eloszlásának csoportosítása a fentiek alapján négyféleképpen történhet.
Az I. fázis előtt meg kell arról bizonyosodni, hogy egyrészt független megfigyelésből származzon a mintaalapunk, másrészt az adatok többdimenziós normális eloszlású kell lennie, harmadrészt elegendő nagyságú minta álljon rendelkezésünkre (Rogalewicz, 2012).
Az I. fázisban, a stabilizáció szakaszában először megbecsüljük az addig ismeretlen átlagvektort és kovarianciamátrixot, a szabályozási határok ismerete után a kiugró értékeket, más néven outliereket azonosítjuk, és el is távolítjuk a mintából. Majd újraszámítjuk a megmaradt adatokból a határokat, mindaddig, míg nem kerül minden adat az ellenőrzési határokon belülre és már nincs megállapítható ok (Rogalewicz, 2012).
A II. fázisban azonban nehéz értelmezni, hogy mi okozhatta a jel tartományán kívülre kerülését. Lehet, hogy azt az egyik minőségjellemző, esetleg kettő vagy több változó együttműködése, vagy a kovariancia megváltozása váltja ki. Néhány módszert már kidolgoztak erre a problémára, amelyek közül megemlíthető a főkomponens-analízis, valamint az eddigi legjobb eljárásnak tartott MYT-felbontás (Mason et al., 1997), melynek lényege a következő: a T^2-statisztika felbontását hajtjuk végre p db derékszögű komponensre, ami után az első változóra nézve kiszámítunk egy feltétel nélküli T^2-et. Ezt követően pedig a többi részre egy feltételes T^2-értéket határozunk meg (Mason et al., 1997, Rogalewicz, 2012).
A vizsgálataink során a T^2-eloszlás hátterét világítottuk át, mivel a szakirodalmakban ellentmondásokkal találkoztunk, valamint nem volt tisztázva az egyes eloszlásokhoz tartozó képletek alakja, ill. jelentése.

Eredmények (javított és újraértelmezett összefüggések)

Csoportosított adatok alapján végzett folyamatszabályozás

A-I) Visszatekintő elemzés eloszlása (I. fázis, Phase I)

Tekintsünk m_I független n (>p) elemű p-dimenziós normális eloszlású kismintát!

$$T_I^2 = \frac{p(m_I-1)(n-1)}{m_I(n-1)-p+1} F(p, m_I(n-1)-p+1) \quad (1)$$

A-II) Aktuális folyamat szabályozásának eloszlása (II. fázis, Phase II)

1. lépés: Az A-I) alapján számolt T_I^2 felhasználásával az m_1 kismintából kihagyunk néhányat: az $m = m_I + (m_1$ – kihagyott kisminták száma).

$$T_{II,1}^2 = \frac{p(m+1)(n-1)}{m(n-1)-p+1} F(p, m(n-1)-p+1) \quad (2)$$

2. lépés: Az első lépés alapján számolt $T_{II,1}^2$ felhasználásával az m_2 kismintából kihagyunk néhányat: $m = m_1 + (m_2$ – kihagyott kisminták száma).

$$T_{II,2}^2 = \frac{p(m+1)(n-1)}{m(n-1)-p+1} F(p, m(n-1)-p+1) \quad (3)$$

i. lépés: Az (i-1) lépés alapján számolt $T_{II,i-1}^2$ felhasználásával az m_i kismintából kihagyunk néhányat: $m = m_{i-1} + (m_i$ – kihagyott kisminták száma).

$$T_{II,i}^2 = \frac{p(m+1)(n-1)}{m(n-1)-p+1} F(p, m(n-1)-p+1) \quad (4)$$

A. Egyedi adatok alapján végzett folyamatszabályozás

B-I) Visszatekintő elemzés eloszlása (I. fázis, Phase I)

Tekintsünk n (>p) elemű p-dimenziós normális eloszlású egyedi adatot!

$$T_I^2 = \frac{(n-1)^2}{n} \beta\left(\frac{p}{2}, \frac{n-p-1}{2}\right) \quad (5)$$

B-II)Aktuális folyamat szabályozásának eloszlása (II. fázis, Phase II)

1. lépés: A B-I) alapján számolt T_I^2 felhasználásával az n_1 számú mintából kihagyunk néhányat: az $n = n_I + (n_1$ – kihagyott minták száma).

$$T_{II,1}^2 = \frac{p(n+1)(n-1)}{n(n-p)} F(p, n-p) \quad (6)$$

2. lépés: Az első lépés alapján számolt $T_{II,1}^2$ felhasználásával az n_2 számú mintából kihagyunk néhányat: $n = n_1 + (n_2$ – kihagyott minták száma).

$$T_{II,2}^2 = \frac{p(n+1)(n-1)}{n(n-p)} F(p, n-p) \quad (7)$$

i. lépés: Az (i-1) lépés alapján számolt $T_{II,i-1}^2$ felhasználásával az n_i számú mintából kihagyunk néhányat: $n = n_{i-1} + (n_i$ – kihagyott minták száma).

$$T_{II,i}^2 = \frac{p(n+1)(n-1)}{n(n-p)} F(p, n-p) \quad (8)$$

Következtetések, javaslatok

A többváltozós folyamatszabályozás alkalmazásának vannak előnyei és hátrányai az egyváltozós folyamatszabályozáshoz képest.

Az USPC-nél az I. fázisnál megállapított szabályozási határ alapján történik a II. fázis ellenőrzése.(A T^2-eloszlásnál jóval egyszerűbb eloszlások alkalmazásával) Vagyis azokat a pontokat jelzi a kártya, amelyek a határon kívül esnek. Így egyszerűbbnek tekinthető a legalább kettő változó külön-külön történő értékelése. Ennél a módszernél nincsenek bonyolult számítások, ellentétben az MSPC-ben használatos pl. MYT-felbontással.

Azonban nem tudhatjuk előre, hogy a vizsgált változók között létezik-e valamilyen fizikai és/vagy statisztikai függőség, ezért érdemes a többváltozós folyamatszabályozás alkalmazása.

Az MSPC bevezetését egy arra alkalmas szoftver implementálásával és validálásával indíthatjuk el. Ennek költségeit nagyobb gyárak, termelő üzemek tudják biztosítani. Az alkalmazásával kialakítható stabil technológiai folyamatok révén produkált egyenletes minőség által termelt nyereség hamar megtéríti a befektetést. Az MSPC bevezetése, az esetleges hiedelmekkel ellentétben, nem jelent egyet a létszámleépítéssel, ugyanis szükség van akkor is a technológiát jól ismerő szakemberekre (pl. az érlelőmesterre), akik az instabil folyamatot eredményező okokat tisztázhatják, és a megfelelő beavatkozást elvégzik.
Kisebb üzemek, amelyek USPC-t alkalmaznak, szintén kiegészíthetik szoftveres minőségbiztosító rendszerüket MSPC-vel, megspórolva a validálás költségeit, bár ebben az esetben az MSPC csak jelzéseket biztosít az automatikus beavatkozás lehetősége nélkül.
Magyarországon nincs elterjedve az MSPC, amellyel hazánkban elsődlegesen közgazdaságtani szakemberek foglalkoztak. Az autóiparban egy főfékhenger vizsgálatát mutatja be egy cikk (Kosztyán et al., 2014). Az élelmiszeriparban pedig a többváltozós folyamatszabályozással kapcsolatban Ittzés András és Zukál Endre mutatott be egy alkalmazási lehetőséget, amely nyers parasztsonka pácolásának a só- és víztartalom alapján történő szabályozásáról szól (Ittzés A. et al., 1999).

Összefoglalás

Megállapíthatjuk, hogy az iparban nem elterjedt a többváltozós folyamatszabályozás alkalmazása. Főbb különbségként az említhető meg, hogy bár egyszerűbb, gazdaságosabb a minőségjellemzőket külön-külön egyváltozós módszerrel megvizsgálni, viszont a jellemzők fizikai és/vagy statisztikai okokra visszavezethető együttváltozása miatt sokkal érdemesebb az MSPC használata, a kevesebb téves riasztás valószínűsége miatt.
Vannak olyan iparágak, ahol szükséges lenne a többváltozós folyamatszabályozás rendszerének kiépítése, például a gyógyszeriparban, autóiparban, valamint az élelmiszeriparban. Az első ábra alapján az üres körrel jelölt ponttal megjelenített terméket az egyváltozós folyamatszabályozás elfogadhatónak minősíti, így másodfajú hibát követve el, azaz az USPC a nullhipotézisben megfogalmazott hibátlan termék minősítést fogadja el, a helyett, hogy az MSPC által szabályozott folyamatnak megfelelően azt elutasítaná. Pl. az élelmiszeriparban, ha kikerül az adott gyárból egy hibás termék, akkor egyrészt a vevő a fogyasztás következtében megbetegedhet, másrészt a gyárnak vissza kell hívnia, meg kell semmisítenie az adott tételt gazdasági károkat eredményezve.
Munkánk első fázisában az MSPC használatához szükséges elméleti ismereteket néztük át, az alkalmazható összefüggések alakjait és szerepüket tisztáztuk. A második fázisban R project-ben megvalósított szimulációs vizsgálatokkal igazoljuk az MSPC előnyeit az USPC-vel szemben.

Irodalom

[1] Sváb J. (1979): *Többváltozós módszerek a biometriában*, Mezőgazdasági Kiadó, Budapest 13 19. (16.)
[2] Kemény S., Papp L., Deák A.(1998): *Statisztikai minőség- (megfelelőség-) szabályozás,* Műszaki Könyvkiadó – Magyar Minőség Társaság, 56-57. és 81-83.
[3] Kosztyán Zs. T., Katona A. I. (2014): Kockázatalapú többváltozós szabályozó kártya kidolgozása a mérési bizonytalanság figyelembe vételével, *Kulturális és társadalmi sokszínűség a változó gazdasági környezetben,* 151-152. és 159-161.
[4] Rogalewicz M.(2012): Some Notes on Multivariate Statistical Process Control, *Management and Production Engineering Review,* 3(4), 80-86.
[5] Ittzés A. (1999): Többváltozós statisztikai folyamatszabályozás, *Minőség és Megbízhatóság,* 33(5), 226-231.

[6] Ittzés A., Zukál E. (1999): Többváltozós folyamatszabályozás alkalmazási lehetőségei a húsiparban, *A Hús, 9(3),* 179-183.
[7] Mason R.L., Tracy N.D., Young J.C., A practical approach for interpreting multivariate T^2 control chart signals, *Journal of Quality Technology*, 29(4), 399., 1997.

SELENITE TREATMENT INDUCES NITRO-OXIDATIVE STRESS AND DECREASES VIABILITY IN INDIAN MUSTARD

Árpád Molnár[1*], Vanda Trifán[1], Gábor Feigl[1], László Erdei[1], Zsuzsanna Kolbert[1]

[1]*Department of Plant Biology, University of Szeged, H-6726 Szeged, Közép fasor 52., Hungary*
e-mail: ajpo314@gmail.com

Abstract

Selenium (Se) is an essential microelement for all living organisms, except higher plants, where it has not been proven yet. Like other micronutriens, non-optimal amounts of Se in organisms has negative effects. Some agricultural crops can accumulate large amounts of Se, that decreases the yield and renders it harmful for consumption. In our study, we examined the long-term effects of selenite on secondary stress processes, in order to reveal molecular mechanisms of Se toxicity.

We examined indian mustard (*Brassica juncea* L.), which is a secondary Se accumulator agricultural crop. Plants were precultivated in hydroponic culture for nine days and treated with 0 μM (control), 20 μM, 50 μM or 100 μM sodium selenite for seven days.

Among reactive nitrogen species, the level of nitric oxide remained at control level in case of all treatment concentrations. The two reactive oxygen species, superoxide radical and hydrogen peroxide had elevated concentrations in case of 100 μM sodium selenite treatment. Peroxynitrite, a molecule connected to both families of reactive molecules showed elevated levels as the effect of all selenite concentrations. Selenite induced lipid peroxidation in the root tips of *Brassica*, while, protein tyrosine nitration only slightly intensified compared to control plants. Viability significantly decreased in root tips of 50 and 100 μM sodium selenite-treated plants.

In supraoptimal concentrations selenite disturbs the natural homeostasis of ROS and RNS resulting in secondary nitro-oxidative stress, which is partly responsible for the Se-induced viability loss.

Introduction

Se is naturally present in the environment; although various natural and anthropogenic factors may influence its content. Anthropogenic factors can rapidly increase Se content in soil to toxic levels; therefore Se is widely examined today. The two main bioactive forms of Se are selenate (SeO_4^-) and selenite (SeO_3^-). Supraoptimal Se content can cause crop yield reduction and *via* accumulator plants it can endanger human health [1]. Selenosis, the disease of elevated Se levels has the following effects: defective nails and skin, hair loss, unsteady gait and paralysis.

Reactive oxygen (ROS) and nitrogen species (RNS) are molecule families which are present under natural conditions. If a stress disrupts their homeostasis, they cause further damages through secondary oxidative and nitrosative stress. Since both the molecules and the harmful processes are similar, as well as they control each other's levels, recently the term nitro-oxidative stress is used [2]. The secondary nitro-oxidative stress can cause notable damages in macromolecules such as proteins and membrane lipids.

Based on the above, it is important to examine environmentally hazardous elements and their toxicity mechanisms, especially in agricultural crops being the first organisms that encounter them. The aim of this study was to characterize the processes behind Se induced nitro-oxidative stress in order to be able to alleviate yield reduction and increase food safety in the future.

Materials and methods

In all cases, approx. two cm-long segments were cut from the root tips and were incubated in 2 mL dye/buffer solutions in Petri-dishes. After the staining procedure, the root samples were prepared on microscopic slides in buffer solution. We used different specific fluorophores for each staining, which is shown below (Table 1).

Fluorophores	**DAF-FM DA**	**DHE**	**DHR**	**Amplex Red**	**FDA**	**Schiff's reagent**
Labelled molecule/ process	Nitric oxide	Superoxide radical	Peroxynitrite	Hydrogen peroxide	Viability	Lipid peroxidation

Table 1. Fluorophores and the examined processes

Although these staining methods allow semi-quantitative determinations, they are reliable tools for *in situ* detection of ROS and RNS, since their specificity were proved *in vivo* and *in vitro*. The roots of the plants labeled with different fluorophores were investigated under a Zeiss Axiovert 200 M inverted microscope (Carl Zeiss Jena, Germany) At least 10–15 root tips were measured in each experiment.

Root tissues of *Brassicajuncea* were grounded with double volume of extraction buffer (50 mM Tris–HCl buffer pH 7.6–7.8) containing 0.1 mM EDTA, 0.1% TritonX-100 and 10% glycerol. After centrifugation at 12,000 rpm for 20 min at 4 °C, the supernatant was stored at -20 °C. Protein concentration was determined using the Bradford (1976) assay with bovine serum albumin as a standard.

10 µg of root and 25 µg of shoot protein extracts per lane were subjected to sodium dodecyl sulphate-polyacrylamide gel electrophoresis (SDS-PAGE) on 12 % acrylamide gels. For western blot analysis, separated proteins were transferred to PVDF membranes using the wet blotting procedure (30 mA, 16h). After transfer, membranes were used for cross-reactivity assays with rabbit polyclonal antibody against 3-nitrotyrosine diluted 1:2000 Immunodetection was performed by using affinity isolated goat anti-rabbit IgG-alkaline phosphatase secondary antibody in dilution of 1:10000, and bands were visualized by using NBT/BCIP reaction. As a positive control nitrated bovine serum albumin was used.

Results and discussion

Nitric oxide levels in root meristems remained similar to control in case of all treatment concentrations (Figure 1. A.).

Mild selenite stress did not affect superoxide levels, but 50 µM sodium selenite decreased it. Contrary, the highest selenite concentration significantly induced the formation of superoxide (Figure 1. B.)

Peroxynitrite is formed in the reaction between nitric oxide and superoxide radical. The levels of peroxynitrite significantly increased in 50 and 100 µM selenite-treated root tips, (Figure 2.A.). Hydrogen peroxide levels increased depending on Se treatment; however only 100 µM sodium selenite resulted in significant difference from control (Figure 2.B.).

We analyzed two markers of nitro-oxidative stress: lipid peroxidation and protein tyrosine nitration. *Brassica juncea* roots had only slightly increased protein nitration compared to control plants. Newly nitrated protein bands could not be observed in treated samples (Figure 3.A.). In case of lipid peroxidation, selenite had a more obvious effect, since every concentration led to the intensification of membrane damage. (Fig 3B).

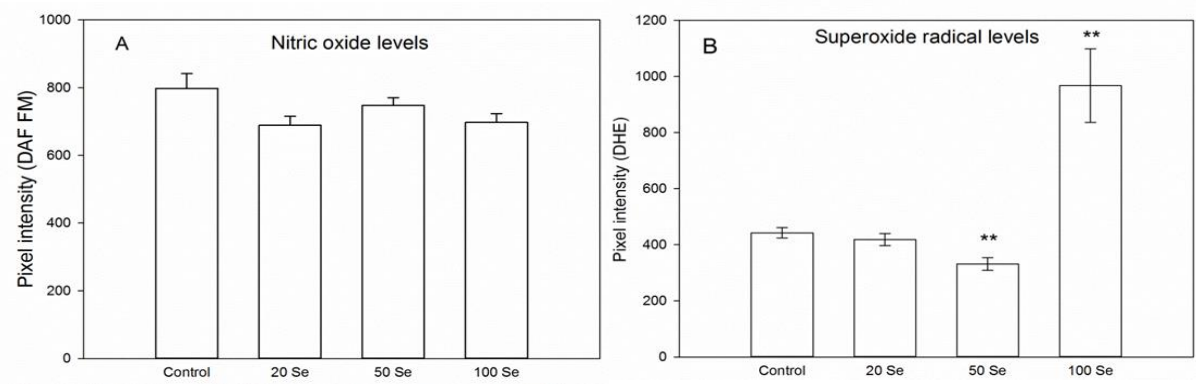

Figure 2. Nitric oxide(A) and superoxide (B) levels in root tips of *B. juncea* treated with 0, 20, 50 or 100 µM selenite for 7 days. Statistically significant differences were determined by Student t -test (**P≤0.01).

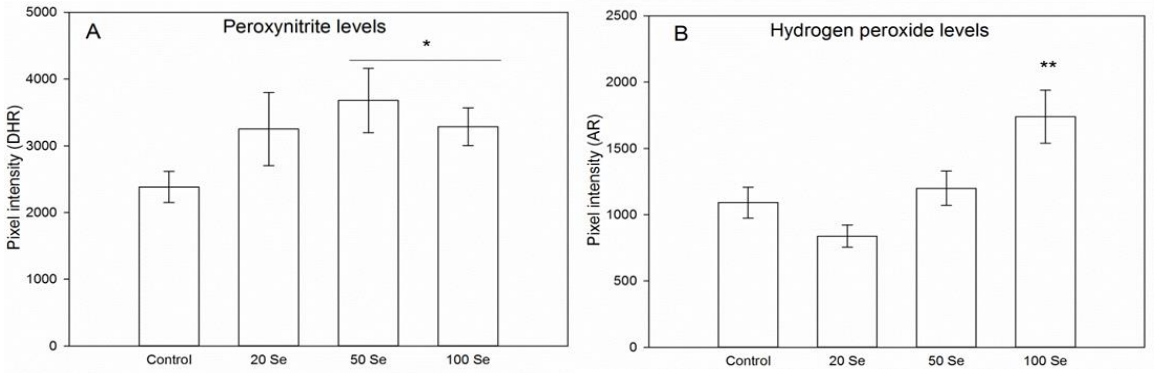

Figure 3. Peroxynitrite (A) and hydrogen peroxide (B) levels in selenite-treated *B. juncea* roots. Statistically significant differences were determined by Student t -test (*P≤0.05, **P≤0.01).

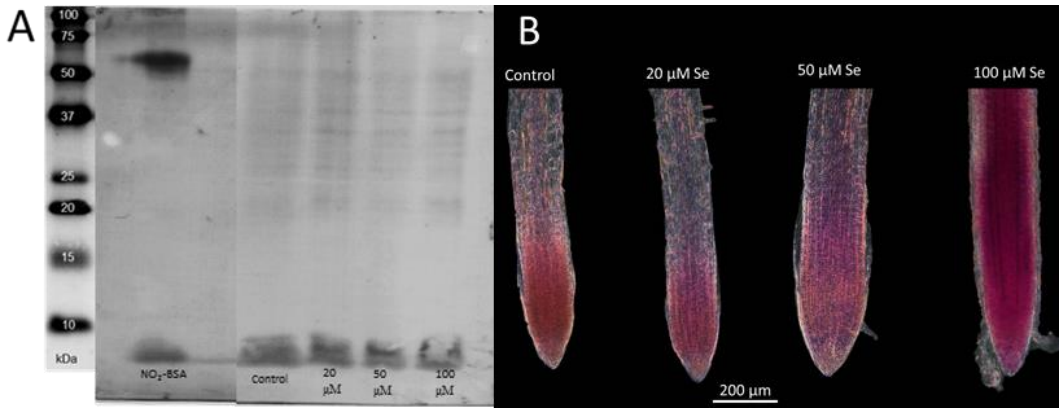

Figure 3. (A) Representative immunoblots showing protein tyrosine nitration in roots of *Brassica juncea* treated with 0, 20, 50 or 100 µM selenite. Commercial nitrated BSA was used as a positive control. (B) Lipid peroxidation in root tips of control and Se-treated *Brassica juncea*. Bar=200 µm

Cell viability in the root meristem is essential to root growth and plant biomass production, thus a decrease in it reflects the overall effect of stress on the organism. In case of sodium selenite, 50 and 100 µM treatment significantly decreased viability compared to control (Figure 4.).

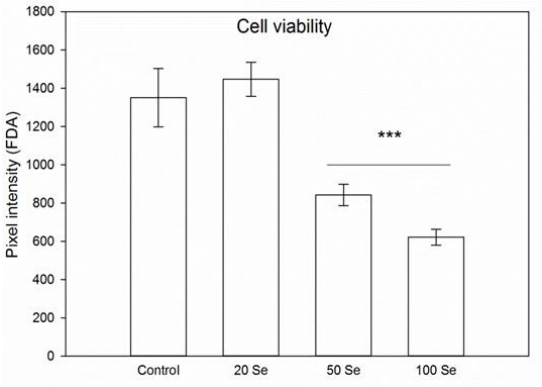

Figure 4. Cell viability in *B. juncea* root meristem. Roots were treated for 7 days with 0, 20, 50 or 100 µM selenite. Statistically significant differences were determined by Student t -test (***P≤0.001).

Conclusion

In case of selenite stress, natural homeostasis of ROS and RNS was disturbed and higher Se concentrations induced nitro-oxidative stress. Nitric oxidelevels remained at control level, but the increase in peroxynitrite showed a slight increase. Most likely, newly generated NO molecules immediately reacted with superoxide radical, forming peroxynitrite. The level of superoxide radical increased only as the effect of 100 µM selenite, and 50 µM sodium selenite decreased it significantly. One mechanism behind this could be the peroxynitite generation, or activation of antioxidant enzimes and other metabolic pathways may be involved. Hydrogen peroxide could be generated from superoxide radical by enzimatic activity. The analyzed oxidative and nitrosative stress markers responded to selenium treatment, which indicates that higher concentrations of Se have harmful effects on plant macromolecules. The observed nitro-oxidative stress processes potentially contributed to the viability loss of root meristem cells, leading to cell death. The slight increase in viability as the effect of 20 µM sodium selenite suggeststhat Se can alleviate stress as an antioxidant.

In this study,for the first time nitration pattern changes where observed in selenium accumulator and tolerant crop plants. The lipid peroxidation proved to be more intense than the protein nitration suggesting that from nitro-oxidative processes, oxidative stress is more severe in selenium accumulator *Brassica* plants.

Acknowledgements

This work was supported by the János Bolyai Research Scholarship of the Hungarian Academy of Sciences and by the National Research, Development and Innovation Fund (Grants no. NKFI-6, K120383 and NKFI-1, PD120962).

References

[1] Kádár I (2013) Szennyvizek, iszapok, komposztok, szervestrágyák a talajtermékenység szolgálatában. Magyar Tudományos Akadémia Agrártudományi Kutatóközpont Talajtani és Agrokémiai Intézete pp. 315-316.

[2] Corpas F.J., Barroso J.B. (2013), Nitro-oxidative stress vs oxidative or nitrosative stress in higher plants. New Phyt., 199(3), 633-635.

VADON TERMŐ ÁFONYA GENOTÍPUSOK ÉS KERESKEDELMI FORGALOMBAN KAPHATÓ ASZALVÁNYOK ANTIOXIDÁNS KAPACITÁSÁNAK VIZSGÁLATA

Molnár Klára[1], Papp Nóra[1], György Zsuzsanna[2], Köbölkuti Zoltán Attila[3], Stefanovits-Bányai Éva[1]

[1] *Szent István Egyetem, Élelmiszertudományi Kar, Alkalmazott Kémia Tanszék, 1118 Budapest, Villányi út 29-43.*
[2] *Szent István Egyetem, Kertészettudományi Kar, Genetika és Növénynemesítés Tanszék , 1118 Budapest, Villányi út 29-43.*
[3] *Szent István Egyetem, Kertészettudományi Kar, Növénytani Tanszék, 1118 Budapest, Villányi út 29-43.*
e-mail: banyai.eva@etk.szie.hu

Abstract
The health benefits of lingonberry (*Vaccinium vitis-idaea*) have been studied extensively. The purported medicinal properties and nutritional benefits have been attributed to a wide range of beneficial compounds. Flavonoids like quercetin, anthocyanin or proanthocyanidin derivatives and phenolic acids like benzoic or chlorogenic acid were described earlier in fruits.In folk medicine, lingonberries have been used for example as a natural remedy for the pain. In the present study, wild lingonberry genotypes were collected to compare their antioxidant capacity with different spectrophotometric methods. The results for wild fruits were compare with a sample purchased from the market. The antioxidant properties of five different dried fruit products were examined. Small variability was found between the wild lingonberry genotypes and little difference was observed between the fruits collected wild and the sample purchased from the market. Among dried fruit products small differences were found in antioxidant capacity.

Bevezetés
Az áfonya (Vaccinium) a hangafélék (erikafélék;Ericaceae) családjának egyik népes nemzettségét alkotja az északi félgömb területein és Európában [1]. A fontosabb áfonyafajok közé tartozó Vörös áfonya (Vaccinium vitis-idaea L.) a Kárpátok és Alpesek övében összefüggő állományban jelennek meg [2]. Számos értékes ásványi anyag (kalcium, magnézium, kálium, nátrium, vas, cink, mangán és foszfor) tartalma mellet, vitaminok (A-,B-,C- és E-vitamin) gazdag forrása. Fontos beltartalmi jellemzői a polifenolok, melyek a növényi anyagcsere másodlagos termékei [3].A vörös áfonyában leginkább megtalálható flavonoidok az antocianidinek és tanninok illetve szerves savak közül az aszkorbinsav, benzoesav, urzolsav és szalicilsav, melyeknek köszönhetően számos egészségügyi pozitívuma ismert[4].Legjelentősebb az akut és krónikus húgyúti fertőzések megelőzése, sejt és érvédő hatása (védi a szervezetünket a káros oxidáció folyamatoktól, óvja testünket az öregedéstől) [5]. Értékessége miatt cukrászati alapanyagként igen elterjed, illetve az üdítőipar, szeszipar és gyógyszeripar területén is nagy kedveltségnek örvend. Munkánk során célunk volt különböző helyről származó vörös áfonya minták antioxidáns kapacitásának összehasonlítása kereskedelemben vásárolt nyers és aszalt mintákkal.

Anyag és módszer

Az antioxidáns kapacitás vizsgálatához négy különböző termőhelyről származó vadon termő vörös áfonyát, ötféle aszalt mintátés egy kereskedelembenkapható friss gyümölcsöt használtunk fel. A vadon termő gyümölcsök közül egy ausztriai ('Ausztria'), míg három romániai ('Románia 1', 'Románia 2', 'Románia 3') termőhelyről származott (1. táblázat).

A vadon termő vörös áfonya mintavételezése az egyes állományokon belül a minimális izolációs távolságot (30m) figyelembe véve, az illető populációt a lehető legjobban reprezentáló növénytakarójú területről, egységes módszerrel történt. A leszedett minták fogyasztási érettségűek voltak.

1. táblázat. A kísérletbe vont vadon termő vörös áfonyák legfontosabb mintagyűjtési paraméterei

No.	Mintavételi helyek	Ország (kód)	Földrajzi koordináták (decimális)	Tengerszint feletti magasság (m)	Élőhelytípus	Mintavételi pontok száma
1	Seckauer Zinken	Ausztria (1)	47.30- 14.75	2370	törpefenyves	4
2	Tinovul Mohos	Románia (1)	46.13- 25.54	1050	tőzegláp	3
3	Tinovul Luci	Románia (2)	46.29- 25.76	1079	tőzegláp	3
4	TinovulFǎntǎna Brazilor	Románia (3)	46.50- 25.26	953	tőzegláp	3

A mérésekhez a kimért nyers és aszalt vörös áfonya szemeket liofilizáltuk, majd dörzsmozsárban elmorzsoltuk. A vizsgálat során a mintákat Milli-Q vízzel extraháltuk. A vízben nem oldódó komponensek miatt az extraktumot centrifugálással ülepítettük. A mérések elvégzéséhez felülúszót használtunk, melyeket eppendorf-csövekben -32 °C-on tároltunk. A minták homogenizálását vortexeléssel valósítottuk meg, és egy órára hűtött ultrahangos vízfürdőbe helyeztük őket.

A minták vizsgálásához a következő módszereket hívtuk segítségül:

- **FRAP:** Benzie és Strain (1996) nevéhez fűződő [6], vasredukálóképességen alapuló módszer. A végeredményeket mmol ASE egyenérték/ 100 g gyümölcsre vonatkoztatva adtuk meg.
- **TPC:**A vizsgálatot Singleton és Rossi (1965) alapján hajtottuk végre [7]. A végeredményeket mmol GSE egyenérték/ 100g gyümölcsre vonatkoztatva adtuk meg.
- **DPPH:** A módszer lényege, hogy a mintában levő antioxidáns hatású vegyületek redukálják a stabil DPPH gyököt (1,1-difenil-2-pikril hidrazil gyök), mely spektrofotometriásan mérhető színváltozással jár [8, 9]. A végeredményeket mmol trolox egyenérték/100 g gyümölcsre vonatkoztatva adtuk meg.
- **Összes monomer antocianintartalom:** Lee és mts. (2005) módszere alapján kiviteleztük a vizsgálatot [10]. A végeredményeket mg cianidin-3-glükozid egyenérték/100 g gyümölcsre vonatkoztatva adtuk meg.

Eredmények és következtetések

A gyümölcsök antioxidáns kapacitását három redukálóképességen alapuló módszerrel (FRAP, TPC, DPPH) határoztuk meg. A több mintavételi pontról, de egy termőhelyről származó minták eredményeit átlagolva az 1. ábrán mutatjuk be. A vadon gyűjtött áfonya gyümölcsök antioxidáns kapacitásának vizsgálata alapján elmondható, hogy az egy termőhelyről, de több mintavételi pontról származó minták között kis különbségeket tapasztaltunk, az egy termőhelyről származó minták homogénnek tekinthetők (1. ábra, A, B, C). Hasonlóan kis különbségeket tapasztaltunk összes monomer antocianintartalom tekintetében is az egy mintavételi helyről származó minták esetében (1. ábra, D). Az eltérő termőhelyről származó minták között kis (közel kétszeres) különbségeket tapasztaltunk antioxidáns kapacitás tekintetében. Általánosságban elmondható, hogy az ausztriai termőhelyről származó mintában mértük a legnagyobb értékeket, melyet a romániai minták követtek. Az általunk piacon vásárolt áfonya minta antioxidáns kapacitása FRAP módszerrel mérve az ausztriai, míg TPC és DPPH módszerekkel a romániai mintákéhoz közelített, összességében a vadon gyűjtött társaihoz hasonló értékekkel rendelkezett. Az összes monomer antocianintartalom meghatározás esetében a 'Románia 1' minta mutatta a legnagyobb értéket, melyhez a kereskedelemben kapható minta állt a legközelebb (1. ábra, D).

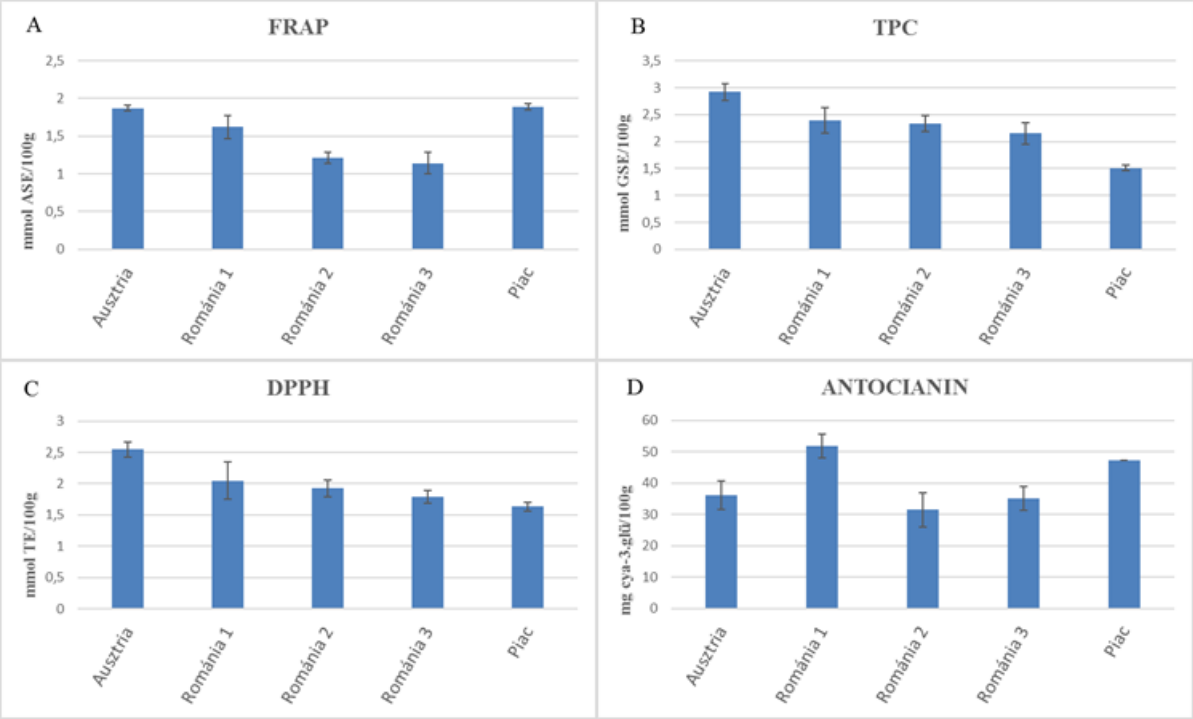

1. ábra. A vadon gyűjtött és kereskedelemben kapható vörös áfonya minták antioxidáns kapacitásának átlagértékei FRAP módszerrel (A), TPC módszerrel (B) és DPPH módszerrel (C)meghatározva és antocianin-tartalmuk (D).

A kereskedelmi forgalomban kapható aszalt vörös áfonya minták antioxidáns kapacitását és összes monomer antocianin-tartalmát a 2. ábrán mutatjuk be. A mintákról megállapítható, hogy mind a négy módszerrel hasonló eredményt kaptunk. Antioxidáns kapacitásban a minták között 1,5-2-szeres különbségeket figyeltünk meg (2. ábra A, B, C). Antocianin-tartalomban közel háromszoros különbséget tapasztaltunk a legkisebb és legnagyobb értékek között (2. ábra D).

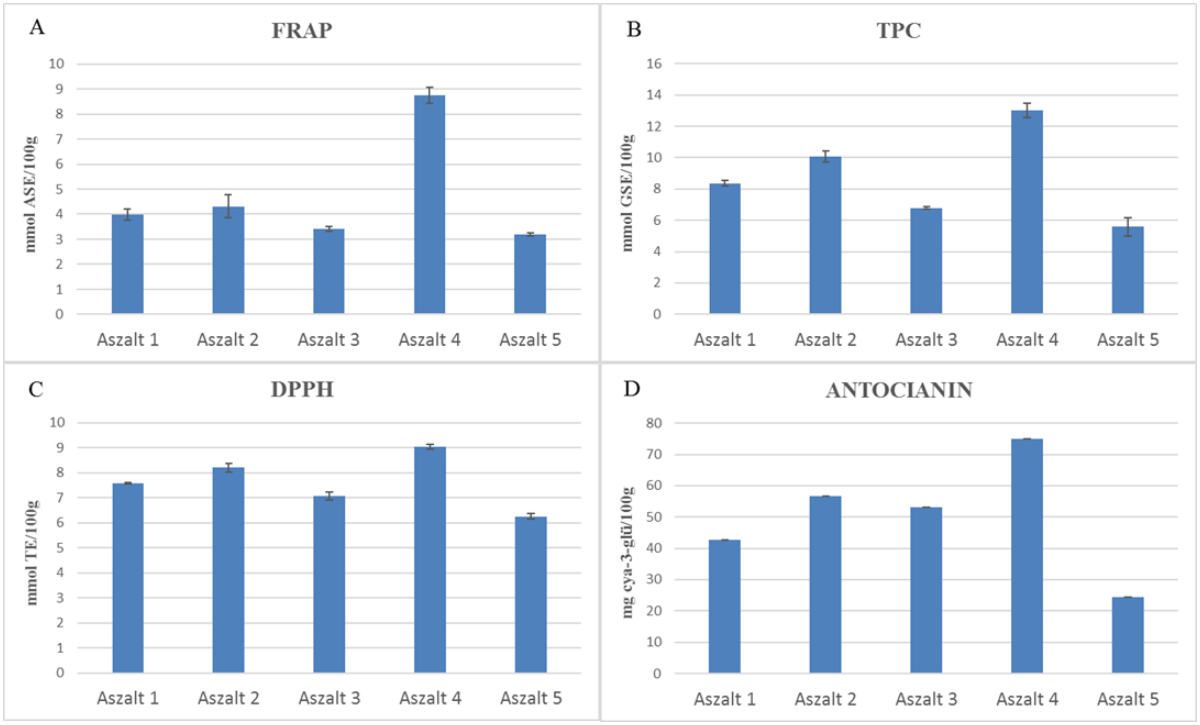

2. ábra. A kereskedelemi forgalomban kapható vörös áfonya aszalványok antioxidáns kapacitása FRAP módszerrel (A), TPC módszerrel (B) és DPPH módszerrel (C) meghatározva és ezek antocianin-tartalma (D).

Összefoglalás

Az antioxidáns mérések eredményeit összevetve, a vadon gyűjtött és kereskedelemben hozzáférhető vörös áfonya minták jelentős eltérést nem mutattak antioxidáns kapacitás tekintetében.Az egy termőhelyről, de különböző mintavételi pontokról származó minták mért értékei között kis különbségeket figyeltünk meg, így ezeket homogénnek tekintettük. A különböző termőhelyekről származó minták redukálóképességében kis variabilitást tapasztaltunk, mely feltehetően a mintaszám bővítésével változna. A kereskedelmi forgalomban kapható aszalt gyümölcsök antioxidáns kapacitásában és antocianin-tartalmában kis különbségek kaptunk. Mivel munkánk kis variabilitás jellemezte a vadon gyűjtött áfonya genotípusokat, a vizsgáltokat szeretnénk kiterjeszteni több termőhelyről származó mintákkal a kiugró beltartalmi értékekkel rendelkező genotípusok keresése érdekében.

Felhasznált irodalom

[1] Kárpáti Z., Terpó A., in: Alkalmazott növényföldrajz, Budapest, 1971
[2] Tőkés Á., M. Deák Sz., Uzonyi D., in: Áfonyák-vadonból a termesztésbe, 2011
[3] Su Z., Pharmaceutical crops. (2012) 3, pp. 7-37
[4] E. Gardner,Britisch Nutrition Foundation Nutrition Bulletin (2014), pp. 223-230
[5] Harvard Health Letter (2013), p. 6.
[6]Benzie, I.F.F., Strain, J.J.,Analytical Biochemistry (1996) 239,70–76.
[7]Huang, D.J., Ou, B.X., Prior, R.L., J. Agr. Food Chem. (2005) 53, pp. 1841-1856
[8]Ayres, G. H.Analytical Chemistry (1949) 21, pp. 652–657.
[9]Sloane, H. J., William, S. G., Applied Spectroscopy (1977) 31, pp. 25–30.
[10]Lee J., Durst R. W., Wrolstad R. E., Journal of AOAC International, (2005),88 pp. 1269-1278.

HIGH-PERFORMANCE LIQUID CHROMATOGRAPHIC STUDY ON THE ENANTIOSEPARATION OF FLUORINE CONTAINING CYCLIC AMINO ACID DERIVATIVES

Tímea Orosz[1], Gyula Lajkó[1,2], Nóra Grecsó, Lóránd Kiss[2], Enikő Forró[2], Ferenc Fülöp[2], Antal Péter[1] and István Ilisz[1]

[1]Department of Inorganic and Analytical Chemistry, University of Szeged, H-6720 Szeged, Dóm tér 7, Hungary
[2]Institute of Pharmaceutical Chemistry, University of Szeged, H-6720 Szeged, Eötvös u. 6, Hungary
e-mail: orosz.ti@chem.u-szeged.hu

Abstract
The stereoisomers of several fluorinated cyclic β^3-amino acid derivatives and their nonfluorinated counterparts were separated on chiral stationary phases containing as chiral selectors cellulose tris-(3,5-dimethylphenyl carbamate), cellulose tris-(3-chloro-4-methylphenyl carbamate), cellulose tris-(4-methylbenzoate), cellulose tris-(4-chloro-3-methylphenyl carbamate), amylose tris-(3,5-dimethylphenyl carbamate) or amylose tris-(5-chloro-2-methylphenyl carbamate). The enantioseparations were carried out in normal-phase mode with n-hexane/alcohol/alkylamine mobile phases in the temperature range 5–40 °C. The effects of the mobile phase composition, the nature and concentration of the alcohol and alkylamine additives, the structures of the analytes and temperature on the separations were investigated.

Introduction
Chirality is eminently important for the modern pharmaceutical industry since many drug compounds are chiral molecules whose stereoisomers usually possess variant toxicological and pharmacological properties. In recent years, fluorine chemistry is an increasing interest in synthetic and medicinal chemistry in recent years because of its considerable impact in drug design. The property changes resulting from the replacement of one or more atoms in a molecule by fluorine may be especially significant from the aspect of biological activity. Fluorinated amino acid derivatives, for example, are of significance in medicinal chemistry in view of their more effective biological properties in comparison with those of their nonfluorinated derivatives: the special characteristics of the C–F bond and the fluorine atom can lead to modified properties as concerns the interactions with active sites of bioreceptors or enzymes [1, 2].

Experimental
The chromatographic system was a 1100 Series HPLC system which was equipped with a solvent degasser, a pump, an autosampler, a column thermostat, a multiwavelength UV–Vis detector and ChemStation chromatographic data software (Agilent Technologies, Waldbronn, Germany), and a corona-charged aerosol detector from ESA Biosciences Inc. (Chelmsford, MA, USA). Chromatography was performed in isocratic mode at a flow rate of 1.0 mL/min and a column temperature of 25 °C. Detection was accomplished with a corona detector. The HPLC columns used were Lux Cellulose-1, Lux Cellulose-2, Lux Cellulose-3, Lux Cellulose-4, Lux Amylose-1 and Lux Amylose-2 (250 × 4.6mm i.d., 5 μm particle size for all columns; Phenomenex, Torrance, CA, USA). The dead-time (t_0) of the column was determined via the injection of tri-t-butylbenzene.

Results and discussion

Effects of the chromatographic conditions on the chiral separation of fluorinated cyclic amino acid derivatives

Compounds investigated in this study were chromatographed on six different chiral stationary phase (CSPs) with mobile phases of n-hexane containing different alcohols (EtOH, PrOH, 2-PrOH, BuOH or t-BuOH) and alkylamine additives. The nature and concentration of the alcohol added were expected to exert considerable effects on the retention, selectivity and resolution, that is, the ratio of the nonchiral and chiral interactions between the CSP and the analytes might depend on these factors. The nonfluorinated derivatives exhibited lower k_1 values than those of the fluorinated ones. The highest α values were observed for the fluorinated derivatives when 2-PrOH was added. The changes in selectivity might be explained by specific changes in the supramolecular structure of the selector. The change caused in the structure of the CSP by the change of the nature and concentration of the alcohol may affect the chiral selectivity of the CSP, depending on the size and structure of the analyte [3].

The six polysaccharide-based CSPs display complementary features, with either some degree of separation efficiency or alternatively probable baseline separation. Separations were carried out with the same mobile phase composition, *n*-hexane–2-PrOH–DEA (90:10:0.1 v/v/v). Of the cellulose-based columns, CSP-3 appeared to be the least effective, since the tris-4-methylbenzoate substitution on the cellulose backbone was disadvantageous in these cases. Comparison of CSP-2 and CSP-4 revealed that k_1 was generally higher on CSP-4 than on CSP-2, while the α and R_S values obtained on CSP-2 were higher. It seems that the nonfluorinated and fluorinated cyclic amino acid derivatives may have stronger nonselective interactions with CSP-4 than with CSP-2. Comparison of the cellulose- and amylose-based selectors substituted with the same tris-(3,5-dimethylphenyl carbamate) (CSP-1 and CSP-5) or similar tris-(3- chloro-4-methylphenyl) carbamate (CSP-2) and amylose tris-(5- chloro-2-methylphenyl) carbamate (CSP-6) moieties demonstrated that k_1 was generally higher on the amylose-based CSPs. Higher α and R_S values were usually obtained on CSP-5 than on CSP-1 indicating more favorable interactions with the selector possessing a helical structure. The selectors' distinct structures and the different positions of the methyl and chlorosubstituents on the aromatic ring in the two selectors affectedthe selector–selectand interactions in different ways, resulting in different chromatographic behavior.

Effect of fluoro substitution

Fluoro substitution on the ring affects the polarity and steric arrangement and therefore the interactions between the selector and the analyte. Nonfluorinated derivatives was observed to have generally smaller k_1 values on all of the columns with the exception of CSP-6, on which the nonfluorinated derivatives were retained more strongly. The higher retention of the fluorinated derivatives was generally accompanied by higher α and R_S values. The fluorinated derivatives are probably capable of H-bonding interactions with the carbamate moiety of the selector. On the cellulose-based CSPs, higher k_1 values were generally obtained for analytes containing a double bond. Enhanced polarity of the molecules may improve the aromatic π–π interactions between the selectand and the selector, resulting in higher k_1 values, but this was not always accompanied by increased selectivity.

Effects of temperature and thermodynamic parameters

In order to investigate the effects of temperature on the chromatographic parameters, a variable-temperature study was carried out on CSP-2 and CSP-6 over the temperature range 5–40 °C. The retention factors and selectivities generally decreased with increasing temperature. All of the van't Hoff plots (ln α vs. 1/T) were linear, with good correlation coefficients. The Δ(ΔH)° and Δ(ΔS)° data exhibit both negative and positive values. When Δ(ΔH)° and Δ(ΔS)° were both negative, the secondeluted enantiomer fitted more strongly into the cavity of the selector, forming a more stable complex than in the case of the first-eluted enantiomer, and the negative entropy was less favorable for enantioseparation. The enantioseparation was enthalpically driven, as in the common case, and the selectivity decreased with increasing temperature. When Δ(ΔH)° and Δ(ΔS)° were both positive, the separation factor increased with increasing temperature, in parallel with decreasing retention. In this case, the change in the adsorption enthalpy with increasing temperature exerted a positive effect on the enantioselectivity. On the other hand, the positive Δ(ΔS°) compensated for the positive Δ(ΔH°) and resulted in a negative Δ(ΔG°). The enantioseparation was entropically driven.

Conclusion

The chromatographic retention behavior and resolution proved to depend on the nature and concentration of the alcohol additive, the temperature and the positions of the substituents. The nature of the alkylamine additives exhibited only slight effects on the chromatographic parameters. Of the studied CSPs, cellulose tris-(3-chloro-4-methylphenyl carbamate) and amylose tris-(3,5-dimethylphenyl carbamate) appeared the best suitable for the direct enantioseparation of the studied derivatives. The values of thermodynamic parameters such as the changes in Δ(ΔH°), Δ(ΔS°) and Δ(ΔG°) proved to depend on the structures of the analytes and on the chiral selector used. Most of the separations were enthalpically driven, but entropically driven separations were also observed.

Acknowledgements

This work was supported by the grants OTKA K 108847. A.P. is grateful to Gen-Lab Kft (Budapest, Hungary) and Phenomenex (Torrance, CA, USA) for the generous gifts of the Lux Cellulose and Amylose columns.

References

[1] Gouverneur V and Müller K. Fluorine in Pharmaceutical and Medicinal Chemistry: From Biophysical Aspects to Clinical Applications. Imperial College Press: London, 2012.

[2] Wang J, Sánchez-Roselló M, Aceña JL, del Pozo C, Sorochinsky AE, Fustero S, Soloshonok VA and Liu H. Fluorine in pharmaceutical industry: fluorinecontaining drugs introduced to the market in the last decade (2001–2011). Chemical Reviews 2014; 114: 2432.

[3] Wang T and Wenslow RM Jr. Effects of alcohol mobile-phase modifiers on the structure and chiral selectivity of amylose tris(3,5- dimethylphenylcarbamate) chiral stationary phase. Journal of Chromatography A 2003; 1015: 99–110.

TRANSFORMATION OF THIACLOPRID, A NEW INSECTICIDE, BY GAMMA RADIOLYSISIN AQUEOUS SOLUTIONS

Georgina Rózsa[1,2], Zsuzsanna Kozmér[1,2], Tünde Alapi[1], Krisztina Schrantz[1], Erzsébet Takács[2], László Wojnárovits[2]

[1]Department of Inorganic and Analytical Chemistry, University of Szeged, H-6720 Szeged, Dómtér 7, Hungary
[2]Radiation Chemistry Department, Centre for Energy Research, Hungarian Academy of Sciences, H-1121 Budapest, Konkoly-ThegeMiklósút 29-33, Hungary
e-mail: rozsa.georgina@chem.u-szeged.hu

Abstract

Degradation of organic pollutants in wastewater by ionizing radiation is an emerging technology. Using this method the transformation of thiacloprid takes place by reactions with free radicals (hydroxyl radical ($^{\bullet}OH$), hydrated electron (e_{aq}^{-}), hydrogen radical ($^{\bullet}H$), and hydroperoxyl radical/superoxide radical anion($HO_2^{\bullet}/O_2^{\bullet-}$)).Gamma (γ)radiolysis is an appropriatemethod to investigate the role of primary radicals in the transformation and degradation of thiacloprid. In this study we examined different reaction conditions (solutions of thiaclopridsaturated with dissolved oxygen or nitrogen or nitrous oxide),in order to investigate the effect of different radical sets formed.

Introduction

The traditional wastewater treatment processesare often not sufficiently effective in fully removing certain contaminants.The advanced oxidation processes (AOPs),including the γ radiolysis,represent an up-to-date technology [1]. Radiation chemistry is nowadays a well-established field of science, because it makes possible to isolate reactions of various radicals with the chemicals of interest.γ radiolysis issuitable for the study of the primary radical induced transformations, as described above.

The present study deals withthiacloprid, an insecticide within the family of neonicotinoids. This compound is widely used for protection of different crops, such as rapeseed, potatoes, sunflower, apple and corn seed dressing. Unfortunately, some representatives of the family of neonicotinoids weakenthe immune system of bees. Another problem is their high stability and good solubility in water (e.g. for thiacloprid: 184mgL^{-1} at 20^{o}C) [2].It consists of a chloronicotinyl ring,thiazole ring andcianoimino group.

During the γ radiolysis, the excited atomic nuclei's energy of excitation gets into ground state by photon emission. The emitted photons are mono-energetic and their energy are similar to the atomic nuclei. During radiolysis, the distribution of radicals in the solution is homogeneous, since they are forming in the whole solution. γ photons with 1.17 and 1.33 MeV energy,which are used in practice,are releasedfrom γ sources (eg. ^{60}Co) by neutroncapturing.

In aqueous solutions irradiated by γ photons the decomposition of water molecules results$^{\bullet}OH$,$e_{aq}^{-}$and (in the lower yield)$^{\bullet}H$, as primary species. These reactive species are surrounded by water molecules in a small volume part, called Spur[3]. The primary radicals are generated (Eq. 1) with yields (G-values) of 0.280, 0.280 and 0.062 μmol J^{-1}, respectively[4, 5].

$$H_2O + \gamma photon \rightarrow {}^{\bullet}OH + e_{aq}^{-} + {}^{\bullet}H \quad (1)$$

Using various dissolved gasses the radical set formed in solutions could be affected and therefore the effect of different species on the transformation or degradation of thiacloprid could be investigated.

In the presence of dissolved oxygen (DO) the reductive primary species ($^{\bullet}H/e_{aq}^{-}$) transform to less reactive $HO_2^{\bullet}/O_2^{\bullet-}$ (Eqs. 2 and 3).

$H^{\bullet} + O_2 \rightarrow HO_2^{\bullet}$ $k_2 = 1.2\times10^{10}$ L mol^{-1} s^{-1}[6](2)

$e_{aq}^{-} + O_2 \rightarrow O_2^{\bullet-}$ $k_3 = 1.9\times10^{10}$ L mol^{-1} s^{-1}[7](3)

The reaction of thiacloprid with e_{aq}^{-} could be examined in the presence of nitrogen (N_2). In nitrous oxide (N_2O) saturated solutions N_2O reacts with the $e_{aq}^{-}$and transforms it to$^{\bullet}OH$, and thereforein this case the examination of $^{\bullet}OH$ induced reaction mechanism of thiaclopridcanbe studied.

$e_{aq}^{-} + N_2O + H_2O \rightarrow N_2 + {}^{-}OH + {}^{\bullet}OH$ $k_4 = 9.1\times10^{8}$L mol^{-1} s^{-1}[5](4)

$^{\bullet}H + N_2O \rightarrow N_2 + {}^{\bullet}OH$ $k_5 = 2.1\times10^{6}$L mol^{-1} s^{-1}[5](5)

Experimental

2.1 Materials and equipment

During our experiments 10^{-4}mol L^{-1}thiacloprid solutions were irradiated by γ-rays of a ^{60}Co source in the presence of different gases (DO, $N_2$and N_2O). Thiacloprid was purchased from Sigma-Aldrich (99.9% purity). In γ radiolysis experiments the 5 mL ampoules with thiacloprid solution were placed to equal distance from the ^{60}Co-γ source of an SSL-01 panoramic type irradiator, to have a dose rate of 0.7 kGy h^{-1} (700 J kg^{-1} h^{-1}). The solutions were irradiated in open ampoules or in sealed ampoules saturated with N_2 or N_2O.

2.2 Analytical methods

Thiacloprid transformation wasfollowedat 242 nm wavelength with UV-Vis spectrophotometry (Agilent 8453 or Agilent 1200) in a 0.5 cm cuvette,as well as by high performance liquid chromatography (Agilent 1100 HPLC equipment using a LiChroCART® C18 reverse-phase column) with diode array detector (DAD). A mixture of methanol (70%) and water (30%) was used as eluent, at a flow rate of 0.6 ml min^{-1}. 20 μL samples were analysed.

Results and discussion

In Figure 1 the transformation kinetic curves of thiacloprid ($c_0 = 1.0\times10^{-4}$mol L^{-1}) are shown in the presence of DO, N_2 and N_2O.

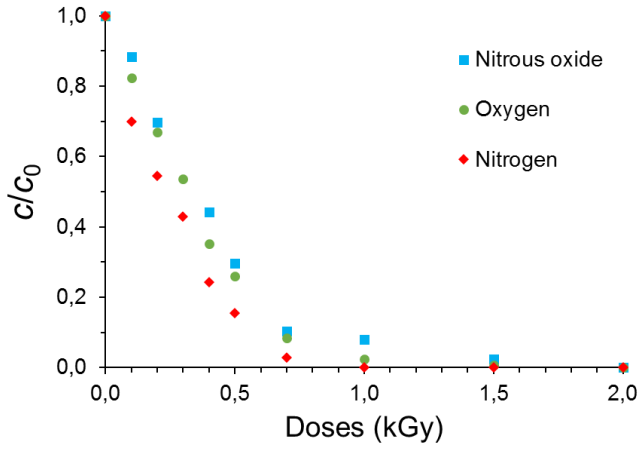

Figure 1. Kinetic curves of thiacloprid ($c_0 = 1.0\times10^{-4}$mol L^{-1}) transformation during γ radiolysis in the presence DO, N_2 and N_2O

The results show slightly increased transformation rate observed in presence of N_2. The initial rates of transformation (r_0) are 3.1×10^{-8}mol L^{-1} s^{-1} in the presence DO, 4.3×10^{-8} mol L^{-1} s^{-1} in the presence N_2 and 2.9×10^{-8}mol L^{-1} s^{-1} in the presence N_2O. Since the reactions of $e_{aq}^-$with thiacloprid were supressedby using DO and N_2O,and in these two cases the transformation rates of thiacloprid were lower than in the solution that did not contain any reactive dissolved gas (N_2 saturated samples),theseresults suggest that beside the $^{\bullet}OH$, e_{aq}^-also contributes to the transformation of thiacloprid.

Furthermore, under all three experimental conditions (DO, N_2O and N_2 saturated solutions) complete transformation of thiaclopridcould be achieved with 1.5 kGy absorbed dose.

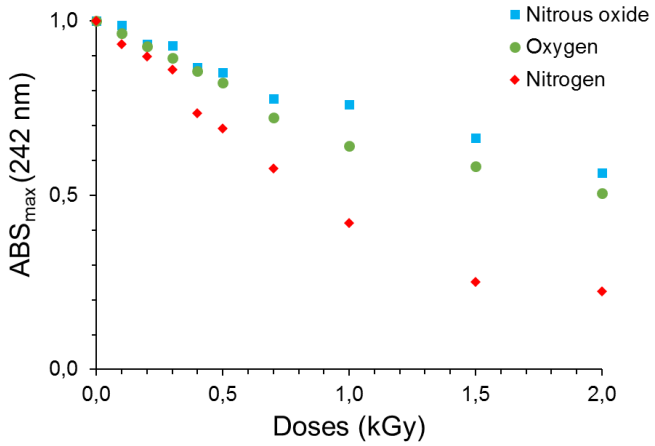

Figure 2. Absorption maximaof 1.0×10^{-4}mol L^{-1}thiacloprid solutions during γ radiolysis in the presence of DO, $N_2$and N_2O

UV-absorption of the thiacloprid solutions during radiolysiswere followedby UV-spectrophotometry between 200 and 350 nm. In the UV spectrum of thiacloprid there is an absorption maximum at 242 nm, and two shoulders around 220 and 270 nm. Based on literature data the strong absorption band with centre at 242 nm (ε_{max}= 18800 mol L^{-1} cm^{-1}) belongs to the 2-thiazolidinecyanamide part of the molecule.

The absorbance maximum changes of the solutionsversus absorbed doses arepresented in Figure 2.The results show that DO and N_2Osaturated solutions contained various intermediates in higher concentration than in N_2 saturated solution. After the total decomposition of thiacloprid (1.5 kGy), the absorbance of the nitrogensaturated solutions was less thanhalf of that of the initial solutions.This results show also thatthe transformationof the thiacloprid and its intermediateswas the most effective in presence of both $^{\bullet}OH$ ande_{aq}^- (in N_2 saturated solution).

The rate constants for the primary radical-induced transformationof thiacloprid will be examined with linear electron accelerator (Linac) in the future.The identification of the main intermediates of thiacloprid transformation will be investigated by HPLC equipped with a quadrupole mass spectrometric detector.

Conclusion

In the present study the effect of dissolved O_2 or N_2O, affecting the radical set formed, were investigated on theγ radiolysis of thiacloprid. Based on the results the dissolved $O_2$and N_2O

reduced slightly the transformation rate of thiacloprid, presumably due to the decreased e_{aq}^- concentration.Consequently, beside $^{\bullet}OH$, e_{aq}^- also contributes to the thiaclopridtransformation.

Acknowledgements
The financial support of the Swiss Contribution (SH7/2/20) is highly appreciated.

References
[1] E. Illés, E. Takács, A. Dombi, K. Gajda-Schrantz, K. Gonter, L. Wojnárovits, Radiation induced degradation of ketoprofen in dilute aqueous solution, Radiat. Phys. Chem., 81 (2012) 1479-1483.
[2] C.A. Morrissey, P. Mineau, J.H. Devries, F. Sanchez-Bayo, M. Liess, M.C. Cavallaro, K. Liber, Neonicotinoid contamination of global surface waters and associated risk to aquatic invertebrates: a review, Environment International, 74 (2015) 291-303.
[3] L. Wojnárovits, Sugárkémia, Akadémiai Kiadó, Budapest, 2007.
[4] G.V. Buxton, The radiation chemistry of liquid water: Principles and applications., in: A. Mozumder, Y. Hatano (Eds.) Charged particle and photon interaction with matter, Marcel Dekker, New York, 2004, pp. 331-365.
[5] J.W.T. Spinks, R.J. Woods, An introduction to radiation chemistry 3rd edition, Wiley-Interscience, New-York, 1990.
[6] G.V. Buxton , C.L. Greenstock , W.P. Helman , B.A. Ross, Critical review of rate constants for reactions of hydrated electrons,hydrogen atoms and hydroxyl radicals ($^{\cdot}OH/^{\cdot}O^-$) in aqueous solution, in: A.I.o.P.a.t.A.C. Society (Ed.)USA, 1988, pp. 513-886.
[7] G.V. Buxton, C.L. Greenstock, W.P. Helman, A.B. Ross, Critical-review of rate constants for reactions of hydrated electrons, hydrogen-atoms and hydroxyl radicals ($^{\cdot}OH/^{\cdot}O^-$) in aqueous-solution, J. Phys. Chem. Ref. Data., 17 (1988) 513-886.

FABRICATION OF SIZE-CONTROLLED COPPER NANOPARTICLES WITH DIFFERENT METHODS

Kriszta Pencz[1*], Koppány L. Juhász[2], András Sápi[2], Ákos Kukovecz[2], Zoltán Kónya[2]

[1]Department of Physical Chemistry and Materials Science, University of Szeged, H-6720 Szeged, Rerrich Béla tér 1., Hungary
[2]Department of Applied and Environmental Chemistry, University of Szeged, H-6720 Szeged, Rerrich Béla tér 1., Hungary
e-mail: penczkriszta92@citromail.hu

Abstract

The opportunity of using photocatalists in photocatalytical reactions is a very exciting and promising topic, thus it is one of the most popular and intensively growing research field in chemical sciences. Photocatalysis can give us alternative options for watersplitting and CO_2 reduction. Copper particles with proper size and shape could be a good candidate for further application.[1,2]

In our work we introduce two different methods for syntetizing copper nanoparticles with different sizes. Our first method is a solvothermal synthesis in nitrate salt bath, the second is a solvochemical method in room temperature (~26°C), in latter case stabilizers are used. The precursors were water-soluble copper salts ($C_{10}H_{16}CuO_4$, $CuSO_4$) in each method, and the reductive components were oleylamine and $NaBH_4$. During the experiments, we studied the effect of the temperature, reaction time and contcentrations of the components. According to our experience, size-controlling of copper nanoparticles is available with these synthesis methods. Our samples were investigated with Transmission Electron Microscopy and with Dynamic Light Scattering.

[1] Zhenni Wang, Guang Yang, Zhaorui Zhang, Mingshang Jin, and Yadong Yin, *ACS Nano, 2016, 10 (4), 4559–4564*

[2] Kendra P. Kuhl, Etosha R. Cave, David N. Abram and Thomas F. Jaramillo, *Energy Environmental Science., 2012, 5, 7050-7059*

ROOM TEMPERATURE ETHANOL SENSOR WITH SUB-PPM DETECTION LIMIT: IMPROVING THE OPTICAL RESPONSE BY USING MESOPOROUS SILICA FOAM

Dániel Sebők[1,*], László Janovák[1], András Sápi[2], Dorina G. Dobó[2,3], Ákos Kukovecz[2,3], Zoltán Kónya[2,4], Imre Dékány[1,5]

[1]Department of Physical Chemistry and Materials Science, University of Szeged, 1 Rerrich square, H-6720 Szeged, Hungary
[2]Department of Applied and Environmental Chemistry, University of Szeged, 1 Rerrich square, H-6720 Szeged, Hungary
[3]MTA-SZTE "Lendület" Porous Nanocomposites Research Group, University of Szeged, 1 Rerrich square, H-6720 Szeged, Hungary
[4]MTA-SZTE Reaction Kinetics and Surface Chemistry Research Group, University of Szeged, 1 Rerrich square, H-6720 Szeged, Hungary
[5]MTA-SZTE Supramolecular and Nanostructured Materials Research Group, University of Szeged, 8 Dóm square, H-6720 Szeged, Hungary
e-mail: sebokd@chem.u-szeged.hu.hu

Abstract

In this paper a low ppm-range ethanol sensor - operating at room temperature - is presented. The three types of ZnO_2 based hybrid thin films as sensor surfaces consist of semiconductor nanoparticles, polyelectrolyte (polyacrylic acid, PAA) and/or mesoporous silica. The thin films were prepared by Layer-by-Layer (LbL) self-assembly method and were subjected to reflectometric interference measurements (RIfS) for testing sensorial application. The sensor investigation showed that the detection limit of the thin films is in the sub-ppm range. Applying mesoporous silica as surface coating or interlayers in the sandwich-structured thin film (ZnO/SF) improved the optical response, but the sensitivity showed non-linear characteristic. The thin film with mixed structure (ZnO/PAA/ZnO/SF) showed linear response in the 0.5-12 ppm range with 0.6 nm /ppm sensitivity and acceptable selectivity.

Introduction

Sensors for volatile organic compounds (VOCs) play an important role in everyday life and industrial safety. These chemical agents are harmful and unhealthy, so the detection of these molecules has a great importance in environmental and health protection, such as in air and water quality control, food industry or – especially in the case of ethanol – the "driving under influence" (DUI) control. The principles, technical solutions, the materials used, the operating temperature ranges and concentration levels are fairly diversified. The studies can be divided into two major groups: room temperature (RT) and high temperature (around 200 and 300 °C) applications. However, it has to be noted that VOC pollutants easily evaporate at room temperature and can be very harmful and carcinogenic already at low concentration, but the most of the RT technical solutions are able to detect ethanol vapour only above 10 ppm concentration.
In this work, we made an attempt to combine the beneficial sensing properties of mesoporous materials and reflectometric interference technique [1-3] to construct a highly sensitive ethanol sensor operating at room temperature.

Experimental

Zinc peroxide nanoparticles with an average diameter of 80 nm were synthesized by the photolysis of zinc acetate dehydrate ($C_4H_6O_4Zn \cdot 2H_2O$, Fluka, a.r.) described in [2]. Poly(acrylic acid) (PAA, M_W = 100000, Sigma, a.r.) was used as a negatively charged polyelectrolyte. Furthermore, SBA-15 and silica foam were used as coatings or negatively charged interlayer materials. Five types of hybrid thin films were prepared by using the ZnO_2 nanoparticles, negatively charged PAA polyelectrolyte and the mesoporous silica samples (see Figure 1.) by the LbL deposition method.

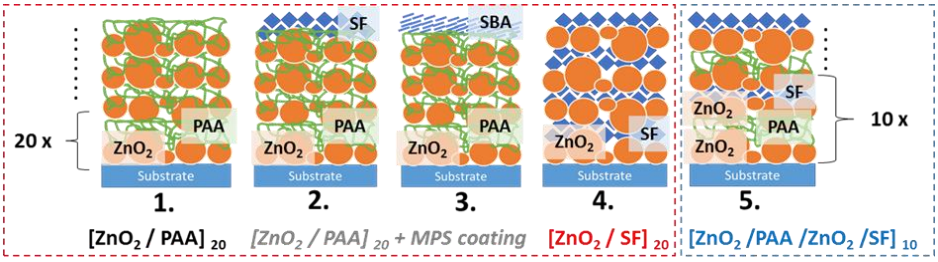

Figure 1. The schematic view of the prepared and applied hybrid thin films.

The specific surface area (BET method) and the total pore volume were determined by the BJH method using a Quantachrome NOVA 2200 gas sorption analyzer by N_2 gas adsorption/desorption at 77 K. SAXS technique was used to investigate the fractal properties and structural parameters of the mesoporous silica components. SAXS curves were recorded with a slit-collimated Kratky compact small-angle system (KCEC/3 Anton-Paar KG, Graz, Austria) equipped with a position-sensitive detector (PSD 50M from M. Braun AG Munich, Germany) containing 1024 channels 55 μm in width. CuK_α radiation ($\lambda_{CuK\alpha}$=0.1542 nm) was generated by a Philips PW1830 X-ray generator operating at 40 kV and 30 mA. The optical and sensorial properties of the thin films were studied by a Nanocalc 2000 spectrophotometer with ADC1000-USB A/Dconverter (Ocean Optics) (see Figure 2.).

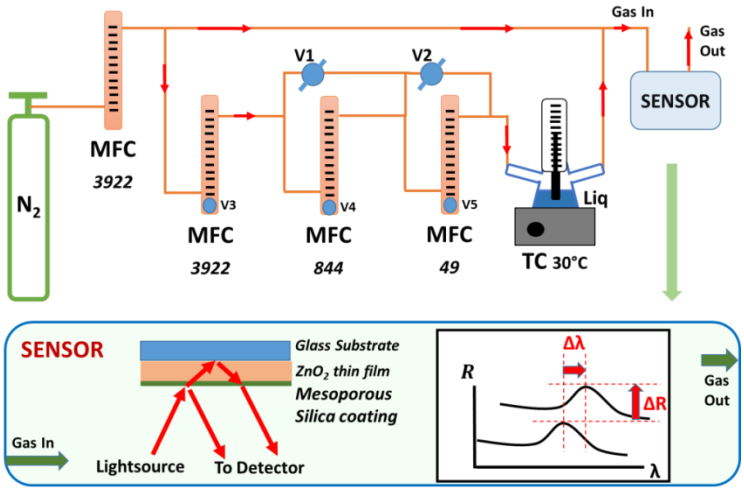

Figure 2. Scheme of the used experimental setup (gas flow system and reflectometric test cell) and the measurement principle.

The sensor responses, Δλ (nm) and ΔR (a.u.) were defined as the wavelength shift of the given extreme of the reflection spectra and the change of the reflection value corresponding to this extreme, respectively.

Results and discussion

The porosity, pore system characteristic and specific surface area are of great importance in the case of mesoporous adsorbents used in sensorial applications, therefore several structural parameters were determined and calculated by using SAXS technique. The double logarithmic plot of the scattering curve is suitable for determining the fractal properties of the material. In the case of SBA-15 the slope is approximately -2 in the higher *h*-range, which indicates a frame-like mass fractal structure, as well as, p = -3.5 for SF sample is characteristic for the surface fractal nature of the mesocellular foam structure. The N_2 adsorption/desorption studies of the silica samples show isotherms with hysteresis loop and pore size distributions between 3 and 10 nm characteristic for mesoporous materials. The specific surface areas and average pore diameters are 798 m^2g^{-1}, 4.2 nm and 666 m^2g^{-1}, 4.6 nm for SBA-15 and SF, respectively. The overall conclusion is that although the structural and fractal nature of these mesoporous materials are significantly different, but the average pore diameters and specific surface areas are similar, and these values appear to be sufficiently high for considerable adsorption capacity and sensorial applications.

The thin films were subjected to reflectometric interference measurements for testing sensorial applications. The measurements were carried out by measuring the shift of the local minimum of reflected intensity near λ=500 nm wavelength. It is λ_{min}=457 nm in the case of $[ZnO_2/PAA]_{20}$, and λ_{min}=507 nm and 568 nm for $[ZnO_2/PAA/ZnO_2/SF]_{10}$ and $[ZnO_2/SF]_{20}$, respectively (these values are valid in the *t=0* measurement point). The raw results (sensorgrams), i.e., the *Δλ vs. t* curves are presented in Figure3 (left side).In the case of *Δλ* curves the responses are positive because of the optical thickness increases due to the vapour adsorption. Significant signal drift can be observed in the case of ZnO_2/PAA, ZnO_2/PAA+coating and ZnO/SF thin films, which is rather disturbing phenomenon: should be drift compensation applied? In this case, not in general. If compensation is used then the responses become nearly independent of concentration; if it is ignored then each measurement step (at the same concentration) results in higher response than the previous one and this fact makes impossible to accurately determine unknown concentrations. As it can be seen on the *Δλ* calibration (response vs. concentration) curves (Figure 3., right side), we did not apply compensation, the responses increase with concentration, even if not linearly. However, in the case of $[ZnO_2/PAA/ZnO_2/SF]_{10}$ hybrid thin film response drift was not observed which resulted a linear Δλ calibration curve (0.586 nm/ppm). In summary, it was found that applying $[ZnO_2/PAA]$, $[ZnO_2/PAA]$+MPS coating or $[ZnO_2/SF]$ structured thin layers mostly failed due to the signal drift and nonlinear sensitivity. The mixed structure of $[ZnO_2/PAA/ZnO_2/SF]$ was devoid of drift and showed linear calibration curves, so this type of hybrid (nanoparticle/polyelectrolyte/mesoporous silica) multilayer is an appropriate structure to apply as sensing surface in reflectometric interference sensor in gas phase.

Based on the presented results the $[ZnO_2/PAA/ZnO_2/SF]_{10}$ thin film was selected for further experiments, such as reproducibility, response time analysis and selectivity. It can be stated that the sensors signal is well reproducible, the sensors response reaches the 90 % of maximum value within 40 s and it is relaxed to 10 % within 80 s. Selectivity test was carried out by using methanol, ethanol, *n*-hexane, toluene and xylene. It was established that in the case of ZnO_2/PAA/SF mixed structure 2-3 times higher response was observed for ethanol than for the

other volatile organic compounds (VOC), although also the affinity to aromatic molecules increased compared to ZnO_2/PAA structure.

Next the $[ZnO_2/PAA/ZnO_2/SF]_{10}$ thin film was subjected to sensorial test in a higher, c=2.46-37 (±0.68) ppm range. The concentration steps (0-50 min) were repeated after a 50 min long baseline stability test. The statement was that the sensor has a fairly stable baseline (without drift), but the Δλ calibration curve showed a slight quadratic deviation from linear behavior.

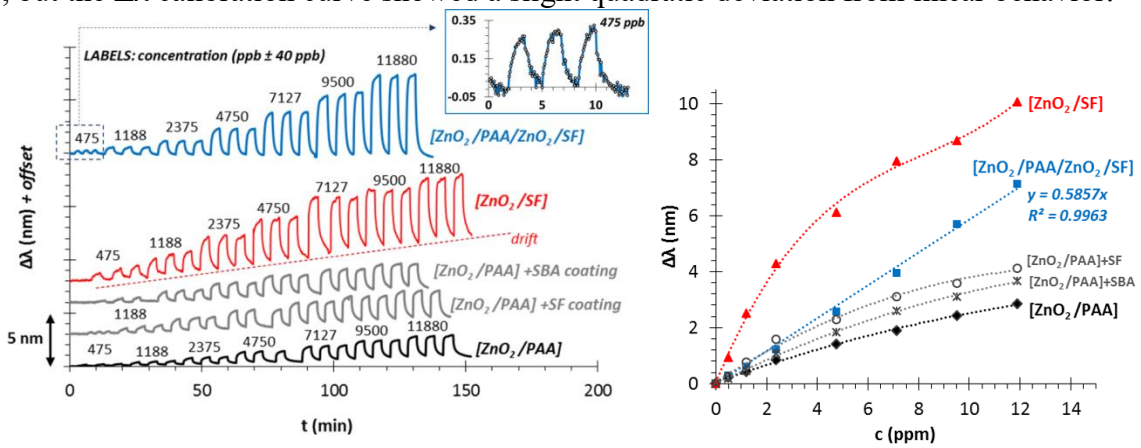

Figure 3. Ethanol sensing tests: *Δλ vs. t* curves for the tested thin films; inset: response of $[ZnO_2/PAA/ZnO_2/SF]_{10}$ mixed structure for c=475 ppb EtOH (left) and ethanol sensing *Δλ(nm) vs. c(ppm)* calibration curves for the prepared thin layers (right) (labels: structure of the thin films and calibration equation for $[ZnO_2/PAA/ZnO_2/SF]_{10}$ mixed structure).

Conclusions

In this work we successfully combined the beneficial sensing properties of mesoporous silica materials and reflectometric interference technique to construct a highly sensitive ethanol sensor operating at room temperature. The structural parameters and fractal properties of the silica samples (SBA-15 and silica foam) were studied by TEM, BET and SAXS techniques: latter methods showed that the specific surface area of the MPSs is over 650 m^2/g. The three types of hybrid thin films, namely ZnO_2/polyelectrolyte (PAA), ZnO_2/mesoporous silica foam (SF) and a mixed, ZnO_2/PAA/ZnO_2/SF structures were subjected to sensorial tests in the gas phase. We showed that the detection limit of the sensor is sub-ppm (< 500 ppb), but only the mixed (ZnO_2/PAA/ZnO_2/SF) nanostructure showed linear sensitivity in the 0.5-11.9 ppm range without response drift, while both the response time and selectivity remain reasonable good. Testing the sensor in extended (up to 40 ppm) concentration range showed a slight quadratic deviation from linear behavior.

Acknowledgements

The authors are very thankful for the financial support from The Hungarian Scientific Research Fund (OTKA) PD 116224. The work was earlier supported by the European Union and the State of Hungary, co-financed by the European Social Fund in the framework of TÁMOP 4.2.4. A/2-11-1-2012-0001 'National Excellence Program'.

References

[1] D. Sebők, Edit Csapó, Nóra Ábrahám, Imre Dékány, Reflectometric measurement of *n*-hexane adsorption on ZnO2 nanohybrid film modified by hydrophobic gold nanoparticles, Appl. Surf. Sci. 333 (2015) 48–53.

[2] D. Sebők, T. Szabó, I. Dékány, Optical properties of zinc peroxide and zinc oxide multilayer nanohybrid films, Appl. Surf. Sci. 255 (2009) 6953–6962.

[3] D. Sebők, I. Dékány, ZnO_2 nanohybrid thin film sensor for the detection of ethanol vapour at room temperature using reflectometric interference spectroscopy, Sensor. Actuat. B-Chem. 206 (2015) 435–442.

LIQUID PHASE HYDROSILYLATION OVER SIZE-CONTROLLED Pt NANOPARTICLES

Dániel Sipos, András Sápi, Dorina G. Dobó

Department of Applied and Environmental Chemistry, University of Szeged, 1 Rerrich square, H-6720 Szeged, Hungary

Abstract

Hydrosilylation reactions give important materials as high potential medical transfer molecules or additives in the rubber industry [1,2]. These reactions were based on homogeneous catalysts in the second half of the last century. Noble metal based heterogeneous catalysts were tested for such reactions since the 90's [3], however the effect of size controlled nanoparticles is unknown. In this study, Platinum nanoparticles with a diameter of 1.6, 4.8, 8.3 nm were anchored onto SBA-15 silica support and tested in phenylacetylene hydrosilylation with triethylene silane. The catalysts were characterized with Inductively Coupled Plasma Mass Spectroscopy (ICP-MS) and Transmission Electron Microscope (TEM). The effect of the size of the Pt nanoparticles on the activity and selectivity of the liquid phase reactions were tested and monitored by Gas Cromatography (GC-MS). Based on our results it can be stated, that the 8.3 nm Pt nanoparticles is 10 times more active compared to the 1.6 nm Pt NPs. We also experienced striking differences in the selectivity of the products based on different sized Pt nanoparticles. Size controlled Pt nanoparticles can be the future for governing hydrosilylation reactions towards high activity and 100% selectivity.

Figure 1.: Schematic of the hydrosylilation reaction

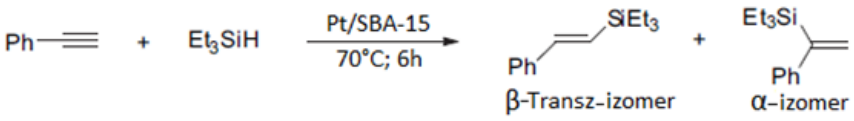

[1] F. Alonso, et al., Journal of Organometallic Chemistry, 2010

[2] B. Marciniec, J. Gulinski, W. Urbaniak, Z.W. Kornetka, Comprehensive Handbook on Hydrosilylation, B. Marciniec (ed) Pergamon Press, Oxford, 754 (1992)

[3] Mario Pagliaro, Rosaria Ciriminna, Valerica Pandarus, and François Béland Eur. J. Org. Chem. 6227–6235, (2013)

SYNTHETISATION AND CHARACTERISATION OF PLATINUM NANOPARTICLES IN A WIDE RANGE OF SIZE

Ákos Szamosvölgyi, Koppány Levente Juhász, András Sápi, Mária Szabó, Dorina Dobó, Ákos Kukovecz, Zoltán Kónya

Department of Applied and Environmental Chemistry, University of Szeged, H-6720 Szeged, Dóm tér 7, Hungary
e-mail: akos.szamosvolgyi@gmail.com

Abstract

Discovering new alternative catalysts for (industrial) organic reactions is an important and challangeing task. Use of transition metals in these kind of reactions has had success since the begining of the 19th century. Development of nanostructure related methods can help us to enhance these reactions. This study showcases different methods that were developed for synthetising nanostructured platinum crystals in a wide range of size. (1-100nm) Production of smaller nanoparticles requires ethylene glycol as solvent, while more robust crystals can be formed in a watery solution. The process could be made either with the use of proctecting organic groups or without; these properties provide good flexibility considering the further usage of the nanoparticles. Characterisation of the nanoparticles involved measurements with Transmission Electron Microscopy and Dynamic Light Scattering, these methods have showed the monodisperse size distribution and spherical geometry of the nanocrystals.

FLAME ATOMIC ABSORPTION SPECTROSCOPY IN MINERAL ANALYSIS OF BARLEY FROM BANAT AREA

Mirela Ahmadi[1], Dorel Dronca[2], Cornelia Milovanov[3], Camelia Tulcan[1], Oana-Maria Boldura[1], Călin Mircu[4], Ioan Huţu[3], Ion Violeta[5], Mihaela Scurtu[5]

[1]Department of Chemistry and Biochemistry, Banat University of Agriculture Sciences and Veterinary Medicine "King Michael I of Romania" from Timisoara (USAMVB), Timisoara – 300645, Calea Aradului 119, România.
[2]Department of Animal and Plant Genetic Improvement, USAMVB, Calea Aradului 119, Timişoara – 300645, România.
[3]Department Animal Production and Veterinary Public Health, USAMVB, Calea Aradului 119, Timişoara – 300645, România.
[4]Department of Genetically Engineering, USAMVB, Calea Aradului 119, Timişoara – 300645, România.
[5] S.C. Scient CromatecPlus – Research Development Innovation Centre for Instrumental Analysis S.R.L., Str. Petre Ispirescu, nr 1, Sat Tancabesti, Com. Snagov, Ilfov – 077167, România.
e-mail: ddronca@animalsci-tm.ro

Abstract
Barley as a cereal grain is very important for animal and human nutrition, being also used in food products technology for fermented or distillated beverages. It has very good nutritional properties for animals and human, being the forth ranks in cultivation and quantity production in the world. The flame atomic absorption spectroscopy (FAAS) is an analysis method for metals, but the laboratory procedure is essential for the final result. Our goal was to analysis the barley content from Banat area with FAAS method using direct determination from the solution after digestion and using a diluted solution. The direct determination for copper content in barley (in mg/Kg, presented as mean and SD) was 4.146±0.205; iron content was 25.657±0.583; manganese determination was 10.391±0.192 and zinc content was 17.911±0.565. The quantity of metals (in mg/Kg, presented as mean and SD) from diluted (5x) samples for copper was 4.463±0.403; for iron was 26.821±1.083; for manganese was 11.136±0.444; for zinc was 18.731±0.665. Comparative evaluation of the mineral content for copper, iron, manganese and zinc showed that the quantitative analysis of five times diluted samples present higher values for all analyzed minerals comparative with direct determination.

Introduction
Barley is a cereal grain, part of the grass family, and it is also known as *Hordeum vulgare*. The importance of barley (cereal grain) is provided by the content of dietary fiber (especially □-glucan) and other complex carbohydrates, well balance of amino acids (tryptophan) and proteins, low lipids, and good source of enzymes, minerals (selenium, copper, manganese, phosphorus, magnesium) and vitamins (thiamine, niacin, especially tocopherols). The mineral content of barley is very important for animal diet and also in beer technology, but this is correlated with the soil and water characteristics from cultivation area (Aldughpassi et al., 2016).
Diabetes people depend on a healthy diet, rich in fibers and characterized by low glycemic index. Naked barley (*Hordeum vulgare*) is a low glycemic index grain, which contains soluble fibre of ß-glucan in higher quantities compared to hulled barley. Naked barley and naked oats were tested for glycemic index, and naked barley presented significant lower glycemic index comparative

with oats (Steele et al., 2013).
The nutraceutical products based on ß-glucan depends very much of the carbohydrate structure. Thus, the chemical structure, the size and the viscosity are characteristics that could be influenced by the germination stage and the processing method (ex. Microwave). Ahmad in 2016, demonstrated experimentally that in germinated barley for ß-glucan was lower compared to ß-glucan obtained from microwave processed barley or from unprocessed barley (Ahmadi, 2016).
Barley is used in. the morning meal for human, because brings fibers and manganese – which is great for nervous system. The regularly consumption of barley can modulate the blood sugar, helps in weight loss – reducing the visceral fat tissue, reduces the blood pressure and cholesterol, reduce the risk of cancer disease and heart diseases, reduce the symptoms of arthritis, has anti-aging properties (Baik and Ullrich, 2008; Olson 2016; Sheikh, 2016; Stanca et al., 2016).

Experimental

Our aim was to analyze the barley cultivated in Timis County, with flame atomic absorption spectroscopy, and to evaluate if the dilution influences the final result.
First stage was to harvest barley from the Timis County field, more precisely from Libling. Then, for flame atomic absorption spectroscopy we made a digestion for every single sample, using azotic acid 65% (15.8mol/l), Merck and Milli-Q water, and then we made the quantitative analyze for copper, iron, manganese and zinc. The analytical determination for minerals was conducted into two directions: the direct analyze and the analyze from dilution (five times dilution). For reading the concentration of copper, iron, manganese and zinc with worked with a Flame Atomic Absorption Spectroscopy and then we calculate the final concentration depending to the quantity of barley took as initial sample for digestion. The accuracy, precision, repeatability and also stability were the results were presented comparatively, and the unit was mg of metal to kg barley. The results were presented as mean (average) and standard deviation (SD).

Results and discussion

Different method of minerals analysis are presented in the literature, referring to different temperature program for digestion, different concentration of azotic acid or even different acid, and of course various analytical equipment. The results of our study are presented in figure 1.

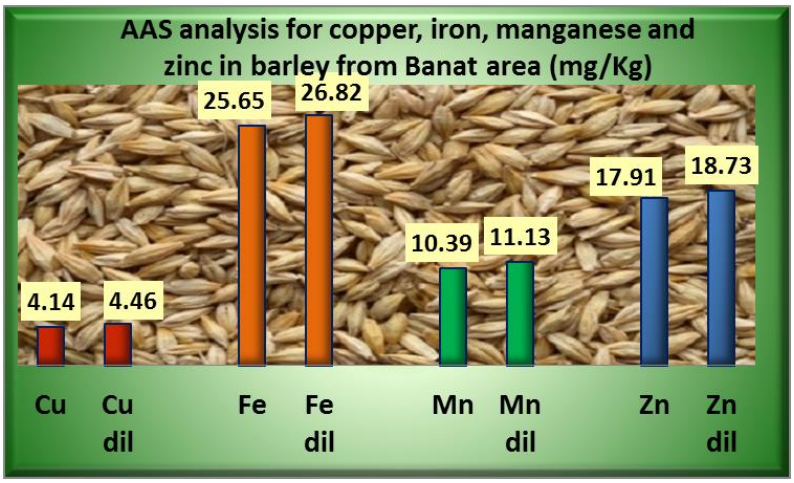

Figure 1. Copper, iron, manganese and zinc AAS analysis in hole barley (*Hordeum vulgare*) from Banat area (direct and 5 times dilluted determination)

All concentrations determination for copper, iron, manganese and zinc, were similar after direct or 5 times diluted determination. Concentrations were calculated as mean (average) and standard deviation in mg/kg, and for direct determination in barley the concentration was: copper content 4.146±0.205; iron 25.657±0.583; manganese 10.391±0.192 and zinc 17.911±0.565; but for diluted (five times) samples for copper was 4.463±0.403; iron was 26.821±1.083; manganese was 11.136±0.444; zinc was 18.731±0.665.

Our results for copper, iron, manganese and zinc concentration from barley were similar with the results presented by other authors in the literature data, even if some condition were not the same (the variety of the barley, the soil composition, the analytical equipment).

The mineral content of different cereals was studied from long time ago, because the chemical mineral composition of cereals is important for the animal and human diet, for the characterization of the soil, and for the fermented and distilled products using barley as substrate.

Thus, Liu and other collaborators presented in 1974 a report of mineral components in milled barley from United States Department of Agriculture, Wisconsin. The results presented 4.0mg/kg copper, 28.0mg/kg iron, 11.0mg/kg manganese, 22.8mg/kg zinc, 257mg/kg calcium, 138mg/kg sodium, 10.2mg/kg aluminum, 0.37mg/kg molybdenum, 1,290mg/kg magnesium, 4,390mg/kg potassium and 2,970mg/kg phosphorus, determined from whole kernel of Atlas barley (Liu et al., 1974). Also, Liu and Zhang in 2010 determined the content of some minerals from hulled barley by ultraviolet and flame atomic absorption spectrometry and the results presented K > S > Mg > Ca > Fe > Na > Zn > Mn > Cu.

There are different methods for investigation of mineral content from grains. Energy dispersive X-ray analysis and neutron activation analysis can also be used for calcium, magnesium, phosphorus and potassium content from different anatomical parts of grains. Thereby, using energy dispersive X-ray method it was investigated the content of calcium related to phosphorus, magnesium and potassium from aleurone cells protein of barley. The results demonstrated that calcium is found in very small quantities compared to P, Mg and K in endosperm. But if the endosperm was used for seedling, the new barley seedlings took over some minerals from endosperm to develop in a new plant (Stewart et al., 1988).

Not only the biomineral plants are important for grain, but heavy metals are also evaluated because the physiology of the plant, crop quality and production is negatively affected; and the quality of cereals are absolutely involved in the quality of food or beverages having the cereals as ingredients. So, heavy metals are contaminants that could be present in the soil and water due to the pollution. Thus, it is very easy for plants to cumulate toxic metals during growing from soil and water. Advanced technologies and analysis techniques involve transcription factors (transcriptomics), metabolites (metabolomics), stress in proteins (proteomics) and mineral elements (ionomics), for evaluate the stress induced by pollution, and also to evaluate the heavy metals tolerance with economic consequences (Singh et al., 2015).

Genetic engineering tries to find new ways to modify the gene of barley, to provide all the nutrients for an optimal growth. Generally, the cereals require macronutrients (nitrogen, phosphorus, potassium, calcium, magnesium, sulphur) and micronutrients (chlorine, boron, iron, manganese, copper, zinc, nickel, and molybdenum). The production of barley is often limited by the phytoavailability of the nutrients, with consequences in the quality of crop (White and Brown, 2010).

New technology provides new challenges in agriculture, food technology, molecular biology and other domains. Thus, the molecular biology work to the gene of cereals, and particularly to barley, modify the genetic characteristic to obtain genetic modify plants that are rich in some

nutrients or are more tolerant for different limiting growth factors (Fujii et al., 2012). One example of this molecular biology technics is genetic modify barley to be more tolerant for aluminum toxicity – this being a very important agriculture characteristic in areas where barley is cultivated on acidic soils, like Middle East.

Conclusion

Crop quality is very important for economic, nutritional, technological point of view. Barley is a grain used in agriculture for food and feed, being used as cereals or for food and beverage technology. The biominerals and heavy metals from barley are important to evaluate the quality and quantity crop, the possibility to use the cereals in human or animal nutrition. *Hordeum vulgare* (barley) is a good vegetal source for benefic minerals, and the barley seedling are taking over the nutrients from endosperm to grow. The distribution of minerals in various anatomical parts is different in grains. For all the samples the concentration of copper, manganese, iron and zinc was in normal limits compared to the literature data. Concentration of the tested biominerals was similar for both direct and dilluted using flame atomic absoption analysis, but for all the minerals from barley (copper, manganese, iron and zinc) th concentration determined after five times dillution was higher then the direct determination.

References

[1] M. Ahmad, A.Gani, A. Shah, A. Gani, F.A. Masoodi, Germination and microwave processing of barley (*Hordeum vulgare* L) changes the structural and physicochemical properties of b-D-glucan and enhances its antioxidant potential, Carbohydrate Polymers, 153(11), 696-702.
[2] A. Aldughpassi, T.M.S. Wollever, E.S.M. Abdel-Aal, Barley, Reference Module in Food Science, Encyclopedia of food and health (2016), 328-331.
[3] B-K. Baik, S.E. Ullrich, Barley for food: characteristic, improvement, and renewed interest, Journal of Cereal Science, 48(2), (2008), 233-242.
[4] M. Fujii, K. Yokosho, N. Yamaji, D. Saisho, M. Yamane, H. Takahashi, K. Sato, M. Nakazono, J.F. Ma, Acquisition of aluminium tolerance by modification of a single gene in barley, Nat. Commun., 3, (2012), 713-722.
[5] D.J. Liu, G.S. Robbins, Y. Pomeranz, Composition and utilization of milled barley products. IV. Mineral components, Cereal Chemistry, 51(3), 309-316.
[6] J. Liu, H.G. Zhang, Determination of nine mineral elements in hulled barley by ultraviolet spectrophotometry and flame atomic absoption spectrometry, Guanq Pu Xue Yu Guang Pu Fen Xi, 30(4), (2010, 1126-9.
[7] S. Olson, Barley Bread can reduce appetite, cut blood glucose level, and lower risk factors for diabetics, Vitality (2016), Febuary 10.
[8] B. Sheikh, The role of prophetic medicine in the management of diabetes mellitus: A review of literature, Journal of Taibah University Medical Sciences, 11(4), (2016), 339-352.
[9] S. Singh, P. Parihar, R. Singh, V.P. Singh, S.M. Prasad, Heavy metal tolerance in plants: role of transcriptomics, proteomics, metabolomics and ionomics, Front Plant Sci., 6, (2015), article 1143, 1-36.
[10] A.M. Stanca, Gianinetti A., Rizza F., Terzi V., Encyclopedia of Food Grains (Second Edition), Vol. 1: The world of food grains (2016) 147-152.
[11] K. Steele, E. Dickin, M.D. Keerio, S. Samad, C. Kambona R. Brook, W. Thomas, G. Frost, Breeding low-glycemic index barley for functional food, Field Crops Research, 154 (2013), 31-39.
[12] A. Stewart, H. Nield, J.N.A. Lott, An investigation of the mineral content of barley grains

and seedlings, Plant Physiol., 86(1), (1988), 93-97.
[13] P.J. White, P.H. Brown, Plant nutrition for sustainable development and globaal health, Ann. Bot., 105(7), (2010), 1073-1080.

EFFECT OF VARIOUS RADICAL TRANSFERS AND SCAVENGERS ON THE TRANSFORMATION OF PHENOL OVER UV IRRADIATED TiO_2

Milán Molnár[a], Krisztina Schrantz[a], Zsuzsanna Kozmér[a], Klára Hernádi[b], Tünde Alapi[a]

[a]Department of Inorganic and Analytical Chemistry, Institute of Chemistry, University of Szeged, Dóm tér 7, H-6720 Szeged, Hungary
[b]Department of Applied and Environmental Chemistry, Institute of Chemistry, University of Szeged, Rerrich Béla tér 1, H-6720 Szeged, Hungary

Abstract
The influence of a radical scavenger methanol (MeOH) and tert-butanol (t-BuOH)) on the transformation rate and radical set during heterogeneous photocatalytic transformation of a simple model compound, phenol (PhOH, 1.0×10^{-4} mol L^{-1}) is discussed in this study. PhOH solutions were treated in the presence of 5.0×10^{-1} mol L^{-1} MeOH and t-BuOH under deoxygenated and O_2-saturated reaction conditions. The rate of transformation of PhOH increased significantly in the presence of dissolved O_2. The radical scavenger materials used strongly reduced the rates of transformation of PhOH both in O_2 saturated and O_2-free solutions.

Bevezetés és célkitűzés
A nehezen átalakítható szerves szennyezőkkel szemben egy lehetséges megoldást kínálnak az olyan oxidációs reakciókon alapuló módszerek, melyek során a szerves szennyezők lebontására alkalmas reaktív részecskéket generálunk vizes oldatokban. Ezeket nevezzük *nagyhatékonyságú oxidációs eljárások*nak. A reaktív részecskék generálására többféle módszer létezik, ilyen például a heterogén fotokatalízis. A heterogén fotokatalízis tervezésének fontos feltétele, hogy megismerjük a rendszerben lejátszódó folyamatokat, a képződő reaktív részecskék, illetve gyökök hozzájárulását a folyamatokhoz. Munkánk során a fenol, mint egyszerű szerkezetű aromás modellmolekula heterogén fotokatalitikus átalakulását vizsgáltuk titán-dioxid (TiO_2) fotokatalizátort alkalmazva, miközben a gyökkészletet gyökfogó anyagok hozzáadásával változtattuk.

Felhasznált anyagok és módszerek
Munkám során $1{,}0\times10^{-4}$ mol dm^{-3} koncentrációjú fenol ((VWR, 99,0%)) oldatot (MILLIPORE Milli-Q Direct 8/16) használtam, melyhez terc-butanolt (VWR, 99,0%) vagy metanolt (VWR, 100,0%) adtam $5{,}0\times10^{-1}$ mol dm^{-3} koncentrációban. Minden esetben 250 cm^3 térfogatú TiO_2 szuszpenziót vizsgáltam, melynek áramoltatását egy PD5001-es típusú Heidolph perisztaltikus pumpa biztosította, 375 $cm^3 \times perc^{-1}$ sebességgel a 25 ± 0,5 °C-ra termosztált (360 mm hosszú, 40 mm külső és 30 mm belső átmérőjű). A mérés során egy GLC303T5/UVA (Lightech) típusú, speciális fluoreszcens réteggel bevont higanygőzlámpát használtam fényforrásként, ezzel sugároztam be a TiO_2 szuszpenziót. A lámpa által kibocsátott fény elsősorban a 300-400 nm hullámhosszúságú tartományba esik, intenzitásának maximuma 365 nm-nél van.
A kísérlet során a 250 cm^3 oldathoz 0,25 g titán-dioxidot (TiO_2, Evonik Aeroxide P25) adtam (1,0 g dm^{-3} volt a szuszpenzió töménysége). Ezután a szuszpenziót minimum 15 percig homogenizáltam ultrahangos szonikálással. Az szuszpenziókon minden esetben 4.5 tisztaságú (99,995%) N_2 gázt vagy 2.5 tisztaságú (99,5%) O_2 gázt buborékoltattam át. A reakciót a lámpa bekapcsolásával indítottam. A mérés során meghatározott időközönként a kezelt szuszpenzióból Eppendorf csövekbe vettem mintát, majd ezeket Dragonlab D2012 típusú centrifugával 2 percig,

15000 rpm fordulatszámon centrifugáltam. Ezután fecskendővel felszívtam a szuszpenziók felülúszóját és 0,20 μm átmérőjű, Sartorius Stedim, Ministart®–plus márkájú fecskendőszűrőn átszűrtem.
A fenol átalakulását egy diódasoros UV-detektorral rendelkező Agilent 1100-as típusú HPLC-berendezés segítségével mértem. Az elválasztáshoz fordított fázisú RP-18 kolonnát alkalmaztam, eluensként 50% MeOH (VWR, 100,0%) és 50% MQ víz elegyét használtam. Az elúció 25 °C-on, 0,900 ml perc^{-1} áramlási sebesség mellett (180 bar), a detektálás pedig 210 nm-es hullámhosszon történt.

Eredmények és értékelésük

Metanol és terc-butanol hatása a fenol átalakulási sebességére

T-BuOH-t és MeOH-t nem tartalmazó oldatokban az oxigén jelenléte számottevően megnövelte a fenol átalakulásának sebességét. Ebben az esetben az O_2 hatékony elektronbefogóként és $^{\bullet}OH$ forrásként egyaránt pozitív hatással van a fenol heterogén fotokatalitikus átalakulására. Ugyanakkor a fenol és lyuk közti közvetlen töltésátmenetet sem akadályozza közvetlenül, csupán a képződött H_2O_2 következtében, ami ugyanakkor szintén hatékony elektronbefogó és $^{\bullet}OH$ forrás egyaránt. Mindemellett az oldott oxigén szerves peroxilgyökökök képződésén keresztül az oldat fázisban is megnövelheti a $HO_2^{\bullet}$ és $O_2^{\bullet-}$ koncentrációját.

1. táblázat *Fenol különböző szakaszokra számolt átalakulási sebességei*

	fenol átalakulási sebessége (×10^{-4} mol dm^{-3} s^{-1})					
	kezdeti szakasz		**töréspont után**		**teljes szakasz**	
	nitrogén	**oxigén**	**nitrogén**	**oxigén**	**nitrogén**	**oxigén**
-	3,70	24,2	3,70	24,2	3,70	24,2
t-BuOH	5,93	6,04	0,18	1,15	0,68	1,55
MeOH	2,97	4,00	0,03	0,07	0,37	0,35

A fenol oxigénmentes közegben mért átalakulásának sebessége arra utal, hogy a fenol átalakulása nem csupán a $^{\bullet}OH$-kel, hanem a fotogenerált töltéshordozókkal való közvetlen reakcióval is indulhat. A pozitív töltésű lyukkal a vízmolekula, a hidroxid-ion, maga a fenol és a képződő H_2O_2 egyaránt elreagálhat. Ebben az esetben, oxigén hiányában a fenolnak, vagy a lyukkal való reakció következtében képződött H_2O_2-nak kell betöltenie az elektronbefogó szerepét. Oldatunk pH-ja a mérés során végig 6 körül volt, azaz a H^+ koncentráció értéke 10^{-6} mol dm^{-3}volt megközelítőleg. Figyelembe véve, hogy a H^+ elektronnal való reakciójának sebességi állandója meglehetősen nagy

$$H^+ + e^-_{aq} \rightarrow {}^{\bullet}H \qquad k_{19} = 2{,}4\times10^{10}\ \text{mol}^{-1}\text{dm}^3\text{s}^{-1}\ [1] \qquad (1)$$

és a képződő $^{\bullet}H$ szintén nagy sebességi állandóval reagál el a fenollal, a H^+-ból képződő $^{\bullet}H$ is szerepet játszhat a fenol átalakulásában

$$\text{fenol} + {}^{\bullet}H \rightarrow \text{hidroxiciklohexadienil gyök} \qquad k_{20} = 1{,}7\times10^{9}\ \text{mol}^{-1}\text{dm}^3\text{s}^{-1}\ [1] \qquad (2)$$

oxigénmentes körülmények között. Oxigén jelenlétében a $^{\bullet}H$ a molekuláris oxigénnel reagál.

$$^{\bullet}H + O_2 \rightarrow HO_2^{\bullet} \qquad k_{21} = 1{,}2\times10^{10}\ \text{mol}^{-1}\text{dm}^3\text{s}^{-1}\ [1] \qquad (3)$$

A t-BuOH-t és MeOH-t $^{\bullet}OH$ gyökfogóként alkalmaztam, 5000-szeres koncentráció feleslegben. Mivel a MeOH és a t-BuOH azonos nagyságrendű és relatíve nagy (10^8 nagyságrendű) sebességi együtthatókkal reagálnak a $^{\bullet}OH$-kel, feltehetően hasonló mértékben csökkentik annak oldatbeli koncentrációját. Feltehetően a t-BuOH és MeOH nem csupán gyökfogóként hat, hanem - három nagyságrenddel nagyobb koncentrációjuknak köszönhetően - a fotokatalizátor felületén is nagyobb valószínűséggel abszorbeálódnak, mint a fenol. (A fenol, a MeOH és a t-BuOH adszorpciója egyaránt igen csekély.)

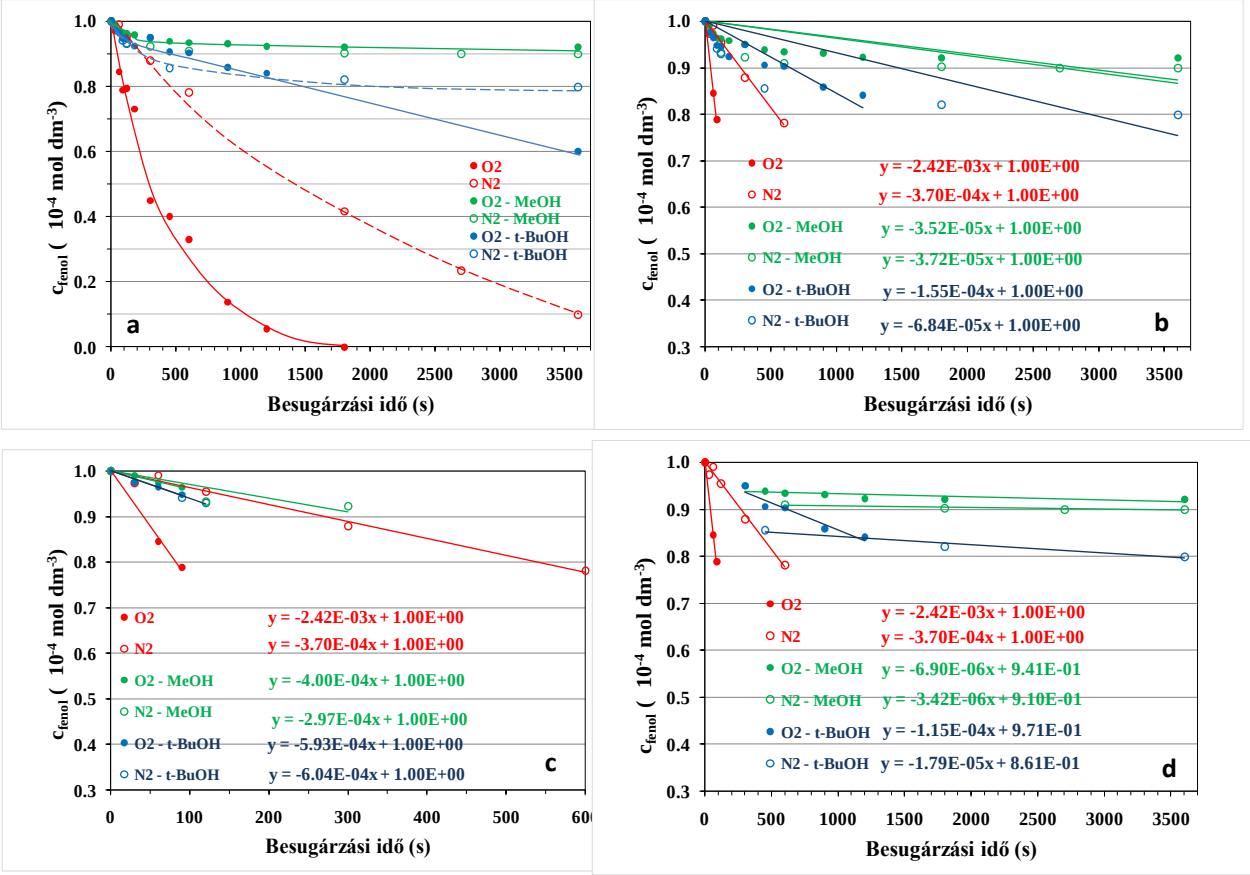

1. ábra *A fenol koncentrációja (c_{fenol} = 1,0×10^{-4} mol dm^{-3}) a besugárzási idő függvényében O_2 mentes és O_2-vel telített (c_{O2} = 2,5×10^{-4} mol dm^{-3}) szuszpenziókban ($c_{t\text{-}BuOH}$ = c_{MeOH} = 5,0×10^{-1} mol dm^{-3}) (a), valamint a 20%-os konverzióig (b), a kezdeti szakaszra (c), és a kezdeti pontok kihagyásával a töréspont utáni szakaszra (d) illesztett egyenesekés azok adatai*

2. táblázat *Fenol, MeOH, t-BuOH és oldott oxigén koncentrációja, valamint azok $^{\bullet}OH$-kel és e^-_{aq}-nal való reakcióinak sebességi állandói és azok szorzatai*

	c (mol dm^{-3})	k (×mol^{-1}dm^{3}s^{-1})		$k_{^{\bullet}OH}$×c	k_{e^-}×c
		$^{\bullet}OH$	e^-_{aq}		
fenol	1,0×10^{-4}	8,4×10^9	3,0×10^7	8,4×10^5	3,0×10^3
t-BuOH	5,0×10^{-1}	6,0×10^8	<4,0×10^5	3,0×10^8	2,0×10^5
MeOH	5,0×10^{-1}	9,7×10^8	<1×10^4	4,9×10^8	5,0×10^3
O_2	2,5×10^{-4}	-	1,9×10^{10}	-	4,8×10^6

Az egyes vegyületek ˙OH-kel és elektronnal való reakcióinak és kiindulási koncentrációinak szorzata, azaz az egyes vegyületeknek a két reaktív részecskével való reakciójának sebessége alapján feltételezhetjük, hogy a beállított reakció körülmények között a ˙OH oxigén jelenlététől függetlenül elsősorban az alkoholokkal reagál el. Mérési eredményeink ezt igazolták, a t-BuOH és MeOH egyaránt szignifikánsan csökkentette a fenol átalakulási sebességét. Ugyanakkor a MeOH valamivel nagyobb mértékben fejtette ki hatását a fenol átalakulási sebességére, mint a t-BuOH. MeOH és t-BuOH hozzáadása során a kinetikai görbe kezdeti szakaszán az átalakulás sebessége szignifikánsan nagyobb, mint a kezdeti szakaszt követő töréspont után. Ennek egyik lehetséges magyarázata, hogy a MeOH és t-BuOH átalakulása jól adszorbeálódó kis szénatomszámú savakat, hangyasavat (MeOH) és oxálsavat eredményez, oxigénmentes körülmények között pedig aldehidek képződhetnek. Ezek jelentősen adszorbeálódva a felületen akadályozzák a közvetlen töltés átmenettel és ˙OH-kel való reakciókkal történő átalakulását a rosszul adszorbeálódó fenolnak. Emellett a MeOH-ból képződő hangyasav és annak deprotonált formája egyaránt igen nagy sebességgel reagál el ˙OH-kel (1.3×10^{8} L mol^{-1} s^{-1} [1]; 3.2×10^{9} L mol^{-1} s^{-1} [1]) és elektronnal (1.4×10^{8} mol^{-1} dm^3 s^{-1} [2]; 8×10^{3} mol^{-1} dm^3 s^{-1} [3]). Azaz nem csak a MeOH hanem a belőle képződő jól adszorbeálódó hangyasav is ˙OH gyökfogóként szerepel.
Oxigénnel telített szuszpenziók esetét vizsgálva t-BuOH jelenlétében a bomlási sebesség oxigén jelenlétében kismértékben nagyobb volt, mint oxigénmentes esetben, míg a MeOH hatása ugyanolyan volt oxigén jelenlététől függetlenül. Ezt azzal értelmezhetjük, hogy oxigén jelenlétében mindkét alkohol elsősorban a ˙OH-kért való versengésen keresztül fejti ki hatását a fenol átalakulási sebességére, mivel ebben az esetben az O_2 az elektronbefogó, ami jelentősen megnövelheti a ˙OH-koncentrációt az oxigénmentes oldathoz képest. Így a fenol és az alkoholok átalakulása is elsősorban a ˙OH-kel való reakciókhoz rendelhető. A t-BuOH-t tartalmazó oldatokban a kinetikai görbe kezdeti szakaszán mért átalakulási sebességek közt szignifikáns különbség nem tapasztalható. Azonban a kinetikai görbe második szakaszán, a töréspont utáni átalakulási sebességeket összehasonlítva, azt látjuk, hogy oxigén jelenlétében a t-BuOH a MeOH-hoz képest kisebb mértékben befolyásolja a fenol átalakulásának sebességét. Ez feltehetően a MeOH-ból és t-BuOH-ból képződő köztitermékek eltérő gyökfogó, elektronbefogó és adszorpciós tulajdonságaival értelmezhető. A két használt alkohol közötti másik fontos különbség azok elektronbefogó tulajdonságával értelmezhető. A t-BuOH alkalmazása során nagyobb a valószínűsége, hogy az elektronbefogóként viselkedve megnöveli a szerves vegyületeknek a fotogenerált lyukkal, vagy az azon képződő ˙OH gyökkel való reakciójának sebességét. Bár a MeOH-ból képződő széncentrumú gyök reaktivitása meghaladja a t-BuOH-ból képződő gyök reaktivitását, feltehetően ezen gyökök szerepe a fenol átalakulásában elhanyagolható az adott körülmények között.

Összefoglalás

Munkánkban a fenol vizes oldatának heterogén fotokatalízisét vizsgáltuk. Az oldott oxigén jelenléte jelentősen megnövelte a fenol átalakulási sebességét az oxigénmentes esetben mérthez képest. Ezt a fotogenerált lyuk-eletronpár rekombinációjának gátlásával, és ennek következtében a rendszerben lévő reaktív részecskék, elsősorban a ˙OH koncentrációjának megnövekedésével értelmezhető. Az alkoholok hozzáadásával a fenol átalakulásának sebessége nagymértékben lecsökkent oxigén jelenlétében és annak távollétében is. Ez egyértelműen azzal magyarázható, hogy a terc-butanol és a metanol is nagymértékben csökkenti a ˙OH-ök koncentrációját.

Irodalomjegyzék

[1] Buxton, G.V.; Greenstock, C.L.; Helman, W.P.; Ross, A.B., J. Phys. Chem. Ref. Data 17 513 – 886, 1988
[2] S. Gordon, E.J. Hart, M.S. Matheson, J. Rabani, J.K. Thomas, Faraday Soc., 36 (1963) 193-205
[3] H. A. Schwarz, J. Phys. Chem. 96 (1992) 8937-8941

SYNTHESIS AND CHARACTERIZATION OF TITANIUM DIOXIDE BASED TERNARY NANOCOMPOSITES FOR PHOTOCATALYTIC HYDROGEN PRODUCTION

Árpád Turcsányi[1], Emília Tálas[2], Szijjártó Gábor[2], Ágnes Veres[1], Imre Dékány[1], András Tompos[2], Tamás Szabó[1]

[1]Department of Physical Chemistry and Materials Science, University of Szeged, H-6720 Szeged, Aradi vértanúk tere 1, Hungary
[2]Institute of Materials and Environmental Chemistry, Research Centre for Natural Sciences, Hungarian Academy of Sciences, H-1117 Budapest, Magyar tudósok körútja 2, Hungary

Abstract

Titanium dioxide based photocatalysts of different graphene oxide (GO) and silver nanoparticle (AgNP) content were prepared and tested in catalytic methanol reformation reaction. Aqueous suspensions of the composite solids obtained by heterocoagulation of alkaline exfoliated GO suspension and slightly acidic TiO_2 suspension showed enhanced sedimentation rate at pH = 6.5-7, when they contained less than 2 wt% graphene oxide. This enables easier catalyst recovery but the suspension needs to be stirred strongly during the catalytic run in order to achieve homogeneous light distribution within the reaction vessel.

The catalytic runs were performed in 6 V/V% methanol/water mixture using 500 mg/L catalyst under UV-illumination. The activity of pure titanium dioxide (Degussa P25) continuously increases and reaches a saturation plateau after 150 min with an activity of 0.12 mmol $H_2/(h \times g_{cat})$. Incorporation of GO into the titanium dioxide matrix by heterocoagulation method results in aggregated suspensions exhibiting an enhancement of the hydrogen evolution rate to the saturation value of 0.17 mmol $H_2/(h \times g_{cat})$. Deposition of different amounts of AgNPs of different sizes onto the surface of titanium dioxide resulted in an even higher photocatalytic activity, reaching 0.25-0.29 mmol $H_2/(h \times g_{cat})$. The combination of AgNP's and GO platelets to obtain ternary TiO_2 based catalysts has not shown any further increase of hydrogen generation rate.

KÜLÖNBÖZŐ ALAKÚ NEMESFÉMEKKEL MÓDOSÍTOTT TiO_2 FOTOKATALIZÁTOROK HATÉKONYSÁGA FOTOKATALITIKUS HIDROGÉNFEJLESZTÉSBEN

Fodor Szilvia[1], Pap Zsolt[2,3,4], Hernádi Klára[1], Kovács Gábor[1,3,4], Lucian Baia[3,4]

1. Department of Applied and Environmental Chemistry, University of Szeged, H–6720 Szeged, Rerrich Béla tér 1, Hungary
2. Institute of Environmental Science and Technology, University of Szeged, H-6720 Szeged, Tisza Lajos körút 103, Hungary
3. Institute for Interdisciplinary Research on Bio-Nano-Sciences, Babeş–Bolyai University, RO-400271, Treboniu Laurean 42, Cluj-Napoca, Romania
4. Faculty of Physics, Babeş-Bolyai University, RO-400084, Mihail Kogălniceanu 1, Cluj-Napoca, Romania
e-mail: fod_szilvia@chem.u-szeged.hu

Abstract
TiO_2 is one of the most frequently used semiconductor photocatalysts, because of its several beneficial properties: physical and chemical stability, nontoxicity, safety, low cost, and resistance to photocorrosion. In the present work we have successfully synthesized differently shaped Pd and Pt nanoparticles deposited onto the surface of commercial photocatalysts: Aldrich anatase, Aldrich rutile, or Evonik Aeroxide P25. The nanocomposites were investigated using DRS, XRD and TEM to uncover morphological, optical, and structural peculiarities of the nanoparticles and the composite photocatalysts.
Finally, we tested their photocatalytic activity in photocatalytic hydrogen production processes and we have correlated the as obtained results with the morphology of Pd and Pt nanoparticles.

Bevezetés
A heterogén fotokatalitikus folyamatokban elengedhetetlen egy félvezető , amelynek a megfelelő hullámhosszon történő megvilágításával, kialakul egy elektron-lyuk páros, hiszen a gerjesztés során egy elektron a vegyértéksávból a vezetési sávba jut fel, maga után hagyva egy pozitív töltésű hibahelyet. Az így keletkezett elektron-lyuk pár hasznosulhat redox folyamatokban, amennyiben jelen van a rendszerben egy elektrondonor és egy elektron akceptor vegyület [1]. A reakció során a szerves szennyező két féle képpen bomolhat el: oxidálódhat a katalizátor felületén, vagy a képződött reaktív gyökökkel.
A titán-dioxid jelenlétében végbemenő fotokatalitikus folyamatok nemcsak szerves szennyezők oxidációjára használhatók fel, hanem oxigénmentes körülmények között lehetőség nyílik vizes oldatokból történő hidrogén gáz fejlesztésére is.A fotokatalitikus hidrogénfejlesztéssorán a rekombinációs idő meghosszabbítására több módszert vizsgáltak, amelyek közül a kompozitkészítés az egyik legígéretesebb eredményekkel kecsegtető alternatíva. A félvezetőket kompozitokba viszik más félvezető oxidokkal (ZnO, WO_3) [2, 3], szén nanoanyagokkal [4] és számos kutatás folyik a nemesfém nanorészecskékkel való hatékonyság növelési kísérletekről is. Ez utóbbi esetén a vezetési sávba feljutó elektron a katalizátor felületére leválasztott nemesfémre kerül át, ahol csapdázódik, majd hasznosul és így megnöveli az elektron-lyuk pár élettartamát a rekombináció visszaszorításával.
Munkánk során ennek a folyamatnak a fejlesztését tűztük ki célul, különböző TiO_2 alapkatalizátor hatékonyságának növelése különböző geometriájú nemesfém nanorészecskék

felvitelével. Az irodalomban fellelhető kutatások szerint nagymértékben javít az aktivitáson az arany nanorészecskével történő módosítás [5-7], de találunk ígéretes eredményeket ezüsttel [8, 9], palládiummal [10, 11] és platinával [12-14]is. Míg egyes kísérletek a rávitt nemesfém mennyiségére [15], vagy a nanorészecskék méretének befolyásoló hatására irányulnak [16], addig a mi kísérleteink a nemesfém alakja által kifejtett hatásra irányultak.

Kísérleti rész

A nemesfém nanorészecskéket minden esetben redukciós eljárással állítottuk elő ($NaBH_4$, etilén-glikol vagy nátrium-citrát adagolással) ahol a hőmérséklettel képesek voltunk befolyásolni az előállított nanorészecskék mérettartományát (a hőmérséklet növelésével csökkent a részecskeméret), míg a hozzáadott alakbefolyásoló anyagok (PVP, CTAB és nátrium-citrát) változtatásával pedig a monodiszperzitást tudtuk szabályozni.

A nemesfémmel adalékolt TiO_2 fotokatalizátor előállítása során a TiO_2 három – kereskedelmi forgalomban kapható − módosulatára (AA, AR és P25) vittünk fel nemesfém nanorészecskéket. Az előállított kompozitokban a nemesfém mindig 1 %-ban került a hordozóra. Az így kapott rendszert homogenizálás céljából 5 percig ultrahangos kezelésnek vetettük alá, majd ezt követően 1 órán keresztül, kevertetés mellett pihentettük.

Eredmények

1. Anyagszerkezeti jellemzések:

Az előállított nemesfém nanorészecskéket elsőként transzmissziós elektronmikroszkópiával vizsgáltuk annak érdekében, hogy felderítsük az előállítási módszer alakszelektivitási eredményességét és az elért mérettartományt.

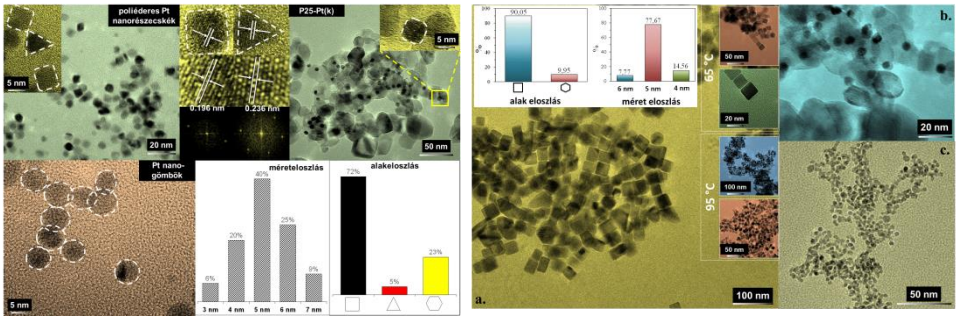

1. ábra: Az előállított nanorészecskék TEM felvételei valamint az alak és méreteloszlás hisztogramjai.

A Pt nanokockák keletkezésekor időnként kialakultak poliéderes és háromszög alapú hasáb részecskék is (1. ábra), de az alakeloszlást megvizsgálva 72 %-os hatékonyságot mutatott a nanokockák képződése. A részecskeméret gyakorlatilag megegyezett, 5±1,5 nm körüli átlagos részecskeméretet tapasztaltunk. A nanogömbök alakszelektivitása egyértelműen leolvasható a felvételekből és a részecskeméret is megfelelő (5 nm) így a kompozitban kapott eredmények összehasonlíthatóvá válnak a nanokockákkal.

A Pd nanorészecskék esetén az alakszelektivitási stratégiánk jó hatásfokot mutatott, mivel csak 9,95 %-ban jelennek meg dodekaéderes kristályok (200 részecske megszámolása esetén kapott érték), így a 90,05 %-os hozammal előállított nanokockák esetén egyértelműen beszélhetünk alakszelektív előállításról. A nanogömbök esetén is 5 nm körüli a részecskeméret, akárcsak a nanokockák esetén, így az eredmények összehasonlíthatósága nem jelenthet gondot itt sem.

A felvételeken az is megfigyelhető, hogy sikerült az alapkatalizátor felszínére felvinni a nemesfém nanorészecskét.
Ezt követően az optikai tulajdonságok meghatározására diffúzreflexiós spektroszkópiával vizsgáltuk az előállított katalizátorokat.

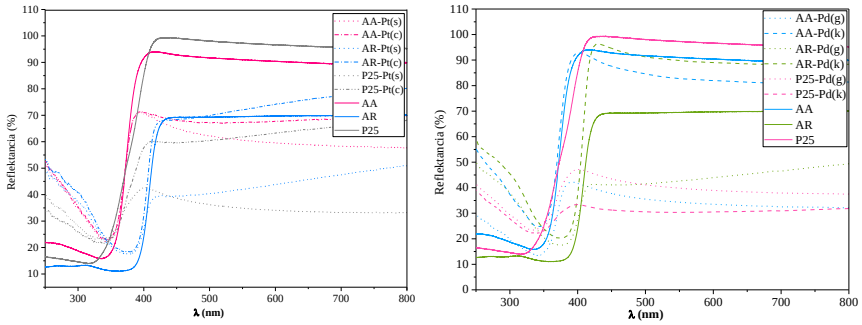

2. ábra: Az alapkatalizátorok és az előállított kompozitok diffúz reflexiós spektrumai.

Minden esetben sikerült befolyásolni a módosított anyagok gerjesztési küszöbeit. Az optikai tulajdonságok módosításának kvantifikálása érdekében kiszámoltuk a kompozit fotokatalizátorok tiltottsáv szélesség értékeit, amelyeketaz **1. táblázatban** foglalunk össze.

1. táblázat: Az előállított katalizátorok számolt tiltottsáv szélesség étkékei (eV).

	P25	**AA**	**AR**
alap	*3,11*	*3,26*	*2,91*
Pt(g)	2,66	3,18	2,82
Pt(k)	2,95	3,20	2,96
Pd(g)	2,99	3,12	2,88
Pd(k)	2,65	3,21	2,98

2. Fotokatalitikus aktivitásvizsgálata

Vizsgáltuk az általunk előállított nanokompozitok fotokatalitikus úton történő hidrogénfejlesztésben mért hatékonyságát. A nemesfémmel nem módosított, kiindulási félvezetők esetén nem fejlődik hidrogén gáz, de abban az esetben, amikor módosítottuk a felületet nemesfém nanorészecskékkel, a leválási túlfeszültség lecsökkenésével − molekuláris oxigén hiányában − az elektron akceptor szerepet a H^+ veszi át, így sikerülhet a hidrogén gáz fejlesztése.

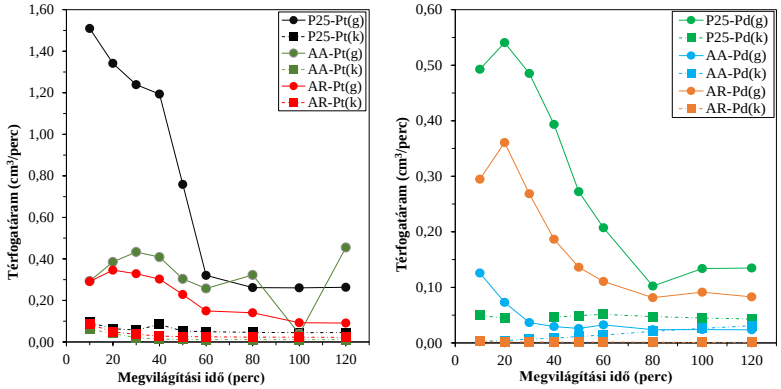

3. ábra: A keletkezett H_2 térfogatárama.

A H_2 fejlődést vizsgáló méréseink során a legnagyobb mennyiségű hidrogén gáz a Pd nanogömbökkel módosított P25 katalizátoron fejlődött, ebben az esetben a keletkező hidrogén térfogatárama a legnagyobb, elérte az 0,54 $cm^3 \cdot perc^{-1}$-es értéket, Pt esetén pedig ez a térfogatáram 1,51 $cm^3 \cdot perc^{-1}$ érték volt, amit szintén a nanogömbökkel történő módosítással értünk el.

Következtetések

A kitűzött céloknak megfelelően sikeres alakszelektív szintéziseket valósítottunk meg, amelyek során 5-8 nm átmérőjű Pd és Pt nanogömböket és nanokockákat állítottunk elő. A sikeresen előállított nanorészecskéket felhasználva 12 új TiO_2 kompozitot készítettünk az alapkatalizátor felület módosításával: P25-Pd(g), P25-Pd(k), AA-Pd(g), AA-Pd(k), AR-Pd(g), AR-Pd(k), P25-Pt(g), P25-Pt(k), AA-Pt(g), AA-Pt(k), AR-Pt(g), AR-Pt(k).

A katalizátorok jellemzését követően fotokatalitikus hidrogénfejlesztő képességüket vizsgáltuk, amely folyamatok során sikerült hidrogén gázt fejleszteni. A legmagasabb érték gömb morfológiájú platinával módosított kompozit esetén 1,51 $cm^3 \cdot perc^{-1}$ érték volt, míg ez palládiummal történő módosított katalizátorok tesztelése során a 0,54 $cm^3 \cdot perc^{-1}$ értéket érte el.

Köszönetnyílvánítás

Fodor Szilvia köszönetet mond a Balassi Intézet, Márton Áron Szakkollégiumának a Tehetséggondozói Szakkollégiumban való támogatásért és a Babeş-Bolyai Tudományegyetemnek a Fiatal Kutatói Kiválósági Ösztöndíjért. Pap Zsolt köszönetet mond a Magyar Tudományos Akadémia Prémium Posztdoktori Pályázatának az anyagi támogatásért. A kutatás anyagi és személyi támogatásáért köszönet illeti a GINOP-2.3.2-15-2016-00013 pályázatot és a Svájci-Magyar együttműködési programot (SH/7/2/20).

References

[1] A. Karci, Chemosphere99 (2014) 1-18.
[2] I. Székely, G. Kovács, L. Baia, V. Danciu, Zs. Pap, Materials9 (2016) 258.
[3] K. Vajda, K. Saszet, Zs. Kedves, Zs. Kása, V. Danciu, L. Baia, K. Magyari, K. Hernádi, G. Kovács, Zs. Pap, Ceram. Int.42 (2016) 3077–3087.
[4] B. Réti, Z. Major, D. Szarka, T. Boldizsár, E. Horváth, A. Magrez, L. Forró, A. Dombi, K. Hernádi, J. Mol. Catal. A: Chem. 414 (2016) 140–147.
[5] A. Bumajdad, M. Madkour, Phys. Chem. Chem. Phys. 16 (2014) 7129–7628.
[6] A. Gazsi, G. Schubert, T. Bánsági, F. Solymosi, J. Photoch. Photobio. A. 271 (2013) 45–55.
[7] Zs. Pap, Zs. R. Tóth, V. Danciu, L. Baia, G. Kovács, Materials8 (2015) 162-180.
[8] C. Zhao, A. Krall, H. Zhao, Q. Zhang, Y. Li, Int. J. Hydrogen Energy. 37 (2012) 9967-9976.
[9] N. Naseri, H. Kim, W. Choi, A.Z. Moshfegh, Int. J. Hydrogen Energy. 37 (2 012) 3056-3065.
[10] I. Chiu, S.-X.Lin, C.-T. Kao, R.-J. Wu, Int. J. Hydrogen Energy. 39 (2014) 14574-14580.
[11] M. Bowker, C. Morton, J. Kennedy, H. Bahruji, J. Greves, W. Jones, P.R. Davies, C. Brookes, P.P. Wells, N. Dimitratos, J. Catal.310 (2014) 10-15.
[12] W. Kim, T. Tachikawa, H. Kim, N. Lakshminarasimhan, P. Murugan, H. Park, T. Majima, W. Choi, Appl. Catal. B. 147 (2014) 642–650.
[13] J. Xing, Y. H. Li, H. B. Jiang, Y. Wang, H. G. Yang, Int. J. Hydrogen Energy. 39 (2014) 1237-1242.
[14] M. P. Languer, F. R. Scheffer, A. F. Feil, D. L. Baptista, P. Migowski, G. J. Machado, D. P. Moraes, J. Dupont, R. Teixeira, D. E. Weibel, Int. J. Hydrogen Energy. 38 (2013) 14440-14450.

[15] V. Iliev, D. Tomova, R. Todorovska, D. Oliver, L. Petrov, D. Todorovsky, M. UzunovaBujnova, Appl. Catal. A. 313 (2006) 115-121.
[16] W. Teoh, L. Madler, D. Beydoun, S. Pratsinis, R. Amal, Chem. Eng. Sci. 60 (2005) 5852-5861.

KERESKEDELMI TIO_2 FOTOKATALIZÁTOROK, ARANY NANOKETRECEKKEL VALÓ MÓDOSÍTÁSA ÉS AKTIVITÁSÁRA VALÓ HATÁSA

Tóth Zsejke-Réka[1], Pap Zsolt[2,3,4], Hernádi Klára[1], Baia Lucian[2,4], Kovács Gábor[1,2,4]

[1]*Department of Applied and Environmental Chemistry, University of Szeged, H-6720 Szeged, Rerrich B. tér 1, Hungary*
[2] *Institute for Interdisciplinary Research on Bio-Nano-Sciences, RO-400271 Cluj-Napoca, Treboniu Laurian 42, Romania*
[3] *Institute of Environmental Science and Technology, H-6720 Szeged, Tisza Lajos krt. 103, Hungary*
[4] *Faculty of Physics, Babeș–Bolyai University, RO-400084 Cluj–Napoca, M. Kogălniceanu 1, Romania*
e-mail: tothzsejkereka@chem.u-szeged.hu

Abstract
Modified TiO_2-based composite photocatalysts were applied in order to degrade phenol and oxalic acid model pollutants. As co-catalysts noble metal nanoparticles (Ag nanoparticles and Au nanocages) were deposited onto the base photocatalysts. The Au nanocages were obtained by both a direct and an indirect synthesis approach, while the composites were fabricated by using either *in-situ* or impregnation techniques for noble metal deposition. The obtained Au/TiO_2 and Ag/TiO_2 composites were characterized by different methods, such as XRD (X-ray Diffraction), TEM (Transmission Electron Microscopy), DRS (Diffuse Reflectance Spectroscopy) and XRF (X-ray fluorescence). The result of our research is that the amount of oxalic acid was lower in case of silver nanoparticles, similarly in the case of phenol degradation to the silver nanoparticles/TiO_2 composites were more active. The gold nanocages composites low conversion value is due to the intermediates adsorption on the surface of TiO_2.

Bevezetés
A jelenleg kifogyóban lévő fosszilis energiaforrások helyettesíthetők H_2-nel, melynek előállítására a fotokatalízis jelentheti a jövőben a megoldást. A folyamathoz elengedhetetlen egy félvezető fotokatalizátor jelenléte. A kutatásaimban a legkutatottabb félvezető fotokatalizátort használtam, és annak is a kereskedelmi előállított fajtáit (P25 [1], Aldrich anatáz (AA), Aldrich rutil (AR)). Előzetes kutatásaink alapján már megfigyeltük, hogyha arany nanorészecskéket választunk le a TiO_2 felületére, akkor nagyobb aktivitást érhetünk el megnövelve a töltésszeparálódás hatásfokát [2]. Azt feltételeztük, hogyha a klasszikus geometriájú (gömb, kocka, rúd, stb.) nemesfém nanorészecskéket kicseréljük egy nagyobb fajlagos felülettel rendelkező geometriára, akkor nagyobb aktivitásbeli különbségek érhetők el a nagyobb elektronátadási felületnek köszönhetően. Ilyen komplex szerkezetű nanoanyagok például a nanoketrecek. Ezek a típusú nanorészecskék a szakirodalom szerint két módon is előállíthatók: indirekt [3] és direkt módszerrel [4]. A indirekt módszerhez elengedhetetlen Ag nanorészecskék előzetes előállítása. Az előbb említett ezüst nanorészecskéket kompozitba vittünk a fent említett TiO_2-kel és megvizsgáltuk a kapott kompozitok fotokatalitikus aktivitását is. Az így nyert, Au/TiO_2 és Ag/TiO_2 nanokompozitok fotokatalitikus aktivitását vizsgálatuk különböző modell szennyezők bontásában. Szerkezeti és morfológiai tulajdonságait XRD, DRS, TEM és XRF segítségével vizsgáltuk.

Kísérleti rész

A kompozit előállítása során három lépcsőben változtattuk az előállítási körülményeket:

a. TiO_2típusa:

A kereskedelemből ismert három TiO_2-ot használtam, amelyek a következő szerkezeti sajátosságokkal rendelkeztek: Evonik Aeroxide P25 (89 % anatáz és 11 % rutil, az elsődleges kristályméret: 25-40 nm), Aldrich anatáz (kristályméret: 200 nm) és Aldrich rutil (kristályméret: 150 nm).

b. A kompozit előállítás módszere:

Két szintézis módszert alkalmaztam a kompozitok előállítására. Az *in situ* (IS) módszer esetében a katalizátor végig jelen van a rendszerben, amíg az impregnálásos (IMP) módszer esetében csak a redukálás után adjuk a rendszerhez az előző pontban említett TiO_2-ot.

c. Arany nanorészecske előállítása:

Az indirekt nanoketrec szintéziséhez az Ag nanorészecskék jelenléte orientálja/templátként hat az Au nanorészecskék kialakítását/kialakítására (ld. 1. ábra).

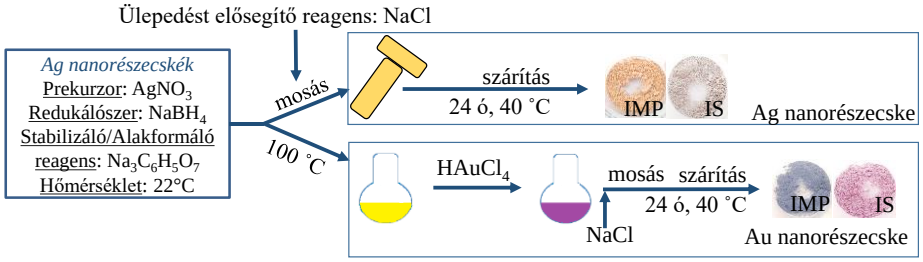

1. ábra: Az Ag nanogömbök (AgNG) és Au nanoketrecek indirekt (AuIND) előállításának sematikus ábrázolása

A direkt nanoketrec szintézis egy lépésben történik a 2. ábra alapján. AA és AR alapú kompozitok esetében a leválasztás nem volt sikeres, mert a nemesfém nanorészecskék nem rögzültek a katalizátor felszínére és külön színes réteget alkottak a beszárítás után. Ezért ezek fotokatalitikus aktivitását nem tudtuk lemérni.

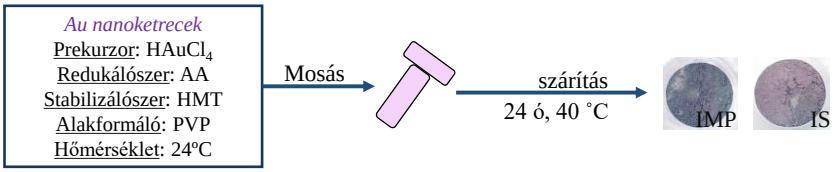

2. ábra: Nanoketrecek direkt (AuDIR) előállításának folyamatábrája

A következő jelölést fogjuk használni a kompozitokhoz, amelyhez figyelembe vesszük a fent említett három változtatott szintézis paramétert:

Nemesfém	Előállított nanorészecske	Kompozit szintézis módszer	TiO_2 típusa
Au	IND/DIR	IMP/IS	P25/AA/AR
Ag	NG	IMP/IS	P25/AA/AR

Táblázat: A továbbiakban használt jelölés

Az így elkészített 8 db. Au/TiO_2 és 6 db. Ag/TiO_2 kompozit szerkezeti tulajdonságának a vizsgálatára a következő berendezéseket használtuk: **TEM** (FEI Technai G2 20 X-TWIN), amellyel meghatározzuk a nanorészecskék alakját és méretét, **XRD** (Rigaku Miniflex II), amellyel meghatározzuk az alapkatalizátorok összetételét és vizsgáljuk a nemesfém jelenlétét,

DRS (JASCO-V650 spektrofotométer -ILV-724 diffúz reflexiós modul), amellyel meghatározzunk az aranyra és az ezüstre jellemző plazmon elnyelési sávokat és **XRF** (Horiba Jobin Yvon XGT-5000), amellyel meghatározzuk az Ag/Au arányát.
A fotokatalitikus mérések során használt körülmények: 6×6 W – UV lámpa ($\lambda_{max} \approx 365$ nm), C_{fenol} = 0,5 mM / $C_{oxálsav}$ = 5 mM, szuszpenzió töménység: 1 g·L^{-1} és megvilágítás ideje 2 óra.

Eredmények és értékelésük
Sikeresen előállítottuk 30 nm-es Ag nanogömböket (3. a. ábra), amelyek a NaCl hozzáadásával agglomerálódtak, majd azokat átalakítottam kb. 5-10 nm-es Au gömbszerű nanoketrecekké (3. b. ábra). Sikeresen előállítottam 25 nm-es nanoketreceket előzetes Ag nanorészecske szintézise nélkül.
A XRD mérések alapján megfigyeltük, hogy a rutil (P25, AR) tartalmú minták esetében csak Ag nanorészecskék keletkeztek, amíg az anatáz (P25, AA) tartalmú minták esetében AgO jelenlétét figyeltük meg. Az Au tartalmú minták esetén csak az aranyra jellemző reflexiókat detektáltuk.

Az XRF mérésekből kiderült, hogy az AuDIR minták esetében 100 %-os volt az Au tartalom, addig az AuIND esetében 99% Au és 1% Ag.

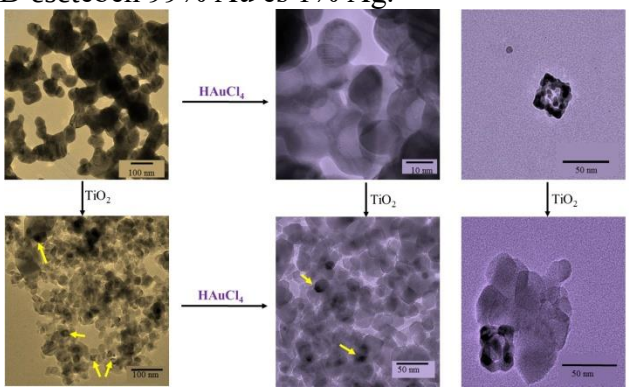

3. **ábra:** a. Ag, b. AuIND, c. Ag/TiO_2, d. AuIND/TiO_2, e AuDIR, f. AuDIR/TiO_2transzmissziós elektronmikroszkópiás felvételei

A DRS mérések kimutatták, hogy az Ag jellemző plazmon elnyelési sávok eltűnnek, majd az Au hozzáadás után újabbak jelennek meg, magasabb hullámhossz tartományban. Ez egy közvetlen bizonyíték arra, hogy a reakció sikeres volt. Az Au/IMP minták esetében (IND, DIR) nem jelenik meg plazmon elnyelési sáv, hiszen a ketrecre jellemző plazmon elnyelési sávok az IR tartományba nyúlnak át. Mindemellett kiszámoltuk a kompozitok tiltottsáv-szélességeit. A tiltottsáv-szélességek értékei azért fontosak, hiszen ha 3 eV alá esik akkor a kompozit akár látható fényben is aktív lehet. A kompozitok esetében azt vettük észre, hogy amíg a P25 tiltottsáv-szélessége 3,17 eV, addig a kompozitok tiltottsáv-szélességei 2,85-2,95 eV közötti értékek között mozog, tehát akár látható fényben is aktív lehet.
Oxálsav (4. a. ábra) esetében 1 óra eltelte után a következő eredményeket figyeltük meg:

- A P25 és AA tartalmú minták mindegyike aktívabbnak bizonyult, mint a kereskedelemből ismert alapkatalizátor párja.
- Az Ag tartalmú minták az IMP szintézis módszer esetében bizonyultak aktívabbnak, amíg az AgO tartalmú kompozitok esetében az IS jelű minták teljesítettek jobban.
- Az AuIND és AuDIR P25-öt tartalmú minták esetében 55-48 % közötti konverzió értékeket értünk el. Az AuIND_AA és AR tartalmú minták esetében függetlenül az alkalmazott kompozit szintézis módszertől egymáshoz közeli értékű konverziókat kaptunk.

- Egy óra eltelte után 8 kompozit bizonyult aktívabbnak, mint a kereskedelmi AR, amely a legaktívabb kereskedelmi katalizátor az oxálsav bontások esetében.
- Fenol (4. b. ábra) bontása esetében 2 óra után a következő eredményeket figyeltük meg:
- Az Ag és AgO tartalmú minták esetében a következő trendet figyeltük meg, figyelembe véve az alapkatalizátorok jellegét: AA>P25>AR.
- A P25 tartalmú minták esetében egyik sem bizonyult aktívabbnak, mint a kereskedelmi párjuk.
- Az AA tartalmú minták esetében mindegyik kompozit hatékonyabban bontotta a fenolt, mint a kereskedelmi AA.
- AR tartalmú kompozitok esetében megközelítőleg egyforma eredményeket értünk el, mint a kereskedelmi AR.

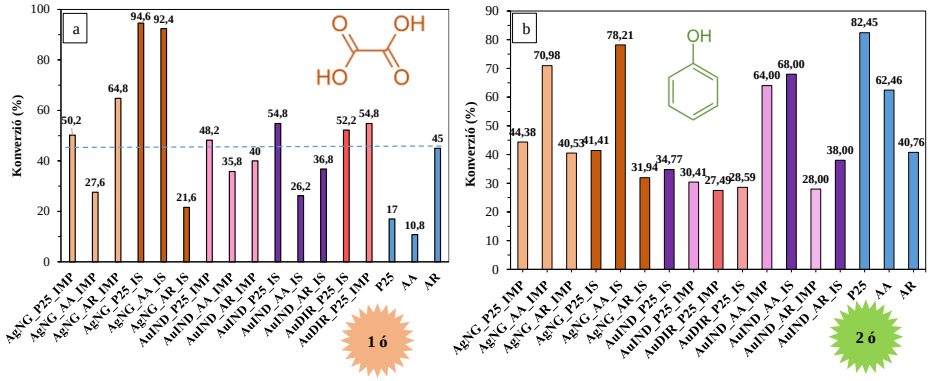

4. **ábra**: A nanokompozitok fotokatalitikus aktivitásának vizsgálata oxálsav (a) és fenol (b) bontásában

Következtetések

Sikeresen állítottunk elő Ag és Au nanorészecskéket és ezeket kompozitba vittük TiO_2-dal (8 db Au/TiO_2 és 6 db Ag/TiO_2 kompozitot). A kapott kompozitokat vizsgáltam XRD, DRS, TEM és XRF módszerek segítségével. A kompozitok fotokatalitikus aktivitását 2 modell szennyező bontásában teszteltük**. Fenol** esetében nem sikerült meghaladni a P25 aktivitását. **Oxálsav** esetében viszont 9 olyan kompozit is volt, amely aktívabbnak bizonyult a kereskedelmi katalizátoroknál. Kettő (Ag_P25_IS és Ag_AA_IS) jelenlétében 1 óra eltelte után 90 %-ot meghaladó konverziót értünk el. A fenti eredményeket figyelembe véve kimondhatjuk, hogy oxálsav bontása esetében az ezüst bizonyult aktívabbnak, mégpedig amikor IS módon vittük a TiO_2 felületére. Ezzel szemben fenol esetében független a kompozit szintézis módszertől az Ag_AA minták bizonyultak a legaktívabbnak. Az arany tartalmú minták esetében a visszaszorított fenol fogyás a köztitermékek adszorbeálódásának tudható be.

Köszönetnyilvánítás

Az elkészített TEM felvételekért köszönet illeti: Réti Balázs és Kecsenovity Egon. P. Zs. köszönetet mond a MTA Prémium Posztdoktori pályázatának az anyagi támogatásért. A szerzők szeretnék megköszöni a GINOP-2.3.2-15-2016-00013 nevű pályázatnak az anyagi támogatást. T. Zs-R köszönetet mond a Márton Áron Szakkollégiumnak, valamint a BBTE által nyújtott kutatói ösztöndíjnak.

Irodalomjegyzék

[1] B. Ohtani, O.O Prieto-Mahaney, D. Li, R. Abe, Journal Photochemistry and Photobiology A: Chemistry, 216(2010) 179–182.
[2] Zs. Pap & Zs. R. Tóth, V. Danciu, L. Baia, G. Kovács, Materials, 8(2015) 162-180.

[3] Y. Sun, Y. Xia, Journal of American Chemical Society, 126 (2004) 3892-3901.
[4] Y. Zhang, Y. Sun, Z. Liu, F. Xu, K. Cui, Y. Shi. Z. Wen, Z. Li, Journal of Electroanalytical Chemistry, 656 (2011) 23–28.

CHARACTERIZATION BY SOFT IONIZATION MASS SPECTROMETRY METHODS OF MONO- AND OLIGOSACCHARIDES FUNCTIONALIZED AT THE ANOMERIC CENTER

Loreta Andrea Božin[1#], Mihai-Cosmin Pascariu[1,2#], Anca Dragomirescu[1], Georgeta Simu[1], Nicolae Dincă[3], Eugen Sisu[1*]

[1] "Victor Babeş" University of Medicine and Pharmacy of Timisoara, Faculty of Medicine, 2 Eftimie Murgu Sq., RO-300041, Timisoara, Romania
[2] "Vasile Goldiş" Western University of Arad, Faculty of Pharmacy, 86 Liviu Rebreanu, RO-310045, Arad, Romania, [#]equal contribution
[3] "Aurel Vlaicu" University of Arad, Faculty o Food Engineering, Tourism and Environmental Protection, 2 Elena Drăgoi, RO-310330, Arad, Romania
e-mail: sisueugen@umft.ro

Abstract
In order to obtain oligosaccharides functionalized with amine groups, aliphatic diamines and polyamines were coupled with maltose by using reductive amination reactions. The synthesized compounds were characterized through electrospray ionization mass spectrometry (ESI-MS), while finer structural details were obtained by using MS^2.

Introduction
In the hands of organic chemists, the reductive amination reaction is a powerful tool for building C-N bonds. Its importance is revealed by the fact that volume 59 of Organic Reactions series *(Ed. L.E. Overman et al. - John Wiley & Sons, 2002*) is completely dedicated to the reductive amination reaction, which uses boranes and their derivatives as reducing agents (2100 reference citations). A multitude of substrates, including aliphatic, aromatic and mixed aldehydes, but also aliphatic and aromatic ketones, can be reductively aminated with primary or secondary amines belonging to the aliphatic or aromatic series, and even by using the ammonium ion.
Dedicated literature abounds with sugar compounds modified with amines, especially in relation with the processes of analytical detection of biological trace samples. The attachment of aromatic amines (some possessing fluorescence) allows the detection of sugars by using high performance liquid chromatography (HPLC) and capillary electrophoresis (CE) techniques.
Keeping in mind our experience regarding the analysis and derivatization of dextrans and maltodextrins [1-3], we set out to synthesize some maltoses aminated with different aliphatic amine components. In this paper, the obtained results regarding the derivatization through reductive amination of maltose, as well as the analysis through electrospray ionization mass spectrometry of the obtained compounds, are presented.

Experimental
The reactions took place in round flasks made of glass, which were equipped with magnetic stirrers, heating sources and straight condensers. The reagents ratios vary depending on the amine, while the working temperature (45-90 °C) depends on the solubility of the participating reacting species. The progress of the reaction was monitored through TLC, visualization of spots being made with 5% ethanolic ninhydrin. The isolated compounds were purified by ion exchange chromatography, using ammonium hydroxide solutions of various concentrations as mobile phases. The products were finally brought in solid state through lyophilization. Before being

subjected to physical-chemical analysis, the products were investigated regarding their purity through TLC and for identity by reacting them with ninhydrin, all compounds giving positive results during these tests.

The spectral characterization through HCIT-MS analysis of maltose derivatives, obtained following the reductive amination reaction with different amine components, was done on a High Capacity Ion Trap (HCIT) Ultra PTM instrument (Bruker Daltonik, Bremen, Germany), belonging to the Institute of Chemistry Timișoara of Romanian Academy and courtesy of dr. Gh. Ilia. In all cases, the samples were injected in the spectrometer with the help of a microsyringe, attached to a push-syringe, with a speed of 250 μL h^{-1}. Nitrogen was used as a nebulizer gas, with a flowrate of 5 L min^{-1} and at 7 p.s.i., and at a 300 °C desolvation temperature. The instrument was programmed to operate in positive ion mode, at an ESI potential of 3.0 kV.

For the analysis, the samples were dissolved in MeOH/H_2O (1:1 v/v) to a concentration of 5-7 pmol μL^{-1} (stock solutions), which were diluted as needed.

Results and discussion

The reactions that occur during the derivatization of maltose through reductive amination are presented in **Scheme 1**, while the reaction conditions, which depend on the amine being used, are presented in **Table 1**.

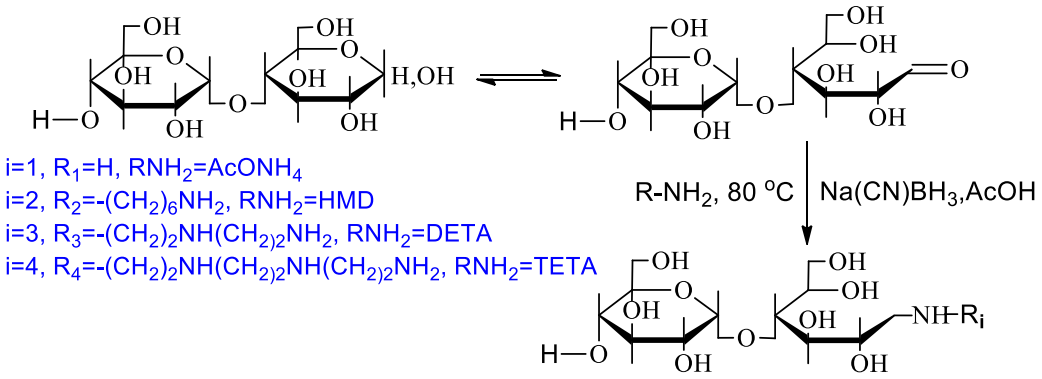

Scheme 1. The reductive amination reactions of maltose with different amine components

Table 1. The reaction conditions for derivatization of maltose with various amine components

No.	Aliphatic amine (mol)	Substrate (mol)	Reducing agent (mol)	Acid (mol)	Time (h)	Control MS	Chemical control
1	**$AcONH_4$**	**maltose**	$Na(CN)BH_3$	AcOH	25	$[M+H]^+$	$Ny^{\#}$
	$15 \cdot 10^{-3}$	$1.5 \cdot 10^{-3}$	$20 \cdot 10^{-3}$	$21 \cdot 10^{-3}$		344.00	+
2	**HMD**	**maltose**	$Na(CN)BH_3$	AcOH	24	$[M+H]^+$	
	$92 \cdot 10^{-3}$	$9 \cdot 10^{-3}$	$18 \cdot 10^{-3}$	$50 \cdot 10^{-3}$		443.00	+
3	**DETA**	**maltose**	$Na(CN)BH_3$	AcOH	120	$[M+H]^+$	
	$90 \cdot 10^{-3}$	$3 \cdot 10^{-3}$	$9 \cdot 10^{-3}$	$30 \cdot 10^{-3}$		430.00	+
4	**TETA**	**maltose**	$Na(CN)BH_3$	AcOH	74	$[M+H]^+$	
	$210 \cdot 10^{-3}$	$9 \cdot 10^{-3}$	$20 \cdot 10^{-3}$	$120 \cdot 10^{-3}$		473.00	+

$^{\#}$Ny - ninhydrin (ethanolic solution of ninhydrin)

In all cases, the $[M+H]^+$ pseudomolecular ion's peak was revealed (see **Table 1**). This was isolated and fragmented through CID, obtaining the MS^2 spectrum (and also, whenever possible, the MS^3 and even the MS^4 spectrum), which gave the minimal number of structural data (characteristic fragmentations for the sugar and, respectively, the amine component). To give an example, the MS^2 and, respectively, MS^3 spectra of the product obtained after amination of maltose with ammonium acetate are shown in **Figs. 1** and **2**. To facilitate the assignments, the main fragmentations of the analyzed product are presented in **Scheme 2**. The MS^3 spectrum of the P fragment (see **Scheme 2**), which is also the base peak, gives all structural details that confirm the structure of the synthesized product.

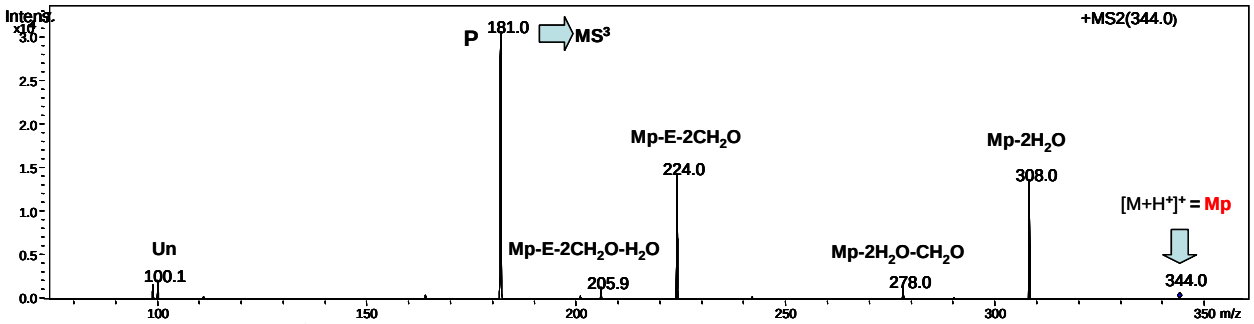

Figure 1. The MS^2 spectrum obtained after (+)-ESI-HCIT-MS analysis of the aminated derivative of maltose, following ammonium acetate reductive amination

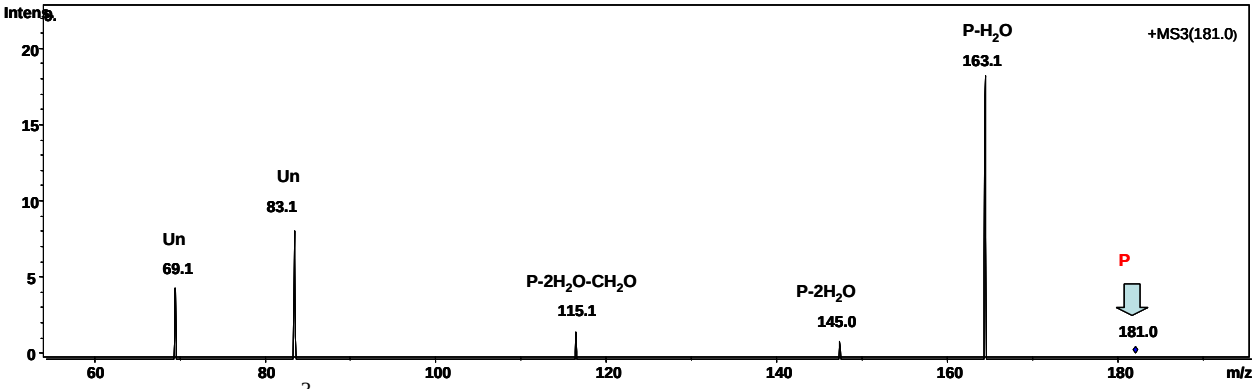

Figure 2. The MS^3 spectrum obtained after (+)-ESI-HCIT-MS analysis of the aminated derivative of maltose, following ammonium acetate reductive amination

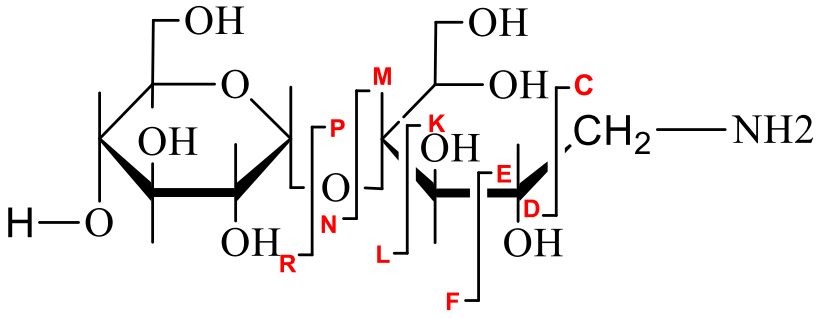

Scheme 2. Fragmentation possibilities for the aminated derivative of maltose, obtained through the reductive amination with ammonium acetate

Conclusions

The derivatization of the anomeric site through attachment of aliphatic amines is done in mild conditions with satisfying yields and with procedures that were established by this research. The determination of the mass spectrometry conditions for ESI-HCIT-MS analysis of the aminated derivatives of maltose gives clear, sharp and reproducible spectra. Owing to the reactivity of the free amine groups, the thus obtained aminated derivatives can be used in many complexation reactions with hydrophilic agents.

Acknowledgements

This work was supported by the Romanian National Authority for Scientific Research (CNCS-UEFISCDI) through project PN-II-PCCA-2011-142. Part of the research was performed at the Center of Genomic Medicine from the 'Victor Babes' University of Medicine and Pharmacy of Timisoara, POSCCE 185/48749, contract 677/09.04.2015.

References

[1] I. Sisu, V. Udrescu, C. Flangea, S. Tudor, N. Dincă,L. Rusnac, A.D. Zamfir, E. Sisu, Cent. Eur. J. Chem. 7 (2009) 66.
[2] E. SiSu, W.T.E. Bosker, W. Norde, T.M. Slaghek, J.W. Timmermans, J. Peter-Katalinic, M.A. Cohen-Stuart, A.D. Zamfir, Rapid Commun. Mass Spectrom. 20 (2006) 209.
[3] I. Perdivara, E. SiSu, I. Sisu, N. Dincă, K.B. Tomer, M. Przybylski, A.D. Zamfir, Rapid Commun. Mass Spectrom. 22 (2008) 773.